Pertanika Journal of

TROPICAL AGRICULTURAL SCIENCE

JTAS

VOL. 48 (3) MAY. 2025

PERTANIKA JOURNALS

A scientific journal published by Universiti Putra Malaysia Press

Pertanika Journal of Tropical Agricultural Science
Pertanika Journal of Tropical Agricultural Science

PERTANIKA JOURNAL OF TROPICAL AGRICULTURAL SCIENCE

About the Journal

Overview

Pertanika Journal of Tropical Agricultural Science is an official journal of Universiti Putra Malaysia. It is an open-access online scientific journal. It publishes the scientific outputs. It neither accepts nor commissions third party content.

Recognised internationally as the leading peer-reviewed interdisciplinary journal devoted to the publication of original papers, it serves as a forum for practical approaches to improving quality in issues pertaining to tropical agriculture and its related fields.

Pertanika Journal of Tropical Agricultural Science currently publishes 6 issues per year (*January, February*, *May*, *June, August*, and *November*). It is considered for publication of original articles as per its scope. The journal publishes in **English** and it is open for submission by authors from all over the world.

The journal is available world-wide.

Aims and scope

Pertanika Journal of Tropical Agricultural Science aims to provide a forum for high quality research related to tropical agricultural research. Areas relevant to the scope of the journal include agricultural biotechnology, biochemistry, biology, ecology, fisheries, forestry, food sciences, genetics, microbiology, pathology and management, physiology, plant and animal sciences, production of plants and animals of economic importance, and veterinary medicine.

History

Pertanika was founded in 1978. Currently, as an interdisciplinary journal of agriculture, the revamped journal, *Pertanika* Journal of Tropical Agricultural Science now focuses on tropical agricultural research and its related fields.

Vision

To publish journals of international repute.

Mission

Our goal is to bring the highest quality research to the widest possible audience.

Quality

We aim for excellence, sustained by a responsible and professional approach to journal publishing. Submissions are guaranteed to receive a decision within 90 days. The elapsed time from submission to publication for the articles averages 180 days. We are working towards decreasing the processing time with the help of our editors and the reviewers.

Abstracting and indexing of Pertanika

Pertanika Journal of Tropical Agricultural Science is now over 47 years old; this accumulated knowledge has resulted in *Pertanika* Journal of Tropical Agricultural Science being abstracted and indexed in Journal Citation Reports (JCR-Clarivate), SCOPUS (Elsevier), BIOSIS, National Agricultural Science (NAL), Google Scholar, MyCite and ISC.

Citing journal articles

The abbreviation for *Pertanika* Journal of Tropical Agricultural Science is *Pertanika J. Trop. Agric. Sci*.

Publication policy

Pertanika policy prohibits an author from submitting the same manuscript for concurrent consideration by two or more publications. It prohibits as well publication of any manuscript that has already been published either in whole or substantial part elsewhere. It also does not permit publication of manuscript that has been published in full in proceedings.

Code of Ethics

The *Pertanika* journals and Universiti Putra Malaysia take seriously the responsibility of all its journal publications to reflect the highest publication ethics. Thus, all journals and journal editors are expected to abide by the journal's codes of ethics. Refer to *Pertanika*'s **Code of Ethics** for full details, available on the official website of *Pertanika*.

Originality

The author must ensure that when a manuscript is submitted to *Pertanika*, the manuscript must be an original work. The author should check the manuscript for any possible plagiarism using any program such as Turn-It-In or any other software before submitting the manuscripts to the *Pertanika* Editorial Office, Journal Division.

All submitted manuscripts must be in the journal's acceptable **similarity index range**:
≤ 20% – *PASS*; **> 20%** – *REJECT*.

International Standard Serial Number (ISSN)

An ISSN is an 8-digit code used to identify periodicals such as journals of all kinds and on all media–print and electronic. All *Pertanika* journals have an e-ISSN.

Pertanika Journal of Tropical Agricultural Science: e-ISSN 2231-8542 (Online).

Lag time

A decision on acceptance or rejection of a manuscript is expected within 90 days (average). The elapsed time from submission to publication for the articles averages 180 days.

Authorship

Authors are not permitted to add or remove any names from the authorship provided at the time of initial submission without the consent of the journal's Chief Executive Editor.

Manuscript preparation

For manuscript preparation, authors may refer to *Pertanika*'s **INSTRUCTION TO AUTHORS**, available on the official website of *Pertanika*.

Editorial process

Authors who complete any submission are notified with an acknowledgement containing a manuscript ID on receipt of a manuscript, and upon the editorial decision regarding publication.

Pertanika follows a double-**blind peer review** process. Manuscripts deemed suitable for publication are sent to reviewers. Authors are encouraged to suggest names of at least 3 potential reviewers at the time of submission of their manuscripts to *Pertanika,* but the editors will make the final selection and are not, however, bound by these suggestions.

Notification of the editorial decision is usually provided within 90 days from the receipt of manuscript. Publication of solicited manuscripts is not guaranteed. In most cases, manuscripts are accepted conditionally, pending an author's revision of the material.

The journal's peer review

In the peer review process, 2 or 3 referees independently evaluate the scientific quality of the submitted manuscripts. At least 2 referee reports are required to help make a decision.

Peer reviewers are experts chosen by journal editors to provide written assessment of the **strengths** and **weaknesses** of written research, with the aim of improving the reporting of research and identifying the most appropriate and highest quality material for the journal.

Operating and review process

What happens to a manuscript once it is submitted to *Pertanika*? Typically, there are 7 steps to the editorial review process:

Pertanika Journal of Tropical Agricultural Science
Pertanika Journal of Tropical Agricultural Science

Pertanika Journal of Tropical Agricultural Science
Pertanika Journal of Tropical Agricultural Science

1. The journal's Chief Executive Editor and the Editor-in-Chief examine the paper to determine whether it is relevance to journal needs in terms of novelty, impact, design, procedure, language as well as presentation and allow it to proceed to the reviewing process. If not appropriate, the manuscript is rejected outright and the author is informed.

2. The Chief Executive Editor sends the article-identifying information having been removed, to 2 or 3 reviewers. They are specialists in the subject matter of the article. The Chief Executive Editor requests that they complete the review within 3 weeks.

   Comments to authors are about the appropriateness and adequacy of the theoretical or conceptual framework, literature review, method, results and discussion, and conclusions. Reviewers often include suggestions for strengthening of the manuscript. Comments to the editor are in the nature of the significance of the work and its potential contribution to the research field.

3. The Editor-in-Chief examines the review reports and decides whether to accept or reject the manuscript, invite the authors to revise and resubmit the manuscript, or seek additional review reports. In rare instances, the manuscript is accepted with almost no revision. Almost without exception, reviewers' comments (to the authors) are forwarded to the authors. If a revision is indicated, the editor provides guidelines to the authors for attending to the reviewers' suggestions and perhaps additional advice about revising the manuscript.

4. The authors decide whether and how to address the reviewers' comments and criticisms and the editor's concerns. The authors return a revised version of the paper to the Chief Executive Editor along with specific information describing how they have answered' the concerns of the reviewers and the editor, usually in a tabular form. The authors may also submit a rebuttal if there is a need especially when the authors disagree with certain comments provided by reviewers.

5. The Chief Executive Editor sends the revised manuscript out for re-review. Typically, at least 1 of the original reviewers will be asked to examine the article.

6. When the reviewers have completed their work, the Editor-in-Chief examines their comments and decides whether the manuscript is ready to be published, needs another round of revisions, or should be rejected. If the decision is to accept, the Chief Executive Editor is notified.

7. The Chief Executive Editor reserves the final right to accept or reject any material for publication, if the processing of a particular manuscript is deemed not to be in compliance with the S.O.P. of *Pertanika.* An acceptance notification is sent to all the authors.

   The editorial office ensures that the manuscript adheres to the correct style (in-text citations, the reference list, and tables are typical areas of concern, clarity, and grammar). The authors are asked to respond to any minor queries by the editorial office. Following these corrections, page proofs are mailed to the corresponding authors for their final approval. At this point, **only essential changes are accepted**. Finally, the manuscript appears in the pages of the journal and is posted on-line.

Pertanika Journal of

TROPICAL AGRICULTURAL SCIENCE

Vol. 48 (3) May. 2025

PERTANIKA JOURNALS

A scientific journal published by Universiti Putra Malaysia Press

PJTAS

***Pertanika* Journal of Tropical Agricultural Science**

AN INTERNATIONAL PEER-REVIEWED JOURNAL

EDITORIAL OFFICE
JOURNAL DIVISION
Putra Science Park
1st Floor, IDEA Tower II
UPM-MTDC Technology Centre
Universiti Putra Malaysia
43400 Serdang, Selangor Malaysia

General Enquiry
Tel. No: +603 9769 1622
E-mail: executive_editor.pertanika@upm.edu.my
URL: http://www.pertanika.upm.edu.my

PUBLISHER
UPM PRESS
Universiti Putra Malaysia
43400 UPM, Serdang, Selangor, Malaysia
Tel: +603 9769 8855
E-mail: dir.penerbit@upm.edu.my
URL: http://penerbit.upm.edu.my

ABSTRACTING AND INDEXING OF PERTANIKA JOURNALS

The journal is indexed in Journal Citation Reports (JCR-Clarivate), SCOPUS (Elsevier), BIOSIS, National Agricultural Science (NAL), Google Scholar, MyCite and ISC.

Pertanika Journal of Tropical Agricultural Science
Vol. 48 (3) May. 2025

Contents

Foreword

Welcome to the third issue of 2025 for the Pertanika Journal of Tropical Agricultural Science (PJTAS)!

PJTAS is an open-access journal for studies in Tropical Agricultural Science published by Universiti Putra Malaysia Press. It is independently owned and managed by the university for the benefit of the world-wide science community.

This issue contains 21 articles: four review articles; two short communications; and the rest are regular articles. The authors of these articles come from different countries namely Afghanistan, Bhutan, Indonesia, Japan, Malaysia, Nigeria, Taiwan, Thailand and Vietnam.

A regular article entitled "Development of Herbal Tea Product Based on *Crossandra infundibuliformis* and *Justicia betonica* Leaves for Functional Drink: Antioxidant Activity, Sensory Evaluation, and Nutritional Value" aims to determine antioxidant activity in extracts, including sensory evaluation of herbal tea products from both *Crossandra infundibuliformis* and *Justicia betonica*. Leaf extracts were taken to determine total extractable phenolic content (TPC), total extractable flavonoid content (TFC), and antioxidant activity, including compound contents, using the high-performance liquid chromatography (HPLC) technique. The results showed that *C. infundibuliformis* extract exhibited a higher activity value for TPC, TFC, and antioxidant activity than *J. betonica*. Moreover, the *C. infundibuliformis* and *J. betonica* leaf extracts contained eight and nine types of phenolic and flavonoid compounds, respectively. Further details of this study are found on the page 719.

A selected article entitled "Effect of Solid-State Fermentation on Nutritional Value of Pineapple Leaves" assessed how pineapple leaves, often discarded as waste, were valorised using solid-state fermentation (SSF) to enhance their nutritional value for animal feed. This study investigated the enrichment of pineapple leaf nutritional values using SSF. The process parameters such as fermentation time, inoculum type and size, additional carbon source and particle size were optimized using the one-factor-at-a-time (OFAT) method. SSF proved to enhance the nutrient content of pineapple leaves, offering an alternative nutrient source for animal feed. The detailed information of this article is available on the page 767.

A study by Norlyiana and team entitled "*Bazzania spiralis* Extracts Exhibit Effective Toxicity and Oviposition Deterrence against *Bemisia Tabaci*" analyzed the insecticidal potential of crude methanol extracts from the liverwort *B. spiralis* against *B. tabaci*. The silverleaf whitefly, *B. tabaci*, is a major agricultural pest that has developed resistance to many synthetic pesticides, necessitating the search for effective, eco-friendly alternatives. The results indicate that *B. spiralis* extracts may serve as a natural alternative to synthetic pesticides for managing *B. tabaci*. However, further studies are required to isolate the active compounds, evaluate their effectiveness under field conditions, and assess their environmental persistence and impact on beneficial insects. Full information on this study is presented on the page 1055.

We anticipate that you will find the evidence presented in this issue to be intriguing, thought-provoking and useful in reaching new milestones in your own research. Please recommend the journal to your colleagues and students to make this endeavour meaningful.

All the papers published in this edition underwent Pertanika's stringent peer-review process involving a minimum of two reviewers comprising internal as well as external referees. This was to ensure that the quality of the papers justified the high ranking of the journal, which is renowned as a heavily-cited journal not only by authors and researchers in Malaysia but by those in other countries around the world as well.

We would also like to express our gratitude to all the contributors, namely the authors, reviewers and Editorial Board Members of PJTAS, who have made this issue possible.

PJTAS is currently accepting manuscripts for upcoming issues based on original qualitative or quantitative research that opens new areas of inquiry and investigation.

Editor-in-Chief
Mohamed Thariq Hameed Sultan

Pertanika J. Trop. Agric. Sci. 48 (3): 667 - 683 (2025)

PERTANIKA JOURNALS

TROPICAL AGRICULTURAL SCIENCE

Journal homepage: http://www.pertanika.upm.edu.my/

Review Article

Home-based Foods in Malaysia: A Food Safety Perspective

Subashini Pallianysamy[1,4], Noor Azira Abdul-Mutalib[2,3], Ungku Fatimah Ungku Zainal Abidin[2], Nor Khaizura Mahmud @ Ab Rashid[1,3] and Nurul Hawa Ahmad[1,3]*

[1]Department of Food Science, Faculty of Food Science and Technology, Universiti Putra Malaysia, 43300 Serdang, Selangor, Malaysia
[2]Department of Food Service and Management, Faculty of Food Science and Technology, Universiti Putra Malaysia, 43300 Serdang, Selangor, Malaysia
[3]Laboratory of Food Safety and Food Integrity, Institute of Tropical Agriculture and Food Security, Universiti Putra Malaysia, 43300 Serdang, Selangor, Malaysia
[4]Food Safety and Quality Division, Ministry of Health, 62675 Putrajaya, Malaysia

ABSTRACT

Home-based food businesses are trending among the new generation of food entrepreneurs, particularly during and after the COVID-19 pandemic. This review aims to provide a general scenario of home-based food businesses in Malaysia, possible contamination sources associated with home-based food and foodborne pathogens that can be linked to common food in Malaysia. Home -based food business is an integral part of food supply chain sells through local markets, online platforms, delivery services or direct pick up whereby food safety is a critical component to be taken care of. This review paper explores initiatives by Ministry of Health in order to create awareness and safety measures in different level of food business. This review also highlights current home-based food guidelines in Malaysia and the knowledge, practice, and attitude (KAP) linked to food operators in Malaysia. This paper also synthesizing current research associated with KAP food handlers and provides insights of future direction of improving food safety systems particularly for home-based food business.

Keywords: Food safety, home-based food business, home-based food, KAP study

ARTICLE INFO

Article history:
Received: 12 July 2024
Accepted: 02 September 2024
Published: 16 May 2025

DOI: https://doi.org/10.47836/pjtas.48.3.01

E-mail addresses:
gs64207@student.upm.edu.my (Subashini Pallianysammy)
n_azira@upm.edu.my (Noor Azira Abdul-Mutalib)
ungkufatimah@upm.edu.my (Ungku Fatimah Ungku Zainal Abidin)
norkhaizura@upm.edu.my (Nor Khaizura Mahmud Ab Rashid)
nurulhawa@upm.edu.my (Nurul Hawa Ahmad)
*Corresponding author

e-ISSN: 2231-8542

INTRODUCTION

A home-based food (HBF) business is any business that sells products from their home (Mason et al., 2011). HBF can be operated by the business owner, individually or with workers (Dahari et al., 2019). Home-based Food Guidelines by the Ministry of Health, Malaysia, defines home-based food as "food prepared at home for selling purposes."

The booming of HBF businesses is evident, especially during the COVID-19 pandemic (Tarmazi et al., 2021). Following the Malaysian government's Movement Control Order (MCO), most people are confined at home and face many outdoor restrictions. MCO has caused many economic activities to slow down, consequently forcing many people to lose their occupations. Nevertheless, some unemployed have started HBF to meet their financial need in line with the great demand of consumers looking for food delivery services during MCO. In 2024, Malaysia's online food delivery revenue will reach USD 2.77 billion, with an expected increase of up to USD 4.63 billion in market volume by 2029 (Statista, 2024).

The Malaysian government has introduced numerous initiatives, such as PRIHATIN and PENJANA Economic Stimulus Package, to facilitate HBF business. Pemulih NewBiz Financing Fund allocated RM50 million in 2022 via Agro Bank to support new HBF businesses (Gimino, 2022). However, the dine-in operation has resumed in Malaysia during the transition period from pandemic to endemic state. Nevertheless, the emergence of e-commerce and social media has caused HBF's business to grow sustainably, particularly for individuals needing household income (Lee, 2021).

Malaysia's economy is recovering momentum post-MCO, but the global inflation crisis has tremendously altered consumer purchasing behavior. The National inflation rate increased to 3.2% in December 2022, as reported by the Department of Statistics Malaysia (2021). More retail owners shifted their businesses to home-based settings to minimize operation costs (Zhang et al., 2022). One of the possible reasons for HBF operators to sustain their business operations at home could be because they may feel that it is still more practical and accommodating to generate income (Zhang et al., 2022). Considering numerous initiatives by the Malaysian government to support solo entrepreneurs, including HBF operators, it can be anticipated that these initiatives may accelerate the growth of HBF in the future (Topimin & Hashim, 2021).

Unfortunately, many foodborne outbreaks are linked to home-based food (Azanza et al., 2018; Byrd-Bredbenner et al., 2013). In May 2020, 48 illnesses and one death were reported in the northeast state of Malaysia due to the consumption of a local dessert called *pudding buih* (bubbled pudding). The egg-based pudding was most likely contaminated with *Salmonella* as raw egg white was used. Furthermore, there is no cooking step prior to consumption ("*Puding Buih* food poisoning," 2020). Affected individuals bought the delicacy via an online platform operated by HBF traders. A recurrent episode of *pudding buih* food poisoning occurred in 2022, where in this case, the home-prepared dessert was

sold at a local stall. This incident affected two children ("Food poisoning: samples of *pudding buih* sent to a lab for analysis," 2022).

On top of that, major food poisoning cases have been reported in Malaysia between May and July 2024. In May 2024, 65 primary school students in Kedah were sick after consuming flat noodle soup ("Sixty-five Sungai Petani primary school pupils suffer food poisoning," 2024). About a month later, two deaths (a two-year-old girl and a 17-year-old male) and 22 illnesses were reported due to spoiled fried noodles and eggs in Selangor. Eighty-two suffer food poisoning symptoms from consuming fried noodles and eggs. Meanwhile, in Johor, breaded fried chickens sold in a school canteen have been implicated in causing food poisoning symptoms to 90 students and nine staff members ("Batu Pahat school canteen ordered shut over food poisoning – Johor exco," 2024). Lastly, a typhoid outbreak in Kelantan has affected ten high school students with abdominal pain, vomiting, and diarrhea (Abdullah, 2024). A mass screening of 1000 individuals led to three food handlers being identified as the source of the outbreak ("Three food handlers identified as the source of the typhoid outbreak at Kelantan school," 2024).

Although the etiologic agents of these foodborne illnesses were not fully reported, the implicated foods might have been contaminated with foodborne pathogens that otherwise can be inactivated by proper cooking procedures or controlled via hygienic handling and appropriate storage conditions. Given that the home environment may not optimally support food preparation, handling, or storage safety protocols (Farias et al., 2020), and food safety practices heavily rely on HBF operators, a more sustainable approach is needed by immersing food safety culture in HBF business. Food safety culture fosters human behavioral changes toward food safety practices (Global Food Safety Initiative, 2018). This concept covers many aspects of food safety, including the first-in-first-out principle of raw materials, cleaning and sanitation, record keeping, and allergen control. Food safety culture adopts the mentality of 'this is the right thing to do," which is greatly aligned with Sustainable Development Goals (SDGs) of responsible consumption and production (SDG 12). By quality education (SDG 4), partnerships for goals (SDG 17), and good health and well-being (SDG 3), food safety culture can be fostered via strategic efforts from government, private, and community segments in reducing food poisoning cases in Malaysia.

POSSIBLE CONTAMINATION SOURCES OF HOME-BASED FOOD

Raw Materials

Perishable goods such as fruits, vegetables, meat, poultry, and dairy products have a short shelf-life. Maintaining perishable goods in a cold environment can minimize the risk of foodborne illnesses, delay the growth of spoilage microorganisms and maintain product quality. Limited cold storage spaces at home may yield an excessive load of refrigerators and

freezers, which consequently prevent the cold storage environment from being maintained below 4°C and -18°C, respectively (United States Department of Agriculture [USDA], 2023). Bulk storage of perishable goods may increase the risk of microbial proliferation. Malaysia is a tropical country where the indoor temperature can range between 21°C to 37°C, with high humidity and high solar irradiation (Gou et al., 2018). Thawing meat, poultry and seafood by submerging frozen products in a kitchen sink or basin at ambient conditions can cause proliferation of foodborne pathogens and spoilage microorganisms (USDA, 2023). With the upward trajectory of global warming, Malaysia likely will continue to face heat wave threats that could increase the risk of foodborne pathogen growth.

Dry ingredients such as anchovy, flour, rice, spices, and dried fruits may have a longer shelf life than perishable goods. However, bacterial spores and mycotoxins are commonly found in dry ingredients (Tanushree et al., 2019). Spores and mycotoxins can survive cooking temperatures. Bacterial spores may germinate after cooking and proliferate in finished products if not stored properly (Navaneethan & Effarizah, 2023). Mycotoxins are potent etiologic agents, and a small number of mycotoxins (ppm or ppb level) can cause severe health symptoms. Obtaining raw materials from reputable suppliers may mitigate the risk, but suppliers only consider bulk purchases, which can be a limiting factor for HBF's business. Extreme weather conditions and uncontrolled relative humidity are major determinants of mold contamination in dry goods (Tanushree et al., 2019).

Cross-contamination

Cross-contamination occurs when a contaminated entity encounters an uncontaminated entity. Three possible routes for cross-contamination could happen at home kitchens: contamination from food-to-food, person-to-food, and surface-to-food. For instance, food-to-food cross-contamination may occur when raw meat and poultry are stored with ready-to-eat foods. Raw juices may spread on cooked or ready-to-eat food if placed or stored near one another without proper control. Food handlers who have poor hygiene can cause person-to-food cross-contamination. Food handlers who handle raw ingredients and ready-to-eat food without hand washing can transfer foodborne pathogens to ready-to-eat foods. Surface-to-food contamination is likely to happen when the same utensils, such as a chopping board and knife, are simultaneously used for raw meat and poultry and ready-to-eat fresh salad vegetables (Kirchner et al., 2021). A study by Borrusso and Quinlan (2017) found that contamination of foodborne pathogens was significantly associated with unsafe or unsanitary conditions of home kitchens in Philadelphia, with 45% of home kitchens detected with multiple foodborne pathogens such as *Escherichia coli, Staphylococcus aureus, Salmonella, Campylobacter, and Listeria monocytogenes.*

Consumers commonly use food delivery services to shuttle food items from merchants to end customers due to several accommodating factors (Keeble et al., 2020). A generalized

framework of food delivery service in Malaysia has been extensively described by Ahmad and Zainal (2021), demonstrating a triad connection between customers, food delivery services, and merchants. There are multiple activities involved between each connection point, such as how customers order food via online platforms and how e-hailing riders deliver food to customers' doorsteps. Most importantly, many instances within those activities can introduce cross-contamination, which may put HBF businesses at risk. First, improper HBF food packaging may cause spills, allowing cross-contact with unsanitary delivery bags or vehicle surfaces. Furthermore, most riders use self-owned vehicles, and the sanitary conditions of the vehicles and reusable delivery bags heavily rely on the rider's self-inspection and food safety self-awareness. Secondly, cross-contamination may occur when non-food items, food items, raw foods, and cooked foods are not well segregated in a delivery bag. For instance, tempering frozen raw foods may cause leakage of raw juice and cross-contact with cooked foods. Lastly, cross-contamination could be attributed merely to the deliverers' lack of food safety knowledge, practices, and attitude, most likely due to noncompulsory food safety training for riders (Hishamudin et al., 2024). On top of cross-contamination incidences, food safety risk for HBF may be escalated when foods are exposed to time-temperature abuse conditions.

Kitchen Space and Layout

Urban housing development in Malaysia is largely focused on low-medium income earners. The size of affordable housing is between 614 to 1195 square feet for apartments and ⩽1900 square feet for landed houses (Construction Industry Development Board Malaysia, 2020). It strongly suggests that the home kitchen has limited space and may not be sufficient to establish specific food preparation, handling, packaging, and storage zones. The home kitchen also serves as a communal space for school, work, laundry and social activities. The home kitchen is accessible to family and nonfamily members and pets so they can roam around freely. Owing to heterogeneous resident profiles and the many ways that kitchen areas are used, foods prepared by HBF operators can pose food safety risks due to a variety of sources of cross-contamination (Wills et al., 2015). In addition to space, the home kitchen design and layout vary depending on the user. Coordination of kitchen cabinets, appliances, and waste containers (hazardous or nonhazardous) is based on the homeowner's preference, which may not be ideal for hygienic design.

In terms of premise setting, Food Standards Australia and New Zealand require that kitchen layout and space are enough for people to work without contaminating food and to separate cooked food away from raw food (Food Standards Australia and New Zealand, 2021). In EU countries, Mihalache et al. (2022) proposed a 'food safety triangle's kitchen design that may support food hygiene practices, contrasting with an ergonomic kitchen design. The food safety triangle design consists of a handwashing sink, countertop and

stove, with the distance between each apex less than 1 m. Although more studies are needed to correlate kitchen design with food safety practices, it can be inferred that ideal kitchen design should minimize cross-contamination during food preparation and handling.

POSSIBLE FOODBORNE PATHOGENS ASSOCIATED WITH HOME-BASED FOOD

Malaysia has various local cuisines, predominantly consisting of rice and wheat-based food as carbohydrate sources and fish, egg, and chicken as protein sources (Goh et al., 2020). Guidelines for food poisoning investigation in Malaysia (Food Safety and Quality Division, 2024) have outlined potential foodborne pathogens that could be tested according to the type of common foods in Malaysia (Table 1). *Salmonella* remains a major concern in Malaysia because many food poisoning episodes have been associated with it.

Table 1
Foodborne pathogens that can be associated with foods commonly consumed in Malaysia

Food group	Specific food	Pathogen*								
		Salmonella	***Escherichia coli* O157:H7**	***Bacillus cereus***	***Diarrheal Bacillus* spp.**	***Listeria monocytogenes***	**Clostridium perfringens**	**Vibrio cholerae**	**Vibrio parahaemolyticus**	**Staphylococcus aureus**
Cereal and grains	White rice			/	/					
	Fried rice			/	/					
	Roti canai ǂ			/	/					
	Noodle			/	/					
	Pasta			/	/					
Poultry	Fried chicken	/								/
	Chicken nugget	/								/
	Chicken ball	/								/
	Chicken frankfurter	/								/
	Steamed chicken	/								/
	Chicken in broth	/					/	/		/
	Chicken *gulai* ǂ	/					/			/

Table 1 *(continue)*

Food group	Specific food	Pathogen*								
		Salmonella	***Escherichia coli* O157:H7**	***Bacillus cereus***	***Diarrheal Bacillus* spp.**	***Listeria monocytogenes***	**Clostridium perfringens**	**Vibrio cholerae**	**Vibrio parahaemolyticus**	**Staphylococcus aureus**
Egg	Hard/Half boiled egg	/								
	Fried egg	/								
	Salted egg	/								
	Egg *gulai* ǂ	/								
Meat	Meatball	/	/							
	Sausage	/	/							
	Meat in broth	/	/				/	/		
	Meat *gulai* ǂ	/	/				/			
Seafood	Fishball	/							/	
	Dried/Salted fish	/							/	
	Fried fish	/							/	
	Fish *gulai* ǂ	/							/	
	Cockles	/							/	
Vegetables	*Ulam* ǂ	/								
	Kerabu ǂ	/								
	Stir-fry vegetables	/								
Milk	UHT/ pasteurized milk	/				/				
	Pudding	/				/				

Note. ǂ*Roti canai:* Malaysian flatbread; *Gulai:* spicy/mild stew that may use spices, condiments, or coconut milk; *ulam:* traditional/common vegetables that can be eaten raw or boiled; *kerabu*: pickled salad that may incorporate shredded coconut, seafood (cockles/squid), or beef tripe. *The limit of detection (LOD) of *Salmonella*, *Vibrio cholerae*, *and Vibrio parahaemolyticus* is 0.04 CFU/g and limit of quantification (LOQ) of *Bacillus cereus*, *Escherichia coli*, *Staphylococcus aureus* is 100 CFU/g according to Food Safety and Quality (2019); LOD and LOQ of *Listeria monocytogenes* are according to ISO 11290-2:2017; no specified LOQ for *Clostridium perfringens* stated in FSQ (2019), but a maximum of 1-log increase is permitted during Ready-to-Eat meat and poultry production based on United States Department of Agriculture Food Safety Inspection Service (2021)

HOME-BASED FOOD OPERATORS AND HANDLERS

Food handlers from various food services play an important role in food safety because they may introduce pathogens into foods during production, processing, distribution, and preparation (Azanza et al., 2019). Food handlers are individuals directly involved in food preparation, come into contact with food or food contact surfaces, and handle packaged or unpackaged food or appliances in any food premises (Act 281, Food Act 1983). According to Malaysian Food Hygiene Regulations 2009, every personnel defined as a food handler shall undergo food handler training provided by a recognized school of food handler training and must be vaccinated for the Typhoid vaccine. These requirements also apply to home-based food handlers, but awareness of these requirements among home-based food operators and handlers is still questionable. Therefore, studies conducted where food handlers became the main target of most researchers because they were the key players determining and controlling the best practices of food hygiene in food establishments.

Given the dynamic nature of their HBF businesses, Razak et al. (2022) suggested introducing a specific category for home-based food handlers under the Food Hygiene Regulations 2009. Such regulation may mitigate home-based operators' reluctance to register and follow food safety recommendations to save costs. Another issue that can be mitigated includes hiring foreign part-time workers who do not possess legal working permits, as they are willing to accept low wages (Abd Rahim et al., 2017). Illegal foreign workers may not be eligible for Typhoid vaccination, which can increase the risk of spreading diseases. Helpers among acquaintances who are not committed to full-time home-based operators should also be considered as food handlers. Sick food handlers may be in contact with food preparation, cooking, or packaging due to ignorance of good hygienic practices. In this sense, measuring their knowledge and awareness is highly important, especially for home-based food handlers. Food poisoning is a public health problem in Malaysia and among the top five communicable diseases in Malaysia, which spread through contaminated food, water and food handlers. Thus, there is a need to ensure that the HBF operators understand standard food safety protocols and adhere to requirements by the Malaysia Ministry of Health to protect public health.

Food Safety Awareness

In Malaysia, the data on food poisoning cases related to home-based food are lacking. Furthermore, not all food poisoning cases are being reported. So, the exact number of food poisoning incidents associated with home-based food is unknown. Most home-based food businesses do not have a business license, and consumers do not know the level of hygiene being practiced by home-based food handlers. Therefore, further studies on the safety of the food produced from home-kitchen have been conducted from various perspectives to improve the service and safety of the food produced from home kitchens.

Customers sometimes rely on testimonies to drive their purchasing decisions because there is no accessible tool or guideline to assess the safety and cleanliness of home-based food (Iblasi et al., 2016).

Unlike HBF, the food industry in Malaysia must execute food safety assurance programs such as Good Manufacturing Practice (GMP), Hazard Critical Control Points (HACCP), ISO 22000, or *Makanan Selamat Tanggungjawab Industri* (MeSTI). In particular, MeSTI is designed for small and medium enterprises (SMEs) to meet food safety requirements minimally in compliance with the Food Hygiene Regulations 2009. Under the MeSTI scheme, food manufacturing premises must be physically audited, given free consultation by Ministry of Health (MOH) officers, approved for operation and monitored after a year of certificate issuance (Food Safety and Quality Division, 2023). In addition, MOH has also introduced *Bersih, Selamat dan Sihat* (BeSS) recognition to encourage food premises such as food kiosks, cafeterias, school canteen, and restaurants, practice food safety standards and promote healthier food options (Food Safety and Quality Division, 2024). Apart from this, MOH initiated the Trust MyCatering Certification, which recognizes that the catering industries comply with food safety elements under the Food Hygiene Regulations 2009 (Food Act 1983). This certification is also applicable to HBF operators who are doing catering business using home kitchens as their business facilities.

Halal certification is a major concern in Malaysia's food and beverage industry and worldwide. It ensures religious compliance, safety, and hygiene compliance. Halal Certification boosts sales and influences customers' purchasing decisions (Yusuf et al., 2017). No halal certification is provided for home-based food products, yet claims of halal home-based food are mushrooming on social media. This statement can create misunderstandings and confusion among customers, thus causing food safety awareness to be prejudged.

In 2020, MOH conducted a pilot project on home-based food operators in Malaysia. A total of 114 out of 410 (27.8%) home-based food operators were approved after going through the approval process from MOH (Figure 1). All participants were briefed on the food safety requirements, and the MOH officers verified their kitchens before approval was granted (Ministry of Health, 2021). There are several reasons why participants who enrolled in the pilot project were unable to be listed under MOH. Some of the reasons include i) HBF operators could not fulfill all requirements from MOH, ii) low commitments from the HBF operators who did not respond to do corrective actions to get approved, iii) HBF just a hobby or temporary business to get extra income for some operators, as they may acquire a permanent job after the pandemic was over. Therefore, MOH has taken necessary steps to educate and regulate home-based food operators in Malaysia by encouraging them to register themselves under a database system called Fosim Domestic to monitor them effectively.

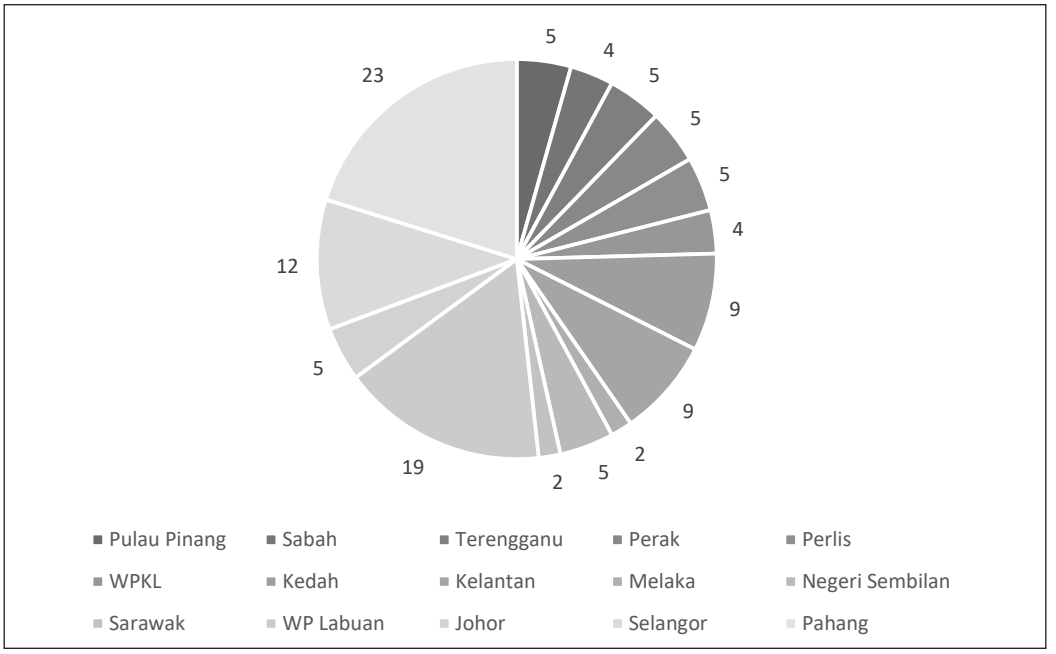

Figure 1. Recognition for home-based listing in the pilot project in Malaysia (Food Safety Quality Division, 2021)

Ministry of Health Malaysia (MOH) has taken the initiative to educate home-based food operators by providing them with specific guidelines for home-based food operators. The Ministry of Health launched a new home-based food listing scheme to encourage home-based food operators to comply with the Food Act 1983 and Food Regulations 1985; Food Hygiene Regulations 2009. Under this guideline, all the home-based food operators are required to undergo Food Handlers training, get vaccinated for typhoid, implement all the food safety measures as in the guidelines, and perform self-monitoring according to the home-based food operator checklist. In 2021, home-based food safety guidelines were also published in the same year as the main reference document for the listing scheme (Ministry of Health, 2021). HBF operators listing specifically initiated to formalize activities as well as food safety control measures. While food safety assurance program implementation may be challenging to HBF operators, relevant food safety standards need to be implemented by HBF operators because any violations by HBF will be treated as any other food handlers and compounded according to the Food Act 1983.

Food safety surveillance is crucial in ensuring that food prepared, sold, or imported into the market meets the standards set by the Food Act 1983. Routine food safety monitoring is conducted by MOH, in which ready-to-eat foods collected from food premises are commonly tested for the presence of foodborne pathogens, including *Bacillus cereus*, *Staphylococcus aureus*, *Salmonella*, and *Escherichia coli*. Microbiological analyses

are conducted in accredited laboratories and are performed according to respective ISO methods (Standards Malaysia, 2024). On top of routine monitoring, a large-scale seasonal inspection such as food stalls and bazaars during Ramadan (Muslim's fasting month) is also conducted. In 2022, for instance, the Food Safety and Quality Division (FSQD) undertook national-level enforcement, given the increased volume and variety of food sold. Out of 12,934 premises inspected, 38 were ordered to shut their operations due to incompliance with the regulations (Food Safety and Quality Division, 2022).

Knowledge, Attitude, and Practice (KAP)

Knowledge, attitude, and practice (KAP) is survey-based research and the most common method used to evaluate the relationship between knowledge, attitude, and practice of food handlers in various fields of the food business. Food safety knowledge and attitudes are the most important cognitive factors that can influence food safety practices, and multiple studies use KAP models to study correlations between food safety knowledge and attitude (Baser et al., 2017; Lim et al., 2016). In Malaysia, KAP studies have been conducted on food handlers in all kinds of food service industries, as illustrated in Table 2.

Although food safety knowledge is important to prevent foodborne illness in home kitchens, approximately 50% of the reported studies on food handlers were not necessarily translated into practice (da Cunha et al., 2019). As mentioned in Food Hygiene Regulations 2009, food handlers in Malaysia must undergo training. However, further studies need to be conducted on the effectiveness of the training provided and evaluate the attitude of home-based food handlers towards food safety. Several studies also show that the level of knowledge did not solely contribute to or influence the level of attitude (Ahmed et al., 2021). These findings revealed that there could be other factors, including environment, job satisfaction, and the relationship between employees and supervisors in a proper food establishment. Therefore, sociodemographic profiles that influence the variables should also be extended to other factors.

Researchers could utilize cross-sectional studies to compare the knowledge, attitude, and self-reported practices (KAP) of food safety assessments focusing on food handlers

Table 2
Example of knowledge, attitude and practice (KAP) score of food handlers in different food service facilities in Malaysia

Sectors	Knowledge (mean)	Attitude (mean)	Practice (mean)
Cafeterias at residential colleges	~57.8%	~76.9%	~66.5%
Hospitals	<90%	<70%	<35%
Restaurants or kiosk	<84%	<82%	<77%
Hawker centers	<84.1%	<67.9%	<74%

Note. Scores between 0 to 40: poor, 41 to 70: fair, 71 to 80: Good

in food service industries (Nee & Sani, 2011; Lee et al., 2017). Cross-sectional studies are conducted involving a certain group of people at one point in time. Cross-sectional studies involve face-to-face interviews, online surveys through Facebook, WhatsApp, and Instagram, or self-reported survey questionnaires distributed by survey companies (Amodio et al., 2022). The sample size varies based on population, location, and time frame needed to complete the survey. Relevant studies (Amodio et al., 2022) are mostly self-reported, based on what is being answered by the respondents, which may be reported differently from actual practice. It may be fit for other food businesses. However, for home-based food businesses, it is suggested to conduct a qualitative study in the explanatory method to study in detail the nature of the business and other contributing factors since home-based food businesses are considered a new emerging business that needs to be explored to provide new insight into the business for necessary actions. Because KAP studies are self-reported data, the findings of KAP studies can be further validated using microbiological assessment of home-based food produced. Observation via online or physical demonstration can be used to evaluate hygienic practices more effectively. The findings of the KAP study are valuable input towards improving existing training modules.

CONCLUSION

Summary

The home-based food business (HBF) is considered part of the food supply chain. Past incidents have revealed that food handlers in Malaysia still lack food safety knowledge, have an inadequate understanding of handling raw materials and have poor hygiene practices. Various factors, including home-kitchen size, layout, location, and usage, can also be considered contributing factors. Yet, there are still limited studies that can strongly correlate the factors mentioned and the contamination sources of home-based food. Home-based food guidelines by the Ministry of Health, Malaysia, are designed to equip HBF operators with a basic knowledge of hygienic food preparation. Given that the HBF operators have various sociodemographic backgrounds, it is critical to measure their level of understanding to comply with the current requirements.

Future Perspective and Recommendations

Nowadays, greater internet literacy and accessibility allow customers to purchase food from HBF businesses from the comfort of their smartphones. HBF operators no longer wait for walk-in customers because e-hailing companies can deliver the food to their customers' doors. With this ongoing demand, HBF operators can reach a larger market size and generate more income. HBF also plays a critical role as one of Malaysia's food supply chain niches. Nevertheless, there is no scheduled monitoring or inspection of HBF operations via the voluntary HBF listing scheme of the Ministry of Health Malaysia. One

approach that may mitigate the risk of foodborne illness for HBF business is establishing a set of maximum limits covering kitchen occupancy, food preparation and storage capacity, and revenue range. Once the maximum limits have been reached and sustained over a reasonable period, regulatory bodies can urge HBF businesses to convert their businesses to a commercial scale because commercial food businesses abide by existing food laws and regulations in Malaysia. To do this, HBF operators must be listed in the scheme. An appropriate enforcement approach must also be designed so that it is feasible for the authorities to carry out the policy and straightforward enough for HBF operators to understand it.

ACKNOWLEDGEMENTS

The authors thank the Food Safety and Quality Division, Ministry of Health Malaysia and the Hadiah Latihan Persekutuan scholarship for financially supporting Subashini Pallianysamy.

REFERENCES

Abd Rahim, S. A., Nawawi, A., & Puteh Salin, A. S. A. (2017). Internal control weaknesses in a cooperative body: Malaysian experience. *International Journal of Management Practice*, *10*(2), 131-151. https://doi.org/10.1504/IJMP.2017.083082

Abdullah, S. M. (2024, July 16). Ten secondary students in Kelantan test positive for typhoid, outbreak under control. *New Straits Times*. https://www.nst.com.my/news/nation/2024/07/1077584/10-secondary-students-kelantan-test-positive-typhoid-outbreak-under

Ahmad, N. N. N., & Zainal, A. S. A. S. (2021) Online food delivery services: Make or break the halal supply chain? *Journal of Food and Pharmaceutical Sciences*, *9*(1), 384-394. https://doi.org/10.22146/jfps.1149

Ahmed, M. H., Akbar, A., & Sadiq, M. B. (2021). Cross sectional study on food safety knowledge, attitudes, and practices of food handlers in Lahore district, Pakistan. *Heliyon*, *7*, e08420. https://doi.org/10.1016/j.heliyon.2021.e08420

Amodio, E., Calamusa, G., Tiralongo, S., Lombardo, F., & Genovese, D. (2022). A survey to evaluate knowledge, attitudes, and practices associated with the risk of foodborne infection in a sample of Sicilian general population. *AIMS Public Health*, *9*(3), 458-470. https://doi.org/10.3934/publichealth.2022031

Azanza, M. P. V, Membrebe, B. N. Q., Sanchez, R. G. R., Estilo, E. E. C., Dollete, U. G. M., Feliciano, R. J., & Garcia, N. K. A. (2019). Foodborne disease outbreaks in the Philippines (2005 – 2018). *Philippines Journal of Science*, *148*(2), 317–336.

Baser, F., Ture, H., Abubakirova, A., Sanlier, N., & Cil, B. (2017). Structural modeling of the relationship among food safety knowledge, attitude and behavior of hotel staff in Turkey. *Food Control*, *73*, 438-444. https://doi.org/10.1016/j. foodcont.2016.08.032

Batu Pahat school canteen ordered shut over food poisoning – Johor exco. (2024, July 1). *Bernama*. https://www.bernama.com/en/news.php/news.php?id=2312957

Borrusso, P. A., & Quinlan, J. J. (2017). Prevalence of pathogens and indicator organisms in home kitchens and correlation with unsafe food handling practices and conditions. *Journal of Food Protection*, *80*(4), 590-597. https://doi:10.4315/0362-028X.JFP-16-354

Byrd-Bredbenner C., Berning J., Martin-Biggers J., & Quick, V. (2013). Food safety in home kitchens: A synthesis of the literature. *International Journal Environmental Research Public Health*, *10*(9), 4060-4085. https://doi.org/10.3390/ijerph10094060

Construction Industry Development Board Malaysia. (2020). *CIBD affordable housing design standard for Malaysia*. https://www.cidb.gov.my/wp-content/uploads/2022/07/205-CIDB-Affordable-housing-design-standard-for-malaysia-min.pdf

da Cunha, D. T., de Rosso, V. V., Pereira, M. B., & Stedefeldt, E. (2019). The differences between observed and self-reported food safety practices: A study with food handlers using structural equation modeling. *Food Research International*, *125*, 108637. https://doi.org/10.1016/J.FOODRES.2019.108637

Dahari, Z. (2019). Key success factors of home-based business among female entrepreneur in Saudi Arabia. *Asia-Pacific Joournal of Business Review*, *3*(2), 43-66. https://doi.org/10.20522/APJBR.2019.3.2.43

Department of Statistic Malaysia. (2022). *Press release consumer price index Malaysia December 2021*. https://Www.Dosm.Gov.My/V1/Index.Php?R=Column/Cthemebycat&Cat=106&Bul_Id=N1rkrdj1awtlu3l5y0m3ostzt21dzz09&Menu_Id=Bthzthqxn1zqmvf6a2i4rkzondfkqt09.

da Silva Farias, A., da S., de Almeida Akutsu, R. D. C. C., Botelho, A. B. A., & Zandonadi, R. P. (2019). Good practices in home kitchens: Construction and validation of an instrument for household food-borne disease assessment and prevention. *International Journal of Environmental Research and Public Health*, *16*(6), 1005. https://doi.org/10.3390/IJERPH16061005

Eighty-two suffer food poisoning symptoms from consuming fried noodles and eggs. (2024, Jun 12). *The Sun*. https://thesun.my/local-news/82-suffer-food-poisoning-symptoms-from-consuming-fried-noodles-and-eggs-HA12561017

Food poisoning: Samples of pudding buih sent to lab for analysis. (2022, April 10). *The Star*. https://www.thestar.com.my/news/nation/2022/04/10/food-poisoning-samples-of-039puding-buih039-sent-to-lab-for-analysis

Food Safety and Quality. (2024). *BeSS guidelines and applications*. https://hq.moh.gov.my/fsq/permohonan-garis-panduan-bess?

Food Safety and Quality (2023). *MeSTI*. https://hq.moh.gov.my/fsq/mesti

Food Safety and Quality Division. (2021). *Annual report FSQP*. https://hq.moh.gov.my/fsq/laporan-tahunan-pkkm

Food Safety and Quality Division. (2022). *Annual report FSQP*. https://hq.moh.gov.my/fsq/laporan-tahunan-pkk1

Food Safety and Quality. (2019). *Guidelines for investigation of food poisoning incidents based on Hazard Analysis Critical Control Point (HACCP) concept (Edition 2019).* https://hq.moh.gov.my/fsq/garis-panduan-berdasarkan-haccp

Gimino, G. (2022, August 6). PM: RM50mil allocated for aspiring home food business owners. *The Star*. https://www.thestar.com.my/news/nation/2022/08/06/pm-rm50mil-allocated-for-aspiring-home-food-business-owners

Global Food Safety Initiative. (2018). *A culture of food safety - A position paper from the Global Food Safety Initiative (GSFI)*. https://mygfsi.com/wp-content/uploads/2019/09/GFSI-Food-Safety-Culture-Full.pdf

Goh, E. V., Azam-Ali, S. McCullogh, F., & Mitra, S. R. (2020). The nutrition transition in Malaysia; key drivers and recommendations for improved health outcomes. *BMC Nutrition*, *6*, 32. https://doi.org/10.1186/s40795-020-00348-5

Gou, Z., Gamage, W., Lau, S. S. Y., & Lau, S. S. Y. (2018). An investigation of thermal comfort and adaptive behaviors in naturally ventilated residential buildings in tropical climates: A pilot study. *Buildings*, *8*(1), 1-17. https://doi.org/10.3390/buildings8010005

Hishamuddin, N. S., Mustafa, E., & Sadiman, M. Q. (2024). Examining food safety practices of food delivery riders using the KAP Theory. *Journal of Tourism, Hospitality & Culinary Arts*, *16*(1), 968-980.

Iblasi, W. N., Dojanah M. K., & Bader, S. A. A.-Q. (2016). The impact of social media as a marketing tool on purchasing decisions (Case Study on SAMSUNG for Electrical Home Appliances). *International Journal of Managerial Studies and Research*, *4*(1), 14-28.

Keeble, M., Adams, J., Sacks, G., Vanderlee, L., White, C. M., Hammond, D. & Burgoine, T. (2020). Use of online food delivery services to order food prepared away-from-home and associated sociodemographic characteristics: A cross-sectional, multi-country analysis. *International Journal of Environmental Research and Public Health*, *17*(14), 5190. https://doi.org/10.3390/ijerph17145190

Kirchner, M., Goulter, R. M., Chapman, B. J., Clayton, J., & Jaykus, L-A. (2021). Cross-contamination on atypical surfaces and venues in food service environments. *Journal of Food Protection*, *84*(7), 1239-1251. https://doi.org/10.4315/JFP-20-314

Lee, H. K., Abdul Halim, H., Thong, K. L., & Chai, L. C. (2017). Assessment of food safety knowledge, attitude, self-reported practices, and microbiological hand hygiene of food handlers. *International Journal of Environmental Research and Public Health*, *14*(1), 55. https://doi.org/10.3390/ijerph14010055

Lee, J. (2021, May 29). E-commerce growth requires delivery service providers to move fast to meet surge in demand. *The Star*. https://www.thestar.com.my/business/smebiz/2021/05/29/e-commerce-growth-requires-delivery-service-providers-to-move-fast-to-meet-surge-in-demand

Lim, T.-P, Chye, F. Y., Sulaiman, M. R., Mohd Suki, N., & Lee, J.-S (2016). A structural modeling on food safety knowledge, attitude, and behaviour among Bum Bum Island community of Semporna, Sabah. *Food Control*, *60*, 241-246. https://doi.org/10.1016/j.foodcont.2015.07.042

Ministry of Health Malaysia. (2021). *Home-based food safety guidelines*. http://fsq.moh.gov.my/v6/xs/page.php?id=441000695

Ministry of Health Malaysia (2020). *Annual report 2020, food safety and quality division*. http://fsq.moh.gov.my/v6/xs/page.php?id=21.

Mason, C. M. Carter, S., & Tagg, S. (2011). Invisible businesses: The characteristics of home-based businesses in the United Kingdom. *Regional Studies*, *45*(5), 625–639. https://doi.org/10.1080/00343401003614241

Mihalache, O. A., Dumitraşcu, L., Nicolau, A. I., & Borda, D. (2021). Food safety knowledge, food shopping attitude and safety kitchen practices among Romanian consumers: A structural modelling approach. *Food Control*, *120*, 107545. https://doi.org/10.1016/J.FOODCONT.2020.107545

Mihalache, O. A., Møretrø, T., Borda, D., Dumitraşcu, L., Neagu, C., Nguyen-The, C., Maître, I., Didier, P., Teixeira, P., Lopes Junqueira, L. O., Truninger, M., Izsó, T., Kasza, G., Skuland, S. E., Langsrud, S., & Nicolau, A. I. (2022). Kitchen layouts and consumers' food hygiene practices: Ergonomics versus safety. *Food Control*, *131*, 108433. https://doi.org/10.1016/J.FOODCONT.2021.108433

Mucinhato, R. M. D., da Cunha, D. T., Barros, S. C. F., Zanin, L. M., Auad, L. I., Weis, G. C. C., Saccol, A. L. de F., & Stedefeldt, E. (2022). Behavioral predictors of household food-safety practices during the COVID-19 pandemic: Extending the theory of planned behavior. *Food Control*, *134*, 108719. https://doi.org/10.1016/j.foodcont.2021.108719

Navaneethan Y., & Effarizah, M. E. (2023). Post-cooking growth and survival of *Bacillus cereus* spores in rice and their enzymatic activities leading to food spoilage potential. *Foods*, *12*(3), 626. https://doi.org/10.3390/foods12030626.

Nee, S. O., & Sani, N. A. (2011). Assessment of Knowledge, Attitudes and Practices (KAP) among food handlers at residential colleges and canteen regarding food safety. *Sains Malaysiana*, *40*(4), 403-410.

'Puding Buih' food poisoning case due to use of expired eggs. (2020, May 31). *Malay Mail*. https://www.malaymail.com/news/malaysia/020/05/31/puding-buih-food-poisoning-case-due-to-use-of-expired-eggs-says-terengganu/1871122

Razak, S. S. A., Tuan, L. Y., & Lau, T. C. (2022). Food safety legal issues in home-based food business. *International Journal of Academic Research in Business and Social Sciences*, *12*(1), 2600–2610. https://doi.org/10.6007/IJARBSS/v12-i1/12133

Reuschke, D., & Mason, C. (2022). The engagement of home-based businesses in the digital economy. *Futures*, *135*, 102542. https://doi.org/10.1016/J.FUTURES.2020.102542

Sixty-five Sungai Petani primary school pupils suffer food poisoning. (2024, May 21). *The Star*. https://www.thestar.com.my/news/nation/2024/05/21/65-sungai-petani-primary-school-pupils-suffer-food-poisoning

Standards Malaysia. (2024). *Microbiology, nucleic acid, chemical & genetically modified (G.M.O) SAMM No. 267*. https://www.jsm.gov.my/images/3-accreditation/resources/samm/document/SC_1.7_-_Specific_Criteria_Molecular_Testing_Final.pdf

Statista. (2024). *Online food delivery-Malaysia*. https://www.statista.com/outlook/emo/online-food-delivery/malaysia

Tanushree, M. P., Sailendri, D., Yoha, K. S., Moses, J. A. & Anandharamakrishnan, C. (2019). Mycotoxin contamination in food: An exposition on spices. *Trends in Food Science and Technology*, *93*, 69-80. https://doi.org/10.1016/j.tifs.2019.08.010

Tarmazi, S. A. A., & Ali, N. M. (2021). The purchase intention of online home-based food products among Kelantanese. *Journal of Tourism, Hospitality & Culinary Arts*, *13*(3), 128-138.

Three food handlers identified as source of typhoid outbreak at Kelantan school. (2024, July 4). *The Star*. https://www.thestar.com.my/news/nation/2024/07/04/three-food-handlers-identified-as-source-of-typhoid-outbreak-at-kelantan-school

Topimin, S., Hashim, M., & Rahayu, S. (2021). An overview of government business support programmes for micro and small businesses in Malaysia during the COVID-19 crisis. *Malaysian Journal of Business and Economics*, *8*(2), 7-14. https://doi.org/10.51200/mjbe.vi.3659

United States Department of Agriculture Food Safety and Inspection Service. (2021). *FSIS stabilization guideline for meat and poultry products (Revised Appendix B), Guideline ID FSIS-GD-2021-0013*. https://www.fsis.usda.gov/sites/default/files/media_file/2021-12/Appendix-B.pdf

Wills, W. J., Meah, A., Dickinson, A. M., & Short, F. (2015). I don't think I ever had food poisoning'. A practice-based approach to understanding foodborne disease that originates in the home. *Appetite*, *85*, 118-125. https://doi.org/10.1016/j.appet.2014.11.022

Yusuf, A. H., Oyelakin, I. O., Abdul Shukor, S., & Ahmad Bustamam, U. S. (2017). The role of halal certification in business performance in Selangor: A study on kopitiams. *Malaysian Management Journal*, *21*, 1-22. https://doi.org/10.32890/mmj.21.2017.9052

Zhang, T., Gerlowski, D., & Acs, Z. (2022). Working from home: Small business performance and the COVID-19 pandemic. *Small Business Economics*, *58*, 611636. https://doi.org/https://doi.org/10.1007/s11187-021-00493-6

Pertanika J. Trop. Agric. Sci. 48 (3): 685 - 693 (2025)

PERTANIKA JOURNALS

TROPICAL AGRICULTURAL SCIENCE

Journal homepage: http://www.pertanika.upm.edu.my/

Short Communication

Assessing the Growth Performance of *Holothuria scabra* Juveniles in Concrete Tanks with a Diet of *Ulva lactuca*

Syed Mohamad Azim Syed Mahiyuddin[1], Muhammad Asyraf Abd Latip[1]*, Najihah Mohamad Nasir[1], Khairudin Ghazali[1], Che Zulkifli Che Ismail[2] and Zaidnuddin Ilias[3]

[1]*Pusat Penyelidikan Marikultur Langkawi, Kompleks Perikanan Bukit Malut, 07000 Langkawi, Kedah, Malaysia*
[2]*Fisheries Research Institute Pulau Sayak, 08000 Kota Kuala Muda, Kedah, Malaysia*
[3]*Fisheries Research Institute (FRI Batu Maung), Jalan Batu Maung, 11960 Batu Maung, Penang, Malaysia*

ABSTRACT

Managing density is critical in farming sandfish (*Holothuria scabra*), significantly affecting their growth and survival. Larval sandfish are initially reared in high-density fiber tanks, but as they develop into juveniles, they require larger and more spacious tanks to support growth. This study observes and analyzes the growth performance of *H. scabra* juveniles reared in concrete tanks with a diet of *Ulva lactuca*. Approximately 200 hatchery-produced sandfish juveniles, aged 40 days with a mean length of 1.03 ± 0.43 cm, were reared in Netlon cages (16 m²) and placed in a large concrete tank with sandy sediment. They were fed weekly with 500 g of macroalgae *U. lactuca*. During the first 30 days, the juveniles showed slight growth to 3.20 ± 0.93 cm, further increasing to 4.82 ± 1.08 cm and 4.89 ± 1.13 cm at 60 and 90 days of rearing, respectively. The specific growth rate (SGR) calculated on day 90 was 1.75 ± 0.21% day^{-1}, and the survival rate recorded was 41%. In conclusion, the use of Netlon cages demonstrated positive results in sandfish growth and their suitability for sandy sediment conditions at the bottom of the tank, replicating their natural habitat. Additionally, the findings indicate that feeding sandfish with seaweed powder from the *U. lactuca* species contributes to improved growth.

Keywords: Holothuria scabra, juveniles, sandfish, *Ulva lactuca*

ARTICLE INFO

Article history:
Received: 09 July 2024
Accepted: 04 September 2024
Published: 16 May 2025

DOI: https://doi.org/10.47836/pjtas.48.3.02

E-mail addresses:
syedazim@dof.gov.my (Syed Mohamad Azim Syed Mahiyuddin)
m.asyrafabdlatip@gmail.com (Muhammad Asyraf Abd Latip)
najihahnasir@dof.gov.my (Najihah Mohamad Nasir)
khairudin@dof.gov.my (Khairudin Ghazali)
che.zulkifli@dof.gov.my (Che Zulkifli Che Ismail)
zaiali71@gmail.com (Zainuddin Ilias)
*Corresponding author

e-ISSN: 2231-8542

INTRODUCTION

Holothuria scabra (*H. scabra*) (Jaeger, 1833) is generally known as sandfish (sea cucumber), which was listed as an endangered (EN) species under the International Union for Conservation of Nature (IUCN) Red List due to its declining wild stock in the natural habitat (Barclay et al., 2017; Han et al., 2016). The market prices of sea cucumber are slightly higher compared with other marine species because of demand and a limited number of wild stocks. Over the years, the increasing demand for high-market-value sea cucumbers has led to overexploitation in their natural habitat. Some cases of extinction have been reported in the original habitat (Wolfe & Byrne, 2022). Normally, sea cucumbers are popular for extraction and use as medicinal supplements, especially in Southeast Asia. It is believed that one of the nutritional benefits of sea cucumber is its ability to cure internal bleeding and improve health (Pangestuti & Arifin, 2018). There was a study that reported the presence of antimicrobial steroidal sapogenins in sandfish is an active agent that can actively fight against bacteria such as *Aeromonas hydrophila*, *Escherichia coli*, *Enterococcus* sp., *Klebsiella pneumoniae*, *Pseudomonas aeruginosa*, *Salmonella typhi*, *Staphylococcus aureus*, *Vibrio harveyi*, and fish-borne mold, *Aspergillus* sp. (Adam et al*.,* 2022; Nugroho et al., 2022).

Meanwhile, in Japan and China, sea cucumbers are a delicacy served as a luxury and exotic food, especially during festivals. The composition of sandfish that is high in protein content (43.23% to 48.27%) and low in fat (4.6% to 5.66%) makes it an option as an exotic food besides serving as a medicinal treatment (Rasyid et al*.,* 2020). A culture technique for sea cucumber was introduced in Japan for the Stichopus japonicus to address the over-exploitation of sea cucumber and support its conservation (Imai et al., 1950). Later, the culture of sea cucumber was developed to other species from families of Holothuroidea and Stichopodidae, such as *H. scabra* (Militz et al., 2018), *H. fuscogilva* (Arriesgado et al., 2022), *Stichopus horrens* (Hu et al., 2013) and *Stichopus vastus* (Sulardiono et al., 2012), all of which were studied according to market value and demand. According to the Food and Agriculture Organization of the United Nations (FOA) (2018), the aquaculture world produced 130,000 metric tonnes of *Apostichopus japonicus*, which would increase to 205,000 metric tonnes in 2016. Increasing global production trends are one of the factors that increase the supply of sea cucumbers throughout the year to meet the supply-demand.

The nursing technique of sea cucumber is quite different from that of other marine species because of its life cycle. Preparing nursing sea cucumber seeds requires technology and some modifications for seed growth, depending on their life cycle phases. After the eggs are fertilized, they will self-develop to become larvae known as auricularia, with algae as their main food, such as *Isochrysis* sp. (Abdelaty et al., 2021), *Nannochloropsis* sp. and *Chaetoceros calcitrans* (Abidin et al., 2019). However, until today, the study of the culture of sea cucumbers is still in progress due to issues of low survival rate reported, especially

at the metamorphosis and pentactula stages (Yu et al., 2022). Furthermore, there are some issues of grow-out and broodstock maturation: sea cucumber growth and declining weight when induced in a tank (Sembiring et al., 2018).

After the eggs fully hatch, the larvae auricularia swim in the water and undergo a metamorphic phase to transform from larvae to adults (pentactula) within 20–30 days. The newly adult pentactula sinks and attaches to the substrate in the tank to complete its development and transform to become a juvenile. Early rearing of larvae and juveniles is the most critical phase and requires a solution to address the issue of their low survival rate. The study of algae concentration fed on larvae was done by Militz et al. (2018), where it was reported that the larvae quality depended on the larvae concentration and water quality. Meanwhile, the study of food nutrition and rearing density was conducted by Lavitra et al. (2009), demonstrating that the extracts of *S. latifolium* provided the best survival rate for juveniles of sandfish, where the rearing density suggested is between 300 and 450 individuals m^{-2}. Recent research by Mahiyuddin et al. (2024) found that juveniles showed improved growth rates when reared at lower densities and fed *Spirulina*. Besides, a study of nursing was also carried out by Lavitra et al. (2015), showing that the high mortality was caused by the crab (predator), *Thalamita crenata*, where it was suggested to employ covered pens for protection against predators.

According to Rakotonjanahary et al. (2016), using marine sediment to nurse sandfish juveniles showed positive results during the study period. This study aims to obtain and observe the survival rate and growth performance of juvenile sandfish fed with *Ulva lactuca* in cages and the use of marine sediment at the bottom layers to create an environment similar to their natural habitat.

MATERIALS AND METHODS

Preparation for Concrete Tank

This study was conducted in a concrete nursery tank with a total area of a tank of 100 m^2 (10 m × 10 m) and a total volume of water of 40 tonnes. Netlon cage was set up in a tank with a total area of 16 m^2 (8 m × 2 m), where it was covered with marine sediment from the finest sediment and mud at a ratio of 50:50 at the bottom of the tank at 20 cm depth (Figure 1). The total height of the cage is 60 cm; 20 cm of the wall cage was planted at the bottom of the tank. The tank was covered with a 70% sunshade net.

Figure 1. The Netlon cage used for this experiment (8 m × 2 m)

Specific Growth Rate and Survival Rate with *Ulva lactuca* Diet

The juveniles of sandfish were produced by inducing the broodstock using the algae bath method. Meanwhile, these wild broodstock were collected from Desaru, Johor (southern part of Peninsular Malaysia). The larvae were reared in the tank until they developed into the juvenile stage, fed with *Chaetoceros* sp. Next, approximately 200 individuals of the same batch juveniles aged 40 days with a mean length of 1.03 ± 0.43 cm were collected and nursed in the tank, with a stocking density of 13 individuals per square meter. Water quality (salinity, alkalinity, temperature, ammonia, nitrate, and dissolved oxygen) was taken weekly, and the juveniles were fed weekly with seaweed powder *U. lactuca* at 31.25 gm^{-2} (500 g/week/cage). Water exchange in the tank was done every two days at 30% of the total volume. Sampling was done on the first week of every month by recording the different lengths of the sandfish juveniles. A number of 50 individuals were collected for every sampling session. At the end of this study, the specific growth rate (SGR) and survival rate (SR) of juvenile sandfish were estimated based on Indriana et al. (2017).

RESULTS AND DISCUSSION

Based on Table 1, the juveniles had a mean length of 1.03 ± 0.43 cm at the beginning of the experiment. After the first month (30th day) of rearing in a cage, the mean length of juveniles showed a threefold growth from the initial length to 3.2 ± 0.93 cm, with a specific growth rate of 3.83 ± 0.56% day^{-1}. Sampling for the second month (60th day) showed the mean length of juveniles increased four times from initial size to 4.82 ± 2.57 cm, where the specific growth rate is 2.58 ± 0.25% day^{-1}. The juveniles continued growing in the third month (90th day) (Figure 2) of rearing when the mean length reached 4.89 ± 1.13 cm, with a specific growth rate of 1.75 ± 0.21% day^{-1}. However, in the last month of the experiment (120th day of rearing), the mean length dropped to 3.40 ± 1.16 cm, and the specific growth rate also declined to 1.03 ± 0.12% day^{-1} across the rearing period. Based on the result, the highest mean length was recorded in the third month after the 90th day of rearing. Meanwhile, the best specific growth rate was recorded on the first month of rearing (30th day), which was 3.77% per day. The survival rate of epibenthic juveniles of sandfish in the cage declined by more than 50% across the rearing period.

Table 1
Survival rate, mean length (cm), and specific growth rate of juvenile sandfish

Rearing days	Mean length (cm)	Specific growth rate (%/day)	Survival rate (%)	Mortality rate (%)
0	1.03 ± 0.43	0		
30	3.20 ± 0.93	3.83 ± 0.56		
60	4.82 ± 1.08	2.58 ± 0.25		
90	4.89 ± 1.13	1.75 ± 0.21		
120	3.40 ± 1.16	1.03 ± 0.12	41	59

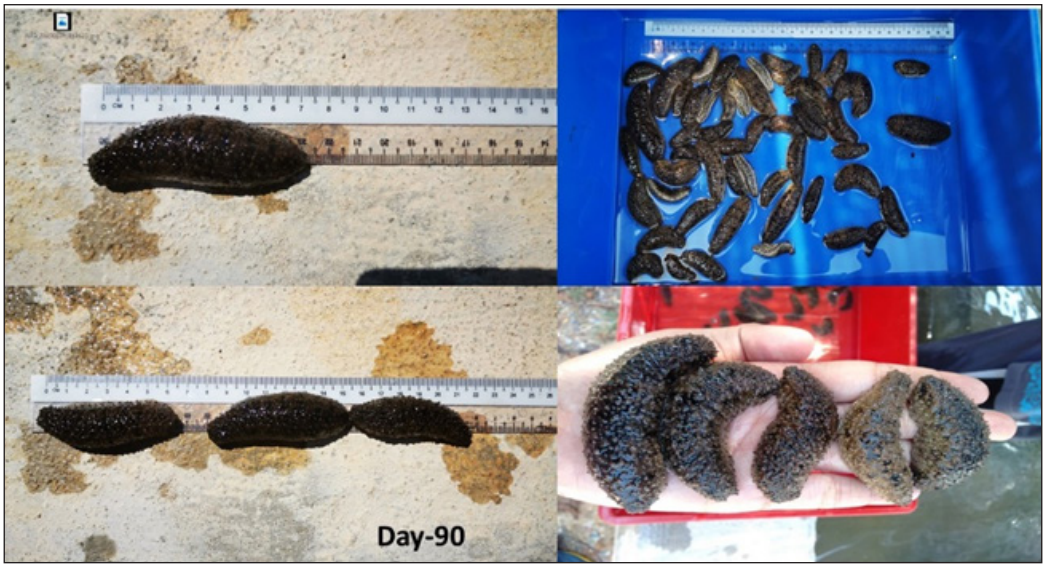

Figure 2. The increased size and length of juveniles on day 90 of rearing

The initial number of individual juveniles reared was 200 individuals. On the 120th day of rearing, the number of juveniles left was 82, with a survival rate and mortality rate of 41% and 59%, respectively. Based on Table 2, the average water parameter of the tank during the experiment was 31.4°C ± 1.9°C, where salinity was recorded at 31.53 ± 2.20 ppt due to dry season, alkalinity was at pH 8.10 ± 0.09, and dissolved oxygen was 4.47 ± 0.45 ppm. Meanwhile, the test for ammonia (NH_3) and nitrate (NO_2) were below 0.05 ppm. Generally, there are no wide variations or drastic changes in the water parameters or their rearing period.

Table 2
Water parameters along with the rearing period of sea cucumber Holothuria scabra

Parameter	Mean ± SD
Salinity (ppt)	31.53 ± 2.20
pH	8.10 ± 0.09
Temperature (°C)	31.40 ± 1.90
Ammonia	< 0.05
Nitrate	< 0.05
Dissolve oxygen (ppm)	4.47 ± 0.45

The result of the present study shows the survival rate is similar to the study of the effect of food quality and rearing density juveniles of sandfish by Lavitra et al. (2009), which was within 34% to 66% survival rate in an eight-week trial period, while the control test (without any artificial food supply) had dropped to 7% survival rate. Research for optimizing the growth of *H. scabra* juveniles during the nursery phase was done by (Rakotonjanahary et al., 2016), who reported that the use of marine sediment substrate and tilapia in co-culture resulted in better performance after seven weeks of rearing from an initial mean weight of 0.03 g to the highest weight of 9.01 ± 4.23 g in seven weeks. This

suggested that rearing juveniles of sandfish requires an artificial diet and marine sediment to enhance the growth of juveniles.

According to Robinson et al. (2013), the study of the role of sand as substrate and dietary component for juvenile sea cucumber *H. scabra* was confirmed to have a positive effect on juvenile growth when sand is provided as a substrate; this is proven when the growth was observed to be positive, and the survival rate was 100% when sand was used as substrate in the tank, compared with sandfish reared in bare tanks. Based on the results and other studies, using marine sediment as substrate is necessary to provide similarity of its natural habitat and shelter for nursing the sandfish. The substrate at the bottom inhibits the sandfish from developing, completing its life cycle, and transforming into its final stage. Generally, adult sandfish have a special characteristic: the burying behavior based on the tank's feeding cycle and temperature conditions. Wolkenhauer (2008) demonstrated that the sandfish was active between 13:00 and 22:00 and became passive between 01:00 and 09:00, which is attributable to the temperature condition. It indicates that temperature was significantly and positively correlated to the sandfish feeding and burying behavior. Moreover, sandfish could act as bioremediation in the tank and sea pen by consuming unused organic deposits.

The positive growth performance was also supported by *Ulva lactuca* as the main food source for juveniles. Sandfish need to be fed artificial food in a controlled system to support their nutrient and protein requirements. A food test study by Lavitra et al. (2009) showed that sandfish fed with *Sargassum latifolium* resulted in the best growth rate of more than 50% compared with that when fed with *Thalassia hemprichii, Thalassodendron ciliatum, Syringodium isoetifolium*, and organic biofilm. From the present study's findings, sandfish can digest and absorb nutrients from seaweed after the seaweed is fully decomposed on the sediment. Normally, based on observation, seaweed requires 2–4 days to decompose and form a layer at the bottom. Furthermore, a study on feeding sandfish with seagrass *Cymodocea* sp. registered growth in length and weight (Arnull et al., 2021).

Lavitra et al.'s (2010) study reported that water temperature does not affect the survival of endobenthic sandfish. However, it predominantly affects their growth (high temperature > 30°C), which favors greater growth. However, sandfish are known to survive at 39°C; they turn weak when the temperature reaches 41°C and eventually die. Compared with water parameters in this study, the water temperature was slightly high at 31.4°C ± 1.9°C, which is a good range for promoting the growth of juveniles of sandfish. However, the declining growth performance after the 90th day of rearing may be attributable to the competition among sandfish juveniles with other marine organisms, such as gastropods, for food and space. Gastropods are widely found in tanks after three months of rearing, and their presence may affect the growth of juvenile sandfish, which needs further study.

CONCLUSION

Utilizing marine sediment as a substrate and incorporating *U. lactuca* into the diet of sandfish juveniles can significantly enhance their survival and growth. Sandfish juveniles at 0.5–1.0 cm sizes can be introduced to *U. lactuca* as an alternative diet when commercial seaweed powders, such as *Sargassum*, are unavailable. Furthermore, in-tank sandfish farming offers a more robust solution compared to pen culture in addressing the challenges posed by climate change, ensuring a more sustainable and resilient aquaculture practice.

ACKNOWLEDGMENTS

The greatest gratitude goes to the Fisheries Research Institute, Department of Fisheries Malaysia (Grant no. P21300040170501), which has funded the sustainability of this project. The authors gratefully thank Pusat Penyelidikan Marikultur Langkawi staff members, including Hairul Hafiz Mahsol, Latifah Zaidi, and Khadijah Adnan, who were directly or indirectly involved in this paper.

REFERENCES

Abdelaty, M., Al-Solami, L., Al-Harbi, M., & Abu El-Regal, M. (2021). Utilization of different types of microalgae to improve hatcheries production of the sea cucumber *Holothuria scabra* Jaeger, 1833 in the Red Sea, KSA. *Egyptian Journal of Aquatic Biology and Fisheries*, *25*(2), 193-204. https://doi.org/10.21608/ejabf.2021.161824

Abidin, N. A., Shaleh, S. M., Ching, F. F., Othman, R., Manjaji-Matsumoto, M., Mustafa, S., & Senoo, S. (2019). Appropriate diet and stocking density for sea cucumber (*Holothuria scabra*) larvae rearing. *Journal of Physics: Conference Series*, *1358*(1), 012015. https://doi.org/10.1088/1742-6596/1358/1/012015

Adam, M., Achmad, H., Tanumihardja, M., Ramadhan, S. R. J., & Masyta, N. (2022). The benefits of golden sea cucumber (*Stichopus hermanni*) as an alternative antimicrobial material in oral health. *Journal of International Dental and Medical Research*, *15*(4), 1806-1815.

Arnull, J., Wilson, A. M. W., Brayne, K., Dexter, K., Donah, A.G., Gough, C. L., Klückow, T., Ngwenya, B., & Tudhope, A. (2021). Ecological co-benefits from sea cucumber farming: *Holothuria scabra* increases growth rate of seagrass. *Aquaculture Environment Interactions*, *13*, 301-310. https://doi.org/10.3354/aei00409

Arriesgado, D. M., Uba, K. I. N., Tubio, E. G., Navarro, V. R., Bucay, D. M., Besoña, J. F., Magcanta-Mortos, M. L. M., & Uy, W. H. (2022). Spawning, larval development, and juvenile rearing of white teatfish *Holothuria fuscogilva* in the hatchery in the Philippines. *Philippine Journal of Science*, *151*(6B), 2555-2566. https://doi.org/10.56899/151.6B.19

Barclay, K., Voyer, M., Mazur, N., Payne, A. M., Mauli, S., Kinch, J., Fabinyi, M., & Smith, G. (2017). The importance of qualitative social research for effective fisheries management. *Fisheries Research*, *186*, 426-438. https://doi.org/10.1016/j.fishres.2016.08.007

Food and Agriculture Organization of the United Nations. (2018). *The state of world fisheries and aquaculture 2018: Meeting the sustainable development goals*. https://www.fao.org/3/i9540en/I9540EN.pdf

Han, Q., Keesing, J. K., & Liu, D. (2016). A review of sea cucumber aquaculture, ranching, and stock enhancement in China. *Fisheries Science and Aquaculture*, *24*(4), 326-341. https://doi.org/10.1080/23308249.2016.1193472.

Hu, C., Li, H., Xia, J., Zhang, L., Luo, P., Fan, S., Peng, P., Yang, H., & Wen J. (2013). Spawning, larval development and juvenile growth of the sea cucumber *Stichopus horrens*. *Aquaculture*, *404*, 47-54. https://doi.org/10.1016/j.aquaculture.2013.04.007

Imai, I., Inaba, D. I., Sato, R., & Hatanaka, M. (1950). The artificial rearing of the transparent flagellate larvae of *Stichopus japonicus*. *Tohoku Daigaku Nogakuhu Kenkyo Iho*, *2*(2), 269-277.

Indriana, L. F., Firdaus, M., & Munandar, H. (2017). Survival rate and growth of juvenile sandfish (*Holothuria scabra*) in various rearing conditions. *Marine Research in Indonesia*, *42*(1), 11-18. https://doi.org/10.14203/mri.v41i2.156

Lavitra, T., Fohy, N., Gestin, P. G., Rasolofonirina, R., & Eeckhaut I. (2010). Effect of water temperature on the survival and growth of endobenthic *Holothuria scabra* (Echinodermata: Holothuroidea) juveniles reared in outdoor ponds. *SPC Beche-de-mer Information Bulletin*, *30*, 25-28.

Lavitra, T., Rasolofonirina, R., Jangoux, M., & Eeckhaut I. (2009). Problems related to the farming of *Holothuria scabra* (Jaeger, 1833). *SPC Beche-de-mer Information Bulletin*, *29*, 20-30.

Lavitra, T., Tsiresy, G., Rasolofonirina, R., & Eeckhaut, I. (2015). Effect of nurseries and size of released *Holothuria scabra* juveniles on their survival and growth. *SPC Beche-de-mer Information Bulletin*, *35*, 37-41.

Mahiyuddin, S. M. A. S., Abd Latip, M. A., Ilias, Z., Ghazali, K., & Sin, N. D. N. (2024). Survival rate and growth performance of *Holothuria scabra* towards different stocking densities and feeding with *Spirulina*. *Pertanika Journal of Tropical Agricultural Science*, *47*(1), 191-199. https://doi.org/10.47836/pjtas.47.1.14

Militz, T. A., Leini, E., Duy, N. D. Q., & Southgate, P. C. (2018). Successful large-scale hatchery culture of sandfish (*Holothuria scabra*) using micro-algae concentrates as a larval food source. *Aquaculture Reports*, *9*, 25-30. https://doi.org/10.1016/j.aqrep.2017.11.005

Nugroho, A., Harahap, I. A., Ardiansyah, A., Bayu, A., Rasyid, A., Murniasih, T., Setyastuti, A., & Putra, M. Y. (2022). Antioxidant and antibacterial activities in 21 species of Indonesian sea cucumbers. *Journal of Food Science and Technology*, *59*, 1-10. https://doi.org/10.1007/s13197-021-05007-6

Pangestuti, R., & Arifin, Z. (2018). Medicinal and health benefit effects of functional sea cucumbers. *Journal of Traditional and Complementary Medicine*, *8*(3), 341-351. https://doi.org/10.1016/j.jtcme.2017.06.007

Rakotonjanahary, F., Lavitra, T., Fohy, N., & Eeckhaut I. (2016). Assays for optimising the growth of *Holothuria scabra* juveniles during the nursery phase. *SPC Beche-de-mer Information Bulletin*. https://www.vliz.be/imisdocs/publications/346007.pdf

Rasyid, A., Murniasih, T., Putra, M. Y., Pangestuti, R., Harahap, I. A., Untari, F., & Sembiring, S. B. (2020). Evaluation of nutritional value of sea cucumber *Holothuria scabra* cultured in Bali, Indonesia. *Aquaculture, Aquarium, Conservation & Legislation*, *13*(4), 2083-2093.

Robinson, G., Slater, M. J., Jones, C. L., & Stead, S. M. (2013). Role of sand as substrate and dietary component for juvenile sea cucumber *Holothuria scabra*. *Aquaculture*, *392*, 23-25. https://doi.org/10.1016/j.aquaculture.2013.01.036

Sembiring, S. B. M., Wibawa, G. S., Giri, I. N. A., & Hutapea, J. H. (2018). Reproduction and larval rearing of sandfish (*Holothuria scabra*). *Marine Research in Indonesia*, *43*(1), 11-17. https://doi.org/10.14203/mri.v43i1.267

Sulardiono, B., Prayitno, S. B., & Hendrarto, I. B. (2012). The growth analysis of *Stichopus vastus* (Echinodermata: Stichopodidae) in Karimunjawa waters. *Journal of Coastal Development*, *15*, 315-323.

Wolfe, K., & Byrne, M. (2022). Overview of the Great Barrier Reef Sea cucumber fishery with focus on vulnerable and endangered species. *Biological Conservation*, *266*, 109451. https://doi.org/10.1016/j.biocon.2022.109451

Wolkenhauer, S. M. (2008). Burying and feeding activity of adult *Holothuria scabra* (Echinodermata: Holothuroidea) in a controlled environment. *SPC Beche-de-mer Information Bulletin*, *27*, 25-28.

Yu, Z., Wu, H., Tu, Y., Hong, Z., & Luo, J. (2022). Effects of diet on larval survival, growth, and development of the sea cucumber *Holothuria leucospilota*. Aquaculture Nutrition, *2022*(1), 8947997. https://doi.org/10.1155/2022/8947997

Pertanika J. Trop. Agric. Sci. 48 (3): 695 - 718 (2025)

PERTANIKA JOURNALS

TROPICAL AGRICULTURAL SCIENCE

Journal homepage: http://www.pertanika.upm.edu.my/

Review Article

Comprehensive Hormonal Profiling in Post-partum Dairy Buffaloes: Insights, Challenges, and Future Perspectives

Dayang Ayu Syamilia Che Roi and Noor Syaheera Ibrahim*

School of Animal Science, Aquatic Science, and Environment, Faculty of Bioresources and Food Industry, Universiti Sultan Zainal Abidin, Besut Campus, 22200 Besut, Terengganu, Malaysia

ABSTRACT

This review paper aims to provide a comprehensive overview of hormonal profiling in post-partum dairy buffaloes, elucidating its significance in reproductive management, milk production, and overall herd health. We discuss the hormonal changes occurring during the post-partum period, factors influencing these changes, current methods of hormonal assessment, and their applications in reproductive and productive efficiency. Furthermore, we address challenges and gaps in existing research and propose future directions for advancing hormonal profiling techniques in dairy buffalo management.

Keywords: Dairy buffalo, oestradiol, hormone profiling, post-partum, progesterone

INTRODUCTION

Importance of the Post-partum Period in Dairy Buffalo

The buffalo has earned the nickname "The Black Gold" due to its high worth and potential for growth and progress (Bilal et al., 2006). The buffalo *(Bubalus bubalis)* exhibits a reproductive cycle influenced by the seasons. During the late summer and early autumn, their sexual activity is triggered by the reduction in daylight hours (short days), as stated by Sethi et al. (2021). Their reproductive success heavily influences the profitability of dairy herds. Reproductive efficiency directly impacts the milk each cow produces during their time in the herd. It, in turn, affects the profitability and lifespan of the cow within the herd.

ARTICLE INFO

Article history:
Received: 23 July 2024
Accepted: 13 September 2024
Published: 16 May 2025

DOI: https://doi.org/10.47836/pjtas.48.3.03

E-mail addresses:
sl4649@putra.unisza.edu.my (Dayang Ayu Syamilia Che Roi)
syaheeraibrahim@unisza.edu.my (Noor Syaheera Ibrahim)
*Corresponding author

e-ISSN: 2231-8542

The post-partum phase is crucial in animal reproduction, and its length affects reproductive effectiveness. Following parturition, it is typical for an animal to experience a lack of cyclicity. However, if this time persists for an extended duration, it becomes problematic and diminishes the animal's reproductive effectiveness (Sethi et al., 2021). Animals experience a delay in returning to their normal reproductive cycle due to low energy levels, depleted body reserves, and post-partum diseases. The typical process of follicular growth involves the stages of follicular recruitment, deviation, selection, growth, and ovulation. If any of these processes fail, the post-partum period will be prolonged.

Overview of Hormonal Changes During the Post-partum Period

Post-partum buffaloes experience hormonal changes, specifically in oestradiol (E2) and progesterone (P4) levels, which affect the quality of oocytes and influence reproductive stages, including oestrous, anoestrous, and cystic pathologies (Kumar et al., 2015). In Jaffarabadi buffaloes, the level of progesterone in the blood decreases before giving birth and reaches its highest point on the day of calving. In contrast, cortisol levels are highest when giving birth, and Prostaglandin F2α Metabolite (PGFM) dramatically increases after parturition, as stated by Dhami et al. (2019). The initial post-partum phase can result in a negative energy balance (NEB) because of metabolic stress generated by reduced feed intake of dry matter and heightened energy requirements during calving and the onset of lactation.

Significant variations in E2 concentrations have been observed in serum and follicular fluid, suggesting ongoing follicular development and regression in anoestrous animals. The reduced E2 levels in cystic animals are likely due to insufficient luteinizing hormone (LH) levels (Wathes et al., 2007). Reported P4 levels align with existing literature, showing a decrease during oestrous (Honparkhe et al., 2008). Dhami et al. (2019) documented a notable decline in plasma P4 levels and a simultaneous increase in E2 levels during calving. Subsequently, both hormones decreased in the early post-partum period, followed by an increase between days 30–60 post-partum, coinciding with the return of ovarian follicles and corpus luteum (CL) formation. Additionally, Dhami et al. (2019) observed a significant rise in plasma cortisol levels on the calving day compared to seven days before and after, indicating heightened stress during calving.

This review paper aims to determine and study the hormones involved, the changes in hormones, and the factors influencing hormonal profiles in post-partum dairy buffaloes. It will also provide strategies and future directions in the hormonal profiling of dairy buffaloes.

HORMONAL INVOLVED IN POST-PARTUM DAIRY BUFFALOES

Ovarian Hormone (Progesterone)

Progestogens are a class of hormones with comparable physiological functions, with P4 being the most significant. P4 regulates the oestrous cycles. Studies by Ahmad et al.

(1977), Mondal and Prakash (2003), and Mondal et al. (2003) have consistently found that the peripheral plasma P4 profile in buffalo closely resembles that of cattle. The study conducted by Saqib et al. (2021) demonstrated that P4 significantly impacts metabolic status, stress levels, milk supply, and reproductive cyclicity. During the post-partum period, there is a change in P4 levels. Ahmad et al. (1977) stated that P4 levels exhibit synchronous fluctuations with the expansion and regression of CL in cycling buffalo because CL is the origin of P4. Batra et al. (1979) reported that P4 levels regularly increase in animals who successfully conceive but fall three days before the second oestrous in those who fail to conceive. The decrease in P4 levels varies depending on when the CL regresses.

Besides that, according to Srivastava et al. (1999), the peripheral plasma P4 levels can vary throughout the seasons. In hotter months, P4 levels are lower during oestrous, and the mid-luteal phases compared to cooler months. Rao and Pandey (1982) propose that lower P4 levels during summer lead to reduced oestrous expression and lower conception rates. Terzano et al. (2012) discovered a substantial increase in P4 levels throughout the summer in comparison to winter. Extended exposure to high temperatures might increase the levels of P4 in the peripheral plasma because of the activity of the adrenal cortex caused by stress (Abilay et al., 1975). Furthermore, P4 levels may differ depending on an individual's nutritional state (Ronchi et al., 2001). Insufficient nourishment in buffaloes, compounded by elevated ambient temperatures, may result in an extended period of reproductive dormancy.

Ovarian Hormone (Oestradiol)

Oestrogens, particularly E2, are endogenous hormones synthesized by the ovary and conveyed by carrier proteins. They influence the central nervous system, resulting in the manifestation of oestrous behaviour in females. The E2 profile in buffalo peripheral plasma is comparable to that in cattle. Riverine and swamp buffaloes have similar E2 profiles during the oestrous cycle (Mondal et al., 2006). The higher levels of E2 in milk compared to plasma have led to an investigation of whether the mammary gland is responsible for absorbing E2 or if the hormone is partially produced inside the mammary tissue. The levels of E2 in the ovarian follicular fluid are markedly higher than in the peripheral circulation (Palta et al., 1998). There is a positive correlation between the E2 levels and the size of the follicle. A study by Palta et al. (1998) found that the level of E2 in large follicles is considerably greater than in medium follicles, whereas medium follicles have higher E2 levels than small follicles. However, Parmar and Mehta (1994) found that the medium-sized follicles had considerably elevated levels of E2 compared to small and large follicles.

Weather conditions also influence the level of E2 plasma (Ronchi et al., 2001). A study by Rao and Pandey (1983) revealed that E2 levels were lower during the summer months compared to the colder months when examining several seasons (hot-dry, hot-humid, warm

and cold). Rao and Pandey (1982) determined that the main reason for a higher occurrence of silent oestrous during the summer is the decreased peak levels of E2 during oestrous, along with decreasing levels of P4.

Pituitary Hormone (Prolactin)

The rise in peripheral plasma prolactin levels during the summer season, in contrast to the winter season, has been linked to the impact of photoperiod on the functioning of prolactin in the pineal glands, as shown by various studies (Mondal et al., 2006). Besides photoperiod, the surrounding temperature significantly affects the prolactin levels. The diurnal fluctuations in prolactin levels were more obvious in summer than in winter, mostly because of the greater difference in ambient temperature between morning, noon, evening, and night. Increased prolactin levels during the summer seasons are believed to interfere with the reproduction cycle and fertility. The reason for this is that prolactin has a direct effect on the synthesis of ovarian steroids by altering the quantity of LH receptors. Besides that, it also obstructs the regular release of LH from the brain and prevents the beneficial effects of oestrogen on LH secretions (Mondal et al., 2006). Singh and Madan (1993) demonstrated that lactation influenced prolactin levels. It was noted that non-lactating buffaloes had higher levels of prolactin throughout the summer compared to lactating ones and vice versa during winter. Furthermore, observations have shown that parity influences peripheral prolactin levels, with multiparous buffaloes exhibiting higher levels on the day of oestrous compared to primiparous buffaloes. Research by Mondal et al. (2006) demonstrated that the quantities of prolactin in milk are more substantial compared to those in plasma, suggesting a possible transfer of prolactin from plasma to milk.

Pituitary Hormone (Follicle Stimulating Hormone)

Follicle-stimulating hormone (FSH) promotes the follicle's development and oestrogen production by granulosa cells in the ovarian follicles. The highest levels of FSH coincided with LH and lasted six to nine hours (Seren et al., 1994). Nevertheless, they noticed that the highest peak of FSH occurs on the tenth day after oestrous, and the last increase is shown on the fourth and fifteenth days after oestrous. After the simultaneous increase of FSH and LH before ovulation, LH levels quickly return to their original levels, and FSH levels gradually decline (Kaker et al., 1980). It has been noted that a reduction in the secretion of LH is associated with the cessation of dominance and the end of the follicular wave, resulting in the absence of ovulation. Weather conditions also influence FSH levels (Prakash et al., 1997). Studies by Janakiraman et al. (1980) have demonstrated that levels of FSH are significantly higher during the oestrous and luteal phases in the peak breeding seasons in Surti buffaloes compared to the equivalent phases in the medium and low breeding seasons.

Pituitary Hormone (Luteinizing Hormone)

LH is essential for evaluating ovarian activity, as its surge prior to ovulation is responsible for the follicular wall's rupture and the egg's release. The radioimmunoassay (RIA) or enzyme-linked immunosorbent assay (ELISA) technique has been used to clearly identify a pre-ovulatory LH increase in buffalo. Like cattle (Rahe et al., 1980), the LH levels in the peripheral blood stay normal for the whole oestrous cycle. The time interval between the highest point of E2 hormone and the highest point of LH hormone has been recorded to be 14–15 hours. However, the duration of LH peak has been estimated to be around 6–12 hours in Mediterranean Italian buffaloes (Seren et al., 1994). Besides that, Terzano et al. (2012) reported an 8-hour interval between the LH surge and the onset of oestrous.

Like other animals, buffalo have changes in peripheral LH levels due to seasonal variations. Rao and Pandey (1983b) showed that LH levels peak on the day of oestrous during cooler months as opposed to hotter months. The variation in LH production in response to E2 can be explained by the failure of the hypothalamohypophyseal axis to consistently enhance LH secretion. Terzano et al. (2012) found that the frequency and amplitude of pulses during the follicular phase exhibit a considerable increase in winter compared to summer seasons. Terzano et al. (2012) discovered that in the summer, the absence of ovarian activity and the lack of pre-ovulatory surge are linked to reduced levels of basal LH. However, Kaker et al. (1980) stated that the average peak of LH levels during ovulation was similar in hot and cool months. The occurrence of silent oestrous during summer can be ascribed to the reduction in the maximum level of LH and the decrease in the P4 level (Rao & Pandey, 1982).

Thyroid Hormone

Thyroid hormones (TH) are involved in the complex hormonal process that regulates steroidogenesis in the ovary. Jorritsma et al. (2003) revealed a correlation between lower triiodothyronine (T3) levels, reduced E2 levels, and decreased oestrous expression. Female animals may experience reproductive issues because of abnormal thyroid function. According to Mutinati et al. (2010), TH directly impacts ovarian function in cattle by influencing the activity of granulosa and thecal cells. Additionally, TH has a substantial effect on the growth of embryos in cattle before and after implantation. Keisler and Lucy (1996) found that artificially induced hypothyroidism negatively affects the rate of conception in dairy cattle. A study by Ghuman et al. (2011) found that even a small amount of thyroid activity in lactating buffaloes can impact their fertility.

Adrenal Hormone (Cortisol)

Cortisol quantifies the overall stress levels in animals (Sampath et al., 2004). The decrease in stress is probably linked to an increase in blood P4 levels. Saqib et al. (2021) discovered

a negative correlation between cortisol and P4 levels. Therefore, it verifies the different functions of the hypothalamus-pituitary-adrenal and hypothalamus-pituitary-gonadal axes. The findings of Saqib et al. (2021) are consistent with the observations made by Mishra et al. (2007), which showed a gradual decrease in blood cortisol levels as the number of post-partum days increased. During the day of oestrous, the cortisol levels in the peripheral plasma reach their highest point because of stress caused by excessive physical activity and the tension related to the oestrous cycle. Saqib et al. (2021) discovered that dairy buffaloes in the later stages of lactation experience enhanced metabolic function, productivity, and reproductive performance while also experiencing decreased stress levels. It demonstrates their capacity to adjust to metabolic, productive, reproductive, and stress-related requirements following parturition.

Insulin-like Growth Factors

Insulin-like growth factor-I (IGF-I) plays a crucial role in the hormonal alterations in mammary gland output following parturition. The liver synthesizes IGF-I in response to growth hormone (GH) and is crucial in regulating development and lactation (Renaville et al., 2002). Multiple IGF-binding proteins (IGFBP) that efficiently suppress IGF activity (LeRoith et al., 2021). In addition, GH opposes the impact of insulin on the body and triggers the secretion of IGF-I. Antagonizing insulin leads to a nutritional partitioning effect, which promotes lean tissue formation and milk secretion (Lucy, 2008). According to Scaramuzzi et al. (2006), GH, IGF-I, and insulin can improve the function of gonadotropin receptors, hence increasing the effectiveness of gonadotropin action. Every hormone could directly influence the ovary by attaching to certain hormone receptors. Metabolic functions like lactation are linked to reproductive processes through a hormonal pathway involving GH, IGF-I, and insulin.

Challenges and Limitation

All hormones face the challenge of the weather. For example, weather conditions can impact plasma E2 levels (Mondal et al., 2006). When comparing E2 levels across different seasons, it was shown that E2 levels were lower during the summer months and the cooler months (Rao & Pandey, 1983). They determined that the main reason for a higher occurrence of silent oestrous during the summer is the decreased peak levels of E2 during oestrous, along with decreasing concentrations of P4.

Furthermore, variables like limited energy intake, decreased body reserve, and post-partum disorders might hinder the process of uterine involution and subsequently delay the restoration of cyclicity. Hence, parturition and the subsequent period are crucial in resuming reproductive function and returning to the normal reproductive cycle (Dhami et al., 2019). An uncomplicated calving process increases the likelihood of a quick return

to normal ovarian activity after giving birth. Besides that, it is preferable to have a short NEB. Fertility can be influenced by various factors related to nutrition, management, and the environment (Parmar et al., 2012). The transitional period and early post-partum phase impose biochemical and physiological stress.

HORMONAL CHANGES IN POST-PARTUM DAIRY BUFFALOES

Changes in Progesterone and Oestradiol

In dairy buffaloes, ovarian hormones like P4 and E2 play an important role in determining the oestrous cycle. During the post-partum period, dairy buffaloes undergo substantial physiological and hormonal changes. In the early post-partum stage, there is typically an NEB produced by metabolic stress due to a decrease in the amount of dry matter intake (DMI) and an increase in energy needs during calving and the start of lactation (Mishra et al., 2007; Saqib et al., 2021). The P4 and E2 synthesis patterns may often appear antagonistic, but both are needed for oestrous and ovulation in the buffalo ovarian cycle.

The P4 profiles can be categorised into three basic patterns: normal cycle, prolonged luteal function, and delayed ovulation (McCoy et al., 2006). Others have reported that there are six types of different ovulatory activities based on P4 profiles during post-partum which are normal, delayed or anovulation, cessation or cyclicity, prolonged luteal phase, short luteal phase, and irregular profiles (Opsomer et al., 1998). When calving, the levels of P4 and E2 decreased gradually to their lowest levels, indicating full luteolysis, as shown in Figure 1. The P4 levels decline progressively from the time of calving to the post-partum

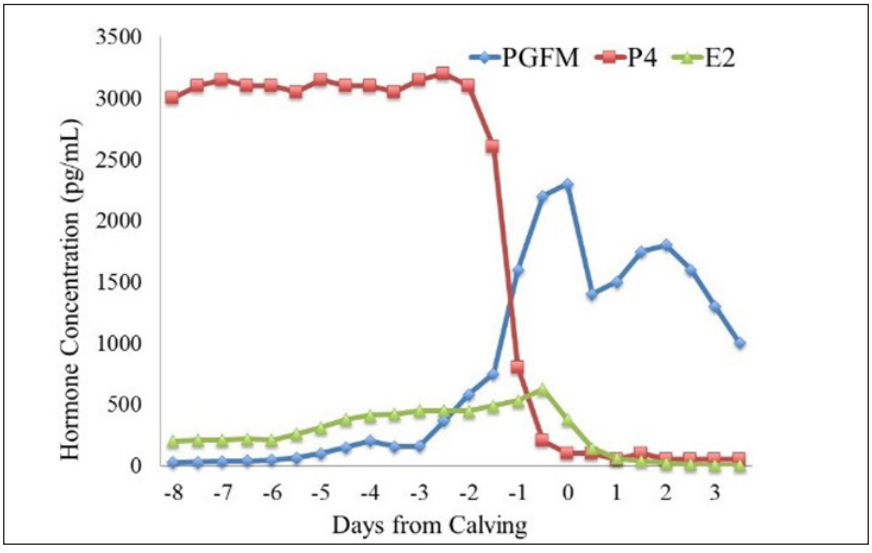

Figure 1. Hormone PGFM, P4 and E2 during the transition period (Mattos et al., 2004; Wiltbank et al., 2016)

period, reaching their minimum point on day 6 (Bahga, 1989) to day 15 (El-Belely et al., 1988). It suggests that the CL of pregnancy has fully regressed. Patel et al. (2020) proposed an extended duration of 3 to 29 days for the complete regression of CL. The decline of CL after calving, as shown by P4 levels on the third day after calving, did not show any variation between milked buffaloes and suckled, according to Arya and Madan (2001). P4 levels remain at a basal level for a varied period of post-partum, but there may be a temporary increase before the resumption of cyclic activity. In late lactation and post-partum stages, buffaloes exhibited improved blood metabolite, P4, and stress levels. The level of P4 rises and falls in sync with the growth and decline of the CL since CL is the source of P4 in cycling bovine (Ahmad et al., 1977).

E2 plays a crucial role in activating the gonadotrophin surge involving the release of GnRH from the hypothalamus and the LH and FSH surge from the anterior pituitary gonadotrophin cells leading to ovulation (Boer et al., 2011). It is well known that E2 is secreted and synthesized by granulosa cells. During post-partum, E2 levels in the blood experienced a considerable decline within the first 24–72 hours. Arya and Madan (2001) stated that basal levels were measured between 2 to 7 days after calving. After this time frame, the levels only had minor fluctuations until day 45 post-partum. Tiwari et al. (1995) showed that the amounts of E2 were higher in buffaloes that were milked compared to those who were suckled. The fluctuations in overall oestrogen levels seen in non-cycling buffaloes during the initial 75 days post-partum are likely indicative of cycles of follicular growth and atresia (Terzano et al., 2012).

Challenges and Limitation

The transition phase, which encompasses the period from late gestation to early post-partum and lasts 6 to 8 weeks, can lead to metabolic disturbances that directly and indirectly impact fertility. Challenging transitions during this period can adversely affect future reproduction (Chapinal et al., 2012). Inadequacies in either the nutritional or non-nutritional aspects of management elevate the likelihood of periparturient metabolic disorders and viral diseases, leading to a decrease in eventual fertility.

P4 and E2 are essential for post-partum dairy buffaloes as they significantly impact oestrous expression and fertility. Inadequate levels can impede the regularity of reproductive cycles and the ability to conceive, affecting reproduction's overall success. Besides that, dairy buffaloes may have P4 insufficiency after parturition during low breeding seasons. It can harm their reproductive efficiency, resulting in silent oestrous and lower conception rates. These effects are evident from the analysis of milk P4 profiles. The reason for this is the insufficient performance of the CL in producing optimal levels of P4. E2 is pivotal in initiating the gonadotrophin surge and ovulation and promoting oestrous behaviour. Consequently, E2 indirectly coordinates the timing of mating and ovulation (Taher &

Hussain, 2022). According to Wathes et al. (2007), the hormonal levels needed for regular oestrous cycles and the return of fertility after calving are gradually returned. Lastly, Failure to recognize oestrous might lead to increased days open, resulting in severe economic losses.

METHODS OF HORMONAL ASSESSMENT

Blood Hormone Assays

Monitoring reproductive cycles and diagnosing the cause of poor reproductive performance in dairy animals is imperative to measuring P4 and E2. There is a need for assays that are easily accessible, can be replicated, provide precise results, and do not involve the use of radiation to measure the levels of P4 and E2 in blood. The dependability and precision of radioimmunoassay (RIA) have made it the preferred method for measuring hormones in dairy buffalo serum, establishing it as the gold standard. RIA presents potential health hazards, has a restricted lifespan, and produces hazardous waste. Using radioactive isotopes in RIA comes with several constraints. Skenandore et al. (2017) propose that ELISA could serve as a feasible alternative. However, it is worth noting that this method may be influenced by various components present in the sample. Sample materials can disrupt enzymeimmunoassay (EIA) methods instead of hormones being tested (Tate & Ward, 2004). Liquid chromatography tandem-mass spectrometry (LC-MS/MS) is the most advanced method for measuring steroid levels in serum. However, it can be costly, time-consuming, and requires specialized expertise, limiting accessibility. Tahir et al. (2013) propose that the chemiluminescence-immunoassay (CLIA) represents a contemporary approach to hormone analysis. Navarro et al. (2022) found that CLIA is more sensitive, faster, and cheaper. P4 levels are commonly measured in human medicine. CLIA's advanced automation enables a high volume of daily analyses, resulting in cost-effectiveness and decreased reliance on human intervention.

Milk Hormone Assays

Milk P4 levels in dairy cows are commonly measured in developed countries to minimize the need for stressful procedures like blood collection, rectal palpation and ultrasound inspection (Wu et al., 2014). Monitoring hormonal changes during bovine pregnancy requires assessing sex hormones in milk (Regal et al., 2012). Measuring P4 in milk presents challenges in sample preservation and varying milk fat content (Comin et al., 2005). However, it offers a simple sampling method. LC-MS/MS is highly regarded for its ability to detect steroids with precision, sensitivity, and accuracy. Electro-spray-ionization linked to tandem mass spectrometry (ESI-MS/MS) is commonly employed for steroid identification in many applications (Regal et al., 2012). Typically, endogenous hormones are non-polar and difficult to ionize using ESI. Derivatization techniques are employed to modify the

chemical structure of analytes, facilitating their ionization (Higashi & Shimada, 2004; Regal et al., 2012). Other methods for measuring hormones in milk include ELISA, RIA, and GC-MS, in addition to LC-MS/MS. ELISA is a solid approach technique for testing ovarian cyclicity. This method helps to accurately determine the periods of oestrous and post-breeding, providing the advantages of accuracy and ease of use. A study by Jouan et al. (2006) discovered that using RIA acquired the most dependable data. As previously said, RIA is considered the benchmark. However, it poses risks to human health. Gas chromatography-mass spectrometry (GC-MS) methods offer superior sensitivity and selectivity compared to immunoassays. Nevertheless, these methods usually need laborious derivatization procedures. Thus, Santen et al. (2007) regarded the combination of GC-MS and LC-MS/MS as the most precise methodology.

Applications of Hormonal Profiling in Dairy Buffalo Management

Buffalo has historically been criticized for having a poorer reproductive capacity than *Bos taurus* cattle. Their extended generation gap, caused by lengthy calving intervals (Singh et al., 2000), has been considered a significant barrier impeding genetic advancement in this species. The calving interval in buffalo is influenced by reproductive issues on the female side and management practices. The importance of CL, a temporary endocrine structure on the ovary, in regulating animal reproductive cycles has been well established (Diaz et al., 2002). P4, produced by the CL, is a reliable indicator of luteal function in dairy cows. It can be measured in milk or blood. E2 impacts the central nervous system and can influence oestrous behaviour. Measuring milk P4 and E2 levels is a straightforward and efficient method for monitoring oestrous, ovarian dysfunction, embryonic death, and pregnancy, particularly in rural settings (Osman et al., 2010). Monitoring P4, oestrogen, total protein, cholesterol, calcium, and phosphorus levels in hormone profiling helps assess dairy buffaloes' reproductive status and health (Patel et al., 2020). Additionally, it can detect hormone misuse, assist in veterinary control and ensure food safety.

Challenges and Limitation

Limitations exist in hormonal profiling for dairy buffalo management. These limitations include the possibility of misdiagnosis caused by non-functioning or cystic ovaries. Accurate diagnosis may require multiple milk samples (Osman et al., 2010). Sampling, stress effects, hormone fluctuations, and post-partum diseases can complicate the process (El-Belely et al., 1988). Buffaloes' aggressive temperament and size make handling and sampling challenging. Insufficient CL activity can lead to decreased P4 levels, which can impact reproductive performance and the ability to detect silent oestrous. Various factors hinder the widespread adoption of hormone profiling, such as budget constraints, farmers' hesitancy to disclose production levels and high costs.

FACTORS INFLUENCING HORMONAL PROFILES

Various factors were documented during this review. Figure 2 summarizes factors influencing the hormonal profiles in dairy buffaloes. Some additional challenges and limitations were presented.

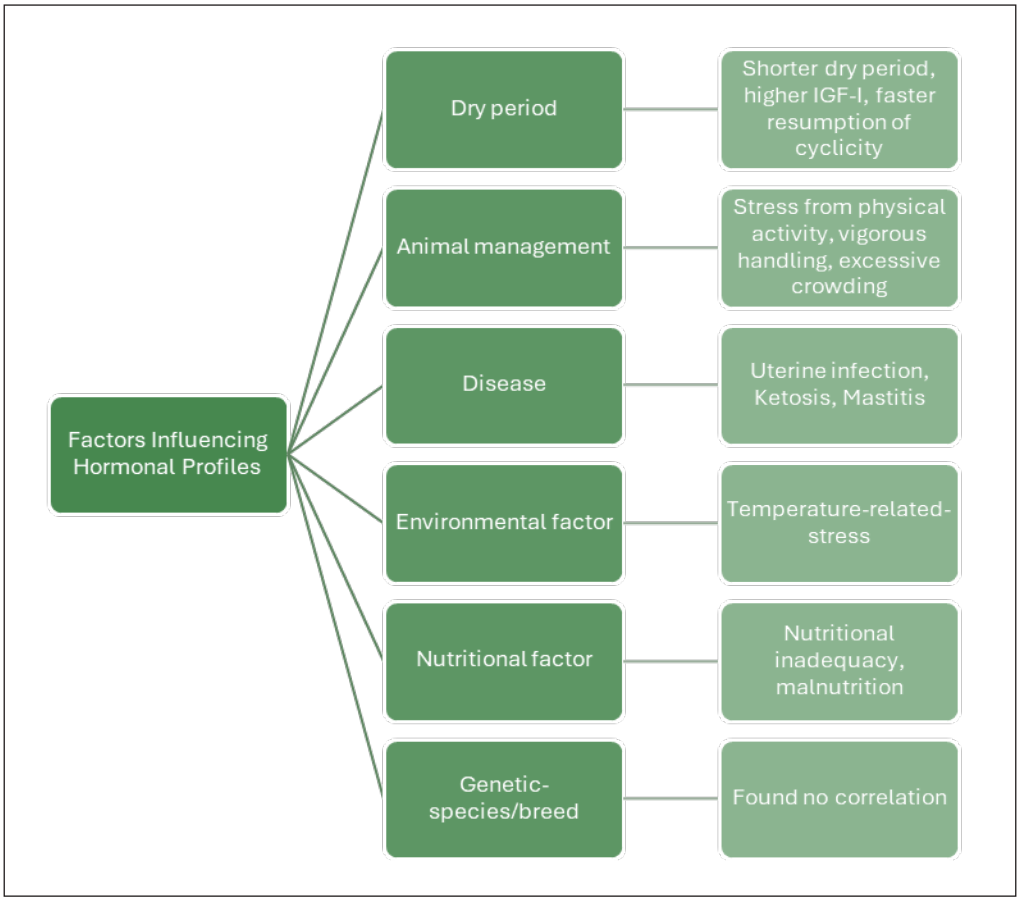

Figure 2. Schematic diagram of factors influencing the hormonal profiles in dairy buffaloes

Dry Period

The dry period is when cows are not milked before calving. Traditionally, this period lasts approximately six to eight weeks (Kok et al., 2019). The dry period serves several tasks. The primary purposes are to administer antibiotics to cows with persistent subclinical mastitis (Bradley & Green, 2001), provide a period of rest for the cow before giving birth to the next calf (Kok et al., 2017), and optimize milk production in the subsequent lactation. A dry period can be regarded as a directly observed economic characteristic of practical importance in dairy farming. The reduction in dry period length lowers milk production

after giving birth. However, several researchers observed enhanced milk production in cows either through shortened (Pezeshki et al., 2007) or wholly eliminated dry period (Andersen et al., 2005).

During the dry period, cows exhibited favourable alterations in their hormone profile, characterized by reduced cortisol levels and higher antioxidant status. The alterations led to a rise in milk production during the initial phases of lactation (Bogolyubova et al., 2021). Mollo et al. (2021) stated that the duration of the dry period affects the hormone profile in dairy cows (Figure 2). They found that shorter dry periods are linked to increased levels of insulin-like growth factor-I and a faster resumption of ovarian cyclicity, ultimately improving milk output. A shorter dry period does not affect reproductive performance other than accelerating the return of ovarian cyclicity and improving milk production.

Animal Management

Effective management is crucial for successfully bringing up buffaloes during the summer months. This weakness is further intensified during the hotter season, as seen by Rensis and Scaramuzzi (2003). It is characterized by less apparent signs of oestrus that last a shorter duration. Buffaloes typically display oestrus mainly during the nighttime or early morning hours, sometimes unnoticed by many farmers. Traditional methods of observation are inadequate for identifying oestrus in these animals (Beg & Totey, 1999), leading to longer mating durations in the warmer months. Implementing breeding management approaches such as controlled internal drug release (CIDR) and Ovsynch protocols substantially impacts plasma progesterone levels in buffaloes but does not affect cholesterol and protein profiles (Savalia et al., 2014). Mondal et al. (2010) noted that buffalo management can influence hormone profiles during the oestrous cycle. Factors such as stress from physical activity and oestrous can alter buffalo's cortisol, T3, and T4 levels. Physical activity includes vigorous handling, excessive crowding, and demanding labour.

Diseases

Post-partum infections can affect hormone levels in dairy buffaloes, which can, in turn, affect ovarian function and reproductive efficiency. Ketosis, a serious condition, decreases milk production while lactation (Fiore et al., 2018). Mastitis hampers reproductive success by triggering a systemic immune response and hormonal changes (Risco & Dahl, 2018). According to Wang et al. (2021), it has been found that this phenomenon can cause delays in the reproductive cycle, decrease pregnancy rates, and elevate the risk of abortion. Mastitis can cause damage to follicles, hinder oocyte development, and decrease ovulation capability; it prolongs the time between oestrous cycles, reduces the luteal phase, and impacts embryo development (Edelhoff et al., 2020).

Environmental Factors

Environmental conditions directly influence the neuroendocrine system in buffalo. Buffaloes are highly vulnerable to thermal stress, particularly when exposed to direct sunlight, due to their limited ability to cool themselves through sweat glands, which are present in low numbers. Due to their sparse hair coat, they have minimal protection (Cockrill, 1993). The situation is further intensified by high relative humidity (Misra et al., 1963). Thermal stress induces hyperprolactinemia, decreased frequency of LH, impaired follicle development, and reduced synthesis of oestradiol in anoestrus buffaloes (Heranjal et al., 1979), resulting in ovarian inactivity.

The manifestation and strength of oestrus and heat in buffaloes are diminished during the summer compared to winter, exhibiting a daily pattern (Madan & Prakash, 2007). Increased ambient temperature also reduces the length of oestrus and the manifestation of oestrus symptoms (Upadhyay et al., 2007). The amount of plasma progesterone and its cyclic fluctuations significantly impact oestrus expression, primarily caused by the cyclic changes in the corpus luteum (Bachlaus et al., 1979). The hot months resulted in low levels of progesterone, oestradiol, and luteinizing hormones in buffaloes, reducing oestrus expression and low conception rates (Rao & Pandey, 1982, 1983). The study conducted by Upadhyay et al. (2007) found that during the summer season, the level of follicle-stimulating hormone in buffaloes was lower compared to the breeding season. It suggests that the main reason for the reduced reproductive efficiency of buffaloes during the summer is temperature-related stress.

Nutritional Factors

Typically, dietary factors are commonly associated with post-partum hormonal alterations in bovines. However, diet is merely one of the factors contributing to the seasonal nature of buffalo reproduction (Zicarelli, 1997). According to Cockrill (1993), it is considered a challenge to the development of buffalo. In Egypt, around 36.5% of non-pregnant buffaloes had ovarian inactivity, likely caused by probable nutritional inadequacy (Heranjal et al., 1979). Buffaloes frequently suffer from malnutrition due to the scarcity of nutrients, particularly protein, as tropical forages get lignified throughout the summer months. In addition, elevated temperature also results in a reduction in the amount of food consumed, which is a crucial aspect of the animal's ability to regulate heat (Rahe et al., 1980). The species may experience a decline in body condition and encounter various reproductive limitations due to nutritional restrictions and reduced voluntary feed intake during heat stress.

Genetic-species Breed

Cruz (2007) identifies the Murrah, Mediterranean, Jaffarabadi, Nili-Ravi, Surti, Kundi, Mehsana, Bhadawari and Nagpuri as the leading buffalo breeds in Asia. According to Harun-Or-Rashid et al. (2019), there are no significant differences in oestrogen and P4 levels on day 0 of the oestrous cycle among local, crossbred, Nili-Ravi and Murrah (Figure 3). Earlier, Arora and Pandey (1982) observed that baseline P4 levels during oestrous ranged from 0.1 to 0.3 ng/ml, stabilising around 1 ng/ml for the subsequent 3-4 days. Mondal et al. (2010) found that plasma P4 levels in buffaloes during the oestrous cycle ranged from 0.30 ± 0.06 to 1.94 ± 0.03 ng/ml.

Puberty is initiated by the release of GnRH from the brain, which subsequently increases the secretion of LH. GnRH is vital in regulating LH release, follicular development, and steroid hormone production. Harun-Or-Rashid et al. (2019) observed no significant variations in the duration of the oestrous cycle among local, crossbred Nili-Ravi and Murrah (Figure 3). Mujawar et al. (2019) found that Marathwadi buffaloes have an oestrous cycle duration of 21.25 ± 2.37 days. Various factors, including environmental conditions, nutrition, and abnormalities in ovarian hormones, can affect the duration of the oestrous cycle.

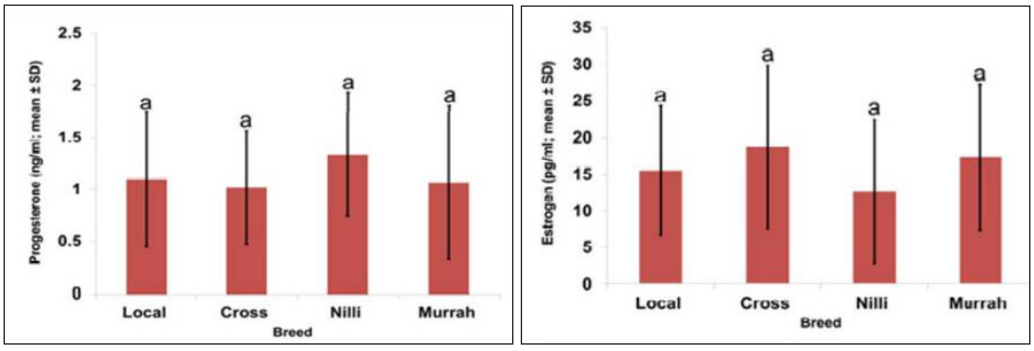

Figure 3. Comparative analysis of ovarian characteristics in several buffalo breeds: (Left) progesterone and (Right) oestrogen levels. Results indicated there is no significant difference ($p > 0.05$) (Harun-Or-Rashid et al., 2019)

Challenges and Limitation

Based on the schematic diagram (Figure 2), buffalo hormonal profiles face difficulties with irregularities in P4, E2, and cortisol levels, as well as metabolic disruptions. Buffalo fertility can be negatively affected by factors, including oxidative stress. In addition, lower LH levels during the oestrous cycle, particularly in warmer months caused by heat stress, impede the initiation of oestrous and reproductive success (Madan & Prakash, 2019). Inconsistent post-partum ovarian activity can result in low P4 levels, leading to conditions like anoestrous, abnormal cycles, and silent heat behaviours (Souza et al., 1997).

In tropical climates, silent heat frequently occurs, which is strongly associated with deficits in management and nutrition, specifically in terms of energy, protein, and minerals (Vale et al., 1988). Furthermore, it is commonly acknowledged that post-partum luteal phases with low progesterone levels might considerably affect the hypothalamic-pituitary-gonadal axis activation (Cable & Grider, 2020). Common irregularities in the oestrous cycle often disrupt fertility. These include shortened or prolonged cycles, silent heat, dysfunctional or persistent CL, inactive ovaries, or ovarian dystrophy. Disturbances like these can hinder heat detection, resulting in lower conception rates and a longer post-partum period. In addition, an NEB during a post-partum period can suppress the quantity and frequency of LH pulses, affecting the stimulation of milk letdown (Souza et al., 1997).

STRATEGIES FOR OVERCOMING CHALLENGES IN HORMONE PROFILING OF DAIRY BUFFALOES

The steroid hormone serves as the principal biomarker indicating the reproductive condition of female animals. Existing methodologies for evaluating the hormone progesterone rely primarily on (enzyme) immunoassays; however, these methods are very expensive for routine screening programs due to their associated labour costs and the necessity for laboratory infrastructure and equipment (Posthuma-Trumpie et al., 2009). It is crucial to know the hormone profiles in dairy buffalo as they have a significant impact on reproductive and production systems. When a dairy animal does not conceive within an optimal timeframe, the farmer faces substantial economic problems, resulting in reduced calf production and milk yield (Bisen et al., 2018). Therefore, it is crucial to enhance the buffaloes' reproductive capabilities managed by small-scale farmers by applying assisted reproductive technologies (Ghuman & Dhami, 2022). Several strategies have been proposed, indicating that hormone profiles in buffaloes can be evaluated by delving deeper into the latest innovations in diagnostic tools and data analytical techniques.

High-performance liquid chromatography (HPLC), gas chromatography, and mass spectrometry represent the analytical methodologies employed to measure progesterone levels in milk (Jang et al., 2017). Applying these methodologies requires extensive sample preparation, a huge financial investment, and skilful personnel adept at operating the laboratory staff to yield the desired outcomes. Limitations such as read-out times, sensitivity, and specificity are inherent drawbacks of lateral flow technology and ELISA kits, which have been used to detect milk progesterone (Wu et al., 2014). Daems et al. (2017) recently introduced a Surface Plasmon Resonance (SPR) biosensor to identify progesterone in dairy milk. This SPR is a competitive inhibition assay with a 0.5 ng/mL detection threshold. Nevertheless, SPR requires a high cost, and it remains a laboratory-centric technique that needs integration with automated milking systems for optimal monitoring (Jang et al., 2017). However, no deployable sensors are available for the on-site assessment of hormone levels in milk.

Enzyme-linked immunosorbent assay (ELISA) is a widely used assay methodology for identifying and quantifying various biological entities due to its remarkable sensitivity and specificity (Song et al., 2023). Frequently, this technique needs the use of substantial and costly laboratory apparatus, which poses challenges for rapid execution at the point-of-care (POC). To enhance portability and user-friendliness, a portable diagnostic system using a Raspberry Pi imaging sensor can rapidly detect progesterone in milk samples, as Jang et al. (2017) outlined. Compared to conventional ELISA assays for progesterone and a commercially accessible plate reader, the proposed POC device demonstrated superior performance metrics while significantly improving portability and simplifying the operation, thus eliminating the requirement for skilful laboratory personnel. The POC reader stands as the sole readily usable portable instrument available to farmers for monitoring the progesterone levels in their herd's milk for various reproductive assessments, effectively addressing a gap with considerable market implications (Jang et al., 2017). Despite all the pros, POC devices need additional validation across a variety of environmental settings to guarantee stable performance within different agricultural systems.

FUTURE DIRECTION

Prospective investigations in hormonal profiling involve integrating endocrinology, cutting-edge agricultural technologies and data science. This amalgamation has the potential to yield a lasting influence on reproduction and productivity across various environmental contexts. Furthermore, subsequent studies are recommended to prioritise advancing diagnostic tools that incorporate artificial intelligence, ensuring they are economically viable and accessible to small-scale farmers, particularly in developing nations such as India and Pakistan, where dairy buffaloes constitute a significant sector of the dairy industry.

CONCLUSION

Ovarian steroid hormones P4 and E2 are pivotal for regulating the oestrous cycle and fertility in dairy buffaloes. Post-partum buffaloes undergo hormonal changes characterized by decreased P4 and E2 levels. These changes are because of reduced DMI and increased energy demands. Normal oestrous cycles and ovulation rely on the appropriate levels of these hormones. Levels of P4 can vary, which can affect the regularity of the menstrual cycle, the duration of luteal function, and the timing of ovulation. E2 triggers the gonadotropin surge needed for ovulation.

Proper nutrition and health management during the transition from late gestation to early post-partum is important to avert metabolic disturbances that may impact fertility. Optimal hormone levels are pivotal for preventing silent oestrous and enhancing conception rates. Monitoring P4 and E2 levels is required in diagnosing reproductive issues. Methods

such as RIA can have potential health and environmental risks. ELISA, LC-MS/MS and CLIA are safer and most cost-effective alternatives.

Optimizing milk production and ensuring sufficient rest are key considerations when managing the 6-8 weeks dry period before calving. Managing buffaloes during hot seasons is crucial because their sensitivity to heat impacts the ability to detect oestrous and hormone levels. Mastitis, ketosis, and environmental factors like heat and humidity can disrupt hormonal balance and decrease fertility. Nutritional deficiencies further impair reproductive health during heat stress. It is important to address reproductive challenges through precise hormonal monitoring and improved management practices to enhance reproductive efficiency and productivity in dairy buffaloes. Genetic factors do not directly influence hormone levels.

ACKNOWLEDGEMENTS

The authors thank the Malaysian Ministry of Higher Education (MOHE) and Universiti Sultan Zainal Abidin for financially supporting the present work through the Fundamental Research Grant Scheme, grant number FRGS/1/2023/WAB04/UNISZA/02/8, entitled 'Mechanistic Understanding on Hormonal Adaptation and Metabolic Pathway During Postpartum Period of Dairy Buffaloes in Malaysia.'

REFERENCES

Abilay, T. A., Johnson, H. D., & Madan, M. (1975). Influence of environmental heat on peripheral plasma progesterone and cortisol during the bovine estrous cycle. *Journal of Dairy Science*, *58*(12), 1836–1840. https://doi.org/10.3168/jds.S0022-0302(75)84795-3

Ahmad, A., Agarwal, S. P., Agarwal, V. K., Rahman, S. A., & Laumas, K. R. (1977). Steroid hormones: Part II. Serum progesterone concentration in buffaloes. *Indian Journal of Experimental Biology*, *15*(8), 591–593.

Andersen, J. B., Madsen, T. G., Larsen, T., Ingvartsen, K. L., & Nielsen, M. O. (2005). The effects of dry period versus continuous lactation on metabolic status and performance in periparturient cows. *Journal of Dairy Science*, *88*(10), 3530-3541. https://doi.org/10.3168/jds.S0022-0302(05)73038-1

Arora, R. C., & Pandey, R. S. (1982). Pattern of plasma progesterone, oestradiol-17β, luteinizing hormone and androgen in non-pregnant buffalo (*Bubalus bubalis*). *European Journal of Endocrinology*, *100*(2), 279–284. https://doi.org/10.1530/acta.0.1000279

Arya, J. S., & Madan, M. L. (2001). Post-partum gonadotropins in suckled and weaned buffaloes. *Indian Veterinary Journal*, *78*(5), 406-409.

Bachlaus, N. K., Arora, R. C., Prasad, A., & Pandey, R. S. (1979). Plasma levels of gonadal hormones in cycling buffalo heifers. *Indian Journal of Experimental Biology*, *17*(8), 823-825.

Bahga, C. S. (1989). Plasma progesterone concentration and reproductive function relative to thyroid activity in postpartum buffaloes (*Bubalus bubalis*). *Veterinary Research Communications*, *13*(6), 407–412. https://doi.org/10.1007/BF00402560

Batra, S. K., Arora, R. C., Bachlaus, N. K., & Pandey, R. S. (1979). Blood and milk progesterone in pregnant and nonpregnant buffalo. *Journal of Dairy Science*, *62*(9), 1390-1393. https://doi.org/10.3168/jds.S0022-0302(79)83434-7

Beg, M. A., & Totey, S. M. (1999). The oestrous cycle, oestrous behaviour and the endocrinology of the oestrous cycle in the buffalo (*Bubalus bubalis*). *Animal Breeding Abstracts*, *66*(9), 329–337.

Bilal, M. Q., Suleman, M., & Raziq, A. (2006). Buffalo: Black gold of Pakistan. *Livestock Research for Rural Development*, *18*(128), 1-16.

Bisen, A., Shukla, S. N., Shukla, M. K., & Mishra, A. (2018). Fertility response using timed insemination protocols in sub-oestrus buffaloes. *Journal of Animal Research*, *8*(3), 417-421.

Boer, H. M. T., Röblitz, S., Stötzel, C., Veerkamp, R. F., Kemp, B., & Woelders, H. (2011). Mechanisms regulating follicle wave patterns in the bovine estrous cycle investigated with a mathematical model. *Journal of Dairy Science*, *94*(12), 5987–6000. https://doi.org/10.3168/jds.2011-4400

Bogolyubova, N. V., Romanov, V. N., & Bagirov, V. A. (2021). Metabolic profile of cows during feeding correction in the late dry period and early lactation. *Russian Agricultural Sciences*, *47*, 155-160. https://doi.org/10.3103/s1068367421020026

Bradley, A. J., & Green, M. J. (2001). An investigation of the impact of intramammary antibiotic dry cow therapy on clinical coliform mastitis. *Journal of Dairy Science*, *84*(7), 1632-1639. https://doi.org/10.3168/jds.S0022-0302(01)74598-5

Cable, J. K., & Grider, M. H. (2020). *Physiology, progesterone*. National Library of Medicine. https://www.ncbi.nlm.nih.gov/books/NBK558960/

Chapinal, N., LeBlanc, S. J., Carson, M. E., Leslie, K. E., Godden, S., Capel, M., Santos, J. E. P., Overton, M. W., & Duffield, T. F. (2012). Herd-level association of serum metabolites in the transition period with disease, milk production, and early lactation reproductive performance. *Journal of Dairy Science*, *95*(10), 5676-5682. https://doi.org/10.3168/jds.2011-5132

Cockrill, W. R. (1993). Developing the water buffalo: A decade of promise. *Buffalo Journal*, *9*(1), 1–11.

Comin, A., Renaville, B., Marchini, E., Maiero, S., Cairoli, F., & Prandi, A. (2005). Technical Note: Direct enzyme immunoassay of progesterone in bovine milk whey. *Journal of Dairy Science*, *88*(12), 4239-4242. https://doi.org/10.3168/jds.S0022-0302(05)73110-6

Cruz, L. C. (2007). Trends in buffalo production in Asia. *Italian Journal of Animal Science*, *6*(SUPPL. 2), 9-24. https://doi.org/10.4081/ijas.2007.s2.9

Daems, D., Lu, J., Delport, F., Mariën, N., Orbie, L., Aernouts, B., Adriaens, I., Huybrechts, T., Saeys, W., Spasic, D., & Lammertyn, J. (2017). Competitive inhibition assay for the detection of progesterone in dairy milk using a fiber optic SPR biosensor. *Analytica Chimica Acta*, *950*, 1–6. https://doi.org/10.1016/j.aca.2016.11.005

Dhami, A. J., Vala, K. B., Kavani, F. S., Parmar, S. C., Raval, R. J., Sarvaiya, N. P., & Gajbhiye, P. U. (2019). Impact of bypass fat and mineral supplementation peripartum on plasma profile of steroid hormones PGFM and postpartum fertility in Jaffarabadi buffaloes. *Indian Journal of Animal Research*, *53*(8), 1042-1048. https://doi.org/10.18805/ijar.b-3631

Diaz, F. J., Anderson, L. E., Wu, Y. L., Rabot, A., Tsai, S. J., & Wiltbank, M. C. (2002). Regulation of progesterone and prostaglandin F2α production in the CL. *Molecular and Cellular Endocrinology*, *191*(1), 65–80. https://doi.org/10.1016/S0303-7207(02)00056-4

Edelhoff, I. N. F., Pereira, M. H. C., Bromfield, J. J., Vasconcelos, J. L. M., & Santos, J. E. P. (2020). Inflammatory diseases in dairy cows: Risk factors and associations with pregnancy after embryo transfer. *Journal of Dairy Science*, *103*(12), 11970-11987. https://doi.org/10.3168/jds.2020-19070

El-Belely, M. S., Zaki, K., & Grunert, E. (1988). Plasma profiles of progesterone and total oestrogens in buffaloes (Bubalus bubalis) around parturition. *The Journal of Agricultural Science*, *111*(3), 519–524. https://doi.org/10.1017/s0021859600083726

Fiore, E., Arfuso, F., Gianesella, M., Vecchio, D., Morgante, M., Mazzotta, E., Badon, T., Rossi, P., Bedin, S., & Piccione, G. (2018). Metabolic and hormonal adaptation in Bubalus bubalis around calving and early lactation. *PLoS ONE*, *13*(4), e0193803. https://doi.org/10.1371/JOURNAL.PONE.0193803

Ghuman, S. P. S., & Dhami, D. S. (2022). Seasonal variation in AI and pregnancy rate in buffalo and improving their fertility status following application of FTAI during non-breeding season. *The Indian Journal of Animal Reproduction*, *38*(1), 4–8.

Ghuman, S. P. S., Singh, J., Honparkhe, M., Ahuja, C. S., Dhami, D. S., Nazir, G., & Gandotra, V. K. (2011). Differential fertility in dairy buffalo: Role of thyroid and blood plasma biochemical milieu. *Iranian Journal of Applied Animal Science*, *1*(2), 105–109.

Harun-Or-Rashid, M., Sarkar, A. K., Hasan, M. M. I., Hasan, M., & Juyena, N. S. (2019). Productive, reproductive, and estrus characteristics of different breeds of buffalo cows in Bangladesh. *Journal of Advanced Veterinary and Animal Research*, *6*(4), 553-560. https://doi.org/10.5455/javar.2019.f382

Heranjal, D. D., Sheth, A. R., Desai, R., & Rao, S. S. (1979). Serum gonadotrophins and prolactin in anoestrus buffaloes. *Indian Journal of Dairy Science*, *32*, 383–385.

Higashi, T., & Shimada, K. (2004). Derivatization of neutral steroids to enhance their detection characteristics in liquid chromatography-mass spectrometry. *Analytical and Bioanalytical Chemistry*, *378*, 875-882. https://doi.org/10.1007/s00216-003-2252-z

Honparkhe, M., Singh, J., Dadarwal, D., Dhaliwal, G. S., & Kumar, A. (2008). Estrus induction and fertility rates in response to exogenous hormonal administration in postpartum anestrous and subestrus bovines and buffaloes. *Journal of Veterinary Medical Science*, *70*(12), 1327-1331. https://doi.org/10.1292/jvms.70.1327

Janakiraman, K., Desai, M. C., Amin, D. R., Sheth, M., & Wadadekar, K. B. (1980). Serum gonadotropin levels in buffaloes in relation to phases of oestrous cycle and breeding periods. *Indian Journal of Animal Sciences*, *50*(8), 601–606.

Jang, H., Ahmed, S., & Neethirajan, S. (2017). GryphSens: A smartphone-based portable diagnostic reader for the rapid detection of progesterone in milk. *Sensors*, *17*(5), 1079. https://doi.org/10.3390/s17051079

Jorritsma, R., Wensing, T., Kruip, T. A. M., Vos, P. L. A. M., & Noordhuizen, J. P. T. M. (2003). Metabolic changes in early lactation and impaired reproductive performance in dairy cows. *Veterinary Research*, *34*(1), 11–26. https://doi.org/10.1051/vetres:2002054

Jouan, P.-N., Pouliot, Y., Gauthier, S. F., & Laforest, J.-P. (2006). Hormones in bovine milk and milk products: A survey. *International Dairy Journal*, *16*(11), 1408–1414. https://doi.org/10.1016/j.idairyj.2006.06.007

Kaker, M. L., Razdan, M. N., & Galhotra, M. M. (1980). Serum LH concentrations in cyclic buffalo (*Bubalus bubalis*). *Reproduction*, *60*(2), 419–424. https://doi.org/10.1530/jrf.0.0600419

Keisler, D. H., & Lucy, M. C. (1996). Perception and interpretation of the effects of undernutrition on reproduction. *Journal of Animal Science*, *74*(suppl_3), 1–17. https://doi.org/10.2527/1996.74suppl_31x

Kok, A., Chen, J., Kemp, B., & van Knegsel, A. T. M. (2019). Review: Dry period length in dairy cows and consequences for metabolism and welfare and customised management strategies. *Animal*, *13*(S1), s42-s51. https://doi.org/10.1017/S1751731119001174

Kok, A., van Hoeij, R. J., Tolkamp, B. J., Haskell, M. J., van Knegsel, A. T. M., de Boer, I. J. M., & Bokkers, E. A. M. (2017). Behavioural adaptation to a short or no dry period with associated management in dairy cows. *Applied Animal Behaviour Science*, *186*, 7-15. https://doi.org/10.1016/j.applanim.2016.10.017

Kumar, S., Balhara, A. K., Kumar, R., Kumar, N., Buragohain, L., Baro, D., Sharma, R. K., Phulia, S. K., & Singh, I. (2015). Hemato-biochemical and hormonal profiles in post-partum water buffaloes (*Bubalus bubalis*). *Veterinary World*, *8*(4), 512-517. https://doi.org/10.14202/vetworld.2015.512-517

LeRoith, D., Holly, J. M. P., & Forbes, B. E. (2021). Insulin-like growth factors: Ligands, binding proteins, and receptors. *Molecular Metabolism*, *52*, 101245. https://doi.org/10.1016/j.molmet.2021.101245

Lucy, M. C. (2008). Functional differences in the growth hormone and insulin-like growth factor axis in cattle and pigs: Implications for post-partum nutrition and reproduction. *Reproduction in Domestic Animals*, *43*(SUPPL.2), 31-39. https://doi.org/10.1111/j.1439-0531.2008.01140.x

Madan, M. L., & Prakash, B. S. (2007). Reproductive endocrinology and biotechnology applications among buffaloes. *Society of Reproduction and Fertility Supplement*, *6*, 261-281

Madan, M., & Prakash, B. (2019). Reproductive endocrinology and biotechnology applications among buffaloes. *Bioscientifica Proceedings*, *6*(1), 261-281. https://doi.org/10.1530/biosciprocs.6.017

Mattos, R., Staples, C. R., Arteche, A., Wiltbank, M. C., Diaz, F. J., Jenkins, T. C., & Thatcher, W. W. (2004). The effects of feeding fish oil on uterine secretion of PGF 2α, milk composition, and metabolic status of periparturient Holstein cows. *Journal of Dairy Science*, *87*(4), 921-932. https://doi.org/10.3168/jds.S0022-0302(04)73236-1

McCoy, M. A., Lennox, S. D., Mayne, C. S., McCaughey, W. J., Edgar, H. W. J., Catney, D. C., Verner, M., Mackey, D. R. & Gordon, A. W. (2006). Milk progesterone profiles and their relationship with fertility, production and disease in dairy cows in Northern Ireland. *Animal Science*, *82*(2), 213–222. https://doi.org/10.1079/ASC200526

Mishra, A., Pankaj, P. K., Roy, B., Sharma, I. J., & Prakash, B. S. (2007). Antigonadotrophic effects of prolactin in relation to commencement of cyclicity, milk yield and blood metabolites in postpartum lactating riverine buffaloes (*Bubalus Bubalis*). *Buffalo Bulletin*, *26*(3), 77-86.

Misra, M. S., Sengupta, B. P., & Roy, A. (1963). Physiological reactions of buffalo cows maintained in two different housing conditions during summer months. *Indian Journal of Dairy Science*, *16*, 203–215.

Mollo, A., Agazzi, A., Prandi, A., Fusi, J., Amicis, I. D. E., & Probo, M. (2021). Metabolic and production parameters of dairy cows with different dry period lengths and parities. *Acta Veterinaria Hungarica*, *69*(4), 354-362. https://doi.org/10.1556/004.2021.00049

Mondal, S., & Prakash, B. S. (2003). Peripheral plasma progesterone concentration in relation to estrus expression in Sahiwal cows. *Indian Journal of Physiology and Pharmacology*, *47*(1).

Mondal, S., Prakash, B. S., & Palta, P. (2003). Relationship between peripheral plasma inhibin and progesterone concentrations in Sahiwal cattle (Bos Indicus) and Murrah buffaloes (*Bubalus bubalis*). *Asian-Australasian Journal of Animal Sciences*, *16*(1), 6-10. https://doi.org/10.5713/ajas.2003.6

Mondal, S., Prakash, B. S., & Palta, P. (2006). Endocrine aspects of oestrous cycle in buffaloes (*Bubalus bubalis*): An overview. *Asian-Australasian Journal of Animal Sciences*, *20*(1), 124–131. https://doi.org/10.5713/ajas.2007.124

Mondal, S., Suresh, K. P., & Nandi, S. (2010). Endocrine profiles of oestrous cycle in buffalo: A meta-analysis. *Asian-Australasian Journal of Animal Sciences*, *23*(2), 169–174. https://doi.org/10.5713/ajas.2010.90193

Mujawar, A., Razzaque, W., Ramteke, S., Patil, A., Ali, S., Bhikane, A., Khan, M., & Mogal, I. (2019). Estrus induction and fertility response in postpartum anoestrus Marathwadi buffaloes using hormonal protocol along with vitamin e and selenium. *International International Journal of Livestock Research*, *9*(3), 289-295.

Mutinati, M., Desantis, S., Rizzo, A., Zizza, S., Ventriglia, G., Pantaleo, M., & Sciorsci, R. L. (2010). Localization of thyrotropin receptor and thyroglobulin in the bovine corpus luteum. *Animal Reproduction Science*, *118*(1), 1-6. https://doi.org/10.1016/j.anireprosci.2009.05.019

Navarro I., Kozicki, L. E., Weber, S. H., Saporski Segui, M., Camargo, C. E., Gomes Bergstein-Galan, T., Weiss, R. R., & Ricci Catalano, F. A. (2022). Serum progesterone profile in the oestrous cycle of mares determined using immuno chemiluminescence (CLIA). *Pferdeheilkunde Equine Medicine*, *38*(5), 413–419. https://doi.org/10.21836/PEM20220502

Opsomer, G., Coryn, M., Deluyker, H., & De Kruif, A. (1998). An analysis of ovarian dysfunction in high yielding dairy cows after calving based on progesterone profiles. *Reproduction in Domestic Animals*, *33*(3–4). https://doi.org/10.1111/j.1439-0531.1998.tb01342.x

Osman, K., El-Regalaty, H., Fekry, A., Farghaly, H., & Aboul-Ela, H. (2010). Use of milk progesterone assay for monitoring ovulation, ovarian cycles and pregnancy in buffalo. *Journal of Animal and Poultry Production*, *1*(5), 163–174. https://doi.org/10.21608/jappmu.2010.86199

Palta, P., Bansal, N., Manik, R. S., Prakash, B. S., & Madan, M. L. (1998). Interrelationships between follicular size, estradiol-17β, progesterone and testosterone concentrations in individual buffalo ovarian follicles. *Asian-Australasian Journal of Animal Sciences*, *11*(3), 293–299. https://doi.org/10.5713/ajas.1998.293

Parmar, A., & Mehta, V. (1994). Seasonal endocrine changes in steroid hormones of developing ovarian follicles in Surti buffaloes. *Indian Journal of Animal Sciences*, *64*. https://epubs.icar.org.in/index.php/IJAnS/article/view/30252

Parmar, K., Shah, R. G., Tank, P. H., & Dhami, A. J. (2012). Effect of hormonal and non-hormonal treatment on reproductive efficiency and plasma progesterone, biochemical and macromineralsprofile in postpartum

anoestrus buffaloes. *The Indian Journal of Field Veterinarians*, *8*, 48–54. http://doi.org/10.1038/nrmicro2577

Patel, B. R., Panchal, M., Dhami, A., Sarvaiya, N., & Pathan, M. (2020). Comparative plasma endocrine, metabolic and mineral profile of cyclic, acyclic, endometritic and pregnant buffaloes. *The Indian Journal of Veterinary Sciences and Biotechnology*, *15*(04), 80-83. https://doi.org/10.21887/ijvsbt.15.4.2

Pezeshki, A., Mehrzad, J., Ghorbani, G. R., Rahmani, H. R., Collier, R. J., & Burvenich, C. (2007). Effects of short dry periods on performance and metabolic status in holstein dairy cows. *Journal of Dairy Science*, *90*(12), 5531-5541. https://doi.org/10.3168/jds.2007-0359

Posthuma-Trumpie, G. A., Van Amerongen, A., Korf, J., & Van Berkel, W. J. H. (2009). Perspectives for on-site monitoring of progesterone. *Trends in Biotechnology*, *27*(11), 652–660. https://doi.org/10.1016/j.tibtech.2009.07.008

Prakash, B. S., Palta, P., Bansal, N., Manik, R. S., & Madan, M. L. (1997). Development of a sensitive, direct enzyme immunoassay for progesterone determination in follicular fluid from individual buffalo ovarian follicles. *Indian Journal of Animal Sciences*, *67*(8). https://epubs.icar.org.in/index.php/IJAnS/article/view/34882

Rahe, C. H., Owens, R. E., Fleeger, J. L., Newton, H. J., & Harms, P. G. (1980). Pattern of plasma luteinizing hormone in the cyclic cow: Dependence upon the period of the cycle. *Endocrinology*, *107*(2), 498–503. https://doi.org/10.1210/endo-107-2-498

Rao, L. V., & Pandey, R. S. (1982). Seasonal changes in plasma progesterone concentrations in buffalo cows (*Bubalus bubalis*). *Journal of Reproduction and Fertility*, *66*(1), 57-61. https://doi.org/10.1530/jrf.0.0660057

Rao, L. V., & Pandey, R. S. (1983). Seasonal variations in oestradiol-17β and luteinizing hormone in the blood of buffalo cows (*Bubalus bubalis*). *Journal of Endocrinology*, *98*(2), 251-255. https://doi.org/10.1677/joe.0.0980251

Regal, P., Cepeda, A., & Fente, C. A. (2012). Development of an LC-MS/MS method to quantify sex hormones in bovine milk and influence of pregnancy in their levels. *Food Additives and Contaminants - Part A*, *29*(5), 770–779. https://doi.org/10.1080/19440049.2011.653989

Renaville, R., Hammadi, M., & Portetelle, D. (2002). Role of the somatotropic axis in the mammalian metabolism. *Domestic Animal Endocrinology*, *23*(1-2), 351–360. https://doi.org/10.1016/s0739-7240(02)00170-4

Rensis, F. D., & Scaramuzzi, R. J. (2003). Heat stress and seasonal effects on reproduction in the dairy cow—a review. *Theriogenology*, *60*(6), 1139–1151. https://doi.org/10.1016/S0093-691X(03)00126-2

Risco, C., & Dahl, M. (2018). Effect of inflammatory response related to mastitis on dairy cattle reproduction. *Clinical Theriogenology*, *10*(3), 253–257.

Ronchi, B., Stradaioli, G., Verini Supplizi, A., Bernabucci, U., Lacetera, N., Accorsi, P. A., Nardone, A. & Seren, E. (2001). Influence of heat stress or feed restriction on plasma progesterone, oestradiol-17β, LH, FSH, prolactin and cortisol in Holstein heifers. *Livestock Production Science*, *68*(2–3), 231–241. https://doi.org/10.1016/S0301-6226(00)00232-3

Sampath, K., Praveen, U., & Kharaiah, M. C. (2004). Effect of strategic supplementation of finger millet straw on milk yield in crossbred cows on farm trial. *Indian Journal of Dairy Science*, *57*(3), 192–197.

Santen, R. J., Demers, L., Ohorodnik, S., Settlage, J., Langecker, P., Blanchett, D., Goss, P. E., & Wang, S. (2007). Superiority of gas chromatography/tandem mass spectrometry assay (GC/MS/MS) for estradiol for monitoring of aromatase inhibitor therapy. *Steroids*, *72*(8), 666–671. https://doi.org/10.1016/j.steroids.2007.05.003

Saqib, M. N., Qureshi, M. S., Suhail, S. M., Khan, R. U., Bozzo, G., Ceci, E., Laudadio, V., & Tufarelli, V. (2021). Association among metabolic status, oxidative stress, milk yield, body condition score and reproductive cyclicity in dairy buffaloes. *Reproduction in Domestic Animals*, *57*(5), 498-504. https://doi.org/10.1111/rda.14086

Savalia, K. K., Dhami, A. J., Hadiya, K. K., Patel, K. R., & Sarvaiya, N. P. (2014). Influence of controlled breeding techniques on fertility and plasma progesterone, protein and cholesterol profile in true anestrus and repeat breeding buffaloes. *Veterinary World*, *7*(9), 727–732. https://doi.org/10.14202/vetworld.2014.727-732

Scaramuzzi, R. J., Campbell, B. K., Downing, J. A., Kendall, N. R., Khalid, M., Muñoz-Gutiérrez, M., & Somchit, A. (2006). A review of the effects of supplementary nutrition in the ewe on the concentrations of reproductive and metabolic hormones and the mechanisms that regulate folliculogenesis and ovulation rate. *Reproduction Nutrition Development*, *46*(4), 339–354. https://doi.org/10.1051/rnd:2006016

Seren, E., Parmeggiani, A., Mongiorgi, S., Zicarelli, L., Montemurro, N., Pacelli, C., Campanile, G., Esposito, L., Di Palo, R., Borghese, A., Barile, V. L., Terzano, G. M., Annichiarico, G., Allergrini, S. (1994). Modificazioni endocrine durante il ciclo estrale nella bufala [Endocrine changes during the estrous cycle in buffalo]. *Agricoltura Ricerca*, *153*(1), 17–24.

Sethi, M., Shah, N., Mohanty, T. K., Bhakat, M., Dewry, R. K., Yadav, D. K., Gupta, V. K., & Nath, S. (2021). The induction of cyclicity in postpartum anestrus buffaloes: A review. *Journal of Experimental Zoology India*, *24*(2), 989–997.

Singh, J., & Madan M. L. (1993). RIA of prolactin as related to circadian changes in buffaloes. *Buffalo Journal*, *9*, 159–164.

Singh, J., Nanda, A. S., & Adams, G. P. (2000). The reproductive pattern and efficiency of female buffaloes. *Animal Reproduction Science*, *60-61*, 593–604. https://doi.org/10.1016/s0378-4320(00)00109-3

Skenandore, C. S., Pineda, A., Bahr, J. M., Newell-Fugate, A. E., & Cardoso, F. C. (2017). Evaluation of a commercially available radioimmunoassay and enzyme immunoassay for the analysis of progesterone and estradiol and the comparison of two extraction efficiency methods. *Domestic Animal Endocrinology*, *60*, 61–66. https://doi.org/10.1016/j.domaniend.2017.03.005

Song, J. G., Baral, K. C., Kim, G.-L., Park, J.-W., Seo, S.-H., Kim, D.-H., Jung, D. H., Ifekpolugo, N. L., & Han, H.-K. (2023). Quantitative analysis of therapeutic proteins in biological fluids: Recent advancement in analytical techniques. *Drug Delivery*, *30*(1), 2183816. https://doi.org/10.1080/10717544.2023.2183816

Souza, H. E. M., Silva, A. O. A., Sousa, J. S., Vale, W. G., Borghese, A., Failla, S., & Barile, V. L. (1997). *Progesterone profiles through the postpartum period in milk buffaloes under poor management conditions.*

https://www.semanticscholar.org/paper/Progesterone-profiles-through-the-postpartum-period-Souza-Silva/8c9f10f2a00401015a048ac1ee2361c4729bca55

Srivastava, S. K., Sahni, K. L., Shanker, U., Sanwal, P. C., & Varshney, V. P. (1999). Seasonal variation in progesterone concentration during oestrus cycle in Murrah buffaloes. *Indian Journal of Animal Sciences*, *69*(9).

Taher, J. K., & Hussain, S. O. (2022). Study of estrogen, progesterone and glucose level in cows during overt and silent estrus. *University of Thi-Qar Journal of Agricultural Research*, *11*(1), 79–83. https://doi.org/10.54174/UTJagr.Vo11.N1/09

Tahir, M. Z., Thoumire, S., Raffaelli, M., Grimard, B., Reynaud, K., & Chastant-Maillard, S. (2013). Effect of blood handling conditions on progesterone assay results obtained by chemiluminescence in the bitch. *Domestic Animal Endocrinology*, *45*(3), 141–144. https://doi.org/10.1016/j.domaniend.2013.07.002

Tate, J., & Ward, G. (2004). Interferences in immunoassay. *The Clinical Biochemist. Reviews*, *25*(2), 105–120.

Terzano, G. M., Barile, V. L., & Borghes, A. (2012). Overview on reproductive endocrine aspects in buffalo. *Journal of Buffalo Science*, *1*(2), 126-138. https://doi.org/10.6000/1927-520x.2012.01.02.01

Tiwari, S. R., Pathak, M. M., & Patel, A. V. (1995). Study of ovarian steroids during postpartum period of Surti buffaloes in relation to suckling and milking practices. *Indian Journal Animal Reproduction*, *16*, 5–8.

Upadhyay, R. C., Singh, S. V., Kumar, A., Gupta, S. K., & Ashutosh, A. (2007). Impact of climate change on milk production of murrah buffaloes. *Italian Journal of Animal Science*, *6*(sup2), 1329–1332. https://doi.org/10.4081/ijas.2007.s2.1329

Vale, W. G., Ohashi, O. M., Sousay, J. S., & Ribeiro, H. F. L. (1988). *Studies on the reproduction of water buffalo in the Amazon Basin.* International Atomic Energy Agency Vienna. https://www.researchgate.net/publication/39012709_Studies_on_the_reproduction_of_water_buffalo_in_the_Amazon_Basin

Wang, N., Zhou, C., Basang, W., Zhu, Y., Wang, X., Li, C., Chen, L., & Zhou, X. (2021). Mechanisms by which mastitis affects reproduction in dairy cow: A review. *Reproduction in Domestic Animals*, *56*(9), 1165–1175. https://doi.org/10.1111/rda.13953

Wathes, D. C., Fenwick, M., Cheng, Z., Bourne, N., Llewellyn, S., Morris, D. G., Kenny, D., Murphy, J., & Fitzpatrick, R. (2007). Influence of negative energy balance on cyclicity and fertility in the high producing dairy cow. *Theriogenology*, *68*(suppl. 1), S232-S241. https://doi.org/10.1016/j.theriogenology.2007.04.006

Wiltbank, M. C., Median, R., Ochoa, J., Baez, G. M., Giordano, J. O., Ferreira, J. C. P., & Sartori, R. (2016). Maintenance or regression of the corpus luteum during multiple decisive periods of bovine pregnancy. *Animal Reproduction*, *13*(3), 217-233. https://doi.org/10.21451/1984-3143-AR865

Wu, L., Xu, C., Xia, C., Duan, Y., Xu, C., Zhang, H., & Bao, J. (2014). Development and application of an ELISA kit for the detection of milk progesterone in dairy cows. *Monoclonal Antibodies in Immunodiagnosis and Immunotherapy*, *33*(5), 330-333. https://doi.org/10.1089/mab.2014.0013

Zicarelli, L. (1997). Reproductive seasonality in buffalo. *Proceedings of Third International Course of Biotechnology in Buffalo Reproduction, Naples, Italy*, *4*, 29–52.

Pertanika J. Trop. Agric. Sci. 48 (3): 719 - 731 (2025)

PERTANIKA JOURNALS

TROPICAL AGRICULTURAL SCIENCE

Journal homepage: http://www.pertanika.upm.edu.my/

Development of Herbal Tea Product Based on *Crossandra infundibuliformis* and *Justicia betonica* Leaves for Functional Drink: Antioxidant Activity, Sensory Evaluation, and Nutritional Value

Marasri Junsi*, Sommarut Klamklomjit, Satitpong Munlum and Nantida Dangkhaw

Culinary Arts program, Faculty of Culinary Arts, Dusit Thani College, Bangkok 10250, Thailand

ABSTRACT

Crossandra infundibuliformis and *Justicia betonica*, belonging to the Acanthaceae family, are well-known medicinal herbs in India, Sri Lanka, and Thailand. This study aims to determine antioxidant activity in extracts, including sensory evaluation of herbal tea products from both herbs. Leaf extracts were taken to determine total extractable phenolic content (TPC), total extractable flavonoid content (TFC), and antioxidant activity, including compound contents, using the high-performance liquid chromatography (HPLC) technique. The herbal tea products were prepared for sensory evaluation using the 9-point hedonic scale. The selected tea formula was studied for physicochemical properties and nutritional value. The results showed that *C. infundibuliformis* extract exhibited a higher activity value for TPC, TFC, and antioxidant activity than *J. betonica*. Moreover, the *C. infundibuliformis* and *J. betonica* leaf extracts contained 8 and 9 types of phenolic and flavonoid compounds, respectively. The T2 formula of herbal tea provided the highest sensory evaluation. It showed moisture and water activity contents of less than 7% and 0.6, while the nutritional value provided energy, protein, carbohydrates, sugar, vitamins A and B2, sodium, *β*-carotene, calcium, iron, and ash. Therefore, *C. infundibuliformis* and *J. betonica* can be produced as herbal tea for being a source of antioxidants.

Keywords: Antioxidants, *Crossandra infundibuliformis*, functional drink, herbal tea, *Justicia betonica*

ARTICLE INFO

Article history:
Received: 07 August 2024
Accepted: 30 September 2024
Published: 16 May 2025

DOI: https://doi.org/10.47836/pjtas.48.3.04

E-mail addresses:
marasri_jun@hotmail.com; marasri.ju@dtc.ac.th (Marasri Junsi)
sommarut.kl@dtc.ac.th (Sommarut Klamklomjit)
satitpong.mu@dtc.ac.th (Satitpong Munlum)
nantida.da@dtc.ac.th (Nantida Dangkhaw)
*Corresponding author

INTRODUCTION

The trend of consuming healthy food and drink products has recently become very popular worldwide, including in Thailand. According to Patathananone et al. (2023), consumers are increasingly aware of the importance of consuming healthy food and raw materials from vegetable groups and herbs, which serve as a source of numerous

biological substances for producing healthy food products. Herbal tea ranks among the top three most popularly consumed beverages globally, with an increasing market for functional food products in many countries (Salazar-Campos et al., 2023). Herbal tea is a healthy beverage in the same form and method of consumption as tea. It is also convenient for making and drinking, providing many functional properties that benefit consumers (Phakamus et al., 2018). *Crossandra infundibuliformis* and *Justicia betonica*, native to tropical Asia and Africa, spread throughout India, Sri Lanka, and Thailand (Eapen et al., 2019; Hari et al., 2022). *Crossandra infundibuliformis* is a local plant in Thailand that belongs to the Acanthaceae family.

Researchers use this plant's fresh and dried leaves for their hepatoprotective, antioxidant, antibacterial, antifungal, and anticandidal properties (Hari et al., 2022). According to Naik et al. (2022), the *J. betonica* plant, a member of the Acanthaceae family, possesses analgesic, antimalarial, antioxidant, antimicrobial, and anti-inflammatory properties. In Thailand, these plants have been traditionally utilized in Thai folklore medicine for therapeutic purposes. They were often prepared as herbal extracts or boiled in water to create a drink believed to alleviate coughs, act as a tonic, and counteract toxins in the blood. (Kanchanapoom et al., 2004; Wong-arun et al., 2014). Thai folklore medicine has been useful in both healing fields in ancient times, but the application of these herbs in functional drinks remains unexplored. Furthermore, the combination of both herbs could possibly produce superior functional properties and be beneficial for consumers, particularly antioxidant properties.

Therefore, this study aims to develop herbal tea products as a source of antioxidant drinks from both herbs, focusing on the leaf part in the developing stage, which is ideal for the development of herbal tea. It will be achieved by determining antioxidant activity, including identifying phenolic and flavonoid compounds in both extract herbs and evaluating consumers' sensory experience. Hence, the prototype product can be used to create a nutritious and functional drink containing herbs that are appealing to the general consumer, benefiting entrepreneurs and consumers. Furthermore, the insights gained from this research can be used for commercial applications further.

MATERIALS AND METHODS

Chemicals

The determination chemicals for antioxidant activities and High-Performance Liquid Chromatography (HPLC) analysis were purchased from Sigma-Aldrich, Seelze, Germany. The other chemicals used as analytical grades are from Merck, Darmstadt, Germany; LAB-SCAN, Dublin, Ireland, and Fisher Scientific, Leicestershire, England.

Plant Materials and Preparation

The developing stage of all plant leaves was purchased directly from farmers: *C. infundibuliformis* and *J. betonica* from Chai Nat, Thailand, and *Pandanus amaryllifolius*

from Nakhon Pathom, Thailand. Then, the leaves were rinsed using tap water, allowed to drain, and air-dried for 5-8 days until the moisture content reached 8-10% (w/w) following traditional methods (Ruangyuttikarn et al., 2013). Finally, they were stored in a sealed, dry container for future analysis.

Sample Extraction

C. infundibuliformis and *J. betonica* dried leaves were ground by blender into a fine powder and passed through a sieve with 60 meshes. Afterward, both leaf powders were soaked in hot water at a temperature of 98±1°C with a ratio of 1 per 10 (w/v) for a duration of 1 hr. The liquid should be strained using three layers of gauze and then passed through filter paper (Whatman No. 4). Both filtrated samples were dried in freeze-dried form and kept at 4°C (Ruangyuttikarn et al., 2013) for further study.

Determination of Total Extractable Phenolic Content (TPC), Total Extractable Flavonoid Content (TFC), and Antioxidant Activity

The determination of TPC for both extracts was done using a modified Folin-Ciocalteu by the method of Tan and Kassim (2011), and the standard curves were generated using gallic acid and stated as milligrams of gallic acid equivalent per gram of dried extract (mg GAE/g dried extract). The TFC was determined using the aluminum chloride colorimetric method (Imam et al., 2011) with some modifications, was determined using catechin as the standard and expressed as milligrams of catechin equivalent per gram of dried extract (mg CE/g dried extract).

The antioxidant activity consisting of DPPH, ABTS, and FRAP was determined. The 2,2-diphenyl-1-picrylhydrazyl (DPPH) scavenging activity was assessed in both extracts based on the DPPH assay (Raj et al., 2016). The determination of 2,2'-azino-bis (3-ethylbenzothiazoline-6-sulphonic acid [ABTS]) radical scavenging using the ABTS assay (Pereira et al., 2014) with some modifications and the ferric ion-reducing antioxidant power (FRAP) was determined with some modifications of the method of Tan & Chan (2014). The activity was quantified by comparing the results with a calibration curve using gallic acid as a standard and expressing as milligrams of gallic acid equivalent per gram of dried extract (mg GAE/g dried extract).

Determination of Phenolic and Flavonoid Compounds Using High-performance Liquid Chromatography (HPLC) Technique

The quantitative phenolic and flavonoid compounds of *C. infundibuliformis* and *J. betonica* extracts were measured by HPLC. The determination of the compounds was completed using the HPLC system (Shimadzu, Kyoto, Japan) equipped with an Inersil C18 (250×4.6 mm, GL Sciences, Japan) column. The mobile phase solvent A is composed of 2% (v/v) acetic acid in water, while solvent B consists of 100% (v/v) acetonitrile. The column

temperature was controlled at 30ºC, and solvent A was programmed, keeping a consistent flow rate of 1 ml/min while gradually increasing the proportion of solvent B from 5% to 90% over 75 min. (Liaudanskas et al., 2014). Gallic acid, catechin, chlorogenic acid, caffeic acid, epicatechin, ferulic acid, quercetin, protocatechuic acid, *p*-hydroxybenzoic acid, vanillic acid, *p*-coumaric acid, rutin, caffeine, syringic acid, vanillin, synaptic acid, myricetin, and *trans*-cinnamic acid were used as standard agents.

Preparation of Herbal Tea

Five formulas of the herbal tea prepared from *C. infundibuliformis*, *J. Betonica*, and *P. amaryllifolius* dried leaves at the following ratios: 4:1:0 (T1), 3:1:1 (T2), 2:2:1 (T3), 1:3:1 (T4), and 0:4:1 (T5). All samples were grounded and sifted through a 60-mesh sieve, then soaked in hot water at 85±2ºC for 4-5 min before being taken to the panelists.

Sensory Evaluation of Herbal Tea

The sensory acceptability of herbal tea products was assessed based on appearance, color, odor, flavor, astringent test, and overall liking. This study used regular consumers for the tested panelists. Each sample was coded with three-digit codes and served randomly (10 ml/sample) to the panelists, and the panelists were provided drinking water between sample tests. A 9-point hedonic scale was used to assess the sensory attributes of product samples (Meilgaard et al., 2007). The rating scale extended from 1 (strongly dislike) to 9 (strongly like) and was evaluated by 50 panelists. This research was considered for ethical approval in human research by the Human Research Ethics Committee, Rangsit University (COA. No. RSUERB2023-069).

Physicochemical Properties of the Selected Herbal Tea

The selected herbal tea product was analyzed for its physicochemical properties, including color values, water activity (a_w), and moisture content (%) (Association of Official Analytical Chemists [AOAC], 2019).

Nutritional Value of the Selected Herbal Tea

The selected herbal tea sample underwent analysis to determine its energy content, proximate compositions, and nutritional value. These included protein, fat, fiber, carbohydrates, ash, sugar, *β*-carotene, vitamins A, B1, and B2, and mineral contents of sodium, calcium, and iron. The analysis method used was outlined in the AOAC (2019).

Statistical Analysis

The data was collected to determine the variance analysis (ANOVA) to set up experimental research. The mean comparison was performed using Duncan's multiple-range tests and

the *t*-test. The data was evaluated for statistical significance at a confidence level of 95% ($p<0.05$) using suitable statistical software.

RESULTS AND DISCUSSION

TPC, TFC, and Antioxidant Activity of the *C. infundibuliformis* and *J. betonica* Leaf Extracts

The TPC, TFC, and the activity of antioxidants determined using DPPH, ABTS, and FRAP assays in *C. infundibuliformis* and *J. betonica* leaf extracts are shown in Table 1. This experiment uses the developing leaves of both plants to develop herbal tea as a source of antioxidants. Generally, the stage of plant leaves for making herbal tea was reported to be highly antioxidant in the developing stage of leaves (Chan et al., 2013). The findings indicated that the TPC, TFC, and antioxidant activity of the *C. infundibuliformis* leaf extract was significantly higher than that of the *J. betonica* leaf extract. It may be due to the difference in type and composition, including the quantity of bioactive compounds in plant leaves that lead to antioxidant activity, especially phenolic and flavonoid compounds (Phakamus et al., 2018). In general, phenolic compounds contribute as primary antioxidants, whereas flavonoids serve as primary and secondary antioxidants (Lim et al., 2007). Patil et al. (2014) found that the methanol extract of *C. infundibuliformis* leaves contain high levels of phenolic (98.52 mg of gallic acid/g of extract) and flavonoid (84.59 mg of rutin/g of extract) while, the methanol extract of the entire *J. betonica* plant was observed to have an inhibitory concentration 50 (IC50) of free radical formation at 31.1%, which corresponds to 1671 µg/ml (Manokari et al., 2019). Moreover, the result showed that *C. infundibuliformis* leaf extract was found to have higher TPC and TFC (177.46±3.11 mg GAE/g dried extract and 254.81±1.78 mg CE/g dried extract) than *Thunbergia laurifolia* leaf extract, herbal tea in Thailand, which was reported with the TPC and TFC as 123.68±2.94 GAE/g dried extract and 62.83±2.85 mg CE/g dried extract (Junsi et al., 2017).

Table 1
TPC, TFC, and antioxidant activity of Crossandra infundibuliformis *and* Justicia betonica *leaf extracts*

Activities	**Leaf extracts**	
	Crossandra infundibuliformis	***Justicia betonica***
TPC (mg GAE/g dried extract)	177.46±3.11[a]	115.88±4.19[b]
TFC (mg CE/g dried extract)	254.81±1.78[a]	48.54±1.62[b]
DPPH (mg GAE/g dried extract)	7.50±0.02[a]	4.45±0.16[b]
ABTS (mg GAE/g dried extract)	23.40±0.91[a]	12.42±0.89[b]
FRAP (mg GAE/g dried extract)	45.32±0.86[a]	20.17±0.22[b]

Note. TPC = Total extractable phenolic content, TFC = Total extractable flavonoid content, GAE = Gallic acid equivalent, CE = Catechin equivalent, [a-b] mean within the given range is significantly different ($p<0.05$), values presented are in the form of mean ± standard deviation ($n = 3$)

Furthermore, Nor and Mohd (2013) reported that the TPC of the ethanol extraction from shoots of the green tea and black tea resulted in 80.27±0.61 and 76.93±1.72 mg GAE/g of dry sample weight, which showed the lower TPC than *C. infundibuliformis* leaf extract. However, compared to other research, it highlighted the challenge of reaching a solid conclusion about TPC, TFC, and antioxidant determination in individual plants when using different factors. Generally, variations in TPC and TFC contents, as well as antioxidant activity, can be influenced by several factors such as planting location, extract preparation and determination, and leaf development stage (Pyankov et al., 2001; Stein et al., 2016). The *C. infundibuliformis* and *J. betonica* leaf extracts demonstrated the highest antioxidant activities in the FRAP assay, followed by the ABTS and DPPH assays. The use of boiled water at 98±1°C in this study likely aided in solubilizing and extracting antioxidant compounds from the plant cell structure by disrupting their polarity. This made it easier to measure these compounds using the FRAP and ABTS assays, whereas the DPPH assay was better suited for detecting lipophilic compound groups (Xiao et al., 2017). Cheng et al. (2023) added that the use of hot water extraction ranging from 5 to 120 minutes on various teas, including green, Oolong, black, and scented teas, improved extraction efficiency with increasing water temperature. The study indicated that the highest levels of antioxidants were obtained, particularly at 100ºC. These circumstances can potentially degrade antioxidant compounds that are sensitive to heat (Sharma et al., 2015), and they could impact a greater number of compounds with strong heat tolerance in the sample, making them suitable for tea production. Hence, these results suggest that *C. infundibuliformis* and *J. betonica* leaves are suitable sources of antioxidants.

Phenolic and Flavonoid Contents of *C. infundibuliformis* and *J. betonica* Determined by HPLC

The study utilized HPLC to analyze the phenolic and flavonoid compounds in leaf extracts of *C. infundibuliformis* and *J. betonica*. The analysis involved using 18 standard compounds reported and found in tea and herbal plants (Chandrasekara & Shahidi, 2018; Shaik et al., 2023; Tungmunnithum et al., 2018). The quantification of compounds is based on their respective standard calibration curves (Table 2). The results found that the leaf extract of *C. infundibuliformis* contained eight phenolic and flavonoid compounds in descending order: chlorogenic acid, myricetin, protocatechuic acid, gallic acid, vanillin, caffeic acid, epicatechin, and *p*-coumaric acid. On the other hand, the leaf extract of *J. betonica* contained nine compounds: myricetin, sinapic acid, ferulic acid, gallic acid, protocatechuic acid, chlorogenic acid, *p*-coumaric acid, *trans*-cinnamic acid, and vanillic acid. The type and content of compounds containing phenolic and flavonoid substances influence various biological activities, particularly antioxidant activity.

The study found that the quantity of bioactive compounds in *C. infundibuliformis* leaf extract was generally higher, but the variety of compounds was less than in *J. betonica* leaf extracts. Furthermore, the findings of this research indicate that the leaf extract of

Table 2
Phenolic and flavonoid contents of Crossandra infundibuliformis *and* Justicia betonica *leaf extracts determined by HPLC*

No.	Compounds	Contents (mg/g extract)	
		Crossandra infundibuliformis	***Justicia betonica***
1	Gallic acid	0.70±0.01	0.39±0.01
2	Protocatechuic acid	2.19±0.04	0.35±0.02
3	*p*-Hydroxybenzoic acid	ND	ND
4	Catechin	ND	ND
5	Chlorogenic acid	37.41±0.04	0.31±0.04
6	Caffeine	ND	ND
7	Vanillic acid	ND	ND
8	Caffeic acid	0.43±0.05	ND
9	Syringic acid	ND	ND
10	Epicatechin	0.33±0.01	ND
11	Vanillin	0.63 ± 0.02	0.13±0.02
12	*p*-Coumaric acid	0.04±0.01	0.17±0.03
13	Ferulic acid	ND	0.91±0.03
14	Sinapic acid	ND	0.53±0.06
15	Rutin	ND	ND
16	Myricetin	9.46±0.14	2.85±0.01
17	Quercetin	ND	ND
18	*Trans*-cinnamic acid	ND	0.14±0.01

Note. ND = Not detected, Values presented are in the form of mean ± standard deviation (n = 3)

C. infundibuliformis contains chlorogenic acid and myricetin as its major components. According to Liang and Kitts (2016), chlorogenic acid has been identified as a potent antioxidant. Barzegar (2016) noted myricetin as one of the most significant flavonoids in food with the highest antioxidant activity. In addition, both extracts contain bioactive compounds that offer not only antioxidants but also other biological activities, such as gallic acid, caffeic acid, protocatechuic acid, and sinapic acid, reported to demonstrate properties that fight inflammation, cancer, tumors, mutations, and it also protects the nervous system and has antibacterial effects (Chen, 2016; Sato et al., 2011). However, both extracts reported some bioactive compounds as not detected (ND). The effect in phenolic and flavonoid profiles may be due to several factors, such as plant preparation and extraction, the limit of quantitation (LOQ) of equipment, and the form of the standard compound referenced in the experiment (Tungmunnithum et al., 2018).

Sensory Qualities of Herbal Tea

The sensory attributes of the herbal tea made from dried leaves of *C. infundibuliformis* and *J. betonica*, including appearance, color, odor, flavor, astringent test, and overall liking, were

assessed and are shown in Figure 1. The *P. amaryllifolius* dried leaves (10%) were used in this experiment to improve the overall odor and flavor. It is well-known that a characteristic of this herb is used in Southeast Asian cuisines for food and beverage flavorings (Bhatt et al., 2021). Our preliminary tests revealed that added *P. amaryllifolius* mixed with *C. infundibuliformis* and *J. betonica* dried leaves in herbal tea formulas seemed to exhibit more consumer acceptability. The results of sensory acceptability from the consumer test showed a ranged score of each attribute between neither like nor dislike and moderate scales. The acceptability scores differed significantly ($p<0.05$) for all attributes except for the astringent test. Moreover, the scores indicated that the panelists preferred the herbal tea from formula T2 more than the other formulas. It aligns with the panelists' comments indicating that the T2 tea has a better flavor and odor. This phenomenon may be due to the ratio of leaves in herbal tea products, in which the T2 tea contains most *C. infundibuliformis* leaves (*C. infundibuliformis: J. betonica: P. amaryllifolius*, 3:1:1). In addition, the T2 tea can provide benefits for consumers who drink this herbal tea for health, which is the previous analysis result of antioxidant activity, which showed that the *C. infundibuliformis* leaf extract provides more antioxidant activity than *J. betonica* leaf extract. Therefore, the herbal tea product from the T2 formula was selected to assess the physical and chemical properties and nutritional values.

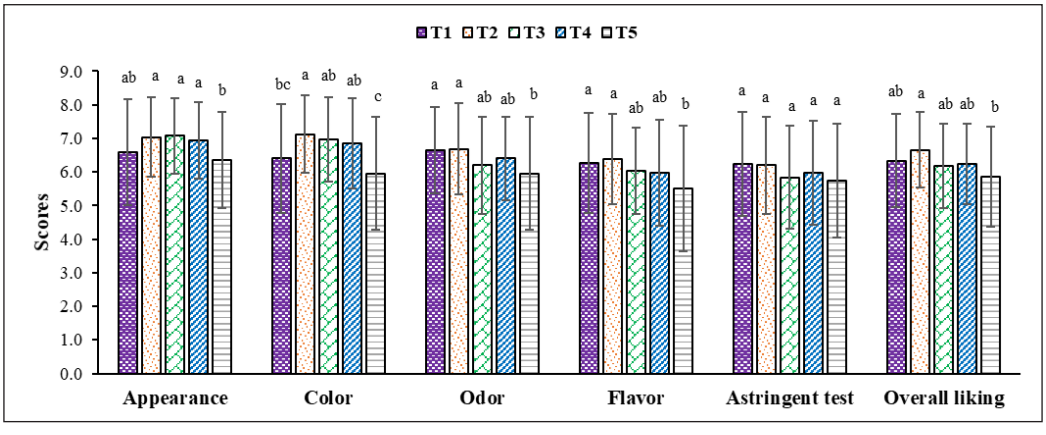

Figure 1. Sensory quality of the five formulas of herbal tea

Note. [a-b] mean within the given range is significantly different ($p<0.05$), values presented are in the form of mean ± standard deviation ($n = 50$)

Physicochemical Properties of the Selected Herbal Tea

The physicochemical properties of the selected herbal tea, *C. infundibuliformis,* and *J. betonica* leaf powders are shown in Table 3. The analysis of the color values revealed that the selected herbal tea powder did not display a significant difference ($p\geq0.05$) compared to *C. infundibuliformis* leaf powder. This result may be due to the ratio of leaf content

Table 3
Physicochemical properties of the leaf powder

Contents	Leaf powder		
	Selected tea	***Crossandra infundibuliformis***	***Justicia betonica***
Color values			
*L**	42.41±0.22[b]	42.72±0.49[b]	44.70±0.40[a]
*a**	-2.69±0.18[a]	-2.78±0.13[a]	-6.39±0.16[b]
*b**	24.13±0.45[b]	21.05±0.18[c]	29.73±0.49[a]
Water activity (a_w)	0.55±0.01[b]	0.55±0.00[b]	0.56±0.00[a]
Moisture content (%)	6.72±0.03[b]	6.46±0.03[c]	6.85±0.03[a]

Note. [a-b] mean within the given range is significantly different (p<0.05), values presented are in the form of mean±standard deviation (n = 3)

in the selected tea formula, which contained the highest content of *C. infundibuliformis* compared with other leaf powders. Moreover, the moisture content in all leaf samples was below 7%, which follows the criteria outlined in the notification of the Ministry of Public Health on tea from plants in Thailand (Thai-Food and Drug Administration, 2021) that specify the dried tea must have a moisture content less than 10% by weight. Furthermore, it was found that the water activity (a_w) content of all samples was less than 0.6. Thus, these conditional properties of the dried leaf powder, especially the selected tea product, could help to prevent the growth of some microorganisms that cause deterioration in the product.

Nutritional Values of the Selected Herbal Tea

Table 4
Nutritional values of the selected herbal tea

Nutrition information	Quantities (per 100 g of powdered tea)
Total energy (kcal)	334.07
Total energy from fats (kcal)	18.99
Total fat (g)	2.11
Saturated fat (g)	0.75
Cholesterol (mg)	ND
Protein (g)	19.60
Total Carbohydrate (g)	59.17
Dietary fiber (g)	41.58
Sugar (g)	1.22
Sodium (g)	0.08
Vitamin A (mg)	2.44
β-Carotene (mg)	14.62
Vitamin B1 (mg)	<0.03
Vitamin B2 (mg)	0.34
Calcium (mg)	1,541.01
Iron (mg)	10.03
Ash (g)	12.03

Note. ND = not detected

The nutritional values of the selected herbal tea are detailed in Table 4. Analyses revealed that the product provided 334.07 kcal of total energy per 100 g of powder and contained protein, carbohydrates, sodium, sugar, and ash at 19.60 g, 59.17 g, 85.31 mg, 1.22 g, and 12.03 g, respectively. The result showed that the product revealed various nutrients such as vitamin A, vitamin B2, *β*-carotene, calcium, and iron. The *β*-carotene is a substance that can be turned into vitamin A and acts

as an antioxidant. It is used in the food industry to provide natural color (Liyanaarachchi et al., 2021). Vitamin A acts as an antioxidant and has been found to protect against Deoxyribonucleic acid (DNA) damage caused by reactive oxygen species (ROS), which is linked to the development of cancer (Fagbohun et al., 2023). Furthermore, Ca is the most prevalent stored nutrient in the human body and is crucial for living organisms because of its vital involvement in a variety of functions (Szlacheta et al., 2020). Fe has also been identified as a crucial trace element for nearly all living organisms, as it plays a crucial role in different metabolic activities, such as DNA creation, respiration, and photosynthesis (Rout & Sahoo, 2015). Moreover, herbal tea contains plant-based nutrients and is low in calories, sugar, and salt, making it suitable for a healthy diet. As a result, herbal tea can provide beneficial nutrients that are appropriate for customers.

CONCLUSION

The research showed that the leaf extract from *C. infundibuliformis* showed greater TPC, TFC, and antioxidant activity when compared to the leaf extract from *J. betonica*. In addition, *C. infundibuliformis* leaf extract found 10 phenolic and flavonoid compounds, ranked from high to low contents as follows: chlorogenic acid, myricetin, protocatechuic acid, gallic acid, vanillin, caffeic acid, rutin, epicatechin, syringic acid, and *p*-coumaric acid, while *J. betonica* leaf extract found 15 compounds, which are as follows: myricetin, sinapic acid, ferulic acid, gallic acid, rutin, *p*-hydroxybenzoic acid, protocatechuic acid, chlorogenic acid, epicatechin, p-coumaric acid, *trans*-cinnamic acid, vanillic acid, vanillin, catechin, and syringic acid, respectively. The T2 formula of herbal tea with mixing *C. infundibuliformis* and *J. betonica* dried leaves and *P. amaryllifolius* at 3:1:1 provided the highest sensory evaluation of the appearance, color, odor, flavor, and overall linking. The nutritional value of selected herbal tea (T2) is the most accepted formula, providing energy, protein, carbohydrates, sugar, vitamin A, B2, sodium, *β*-carotene, calcium, iron, and ash. At the same time, the moisture and water activity contents of the product showed less than 7% and 0.6, respectively. This experiment supported using both herbs as herbal teas for functional drinks. However, the study of the potential single or combined leaf activity that affects other functional properties such as anti-inflammatory, antimicrobial, anti-diabetic, and anti-dote should be further investigated both *in vitro* and *in vivo*.

ACKNOWLEDGMENTS

This research is funded by the Research Institute of Dusit Thani College.

REFERENCES

Association of Official Analytical Chemists (AOAC). (2019). *Official methods of analysis.* (21st ed). Washington DC.

Barzegar, A. (2016). Antioxidant activity of polyphenolic myricetin in vitro cell-free and cell-based systems. *Molecular Biology Research Communications*, *5*(2), 87-95.

Bhatt, V., Barvkar, V. T., Furtado, A., Henry, R. J., & Nadaf, A. (2021). Fragrance in *Pandanus amaryllifolius* Roxb. despite the presence of a betaine aldehyde dehydrogenase 2. *International Journal of Molecular Sciences*, *22*(13), 6968. https://doi.org/10.3390/ijms22136968

Chan, E. W. C., Lye, P. Y., Eng, S. Y., & Tan, Y. P. (2013). Antioxidant properties of herbs with enhancement effects of drying treatments: A synopsis. *Free Radicals and Antioxidants*, *3*(1), 2-6. http://doi.org/10.1016/j.fra.2013.02.001

Chandrasekara, A., & Shahidi, F. (2018). Herbal beverages: Bioactive compounds and their role in disease risk reduction - A review. *Journal of Traditional and Complementary Medicine*, *8*(4), 451-458. https://doi.org/10.1016/j.jtcme.2017.08.006

Chen, C. (2016). Sinapic acid and its derivatives as medicine in oxidative stress-induced diseases and aging. *Oxidative Medicine and Cellular Longevity*, *2016*(1), 3571614. http://doi.org/10.1155/2016/3571614

Cheng, Y., Xue, F., & Yang, Y. (2023). Hot water extraction of antioxidants from tea leaves-optimization of brewing conditions for preparing antioxidant-rich tea drinks. *Molecules*, *28*(7), 3030. https://doi.org/10.3390/molecules28073030

Eapen, J., Ansary, P. Y., Hameed, A. S., Indulekha, V. C., & Resny, A. R. (2019). Phamacognosy of Leaf, Stem and Root of *Justicia betonica* Linn. *International Journal of Research in Ayurveda and Pharmacy*, *10*(1), 44-48. https://doi.org/10.7897/2277-4343.100111

Fagbohun, O. F., Gillies, C. R., Murphy, K. P. J., & Rupasinghe, H. P. V. (2023). Role of antioxidant vitamins and other micronutrients on regulations of specific genes and signaling pathways in the prevention and treatment of cancer. *International Journal of Molecular Sciences*, *24*(7), 6092. https://doi.org/10.3390/ijms24076092

Hari, V. P, Abdul, A. A, Vanitha, M., Ganesan, S., & Gokulnath, K. (2022). Pharmacognostical studies and pharmacological activities of *Crossandra infundibuliformis*. *International Journal of Research and Development in Pharmacy & Life Sciences*, *8*(5), 140. http://doi.org/10.4172/2278-0238.1000140

Imam, M. Z., Akter, S., Mazumder, M. E. H., & Rana, M. S. (2011). Antioxidant activities of different parts of *Musa sapientum* L. ssp. *Sylvestris* fruit. *Journal of Applied Pharmaceutical Science*, *1*(10), 68-72.

Junsi, M., Siripongvutikorn, S., Yupanqui, C. T., & Usawakesmanee, W. (2017). Efficacy of *Thunbergia laurifolia* (rang jued) aqueous leaf extract for specific biological activities using RAW 264.7 macrophage cells as test model. *International Food Research Journal*, *24*(6), 2317-2329.

Kanchanapoom, T., Noiarsa, P., Ruchirawat, S., Kasai, R., & Otsuka, H. (2004). Triterpenoidal glycosides from *Justicia betonica*. *Phytochemistry*, *65*(18), 2613-2618. https://doi.org/10.1016/j.phytochem.2004.06.029

Liang, N., & Kitts, D. D. (2016). Role of chlorogenic acids in controlling oxidative and inflammatory stress conditions. *Nutrients*, *8*, 16. http://doi.org/10.3390/nu8010016

Liaudanskas, M., Viškelis, P., Jakštas, V., Raudonis, R., Kviklys, D., Milašius, A., & Janulis, V. (2014). Application of an optimized HPLC method for the detection of various phenolic compounds in apples from Lithuanian cultivars. *Journal of Chemistry*, *2014*(1), 542121. https://doi.org/10.1155/2014/542121

Lim, Y. Y., Lim, T. T., & Tee, J. J. (2007). Antioxidant properties of several tropical fruits: A comparative study. *Food Chemistry*, *103*(3), 1003-1008. https://doi.org/10.1016/j.foodchem.2006.08.038

Liyanaarachchi, V. C., Premaratne, M., Ariyadasa, T. U., Nimarshana, P. H. V., & Malik, A. (2021). Two-stage cultivation of microalgae for production of high-value compounds and biofuels: A review. *Algal Research*, *57*, 102353. https://doi.org/10.1016/j.algal.2021.102353

Manokari, M., Latha, R., Priyadharshini, S., Cokul, R. M., Beniwal, P., Manjunatha, R. Y., Rajput, B. S., & Shekhawat, M. S. (2019). A comprehensive review on a less explored medicinally important plant *Justicia betonica* L. *World Scientific News*, *131*, 110-122.

Meilgaard, M. C., Civille, G. V., & Carr, B. T. (2007). *Sensory evaluation techniques* (4th ed.). CRC Press.

Naik, S. K., Manjula, B. L., Balaji, M. V., Marndi, S., Kumar, S., & Devi, R. S. (2022). Antibacterial activity of *Justicia betonica* Linn. *Asian Pacific Journal of Health Sciences*, *9*(4), 227-230. https://doi.org/10.21276/apjhs.2022.9.4.45

Nor, Q. I. M. N., & Mohd, F. A. B. (2013). Phytochemicals and antioxidant properties of different parts of *Camellia sinensis* leaves from sabah tea plantation in Sabah, Malaysia. *International Food Research Journal*, *20*(1), 307-312.

Patathananone, S., Pothiwan, M., Uapipatanakul, B., & Kunu, W. (2023). Inhibitory effects of *Vernonia amygdalina* leaf extracts on free radical scavenging, tyrosinase, and amylase activities. *Preventive Nutrition and Food Science*, *28*(3), 302-311. https://doi.org/10.3746/pnf.2023.28.3.302

Patil, K., G., Jaishree, V., & Tejaswi, H. P. (2014). Evaluation of phenolic content and antioxidant property of *Crossandra infundibuliformis* leaves extracts. *American Journal of Plant Sciences*, *5*(9), 1133-1138. http://doi.org/10.4236/ajps.2014.59126

Pereira, A. C. S., Dionísio, A. P., Wurlitzer, N. J., Alves, R. E., Brito, E. S., Silva, A. M. O., Brasil, I. M., & Filho, J. M. (2014). Effect of antioxidant potential of tropical fruit juices on antioxidant enzyme profiles and lipid peroxidation in rats. *Food Chemistry*, *157*(15), 179-185. http://doi.org/10.1016/j.foodchem.2014.01.09012

Phakamus, S., Chokrathok, S., Woraratphoka, J., & Innok, S. (2018). Development of Yanang mixed herb tea products. *Burapha Science Journal*, *23*(3), 1682-1695.

Pyankov, V. I., Ivanov, L. A., & Lambers, H. (2001). Chemical composition of the leaves of plants with different ecological strategies from the boreal zone. *Russian Journal of Ecology*, *32*(4), 221-229. https://doi.org/10.1023/A:1011354019319

Raj, V. K., Kumar, J. R., Balasubramanian, S., Swamy, S. N., Keerthini, D., Shambhavi, N., Kanthesh, B. M., & Avinash, K. O. (2016). Comparative evaluation of hepatoprotective effects of exotic fruits and common vegetables extracts on CCl_4 induced hepatotoxicity: An *in vitro* study. *International Journal of Pharmaceutical Sciences and Research*, *7*(8), 3388-3393. http://doi.org/10.13040/IJPSR.0975-8232.7(8).3388-93

Rout, G. R., & Sahoo, S. (2015). Role of iron in plant growth and metabolism. *Reviews in Agricultural Science*, *3*, 1-24. https://doi.org/10.7831/ras.3.1

Ruangyuttikarn, W., Chattaviriya, P., Morkmek, N., Chuncharunee, S., & Lertprasertsuke, N. (2013). *Thunbergia laurifolia* leaf extract mitigates cadmium toxicity in rats. *Science Asia*, *39*(1), 19-25. https://doi.org/10.2306/scienceasia1513-1874.2013.39.019

Salazar-Campos, J., Salazar-Campos, O., Gálvez-Ruiz, O., Gavidia-Chávez, H., Gavidia-Chávez, M., Irigoin-Guevara, M., & Obregón-Domínguez, J. (2023). Functional properties and acceptability of potentially medicinal tea infusions based on *Equisetum arvense*, *Desmodium molliculum*, and *Mentha piperita*. *Preventive Nutrition and Food Science*, *28*(4), 444-452. https://doi.org/10.3746/pnf.2023.28.4.444

Sato, Y., Itagaki, S., Kurokawa, T., Ogura, J., Kobayashi, M., Hirano, T., Sugawara, M., & Iseki, K. (2011). *In vitro* and *in vivo* antioxidant properties of chlorogenic acid and caffeic acid. *International Journal of Pharmaceutics*, *403*(1-2), 136-138. https://doi.org/10.1016/j.ijpharm.2010.09.035

Shaik, M. I., Hamdi, I. H., & Sarbon, N. M. (2023). A comprehensive review on traditional herbal drinks: Physicochemical, phytochemicals and pharmacology properties. *Food Chemistry Advances*, *3*, 100460. https://doi.org/10.1016/j.focha.2023.100460

Sharma, K., Ko, E. Y., Assefa, A. D., Ha, S., Nile, S. H., Lee, E. T., & Park, S. W. (2015). Temperature-dependent studies on the total phenolics, flavonoids, antioxidant activities, and sugar content in six onion varieties. *Journal of Food and Drug Analysis*, *23*(2), 243-252. https://doi.org/10.1016/j.jfda.2014.10.005

Stein, R. J., Horeth, S., Melo, J. R. F., Syllwasschy, L., Lee, G., Garbin, M. L., Clemens, S., & Krämer, U. (2017). Relationships between soil and leaf mineral composition are element-specific, environment-dependent and geographically structured in the emerging model *Arabidopsis halleri*. *New Phytologist*, *213*(3), 1274-1286. https://doi.org/10.1111/nph.14219

Szlacheta, Z., Wąsik, M., Machoń-Grecka, A., Kasperczyk, A., Dobrakowski, M.., Bellanti, F., Szlacheta, P., & Kasperczyk, S. (2020). Potential antioxidant activity of calcium and selected oxidative stress markers in lead- and cadmium-exposed workers. *Oxidative Medicine and Cellular Longevity*, *2020*, 8035631. https://doi.org/10.1155/2020/8035631

Tan, K. W., & Kassim, M. J. (2011). A correlation study on the phenolic profiles and corrosion inhibition properties of mangrove tannins (*Rhizophora apiculata*) as affected by extraction solvents. *Corrosion Science*, *53*(2), 569-574. http://doi.org/10.1016/j.corsci.2010.09.065

Tan, Y. P., & Chan, E. W. C. (2014). Antioxidant, antityrosinase and antibacterial properties of fresh and processed leaves of *Anacardium occidentale* and *Piper betle*. *Food Bioscience*, *6*, 17-23. http://doi.org/10.1016/j.fbio.2014.03.001

Thai-Food and Drug Administration. (2021). *Announcement of the Ministry of Public Health: Tea from plants*. https://food.fda.moph.go.th/media.php?id=5094383709681172 48&name=P426.PDF

Tungmunnithum, D., Thongboonyou, A., Pholboon, A., & Yangsabai, A. (2018). Flavonoids and other phenolic compounds from medicinal plants for pharmaceutical and medical aspects: An overview. *Medicines*, *5*(3), 93. https://doi.org/10.3390/medicines5030093

Wong-arun, W., Jongkolnee, W., Mengkwang, R., Kwangswat, A., Sukaphat, S., & Duangmala, E. (2014). *The diversity of medicinal plants in Sam Roi Yod FreshWater Marsh*. Rajamangala University of Technology Rattanakosin.

Xiao, H. W., Pan, Z., Deng, L. Z., El-Mashad, H. M., Yang, X. H. Mujumdar, A. S., Gao, Z. J., & Zhang, Q. (2017). Recent developments and trends in thermal blanching: A comprehensive review. *Information Processing in Agriculture*, *4*(2), 101-127. http://doi.org/10.1016/j.inpa.2017.02.001

Pertanika J. Trop. Agric. Sci. 48 (3): 733 - 746 (2025)

PERTANIKA JOURNALS

TROPICAL AGRICULTURAL SCIENCE

Journal homepage: http://www.pertanika.upm.edu.my/

Gamma Ray Irradiation Effects on Embryogenic Calli Growth in Indonesian Taro

Krismandya Ayunda Wardhani[1], Diny Dinarti[1]*, Edi Santosa[1] and Waras Nurcholis[2,3]

[1]Department of Agronomy and Horticulture, Faculty of Agriculture, IPB University, IPB Dramaga Campus, 16680 Bogor, West Java, Indonesia

[2]Department of Biochemistry, Faculty of Mathematics and Natural Science, IPB University, IPB Dramaga Campus, 16680 Bogor, West Java, Indonesia

[3]Tropical Biopharmaca Research Center, IPB University, IPB Taman Kencana Campus, Bogor 16128, West Java, Indonesia

ABSTRACT

Colocasia and Xanthosoma are widely distributed in humid tropical areas and primarily found in moderate to high rainfall areas. In Indonesia, *Colocasia esculenta* var. antiquorum (eddoe taro) and *Xanthosoma undipes* (beneng banten taro) are prominent taro. However, traditional vegetative propagation methods often result in limited phenotypic diversity. Gamma irradiation of embryogenic calli presents a promising approach to induce genetic diversity for taro improvement. This study aimed to assess the radiosensitivity of Indonesian taro explants to gamma-ray irradiation by determining the LD_{50} value and evaluating the impact of the gamma ^{60}Co irradiation dose on the proliferation and growth of taro embryogenic calli. The research adopted a completely randomized factorial design, encompassing eight treatments of Gamma ^{60}Co radiation dose ranging from 0 to 27.5 Gy, combined with two treatment media variations on callus formation, with 12 repetitions each. The results showed that gamma-ray irradiation affected callus formation, embryogenic callus proliferation, and the number of globular phases of somatic embryos in both explants. The LD_{50} for *Colocasia esculenta* explants was determined to be 7.23 Gy, while that for *Xanthosoma undipes* explants was 12.84 Gy. These findings underscore the significant effect of gamma-ray irradiation on explants, elucidating its potential to induce mutations and augment genetic diversity in orphan crop species such as Indonesian taro.

Keywords: Araceae, asparagine, browning, callus, Colocasia, malt extract, somatic embryo, Xanthosoma

ARTICLE INFO

Article history:
Received: 24 June 2024
Accepted: 01 October 2024
Published: 16 May 2025

DOI: https://doi.org/10.47836/pjtas.48.3.05

E-mail addresses:
krismandya_wardhani@apps.ipb.ac.id (Krismandya Ayunda Wardhani)
dinyagh@apps.ipb.ac.id (Diny Dinarti)
edi_santosa@apps.ipb.ac.id (Edi Santosa)
wnurcholis@apps.ipb.ac.id (Waras Nurcholis)
*Corresponding author

INTRODUCTION

The aroids plant family comprises more than 120 genera and 3750 species, and it is widely distributed in humid tropical regions with medium to high rainfall (Vaneker & Slaats, 2012). In addition to their use as ornamental plants, they play a crucial role in horticulture as secondary staples in Asia, the Pacific Islands, and Central South America. Taro is one of the edible aroids found in Indonesia. They serve as staple and functional foods due to their rich starch, fiber, potassium, vitamin C, proteins, glucomannan, and other micronutrients (Cahyanti et al., 2024). Furthermore, taro can thrive in various soil types, including well-drained, dry, and regions with high rainfall (Chaïr et al., 2016; Cahyanti et al., 2022; Chaïr et al., 2016). Some taros in Indonesia are derived from the Alocasia, Colocasia, and Xanthosoma genera.

Colocasia esculenta (L.) Schott var. *antiquorum*, commonly known as eddoe taro, is widely grown in Indonesia owing to its high productivity and delicious tuber taste. The plant has light-green petioles, purple upper parts, and cylindrical tubers (Maretta et al., 2020). Tubers are highly nutritious, containing 3.45% protein, 0.31% fat, 6.07% water, 2.14% ash, 88.03% carbohydrates, and 2.87% fiber (Fidyasari et al., 2017). This taro is also a suitable crop for areas prone to drought as it has good adaptation mechanisms to groundwater fluctuations (Hidayatullah et al., 2020). However, the plant is susceptible to pest attacks, particularly leaf pests, such as grasshoppers (Jayaprakas & Harish, 2022).

The Indigenous beneng banten taro (*X. undipes* K. Koch) is a valuable agricultural commodity in Indonesia, characterized by its large tuber size and high protein and carbohydrate content. It has the potential to be used in various food products and can contribute to food security. The flour contains 82.56% carbohydrates, 3.4% protein, 0.28% and 0.8% fat, and the leaves have been used as a tobacco substitute (Rostianti et al., 2018; Susilawati et al., 2021). As a relatively new domesticated crop, beneng banten taro has yet to undergo significant genetic improvement beyond its wild counterpart (Alghifari et al., 2023).

Despite their nutrient density, historical importance, and wide adaptability, most taro are classified as orphan crops, necessitating genetic improvement. The development of a new cultivar relies on the use of taro germplasm, which demonstrates high genetic diversity and genetic distance. Vegetative propagation in taro leads to a limited range of phenotypic diversity. Prana (2007) noted that traditional crossing methods for breeding *C. esculenta* cultivar take a long time, with plants taking six to eight months to flower after planting. Therefore, enhancing the genetics of taro varieties is not without its challenges, but it is essential for creating new cultivars with promising yields.

An effective strategy for enhancing genetic diversity in taro involves the application of ionizing radiation, such as gamma rays, to induce mutagenesis in embryogenic calli. Gamma-ray irradiation can cause deletions or aberrations in deoxyribonucleic acid

(DNA) owing to its interaction with high-energy electromagnetic radiation. This method is advantageous because embryogenesis originates from individual cells, thus minimizing the formation of chimeric mutants and allowing selection at the cellular level. Gamma rays are important in mutation breeding and in vitro mutagenesis to develop the desired plant traits and increase genetic variability among radiation sources. Gamma-ray mutation induction in embryogenic calli has been applied to enhance temperature resistance in wheat (*Triticum aestivum* L.) and to produce 19 putative mutant plantlets of the Dewata variety, which are believed to be tolerant to high temperatures (Setiawan et al., 2015). Nurilmala et al. (2017) induced somaclonal variation in *C. esculenta* (L.) by exposing shoot explants to gamma irradiation with an LD_{50} of 10 Gy, resulting in up to 51% genetic diversity compared to the parents.

The first step in plant breeding using mutation techniques is to optimize the radiation dose and target radiosensitivity. The radiosensitivity of a plant to gamma-ray irradiation can be evaluated by determining its lethal dose of 50% (LD_{50}). LD_{50} is the radiation that can cause the death of 50% of the exposed plant population. Gamma irradiation has been carried out *in vitro* shoots of cocoyam (*Xanthosoma sagittifolium* L. Schott) with an LD_{50} of 8.7 Gy for the white flesh tuber and 7.6 Gy for the red flesh tuber (Ndzana et al., 2008). Seetohul et al. (2008) showed that 20 Gy of gamma irradiation was lethal to shoot explants of *C. esculenta* (L.). Gamma-ray irradiation doses can positively and negatively affect a given plant. This study aimed to determine the radiosensitivity of two types of taro explants to gamma-ray irradiation and to examine the effect of the irradiation dose on the growth of embryogenic calli.

MATERIALS AND METHODS

Explant Materials and Sample Preparation

The explants used were aseptic plantlets of eddoe taro (*Colocasia esculenta* var. antiquorum) and beneng banten taro (*Xanthosoma undipes* K. Koch) obtained from Tissue Culture Laboratory 3, Department of Agronomy and Horticulture, Faculty of Agriculture, IPB University. The explant was the leaf base of a taro shoot, measuring 10×5×1.5 mm.

Each explant was planted on callus initiation with MS basic media composition (Murashige & Skoog, 1962) enriched with 500 mg L^{-1} malt extract (Merck, Germany), 200 mg L^{-1} l-asparagine (Merck, Germany), 1000 mg L^{-1} cefotaxime antibiotic (Cetaxime, Indonesia), and two levels of plant growth regulator (PGR) addition, TDZ (PhytoTech Labs, USA) and picloram (PhytoTech Labs, USA). Eddoe taro explants were planted on media with the addition of 13.57 µM picloram and 9.04 µM picloram+ 6.81µM TDZ. In comparison, beneng banten taro explants were planted on basic media with PGR added in the form of 4.52 µM picloram+ 6.81µM TDZ and 9.04 µM picloram+ 6.81µM TDZ.

The explants were cultured for three weeks before irradiation to ensure that the taro explants were at the active growth stage for irradiation treatment. Selection was carried out on green and aseptic explants that had uniform growth before being treated with irradiation. Explants were planted in disposable petri dishes measuring 90×90×15 mm, with an explant density of 12 explants per petri dish.

Gamma Ray Irradiation Treatment

Gamma-ray irradiation was performed at the Research and Technology Center for Application of Isotope and Radiation, National Research and Innovation Agency of the Republic of Indonesia, using a ^{60}Co gamma-ray irradiator (Gamma Chamber 4000 Å, Bhabha Atomic Research Centre, India). An irradiation experiment was conducted with ^{60}Co gamma-ray irradiation at 0 (control), 2.5, 5, 7.5, 10, 12.5, 17.5, and 27.5 Gy; the dose rate used was 2.25 Gy/min.

Explant Regeneration

The irradiated explants were then transferred to a new medium with the same composition at a rate of one explant per bottle. Explants were transferred less than 24 h after irradiation to replace the medium that was thought to be toxic to plant cells due to irradiation. Planted explants were stored in a culture room at 23 ± 2°C and a light intensity of 1000 lx. Culture bottles containing explants were maintained by spraying 96% alcohol into the culture bottles every week.

Explant growth was observed every week for eight weeks after irradiation, with the variables being the percentage of explant survival after irradiation, color and condition of the explant after irradiation, percentage of callus, time for callus formation, percentage embryogenic callus, number of somatic embryos (in the globular phase), time for somatic embryo formation, and efficiency of embryogenic callus formation.

This study used a completely randomized design (CRD) with two factors, two combinations of treatment media, and eight combinations of irradiation doses with 12 repetitions in one repetition consisting of one culture bottle with one taro explant; thus, there were 192 observation units for each taro. The data were tested using *F*-test analysis at the α=5% level using Minitab 17 software. The F-test results showing a real effect were further tested using Tukey's range test at the α=5% level. LD_{50} calculations were performed using CurveExpert Professional 2.7.3 software.

RESULTS

Response to Gamma Irradiation

Different gamma-ray doses significantly influenced the formation of calli and somatic embryos (Table 1). Callus formation was observed four weeks after irradiation. Interestingly,

media treatment did not significantly affect callus formation, unlike the irradiation dose, which considerably influenced the percentage of callus formation. The control treatment successfully produced 100% explants with calluses for both taro. In eddoe taro (*C. esculenta* var. antiquorum) explants, an irradiation dose of 17.50 Gy produced a low callus percentage of 20.83%. In contrast, beneng banten taro (*X. undipes*) explants, irradiation doses above 12.50 Gy resulted in low callus percentages of 29.17% (17.50 Gy) and 16.67% (27.50 Gy). Beneng banten taro explants receiving irradiation of 2.50 — 12.50 Gy still formed callus well, with over 85% exhibiting callus. In contrast, this treatment produced a callus percentage of over 33% for eddoe taro.

Table 1
Effect of gamma dose on callus initiation and regeneration in taro

Gamma doses (Gy)	Eddoe taro (*C. esculenta var. antiquorum*)				Beneng banten taro (*X. undipes*)			
	Callus formation[a] (%)	EC induction[b] (%)	Number of $SE^{c}_{(g)}$ ($\bar{x}$)	% EEC[d]	Callus formation[a] (%)	EC induction[b] (%)	Number of $SE^{c}_{(g)}$ ($\bar{x}$)	% EEC[d]
0.00	100.00 a	95.83 a	8.44 a	95.83	100.00 a	100.00 a	24.13 a	100.00
2.50	70.83 ab	50.00 b	4.00 b	66.67	87.50 a	66.67 ab	7.80 b	88.89
5.00	66.67 ab	41.67 b	2.46 bc	71.44	87.50 a	66.67 ab	5.83 b	80.01
7.50	58.33 bc	37.50 bc	1.85 bc	81.82	100.00 a	62.50 abc	6.03 bc	83.33
10.00	70.83 ab	29.17 bc	1.92 c	70.00	95.83 a	58.33 bc	6.00 bc	82.35
12.50	33.33 bc	16.67 bc	2.00 c	57.15	91.67 a	41.67 bcd	3.30 cd	90.92
17.50	20.83 c	16.67 bc	0.88 c	80.03	29.17 b	25.00 cd	1.13 d	100.00
27.50	25.00 c	4.17 c	0.50 c	50.06	16.67 b	8.33 d	0.50 d	66.64
F-Value Gamma doses	**	**	**		**	**	**	
%CV	25.55	27.47	50.55		19.88	25.92	64.07	

Note. (**) has a very significant effect, numbers followed by the same letter in the same column, CV: coefficient of variance, and variables show no significant difference based on Tukey's Studentized Range (HSD) ($p < 0.05$). [a]Callus formation was observed in the fourth week after irradiation. [b]Embryogenic callus induction was observed at the eighth week after irradiation. [c]Number of somatic embryo (globular phase) was observed in the eighth week after irradiation. [d]Efficiency of embryogenic callus formation: %EC induction/% callus formation 100% at the eighth week after irradiation

The induction of embryogenic calli in beneng banten taro and eddoe taro explants was significantly influenced by the level of gamma-ray irradiation. In beneng banten taro explants, a decrease in the ability to induce embryogenic calli below 50% occurred at medium to high doses of irradiation (12.50 — 27.50 Gy), with only 8.33% of embryogenic calli formed at 27.50 Gy. All doses of irradiation on eddoe taro explants reduced the ability of the explants to form embryogenic calli, with a low dose (2.50 Gy) reducing the ability by 50% and a high dose (27.50 Gy) producing only 4.17% embryogenic calli. However,

the efficiency of embryogenic callus induction in both explant types was greater than 50% at all irradiation doses. Even at 17.50 Gy, 100% of the calli produced by beneng banten taro explants induced embryogenic calli in the eighth week after irradiation. The highest irradiation dose (27.50 Gy) for eddoe taro explants reduced the efficiency of embryogenic callus induction by up to 50%.

The dose of gamma irradiation significantly affected the number of somatic embryos produced by taro explants in the globular phase eight weeks after irradiation. The average number of somatic embryos per explant decreased as the gamma irradiation dose increased. The ability of beneng banten taro and eddoe taro explants to produce somatic embryos decreased by 75% compared to that of the non-irradiated treatment. Even though the high-dose irradiation (27.50 Gy) still produced an average number of somatic embryos per explant in all taro explants, it was significantly lower than the low to medium irradiation doses (2.50 — 12.50 Gy) in beneng banten taro and the low dose (2.50 Gy) in eddoe taro.

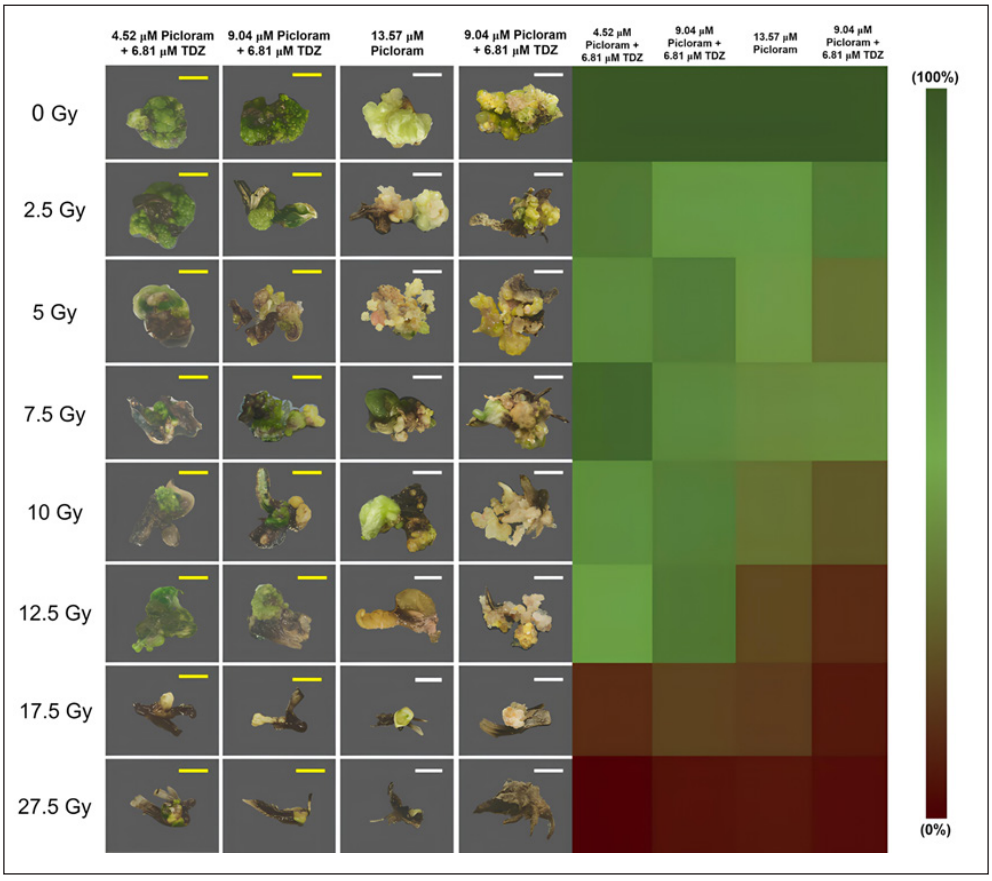

Figure 1. The condition and heatmap of green beneng banten taro (*X. undipes*) and eddoe taro (*C. esculenta* var. antiquorum) explants at eight weeks after irradiation

Note. Yellow bar = Beneng banten taro, White bar = Eddoe taro, Bar = 5 mm

All explant outcomes varied depending on the radiation dose administered after eight weeks of exposure (Figure 1). The control group appeared healthier and greener in color than the other treatment groups. Explants treated with 2.50 — 12.50 Gy of radiation displayed various changes in appearance, such as the callus becoming crumbly or compact, the color of the explant becoming paler, and cell death marked by browning in some parts. In contrast, explants exposed to more than 12.50 Gy of radiation experienced browning and cell death in nearly 80% of samples.

Radio-sensitivity of Taro Explants

The results of this study on the effect of irradiation on taro explant survival are shown in Figure 2. The data revealed that the percentage of explant survival decreased as the irradiation dose increased for both taro. Specifically, gamma irradiation at 12 Gy suppressed the growth of beneng banten taro explants by nearly 50%, whereas a dose of 7.5 Gy suppressed the growth of eddoe taro explants by 50%. However, it is important to note that complete explant death did not occur even at the highest dose level, as 21.59% of beneng banten taro explants and 12.50% of eddoe taro explants remained viable after treatment with 27.50 Gy of irradiation. The differences between control and treated explants were found to be statistically significant ($p \leq 0.05$) for both types of taro, particularly between doses of 12.50 to 27.50 Gy for beneng banten taro and between doses of 7.50 to 27.50 Gy for eddoe taro. Based on these results, the estimated LD_{50} for beneng banten taro explants was 12.84 Gy, whereas the LD_{50} for eddoe taro explants was 7.23 Gy.

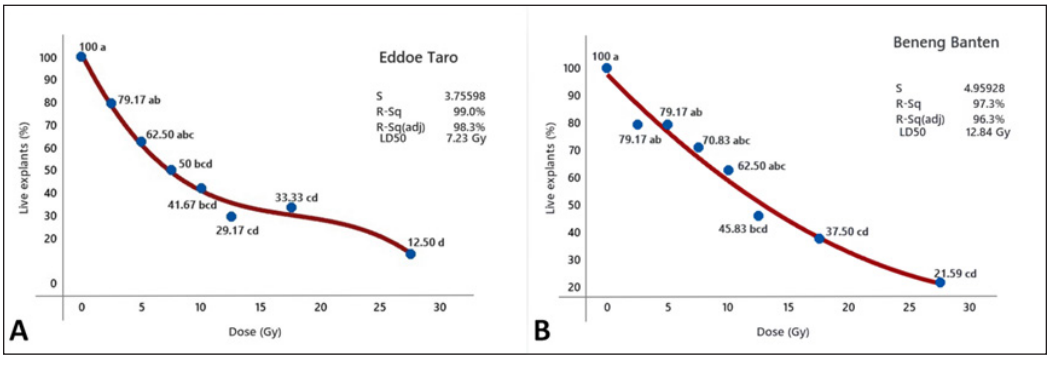

Figure 2. (A) Radiosensitivity curves of eddoe (*C. esculenta* var. antiquorum) and (B) beneng banten (*X. undipes*) taro at eight weeks after irradiation. Numbers followed by the same letter indicate no significant difference based on Tukey's Studentized Range (HSD) ($p < 0.05$)

DISCUSSION

The callus is a type of tissue that forms temporarily through the growth of stem cells. It is an undifferentiated tissue, meaning it has yet to develop into a specific tissue type. Differences

in callus formation may indicate changes in irradiated explants, reflecting their ability to survive radiation-induced cellular damage and resume growth. In this study, low doses of gamma irradiation support callus formation, as demonstrated in *Metroxylon sagu* by adding callus biomass in the 10 Gy gamma irradiation treatment (Riyadi & Sumaryono, 2017). Low doses of gamma rays have a positive effect on the growth of various plants, such as *Hordeum vulgare* L. seeds (Volkova et al., 2019) and shoot formation in bananas (Ali et al., 2020). The positive effect of low doses of gamma irradiation on growth and development may be due to better mobilization of proteins and metabolites and modulation of reactive oxygen species (ROS) levels. There is evidence that ROS could be a crucial molecule that acts as a hub in various phytohormonal cascades connected to changes in phytohormone signaling pathways (Geras'kin et al., 2017; Sewelam et al., 2016).

The influence of gamma irradiation on embryogenic callus induction in explants is thought to be related to the death of explants caused by irradiation, particularly high-dose irradiation. Gamma irradiation at high doses can result in cell disruption and explant death. However, this can also lead to creating more mutant variants through the induction of chromosomal and DNA damage (Agisimanto et al., 2016). Despite this, the relatively high efficiency of embryogenic callus induction in this study suggests that the administered irradiation dose did not affect the callus redifferentiation process into embryogenic calli, which is meristematic and has the potential to develop into somatic embryos. Litz (2004) emphasized the importance of limited proliferation cycles due to irradiation to ensure cell recovery for further development. Similarly, decreased responses to embryogenic callus induction following gamma irradiation have been observed in *Saccharum officinarum* (Hapsoro et al., 2018) and *Agave tequilana* (Valencia-Botín et al., 2020).

Somatic embryos are ideal for mutagenesis because they are derived from a single cell and are thus not susceptible to chimeric development. The decrease in the average number of globular-phase somatic embryos was attributed to a decline in the number of embryogenic calli that could be induced by gamma-ray irradiation. When subjected to high levels, gamma rays produce and accumulate ROS, which damage plant tissues (Liu et al., 2021). Another study found that gamma irradiation resulted in the degradation of the indoleacetic dehydrogenase enzyme, which is crucial for IAA synthesis. Degradation of this enzyme leads to a browning reaction in explants and reduces the regeneration capacity of the plant (Rosmala et al., 2022). Gamma irradiation also decreased the average number of somatic embryos in *M. sagu* (Riyadi & Sumaryono, 2017), *Panax ginseng* (Lee et al., 2019), and *Coffea* spp. (Bado et al., 2021), and *Catharanthus roseus* (Mujib et al., 2022).

Using gamma rays as a mutational agent has benefited plant breeding and germplasm collection. However, high doses of gamma irradiation can hinder the development of living plants, such as *A. tequilana* (Valencia-Botín et al., 2020) and *Philodendron billietiae* (Maikaeo et al., 2024). On the other hand, it can also promote a broader range of genetic diversity, as observed in *Typhonium flagelliforme* (Sianipar et al., 2017), *Etlingera elatior*

(Azzahra et al., 2018), *Vanilla planifolia* (Serrano-Fuentes et al., 2022), and *Zamioculcas zamiifolia* (Beyramizadeh et al., 2023).

Many studies have shown that the exposure of plants to high doses of radiation can harm their growth. It can include hindering germination and causing negative outcomes, such as chromosomal abnormalities, which may eventually result in plant death (Gudkov et al., 2019; Jan et al., 2011; Tan et al., 2023). A common indication of explant death resulting from irradiation is color change. During high-dose irradiation, the explant changes color from green to brown or black due to ROS. As mutagenic agents, gamma rays produce biological effects through the interactions of atoms or molecules in cells, particularly with water. Gamma irradiation can increase the production of reactive ROS, including superoxide anions, hydrogen peroxide, and hydroxyl radicals. This increase in ROS can trigger oxidative stress in various cellular components, resulting in chloroplast deformation, plasmalemma disintegration, and nuclear membrane rupture (Gill & Tuteja, 2010). The accumulation of excess ROS, accompanied by organelle disorganization, leads to cell death, which can be observed in a brownish color (Sharma et al., 2012). The browning and death of calli due to gamma irradiation also occur in *Allium sativum* L. (Maryono, 2020) and *Amorphophallus paeoniifolius* (Rivai et al., 2022).

It is crucial to determine the radiosensitivity of plants before implementing large-scale irradiation processes. Several factors, including planting material, plant genotype, degree of polyploidy, cell development stage, tissue age, and post-irradiation conditions, influence the optimal dosage of gamma rays for mutagenesis. Therefore, conducting radiation sensitivity studies such as LD_{50} determination is essential before incorporating gamma rays into breeding programs (Datta, 2019; Datta, 2023). In vitro, gamma irradiation was conducted on cocoyam shoots (*X. sagittifolium* L. Schott) with an LD_{50} of 8.7 Gy for white-fleshed tubers and 7.6 Gy for red-fleshed tubers (Ndzana et al., 2008). The effective dose (LD_{30}) in cultures of taro shoots (*C. esculenta* (L.)) was found to be 7.65 Gy, causing a 30% reduction in growth. Furthermore, 20 Gy gamma irradiation is lethal to taro shoot explants (Seetohul et al., 2008).

The present study produced a higher LD_{50} than previous research on taro families that utilized irradiation despite employing shoot base explants as the planting material. This difference is attributable to adding malt extract and l-asparagine to the media, which serve as additional carbohydrates and amino acid sources. Malt extract contains approximately 90% carbohydrates, amino acids, and phenolic compounds, such as ferulic acid (Chaves et al., 2019). L-asparagine is an adaptable amino acid that participates in several biological processes, such as plant growth and adjustment to environmental stressors (Han et al., 2022). In addition to inducing somatic embryos, these two components are thought to facilitate cell adaptation, particularly in cell walls that experience oxidative stress due to the induction of gamma rays. Numerous studies have shown that plant cells possess several mechanisms for coping with oxidative stress. These mechanisms include activating

and synthesizing antioxidants, enzymes, and non-enzymatic substances. Some of these substances can reduce the catalytic activity of transition metals, such as polysaccharides in cell walls and structural proteins (Gill & Tuteja, 2010; Hassinen et al., 2011; Zagorchev et al., 2013). Consequently, gamma irradiation at the highest dose (27.5 Gy) did not result in the complete death of the explants.

CONCLUSION

In this study, gamma irradiation affected the initiation and proliferation of embryogenic calli in eddoe and beneng banten taro plants. Specifically, the LD_{50} for eddoe taro explants was 7.23 Gy, while the LD_{50} for beneng banten taro explants was 12.84 Gy. Additional studies are necessary to investigate the effects of adding malt extract and l-asparagine on the survival of explants. The results showed that lower doses of gamma irradiation can increase explants' ability to form calluses, whereas higher doses can decrease their capacity to redifferentiate into globular-phase somatic embryos. Using gamma rays for mutation induction is a potential method for increasing genetic diversity or improving orphan crop plant species, such as Indonesian taro.

ACKNOWLEDGEMENTS

Thanks to the Malaysian Agriculture Research and Development Institute (MARDI) for supporting the financial schemes through the FAO-Benefit Sharing Fund (BSF) 2019−2023.

REFERENCES

Agisimanto, D., Noor, N. M., Ibrahim, R., & Mohamad, A. (2016). Gamma irradiation effect on embryogenic callus growth of *Citrus reticulata* cv. Limau Madu. *Sains Malaysiana*, *45*(3), 329–337.

Alghifari, A. F., Santosa, E., & Susila, A. D. (2023). Growth and production beneng taro (*Xanthosoma undipes* K. Koch) accessions on several status of soil organic carbon. *Jurnal Agronomi Indonesia*, *51*(1), 17–26. https://doi.org/10.24831/ija.v51i1.44975

Ali, M., Nizamani, G. S., Khan, M. T., Yasmeen, S., Siddiqui, A., Khan, I. A., Nizamani, M. R. Nizamani, F., Siddiqui, M. A., & Khaskheli, M. A. (2020). Implications of *in vitro* mutagenesis in banana (*Musa spp*.). *Pure and Applied Biology*, *9*(1), 1230−1241. http://doi.org/10.19045/bspab.2020.90003

Azzahra, E. I., Aisyah, S. I., Dinarti, D., & Krisantini, K. (2018). In vitro mutagenesis of *Etlingera elatior* by gamma ray intermittent irradiation. *Journal of Tropical Crop Science*, *5*(3), 111–118. https://doi.org/10.29244/jtcs.5.3.111-118

Bado, S., Maghuly, F., Varzea, V., & Laimer, M. (2021). Mutagenesis of *in vitro* explants of *Coffea* spp. to induce fungal resistance. In S. Sivasankar, E. Noel, Jankuloski & I. Ingelbrecht (Eds.), *Mutation breeding, genetic diversity and crop adaptation to climate change* (pp. 344–352). CABI. https://doi.org/10.1079/9781789249095.0036

Beyramizadeh, E., Arminian, A., & Fazeli, A. (2023). Evaluating the effect of gamma rays on Zamiifolia (*Zamioculcas zamiifolia*) plant in vitro and genetic diversity of the resulting genotypes using the ISSR marker. *Scientific Reports*, *13*(1), 8308. https://doi.org/10.1038/s41598-023-35618-2

Cahyanti, L. D., Sopandie, D., Santosa, E., & Purnamawati, H. (2022). Variability response of growth of 17 taro genotype under drought and flooding. *Jurnal Agronomi Indonesia*, *50*(2), 164–171. https://doi.org/10.24831/jai.v50i2.41814

Cahyanti, L. D., Sopandie, D., Santosa, E., & Purnamawati, H. (2024). Diversity of 17 genotypes of taro based on anatomy and nutritional value of tuber. *Hayati Journal of Biosciences*, *31*(3), 465–473. https://doi.org/10.4308/hjb.31.3.465-473

Chaïr, H., Traore, R. E., Duval, M. F., Rivallan, R., Mukherjee, A., Aboagye, L. M., Van Rensburg, W. J., Andrianavalona, V., Pinheiro de Carvalho, M. A. A., Saborio, F., Sri Prana, M., Komolong, B., Lawac, F., & Lebot, V. (2016). Genetic diversification and dispersal of taro (*Colocasia esculenta* (L.) Schott). *PLOS ONE*, *11*(6), e0157712. https://doi.org/10.1371/journal.pone.0157712

Chaves, D. F. S. (2019). Malt extract as a healthy substitute for refined sugar. *American Journal of Biomedical Science & Research*, *4*(1), 52–53. https://doi.org/10.34297/ajbsr.2019.04.000758

Datta, S. K. (2019). Determination of radiosensitivity: Prerequisite factor for induced mutagenesi*s*. In C. P. Malik & P. C. Trivedi (Eds.), *Harnessing plant biotechnology and physiology to stimulate agricultural growth* (pp. 51 — 70). Agrobios.

Datta, S. K. (2023). Technology package for induced mutagenesis. *Journal of Biology and Nature*, *15*(1), 70–88. https://doi.org/10.56557/joban/2023/v15i18077

Fidyasari, A., Sari, R. M., & Raharjo, S. J. (2017). Identifikasi komponen kimia pada Umbi Bentul (Colocasia esculenta (L.) Schoot) sebagai pangan fungsional [Chemical component identification of (*Colocasia esculenta* (L.) Schoot) as functional food]. *Amerta Nutrition*, *1*(1), 14. https://doi.org/10.20473/amnt.v1i1.2017.14-21

Geras'kin, S., Churyukin, R., & Volkova, P. (2017). Radiation exposure of barley seeds can modify the early stages of plants' development. *Journal of Environmental Radioactivity*, *177*, 71–83. https://doi.org/10.1016/j.jenvrad.2017.06.008

Gill, S. S., & Tuteja, N. (2010). Reactive oxygen species and antioxidant machinery in abiotic stress tolerance in crop plants. *Plant Physiology and Biochemistry*, *48*(12), 909–930. https://doi.org/10.1016/j.plaphy.2010.08.016

Gudkov, S. V., Grinberg, M. A., Sukhov, V., & Vodeneev, V. (2019). Effect of ionizing radiation on physiological and molecular processes in plants. *Journal of Environmental Radioactivity*, *202*, 8–24. https://doi.org/10.1016/j.jenvrad.2019.02.001

Han, M., Wang, S., Wu, L., Feng, J., Si, Y., Liu, X., & Su, T. (2022). Effects of exogenous l-asparagine on poplar biomass partitioning and root morphology. *International Journal of Molecular Sciences*, *23*(21), 13126. https://doi.org/10.3390/ijms232113126

Hapsoro, D., Inayah, T., & Yusnita. (2018). Plant regeneration of sugarcane (*Saccharum officinarum* L.) calli in vitro and its response to gamma irradiation. *ISSAAS Journal*, *24*(1), 58–66.

Hassinen, V. H., Tervahauta, A. I., Schat, H., & Kärenlampi, S. O. (2010). Plant metallothioneins – metal chelators with ROS scavenging activity? *Plant Biology*, *13*(2), 225–232. https://doi.org/10.1111/j.1438-8677.2010.00398.x

Hidayatullah, C. S. R., Santosa, E., Sopandie, D., & Hartono, A. (2020). Phenotypic plasticity of eddoe and dasheen taro genotypes in response to saturated water and dryland cultivations. *Biodiversitas*, *21*(10), 4550–4557. https://doi.org/10.13057/biodiv/d211012

Jan, S., Parween, T., Siddiqi, T. O., & Mahmooduzzafar. (2010). Gamma radiation effects on growth and yield attributes of *Psoralea corylifolia* L. with reference to enhanced production of psoralen. *Plant Growth Regulation*, *64*(2), 163–171. https://doi.org/10.1007/s10725-010-9552-z

Jayaprakas, C. A., & Harish, E. R. (2022). Pests and their management in minor tuber crops. In. M. Mani (Eds.), *Trends in horticultural entomology* (pp. 1109–1137). Springer. https://doi.org/10.1007/978-981-19-0343-4_48

Lee, J. W., Jo, I. H., Kim, J. U., Hong, C. E., Bang, K. H., & Park, Y. D. (2019). Determination of mutagenic sensitivity to gamma rays in ginseng (*Panax ginseng*) dehiscent seeds, roots, and somatic embryos. *Horticulture, Environment, and Biotechnology*, *60*(5), 721–731. https://doi.org/10.1007/s13580-019-00164-2

Litz, R. E. (2004). Effect of gamma irradiation on embryogenic avocado cultures and somatic embryo development. *Plant Cell Tissue and Organ Culture*, *77*, 139–147. https://doi.org/10.1023/B:TICU.0000016817.65358.77

Liu, H., Li, H., Yang, G., Yuan, G., Ma, Y., & Zhang, T. (2021). Mechanism of early germination inhibition of fresh walnuts (*Juglans regia*) with gamma radiation uncovered by transcriptomic profiling of embryos during storage. *Postharvest Biology and Technology*, *172*, 111380. https://doi.org/10.1016/j.postharvbio.2020.111380

Maikaeo, L., Puripunyavanich, V., Limtiyayotin, M., Orpong, P., & Kongpeng, C. (2024). Micropropagation and gamma irradiation mutagenesis in *Philodendron billietiae*. *Thai Journal of Agricultural Science*, *57*(1), 11−19.

Maretta, D., Sobir, S., Helianti, I., Purwono, P., & Santosa, E. (2020). Genetic diversity in eddoe taro (*Colocasia esculenta* var. *antiquorum*) from Indonesia based on morphological and nutritional characteristics. *Biodiversitas, 21*(8), 3525-3533. https://doi.org/10.13057/biodiv/d210814

Maryono, M. Y. (2020). Somatic embryogenesis on irradiated callus of garlic (*Allium sativum* L.). *Journal of Physics: Conference Series*, *1436*(1), 012115. https://doi.org/10.1088.1742-6596/1436/1/012115

Mujib, A., Fatima, S., & Malik, M. Q. (2022). Gamma ray–induced tissue responses and improved secondary metabolites accumulation in *Catharanthus roseus*. *Applied Microbiology and Biotechnology*, *106*(18), 6109–6123. https://doi.org/10.1007/s00253-022-12122-7

Murashige, T., & Skoog, F. (1962). A revised medium for rapid growth and bio assays with tobacco tissue cultures. *Physiologia Plantarum*, *15*(3), 473–497. https://doi.org/10.1111/j.1399-3054.1962.tb08052.x

Ndzana, X., Zok, S., & Sama, A. E. (2008). Preliminary study on radiation sensitivity of *in vitro* cultures of Xanthosoma (macabo) in Cameroon. *Plant Mutation Report*, *2*(1), 10–12.

Nurilmala, F., Hutagaol, R. P., Widhyastini, I. M., Widyastuti, U., & Suharsono, S. (2017). Somaclonal variation induction of bogor taro (*Colocasia esculenta*) by gamma irradiation. *Biodiversitas*, *18*(1), 28-33. https://doi.org/10.13057/biodiv/d180105

Prana, M. S. (2007). Study on flowering biology of taro (*Colocasia esculenta* (L.) Schott.). *Biodiversitas*, *8*(1), 63-66. https://doi.org/10.13057/biodiv/d080113

Rivai, R. R., Isnaini, Y., & Yuzammi. (2022). Elucidation of the radiosensitivity level of *Amorphophallus paeoniifolius* (Dennst.) Nicolson embryogenic callus induced by gamma ray irradiation. *Biology and Life Sciences Forum*, *11*(1), 93. https://doi.org/10.3390/IECPS2021-11951

Riyadi, I., & Sumaryono, S. (2017). Effect of gamma irradiation on the growth and development of sago palm (*Metroxylon sagu* Rottb.) calli. *Indonesian Journal of Agricultural Science*, *17*(1), 35−40. https://doi.org/10.21082/ijas.v17n1.2016.p35-40

Rosmala, A., Sukma, D., & Khumaida, N. (2022). Effect of gamma irradiation on callus of handeuleum (*Graptophillum pictum* L. Griff) Kalimantan and Papua accession. *Indonesian of Journal Horticulture*, *13*(1), 23–28. https://doi.org/10.29244/jhi.13.1.23-28

Rostianti, T., Hakiki, D. N, Ariska, A., & Simantri. (2018). Karakterisasi sifat fisikokimia tepung talas beneng sebagai biodiversitas pangan lokal Kabupaten Pandeglang [Characterization of the physicochemical properties of beneng taro flour as local food biodiversity in Pandeglang Regency]. *Gorontalo Agriculture Technology Journal*, *1*(2), 1-7. https://doi.org/10.32662/gatj.v1i2.410

Seetohul, S., Puchooa, D., & Ranghoo-Sanmukhiya, V. M. (2008). Genetic improvement of taro (*Colocasia esculenta* var. *esculenta*) through in vitro mutagenesis. *University of Mauritius Research Journal*, *13A*, 79–89.

Serrano-Fuentes, M. K., Gómez-Merino, F. C., Cruz-Izquierdo, S., Spinoso-Castillo, J. L., & Bello-Bello, J. J. (2022). Gamma radiation (^{60}Co) induces mutation during in vitro multiplication of vanilla (*Vanilla planifolia* Jacks. ex Andrews). *Horticulturae*, *8*(6), 503. https://doi.org/10.3390/horticulturae8060503

Setiawan, R. B., Khumaida, N., & Dinarti, D. (2015). Induksi mutasi kalus embriogenik gandum (*Triticum aestivum* L.) melalui iradiasi sinar gamma untuk toleransi suhu tinggi [Mutation induction on embryogenic callus of wheat (*Triticum aestivum* L.) through gamma ray irradiation for high temperature tolerance]. *Jurnal Agronomi Indonesia*, *43*(1), 36. https://doi.org/10.24831/jai.v43i1.9589

Sewelam, N., Kazan, K., & Schenk, P. M. (2016). Global plant stress signaling: Reactive oxygen species at the cross-road. *Frontiers in Plant Science*, *7*, 187. https://doi.org/10.3389/fpls.2016.00187

Sharma, P., Jha, A. B., Dubey, R. S., & Pessarakli, M. (2012). Reactive oxygen species, oxidative damage, and antioxidative defense mechanism in plants under stressful conditions. *Journal of Botany*, *2012*(1), 217037. https://doi.org/10.1155/2012/217037

Sianipar, N. F., Purnamaningsih, R., Gumanti, D. L., Rosaria, & Vidianty, M. (2017). Analysis of gamma irradiated-third generation mutants of rodent tuber (*Typhonium flagelliforme* Lodd.) based on morphology, RAPD, and GC-MS markers. *Pertanika Journal of Tropical Agricultural Science*, *40*(1), 185−202.

Susilawati, P. N., Yursak, Z., Kurniawati, S., & Saryoko, A. (2021*). petunjuk teknis budidaya dan pengolahan varietas Talas Beneng* [Technical guideline of cultivation and processing of Beneng Taro variety]. Balai

Pengkajian Teknologi Pertanian. https://hortikultura.pertanian.go.id/wp-content/uploads/2024/10/Juknis-Budidaya-dan-Pengolahan-Paspa-Varietas-Beneng_watermark.pdf

Tan, Y., Duan, Y., Chi, Q., Wang, R., Yin, Y., Cui, D., Li, S., Wang, A., Ma, R., Li, B., Jiao, Z., & Sun, H. (2023). The role of reactive oxygen species in plant response to radiation. *International Journal of Molecular Sciences*, *24*(4), 3346. https://doi.org/10.3390/ijms24043346

Valencia-Botín, A. J, Ramírez-Serrano, C., Virgen-Calleros, G., Pimienta-Barrios, E., Rodríguez-Guzmán, E, Angeles-Espino, A. (2020). Indirect somatic embryogenesis on mutans of *Agave tequilana* weber cultivar blue induced with ^{60}Co gamma rays. *Tropicaland Subtropical Agroecosystems*, *23*, 1−9. https://doi.org/10.56369/tsaes.3216

Vaneker, K., & Slaats, E. (2012). Mapping edible aroids. *Iridescent*, *2*(3), 34–45. https://doi.org/10.1080/19235003.2012.11428513

Volkova, P. Y., Duarte, G. T., Soubigou-Taconnat, L., Kazakova, E. A., Pateyron, S., Bondarenko, V. S., Bitarishvili, S. V., Makarenko, E. S., Churyukin, R. S., Lychenkova, M. A., Gorbatova, I. V., Meyer, C., & Geras'kin, S. A. (2019). Early response of barley embryos to low- and high-dose gamma irradiation of seeds triggers changes in the transcriptional profile and an increase in hydrogen peroxide content in seedlings. *Journal of Agronomy and Crop Science*, *206*(2), 277–295. https://doi.org/10.1111/jac.12381

Zagorchev, L., Seal, C., Kranner, I., & Odjakova, M. (2013). A central role for thiols in plant tolerance to abiotic stress. *International Journal of Molecular Sciences*, *14*(4), 7405–7432. https://doi.org/10.3390/ijms14047405

Pertanika J. Trop. Agric. Sci. 48 (3): 747 - 766 (2025)

PERTANIKA JOURNALS

TROPICAL AGRICULTURAL SCIENCE

Journal homepage: http://www.pertanika.upm.edu.my/

In-silico and Phylogenetic Analysis of Acetate: Succinate COA-Transferase (ASCT) from *Angiostrongylus malaysiensis*

Quincie Sipin[1], Suey Yee Low[1], Wan Nur Ismah Wan Ahmad Kamil[2], Kiew-Lian Wan[3], Mokrish Ajat[4], Juriah Kamaludeen[5,6], Sharifah Salmah Syed-Hussain[7], Nur Indah Ahmad[1] and Nor Azlina Abdul Aziz[1]*

[1]Department of Veterinary Pathology and Microbiology, Faculty of Veterinary Medicine, Universiti Putra Malaysia, 43400 Serdang, Malaysia

[2]Department of Microbiology, Faculty of Biotechnology and Biomolecular Sciences, Universiti Putra Malaysia, 43400 Serdang, Malaysia

[3]Department of Biological Sciences and Biotechnology, Faculty of Science and Technology, Universiti Kebangsaan Malaysia, 43600 Bangi, Selangor, Malaysia

[4]Department of Veterinary Preclinical Science, Faculty of Veterinary Medicine, Universiti Putra Malaysia, 43400 Serdang, Malaysia

[5]Department of Animal Science and Fishery, Faculty of Agriculture Science and Forestry, Universiti Putra Malaysia Bintulu Sarawak Campus, 97008 Bintulu, Sarawak, Malaysia

[6]Institute of Tropical Agriculture and Food Security, Universiti Putra Malaysia, 43400 Serdang, Selangor, Malaysia

[7]Department of Veterinary Clinical Studies, Faculty of Veterinary Medicine, Universiti Putra Malaysia, 43400 Serdang, Malaysia

ABSTRACT

The zoonotic capability of *Angiostrongylus malaysiensis* was recently observed after several years of doubt. This parasite was found in a high burden of Malaysian rats, which is alarming. There is currently no effective treatment for human neuroangiostrongyliasis. Acetate: succinate CoA-transferase (ASCT) enzyme catalyses acetate production in helminth parasites. ASCT was classified into three subfamilies within the family I CoA-transferases (IA, IB, and IC). Acetate is an essential metabolic end product of many parasites, making it an attractive drug target since it is absent in mammalian hosts. The current study describes the in-silico analysis conducted for the identification and phylogenetic characterisation of *A. malaysiensis* ASCT and genetic variations between subfamilies of ASCT. The *Am*ASCT was identified from the ongoing de novo transcriptome assembly and annotation

ARTICLE INFO

Article history:
Received: 26 July 2024
Accepted: 01 October 2024
Published: 16 May 2025

DOI: https://doi.org/10.47836/pjtas.48.3.06

E-mail addresses:
quinciesipin@gmail.com (Quincie Sipin)
eulynnlow96@gmail.com (Suey Yee Low)
wn_ismah@upm.edu.my (Wan Nur Ismah Wan Ahmad Kamil)
klwan@ukm.edu.my (Kiew-Lian Wan)
mokrish@upm.edu.my (Mokrish Ajat)
juriahk@upm.edu.my (Juriah Kamaludeen)
ssalmah@upm.edu.my (Sharifah Salmah Syed-Hussain)
nurindah@upm.edu.my (Nur Indah Ahmad)
azlinaaziz@upm.edu.my (Nor Azlina Abdul Aziz)
*Corresponding author

of adult *A. malaysiensis*. The analysis of *Am*ASCT physiochemical properties, multiple sequence alignment and phylogenetic relations with the ASCTs of other helminths are conducted using standard bioinformatic tools. Pairwise comparisons between subfamilies of ASCT have also been conducted in silico. *Am*ASCT has the conserved regions of the family I CoA-transferases and is clustered with subfamily IB of ASCT. From the pairwise analysis, subfamilies IB and IC were most closely related between the three subfamilies. *Am*ASCT was predicted to be overall hydrophilic and stable in a neutral to slightly alkaline environment within the parasite. The phylogenetic analysis confirmed that *Am*ASCT belongs to subfamily IB of ASCTs. Further study on the biochemical activity of ASCT in *A. malaysiensis* is required to determine its enzymatic function.

Keywords: Acetate: succinate CoA-transferase (ASCT), acetate production, *Angiostrongylus malaysiensis*

INTRODUCTION

Human neuroangiostrongyliasis, caused by the rat lungworm, is a food-borne parasitic zoonosis distributed worldwide and endemic to Asia and the Pacific Basin. However, it has been reported in new regions beyond its traditional endemic range (Eamsobhana, 2014). The prime causative agent of human neuroangiostrongyliasis is *Angiostrongylus cantonensis* (Wang et al., 2008). Recently, *A. malaysiensis*, formerly known as the Malaysian strain of *A. cantonensis*, was revealed to be zoonotic after several years of doubt (Watthanakulpanich et al., 2021), increasing the risk of human neuroangiostrongyliasis infection. The newly found zoonotic capability of *A. malaysiensis* is alarming, given its high prevalence in rats in Malaysia (Low et al., 2023). There is currently no effective treatment for human neuroangiostrongyliasis. Current treatment focuses on alleviating pain, inflammation, and intracranial pressure in infected individuals (Sawanyawisuth et al., 2008; Slom et al., 2002). Although anthelmintics have been extensively used, their effectiveness is debatable (Murphy et al., 2013), as they leave the disease without an efficient cure. A new, effective approach is needed for treating this disease.

The complex life cycle of parasites enables them to inhabit more than one host organism throughout their life cycle. Most parasites have a complex life cycle, including free-living and distinct stages inhabiting one or more host organisms. As a result, parasites are forced to modify their metabolism to survive in habitats where nutrients and oxygen are scarce. These parasites have evolved metabolic strategies that produce acetate from acetyl-CoA as an essential metabolic product (Tielen et al., 2002). Two pathways of acetate formation from acetyl-CoA have been found in parasites and are catalysed by either a cytosolic acetyl-CoA synthetase (ACS) or an organellar acetate: succinate CoA-transferase (ASCT). Furthermore, the ACS pathway has been reported only in parasitic protists (Reeves et al., 1977; Sánchez et al., 2000; Stechmann et al., 2008), while the ASCT pathway was previously found in both helminths and protists (Steinbüchel & Müller, 1986; Saz et al., 1996; van Hellemond et al., 1998).

To date, all acetate/succinate CoA-transferases (ASCTs) found in eukaryotes are family I CoA-transferases that are distinguished by the catalysis of CoA group transfer, which involves the presence of a glutamate residue in the enzyme's active site (Heider, 2001). Recently, the corresponding ASCT genes were identified and characterised in two protists, *Trypanosoma brucei* (Rivière et al., 2004) and *Trichomonas vaginalis* (van Grinsven et al., 2008), and in the helminth *Fasciola hepatica* (van Grinsven et al., 2009). The ASCT genes from the three parasites showed little sequence homology, classifying them into three different subfamilies of family I CoA-transferases: *T. brucei* in subfamily IA, *F. hepatica* in subfamily IB, and *T. vaginalis* in subfamily IC (Tielens et al., 2010).

Acetate is a prime candidate for developing new antiparasitic medications because it is a crucial byproduct of the energy metabolism of many parasites absent in their mammalian hosts. Identifying and characterising acetate-producing enzymes in rat lungworms is crucial for developing new and effective drugs to treat human neuroangiostrongyliasis. Here, we conducted a phylogenetic and physiochemical characterisation of the identified putative gene sequence of *A. malaysiensis* ASCT (AmASCT) obtained from our ongoing transcriptomic data analysis and further analysed the genetic variations among the three subfamilies of ASCTs.

METHODS

In-silico Analysis

Identification of Putative A. malaysiensis *ASCT (AmASCT)*

Putative A*m*ASCT was identified through ongoing transcriptomic analysis of adult *A. malaysiensis*. In short, the raw RNA-seq reads obtained were subjected to quality control using Trimmomatic (Galaxy version 0.39) (Bolger et al., 2014) and de novo transcriptome assembly using Trinity (Grabherr et al., 2011). Coding regions were predicted using TransDecoder (Galaxy version 5.5.0) (Haas et al., 2013). Subsequently, the assembled transcripts and predicted coding regions were subjected to homology-based similarity search using BLASTx and BLASTp against the latest non-redundant protein sequence (nr) database in the DIAMOND alignment tool (Galaxy version 2.0.15) (Buchfink et al., 2014). Hmmscan (Galaxy version 3.4) (Finn et al., 2011) searches were conducted using the protein family database (Pfam-A) database as a query, and TMHMM software (Galaxy version 0.0.17) (Cock et al. 2013) was used for transmembrane domains detection. Trinotate (Galaxy version 3.2.2) (Grabherr et al., 2011) integrated the BLAST, hmmscan, and TMHMM results.

A BLASTp search (Camacho et al., 2009) using *F. hepatica*'s ASCT gene (accession no. ACF06126.1) (van Grinsven et al., 2009) as a query was conducted against the nr database of *A. cantonensis*. The GenBank accession number of the top BLASTp hit was retrieved

and searched against the Trinotate integrated annotation results previously obtained. The gene sequence of the putative *Am*ASCT was retrieved from the Trinotate result for further analysis.

*Validation of the Obtained A*m*ASCT*

Several bioinformatic tools and molecular techniques were employed to validate the identified *Am*ASCT. The initial bioinformatic validation involved utilising BLASTx search by using the obtained putative *Am*ASCT gene sequence as a query against the nr database of *F. hepatica* to ensure whether the putative *Am*ASCT is a homolog to the previously characterised ASCT of *F. hepatica* (accession no. ACF06126.1) (van Grinsven et al., 2009). In addition, ORFfinder in the National Center for Biotechnology Information (NCBI) websites (https://www.ncbi.nlm.nih.gov/orffinder/) was used to identify and analyse the open reading frame (ORF) of the *Am*ASCT gene, aiding in the prediction of coding regions and potential functional domains.

Following the bioinformatic validation, molecular techniques were employed to confirm the presence of the putative *Am*ASCT gene at the transcript and deoxyribonucleic acid (DNA) levels. Polymerase chain reaction (PCR), agarose gel electrophoresis, and Sanger sequencing were conducted. Briefly, adult *A. malaysiensis* worms collected from Low et al. (2023) were used for total ribonucleic acid (RNA) extraction using Trizol reagent (Thermo Fisher Scientific, USA), followed by cDNA synthesis using RevertAid™ First Strand cDNA Synthesis Kit (Toyobo, Japan) according to the manufacturer's instructions. Subsequently, the cDNA was used in polymerase chain reaction (PCR) amplification using a set of primers (forward: 5'-ATGCTGTGTCGGCTCTCATCC-3' and reverse: 5'-TTAGTCCACTTCAAGGCATC-3'). PCR was carried out in a thermal cycler with the cycling conditions set as follows: 94°C for 2 min, followed by 35 cycles of denaturation at 94°C for 30 sec, annealing at 55°C for 30 sec and extension at 72°C for 1 min. The cycling condition was ended with a final extension at 72°C for 5 min. Next, 1.5% agarose mixed with 1x TAE buffer was prepared, and the PCR product was electrophoresed (400W/80V) for 60 minutes and visualised under a UV transilluminator. Each primer's PCR product and 10 µl (10 µM) were outsourced to Apical Scientific Sdn. Bhd. (Selangor, Malaysia) for purification and sanger sequencing.

*Physiochemical Profiling of A*m*ASCT*

The putative *Am*ASCT's gene sequence was retrieved and subjected to physiochemical characterisation using ExPASy's ProtParam tool (Wilkins et al., 1999). The default configuration of the ProtParam tool was utilised to obtain the putative *Am*ASCT's molecular mass, theoretical isoelectric point (pI), amino acid composition, aliphatic index, and grand average of hydropathy (GRAVY).

Phylogenetic Analysis

Retrieval of ASCT Protein Sequences from Other Helminths

Before multiple sequence alignment and phylogenetic analysis, ASCT gene sequences from other helminth parasites were retrieved from the NCBI GenBank. BLASTp searches using previously characterised ASCTs of *T. brucei* (accession no. EAN79240) (Rivière et al., 2004), *F. hepatica* (accession no. ACF06126.1) (van Grinsven, 2009), and *T. vaginalis* (accession no. XP_001330176) (van Grinsven, 2008) were conducted against the nr database of helminth parasites. Sequences with an E value smaller than 20 (E^{-20}) were retrieved. If multiple parasites of the same species were found as a hit, only the sequence with the highest hit was retrieved.

Multiple Sequence Alignment and Phylogenetic Analysis

Multiple sequence alignment was conducted using the putative *Am*ASCT obtained in this study, the previously characterised ASCT protein sequences of *T. brucei*, *F. hepatica*, and *T. vaginalis*, and the retrieved ASCT protein sequences from other helminth parasites. Multiple sequence alignment was carried out using ClustalW (Thompson et al., 1994), and all sequences without the conserved ExG and GxGGxxD motifs of the family I CoA-transferases were removed. The aligned protein sequences of ASCTs were used for phylogenetic tree construction through the neighbour-joining (NJ) method in Molecular Evolutionary Genetics Analysis version 11 (MEGA11) software (Tamura et al., 2021). Pairwise comparisons to infer genetic variation within and between the three subfamilies of the family I CoA-transferases were also performed using MEGA11 software.

RESULTS AND DISCUSSION

Identification of the *A. malaysiensis* ASCT Gene Sequence

The ASCT sequence of *A. malaysiensis* was identified from our ongoing transcriptomic data analysis of adult *A. malaysiensis*. A BLASTP search conducted against the nr database of A. cantonensis using the previously characterised ASCT of *F. hepatica* (accession no. ACF06126.1) resulted in one blast hit (accession no. KAE9415559.1) that could be the putative ASCT of *A. cantonensis*. The previously characterised ASCT of *F. hepatica* was used as a query since it is a helminth parasite that could have genetic information similar to that of *A. malaysiensis*. In contrast, the other previously characterised parasites, *T. brucei* and *T. vaginalis*, are parasitic protists. Moreover, the nr database of *A. cantonensis* was searched against this gene due to the minimal protein and nucleotide sequences of *A. malaysiensis* being available in public databases. In addition, the reference genome of *A. malaysiensis* has yet to be sequenced. In contrast, the reference genome of *A. cantonensis*

is available in the NCBI GenBank (accession no. MQTX01000177.1, Xu et al., 2019). In addition, *A. cantonensis* is closely related to *A. malaysiensis,* and their morphological and genetic information is highly similar (Chan et al., 2020; Eamsobhana et al., 2015).

The gene annotation data from the transcriptomic data analysis of *A. malaysiensis* were searched for the gene homolog to the obtained putative *A. cantonensis* ASCT (accession no: KAE9415559.1). However, no similarities were found. For this reason, the putative *A. cantonensis* ASCT (accession no: KAE9415559.1) was further used as a query protein in a BLASTP search against the nr database to find other homologues. The top five hits of the BLASTP search (accession no. KAJ1347515.1, EYC13181.1, KIH58849.1, EYC13183.1, and EYC13182.1) were used further to search the transcriptomic gene annotation data of *A. malaysiensis*. A gene was found to be the homolog of the accession no. EYC13181.1, which could be the putative *A. malaysiensis* ASCT (*Am*ASCT). The complete nucleotide length and the open reading frame (ORF) amino acid sequence length of the putative AmASCT gene were 1413 base pairs (bp) and 470 amino acids (aa), respectively (Figure 1). A BLASTP search conducted using the putative *Am*ASCT protein sequence as a query revealed high similarity with a few other helminth parasites, with *A. cantonensis* (accession no. KAE9415559.1) exhibiting the highest similarity, followed by *Parelaphostrongylus tenuis* (KAJ1347515.1) and *Ancylostoma ceylanicum* (EYC13181). However, these homolog protein hits were described as hypothetical proteins because the gene has never been characterised in any of these helminths.

The putative AmASCTs were annotated as acetyl-CoA hydrolases or acetyl-CoA transferase N-terminal domains according to the protein family database (Pfam) annotation from the transcriptomic gene annotation data. Acetyl-CoA hydrolase (ACH) is one of the four known enzymes catalysing acetate formation from acetyl-CoA. The activity of ACH has been described in plants and animals (Hunt & Alexson, 2008; Zeiher & Randall, 1990). Although ACH activity has been reported in *Ascaris suum parasites* (de Mata et al., 1997), the complementary gene of this enzyme in this nematode parasite has yet to be identified. The CoA-transferase enzyme was previously confused with ACH in *Saccharomyces cerevisiae* (Lee et al., 1989, 1990); this enzyme was subsequently recharacterised as a CoA-transferase due to its minor hydrolase activity and was found to catalyse the transfer of the CoA moiety from succinyl-CoA to acetate, which is a particular characteristic of CoA-transferases (Fleck & Brock, 2009). One of the apparent characteristics of CoA-transferases that is absent in CoA-hydrolases is the glutamate active site for the formation of CoA-ester intermediates via a ping-pong bibi mechanism (Heider, 2001; White & Jencks, 1976). When the glutamate active site was replaced, CoA-transferase was found to be converted into a CoA-hydrolase (Mack & Buckel, 1997).

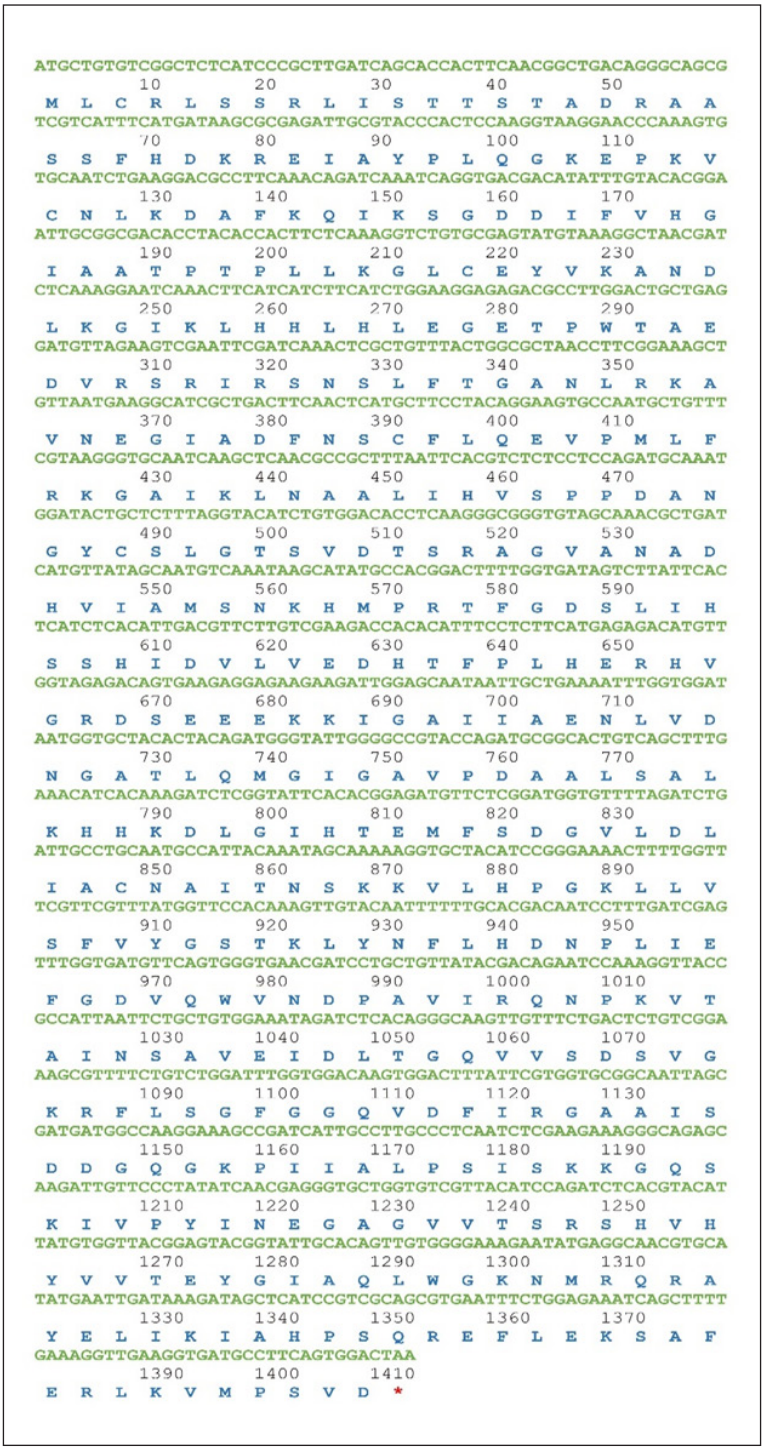

Figure 1. Full-length nucleotide sequence and ORF of the putative *Angiostrongylus malaysiensis* ASCT. The coding region comprises 1413 bp (green) of nucleotides and 470 aa (blue)

Validation of The Obtained Putative *A. malaysiensis* ASCT

Upon conducting the BLASTx search, the putative *Am*ASCT exhibited the ASCT gene of *F. hepatica* as the top hit, indicating a significant alignment and similarity between the two sequences. This BLASTx result demonstrates a high degree of homology between the putative *Am*ASCT and the previously characterised ASCT gene of *F. hepatica* (accession no. ACF06126.1). The positive amplification of the *Am*ASCT gene was confirmed through both PCR and agarose gel electrophoresis. Upon subjecting the PCR product to electrophoresis and visualising it under a UV transilluminator, a distinct and well-defined band was observed at the expected size, indicative of successful amplification of the *Am*ASCT gene and the presence of the gene in transcript and DNA levels. In addition, the obtained Sanger sequencing result of the amplified PCR product confirmed the identity of the putative *Am*ASCT, providing a similar representation of the coding sequence of the putative *Am*ASCT obtained from the de novo transcriptome annotation of adult *A. malaysiensis*. These bioinformatic and molecular approach results validate the reliability of the obtained putative *Am*ASCT gene sequence from the de novo transcriptome annotation data.

Physiochemical Profiling of AmASCT

The physiochemical properties of *Am*ASCT were analysed to understand and predict the enzyme function and behaviour under different conditions. The physiochemical profiling of *Am*ASCT conducted using ExPASy's ProtParam tool revealed several crucial molecular characteristics of *Am*ASCT (Table 1). The computational analysis predicted that *Am*ASCT has a molecular weight of 51.33 kDA, suggesting that the enzyme has a moderate size. The theoretical isoelectric point (pI) of 7.74 indicates that the *Am*ASCT is likely to be neutral or slightly alkaline, which suggests that *Am*ASCT is most stable under such conditions within the parasite. The high aliphatic index (93.79) implies that *Am*ASCT is enriched in hydrophobic amino acids and its adaptation and stability to functioning in hydrophobic environments. Also, the GRAVY score (-0.162) of *Am*ASCT indicates the hydrophilic nature of the enzyme, contributing to its solubility in aqueous environment. Despite containing enriched hydrophobic amino acids as indicated by the high aliphatic index, the overall hydrophilicity of *Am*ASCT may be because of the distribution of hydrophilic residues and charged or polar amino acids presence on its surface.

Table 1
Physiochemical profiling of AmASCT

No. of amino acids	Molecular weight (kDA)	Theoretical isoelectric point (pI)	Aliphatic index	GRAVY
470	51.33	7.74	93.79	- 0.162

Retrieval of ASCT from Helminth Parasites from GenBank

The retrieved amino acid sequences of helminth parasites were subjected to BLASTP searches against the non-redundant helminth protein database using *F. hepatica* (accession no. ACF06126.1), *T. vaginalis* (accession no. XP_001330176), and *T. brucei* (accession no. EAN79240), which represent the three subfamilies of the family I CoA-transferase, as tabulated in Table 1. BLASTP searches revealed 15, 22 and two amino acid sequences of subfamilies IA, IB and IC, respectively, of the family I CoA-transferase. The retrieved amino acid sequence of the helminth parasites in Table 2 shows that most helminth parasites

Table 2
Helminth parasites and their accession numbers of the family I CoA-transferase amino acid sequences with E values less than $1e^{-20}$ *retrieved from the NCBI GenBank*

Subfamily A	Subfamily B		Subfamily C
Ancylostoma ceylanicum (EYC45313)	*Fasciola hepatica* (ACF06126)	*Litomosoides sigmodontis* (VDK78337)	*Caenorhabditis remanei* (EFO99043)
Aphelenchoides bicaudatus (KAI6175034)	*Fasciola gigantica* (TPP58613)	*Toxocara canis* (KHN81999)	*Diploscapter pachys* (PAV69794)
Bursaphelenchus okinawaensis (CAD5205821)	*Heterobilharzia americana* (CAH8437700)	*Bursaphelenchus xylophilus* (CAD5213378)	
Nippostrongylus brasiliensis (VDL75362)	*Schistosoma mansoni* (XP_018648509)	*Acanthocheilonema viteae* (VBB34274)	
Caenorhabditis briggsae (XP_002629737)	*Trichobilharzia regent* (CAH8830533)	*Brugia malayi* (XP_042934641)	
Caenorhabditis elegans (NP_496144)	*Strongyloides ratti* (XP_024501800)	*Pristionchus pacificus* (KAF8362703)	
Meloidogyne enterolobii (CAD2169927)	*Caenorhabditis remanei* (EFP07577)	*Mesocestoides corti* (VDD82102)	
Parelaphostrongylus tenuis (KAJ1371690)	*Parelaphostrongylus tenuis* (KAJ1347515)	*Taenia asiatica* (VDK22328)	
Pristionchus pacificus (KAF8360361)	*Angiostrongylus cantonensis* (KAE9415559)	*Hymenolepis microstoma* (CUU98198)	
Ditylenchus destructor (KAI1702014)	*Enterobius vermicularis* (VDD96370)	*Echinococcus multilocularis* (CDS43154)	
Dracunculus medinensis (VDN53078)	*Steinernema carpocapsae* (TMS35399)	*Rodentolepis nana* (VDO13213)	
Strongyloides ratti (XP_024505624)			
Paragonimus westermani (KAF8572391)			
Clonorchis sinensis (KAG5445983)			
Opisthorchis felineus (TGZ64319)			

have the CoA-transferase enzyme of subfamily IB, followed by subfamily IA and only two in subfamily IC. This finding is in agreement with that of Tielens et al. (2010), who reported that the subfamily IA is found only in trypanosomatid parasites and some metazoan parasites, while the subfamily IC of ASCT is usually possessed only by prokaryotes and fungi. On the other hand, most of the ASCT enzymes of helminth parasites were previously reported to be in subfamily IB of family I CoA-transferases (Tielens et al., 2010).

Multiple Sequence Alignment of Helminth ASCT

Figure 2 presents the multiple amino acid sequence alignments of the putative ASCT gene of *A. malaysiensis* obtained in this study with amino acid sequences of the ASCT gene of other helminth parasites retrieved from the BLASTP searches and the ASCTs of previously characterised parasites. The helminth parasites were grouped into subfamilies based on the query ASCT sequence. Note that although *T. brucei* and *T. vaginalis* are parasitic protists, their ASCT proteins were included in this study as references since their ASCT genes were previously characterised.

According to the multiple amino acid sequence alignments, all the ASCT enzymes of helminth parasites included in this study contained the conserved ExG and GxGGxxD motifs of the ASCTs in the family I CoA-transferases (Tielens et al., 2010). The subfamily

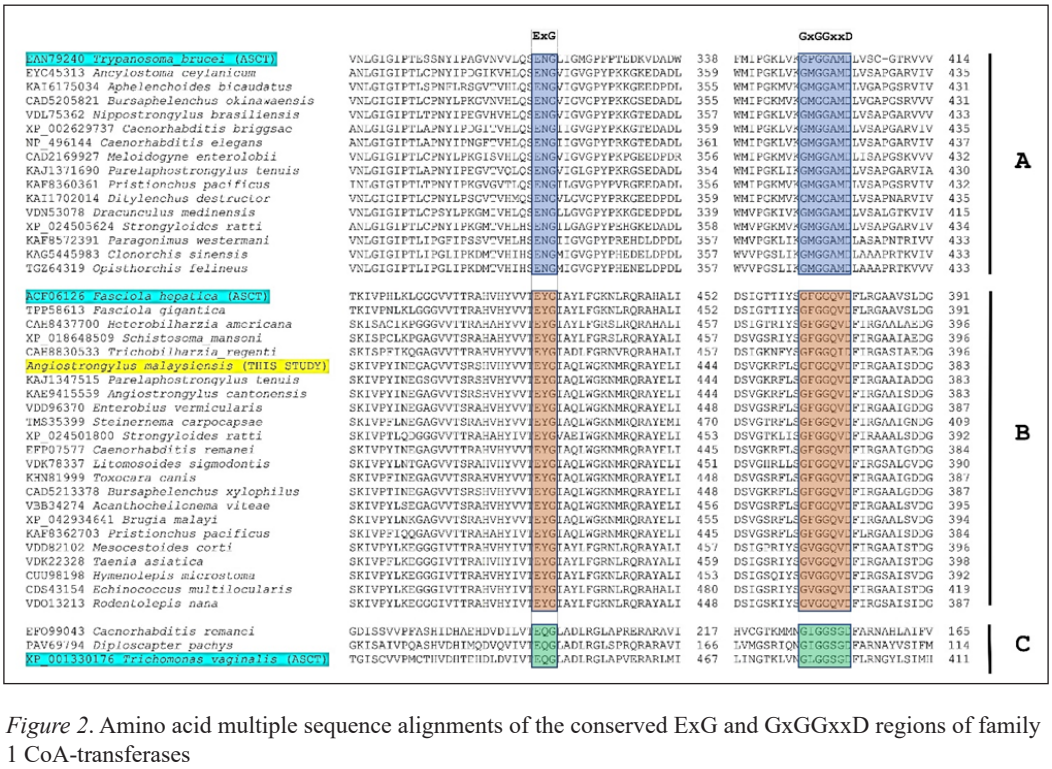

Figure 2. Amino acid multiple sequence alignments of the conserved ExG and GxGGxxD regions of family 1 CoA-transferases

IAs of ASCTs have a broader SENG motif since they are grouped with the mammalian succinyl-CoA:3-ketoacid CoA transferase (SCOT) enzyme (Rivière et al., 2004). This conserved SENG motif contains the glutamate residue active site of CoA-transferase (Rangarajan et al., 2005). On the other hand, ASCTs in subfamily IB and subfamily IC do not have the conserved SENG motif but instead possess a conserved ExG motif, which is believed to be a constituent of the more prominent SENG motif found within subfamily IA (Tielens et al., 2010). All the subfamilies of ASCT have the conserved GxGGxxD motif, an integral component of the oxyanion hole (Rangarajan et al., 2005; Tielens et al., 2010). The relative position of the GxGGxxD motif to the ExG motif was consistent between subfamily IB and IC. However, there was a notable difference in the expression of subfamily IA. In subfamily IA, the ExG motif was located proximal to the N-terminal region, whereas the GxGGxxD motif was situated toward the C-terminal region. The opposite trend occurs in subfamilies IB and IC.

Phylogenetic Analysis of Helminth ASCT

The phylogenetic tree constructed from the multiple amino acid alignment of ASCTs from helminth parasites is presented in Figure 3. The phylogenetic tree showed that the ASCTs of helminth parasites consisted of two clades: subfamilies IB and IC were in the same clade, while subfamily IA was in the other clade. Subfamilies IB and IC were divided into two distinct clusters within their clades. The phylogenetic tree in Figure 2 shows that subfamilies IB and IC are closer to each other than to subfamily IA. The putative *Am*ASCT obtained in this study clustered with the previously characterised ASCT of *F. hepatica* in subfamily IB.

The CoA-transferases responsible for the generation of acetate in parasites have been well-recognised as succinate-dependent enzymes and are thus referred to as acetate/succinate CoA-transferases. The CoA moiety of acetyl-CoA was transferred to succinate, resulting in the production of acetate and succinyl-CoA. To date, all eukaryotic ASCTs found are family I CoA-transferases. These enzymes are distinguished by their ability to transfer CoA groups, which involve a glutamate residue located in the active region of the enzyme (Heider, 2001). The identification and characterisation of the ASCT gene have been conducted in the helminth parasite *F. hepatica* (van Grinsven et al., 2009) and two other protist parasites, *T. brucei* (Rivière et al., 2004) and *T. vaginalis* (van Grinsven et al., 2008). The ASCT genes from these three parasites were found to share little homology, thus characterising them into three different subfamilies of the family I CoA-transferases (Tielens et al., 2010).

The ASCT enzymes of *T. brucei* were classified into subfamily IA of the family I CoA-transferases. ASCT in subfamily IA was found to exhibit significant homology to SCOT. This enzyme plays a crucial role in using ketone bodies inside the mitochondria of the human brain and muscle (Fukao et al., 2004). Among the three subfamilies, only

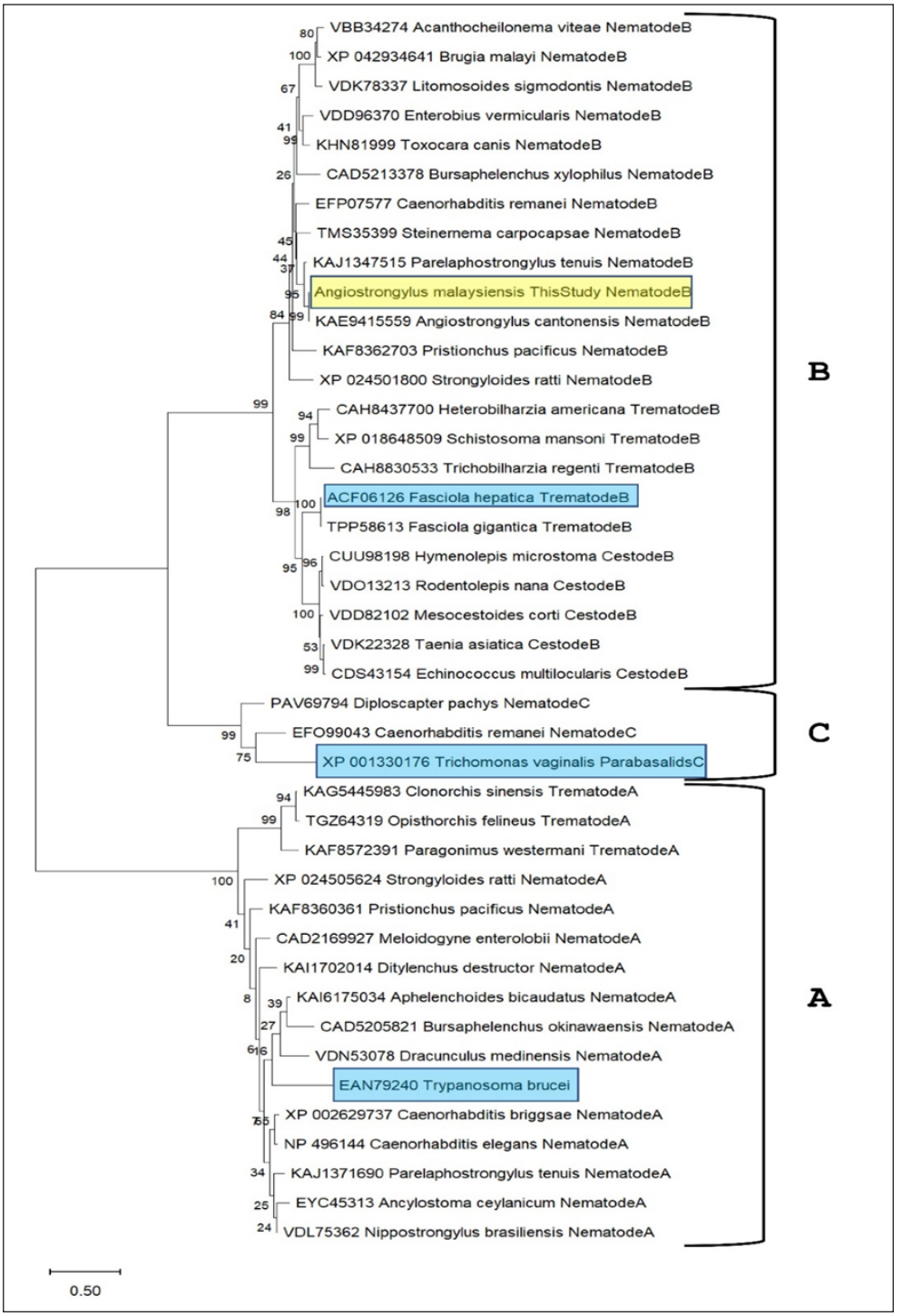

Figure 3. Phylogenetic tree of the ASCT gene of helminth parasites

subfamily IA exhibited homology to enzymes present in mammals. ASCT in subfamily IA occurs in the aerobic mitochondria of trypanosomatids and other metazoans (Rivière et al., 2004). The ASCT enzyme of *F. hepatica* was previously classified into subfamily IB and occurs in the anaerobically functioning mitochondria of metazoan organisms. The ASCTs of parasitic helminths mainly belong to subfamily IB of the family I CoA-transferases (Tielens et al., 2010). ASCT of *T. vaginalis* was classified into the subfamily IC. Unlike those in subfamilies IA and IB, ASCT in subfamily IC did not occur in mitochondria but in anaerobic hydrogenosomes (van Grinsven et al., 2008). Hydrogenosomes are membrane-bound organelles that are involved in the production of hydrogen. These organelles are closely linked to mitochondria, although they develop independently in different protists (Cavalier-Smith & Chao, 1996).

A previous study revealed the possibility that hydrogenosomes and mitochondria are evolutionarily related and that hydrogenosomes have undergone evolutionary changes due to adaptation to anaerobic environments (Martin & Muller, 1998; Roger et al., 1996). The exact evolutionary relationship between mitochondria and hydrogenosomes is currently disputed in the academic community. ASCT coupled with the succinyl-CoA synthase (SCS) cycle is the only catabolic pathway identified in mitochondria and hydrogenosomes. Nevertheless, based on the phylogenetic tree (Figure 3), the mitochondrial ASCT of *T. brucei* in subfamily IA lacks similarity with the hydrogenosomal ASCT of *T. vaginalis* in subfamily IC, as does the mitochondrial ASCT of *F. hepatica* in subfamily IB. Hence, if both mitochondria and hydrogenosomes are evolutionarily related, it may be inferred that the occurrence of ASCT enzyme activity within organelles derived from endosymbiotic events has separately undergone convergent evolution on at least two separate occasions. Additionally, based on the multiple sequence alignment previously discussed in this study (Figure 2), there was a significant difference in the relative location of the oxyanion hole GxGGxxD motif and the active site ExG motif between subfamily IA and subfamilies IB and IC. The positioning of the two conserved motifs is the same in subfamilies IB and IC but different in subfamily IA (Tielens et al., 2010). This relative location of both conserved regions may contribute to positioning the three subfamilies in the phylogenetic tree.

Pairwise analyses were also conducted to infer genetic variations between and within the three subfamilies of the family I CoA-transferases. The genetic variations within subfamilies ranged from 0.04% to 0.85% for subfamily IA (Table 3), 0.005% to 0.78% for subfamily IB (Table 4), and 0.56% to 0.63% for subfamily IC (Table 5). In subfamily IA, the highest genetic variation between helminths was observed between *Caenorhabditis briggsae* and *Opistorchis felineus* (0.760%), while the lowest was observed between *Clonorchis sinensis* and *Opisthorchis felineus* (0.039%). In subfamily IB, the highest genetic variation between helminths was observed between *Trichobilharzia regenti* and *P. pacificus* (0.781%), while the lowest variation was observed between *Fasciola*

Table 3
Pairwise genetic variation in percentage (%) for helminth parasites in subfamily IA*

	T.b	**A.c**	**A.b**	**B.o**	***N.b***	***C.b***	***C.e***	***M.e***	***P.t***	***P.p***	***D.d***	***D.m***	***S.r***	***P.w***	***C.s***	***O.f***
*T.*b																
A.c	0.663															
A.b	0.648	0.341														
B.o	0.665	0.351	0.228													
N.b	0.664	0.112	0.341	0.355												
C.b	0.713	0.149	0.355	0.355	0.176											
C.e	0.720	0.141	0.342	0.348	0.174	0.061										
M.e	0.663	0.324	0.307	0.315	0.329	0.359	0.354									
P.t	0.671	0.172	0.345	0.361	0.163	0.183	0.187	0.345								
P.p	0.680	0.211	0.342	0.338	0.209	0.206	0.197	0.315	0.262							
D.d	0.696	0.314	0.318	0.341	0.325	0.332	0.324	0.268	0.321	0.277						
D.m	0.670	0.336	0.363	0.375	0.346	0.352	0.341	0.361	0.368	0.318	0.335					
S.r	0.706	0.351	0.411	0.410	0.378	0.353	0.335	0.396	0.368	0.366	0.408	0.395				
P.w	0.802	0.671	0.591	0.645	0.651	0.717	0.707	0.664	0.679	0.681	0.662	0.643	0.658			
C.s	0.827	0.682	0.623	0.669	0.683	0.747	0.709	0.663	0.670	0.691	0.678	0.638	0.684	0.289		
O.f	0.846	0.680	0.628	0.667	0.673	0.760	0.725	0.656	0.676	0.702	0.685	0.649	0.706	0.272	0.039	

Note. T.*b = Trypanosoma brucei*, *A.c = Ancylostoma ceylanicum*, *A.b = Aphelenchoides bicaudatus*, *B.o = Bursaphelenchus okinawaensis*, *N.b = Nippostrongylus brasiliensis*, *C.b = Caenorhabditis briggsae*, *C.e = Caenorhabditis elegans*, *M.e = Meloidogyne enterolobii*, *P.t = Parelaphostrongylus tenuis*, *P.p = Pistionchus pacificus*, *D.d = Ditylenchus destructor*, *D.m = Dracunculus medinensis*, *S.r = Strongyloides ratti*, *P.w = Paragonimus westermani*, *C.s = Clonorchis sinensis*, *O.f = Opisthorchis felineus*

Table 4
Pairwise genetic variation in percentage (%) for helminth parasites in subfamily IB*

	F.h	**F.g**	**H.a**	**S.m**	**T.r**	**A.m**	**P.t**	**A.c**	**E.v**	**S.c**	**S.r**	**C.r**	**L.s**	**T.c**	**B.x**	**A.v**	**B.m**	**P.p**	**M.c**	**T.a**	**H.m**	**E.m**	**R.n**
F.h																							
F.g	0.005																						
H.a	0.388	0.392																					
S.m	0.378	0.375	0.170																				
T.r	0.463	0.468	0.277	0.362																			
A.m	0.597	0.597	0.680	0.637	0.689																		
P.t	0.583	0.583	0.680	0.667	0.701	0.057																	
A.c	0.597	0.596	0.681	0.636	0.690	0.005	0.062																
E.v	0.588	0.593	0.667	0.658	0.692	0.242	0.240	0.246															
S.c	0.611	0.617	0.683	0.653	0.705	0.185	0.169	0.189	0.252														
S.r	0.631	0.629	0.698	0.689	0.737	0.346	0.327	0.349	0.355	0.345													
C.r	0.632	0.629	0.669	0.645	0.671	0.174	0.175	0.177	0.281	0.201	0.322												
L.s	0.645	0.644	0.680	0.657	0.714	0.303	0.317	0.302	0.266	0.333	0.381	0.306											
T.c	0.602	0.607	0.670	0.652	0.687	0.198	0.179	0.202	0.129	0.224	0.331	0.220	0.247										
B.x	0.648	0.644	0.690	0.704	0.710	0.281	0.264	0.280	0.290	0.291	0.341	0.291	0.330	0.272									
A.v	0.642	0.641	0.680	0.640	0.720	0.307	0.326	0.304	0.277	0.337	0.386	0.326	0.113	0.271	0.352								
B.m	0.645	0.644	0.682	0.648	0.728	0.300	0.308	0.297	0.247	0.325	0.374	0.290	0.098	0.241	0.328	0.082							
P.p	0.696	0.702	0.725	0.714	0.781	0.316	0.318	0.321	0.295	0.291	0.353	0.275	0.374	0.291	0.401	0.372	0.348						
M.c	0.296	0.295	0.441	0.465	0.505	0.614	0.594	0.610	0.622	0.602	0.632	0.629	0.657	0.633	0.661	0.640	0.646	0.691					
T.a	0.292	0.292	0.432	0.447	0.519	0.634	0.612	0.630	0.642	0.613	0.647	0.656	0.669	0.639	0.658	0.652	0.658	0.701	0.062				
H.m	0.291	0.290	0.444	0.461	0.518	0.613	0.594	0.610	0.614	0.608	0.629	0.629	0.644	0.621	0.664	0.635	0.641	0.693	0.078	0.081			
E.m	0.299	0.298	0.442	0.457	0.521	0.642	0.626	0.637	0.646	0.629	0.653	0.658	0.675	0.643	0.663	0.658	0.666	0.702	0.062	0.025	0.081		
R.n	0.295	0.294	0.463	0.465	0.522	0.620	0.602	0.615	0.623	0.612	0.631	0.639	0.652	0.636	0.671	0.640	0.647	0.695	0.070	0.073	0.028	0.070	

Note. F.h = Fasciola hepatica, F.g = Fasciola gigantica; *H.a = Heterobilharzia americana*; *S.m = Schistosoma mansoni*; *T.r = Trichobilharzia regent*; *A.m = Angiostrongylus malaysiensis*; *P.t = Parelaphostrongylus tenuis*; *A.c = Angiostrongylus cantonensis*; *E.v = Enterobius vermicularis*; *S.c = Steinernema carpocapsae*; *S.r = Strongyloides ratti*; *C.r = Caenorhabditis remanei*; *L.s = Litomosoides sigmodontis*; *T.c = Toxocara canis*; *B.x = Bursaphelenchus xylophilus*; *A.v = Acanthocheilonema viteae*; *B.m = Brugia malayi*; *P.p = Pristionchus pacificus*; *M.c =Mesocestoides corti*; *T.a = Taenia asiatica*; *H.m = Hymenolepis microstoma*; *E.m = Echinococcus multilocularis*; *R.n = Rodentolepis nana*

hepatica and *Fasciola gigantica* (0.005%). Similarly, low variation was observed between *Angiostrongylus malaysiensis* and *Angiostrongylus cantonensis* (0.005%). Although both *C. briggsae* and *O. felineus* are in subfamily IA, *C. briggsae* is a nematode helminth, while *O. felineus* is a trematode. The same is true for *T. regenti* and *P. pacificus* in subfamily IB; *T. regenti* is a trematode, while *P. pacificus* is a nematode. Moreover, *Clonorchis sinensis* and *Opisthorchis felineus* in subfamily IA are both trematodes. In subfamily IB, *F. hepatica* and *F. gigantica* are parasites of the same genus, similar to *A. malaysiensis* and *A. cantonensis*, which explains the slight variation observed between these parasites. There was high genetic variation between parasites in the subfamily IC (Table 5). However, only two ASCT sequences of helminth parasites were found with the addition of the previously characterised ASCT of *T. vaginalis*.

Table 5
Pairwise genetic variation in percentage (%) for helminth parasites in subfamily IC*

	C.r	**D.p**	**T.v**
C.r			
D.p	0.555		
T.v	0.627	0.625	

Note. C.r = Caenorhabditis remanei; *D.p = Diploscapter pachys*; *T.v = Trichomonas vaginalis*

Table 6
Pairwise genetic variation between subfamilies IA, IB, and IC

	IA	**IB**	**IC**
IA			
IB	3.828		
IC	3.651	1.933	

A pairwise genetic comparison between the subfamilies was also conducted, where subfamilies IB and IC were found to be most closely related to each other, with a mean genetic variation between the two groups of 1.933%. Moreover, subfamily IA was found to have more significant genetic variation than both subfamily IB (3.828%) and subfamily IC (3.651) (Table 6). The three subfamilies of the family I CoA-transferases exhibit only remote genetic relationships. Notably, subfamilies 1B and 1C demonstrated a closer genetic affinity to each other than to subfamily 1A.

CONCLUSION

The putative *Am*ASCT identified in this study possessed the ExG motif, which contains the active site's conserved glutamate residue, and the conserved GxGGxxD motif, which is part of the oxyanion hole. Both motifs are characteristic of the family I CoA-transferases. The phylogenetic tree showed that the putative *Am*ASCT gene was clustered with the previously characterised subfamily IB gene of F. hepatica ASCT, suggesting that the putative *Am*ASCT gene is a subfamily IB gene of the family I CoA-transferase. Acetate, a significant byproduct of energy metabolism in many parasites but not in their mammalian hosts, presents an appealing opportunity to advance novel antiparasitic medications. Further biochemical characterisation of this enzyme in rat lungworms and other parasites

is crucial for further understanding its role in parasite energy metabolism for survival in mammalian hosts.

ACKNOWLEDGEMENTS

The authors thank Mr Mohd Noor Md Isa for assistance with transcriptomic data analysis. This study was financially supported by the Fundamental Research Grant Scheme (FRGS) Research Grant (FRGS/1/2019/STG03/UPM/02/16) from the Ministry of Higher Education Malaysia.

REFERENCES

Bolger, A. M., Lohse, M., & Usadel, B. (2014). Trimmomatic: A flexible trimmer for Illumina sequence data. *Journal of Bioinformatics*, *30*(15), 2114–2120. https://doi.org/10.1093/bioinformatics/btu170

Buchfink, B., Xie, C., & Huson, D. H. (2014). Fast and sensitive protein alignment using DIAMOND. *Nature Methods*, *12*(1), 59–60. https://doi.org/10.1038/nmeth.3176

Camacho, C., Coulouris, G., Avagyan, V., Ma, N., Papadopoulos, J., Bealer, K., & Madden, T. L. (2009). BLAST+: Architecture and applications. *BMC Bioinformatics*, *10*, 421. https://doi.org/10.1186/1471-2105-10-421

Cavalier-Smith, T., & Chao, E. E. (1996). Molecular phylogeny of the free-living archezoan *Trepomonas agilis* and the nature of the first eukaryote. *Journal of Molecular Evolution*, *43*(6), 551–562. https://doi.org/10.1007/bf02202103

Chan, A. H. E., Chaisiri, K., Dusitsittipon, S., Morand, S., & Ribas, A. (2020). Mitochondrial ribosomal genes as novel genetic markers for discrimination of closely related species in the *Angiostrongylus cantonensis* lineage. *Acta Tropica*, *211*, 105645. https://doi.org/10.1016/j.actatropica.2020.105645

Cock, P. J. A., Grüning, B. A., Paszkiewicz, K., & Pritchard, L. (2013). Galaxy tools and workflows for sequence analysis with applications in molecular plant pathology. *PeerJ*, *1*, e167. https://doi.org/10.7717/peerj.167

de Mata, Z. S., de Bruyn, B., Saz, H., & Lo, H. S. (1997). Acetyl-CoA hydrolase activity and function in *Ascaris suum* muscle mitochondria. *Comparative Biochemistry and Physiology Part B: Biochemistry and Molecular Biology*, *116*(3), 379–383. https://doi.org/10.1016/s0305-0491(96)00266-0

Eamsobhana, P. (2014). Eosinophilic meningitis caused by *Angiostrongylus cantonensis* – A neglected disease with escalating importance. *Tropical Biomedicine*, *31*(4), 569–578.

Eamsobhana, P., Lim, P., & Yong, H. (2015). Phylogenetics and systematics of *Angiostrongylus* lungworms and related taxa (Nematoda: Metastrongyloidea) inferred from the nuclear small subunit (SSU) ribosomal DNA sequences. *Journal of Helminthology*, *89*(3), 317–325. https://doi.org/10.1017/s0022149x14000108

Finn, R. D., Clements, J., & Eddy, S. R. (2011). HMMER web server: Interactive sequence similarity searching. *Nucleic Acids Research*, *39*, W29–W37. https://doi.org/10.1093/nar/gkr367

Fleck, C. B., & Brock, M. (2009). Re-characterization of *Saccharomyces cerevisiae* Ach1p: Fungal CoA-transferases are involved in acetic acid detoxification. *Fungal Genetics and Biology*, *46*(6-7), 473–485. https://doi.org/10.1016/j.fgb.2009.03.004

Fukao, T., Lopaschuk, G. D., & Mitchell, G. A. (2004). Pathways and control of ketone body metabolism: On the fringe of lipid biochemistry. *Prostaglandins, Leukotrienes and Essential Fatty Acids*, *70*(3), 243–251. https://doi.org/10.1016/j.plefa.2003.11.001

Grabherr, M. G., Haas, B. J., Yassour, M., Levin, J. Z., Thompson, D. A., Amit, I., Adiconis, X., Fan, L., Raychowdhury, R., Zeng, Q., Chen, Z., Mauceli, E., Hacohen, N., Gnirke, A., Rhind, N., di Palma, F., Birren, B. W., Nusbaum, C., Lindblad-Toh, K. … Regev, A. (2011). Full-length transcriptome assembly from RNA-Seq data without a reference genome. *Nature Biotechnology*, *29*(7), 644–652. https://doi.org/10.1038/nbt.1883

Haas, B. J., Papanicolaou, A., Yassour, M., Grabherr, M., Blood, P. D., Bowden, J., Couger, M. B., Eccles, D., Li, B., Lieber, M., MacManes, M. D., Ott, M., Orvis, J., Pochet, N., Strozzi, F., Weeks, N., Westerman, R., William, T., Dewey, C. N. … Regev, A. (2013). De novo transcript sequence reconstruction from RNA-seq using the Trinity platform for reference generation and analysis. *Nature Protocols*, *8*(8), 1494–1512. https://doi.org/10.1038/nprot.2013.084

Heider, J. (2001). A new family of CoA-transferases. *FEBS Letters*, *509*(3), 345–349. https://doi.org/10.1016/S0014-5793(01)03178-7

Hunt, M. C., & Alexson, S. E. (2008). Novel functions of acyl-CoA thioesterases and acyltransferases as auxiliary enzymes in peroxisomal lipid metabolism. *Progress in Lipid Research*, *47*(6), 405-421. https://doi.org/10.1016/j.plipres.2008.05.001

Lee, F. J., Lin, L. W., & Smith, J. A. (1989). Purification and characterization of an acetyl-CoA hydrolase from *Saccharomyces cerevisiae*. *European Journal of Biochemistry*, *184*(1), 21–28. https://doi.org/10.1111/j.1432-1033.1989.tb14985.x

Lee, F. J., Lin, L. W., & Smith, J. A. (1990). A glucose-repressible gene encodes acetyl-CoA hydrolase from *Saccharomyces cerevisiae*. *Journal of Biological Chemistry*, *265*(13), 7413–7418. https://doi.org/10.1016/j.jbc.1990.003

Low, S. Y., Lau, S. F., Ahmad, N. I., Sharma, R. S. K., Rosli, M. Z., Mohd-Taib, F. S., Md. Ajat, M. M., Kamaludeen, J., Syed Hussain, S. S., Wan, K.-L., Salleh, A., & Abdul Aziz, N. A. (2023). A cross-sectional study of *Angiostrongylus malaysiensis* in rats and gastropod hosts from recreational parks in Kuala Lumpur, Malaysia: Detection, risk factors and pathology. *Zoonoses and Public Health*, *70*(7), 636-646. https://doi.org/10.1111/zph.13072

Mack, M., & Buckel, W. (1997). Conversion of glutaconate CoA-transferase from *Acidaminococcus fermentans* into an acyl-CoA hydrolase by site-directed mutagenesis. *FEBS Letters*, *405*(2), 209–212. https://doi.org/10.1016/s0014-5793(97)00187-7

Martin, W., & Müller, M. (1998). The hydrogen hypothesis for the first eukaryote. *Nature*, *392*, 37–41. https://doi.org/10.1038/32096

Murphy, G. S., & Johnson, S. (2013). Clinical aspects of eosinophilic meningitis and meningoencephalitis caused by *Angiostrongylus cantonensis*, the rat lungworm. *Hawaii Journal of Medicine and Public Health*, *72*, 35–40.

Rangarajan, E. S., Li, Y., Ajamian, E., Iannuzzi, P., Kernaghan, S. D., Fraser, M. E., Cygler, M., & Matte, A. (2005). Crystallographic trapping of the glutamyl-CoA thioester intermediate of family I CoA transferases. *Journal of Biological Chemistry*, *280*(52), 42919–42928. https://doi.org/10.1074/jbc.m510522200

Reeves, R. E., Warren, L. G., Susskind, B., & Lo, H. S. (1977). An energy-conserving pyruvate-to-acetate pathway in *Entamoeba histolytica*. *Journal of Biological Chemistry*, *252*, 726–731.

Rivière, L., van Weelden, S. W. H., Glass, P., Vegh, P., Coustou, V., Biran, M., van Hellemond, J. J., Bringaud, F., Tielens, A. G. M., & Boshart, M. (2004). Acetyl CoA-transferase in procyclic *Trypanosoma brucei*. *Journal of Biological Chemistry*, *279*(44), 45337–45346. https://doi.org/10.1074/jbc.m407513200

Roger, A. J., Clark, C. G., & Doolittle, W. F. (1996). A possible mitochondrial gene in the early-branching amitochondriate protist *Trichomonas vaginalis*. *Proceedings of the National Academy of Sciences of the United States of America*, *93*(25), 14618–14622. https://doi.org/10.1073/pnas.93.25.14618

Sánchez, L. B., Galperin, M. Y., Müller, M. (2000). Acetyl-CoA synthetase from the amitochondriate eukaryote *Giardia lamblia* belongs to the newly recognized superfamily of acyl-CoA synthetases (Nucleoside diphosphate-forming). *Journal of Biological Chemistry*, *275*, 5794–5803. https://doi.org/10.1074/jbc.275.8.5794

Sawanyawisuth, K., & Sawanyawisuth, K. (2008). Treatment of angiostrongyliasis. *Transactions of the Royal Society of Tropical Medicine and Hygiene*, *102*(10), 990-996. https://doi.org/10.1016/j.trstmh.2008.04.021

Saz, H. J., deBruyn, B., & de Mata, Z. (1996). Acyl-CoA transferase activities in homogenates of *Fasciola hepatica* adults. *Journal of Parasitology*, *82*(5), 694–696. https://doi.org/10.2307/3283876

Slom, T. J., Cortese, M. M., Gerber, S. I., Jones, R. C., Holtz, T. H., Lopez, A. S., Zambrano, C. H., Sufit, R. L., Sakolvaree, Y., Chaicumpa, W., Herwaldt, B. L., & Johnson, S. (2002). An outbreak of eosinophilic meningitis caused by *Angiostrongylus cantonensis* in travelers returning from the Caribbean. *New England Journal of Medicine*, *346*(9), 668-675. https://doi.org/10.1056/nejmoa012462

Stechmann, A., Hamblin, K., Pérez-Brocal, V., Gaston, D., Richmond, G. S., van der Giezen, M., Clark, C. Graham, & Roger, A. J. (2008). Organelles in *Current Biology*, *18*, 580–585. https://doi.org/10.1016/j.cub.2008.03.037

Steinbüchel, A., Müller, M. (1986). Anaerobic pyruvate metabolism of *Tritrichomonas foetus* and *Trichomonas vaginalis* hydrogenosomes. *Molecular and Biochemical Parasitology*, *20*(1), 57–65. https://doi.org/10.1016/0166-6851(86)90142-8

Tamura, K., Stecher, G., Kumar, S. (2021). MEGA11: Molecular evolutionary genetics analysis version 11. *Molecular Biology and Evolution*, *38*(7), 3022-3027. https://doi.org/10.1093/molbev/msab120

Thompson, J. D., Higgins, D. G., Gibson, T. J. (1994). CLUSTAL W: Improving the sensitivity of progressive multiple sequence alignment through sequence weighting, position-specific gap penalties and weight matrix choice. *Nucleic Acids Research*, *22*(22), 4673-4680. https://doi.org/10.1093/nar/22.22.4673

Tielens, A. G. M., Rotte, C., Van-Hellemond, J. J., Martin, W. (2002). Mitochondria as we don't know them. *Trends in Biochemical Sciences*, *27*, 564–572. https://doi.org/10.1016/s0968-0004(02)02193-x

Tielens, A. G. M., van Grinsven, K. W. A., Henze, K., van Hellemond, J. J., & Martin, W. (2010). Acetate formation in the energy metabolism of parasitic helminths and protists. *International Journal for Parasitology*, *40*(4), 387–397. https://doi.org/10.1016/j.ijpara.2009.12.006

van Grinsven, K. W. A., Rosnowsky, S., van Weelden, S. W. H., Pütz, S., van der Giezen, M., Martin, W., van Hellemond, J. J., Tielens, A. G. M., & Henze, K. (2008). Acetate CoA-transferase in the hydrogenosomes

of *Trichomonas vaginalis*: Identification and characterization. *Journal of Biological Chemistry*, *283*(3), 1411–1418. https://doi.org/10.1074/jbc.m702528200

van Grinsven, K. W. A., van Hellemond, J. J., Tielens, A. G. M. (2009). Acetate CoA-transferase in the anaerobic mitochondria of *Fasciola hepatica*. *Molecular and Biochemical Parasitology*, *164*(1), 74–79. https://doi.org/10.1016/j.molbiopara.2008.11.008

van Hellemond, J. J., Opperdoes, F. R., & Tielens, A. G. M. (1998). Trypanosomatidae produce acetate via a mitochondrial acetate CoA transferase. *Proceedings of the National Academy of Sciences of the United States of America*, *95*(6), 3036–3041. https://doi.org/10.1073/pnas.95.6.3036

Wang, Q.-P., Lai, D.-H., Zhu, X.-Q., Chen, X.-G., & Lun, Z.-R. (2008). Human angiostrongyliasis. *The Lancet Infectious Diseases*, *8*, 621–630. https://doi.org/10.1016/s1473-3099(08)70229-9

Watthanakulpanich, D., Jakkul, W., Chanapromma, C., Ketboonlue, T., Dekumyoy, P., Lv, Z., Chan, A. H. E., Thaenkham, U., & Chaisiri, K. (2021). Co-occurrence of *Angiostrongylus malaysiensis* and *Angiostrongylus cantonensis* DNA in cerebrospinal fluid: Evidence from human eosinophilic meningitis after ingestion of raw snail dish in Thailand. *Food and Waterborne Parasitology*, *24*, e00128. https://doi.org/10.1016/j.fawpar.2021.e00128

White, H., & Jencks, W. P. (1976). Mechanism and specificity of succinyl-CoA:3-ketoacid coenzyme A transferase. *Journal of Biological Chemistry*, *251*(6), 1688–1699. https://doi.org/10.1016/S0021-9258(17)33704-3

Wilkins, M. R., Gasteiger, E., Bairoch, A., Sanchez, J. C., Williams, K. L., Appel, R. D., & Hochstrasser, D. F. (1999). Protein identification and analysis tools in the *ExPASy server*. *Methods in Molecular Biology*, *112*, 531–552. https://doi.org/10.1385/1-59259-584-7:531

Xu, L., Xu, M., Sun, X., Xu, J., Zeng, X., Shan, D., Yuan, D., He, P., He, W., Yang, Y., Luo, S., Wei, J., Wu, X., Liu, Z., Xu, X., Dong, Z., Song, L., Zhang, B., Yu, Z. … Wu, Z. (2019). The genetic basis of adaptive evolution in parasitic environment from the *Angiostrongylus cantonensis* genome. *PLoS Neglected Tropical Diseases*, *13*(11), e0007846. https://doi.org/10.1371/journal.pntd.0007846

Zeiher, C. A., & Randall, D. D. (1990). Identification and characterization of mitochondrial acetyl-coenzyme A hydrolase from *Pisum sativum* L. seedlings. *Plant Physiology*, *94*(1), 20-27. https://doi.org/10.1104/pp.94.1.20

Pertanika J. Trop. Agric. Sci. 48 (3): 767 - 780 (2025)

PERTANIKA JOURNALS

TROPICAL AGRICULTURAL SCIENCE

Journal homepage: http://www.pertanika.upm.edu.my/

Effect of Solid-state Fermentation on Nutritional Value of Pineapple Leaves

Noor Hidayah Othman, Noor Fatihah Abdullah, Siti Nur 'Aisyah Mohd Roslan, Stephanie Peter, Noraziah Abu Yazid, Siti Hatijah Mortan and Rohana Abu*

Faculty of Chemical and Process Engineering Technology, Universiti Malaysia Pahang Al-Sultan Abdullah, Lebuh Persiaran Tun Khalil Yaakob, 26300, Gambang, Kuantan, Pahang, Malaysia

ABSTRACT

Pineapple leaves, a by-product of cultivation, are generally discarded and burned at the farm sites before replanting. As the demand for pineapple products increases yearly, the number of discarded leaves also increases. Valorisation of the leaves through solid-state fermentation (SSF) is a sustainable waste management approach that converts the low-nutrient substrate into valuable resources for animal feed. This study investigated the enrichment of pineapple leaf nutritional values using SSF. The process parameters such as fermentation time, inoculum type and size, additional carbon source and particle size were optimised using the one-factor-at-a-time (OFAT) method. The nutrient compositions were analysed for their total protein, total phenolic, antioxidant activity, reducing sugar and crude fibre using Bradford, Folin–Ciocalteu, DPPH (2,2-diphenyl-1-picrylhydrazyl), DNS (3,5-dinitrosalicylic acid) and AOAC978.10 methods, respectively. The optimal conditions were determined to be a 2 mm leaf particle size, 2% (w/w) *Rhizopus* sp. inoculum, and a fermentation duration of 2 days without the addition of a carbon source. Under these conditions, the nutrient enrichment resulted in a total protein content of 24.14 ± 0.31 mg/g, total phenolics of 11.81 ± 0.50 mg/g, antioxidant activity of 3.17 ± 0.04 mg/g, and a reducing sugar content of 12.03 ± 0.97 mg/g. Crude fibre content decreased from 20.37 ± 1.10% in unfermented leaves to 6.77 ± 0.44% after fermentation, potentially improving nutrient digestibility due to the reduction of indigestible fibre. These results demonstrate that SSF is a promising method to enhance the nutrient content of pineapple leaves, offering an alternative nutrient source for animal feed.

Keywords: Antioxidants, nutrient content, phenolics, pineapple leaves, solid-state fermentation

ARTICLE INFO

Article history:
Received: 07 August 2024
Accepted: 15 October 2024
Published: 16 May 2025

DOI: https://doi.org/10.47836/pjtas.48.3.07

E-mail addresses:
hidayahothman104@gmail.com (Noor Hidayah Othman)
TJ20057@student.ump.edu.my (Noor Fatihah Abdullah)
TJ20066@student.ump.edu.my (Siti Nur 'Aisyah Mohd Roslan)
TJ20041@student.ump.edu.my (Stephanie Peter)
noraziahay@umpsa.edu.my (Noraziah Abu Yazid)
hatijah@umpsa.edu.my (Siti Hatijah Mortan)
rohanaa@umpsa.edu.my (Rohana Abu)
*Corresponding author

INTRODUCTION

Malaysia is one of the pineapple-producing countries, with a total production of 289,763 metric tons from a planting area of 10,567 hectares in 2021. Production increased by 16% compared to 2020, contributing to the country's economic growth alongside other main products such as palm oil and rubber (Malaysian Pineapple Industry Board [MPIB], 2022). Along with this economic growth, the pineapple industry generates a high amount of waste every year due to the high demand for pineapple products. Moreover, the increasing tons of waste is due to the short growth and production cycle of pineapples (de Aquino Gondim et al., 2023). It contributes 45%–65% of the pineapple mass, including leaves, stems, peels, crowns and cores (Difonzo et al., 2019). Usually, the leaf waste is managed through disposal methods like open burning or natural decomposition at the farm sites. These practices raise environmental concerns, such as emissions of greenhouse gases (carbon dioxide and methane) and soil erosion, highlighting the need for a more sustainable waste management solution (Aili Hamzah et al., 2021).

Numerous studies have reported the chemical compositions of pineapple waste, including its nutritional content, volatile compounds and bioactive compounds (Baidhe et al., 2021; Polanía et al., 2023; Roda & Lambri, 2019). In particular, the nutrient content of pineapple leaves contains beneficial nutrients such as total sugar, crude fibre, crude protein, organic acids, phenolic content and antioxidants (Arampath & Dekker, 2019; Awasthi et al., 2022; Nath et al., 2023). However, despite the availability of these nutrient content, studies have reported that the leaves still contain high indigestible fibre and low protein content (Sukri et al., 2023). Current research has focused on utilising pineapple leaves for the production of bio-composite (Tripathi et al., 2022) and biofuel (Chintagunta et al., 2017; Mund et al., 2022).

Pineapple leaves should be converted using innovative approaches to increase their nutritional value, like protein before being utilised as animal feed for a sustainable agriculture system. There is an increasing demand for feed protein in animal production. Therefore, it is essential to explore alternative protein sources other than soybean meal (Kim et al., 2019). There is also a growing interest in the application of solid-state fermentation (SSF) using microbes such as fungi and yeast to improve the protein content of low-nutrient agricultural waste such as peels and pulps for animal feed production (Wang et al., 2023). Besides, SSF offers uncomplicated product recovery, allowing the resulting product to be directly utilised as animal feed (Yafetto et al., 2023). In other words, SSF can improve the quality of agricultural waste while effectively sustainably managing solid waste (Yazid et al., 2017). Therefore, SSF was used in this work to improve the nutrient content in pineapple leaves. The effects of different SSF parameters, including fermentation time, particle size, carbon source and inoculum type on the total protein, total phenolics, antioxidants, reducing sugar and crude fibre, were investigated.

MATERIALS AND METHODS

Materials

Bradford reagent, magnesium sulphate, potassium dihydrogen phosphate, sulfuric acid and hydrochloric acid were obtained from Sigma-Aldrich (St. Louis, USA). Folin-Ciocalteu reagent was purchased from Chemiz (Selangor, Malaysia). 2,2-Diphenyl-1-picrylhydrazyl (DPPH), bovine serum albumin (BSA), dinitrosalisylic acid (DNS) and potassium sodium tartrate were purchased from Macklin (Shanghai, China). Glucose, sodium hydroxide, gallic acid, ascorbic acid, and ethanol were procured from HmbG Chemicals (Hamburg, Germany). Palm oil decanter cake was collected at Banting, Selangor. Effective microorganisms (EM4) and *Rhizopus* sp. were bought from BH Farm (Perak, Malaysia) and Raprima (Bandung, Indonesia), respectively. Longan syrup was obtained from KBK Greenleaf Enterprise (Kedah, Malaysia).

Preparation of Pineapple Leaves Powder

Pineapple leaves were collected at Sweetpine Pineapple farm in Kuantan, Pahang. They were dried under sunlight for three days. After that, they were cut into smaller sizes and dried in an oven at 70°C for 48 h. The dried leaves were ground before sieving through a 4 mm Retsch sieve.

Solid-state Fermentation

Experiments were carried out using the one-factor-at-a-time (OFAT) method to determine the optimum nutrient content in the fermented pineapple leaves. In the SSF, 3% (w/w) of *Rhizopus* sp. was added in a mixture containing 50 g of 4-mm leaves sample and 3% (w/w) of spent coffee ground as a nitrogen source. Subsequently, 45 ml of trace elements consisting of 1 g/L magnesium sulphate, 2 g/L potassium dihydrogen phosphate and 0.4 N hydrochloric acid were added to the mixture (Kupski et al., 2012). Then, 20% (w/v) of the bulking agent was mixed with the mixture before being incubated at 30°C for 3 days. The procedure was repeated at different fermentation parameters such as fermentation time (1–5 days), substrate particle size (2–20 mm), inoculum type (effective microorganism 4, palm decanter cake), inoculum size (1%–5% (w/w)), carbon source (sucrose, molasses, longan syrup) and carbon composition (2.5%–10% (w/w)).

Extraction of Nutrient Content

The nutrient content in unfermented and fermented pineapple leaves was analysed using 5 g of sample extracted with 50 ml of 75% ethanol. The extraction process was carried out through incubation in an ultrasonic water bath at 40°C for 1 h (Azizan et al., 2020). After that, the sample was filtered using Whatman No. 1 paper, and the filtrate was used for further analysis.

Determination of Total Protein Content

The Bradford method determined the protein content (Setti et al., 2020). Briefly, 1.5 ml of Bradford reagent was added to 0.05 ml of the sample in a cuvette. The absorbance of the mixture was measured at a wavelength of 595 nm using a UV-Vis spectrophotometer (Thermo Scientific AquaMate 7100, USA). Bovine serum albumin (BSA) concentrations (0–0.14 mg/ml) were used as the standard reference.

Determination of Total Phenolic Content

The total phenolic content (TPC) was determined using the Folin–Ciocalteu method (Azkia et al., 2023). Briefly, 0.5 ml of the sample was added to 1 ml of 10% Folin-Ciocalteu solution, followed by 1 ml of 10% sodium carbonate solution. The mixture was left in the dark at room temperature for 2 h. The absorbance of the mixture was measured at 760 nm using a UV-Vis spectrophotometer (Thermo Scientific AquaMate 7100, USA). Gallic acid concentrations (0–0.2 mg/ml) were the standard reference. The TPC in the sample was expressed as gallic acid equivalents (GAE) in mg/g.

Determination of Reducing Sugar

Reducing sugar was determined using the dinitrosalisylic acid (DNS) method (Anigboro et al., 2023). Briefly, 3 ml of the sample was added to 3 ml of 1 L solution of DNS reagent containing 10 g DNS, 2 g phenol, 0.5 g sodium sulphite and 10 g sodium hydroxide. The mixture was heated in a boiling water bath for 10 min. After that, 1 ml of a 40% potassium sodium tartrate was added to stabilise the colour developed and allowed to cool at room temperature. The absorbance of the mixture was measured at 575 nm using a UV-Vis spectrophotometer (Thermo Scientific AquaMate 7100, USA). Glucose concentrations (0–2 mg/ml) were used as the standard reference.

Determination of Antioxidant Content

The antioxidant content was determined using a 2,2-Diphenyl-1-picrylhydrazyl (DPPH) assay (Buenrostro-Figueroa et al., 2017). Briefly, 100 ml of the sample was added to 3 ml of 0.55 mM DPPH solution. The mixture was left in the dark for 30 min before measuring the absorbance at 517 nm using a UV-Vis spectrophotometer (Thermo Scientific AquaMate 7100, USA). Ascorbic acid concentrations (0-0.15 mg/ml) were the standard reference. The antioxidant content was expressed in ascorbic acid equivalents in mg/g.

Determination of Crude Fibre

The crude fibre was estimated using the Association of Official Analytical Chemists (AOAC 978.10). Briefly, 1 g of sample was boiled in 1.25% (v/v) sulphuric acid with n-octanol

for 30 min. The solution was filtered, and the residue was washed four times with boiling water. After that, the residue was boiled in 1.25% potassium hydroxide for another 30 min. The solution was filtered again, and the residue was washed four times with boiling water. The residue was transferred to a crucible, dried in an oven at 130°C for 2 h, cooled in a desiccator, and weighed. The crucible containing the ash was dried in a muffle furnace at 525°C for 3 h in a desiccator before reweighing to determine the crude fibre content using Equation 1 (Rivera et al., 2023).

$$\text{Crude fibre (\%)} = \frac{\text{Weight of crucible with fibre - Weight of crucible with ash}}{\text{Weight of sample}} \times 100\% \quad [1]$$

Statistical Analysis

The results were expressed as mean ± standard deviation (SD) from duplicate experiments using Origin 2022 software. For group comparisons, one-way Analysis of variance (ANOVA) was performed using Microsoft Excel 2016 with statistical significance set at $p<0.05$.

RESULTS AND DISCUSSION

The Nutrient Content of Unfermented Pineapple Leaves

Table 1 shows the nutrient content of raw pineapple leaves before fermentation, which served as the control throughout this study. The contents of protein, phenolics, antioxidants and reducing sugar in the unfermented pineapple leaves were 5.30 ± 0.51 mg/g, 9.93 ± 0.17 mg/g, 0.29 ± 0.10 mg/g and 6.67 ± 0.67 mg/g, respectively. The leaves also contained high crude fibre of 20.37%. Previous studies have also demonstrated the low quality of unfermented pineapple waste. Pineapple pulp waste has 0.1 mg/g of total protein and 0.27 mg/g of antioxidants (Hemalatha & Anbuselvi, 2013). The waste mixture containing pulp, peel core and crown has a low phenolic content of 1.12 mg/g (Rashad et al., 2015). The peels and leaves have crude fibre of 13.96%–14.72% (Aruna, 2019; Rivera et al., 2023) and 31% (Zainuddin et al., 2014), respectively. Based on the unfermented results, the use of pineapple waste as animal feed has limitations due to its low levels of beneficial nutrients.

Table 1
Nutrient content of unfermented pineapple leaves (raw)

Nutrient	Content
Total protein (mg/g)	5.30 ± 0.51
Total phenolic (mg/g)	9.93 ± 0.17
Antioxidant activity (mg/g)	0.29 ± 0.10
Reducing sugar (mg/g)	6.67 ± 0.67
Crude fibre (%)	20.37 ± 1.10

Effect of Fermentation Time on the Nutrient Content

Fermentation time is one of the important process variables for accessing protein enrichment in the SSF method. In this study, the highest protein content (13.96 ± 0.43 mg/g) was achieved on day 2, monitored over 5 days of fermentation time, as shown in Figure 1. It represents a 2.6-fold increase compared to unfermented pineapple leaves (5.30 ± 0.51 mg/g). Previous studies have demonstrated that extending fermentation time from 0 to 3 days can maximise protein content up to 2.8-fold in pineapple waste containing peel and core using *Aspergillus niger* and *Trichoderma viride* (Omwango et al., 2013). In another study, the total protein content increased from 30.28 ± 3.52 mg/g to 44.08 ± 4.17 mg/g after 5 days of fermenting brewery spent grain with *Bacillus velezensis* (Zeng et al., 2021). Similarly, the total protein content of dehusked barley increased from 4.76 ± 0.20 mg/g (unfermented) to 9.50 ± 0.16 mg/g after 36 h of co-fermentation with *Rhizopus oryzae* and *Lactobacillus plantarum* (Wang et al., 2020). Typically, long fermentation could yield

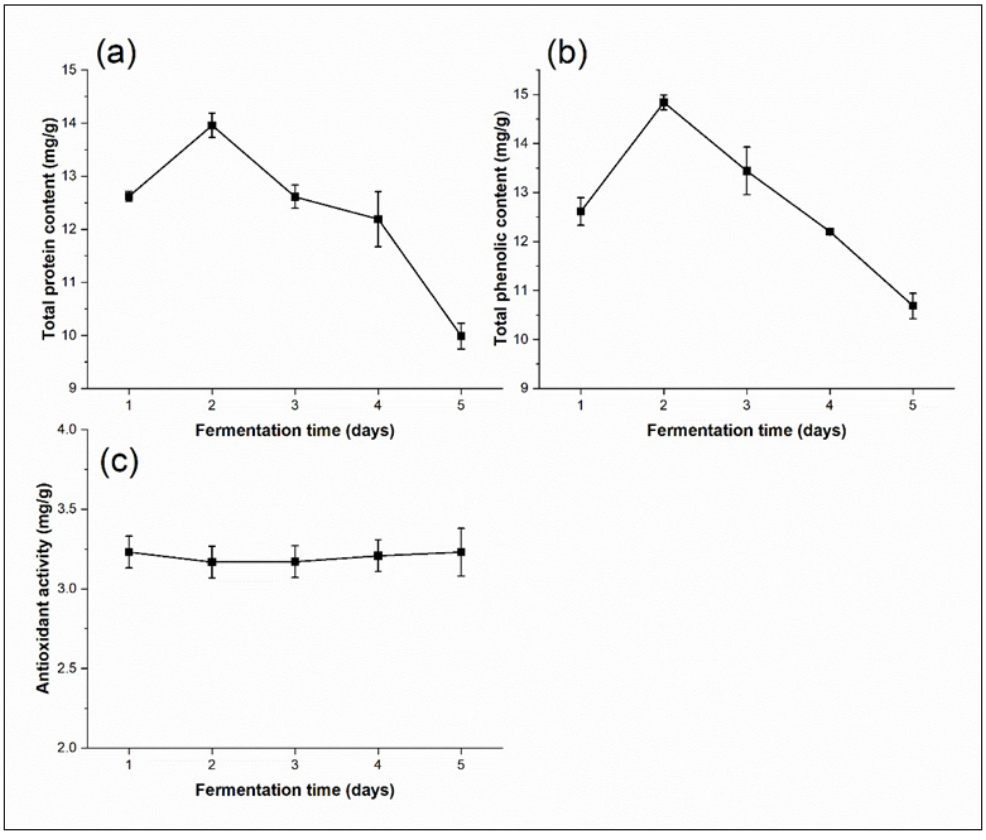

Figure 1. Effect of fermentation time on the nutrient content of fermented pineapple leaves. (a) Total protein content, (b) total phenolic content and (c) antioxidant activity. The value was expressed as the mean ± SD of duplicate experiments

optimal protein content due to fungal growth that secreted more extracellular enzymes during metabolism. However, a prolonged fermentation period may reach a plateau or even decline due to depletion of nutrients, changes in the microbial community or the accumulation of inhibitory by-products (Olorunnisola et al., 2018).

Furthermore, fungal treatment through SSF releases bioactive compounds such as phenolics and antioxidants. This enhancement was due to the degradation of lignocellulosic components, which breaks open phenol rings trapped within the lignin fraction, releasing phenolic compounds with antioxidant activity (Buenrostro-Figueroa et al., 2017). In their study investigating the effect of time, the maximal release of phenolics (4.77 mg/g) and antioxidants (0.53 mg/g) was reported at 36 h of fermentation with *A. niger*. A similar trend was observed in the present study, with total phenolic content increasing from 9.93 ± 0.17 mg/g (unfermented) to 14.84 ± 0.15 mg/g on day 2 of fermentation. Moreover, antioxidant activity on day 2 was 11-fold higher (3.17 ± 0.11 mg/g) compared to unfermented leaves (0.29 ± 0.10 mg/g). Extending the fermentation beyond day 2 did not result in a significant difference in antioxidant activity ($P>0.05$). Previous research has consistently shown that extending fermentation time enhances soluble protein, phenolic content, and antioxidant activity. For example, during SSF using ragi tape and black glutinous rice as substrates, total phenolic compounds increased from day 0 (4.65 mg/g) to day 3 (6.94 mg/g), leading to a 35.24% increase in antioxidant activity (Azkia et al., 2023). Similarly, co-fermentation with *Rhizopus oryzae* and *Lactobacillus plantarum* in dehusked barley from 0 to 36 h demonstrated an increase in soluble protein, phenolics, and antioxidants (Wang et al., 2020).

Effect of Substrate Particle Size on the Nutrient Content

Figure 2 shows the effect of pineapple leaves particle sizes on the nutrient content during SSF. The smallest particle sizes of 2 mm resulted in the highest enrichment of total protein (23.19 ± 0.52 mg/g) and total phenolics (12.61 ± 0.17 mg/g). In contrast, fermentation with the largest particle size led to only a 1.7-fold increase in total protein (9.03 ± 0.48 mg/g) compared to unfermented pineapple leaves (5.30 ± 0.51 mg/g). Similarly, there is no significant difference in antioxidant activity when using different particle sizes for fermentation ($p>0.05$). Smaller particle sizes enhance the surface area-to-volume ratio and improve the accessibility of the substrate to microorganisms, thereby promoting microbial activity and growth (Tosuner et al., 2019). Moreover, the smaller particle of the substrate sizes allows for better mass transfer between solid substrate and air surfaces, leading to a more efficient fermentation rate (Wang et al., 2023). Similarly, studies have shown that smaller particles favour higher nutrient enrichment, such as protein and phenolics in rice bran, whereas larger particles tend to generate more fungal biomass in SSF (Schmidt & Furlong, 2012).

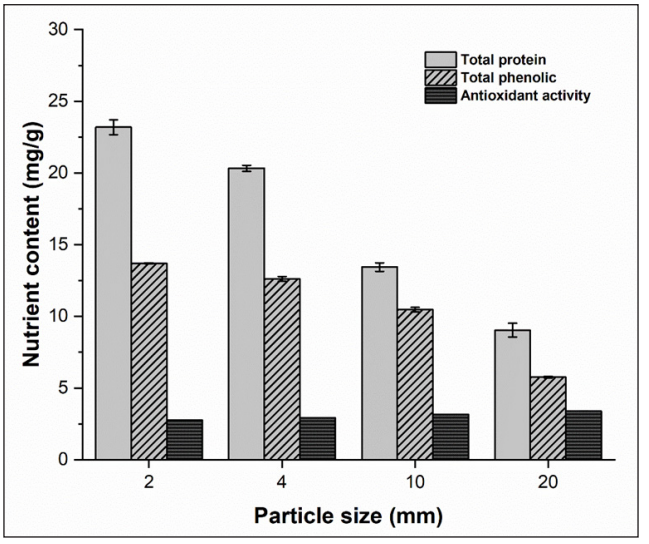

Figure 2. Effect of different particle sizes of substrate on the nutrient content of fermented pineapple leaves. The value was expressed as the mean ± SD of duplicate experiments

Effect of Inoculum Type and Size on the Nutrient Content

The impact of different types of inoculums for nutrient enrichment was evaluated using *Rhizopus* sp., effective microorganism (EM) and palm decanter cake. The results showed that *Rhizopus* sp. produced the highest protein content, followed by EM and decanter cake (Figure 3). The results suggest that all studied microbial inoculants have the potential to enhance protein content in the pineapple leaves. Additionally, raw decanter cake is rich in Indigenous microbes, making it an effective inoculum for promoting nutrient enrichment in the natural substrate (Kanchanasuta & Pisutpaisal, 2016). Besides, EM contains numerous species of microorganisms that can improve the quality of nutrients by utilising agricultural waste as a natural substrate (Hidalgo et al., 2022). The effect of inoculum size, ranging from 1% to 5% (w/w), was also studied to determine their effects on the nutrient content. However, no significant difference in the total protein content was observed despite the varying inoculum sizes within the studied range (p>0.05). The maximum protein content was achieved at 2% (w/w) of *Rhizopus* sp. with 24.14 ± 0.31 mg/g, 3% (w/w) of EM with 16.47 ± 1.19 mg/g and 1% (w/w) of decanter cake with 13.22 ± 0.65 mg/g, representing an increase of 4.5, 3.1 and 2.5 folds, respectively, compared to unfermented leaves. Several studies have shown the enrichment of low protein content in pineapple waste by SSF. The total protein content increased 4.2-fold in pineapple peels after 4 days of SSF using *Trichoderma viride* (Aruna, 2019). At the same time, a 3.5-fold increase in protein content was produced after 2 days of SSF of pineapple pulp by *Saccharomyces cerevisiae* (Correia et al., 2007).

Figure 3 also demonstrates the influence of inoculum type and size on phenolic and antioxidant content in pineapple leaves. All tested inoculum types were able to increase the bioactive compounds concerning the unfermented leaves. However, the inoculum size did not significantly impact the levels of these compounds (p>0.05). Moreover, EM inoculation created favourable conditions for greater phenolic release compared to *Rhizopus* sp. and decanter cake. A recent study has also reported increased phenolic and antioxidant contents in the pineapple peel fermented with *Rhizopus oryzae*, with phenolic content rising from 30 to 52.70 mg GAE/g and antioxidant activity increasing from 37.02% to 61.46% (Rivera et al., 2023). Additionally, SSF of pineapple peel using *A. niger* HT3 resulted in 1.5 times higher DPPH activity (60.28 ± 1.74%) compared to the unfermented peel (Casas-Rodríguez et al., 2024).

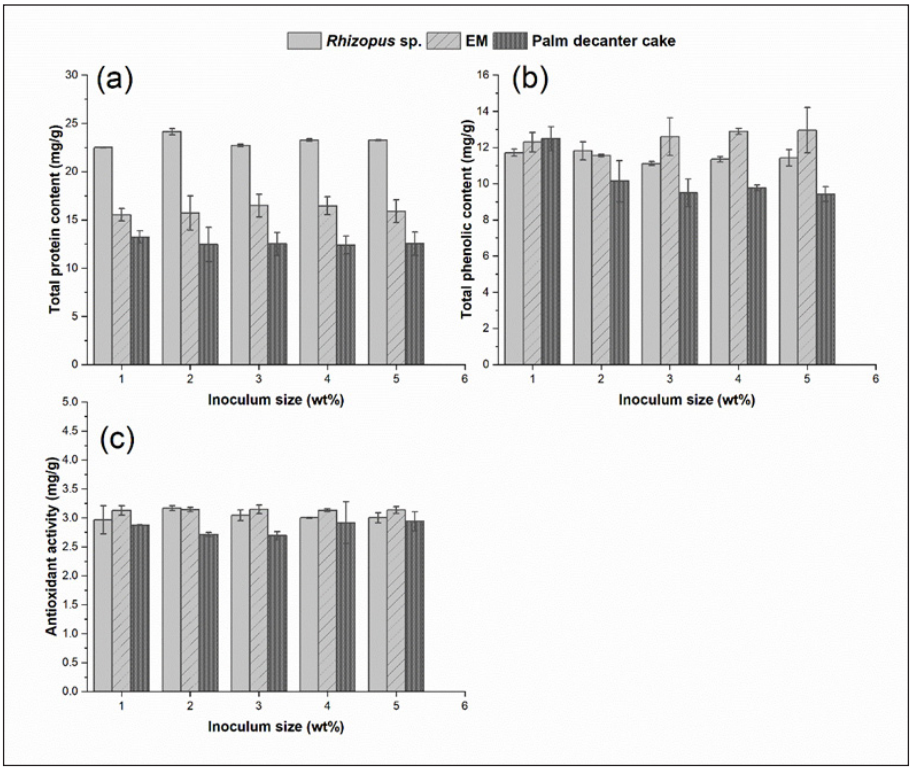

Figure 3. Effect of inoculum types and sizes on the nutrient content of fermented pineapple leaves. (a) Total protein content, (b) total phenolic content, and (c) antioxidant activity. The value was expressed as the mean ± SD of duplicate experiments

Effect of Carbon Source on the Nutrient Content

The impact of different carbon sources, including sucrose, molasses, and longan syrup, on nutrient enrichment in the SSF system using pineapple leaves was examined at varying

compositions (Figure 4). The highest yield of total protein content was achieved at 2.5% (w/w) sucrose with 24.41 ± 0.62 mg/g, followed by molasses (22.09 ± 1.91 mg/g) and longan syrup (17.17 ± 0.12 mg/g), both at 5% (w/w). The availability of sucrose serves to be a more efficient energy source for microorganism growth compared to longan syrup and molasses.

Molasses, a by-product of the sugar industry, is a suitable co-substrate due to its rich carbon content, which includes sucrose (30%–35%), fructose (10%–20%) and glucose (10%–25%) (Jamir et al., 2021). On the other hand, longan syrup contains lower levels of sucrose (14.21%), fructose (3.91%) and glucose (2.77%) (Surin et al., 2014). However, when comparing the SSF without the addition of any carbon source, the total protein content (24.14 ± 0.31 mg/g) showed no significant increase, suggesting that the native carbon sources present in pineapple leaves may be sufficient for microbial activity under certain conditions. The phenolics and antioxidants did not show positive effects in the SSF when additional carbon sources were introduced. Instead, the reduced sugar increased significantly as the carbon content increased.

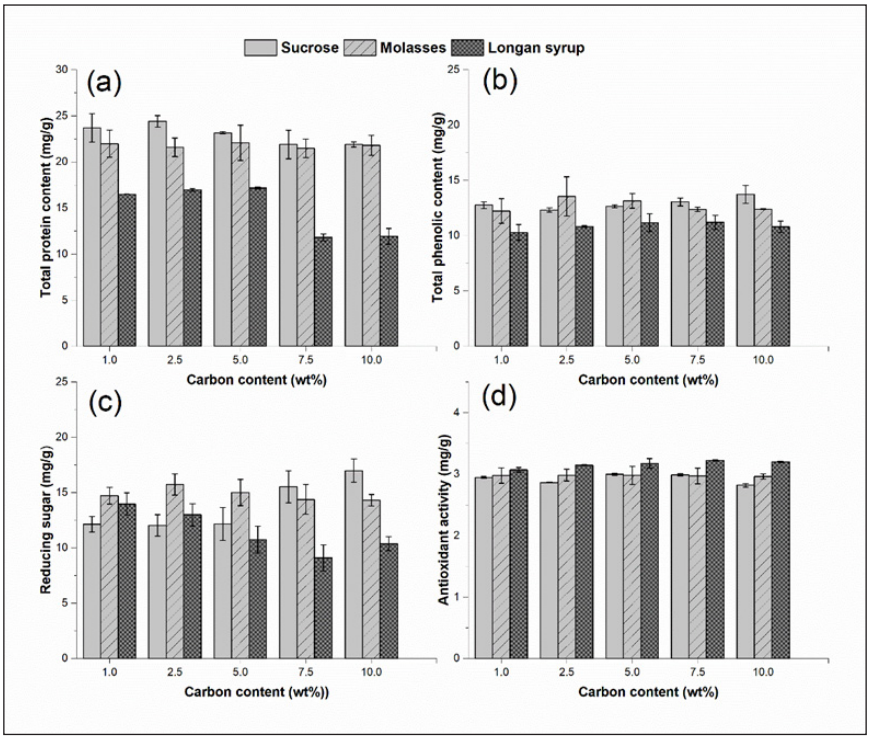

Figure 4. Effect of carbon types and size on the nutrient content of fermented pineapple leaves. (a) Total protein content, (b) total phenolic content, (c) reducing sugar, and (d) antioxidant activity. The value was expressed as the mean ± SD of duplicate experiments

CONCLUSION

The present study investigated the nutrient enrichment in pineapple leaves through solid-state fermentation. The optimal SSF conditions, determined using the OFAT method, were achieved to be 2 mm particle size of pineapple leaves, 2% (w/w) *Rhizopus* sp. inoculum, and a fermentation time of 2 days without the need for an additional carbon source. Under these conditions, the nutrient enrichment resulted in a total protein content of 24.14 ± 0.31 mg/g, total phenolic of 11.81 ± 0.50 mg/g, antioxidant activity of 3.17± 0.04 mg/g and reducing sugar of 12.03 ± 0.97 mg/g. Additionally, crude fibre was reduced from 20.37 ± 1.10% in unfermented leaves to 6.77 ± 0.44% after 2 days of fermentation. The results provide a potential approach to enhance the nutritional value of pineapple leaves through solid-state fermentation, which can be subsequently used for animal feed. Moreover, SSF offers a sustainable solution for improving the quality of agro-industrial waste, addressing solid waste management issues.

ACKNOWLEDGEMENTS

We greatly appreciate the financial support from Universiti Malaysia Pahang Al-Sultan Abdullah through the Fundamental Research Grant (RDU230336).

REFERENCES

Aili Hamzah, A. F., Hamzah, M. H., Che Man, H., Jamali, N. S., Siajam, S. I., & Ismail, M. H. (2021). Recent updates on the conversion of pineapple waste (*Ananas comosus*) to value-added products, future perspectives and challenges. *Agronomy*, *11*, 2221. https://doi.org/10.3390/agronomy11112221

Anigboro, A. A., Ajoh, A. I., Avwioroko, O. J., Ehwarieme, D. A., & Tonukari, N. J. (2023). Solid-state fermentation of cassava (*Manihot esculenta*) peels using *Rhizopus oligosporus*: Application of the fermented peels in yeast production and characterization of α-amylase enzyme produced in the process. *Chemistry Africa*, *6*, 1669–1678. https://doi.org/10.1007/s42250-022-00582-3

Arampath, P. C., & Dekker, M. (2019). Bulk storage of mango (*Mangifera indica* L.) and pineapple (*Ananas comosus* L.) pulp: Effect of pulping and storage temperature on phytochemicals and antioxidant activity. *Journal of the Science of Food and Agriculture*, *99*(11), 5157–5167. https://doi.org/10.1002/jsfa.9762

Aruna, T. E. (2019). Production of value-added product from pineapple peels using solid state fermentation. *Innovative Food Science and Emerging Technologies*, *57*, 102193. https://doi.org/10.1016/j.ifset.2019.102193

Awasthi, M. K., Azelee, N. I. W., Ramli, A. N. M., Rashid, S. A., Manas, N. H. A., Dailin, D. J., Illias, R. M., Rajagopal, R., Chang, S. W., Zhang, Z., & Ravindran, B. (2022). Microbial biotechnology approaches for conversion of pineapple waste in to emerging source of healthy food for sustainable environment. *International Journal of Food Microbiology*, *373*, 109714. https://doi.org/10.1016/j.ijfoodmicro.2022.109714

Azizan, A., Lee, A. X., Abdul Hamid, N. A., Maulidiani, M., Mediani, A., Abdul Ghafar, S. Z., Zolkeflee, N. K. Z., & Abas, F. (2020). Potentially bioactive metabolites from pineapple waste extracts and their antioxidant and α-glucosidase inhibitory activities by ^{1}H NMR. *Foods*, *9*(2), 173. https://doi.org/10.3390/foods9020173

Azkia, M. N., Cahyanto, M. N., Mayangsari, Y., Briliantama, A., Palma, M., & Setyaningsih, W. (2023). Enhancement of phenolic profile and antioxidant activity of black glutinous rice (*Oryza sativa* var. glutinosa) due to tape fermentation. *Arabian Journal of Chemistry*, *16*, 105275. https://doi.org/10.1016/j.arabjc.2023.105275

Baidhe, E., Kigozi, J., Mukisa, I., Muyanja, C., Namubiru, L., & Kitarikawe, B. (2021). Unearthing the potential of solid waste generated along the pineapple drying process line in Uganda: A review. *Environmental Challenges*, *2*, 100012. https://doi.org/10.1016/j.envc.2020.100012

Buenrostro-Figueroa, J. J., Velázquez, M., Flores-Ortega, O., Ascacio-Valdés, J. A., Huerta-Ochoa, S., Aguilar, C. N., & Prado-Barragán, L. A. (2017). Solid state fermentation of fig (*Ficus carica* L.) by-products using fungi to obtain phenolic compounds with antioxidant activity and qualitative evaluation of phenolics obtained. *Process Biochemistry*, *62*, 16–23. https://doi.org/10.1016/j.procbio.2017.07.016

Casas-Rodríguez, A. D., Ascacio-Valdés, J. A., Dávila-Medina, M. D., Medina-Morales, M. A., Londoño-Hernández, L., & Sepúlveda, L. (2024). Evaluation of solid-state fermentation conditions from pineapple peel waste for release of bioactive compounds by *Aspergillus niger* spp. *Applied Microbiology*, *4*, 934–947. https://doi.org/10.3390/applmicrobiol4020063

Chintagunta, A. D., Ray, S., & Banerjee, R. (2017). An integrated bioprocess for bioethanol and biomanure production from pineapple leaf waste. *Journal of Cleaner Production*, *165*, 1508–1516. https://doi.org/10.1016/j.jclepro.2017.07.179

Correia, R., Magalhães, M., & Macêdo, G. (2007). Protein enrichment of pineapple waste with *Saccharomyces cerevisiae* by solid state bioprocessing. *Journal of Scientific and Industrial Research*, *66*, 259–262.

de Aquino Gondim, T., Guedes, J. A. C., Silva, M. F. S., da Silva, A. C., Dionísio, A. P., Souza, F. V. D., do Ó Pessoa, C., Lopes, G. S., & Zocolo, G. J. (2023). Assessment of metabolic, mineral, and cytotoxic profile in pineapple leaves of different commercial varieties: A new eco-friendly and inexpensive source of bioactive compounds. *Food Research International*, *164*, 112439. https://doi.org/10.1016/j.foodres.2022.112439

Difonzo, G., Vollmer, K., Caponio, F., Pasqualone, A., Carle, R., & Steingass, C. B. (2019). Characterisation and classification of pineapple (*Ananas comosus* [L.] Merr.) juice from pulp and peel. *Food Control*, *96*, 260–270. https://doi.org/10.1016/j.foodcont.2018.09.015

Hemalatha, R., & Anbuselvi, S. (2013). Physicohemical constituents of pineapple pulp and waste. *Journal of Chemical and Pharmaceutical Research*, *5*(2), 240–242.

Hidalgo, D., Corona, F., & Martín-Marroquín, J. M. (2022). Manure biostabilization by effective microorganisms as a way to improve its agronomic value. *Biomass Conversion and Biorefinery*, *12*, 4649–4664. https://doi.org/10.1007/s13399-022-02428-x

Jamir, L., Kumar, V., Kaur, J., Kumar, S., & Singh, H. (2021). Composition, valorization and therapeutical potential of molasses: A critical review. *Environmental Technology Reviews*, *10*(1), 131–142. https://doi.org/10.1080/21622515.2021.1892203

Kanchanasuta, S., & Pisutpaisal, N. (2016). Waste utilization of palm oil decanter cake on biogas fermentation. *International Journal of Hydrogen Energy*, *41*, 15661–15666. https://doi.org/10.1016/j.ijhydene.2016.04.129

Kim, S. W., Less, J. F., Wang, L., Yan, T., Kiron, V., Kaushik, S. J., & Lei, X. G. (2019). Meeting global feed protein demand: Challenge, opportunity, and strategy. *Annual Review of Animal Biosciences*, *7*, 221–243. https://doi.org/10.1146/annurev-animal-030117-014838

Kupski, L., Cipolatti, E., Rocha, M. da, Oliveira, M. dos S., Souza-Soares, L. de A., & Badiale-Furlong, E. (2012). Solid-state fermentation for the enrichment and extraction of proteins and antioxidant compounds in rice bran by *Rhizopus oryzae*. *Brazilian Archives of Biology and Technology*, *55*(6), 937–942. https://doi.org/10.1590/S1516-89132012000600018

Malaysian Pineapple Industry Board. (2022). *Laporan tahunan 2021* [2021 Annual report]. https://www.mpib.gov.my/penerbitan/

Mund, N. K., Dash, D., Mishra, P., & Nayak, N. R. (2022). Cellulose solvent–based pretreatment and enzymatic hydrolysis of pineapple leaf waste biomass for efficient release of glucose towards biofuel production. *Biomass Conversion and Biorefinery*, *12*, 4117–4126. https://doi.org/10.1007/s13399-020-01225-8

Nath, P. C., Ojha, A., Debnath, S., Neetu, K., Bardhan, S., Mitra, P., Sharma, M., Sridhar, K., & Nayak, P. K. (2023). Recent advances in valorization of pineapple (*Ananas comosus*) processing waste and by-products: A step towards circular bioeconomy. *Trends in Food Science & Technology*, *136*, 100–111. https://doi.org/10.1016/j.tifs.2023.04.008

Olorunnisola, K. S., Jamal, P., & Alam, M. Z. (2018). Growth, substrate consumption, and product formation kinetics of *Phanerochaete chrysosporium* and *Schizophyllum commune* mixed culture under solid-state fermentation of fruit peels. *3 Biotech*, *8*, 429. https://doi.org/10.1007/s13205-018-1452-3

Omwango, E. O., Njagi, E. N. M., Orinda, G. O., & Wanjau, R. N. (2013). Nutrient enrichment of pineapple waste using *Aspergillus niger* and *Trichoderma viride* by solid state fermentation. *African Journal of Biotechnology*, *12*(43), 6193–6196. https://doi.org/10.5897/AJB2013.12992

Polanía, A. M., Londoño, L., Ramírez, C., Bolivar, G., & Aguilar, C. N. (2023). Valorization of pineapple waste as novel source of nutraceuticals and biofunctional compounds. *Biomass Conversion and Biorefinery*, *13*, 3593–3618. https://doi.org/10.1007/s13399-022-02811-8

Rashad, M. M., Mahmoud, A. E., Ali, M. M., Nooman, M. U., & Al-Kashef, A. S. (2015). Antioxidant and anticancer agents produced from pineapple waste by solid state fermentation. *International Journal of Toxicological and Pharmacological Research*, *7*(6), 287–296.

Rivera, A. M. P., Toro, C. R., Londoño, L., Bolivar, G., Ascacio, J. A., & Aguilar, C. N. (2023). Bioprocessing of pineapple waste biomass for sustainable production of bioactive compounds with high antioxidant activity. *Journal of Food Measurement and Characterization*, *17*, 586–606. https://doi.org/10.1007/s11694-022-01627-4

Roda, A., & Lambri, M. (2019). Food uses of pineapple waste and by-products: A review. *International Journal of Food Science & Technology*, *54*(4), 1009–1017. https://doi.org/10.1111/ijfs.14128

Schmidt, C. G., & Furlong, E. B. (2012). Effect of particle size and ammonium sulfate concentration on rice bran fermentation with the fungus *Rhizopus oryzae*. *Bioresource Technology*, *123*, 36–41. https://doi.org/10.1016/j.biortech.2012.07.081

Setti, L., Samaei, S. P., Maggiore, I., Nissen, L., Gianotti, A., & Babini, E. (2020). Comparing the effectiveness of three different biorefinery processes at recovering bioactive products from hemp (*Cannabis sativa* L.) byproduct. *Food and Bioprocess Technology*, *13*, 2156–2171. https://doi.org/10.1007/s11947-020-02550-6

Sukri, S. A. M., Andu, Y., Sarijan, S., Khalid, H.-N. M., Kari, Z. A., Harun, H. C., Rusli, N. D., Mat, K., Khalif, R. I. A. R., Wei, L. S., Rahman, M. M., Hakim, A. H., Norazmi Lokman, N. H., Hamid, N. K. A., Khoo, M. I., & Doan, H. Van. (2023). Pineapple waste in animal feed: A review of nutritional potential, impact and prospects. *Annals of Animal Science*, *23*(2), 339–352. https://doi.org/10.2478/aoas-2022-0080

Surin, S., Thakeow, P., Seesuriyachan, P., Angeli, S., & Phimolsiripol, Y. (2014). Effect of extraction and concentration processes on properties of longan syrup. *Journal of Food Science and Technology*, *51*(9), 2062–2069. https://doi.org/10.1007/s13197-013-1249-7

Tosuner, Z. V., Taylan, G. G., & Özmıhçı, S. (2019). Effects of rice husk particle size on biohydrogen production under solid state fermentation. *International Journal of Hydrogen Energy*, *44*(34), 18785–18791. https://doi.org/10.1016/j.ijhydene.2018.10.230

Tripathi, A. D., Mishra, P. K., Darani, K. K., Agarwal, A., & Paul, V. (2022). Hydrothermal treatment of lignocellulose waste for the production of polyhydroxyalkanoates copolymer with potential application in food packaging. *Trends in Food Science & Technology*, *123*, 233–250. https://doi.org/10.1016/j.tifs.2022.03.018

Wang, J., Huang, Z., Jiang, Q., Roubík, H., Xu, Q., Gharsallaoui, A., Cai, M., Yang, K., & Sun, P. (2023). Fungal solid-state fermentation of crops and their by-products to obtain protein resources: The next frontier of food industry. *Trends in Food Science & Technology*, *138*, 628–644. https://doi.org/10.1016/j.tifs.2023.06.020

Wang, K., Niu, M., Song, D., Liu, Y., Wu, Y., Zhao, J., Li, S., & Lu, B. (2020). Evaluation of biochemical and antioxidant dynamics during the co-fermentation of dehusked barley with *Rhizopus oryzae* and *Lactobacillus plantarum*. *Journal of Food Biochemistry*, *44*(2), e13106. https://doi.org/10.1111/jfbc.13106

Yafetto, L., Odamtten, G. T., & Wiafe-Kwagyan, M. (2023). Valorization of agro-industrial wastes into animal feed through microbial fermentation: A review of the global and Ghanaian case. *Heliyon*, *9*(4), e14814. https://doi.org/10.1016/j.heliyon.2023.e14814

Yazid, N. A., Barrena, R., Komilis, D., & Sánchez, A. (2017). Solid-state fermentation as novel paradigm for organic waste valorization: A review. *Sustainability*, *9*(2), 224. https://doi.org/10.3390/su9020224

Zainuddin, M. F., Shamsudin, R., Mokhtar, M. N., & Ismail, D. (2014). Physicochemical properties of pineapple plant waste fibers from the leaves and stems of different varieties. *BioResources*, *9*(3), 5311–5324. https://doi.org/10.15376/biores.9.3.5311-5324

Zeng, J., Huang, W., Tian, X., Hu, X., & Wu, Z. (2021). Brewer's spent grain fermentation improves its soluble sugar and protein as well as enzymatic activities using *Bacillus velezensis*. *Process Biochemistry*, *111*, 12–20. https://doi.org/10.1016/j.procbio.2021.10.016

Pertanika J. Trop. Agric. Sci. 48 (3): 781 - 813 (2025)

PERTANIKA JOURNALS

TROPICAL AGRICULTURAL SCIENCE

Journal homepage: http://www.pertanika.upm.edu.my/

Review Article

A Review of Pregnancy Rates in Beef Cattle via Timed Artificial Insemination Utilizing CIDR-based 5 and 7-Day CO-synch Protocols

Jigdrel Dorji[1,2]*, Mark Wen Han Hiew[1] and Nurhusien Yimer[3,4]

[1]Department of Veterinary Clinical Studies, Faculty of Veterinary Medicine, Universiti Putra Malaysia, 43400 Serdang, Selangor, Malaysia

[2]Department of Animal Science, College of Natural Resources, Royal University of Bhutan, Lobesa (14001), Punakha, Bhutan

[3]Department of Veterinary Sciences, School of Medicine, IMU University, Bukit Jalil, 57000, Kuala Lumpur, Malaysia

[4]Veterinary Reproduction Division, Faculty of Veterinary Medicine, Airlangga University, Surabaya 60115, Indonesia

ABSTRACT

Although timed artificial insemination programs (TAI) are widely implemented, the effectiveness of field CO-Synch programs is less known. A clear understanding of overall pregnancy rates (PRs) from controlled internal drug release (CIDR)-based TAI programs like 7-day CO-Synch (7DCOS) or effectiveness of various prostaglandin delivery in 5-day CO-Synch (5DCOS) is not available. This paper aimed to review pregnancy rates in 7DCOS and 5DCOS (with different methods of prostaglandin delivery). An analysis of 74 studies retrieved from Google Scholar, PubMed, and ScienceDirect was done. The TAI-PRs were expressed as Weighted TAI-PR (WTAI-PR) to account for different trial sizes across various studies. The WTAI-PR was 54.91% in cows and 53.50% in heifers under 7DCOS, and 51.75%, 50.38%, and 57.98% for cows and 52.84%, 51.90%, and 58.42% for heifers treated with 5DCOS+CIDR® with a single (25 mg), double (50 mg)/two simultaneous doses (25 mg each) or two separate doses (25 mg, 2-24 hours apart) of prostaglandin (PGF). Other factors like cyclicity at treatment initiation, breeding season, estrus expression before AI, and body condition score affected the TAI-PRs. Although two doses

ARTICLE INFO

Article history:
Received: 18 May 2024
Accepted: 17 October 2024
Published: 16 May 2025

DOI: https://doi.org/10.47836/pjtas.48.3.08

E-mail addresses:
jdorji.cnr@rub.edu.bt (Jigdrel Dorji)
mark@upm.edu.my (Mark Wen Han Hiew)
nurhusienyimerdegu@imu.edu.my (Nurhusien Yimer)
*Corresponding author

e-ISSN: 2231-8542

of PGF were effective, the cost was higher due to the extra labor for handling and purchase of hormones. Both 5DCOS and 7DCOS showed satisfactory pregnancy rates, but progesterone device discomfort due to two additional days (7DCOS) are a welfare concern. There is a lack of studies evaluating these programs in tropical climates. Future research should focus on the effect of unique environmental conditions in the tropics on the success of these protocols.

Keywords: Beef cattle, CIDR, CO-synch, pregnancy rates, timed artificial insemination

INTRODUCTION

The beef production industry plays a crucial role in alleviating poverty and contributes to achieving food security by providing essential nutrients and high-quality proteins, particularly in regions where protein from other sources is limited (McAllister et al., 2020). While one of the fundamental strategies for meeting this increasing demand is via the increase in the number of calves per breeding season, breeders need to optimize their production by reducing the cost of production (Dahlen et al., 2014).

Timed Artificial Insemination (TAI) programs were developed to bypass the need for estrus detection, thereby reducing labor expenses and improving breeding efficiency to overcome these challenges (Colazo & Mapletoft, 2014; Sá Filho et al., 2013). The pioneering TAI protocol, Ovsynch, was first developed in the early 19th century and facilitated the use of embryo transfer and Artificial Insemination at predetermined times by controlling follicular dynamics, the luteal phase, and triggering synchronized ovulation of the dominant follicle (Bó & Baruselli, 2014; Pursley et al., 1995). This protocol is mostly used in intensive systems for dairy cattle, where multiple handling can be realized. However, it is less feasible for beef cattle to be raised in extensive systems with less controlled environments. Frequent handling is costly to breeders and more stressful for cattle. Thus, protocols involving fewer animal handlings are more practical for beef cattle (Colazo & Mapletoft, 2014; Geary et al., 2001).

Timed Artificial Insemination (TAI) protocols relevant to beef cattle, such as 7-day CO-Synch (7DCOS) and 5-day CO-Synch (5DCOS) plus Controlled Internal Drug Release (CIDR), have been developed to reduce animal handling and improve practicality for breeders (Colazo & Mapletoft, 2014). CO-Synch protocols reduce the number of animal handling by injecting a second GnRH Gonadotropin Releasing Hormone (GnRH) concurrently at TAI (Geary et al., 2001). Although CO-Synch programs are commonly utilized, the variability of PRs remains a challenge. For example, TAI-PRs from 7DCOS ranged from 38.2 to 61.1% across studies, indicating that factors such as management practices, environmental conditions, and physiology of cattle significantly affect pregnancy outcomes (Dobbins et al., 2009). Whereas in 5DCOS, Prostaglandin F2α (PGF) is delivered using three methods: single dose, two separate doses, and double dose, but it is difficult to

determine which method is the most effective. Stevenson et al. (2011) reported pregnancy rates of 44.2% (for a single dose), 57.4% (for two separate doses) and 51.8% (for a double dose), again demonstrating the variability of pregnancy outcomes and how different factors affect it. This evidence shows that although various TAI programs are widely studied and implemented, the effectiveness of CO-Synch programs at the field level is less known. Moreover, a clear understanding of pregnancy rates resulting from CIDR-based TAI programs such as 7DCOS or the effectiveness of various PGF delivery in 5DCOS is not available. By clearly understanding CO-Synch protocols, breeders can identify and choose the most effective protocol that benefits them economically.

However, there are practical implications that cattle breeders may face. For instance, one of the major practical challenges faced by breeders is enhancing reproductive efficiency in extensive production systems where the cost of labor for estrus detection is expensive and difficult to manage. Though effective, traditional breeding protocols that require heat detection demand a huge amount of time and labor, which can be impractical for breeders in extensively managed farms (Santos et al., 2022). It is particularly important in regions with scarce labor resources and large cattle heads. Although CO-Synch protocols may offer a potential solution to enhance reproductive efficiency in beef cattle, the cost of drugs, labor and animal handling stress remains a key concern. In addition, different AI protocols will have different cost implications arising from the duration of synchronization, number of animal handlings, and quantity of hormone used. With an increase in global meat demand, the beef cattle industry will have a significant role in future meat supply. Improvement in AI technology will be necessary for enhancing reproduction and increasing the beef cattle population. While such measures might have bigger implications for breeders in top beef exporting countries such as the United States, European Union and Brazil, technological transfer and use of AI by breeders in low-income countries will also become relevant because of increasing meat consumption in these countries.

Therefore, this paper aims to review pregnancy rates in 7DCOS, pregnancy rates obtained from different methods of prostaglandin delivery in 5DCOS and other factors affecting TAI-PRs outside of treatments in TAI programs.

METHODOLOGY

Literature Search Strategy

Literature was retrieved using the keywords: "Estrus Synchronization," "Timed Artificial Insemination," "Pregnancy Rates," 'Beef Cattle," "CO-Synch," "CO-Synch," "CIDR," and "Controlled Internal Drug Release." Data extraction and calculation of Weighted Timed Artificial Insemination Pregnancy Rates (WTAI-PRs) were carried out manually in Microsoft Excel. The details of the literature selection process are presented in Figure 1.

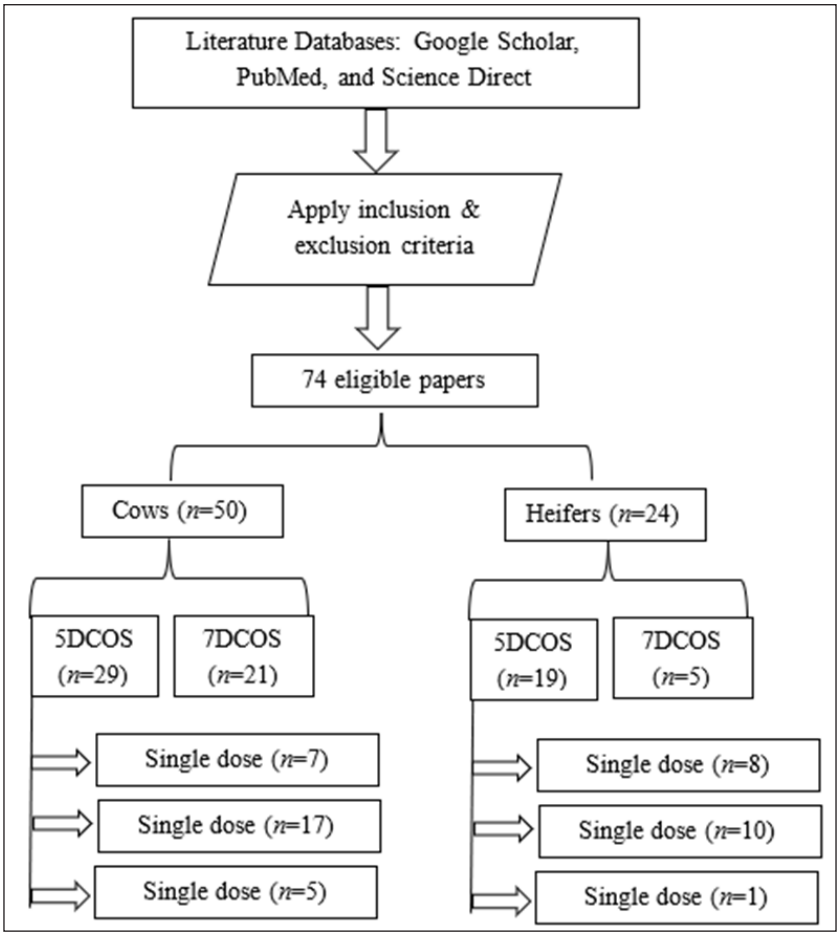

Figure 1. Flowchart for the process of literature selection

Selection of Literature for Review

Inclusion Criteria

This review included CO-Synch programs that relied solely on GnRH and PGF, with an interval of five to seven days between initial GnRH and PGF. The interval duration between CIDR® removal and TAI must be 48 to 72 hours and 56 to 72 hours for 7DCOS and 5DCOS, respectively. Furthermore, CO-Synch programs must exclusively utilize CIDR® as a P4 source. Modified 5DCOS programs (without initial GnRH with a single PGF) were included. Likewise, 5DCOS programs that administered two PGF2α doses (25 mg each) concurrently, a single dose (25 mg), a double dose (50 mg) at CIDR® removal, and two separate doses (25 mg each) at certain time intervals (initial dose at CIDR® removal) were included. And lastly, the studies must be strict on beef cattle.

Exclusion Criteria

The review excluded studies that utilized hormones other than GnRH and PGF, such as eCG (equine chorionic gonadotropin), estradiol benzoate (EB), and hCG (human chorionic gonadotropin). Similarly, studies that utilized intravaginal P4 devices other than CIDR® or that did not utilize any P4 device between initial GnRH and PGF were excluded.

CO-SYNCH PROGRAMS AND VARIATIONS

Beef cattle subjected to 7DCOS received an intravaginal insert (CIDR®) and GnRH at the initiation of synchronization. Seven days later, CIDR® was removed concurrently with an injection of PGF. Fixed-time AI was performed 54 to 60 hours and 48 to 72 hours after the CIDR® removal for heifers and cows, respectively. Cows and heifers subjected to 5DCOS protocol either received an initial GnRH or no GnRH concurrent with CIDR® insertion. At the time of CIDR® removal, cattle received either a single standard dose (25 mg), a single large dose (50 mg)/double dose (2 × 25 mg concurrently), or two separate (2 to 24 hours apart) doses of PGF on D5 (initial dose at CIDR® removal). Fixed time AI occurred 56 to 72 hours and 60 to 72 hours, respectively, for heifers and cows following CIDR® removal. In both protocols, cattle received a second GnRH dose at the time of FTAI

The proestrus period, the time duration between luteolysis and Luteinizing Hormone (LH) surge, was found to be associated with increased TAI-PRs. Bridges et al. (2008) conducted a series of experiments to modify the traditional 7-day Cosynch program by reducing the duration of P4 device exposure from 7 to 5 days to allow an extended proestrus period, resulting in a 5-day Cosynch program. The authors compared TAI-PRs between 7DCOS (proestrus = 60 hours) and 5DCOS (proestrus = 60 hours) programs in these experiments. Their result showed similar TAI-PRs. However, in the two other experiments, when proestrus duration in 5DCOS was increased to 72 hours (60 hours in 7DCOS), TAI-PRs were 13.3% (n=223) and 9.1% (n = 400) higher than 7DCOS program ($p < 0.05$). An increased pregnancy rate in a lengthened proestrus duration in 5DCOS was a result of a lower incidence of ovulating immature follicles and increased gonadotropin exposure to the preovulatory follicle. It leads to increased estradiol concentration before ovulation, a key fertility determinant (Day, 2018). Estradiol is indispensable as it contributes to the expression of uterine genes and proteins, which are responsible for the establishment of pregnancy (Perry, Cushman et al., 2020).

Variations of 7DCOS plus CIDR® Protocol

The initial goal of the 7DCOS program was to breed 48 hours after PGF injection. However, later studies have shown increased conception rates when artificial insemination was performed 54-56 hours after PGF (Bridges et al., 2012). There are several variations in

the interval between PGF and TAI. The 7DCOS program begins with an initial GnRH on D0, PGF on D7, and a second GnRH injection concomitantly on the day of TAI: 60–66 hours (Lansford, 2018), 54–66 hours (Bridges et al., 2012) 60 hours (Bridges et al., 2008), 72 hours (Mellieon et al., 2012; Randi et al., 2021), and 66 hours (Andersen et al., 2021) after the P4 device removal.

Variations of 5DCOS plus CIDR® Protocol

The increased length of proestrus (the duration between PGF and GnRH-induced LH surge or interval from the removal of the P4 device to GnRH/TAI) demonstrated an increased pregnancy rate (Bó et al., 2016; Day, 2018; de la Mata et al., 2018). To allow a longer proestrus, Bridges et al. (2008) modified the traditional 7DCOS by shortening the duration of intravaginal device exposure from 7 to 5 days, resulting in the 5DCOS protocol. However, this modification led to the formation of immature Corpus Luteum (5 days old) on the day of PGF that resists complete luteolysis. Thus, researchers proposed delivering two doses of PGF to completely lyse the young 5-day-old CL. As a result, there have been concerns among researchers that the extra handling of animals and the cost associated with additional PGF may discourage the implementation of the 5DCOS program. Greater pregnancy rates were reported for 5DCOS compared to 7DCOS. However, increased TAI pregnancy rates in the former failed to offset the extra cost associated with additional PGF dose and animal handling (Peel et al., 2010). To reduce the cost of implementing the 5DCOS program, Gunn et al. (2015) conducted a trial with and without a P4 device. Significantly lower pregnancy rates in cows without the P4 device were observed.

Generally, 5DCOS yielded greater TAI-PRs than the 7DCOS program. Several biological mechanisms have been proposed for increased PRs observed in the former program. The reduced P4 exposure in the 5DCOS program improves the development of follicles. It restricts the emergence of older, less viable follicles, which results in the ovulation of younger, healthier follicles with good oocyte quality (Day, 2015). This results in more precise control of ovulation and LH surge because of tighter ovulation synchronization with TAI (Bridges et al., 2018). Additionally, 5DCOS supports the healthy development of CL, which produces a higher concentration of progesterone and is essential for early embryonic development and maintaining pregnancy (Lamb et al., 2006). In contrast, 7DCOS due to extended P4 exposure, risk of ovulating persistent follicles with low-quality oocytes, and weaker CL with low P4 level may lead to early embryonic loss and reduce PRs (Bridges et at., 2010). Although 5DCOS showed greater TAI-PRs compared to 7DCOS, it is suggested that the choice of protocol must be based on the local condition and management practices (Whittier et al., 2013).

One or Two Doses of PGF in the 5DCOS Protocol

Several studies have investigated the need for one or two doses of PGF in a 5DCOS program. Studies have shown improved pregnancy rates when two doses were given six to eight hours apart, with an initial dose administered concomitantly at P4 device removal. For instance, Stevenson et al. (2011) conducted a multi-location study, which included 2420 postpartum beef cows, to compare the effectiveness of single, double and two separate doses of PGF at 8-hour intervals. The highest TAI-PR was observed in cows receiving two PGF doses 8 hours apart, followed by doubled and single doses. A similar study by Kasimanickam et al. (2009) found significantly greater TAI-PRs in cows that received two separate doses of PGF (Dinoprost: 7 hours apart, 69.0%) compared to a single PGF dose (Diniprost: 52.0%) and a single dose of Cloprostenol (54.3%).

Timing of TAI in 7DCOS Protocol

The timing for TAI in the 7DCOS plus CIDR® protocol ranged from 48 to 72 hours after P4 device removal, with varying pregnancy rates. A comparison of FTAI-PR in postpartum beef cows resulting from inseminations performed 54 and 66 hours after CIDR® removal resulted in significantly greater PRs when inseminated at 66 hours (61 vs. 67%, $p = 0.05$) (Busch et al., 2008). Similarly, the pregnancy rate in beef cows after inseminating at 56 and 64 hours after PGF administration was greater compared to 48 hours ($p < 0.01$), but it was not different from 72 hours (Dobbins et al., 2009). The breeding time for beef cows and heifers has been recommended at 60 to 66 hours and 52 to 56 hours after P4 device withdrawal (Johnson et al., 2010). An expert review article published by Bridges et al. (2012) reported an average TAI-PR of 55%, 54%, and 51% when TAI was performed at 48, 54-66, and 72 hours, respectively, after CIDR® removal, with a range of 45 to 66%.

Timing of TAI in 5DCOS Protocol

When 5DCOS was first developed, PR from TAI at 60 and 72 hours after CIDR® removal in postpartum beef cows was 56.8% and 65.3%, respectively (Bridges et al., 2008). Likewise, an acceptable pregnancy rate of (52% to 57%) was achieved using 5DCOS + CIDR® by inseminating at 72 hours after CIDR® withdrawal (Whittier et al., 2010). Whereas most beef heifers were observed to express estrus behaviors 24 hours before TAI occurred. Based on this observation, Kasimanickam et al. (2012) hypothesized that the TAI-PRs in beef heifers would improve if breeding were performed 56 hours after CIDR® removal instead of 72 hours, and this was shown when the TAI-PR was 10.3% higher in heifers inseminated at 56 compared to 72 hours after CIDR® removal.

Comparison of Efficiency and Cost Effectiveness Between 5DCOS and 7DCOS

In general, there are some differences between 5DCOS and 7DCOS in terms of efficiency and cost-effectiveness (Table 1). For instance, higher pregnancy rates were observed in 5DCOS when two PGF were given compared to 7DCOS. However, an extra PGF dose in 5DCOS will increase the overall cost of implementation, and there is a need to assess whether the extra cost offers the advantage of having higher pregnancy rates in 5DCOS compared to the 7DCOS program.

Table 1
Summary comparison of 5DCOS and 7DCOS

Parameter	5DCOS	7DCOS
Pregnancy rates	Slightly higher in some studies (5-10%)	Moderate to high but variable
Hormonal treatments	Require 2PGF	Single PGF
Labor and cost	Higher due to additional treatment	Lower, fewer animal handling
Follicular dynamics	Younger dominant follicle (High Estradiol production)	Older dominant follicle (Low estradiol production)
Corpus luteum (CL) regression	Complete with 2 Prostaglandin F2α (PGF) doses	Single PGF dose
Duration of P4 device exposure	5 Days	7 Days
Cost-effectiveness	Higher cost but effective with two doses of PGF	Lower cost and effective with a single PGF dose

PREGNANCY RATES IN CO-SYNCH PROGRAMS

Based on the inclusion and exclusion criteria, a total of 74 trials were thoroughly reviewed (50 on cows and 24 on heifers). Of these, 48 trials implemented the 5DCOS +CIDR® protocol, while the remaining 26 implemented the 7DCOS+CIDR® protocol (Figure 1). The TAI-PRs were expressed as weighted timed-AI pregnancy rates (WTAI-PR) to account for different trial sizes across various studies. It was calculated as:

$$\text{WTAI-PR (\%)} = (\text{Sum of weighted values}/\text{Total number of animals}) \quad [1]$$

where, weighted values = Number of Animals × TAI-PR%

The consolidated WTAI-PR for different methods of PGF delivery in 5DCOS + CIDR® is presented in (Figure 2, Tables 2, 3, 4, and 5). The highest WTAI-PRs were observed with two separate doses of PGF. Meanwhile, in the 7DCOS program, TAI-PRs between cows and heifers were similar (Figure 3, Table 5). Irrespective of the animal category, the WTAI-PRs among experimental regions varied from 53% to 58.7% for 5DCOS and

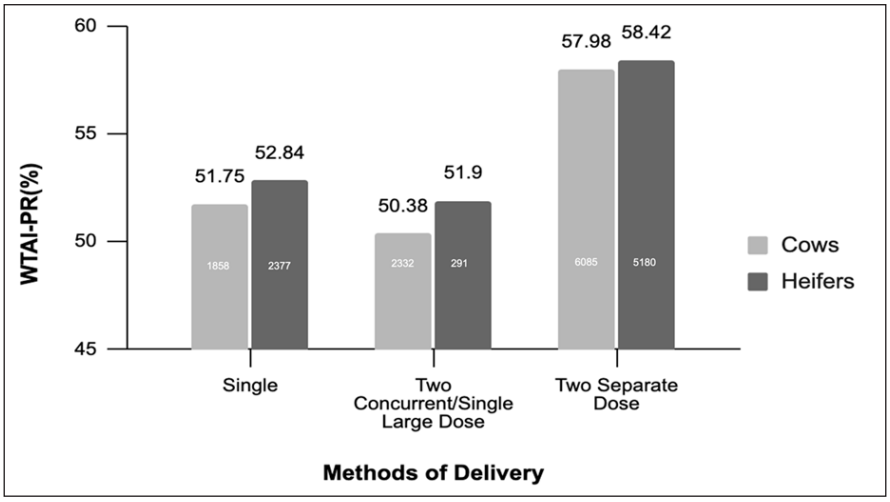

Figure 2. Weighted Timed Artificial Insemination Pregnancy Rates (WTAI-PR) in cows and heifers with 5DCOS +CIDR® program based on different methods of Prostaglandin delivery. The numbers in the center of the bar indicate the total number of animals

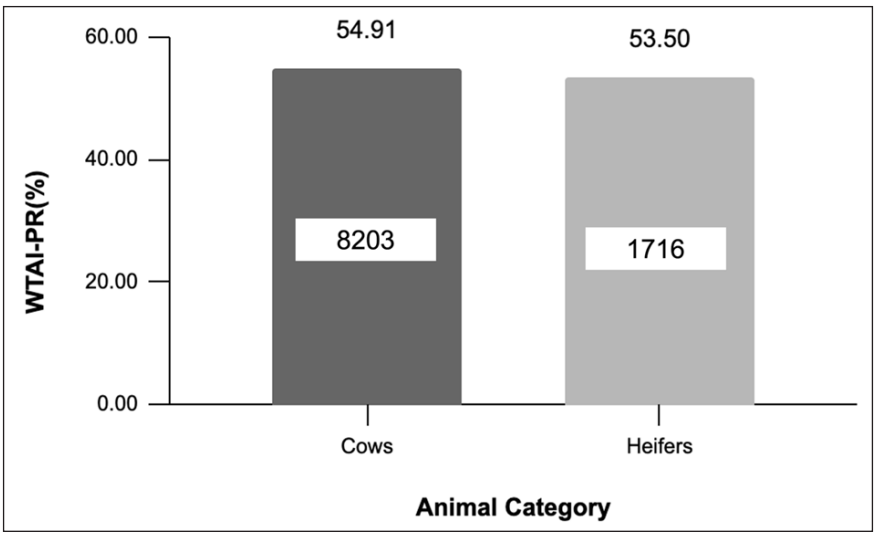

Figure 3. Weighted Timed Artificial Insemination Pregnancy Rates (WTAI-PR) in cows and heifers with the 7DCOS +CIDR® program. The numbers in the center of the bar indicate the total number of animals

7DCOS programs and were similar (Figure 4). Five studies, Russia (*n*=2) and Canada (*n*=2), have been excluded because of regional differences (outside USA). However, their data was included for breed-based TAI-PRs analysis. Among the cattle breeds employed, WTAI-PRs varied from 53.48% to 58.11% and were similar. Table 6 and Table 7 show WTAI-PRs resulting from sex-sorted semen using the 7DCOS program in cows and heifers. The WTAI-PRs varied from 40.67% to 44.14%. However, there were no studies

that employed 5DCOS for sex-sorted semen. Overall, WTAI-PR was 54.91% in cows and 53.50% in heifers under 7DCOS, and 51.75%, 50.38%, and 57.98% for cows and 52.84%, 51.90%, and 58.42% for heifers treated with 5DCOS plus CIDR® with a single (25 mg), double (50 mg)/two simultaneous doses (25 mg each) or two separate doses (25 mg, 2 to 24 hours apart) of prostaglandin (PGF).

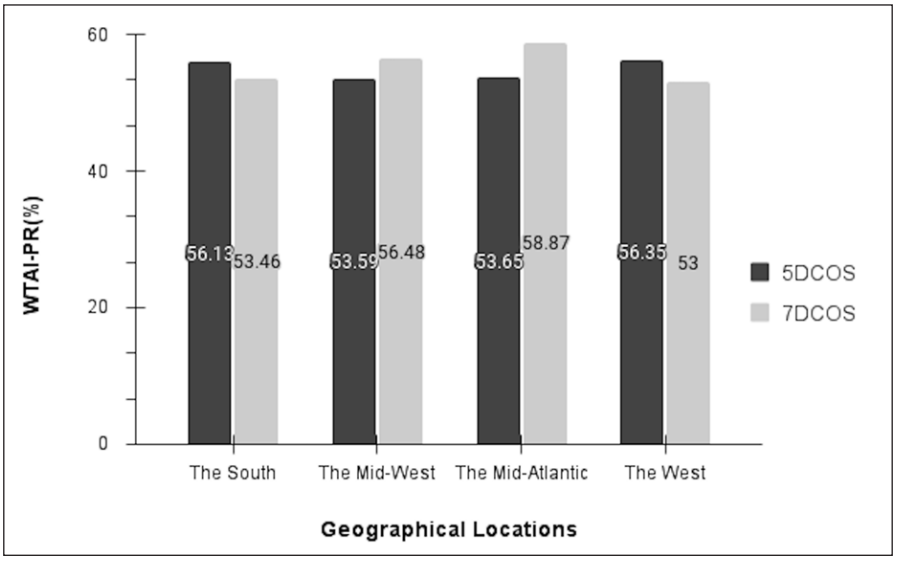

Figure 4. Comparison of Weighted Timed Artificial Insemination Pregnancy Rates (WTAI-PR) between 5DCOS and 7DCOS programs across geographical locations

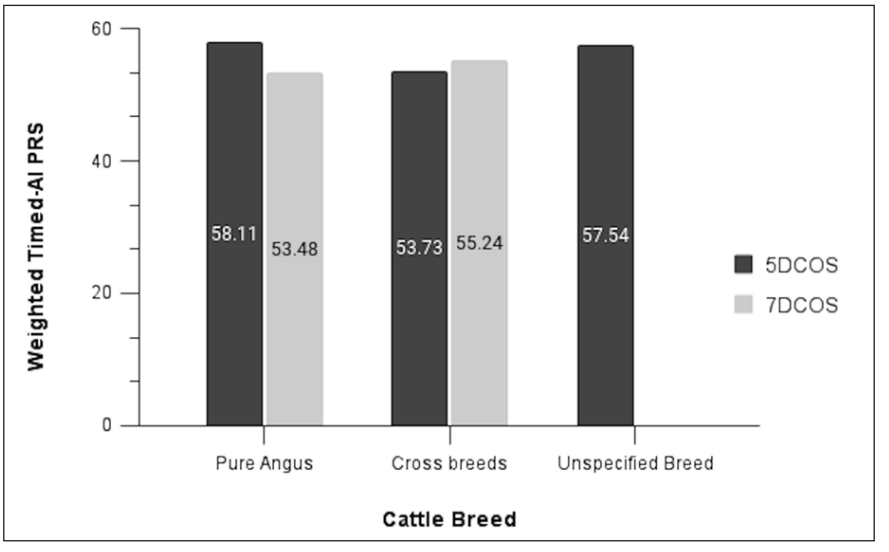

Figure 5. Comparison of weighted timed-AI pregnancy rates between 5DCOS and 7DCOS programs across cattle breeds

Timed AI Pregnancy Rates from Various Published Reports

The Weighted Timed Artificial Insemination Pregnancy Rates (WTAI-PRs) resulting from single (standard), single large dose (double dose), two separate doses (2-24 hours part) of PGF are provided below (Table 2-4). While Table 5 shows WTAI-PRs resulting from 7DCOS + CIDR protocol in beef cattle.

Table 2
WTAI-PR for 5DCOS +CIDR® protocol in beef cattle using a single standard dose of PGF at CIDR® withdrawal

Cows				
n	**PGF to AI (h)**	**TAI-PR (%)**	**Notes**	**Reference(s)**
277	72	52.0	25 mg Dinoprost	Kasimanickam et al. (2009)
271	72	54.3	500 µg Cloprostenol	
197	72	44.2	25 mg Dinoprost	Stevenson et al. (2011)
815	72	48.0	25 mg Dinoprost	Bridges et al. (2012)
100	72	62.0	25 mg (Lutalyse® HighCon, Zoetis)	Corpron et al. (2019)
90	66	63.0	500 µg Cloprostenol (modified 5DCOS)	Macmillan et al. (2020)
108	72	68.0		
WTAI-PRs		51.75	293	
Heifers				
264	72	54.2	25 mg Dinoprost	Peterson et al. (2011)
290	56	50.3	Modified 5DCOS (25 mg Dinoprost)	Kasimanickam et al. (2014)
263	56	59.7	25 mg Dinoprost	
408	72	50.5	Modified 5DCOS (25 mg Dinoprost)	Cruppe et al. (2014)
415	72	54.9	25mg Dinoprost	
144	56-59	63.9	Modified 5DCOS (25 mg Dinoprost)	Ahmadzadeh et al. (2015)
293	56	54.9	25 mg Dinoprost	White et al. (2016)
300	72	41.1	500 µg Cloprostenol	Macmillan et al. (2020)
WTAI-PRs		52.84		

Note. PGF-AI (h) = Time interval between CIDR® removal to TAI, TAI-PR (%) = Pregnancy rates to timed artificial insemination, 5DCOS + CIDR® = Initial GnRH + CIDR® insertion (D0), single PGF (25 mg standard dose on D5) at CIDR® removal, TAI of 72 and 56-72 hours (beef cows and heifers respectively) after CIDR® removal, Modified 5DCOS: Same as standard 5DCOS protocol except without initial GnRH and second PGF

Table 3
WTAI-PR for 5DCOS +CIDR® protocol in beef cattle using a single large dose or two standard doses (i.e., doubled dose) concurrently

Cows				
n	**PGF to AI (h)**	**TAI-PR (%)**	**Notes**	**Reference(s)**
199	72	51.8	50 mg Dinoprost as single dose	Stevenson et al. (2011)
829	72	51.0	Concurrently (2 × 25 mg each)	Bridges et al. (2012)
203	72	51.0	Concurrently (2 × 25 mg each)	Ahmadzadeh et al. (2021)
551	72	49.5	Concurrently (2 × 500 µg Cloprostenol) with 100 µg initial GnRH	Rojas Canadas et al. (2023)
550	72	49.6	Concurrently (2 × 500 µg Cloprostenol) with 200 µg initial GnRH	
WTAI-PRs		50.38		
Heifers				
291	56	51.9	50mg Dinoprost as single dose	White et al. (2016)
WTAI-PRs		51.9		

Note. PGF-AI (H) = Interval from CIDR® removal to TAI (Timed-AI), TAI-PR (%) = Timed AI pregnancy rate, 5DCOS +CIDR® = Initial GnRH + CIDR® insertion (D0), double PGF (Either two doses of 25 mg concurrently or single large dose of 50mg) at CIDR® removal, TAI at 72 and 56-72 hours (for beef cows and heifers respectively) after CIDR® removal

Table 4
WTAI-PRs for 5DCOS +CIDR® protocol in beef cattle using two separate doses of PGF (2 – 24 hours interval; initial PGF at CIDR® removal)

Cows					
n	**PGF-AI (h)**	**TAI-PR (%)**	**PGF Delivery**	**Notes**	**Reference(s)**
111	60	56.8	12 hours later	25 mg each Dinoprost	Bridges et al. (2008)
105	72	80.0	12 hours later	25 mg each Dinoprost	
199	72	65.3	12 hours later	25 mg each Dinoprost	
282	72	69.0	7 hours later	25 mg each Dinoprost	Kasimanickam et al. (2009)
89	72	54.5	3 hours later	500µg Cloprostenol	Johnson et al. (2009)
210	72	67.0	12 hours later	25 mg each Dinoprost	Wilson et al. (2010)
881	72	52.7	2.25±0.05 hours later	25 mg each Dinoprost	Whittier et al. (2010)
901	72	57.2	6.45±0.03 hours later	25 mg each Dinoprost	
217	72	50.3	6 hours later	25 mg each Dinoprost	Peel et al. (2010)
216	72	51.1	12 hours later	25 mg each Dinoprost	
195	72	57.4	8 hours later	25 mg each Dinoprost	Stevenson et al. (2011)
821	72	55	8 hours later	25 mg each Dinoprost	Bridges et al. (2012)
911	72	58.1	6 hours later	25 mg each Dinoprost	Whittier et al. (2013)
438	72	62.3	2 to 10 hours later	N/A	Gunn et al. (2015)

Table 4 *(continue)*

Cows					
n	**PGF-AI (h)**	**TAI-PR (%)**	**PGF Delivery**	**Notes**	**Reference(s)**
100	72	71.0	7-11 hours later	25 mg each Dinoprost	Corpron et al. (2019)
201	72	52.0	8 hours later	25 mg each Dinoprost	Ahmadzadeh et al. (2021)
208	72	61.0	24 hours later	500µg Cloprostenol	Zwiefelhofer et al. (2021)
WTAI-PRs		57.98			
Heifers					
298	72	62.1	6 hours later	25 mg each Dinoprost	Peterson et al. (2011)
554	56	66.2	6 hours later	25 mg each Dinoprost	Kasimanickam et al. (2012)
544	72	55.9	6 hours later	25 mg each Dinoprost	
237	56	50.2	6 hours later	25 mg each Dinoprost (without initial GnRH)	Kasimanickam et al. (2014)
228	56	58.3	6 hours later	25 mg each Dinoprost (with initial GnRH)	
270	72	62.6	> 4 hours later	25 mg each Dinoprost	Bridges et al. (2014)
1887	56	55.5	6 hours later	25 mg each Dinoprost	Kasimanickam et al. (2015)
718	72	57.8	6 hours later	25 mg each Dinoprost	
291	56	63.6	6 hours later	25 mg each Dinoprost	White et al. (2016)
153	72	66.7	24 hours later	500µg Cloprostenol	Zwiefelhofer et al. (2021)
WTAI-PRs		58.42			

Table 5
WTAI-PR to 7DCOS + CIDR® protocol in beef cattle

Cows				
n	**PGF-AI (h)**	**TAI-PR (%)**	**Notes**	**Reference(s)**
539	60	54.0	25 mg Dinoprost	Larson et al. (2006)
365	64	44.7	25 mg Dinoprost	Kasimanickam et al. (2006)
599	60	52.0	25 mg Dinoprost	Kasimanickam et al. (2008)
112	60	52.7	25 mg Dinoprost	Bridges et al. (2008)
111	60	66.7	25 mg Dinoprost	
201	60	56.2	25 mg Dinoprost	
424	54	61.0	25 mg Dinoprost	Busch et al. (2008)
427	66	67.0	25 mg Dinoprost	
89	56	53.4	500 µg, Cloprostenol	Johnson et al. (2009)
736	66	51.5	Fresh semen (25 mg Dinoprost)	Bucher et al. (2009)
719	66	59.0	Frozen semen (25 mg Dinoprost)	

Table 5 *(continue)*

Cows				
n	**PGF-AI (h)**	**TAI-PR (%)**	**Notes**	**Reference(s)**
136	48	38.2	25 mg Dinoprost	Dobbins et al. (2009)
157	56	61.1	25 mg Dinoprost	
170	64	51.8	25 mg Dinoprost	
142	72	47.2	25 mg Dinoprost	
209	66	67.0	25 mg Dinoprost	Wilson et al. (2010)
619	60	54.6	25 mg Dinoprost	Echternkamp & Thallman (2011)
906	66-72	55.1	25 mg Dinoprost	Whittier et al. (2013)
773	66	54.0	25 mg Dinoprost	Mercadante et al. (2015)
383	66	60.0	Conventional semen (500 µg Cloprostenol)	
386	66	44.0	Sexed semen (500 µg Cloprostenol)	
WTAI-PRs		54.91		
Heifers				
531	60	53.0	25 mg Dinoprost	Lamb et al. (2006)
109	54	47.0	25 mg Dinoprost	Busch et al. (2007)
145	57.5	53.0	Without initial GnRH (25 mg Dinoprost)	Ahmadzadeh et al. (2015)
498	54	55.0	25 mg Dinoprost	Mercadante et al. (2015)
433	60	54.2	Lutalyse® HighCon (25 mg Dinoprost)	Kasimanickam et al. (2021)
WTAI-PRs		53.50		

Note. 7DCOS + CIDR® = Initial GnRH + CIDR® insert (D0), PG (single PG, 25mg) on D7, TAI/GnRH: 48–72 and 54–60 hours in cows and heifers respectively after CIDR® removal

Table 6
Cows under 7DCOS (Sex-sorted)

n	**TAI-PR (%)**	**Reference(s)**
187	22.32	MacMurracy et al. (2020)
405	48.00	Thomas et al. (2019)
338	44.00	Andersen et al. (2021)
88	40.20	Aubuchon et al. (2022)
386	44.00	Mercadante et al. (2015)
276	53.30	Crite et al. (2018)
40	55.00	Crite et al. (2018)
n= 1720	WTAI-PRs (44.14)	

Table 7
Heifers under 7DCOS (Sex-sorted)

n	**TAI-PR (%)**	**Reference(s)**
356	36.90	Oosthuizen et al. (2021)
360	42.10	Oosthuizen et al. (2021)
78	51.30	Crite et al. (2018)
n= 794	WTAI-PRs (40.67)	

Table 8
Country and experimental area climatic zones

Country	Authors	Climate
Virginia, USA	Kasimanickam et al. (2009)	Humid, Subtropical
Manhattan, USA	Stevenson et al. (2011)	Humid subtropical
Florida, USA	Mercadante et al. (2015)	Humid subtropical
Colorado, USA	Bridges et al. (2012)	Semi-arid
Moscow, Russia	Corppron et al. (2019)	Humid continental
Alberta, Canada	Macmillan et al. (2020)	Continental
Washington, USA	Peterson et al. (2011)	Temperate
Washington, USA	Kasimanickam et al. (2014)	Temperate
Ohio, USA	Cruppe et al. (2014)	Humid- continental
Idaho, USA	Ahmadzadeh et al. (2015)	Temperate
Washington, USA	White et al. (2016)	Temperate
Manhattan, USA	Stevenson et al (2011)	Humid subtropical
Colorado, USA	Bridges et al. (2012)	Semi-arid
Idaho, USA	Ahmadzadeh et al. (2021)	Temperate
Ohio, USA	Rojas Canadas et al. (2023)	Humid continental
Washington, USA	White et al. (2016)	Temperate
Colorado, USA	Bridges et al. (2008)	Semi-arid
Virginia, USA	Kasimanickam et al. (2009)	Humid subtropical
Manhattan, USA	Johnson et al. (2009)	Humid subtropical
Missouri, USA	Wilson et al. (2010)	Continental
Virginia, USA	Whittier et al. (2010)	Humid subtropical
Colorado, USA	Peel et al. (2010)	Semi-arid
Manhattan, USA	Stevenson et al. (2011)	Humid subtropical
Colorado USA	Bridges et al. (2012)	Semi-arid
Virginia, USA	Whittier et al. (2013)	Humid subtropical
Pardue, USA	Gunn et al. (2015)	Continental
Moscow, Russia	Corpron et al. (2019)	Humid continental
Moscow, Russia	Ahmadzadeh et al. (2021)	Humid continental
Alberta, Canada	Zwiefelhofer et al. (2021)	Continental
Washington, USA	Peterson et al. (2011)	Temperate
Virginia, USA	Kasimanickam et al. (2012)	Humid subtropical
Washington, USA	Kasimanickam et al. (2014)	Temperate
Colorado USA	Bridges et al. (2014)	Semi-arid
Virginia, USA	Kasimanickam et al. (2015)	Temperate
Washington, USA	White et al. (2016)	Temperate
Alberta, Canada	Zwiefelhofer et al. (2021)	Continental
Minnesota, USA	Larson et al. (2006)	Humid continental
Virginia, USA	Kasimanickam et al. (2006)	Humid subtropical
Virginia, USA	Kasimanickam et al. (2009)	Humid subtropical

Table 8 *(continue)*

Country	Authors	Climate
Colorado, USA	Bridges et al. (2008)	Semi-arid
Missouri, USA	Busch et al. (2008)	Continental
Manhattan, USA	Johnson et al. (2009)	Humid subtropical
Virginia, USA	Bucher et al. (2009)	Humid, Subtropical
Manhattan, USA	Dobbins et al. (2009)	Humid subtropical
Missouri, USA	Wilson et al. (2010)	Continental
Nebraska, USA	Echternkamp and Thallman (2011)	Humid continental/semi-arid
Virginia, USA	Whittier et al. (2013)	Humid, Subtropical
Virginia, USA	Whittier et al. (2013)	Humid, Subtropical
Florida, USA	Mercadante et al. (2015)	Humid subtropical
Minnesota, USA	Lamb et al. (2006)	Humid continental
Missouri, USA	Busch et al. (2007)	Continental
Idaho, USA	Ahmadzadeh et al. (2015)	Temperate
Florida, USA	Mercadante et al. (2015)	Humid subtropical
Virginia, USA	Kasimanickam et al. (2021)	Humid subtropical

FACTORS AFFECTING TAI-PREGNANCY RATES

A variety of factors influence the TAI-PRs in cattle, and these can differ based on specific synchronization methods used, management practices, and characteristics of the cattle population. The meta-analysis report by Richardson et al. (2016) revealed that the body condition score, expression of estrus before AI, and cyclicity had the greatest influence on conception rates in beef cows exposed to TAI programs. Some of the key factors impacting TAI-PRs are discussed below.

Body Condition Score (BCS)

The impact of BCS on reproductive performance in cattle has been extensively studied (D'Occhio et al., 2019; Nazhat et al., 2021; Wang et al., 2019). Body condition scores serve as a crucial indicator of the adipose tissue content in cattle, and it is widely acknowledged by both animal scientists and livestock producers as a fundamental element of dairy cow management and is considered a valuable tool for subjectively assessing the levels of body energy reserves (Pfeifer et al., 2021; Roche et al., 2009). Negative energy balance (NEB) affects the resumption of the postpartum ovarian cycle by impeding LH pulse frequency as well as decreasing blood glucose and insulin growth factor-1 (IGF-1), which altogether prevents E2 production by preovulatory follicles (Butler, 2001). In cows with high milk yield, persistent NEB increases the incidence of anestrus due to smaller dominant follicles, leading to insufficient E2 production to cause ovulation (Roche & Diskin, 2001). Inadequate body condition causes failure to resume cyclicity and prolongs the calving interval, a good indicator of herd productivity (Eversole et al., 2005).

Furthermore, cattle with low energy levels fail to express estrus, which is an important indicator of pregnancy success (Wiltbank et al., 1962). For instance, cattle with poor BCS at calving take longer to resume cyclicity (D'Occhio et al., 2019). The overall reproductive parameters such as calving rate, weaning weight, and number of calves weaned are greater in beef cows with BCS > 5 compared to cows with BCS < 5 (1-9 scale) (Cooke et al., 2021). Similarly, Vedovatto et al. (2022) demonstrated greater pregnancy rates and estrus expression in cows with BCS < 5 than BCS < 5 in beef cattle. Furthermore, in suckling beef cows that were exposed to TAI, PRs were greater in high (≥ 3.5) and moderate (2.75–3.25) BCS compared to low (2–2.5) in 1–5 scale BCS) (Nishimura et al., 2018). It was reported that one of the major reasons for suckling beef cows failing to resume cyclicity after calving is due to inadequate BCS at calving time (Crowe et al., 2014). Whittier et al. (2013) also observed lower TAI-PRs for cows with BCS ≤ 4 (49.3%) compared to those > 6 (55.8%).

Apart from BCS alone, understanding other factors that interact together to impact TAI outcomes is crucial in improving herd productivity. For instance, older cows with good BCS may fail to give satisfactory pregnancy rates due to reduced ovulation rates, inadequate GnRH release, and poor egg quality. Similarly, heifers with ideal BCS may not perform well in the tropics due to heat stress. On the other hand, an effective synchronization protocol coupled with good BCS may contribute positively to pregnancy outcomes. For optimizing breeding programs, breeders must be aware of such interactions while implementing TAI programs. Setiaji et al. (2023) reported that BCS and breeding season affected conception rates whereby, cows with BCS 3 and 4 (1 to 5 scale) had better conception rates during autumn, while cows with BCS of 5 showed the highest conception rates during autumn and winter. However, lower rates during spring and summer indicating some seasons have more favorable conception rates than others. Furthermore, the success of postpartum rebreeding is attributed to the combined effect of BCS and nutrient availability in the feed, as higher BCS causes increased plasma P4, which is crucial for maintaining pregnancy (Randel., 1990; Vedovatto et al., 2022).

Expression of Estrus Before TAI

The impact of estrus expression in cattle subjected to TAI programs has been substantially documented. The occurrence of estrus before TAI has a beneficial effect on pregnancy rates. It is attributed to its ability to modify the uterine environment, enhance the number of accessory sperm, improve fertilization rates, and promote embryo survival (Richardson et al., 2016). Additionally, sex steroids alter the composition of cervical mucus during estrus, facilitating the movement of spermatozoa through the cervix to achieve successful fertilization (Tsiligianni et al., 2011). The effect of estrus expression before TAI was revealed in the meta-analysis by Richardson et al. (2016), where beef cows that had exhibited estrus before TAI had 27% greater PRs compared to those not expressing estrus. Similarly, Cedeño

et al. (2020) examined the influence of estrous expression on pregnancy rates in an embryo transfer (ET) program and found that recipient cows that exhibited estrus had a significantly higher PR/ET compared to cows that did not exhibit estrus (39.0% vs. 25.0%) regardless of the type of treatments. They also observed higher calving rates and lower pregnancy losses in recipient cows that exhibited estrus. Furthermore, Sá Filho et al. (2011) demonstrated larger follicle size, greater ovulation rate, larger CL, and a higher P4 concentration in cows that expressed estrus prior to AI. This knowledge is of particular importance in programs that utilize expensive sex-sorted semen. By selectively distributing sex-sorted semen to females that exhibit estrus, the cost per pregnancy may be lowered, and pregnancy rates may be enhanced. In the study by Perry, Walker et al. (2020), higher conception rates for both conventional and sexed-sorted semen were observed in females who exhibited estrus in a TAI program—additionally, Bó and Cedeño. (2018) also observed greater PRs and lower pregnancy losses in cows displaying estrus that utilized embryos generated from *in-vitro* and *in-vivo* methods. Furthermore, the overall TAI-PRs in postpartum cows were significantly higher ($p = 0.01$) in cows that showed estrus behaviors before TAI compared to those that did not (73.0 Vs. 45.0%) (Nash et al., 2012). The results from these studies indicate a positive impact of estrus expression on pregnancy outcomes in a TAI Program.

The expression of estrus is dependent on several factors, irrespective of its detection efficiency. Estradiol from the dominant follicle plays a vital role in inducing sexual behavior in cattle, and it triggers luteinizing hormone surge to cause ovulation. Thus, a hormonal environment that supports intense estrus behaviors is closely associated with timely ovulation and fertilization. The interaction between BCS and estrus expression is well-documented. Cows with higher BCS are more likely to show estrus behaviors than those with low BCS, which, in turn, improves their likelihood of successful breeding (Nazhat et al., 2021). Conversely, cows with low BCS may either fail to express estrus behaviors or lack intensity, resulting in reduced TAI-PRs following synchronization because of low energy reserve, which impacts the production of reproductive hormones. In contrast, over-conditioned cows may suffer from metabolic disorders (Bisinotto et al., 2010).

Stage of Estrous Cycle at the Initiation of the TAI Program

The estrous cycle stage at the initiation of the TAI program can be determined by ultrasound examination to identify the presence or absence of CL. Additionally, transrectal palpation and quantification of milk or blood P4 can be used to determine the presence of CL. Significantly higher PRs were observed in beef heifers that possessed CL at the initiation of the TAI program compared to those that did not (71.3 vs. 59.0%) (Núñez–Olivera et al., 2022). This finding also aligns with the report of Stevenson et al. (2011), where cyclic lactating postpartum beef cows subjected to 5DCOS plus CIDR® protocol had greater TAI-PRs than those not-cycling (53.4 vs. 45.6%). They also observed that those cows

possessing CL at the initiation of the program were 1.5 times more likely to get pregnant. Similarly, the conception rate of cyclic beef cows (66.0%) was significantly higher than that of anestrus cows (53.0%), irrespective of the TAI protocols used (Geary et al., 2001). In the meta-analysis by Borchardt et al. (2020), lactating cows that had functional CL at the initiation of the TAI program had a 10.0% improved PR/AI. A greater TAI-PR was also reported by Mercadante et al. (2015) in suckling beef cows, where cows with CL at the initiation of the TAI program had significantly higher pregnancy rates compared to those that did not (66.3% vs. 39.4%, $p = 0.012$). The increased pregnancy rates in cows with CL may be due to increased endogenous P4 concentration, which improved ovulation synchronization and oocyte/follicle maturation, and due to a positive effect on the endometrium (Bisinotto et al., 2015).

Cyclicity during protocol initiation has been closely linked to animal's BCS. Cattle with BCS of 3-4 (5-scale point) are more likely to be cyclic and better respond to TAI programs. Furthermore, cyclicity is not only affected by BCS but also impacts how cows respond to hormonal treatments in TAI programs (Lucy, 2007). The likelihood of estrus rates in heifers synchronized using a modified 5DCOS program revealed a significant interaction between the presence of corpus luteum, the treatment protocol, and eCG treatment (Macmillan et al., 2020). CL on the ovary indicates a normal estrous cycle in cattle. It serves as an important source of P4, which in turn improves estrus synchronization, which is one of the possible reasons for stimulating puberty in heifers and helps resume postpartum estrus in cows supplemented with P4 at the initiation of synchronization (Kasimanickam et al., 2020).

Breeding Season

The impact of TAI programs on pregnancy rates was variable across several breeding seasons. It suggests that the efficacy of treatment protocols depends on the breeding season under consideration. For instance, a significant effect of the breeding season on pregnancy rates was observed in suckled beef cows (Bilbao et al., 2019; Randi et al., 2021). The conception rate for dairy cattle after the first post-calving insemination was lowest during the summer (Souames & Berrama, 2020) and this may be attributed to the increased ambient temperature leading to heat stress as it negatively impacts fertilization and embryo survival. Spring is commonly targeted for cattle breeding as it allows calves to be born in more favorable weather conditions that minimize the risks of cold stress to newborns and increase calf survivability (Keskin et al., 2016).

However, in tropical regions of the world, cattle breeding requires careful consideration of environmental, nutritional, and reproductive factors, as extreme heat and rainfall may negatively affect fertility. Targeting cooler and drier months of the year can help reduce heat stress and improve pregnancy rates. Additionally, scheduling breeding after the rainy season will ensure sufficient fodder availability to maintain a healthy body condition score.

Anestrus is a common condition among cattle in tropical regions characterized by shorter estrus periods, mostly occurring at night, affecting AI programs. The use of hormonal treatments consisting of progesterone device, GnRH, PGF, eCG, and Estradiol benzoate results in consistent pregnancy rates in *Bos indicus* cows adapted in this region and could be an alternative to improve breeding efficiency (Baruselli et al., 2004).

Environmental and Management Factors

Environmental and managemental factors play a vital role in TAI-PRs in beef cows by influencing cows' physiology, reproductive efficiency, and overall herd fertility. Extreme temperature, particularly heat stress, impairs ovarian functions, reduces oocyte quality, affects embryo development, and lowers PRs (De Rensis & Scaramuzzi, 2003). Deficiency of nutrients and inadequate BCS cause a delay in estrus expression with poor response to synchronization, leading to reduced conception rates (Bó et al., 2002). Furthermore, management practices such as poor estrus detection, improper animal handling during synchronization and AI, and faults in semen storage or handling can lower AI success (Diskin & Morris, 2008). Proper herd management, optimizing nutritional requirements, and reducing stress are essential to enhancing TAI-PRs in beef cows.

LIMITATIONS

Exclusive Focus on Beef Cattle

The techniques examined in this review solely relied on data obtained from beef cattle studies, which may restrict the results' applicability to other cow populations and breeds. Further studies should strive to include a broader spectrum of cattle demographics in conducting a more thorough and complete assessment.

Restriction to CIDR® as a Progesterone Source

The review selectively considered manuscripts that employed CIDR® as the source of progesterone, which may have restricted the findings' applicability to other progesterone devices. Future reviews could incorporate a more diverse range of progesterone devices to provide a more holistic understanding of the efficacy of different protocols.

Inclusion of Data from Sex-sorted Semen

Pregnancy rates resulting from sexed semen are usually lower than conventional semen. Thus, the inclusion of data from sexed sorted semen may have contributed nuance to the overall findings. Future reviews should consider adding information for non-conventional semen.

Potential Biases in Reviewed Studies

The overall WTAI-PRs reported in our review may also be limited because of potential biases. Firstly, the trial size of the reviewed papers ranged from a minimum of 40 to a maximum of 1887 across studies. The applicability of results from a small trial size may affect the reliability of the findings and complicate application in a larger population in the practical setting. Secondly, most studies reviewed were from the states of the United States of America, where heat stress is seasonal, unlike in the tropics, where heat stress is year-round, which may negatively affect breeding outcomes. Thirdly, the type of cattle breeds used for experiments are mostly exotic or their crosses. Such results cannot be generalized to *Bos indicus* and other local breeds in tropical regions. Lastly, most reviewed studies do not specify the management practices of experimental animals. Therefore, our WTAI-PRs were unable to account for the effect of different management practices, including diet, humidity, and type of husbandry practices.

DISCUSSION

This paper reviewed pregnancy rates in 7DCOS and pregnancy rates obtained from different methods of prostaglandin delivery in 5DCOS. Other factors besides the treatments used in TAI programs were also observed. A WTAI-PR of 54.91% and 53.5% in 7DCOS for cows and heifers were observed (Figure 3). The WTAI-PR for 5DCOS were reviewed separately for single, double, and two separate doses, with the results showing 51.75% and 52.84% (single dose), 50.38% and 51.90% (double), and 57.98% and 58.42% (two separate doses) for cows and heifers respectively (Figure 2). Outside of these treatment protocols, factors such as body condition score, breeding season, estrus expression prior to TAI, and cyclicity prior to treatment initiation also influenced TAI-PRs. The WTAI-PRs based on geographical locations of the experiment and cattle breed is shown in Figure 4 and 5 respectively.

Although the increased length of proestrus indicated by the duration between PGF and GnRH-induced LH surge or the interval from the ejection of P4 device to GnRH/TAI should show increased pregnancy rates (Bó et al., 2016; Day, 2018; de la Mata et al., 2018), WTAI-PRs in both 7DCOS and 5DCOS when PGF is delivered in a single and double dose were comparable. It shows that reducing the number of synchronization durations (from a minimum of nine days in 7DCOS to eight days in 5DCOS) and CIDR® exposure duration (from seven days in 7DCOS to five days in 5DCOS) has no impact on TAI-PRs. However, two separate PGF doses had a higher WTAI-PR in 5DCOS compared to 7DCOS, in which PGF is always delivered as a one-time dose (single and double). Reducing the P4 device exposure from seven days to five resulted in a young immature corpus luteum that resisted complete luteolysis, and two PGF doses in 5DCOS are required (Bridges et al., 2012). However, WTAI-PR for both 7DCOS and 5DCOS were within the range reported for TAI-PRs (Bó et al., 2018).

While most evidence of PRs through CO-Synch programs is based on experimental research with different trial sizes, they do not truly understand the program's overall effect on PRs. This review employed a weighted average approach to provide a more reliable estimate of pregnancy rates under CO-Synch programs. This method of weighted timed artificial insemination accounts for the disparity in animal numbers across studies by dividing trial sizes in each study in the review by the sum of all the trial sizes, thereby enabling all the studies reviewed to have the same animal numbers.

Beef farmers were seen to be slow in adopting AI technology primarily because of the labor-intensive nature of the tasks involved and the considerable time needed for detecting heat (Colazo & Mapletoft. 2014). Although labor can be saved with TAI programs, multiple doses (especially two separate) are needed to increase PRs under 5DCOS, which involves extra labor for animal handling and added hormonal costs. The advent of TAI programs has enhanced pregnancy rates because cattle are inseminated irrespective of estrus expression prior to AI (Colazo & Mapletoft, 2014). With two separate PGF doses in 5DCOS, TAI is more effective in achieving high pregnancy rates. Since beef cattle are typically raised in extensive systems where less time is spent monitoring them compared to dairy cattle, synchronization programs that depend on heat detection are not feasible (Taponen, 2009). Beef farmers would have to incur added costs just to improve PRs. It could lead to a further decrease in adoption rates of AI technology among beef producers.

As this review focused on beef cattle, the applicability of results to other cattle breeds not bred for beef is limited. Focus was made on CO-Synch programs mainly because there is a lack of understanding of the average effect of CO-Synch programs on pregnancy rates in beef cattle. Additionally, CO-Synch programs are mostly implemented in beef cattle compared to dairy cattle (Colazo & Mapletoft, 2014). This review's applicability is also limited to CIDR® and no other progesterone devices such as PRID, PRID-Delta, and TRIU-B. CIDR® mainly due to its widespread adoption and effectiveness in releasing progesterone. Furthermore, CIDR® has regulatory approval and standardization, providing consistent synchronization outcomes in breeding programs (Klabnik & Horn, 2023).

Results obtained from our review are not applicable outside the use of conventional semen. Sex-sorted semen is prevalent in 7DCOS, and PRs are relatively lower than conventional semen in both cows and heifers. Sex-sorted semen via 7DCOS showed WTAI-PR of 44.14% and 40.67% in cows and heifers, respectively (Tables 6 -7).

Despite discussing different hormonal inductions and ART such as Ovsynch, 7DCOS and 5DCOS, these methods basically fall under ART in cattle and remain a hot subject, particularly in farms managed in precision and tuned to profit from high-quality animals. Because this is actively being pursued in two types of cattle industries (dairy and specialized beef cattle breeding farms), rates of use of CO-Synch protocols in beef cattle are understandably lower for sex-sorted semen. Our review used fewer publications

since publications are also far apart in dates. Although AI technology is not new, and in the 90 years of its use, the achievement of more than 50% PR from hormonally induced ovulation + AI can teach us important lessons. In this review, results of the percentage of PRs have been sought from data involving thousands of animals, and the highest rate for this protocol is settled at this point. Even in beef cattle, the focus of using ART should never be for common farms and/or common breeds. However, ART might be an important tool to quickly propagate high-quality beef cattle to impact population size and contribute to the industry. This review provides a guide as to when the CO-Synch protocols would be an important tool for the beef cattle industry and which protocols would be a choice in achieving higher PRs.

Most papers that were reviewed took place in temperate and sub-tropical climates, and therefore, the results cannot be generalized to countries with tropical conditions (Table 8). This review attempted to look at the application of CO-Synch protocols in the tropics, but this proved difficult given the lack of publications in tropical climates. Nevertheless, a good number of studies have been carried out in some of the states in the United States of America that have humid subtropical climate zones. It indicates an opportunity for breeders to explore the potential of CO-Synch programs in the tropics due to the closely related climatic zone.

CO-Synch protocols are unsuitable for extensive beef cattle farming, whereby the animals' body condition is determined largely by environmental factors. Careful management of environmental conditions such as heat stress and adequate nutrition are still required for intensive beef cattle farms in the tropics. In general, 7DCOS would be appropriate for both intensive and extensive beef farms, provided beef farmers are willing to invest labor and time. The employment of 5DCOS with two doses of PGF may increase the number of animal handlings, which may negatively impact the farm's profitability. Therefore, a modified version with a single-double-dosed PGF would be an alternative to reduce the number of animal handlings.

While the reviewed studies show various P4-based TAI programs, it is important to note that these studies were conducted mostly under controlled experimental conditions that may not fully reflect real-world breeding environments. For instance, common tropical climate features such as excessive heat and humidity are not accounted which may potentially limit the generalizability of findings to regions where such conditions exist (De Rensis & Scaramuzzi, 2003). Furthermore, some studies used optimally managed herds with good nutrition, estrus detection, and AI techniques, which may not reflect more variable management practices encountered by cattle breeders. Although various P4 devices are available for use, this review specifically focused on CIDR (Reason cited elsewhere in this review) with exposure duration of either 5 (5DCOS) or 7 (7DCOS) days. However, the articles reviewed herein did not assess the long-term impact of CIDR devices, especially

for management systems that are under-resourced. Likewise, the efficacy of CIDR-based programs in minimizing early embryonic loss and improving PRs in tropical regions remains underexplored. Since the absorption rates of P4 and response to hormonal induction may vary under extreme heat stress, future research should aim to assess the reproductive performance of different P4 devices in tropical regions (Bó et al., 2002). Additionally, most studies focused on immediate TAI success rates without long-term follow-up on reproductive efficiency and health. It may result in an insufficient understanding of the implications of treatment protocols in real-world settings. Most studies in TAI protocols are focused on the effectiveness of TAI programs on PRs without studying the economic implications of these protocols. So, future studies should study CO-Synch protocols' cost-effectiveness and economic efficiency.

CO-Synch protocols are not commonly employed in Malaysia, with reported lower pregnancy rates of 18-23.3% using the CIDR-based TAI program (Azizah et al., 2014; Malik et al., 2012). With the growing enthusiasm for genetic improvement in Malaysian cattle through AI, future studies could look at the use of CO-Synch protocols in Malaysia as the demand for better genetics increases. Although CO-Synch programs are predominant in the Western world in temperate climates, it would be a good opportunity for beef producers to use native beef cattle well adapted to the warm tropics like the Kedah-Kelantan and their crossbreeds.

CONCLUSION

This review examined the reproductive outcomes associated with 5DCOS and 7DCOS plus CIDR® protocols in beef cattle. The importance of selecting the most appropriate PGF administration method in the 5DCOS protocol to optimize reproductive success in cattle production and factors other than the protocols themselves when implementing TAI protocols, such as body condition, breeding season, nutritional management, and estrus expression before AI, were highlighted. The CO-Synch programs looked at had different trial sizes, and this variability did not provide a true understanding of the program's overall effect on PRs. Therefore, this review employed a weighted average approach. As beef cattle are typically raised in extensive systems where less time is spent monitoring, synchronization programs that depend on heat detection are not feasible for beef cattle. Additional costs would be incurred to employ programs like the 5DCOS with two separate PGF injections. The increase in economic cost for extra animal handling and hormone purchase might discourage adoption rates of AI technology among beef producers. Among the protocols presented, 7DCOS would be appropriate for both intensive and extensive beef farms, provided farmers are willing to invest time and labor.

ACKNOWLEDGEMENTS

The authors extend our heartfelt gratitude to the Universiti Putra Malaysia for providing access to electronic databases and facilitating full access to scientific papers.

REFERENCES

Ahmadzadeh, A., Corpron, M., Hall, J. B., Ahmadzadeh, A., & Dalton, J. (2021). 234 pregnancy and hormonal response in suckled beef cows administered high-concentration prostaglandin F2α in a 5-day CO-Synch + CIDR synchronization program. *Journal of Animal Science, 99*(Supplement 3), 122–123. https://doi.org/10.1093/jas/skab235.224

Ahmadzadeh, A., Gunn, D., Hall, J. B., & Glaze, J. B. (2015). Evaluation of treatment with a 5-day versus 7-day controlled internal drug-release insert on reproductive outcomes of beef heifers using a modified timed–artificial insemination protocol. *The Professional Animal Scientist*, *31*(3), 270–277. https://doi.org/10.15232/pas.2014-01378

Andersen, C. M., Bonacker, R. C., Smith, E. G., Spinka, C. M., Poock, S. E., & Thomas, J. M. (2021). Evaluation of the 7 & 7 Synch and 7-day CO-Synch + CIDR treatment regimens for control of the estrous cycle among beef cows prior to fixed-time artificial insemination with conventional or sex-sorted semen. *Animal Reproduction Science*, *235*, 106892. https://doi.org/10.1016/j.anireprosci.2021.106892

Aubuchon, K. W., Odde, J. A., Bronkhorst, C., Bortoluzzi, E. M., Goering, M. J., Fike, K. E., & Odde, K. G. (2022). Field trial assessing the use of sex-sorted semen in beef cattle. *Kansas Agricultural Experiment Station Research Reports*, *8*(1), 14. https://doi.org/10.4148/2378-5977.8233

Azizah, A., Ariff, O. M., Ahmad Nazri, A. R., Wahid, H., Ahmad, J., & Saadiah, J. (2014). Pregnancy rate from timed-artificial insemination and natural service of oestrus synchronized Kedah-Kelantan and crossbred cows in two management systems. *Malaysian Journal of Animal Science*, *17*(2), 11-21.

Baruselli, P. S., Reis, E. L., Marques, M. O., Nasser, L. F., & Bó, G. A. (2004). The use of hormonal treatments to improve reproductive performance of anestrous beef cattle in tropical climates. *Animal reproduction science*, *82*, 479-486. https://doi.org/10.1016/j.anireprosci.2004.04.025

Bilbao, M. G., Zapata, L. O., Harry, H. R., Wallace, S. P., Farcey, M., Gelid, L., Palomares, R. A., Ferrer, M. S., & Bartolome, J. (2019). Comparison between the 5-day CO-Synch and 7-day estradiol-based protocols for synchronization of ovulation and timed artificial insemination in suckled Bos taurus beef cows. *Theriogenology*, *131*, 72–78. https://doi.org/10.1016/j.theriogenology.2019.01.027

Bisinotto, R. S., Greco, L. F., Ribeiro, E. S., Martinez, N., Lima, F. S., Staples, C. R., & Santos, J. E. P. (2018). Influences of nutrition and metabolism on fertility of dairy cows. *Animal Reproduction (AR)*, *9*(3), 260-272.

Bisinotto, R., Lean, I., Thatcher, W., & Santos, J. (2015). Meta-analysis of progesterone supplementation during timed artificial insemination programs in dairy cows. *Journal of Dairy Science*, *98*(4), 2472–2487. https://doi.org/10.3168/jds.2014-8954

Bó, G. A., & Baruselli, P. S. (2014). Synchronization of ovulation and fixed-time artificial insemination in beef cattle. *Animal*, *8*(s1), 144–150. https://doi.org/10.1017/s1751731114000822

Bó, G. A., & Cedeño, A. (2018). Expression of estrus as a relevant factor in fixed-time embryo transfer programs using estradiol/progesterone-based protocols in cattle. *Animal Reproduction*, *15*(3), 224–230. https://doi.org/10.21451/1984-3143-AR2018-0060

Bó, G. A., Baruselli, P. S., Moreno, D., Cutaia, L., Caccia, M., Tríbulo, R., & Mapletoft, R. J. (2002). The control of follicular wave development for self-appointed embryo transfer programs in cattle. *Theriogenology*, *57*(1), 53-72. https://doi.org/10.1016/S0093-691X(01)00657-4

Bó, G. A., de la Mata, J. J., Baruselli, P. S., & Menchaca, A. (2016). Alternative programs for synchronizing and resynchronizing ovulation in beef cattle. *Theriogenology*, *86*(1), 388–396. https://doi.org/10.1016/j.theriogenology.2016.04.053

Borchardt, S., Pohl, A., & Heuwieser, W. (2020). Luteal presence and ovarian response at the beginning of a timed artificial insemination protocol for lactating dairy cows affect fertility: A meta-analysis. *Animals*, *10*(9), 1551. https://doi.org/10.3390/ani10091551

Bridges, A., Lake, S., Lemenager, R., & Claeys, M. (2008). *Timed artificial insemination in beef cows: What are the options?* Purdue University. https://www.extension.purdue.edu/extmedia/as/as_575_w.pdf

Bridges, G. A., Ahola, J. K., Brauner, C., Cruppe, L. H., Currin, J. C., Day, M. L., Gunn, P. J., Jaeger, J. R., Lake, S. L., & Lamb, G. C. (2012). Determination of the appropriate delivery of prostaglandin F2α in the five-day CO-Synch + controlled intravaginal drug release protocol in suckled beef cows. *Journal of Animal Science*, *90*(13), 4814–4822. https://doi.org/10.2527/jas.2011-4880

Bridges, G. A., Helser, L. A., Grum, D. E., Mussard, M. L., Gasser, C. L., & Day, M. L. (2008). Decreasing the interval between GnRH and PGF2α from 7 to 5 days and lengthening proestrus increases timed-AI pregnancy rates in beef cows. *Theriogenology*, *69*(7), 843-851. https://doi.org/10.1016/j.theriogenology.2007.12.011

Bridges, G. A., Lake, S. L., Kruse, S. G., Bird, S. L., Funnell, B. J., Arias, R., Walker, J. A., Grant, J. K., & Perry, G. A. (2014). Comparison of three CIDR-based fixed-time AI protocols in beef heifers. *Journal of Animal Science*, *92*(7), 3127–3133. https://doi.org/10.2527/jas.2013-7404

Bridges, G. A., Mussard, M. L., Burke, C. R., & Day, M. L. (2010). Influence of the length of proestrus on fertility and endocrine function in female cattle. *Animal reproduction science, 117*(3-4), 208-215. https://doi.org/10.1016/j.anireprosci.2009.05.002

Bucher, A., Kasimanickam, R., Hall, J. B., DeJarnette, J. M., Whittier, W. D., Kähn, W., & Xu, Z. (2009). Fixed-time AI pregnancy rate following insemination with frozen-thawed or fresh-extended semen in progesterone supplemented CO-Synch protocol in beef cows. *Theriogenology*, *71*(7), 1180–1185. https://doi.org/10.1016/j.theriogenology.2008.12.009

Busch, D. C., Schafer, D. J., Wilson, D. J., Mallory, D. A., Leitman, N. R., Haden, J. K., Ellersieck, M. R., Smith, M. F., & Patterson, D. J. (2008). Timing of artificial insemination in postpartum beef cows following administration of the CO-Synch + controlled internal drug-release protocol. *Journal of Animal Science*, *86*(7), 1519–1525. https://doi.org/10.2527/jas.2008-0925

Busch, D. C., Wilson, D. J., Schafer, D. J., Leitman, N. R., Haden, J. K., Ellersieck, M. R., Smith, M. F., & Patterson, D. J. (2007). Comparison of progestin-based estrus synchronization protocols before fixed-time artificial insemination on pregnancy rate in beef heifers. *Journal of Animal Science*, *85*(8), 8. https://doi.org/10.2527/jas.2006-845

Butler, W. R. (2001). Nutritional effects on resumption of ovarian cyclicity and conception rate in postpartum dairy cows. *BSAP Occasional Publication*, *26*(1), 133–145. https://doi.org/10.1017/S0263967X00033644

Rojas Canadas, E., Battista, S. E., Kieffer, J. D., Wellert, S. R., Mussard, M. L., & Garcia-Guerra, A. (2023). GnRH dose at initiation of a 5-day CO-Synch + P4 for fixed time artificial insemination in suckled beef cows. *Animal Reproduction Science*, *250*, 107210. https://doi.org/10.1016/j.anireprosci.2023.107210

Cedeño, A., Tríbulo, A., Tríbulo, R. J., Andrada, S., Mapletoft, R. J., & Bó, G. A. (2020). Effect of estrus expression or treatment with GnRH on pregnancies per embryo transfer and pregnancy losses in beef recipients synchronized with estradiol/progesterone-based protocols. *Theriogenology*, *157*, 378–387. https://doi.org/10.1016/j.theriogenology.2020.08.023

Colazo, M. G., & Mapletoft, R. J. (2014). A review of current timed-AI (TAI) programs for beef and dairy cattle. *The Canadian Veterinary Journal = La Revue Veterinaire Canadienne*, *55*(8), 772–780.

Cooke, R. F., Lamb, G. C., Vasconcelos, J. L. M., & Pohler, K. G. (2021). Effects of body condition score at initiation of the breeding season on reproductive performance and overall productivity of Bos taurus and Bos indicus beef cows. *Animal Reproduction Science*, *232*, 106820. https://doi.org/10.1016/j.anireprosci.2021.106820

Corpron, M. R., Menegatti Zoca, S., Reynolds, M., Carnahan, K., Hall, J. B., & Ahmadzadeh, A. (2019). Evaluating the effects of a high-concentration dose of prostaglandin F2α in a 5-d CO-Synch + controlled internal drug release protocol on fertility in beef cows. *Translational animal science*, *3*(Suppl 1), 1754–1757. https://doi.org/10.1093/tas/txz081

Crites, B. R., Vishwanath, R., Arnett, A. M., Bridges, P. J., Burris, W. R., McLeod, K. R., & Anderson, L. H. (2018). Conception risk of beef cattle after fixed-time artificial insemination using either SexedUltra™ 4M sex-sorted semen or conventional semen. *Theriogenology*, *118*, 126-129. https://doi.org/ 10.1016/j.theriogenology.2018.05.003

Crowe, M. A., Diskin, M. G., & Williams, E. J. (2014). Parturition to resumption of ovarian cyclicity: Comparative aspects of beef and dairy cows. *Animal*, *8*, 40–53. https://doi.org/10.1017/s1751731114000251

Cruppe, L. H., Day, M. L., Abreu, F. M., Kruse, S. G., Lake, S., Biehl, M.V., Cipriano, R.S., Mussard, M.L. & Bridges, G. A. (2014). The requirement of GnRH at the beginning of the five-day CO-Synch + controlled internal drug release protocol in beef heifers. *Journal of Animal Science*, *92*(9), 4198–4203. https://doi.org/10.2527/jas.2014-7772

D'Occhio, M. J., Baruselli, P. S., & Campanile, G. (2019). Influence of nutrition, body condition, and metabolic status on reproduction in female beef cattle: A review. *Theriogenology*, *125*, 277–284. https://doi.org/10.1016/j.theriogenology.2018.11.010

Dahlen, C., Larson, J., & Lamb, G. C. (2014). Impacts of reproductive technologies on beef production in the United States. In *Current and future reproductive technologies and world food production* (pp. 97–114). Springer. https://doi.org/10.1007/978-1-4614-8887-3_5

Day, M. L. (2015). State of the art of GnRH-based timed AI in beef cattle. *Animal Reproduction*, *12*(3), 473-478.

De La Mata, J. J., Núñez-Olivera, R., Cuadro, F., Bosolasco, D., De Brun, V., Meikle, A., Bó, G. A., & Menchaca, A. (2018). Effects of extending the length of pro-oestrus in an oestradiol- and progesterone-based oestrus

synchronisation program on ovarian function, uterine environment and pregnancy establishment in beef heifers. *Fertility and Development, 30*(11), 1541-1552. https://doi.org/10.1071/rd17473

De Rensis, F., & Scaramuzzi, R. J. (2003). Heat stress and seasonal effects on reproduction in the dairy cow—A review. *Theriogenology*, *60*(6), 1139-1151. https://doi.org/10.1016/S0093-691X(03)00126-2

Diskin, M. G., & Morris, D. G. (2008). Embryonic and early foetal losses in cattle and other ruminants. *Reproduction in Domestic Animals*, *43*, 260-267. https://doi.org/10.1111/j.1439-0531.2008.01171.x

Dobbins, C. A., Eborn, D. R., Tenhouse, D. E., Breiner, R. M., Johnson, S. K., Marston, T. T., & Stevenson, J. S. (2009). Insemination timing affects pregnancy rates in beef cows treated with CO-Synch protocol including an intravaginal progesterone insert. *Theriogenology, 72*(7), 1009-1016. https://doi.org/10.1016/j.theriogenology.2009.06.025

Echternkamp, S. E., & Thallman, R. M. (2011). Factors affecting pregnancy rate to estrous synchronization and fixed-time artificial insemination in beef cattle. *Journal of animal science*, *89*(10), 3060–3068. https://doi.org/10.2527/jas.2010-3549

Eversole, D. E., Browne, M. F., Hall, J. B., & Dietz, R. E. (2009). *Body condition scoring beef cows.* https://vtechworks.lib.vt.edu/server/api/core/bitstreams/dacc5413-82f2-4c0e-b5b6-d89b9e5837da/content

Geary, T. W., Whittier, J. C., Hallford, D. M., & MacNeil, M. D. (2001). Calf removal improves conception rates to the Ovsynch and CO-Synch protocols. *Journal of Animal Science*, *79*(1), 1-4. https://doi.org/10.2527/2001.7911

Gunn, P. J., Lemenager, R., & Bridges, A. (2015). Efficacy of the 5-day CO-Synch estrous synchronization protocol with or without the inclusion of a controlled internal drug release device in beef cows. *Iowa State University Animal Industry Report*, *12*(1), 1-3. https://doi.org/10.31274/ans_air-180814-1270

Johnson, S. K., Funston, R. N., Hall, J. B., Lamb, G. C., Lauderdale, J. W., Patterson, D., & Perry, G. (2010). Protocols for synchronization of estrus and ovulation. In *Proceedings Applied Reproductive Strategies in Beef Cattle San Antonio, TX* (pp. 262-270). Beed Reproduction Task Force. https://beefrepro.org/wp-content/uploads/2020/09/22-protocols.pdf

Johnson, S. K., Jaeger, J. R., Harmoney, K. R., & Bolte, J. W. (2009). Comparison of a modified 5-day CO-Synch plus CIDR protocol with CO-Synch plus CIDR in mature beef cows. In *Proceedings, Western Section* (p. 248). American Society of Animal Sciences. https://www.asas.org/docs/western-section/2009-western-section-proceedings.pdf?sfvrsn=0#page=243

Kasimanickam, R. K., Firth, P., Schuenemann, G. M., Whitlock, B. K., Gay, J. M., Moore, D. A., Hall, J. B., & Whittier, W. D. (2014). Effect of the first GnRH and two doses of PGF2α in a 5-day progesterone-based CO-Synch protocol on heifer pregnancy. *Theriogenology*, *81*(6), 797-804. https://doi.org/10.1016/j.theriogenology.2013.12.023

Kasimanickam, R. K., Kasimanickam, V. R., Oldham, J., & Whitmore, M. (2020). Cyclicity, estrus expression and pregnancy rates in beef heifers with different reproductive tract scores following progesterone supplementation. *Theriogenology*, *145*, 39-47. https://doi.org/10.1016/j.theriogenology.2020.01.028

Kasimanickam, R., Asay, M., Firth, P., Whittier, W. D., & Hall, J. B. (2012). Artificial insemination at 56 h after intravaginal progesterone device removal improved AI pregnancy rate in beef heifers synchronized

with five-day CO-Synch + controlled internal drug release (CIDR) protocol. *Theriogenology*, *77*(8), 1624-1631. https://doi.org/10.1016/j.theriogenology.2011.12.007

Kasimanickam, R., Collins, J. C., Wuenschell, J., Currin, J. C., Hall, J. B., & Whittier, D. W. (2006). Effect of timing of prostaglandin administration, controlled internal drug release removal and gonadotropin releasing hormone administration on pregnancy rate in fixed-time AI protocols in crossbred Angus cows. *Theriogenology*, *66*(2), 166–172. https://doi.org/10.1016/j.theriogenology.2005.10.019

Kasimanickam, R., Day, M. L., Rudolph, J. S., Hall, J. B., & Whittier, W. D. (2009). Two doses of prostaglandin improve pregnancy rates to timed-AI in a 5-day progesterone-based synchronization protocol in beef cows. *Theriogenology*, *71*(5), 762-767. https://doi.org/10.1016/j.theriogenology.2008.09.049

Kasimanickam, R., Hall, J. B., Currin, J. F., & Whittier, W. D. (2008). Sire effect on the pregnancy outcome in beef cows synchronized with progesterone based Ovsynch and CO-Synch protocols. *Animal Reproduction Science*, *104*(1), 1–8. https://doi.org/10.1016/j.anireprosci.2007.01.003

Kasimanickam, R., Kasimanickam, V., & Kappes, A. (2021). Timed artificial insemination strategies with or without short-term natural service and pregnancy success in beef heifers. *Theriogenology*, *166*, 97–103. https://doi.org/10.1016/j.theriogenology.2021.02.023

Kasimanickam, R., Schroeder, S., Hall, J. B., & Whittier, W. D. (2015). Fertility after implementation of long- and short-term progesterone-based ovulation synchronization protocols for fixed-time artificial insemination in beef heifers. *Theriogenology*, *83*(7), 1226–1232. https://doi.org/10.1016/j.theriogenology.2015.01.004

Keskin, A., Mecitoğlu, G., Bilen, E., Guner, B., Orman, A., Okut, H., & Gumen, A. (2016). The effect of ovulatory follicle size at the time of insemination on pregnancy rate in lactating dairy cows. *Turkish Journal of Veterinary & Animal Sciences*, *40*(1), 68–74. https://doi.org/10.3906/vet-1506-59

Klabnik, J., & Horn, E. (2023). When the plan goes awry: How to negotiate estrus synchronization errors in beef cattle. *Clinical Theriogenology*, *15*, 1-9. http://doi.org/10.58292/CT.v15.9265

Lamb, G. C., Larson, J. E., Geary, T. W., Stevenson, J. S., Johnson, S. K., Day, M. L., Ansotegui, R. P., Kesler, D. J., DeJarnette, J. M., & Landblom, D. G. (2006). Synchronization of estrus and artificial insemination in replacement beef heifers using gonadotropin-releasing hormone, prostaglandin F2α, and progesterone. *Journal of Animal Science*, *84*(11), 3000–3009. https://doi.org/10.2527/jas.2006-220

Lansford, A. (2018). *Supplementation and reproductive strategies for beef females as part of a may-calving herd in the Nebraska Sandhills.* [Master's thesis, University of Nebraska-Lincoln, USA]. Theses and Dissertations in Animal Science. https://digitalcommons.unl.edu/animalscidiss/159/

Larson, J. E., Lamb, G. C., Stevenson, J. S., Johnson, S. K., Day, M. L., Geary, T. W., Kesler, D. J., DeJarnette, J. M., Schrick, F. N., DiCostanzo, A., & Arseneau, J. D. (2006). Synchronization of estrus in suckled beef cows for detected estrus and artificial insemination and timed artificial insemination using gonadotropin-releasing hormone, prostaglandin F2α, and progesterone. *Journal of Animal Science*, *84*(2), 332-342. https://doi.org/10.2527/2006.842332x

Lucy, M. C. (2007). Fertility in high-producing dairy cows: Reasons for decline and corrective strategies for sustainable improvement. *Society of Reproduction and Fertility supplement*, *64*, 237-254. https://doi.org/10.5661/rdr-vi-237

Macmillan, K., Gobikrushanth, M., Sanz, A., Bignell, D., Boender, G., Macrae, L., Mapletoft, R. J., & Colazo, M. G. (2020). Comparison of the effects of two shortened timed-AI protocols on pregnancy per AI in beef cattle. *Theriogenology*, *142*, 85–91. https://doi.org/10.1016/j.theriogenology.2019.09.038

Malik, A., Wahid, H., Rosnina, Y., Kasim, A., & Sabri, M. (2012). Effects of timed artificial insemination following estrus synchronization in postpartum beef cattle. *Open Veterinary Journal*, *2*(1), 1-5.

McAllister, T. A., Stanford, K., Chaves, A. V., Evans, P. R., Eustaquio de Souza Figueiredo, E., & Ribeiro, G. (2020). Nutrition, feeding and management of beef cattle in intensive and extensive production systems. In F. W. Bazer, G. C. Lamb & G. Wu (Eds.), *Animal agriculture* (pp. 75–98). Academic Press. https://doi.org/10.1016/B978-0-12-817052-6.00005-7

Mellieon, H. I., Pulley, S. L., Lamb, G. C., Larson, J. E., & Stevenson, J. S. (2012). Evaluation of the 5-day versus a modified 7-day CIDR breeding program in dairy heifers. *Theriogenology*, *78*(9), 1997-2006. https://doi.org/10.1016/j.theriogenology.2012.07.014

Mercadante, V. R. G., Kozicki, L. E., Ciriaco, F. M., Henry, D. D., Dahlen, C. R., Crosswhite, M. R., Larson, J. E., Voelz, B. E., Patterson, D. J., Perry, G. A., Funston, R. N., Steckler, T. L., Hill, S. L., Stevenson, J. S., & Lamb, G. C. (2015). Effects of administration of prostaglandin F2α at initiation of the seven-day CO-Synch + controlled internal drug release ovulation synchronization protocol for suckled beef cows and replacement beef heifers. *Journal of Animal Science*, *93*(11), 5204–5213. https://doi.org/10.2527/jas.2015-8967

Nash, J. M., Mallory, D. A., Ellersieck, M. R., Poock, S. E., Smith, M. F., & Patterson, D. J. (2012). Comparison of long- versus short-term CIDR-based protocols to synchronize estrus prior to fixed-time AI in postpartum beef cows. *Animal Reproduction Science*, *132*(1–2), 11–16. https://doi.org/10.1016/j.anireprosci.2012.03.013

Nazhat, S. A., Aziz, A., Zabuli, J., & Rahmati, S. (2021). Importance of body condition scoring in reproductive performance of dairy cows: A review. *Open Journal of Veterinary Medicine, 11*(07), 272-288. https://doi.org/10.4236/ojvm.2021.117018

Nishimura, T. K., Martins, T., da Silva, M. I., Lafuente, B. S., de Garla Maio, J. R., Binelli, M., Pugliesi, G., & Saran Netto, A. (2018). Importance of body condition score and ovarian activity on determining the fertility in beef cows supplemented with long-acting progesterone after timed-AI. *Animal Reproduction Science*, *198*, 27–36. https://doi.org/10.1016/j.anireprosci.2018.08.042

Núñez–Olivera, R., Bó, G. A., & Menchaca, A. (2022). Association between length of proestrus, follicular size, estrus behavior, and pregnancy rate in beef heifers subjected to fixed–time artificial insemination. *Theriogenology*, *181*, 1–7. https://doi.org/10.1016/j.theriogenology.2021.12.028

Oosthuizen, N., Fontes, P. L. P., Oliveira Filho, R. V., Dahlen, C. R., Grieger, D. M., Hall, J. B., ... & Lamb, G. C. (2021). Pre-synchronization of ovulation timing and delayed fixed-time artificial insemination increases pregnancy rates when sex-sorted semen is used for insemination of heifers. *Animal Reproduction Science*, *226*, 106699. https://doi.org/10.1016/j.anireprosci.2021.106699

Peel, R. K., Whittier, J. C., Enns, R. M., Grove, A. V., & Seidel, G. E. (2010). Effect of 6- versus 12-hour interval between 2 prostaglandin F2α injections administered with 5-day CO-Synch + controlled internal drug-release protocol on pregnancy rate in beef cows. *The Professional Animal Scientist*, *26*(3), 307-312. https://doi.org/10.15232/S1080-7446(15)30598-2

Perry, G. A., Cushman, R. A., Perry, B. L., Schiefelbein, A. K., Northrop, E. J., Rich, J. J., & Perkins, S. D. (2020). Role of preovulatory concentrations of estradiol on timing of conception and regulation of the uterine environment in beef cattle. *Systems Biology in Reproductive Medicine*, *66*(1), 12-25. https://doi.org/10.1080/19396368.2019.1695979

Perry, G. A., Walker, J. A., Rich, J. J. J., Northrop, E. J., Perkins, S. D., Beck, E. E., Sandbulte, M. D., & Mokry, F. B. (2020). Influence of SexcelTM (gender ablation technology) gender-ablated semen in fixed-time artificial insemination of beef cows and heifers. *Theriogenology*, *146*, 140–144. https://doi.org/10.1016/j.theriogenology.2019.11.030

Peterson, C., Alkar, A., Smith, S., Kerr, S., Hall, J. B., Moore, D., & Kasimanickam, R. (2011). Effects of one versus two doses of prostaglandin F2alpha on AI pregnancy rates in a 5-day, progesterone-based, CO-Synch protocol in crossbred beef heifers. *Theriogenology*, *75*(8), 1536-1542. https://doi.org/10.1016/j.theriogenology.2010.12.017

Pfeifer, L. F. M., Rodrigues, W. B., & Nogueira, E. (2021). Relationship between body condition score index and fertility in beef cows subjected to timed artificial insemination. *Livestock Science*, *248*, 104482. https://doi.org/10.1016/j.livsci.2021.104482

Pursley, J. R., Mee, M. O., & Wiltbank, M. C. (1995). Synchronization of ovulation in dairy cows using PGF2α and GnRH. *Theriogenology*, *44*(7), 915-923. https://doi.org/10.1016/0093-691X(95)00279-H

Randel, R. D. (1990). Nutrition and postpartum rebreeding in cattle. *Journal Of Animal Science*, *68*(3), 853-862. https://doi.org/10.2527/1990.683853x

Randi, F., Kelly, A. K., Parr, M. H., Diskin, M. G., Lively, F., Lonergan, P., & Kenny, D. A. (2021). Effect of ovulation synchronization program and season on pregnancy to timed artificial insemination in suckled beef cows. *Theriogenology*, *172*, 223–229. https://doi.org/10.1016/j.theriogenology.2021.06.021

Richardson, B. N., Hill, S. L., Stevenson, J. S., Djira, G. D., & Perry, G. A. (2016). Expression of estrus before fixed-time AI affects conception rates and factors that impact expression of estrus and the repeatability of expression of estrus in sequential breeding seasons. *Animal Reproduction Science*, *166*, 133–140. https://doi.org/10.1016/j.anireprosci.2016.01.013

Roche, J. F., & Diskin, M. G. (2001). Resumption of reproductive activity in the early postpartum period of cows. *BSAP Occasional Publication*, *26*(1), 31–42. https://doi.org/10.1017/S0263967X00033577

Roche, J. R., Friggens, N. C., Kay, J. K., Fisher, M. W., Stafford, K. J., & Berry, D. P. (2009). Invited review: Body condition score and its association with dairy cow productivity, health, and welfare. *Journal of Dairy Science*, *92*(12), 5769-5801. https://doi.org/10.3168/jds.2009-2431

Sá Filho, M. F., Santos, J. E. P., Ferreira, R. M., Sales, J. N. S., & Baruselli, P. S. (2011). Importance of estrus on pregnancy per insemination in suckled Bos indicus cows submitted to estradiol/progesterone-based timed insemination protocols. *Theriogenology*, *76*(3), 455–463. https://doi.org/10.1016/j.theriogenology.2011.02.022

Santos, C. A. D., Landim, N. M. D., Araújo, H. X. D., & Paim, T. D. P. (2022). Automated systems for estrous and calving detection in dairy cattle. *AgriEngineering, 4*(2), 475-482. https://doi.org/10.3390/agriengineering4020031

Setiaji, A., Oikawa, T., & Arakaki, D. (2023). Relation between body condition score and conception rate of Japanese Black cows. *Animal bioscience*, *36*(8), 1151. https//doi.org/10.5713/ab.22.0329

Souames, S., & Berrama, Z. (2020). Factors affecting conception rate after the first artificial insemination in a private dairy cattle farm in North Algeria. *Veterinary World, 13*(12), 2608–2611. https://doi.org/10.14202/vetworld.2020.2608-2611

Stevenson, J. S., Pulley, S. L., Mellieon, H. I., Olson, K. C., Johnson, S. K., Grieger, D. M., Jaeger, J. R., & Breiner, R. M. (2011). Optimizing a new 5-day CIDR-CO-Synch timed artificial insemination program. *Kansas Agricultural Experiment Station Research Reports*, (1), 14–17. https://doi.org/10.4148/2378-5977.2880

Taponen, J. (2009). Fixed-time artificial insemination in beef cattle. *Acta Veterinaria Scandinavica*, *51*, 1-6. https://doi.org/10.1186/1751-0147-51-48

Thomas, J. M., Locke, J. W. C., Bonacker, R. C., Knickmeyer, E. R., Wilson, D. J., Vishwanath, R., ... & Patterson, D. J. (2019). Evaluation of SexedULTRA 4M™ sex-sorted semen in timed artificial insemination programs for mature beef cows. *Theriogenology*, *123*, 100-107. https://doi.org/10.1016/j.theriogenology.2018.09.039

Tsiligianni, T., Amiridis, G. S., Dovolou, E., Menegatos, I., Chadio, S., Rizos, D., & Gutierrez–Adan, A. (2011). Association between physical properties of cervical mucus and ovulation rate in superovulated cows. *Canadian Journal of Veterinary Research = Revue Canadienne de Recherche Veterinaire*, *75*(4), 248–253.

Vedovatto, M., Lecciolli, R. B., Lima, E. D. A., Rocha, R. F. A. T., Coelho, R. N., Moriel, P., da Silva, L. G., Ferreira, L. C. L., da Silva, A. F., Alves dos Reis, W. V., de Oliveira, D. M., & Franco, G. L. (2022). Impacts of body condition score at beginning of fixed-timed AI protocol and subsequent energy balance on ovarian structures, estrus expression, pregnancy rate and embryo size of Bos indicus beef cows. *Livestock Science*, *256*, 104823. https://doi.org/10.1016/j.livsci.2022.104823

Wang, Y., Huo, P., Sun, Y., & Zhang, Y. (2019). Effects of body condition score changes during peripartum on the postpartum health and production performance of primiparous dairy cows. *Animals*, *9*(12), 1159. https://doi.org/10.3390/ani9121159

White, S. S., Kasimanickam, R. K., & Kasimanickam, V. R. (2016). Fertility after two doses of PGF2α concurrently or at 6-hour interval on the day of CIDR removal in 5-day CO-Synch progesterone-based synchronization protocols in beef heifers. *Theriogenology*, *86*(3), 785-790. https://doi.org/10.1016/j.theriogenology.2016.02.032

Whittier, W. D., Currin, J. F., Schramm, H., Holland, S., & Kasimanickam, R. K. (2013). Fertility in Angus cross beef cows following 5-day CO-Synch + CIDR or 7-day CO-Synch + CIDR estrus synchronization and timed artificial insemination. *Theriogenology*, *80*(9), 963-969. https://doi.org/10.1016/j.theriogenology.2013.07.019

Whittier, W. D., Kasimanickam, R. K., Currin, J. F., Schramm, H. H., & Vlcek, M. (2010). Effect of timing of second prostaglandin F2α administration in a 5-day, progesterone-based CO-Synch protocol on AI pregnancy rates in beef cows. *Theriogenology*, *74*(6), 1002-1009. https://doi.org/10.1016/j.theriogenology.2010.04.029

Wilson, D. J., Mallory, D. A., Busch, D. C., Leitman, N. R., Haden, J. K., Schafer, D. J., Ellersieck, M. R., Smith, M. F., & Patterson, D. J. (2010). Comparison of short-term progestin-based protocols to synchronize estrus and ovulation in postpartum beef cows. *Journal of Animal Science*, *88*(6), 2045–2054. https://doi.org/10.2527/jas.2009-2627

Wiltbank, J. N., Rowden, W. W., Ingalls, J. E., Geegoey, K. E., & Koch, R. M. (1962). Effect of energy level on reproductive phenomena of mature hereford cows. *Journal of Animal Science*, *21*(2), 219–225. https://doi.org/10.2527/jas1962.212219x

Zwiefelhofer, E. M., Macmillan, K., Gobikrushanth, M., Adams, G. P., Yang, S. X., Anzar, M., Asai-Coakwell, M., & Colazo, M. G. (2021). Comparison of two intravaginal progesterone-releasing devices in shortened-timed artificial insemination protocols in beef cattle. *Theriogenology*, *168*, 75–82. https://doi.org/10.1016/j.theriogenology.2021.03.023

Pertanika J. Trop. Agric. Sci. 48 (3): 815 - 836 (2025)

PERTANIKA JOURNALS

TROPICAL AGRICULTURAL SCIENCE

Journal homepage: http://www.pertanika.upm.edu.my/

Effects of Different Pasteurisation Temperatures and Time on Microbiological Quality, Physicochemical Properties, and Vitamin C Content of Red Dragon Fruit (*Hylocereus costaricensis*) Juice

Sharrvesan Thanasegaran and Norlia Mahror*

Food Technology Division, School of Industrial Technology, Universiti Sains Malaysia, 11800 Penang, Pulau Pinang, Malaysia

ABSTRACT

This study examines the effects of different pasteurisation temperatures and times on red dragon fruit juice's microbiological quality, physicochemical properties, and vitamin C content. Microbial analysis used the spread plate technique to determine total plate count (TPC) and yeast and mould count (YMC). Physicochemical properties were assessed through pH, titratable acidity (TA), colour, and total soluble solids (TSS). Vitamin C content was measured using iodometric titration. Pasteurisation at 80°C for 60 s achieved the lowest TPC (3.56 log CFU/mL) compared to 6 log CFU/mL in unpasteurised juice. All pasteurised samples showed YMC below 2 log CFU/mL, demonstrating effective microbial control. However, no significant differences ($p > 0.05$) were observed in TPC between 60°C and 80°C. Pasteurisation caused only slight changes in pH and TSS, with higher temperature (80°C) resulting in lighter juice colour, indicating potential pigment breakdown. Vitamin C, being heat-sensitive, decreased significantly as temperature and time increased, with a maximum reduction of 30.82 mg/100 mL at 80°C for 60 s. During 28 days of storage at 4°C, juice pasteurised at 60°C for 60 s maintained microbial loads within acceptable limits. TA increased slightly, and pH levels shifted from 5.05 to 4.98. TSS remained stable, while colour difference (ΔE) increased, indicating noticeable changes. Low-temperature pasteurisation (60°C for 60 s) resulted in minimal vitamin C loss (9.36%) compared to 80°C (17.59%). In conclusion, pasteurising at 60°C for 60 s effectively balances microbial quality, physicochemical properties, and vitamin C preservation.

Keywords: Microbiological quality, pasteurisation, physicochemical properties, red dragon fruit, vitamin C

ARTICLE INFO

Article history:
Received: 24 September 2024
Accepted: 11 November 2024
Published: 16 May 2025

DOI: https://doi.org/10.47836/pjtas.48.3.09

E-mail addresses:
sharrvesank@gmail.com (Sharrvesan Thanasegaran)
norlia.mahror@usm.my (Norlia Mahror)
*Corresponding author

e-ISSN: 2231-8542

INTRODUCTION

Red dragon fruit (*Hylocereus costaricensis*) is a tropical fruit endemic to Central and South America that belongs to the Cactaceae family (Harivainda et al., 2008). Red dragon fruit is rich in vitamins, minerals and antioxidants, with vitamin C being a key component contributing to its nutritional value (Susilo et al., 2021). Due to its health benefits and diverse applications in the food industry, red dragon fruit has gained global market appeal (Nguyen, 2020). However, the perishable nature poses significant challenges in postharvest handling, processing, and distribution. Factors such as microbial contamination, enzymatic activity, and oxidation can quickly degrade its quality and safety (Jalgaonkar et al., 2022).

Pasteurisation is a critical step in fruit juice processing to ensure microbiological safety and the overall quality of the product. In this context, fruit juices are pasteurised at different combinations of temperature (more or less than 80°C) and time (more or less than 30 s) (Petruzzi et al., 2017). High temperatures could create structural changes and impair sensory attributes, emphasising the need to retain the original characteristics of the fruit juice. Despite extensive studies on other fruit juices, limited research exists on the effects of pasteurisation specific to dragon fruit juice. Liaotrakoon (2013) investigated the impact of heat treatment on the physicochemical properties, microbial destruction, antioxidative properties and rheological parameters. This study applied thermal treatments to dragon fruit purees at temperatures ranging from 50 to 90°C for 0 to 60 min. In comparison to the initial value, heated dragon fruit purees retained a comparatively high level of vitamin C. During thermal treatment, the betacyanin pigment of the red-flesh dragon fruit puree degraded from betanin to neobetanin.

Total plate count (TPC) and yeast and mold count (YMC) provide insight into the microbial load in juice but do not differentiate between beneficial, pathogenic, or spoilage microorganisms. Therefore, high TPC and YMC values indicate potential spoilage and are useful for evaluating shelf life and guiding quality control measures. Research by Mandha et al. (2023) found that the physicochemical, microbial and qualitative parameters of watermelon, pineapple, and mango juices differed significantly. For example, pasteurisation negatively affects watermelon juice colour and significantly reduces vitamin C content after 10 min ($p < 0.05$). Thus, analysing different pasteurisation times is crucial to optimise the quality of dragon fruit juice. In addition, evaluating the physicochemical properties after pasteurisation and the shelf life of the thermally treated juice is important to prove that pasteurisation can maintain the juice's valuable properties. A study by Rabie et al. (2014) concluded that pasteurised juice stored at 4°C had a longer storage life of at least 21 days than fresh juice and better-preserved physicochemical properties. Storage studies are significant for estimating fruit juice's shelf life and pasteurised fruit juices' marketability over extended periods such as 90 and 180 days of storage (Wurlitzer et al., 2019).

High-temperature pasteurisation ranges from 72°C to 90°C, while low-temperature pasteurisation is about 63°C (Petruzzi et al., 2017). Low-temperature long-time (LTLT)

pasteurisation, at about 63°C, effectively removes microorganisms using less energy, thus supporting sustainable juice production (Myer et al., 2016). On the other hand, high-temperature pasteurisation requires more energy due to the rapid heating and sustained high temperatures (Ağçam et al., 2018). Besides, studies suggested that pasteurisation conditions differ based on juice characteristics (Petruzzi et al., 2017). For instance, Saikia et al. (2016) found that watermelon juice pasteurised at 60°C for 30 s had low total soluble solids after refrigeration, while Ahmad et al. (2015) noted a significant decrease in vitamin C content in guava juice at 85°C for 60 s. In mango and watermelon juices, pasteurisation at 80°C for 60 s reduced TPC and YMC to below 1 log CFU/mL (Mandha et al., 2023).

Despite extensive studies analysing the pasteurisation of other juices, limited research exists on how temperature and time variations during pasteurisation affect red dragon fruit juice's quality and shelf life. The energy efficiency and sustainability of different pasteurisation conditions for red dragon fruit juice require further investigation. Hence, this study aims to evaluate the effects of both low (60°C) and high (80°C) pasteurisation temperatures for 30 s and 60 s on the microbiological and physicochemical quality as well as the vitamin C content of dragon fruit juice.

MATERIALS AND METHODS

Materials and Reagents

Fully ripened red dragon fruits from Vietnam and aluminium foil were purchased from Lotus, Sungai Dua (Penang, Malaysia). Buffered peptone water (BPW), plate count agar (PCA), and Dichloran Rose-Bengal Chloramphenicol Agar (DRBC) were obtained from HiMedia (Mumbai, India). Sodium hydroxide (NaOH) and ethanol were sourced from Classic Chemical Sdn. Bhd. (Malaysia) and phenolphthalein powder from HmbG Chemical (Malaysia). Potassium iodide, iodine, and soluble starch were acquired from R&M Chemical (London, UK) and ascorbic acid from HiMedia (Mumbai, India).

Preparation of Red Dragon Fruit Juice

Red dragon fruits were cleaned, peeled, and sliced before being juiced using a fruit juice extractor (Hanabishi, Malaysia). The juice was then sieved to achieve a uniform puree. In the first phase, 400 mL of juice samples were divided into five beakers, with one serving as the control while the others were prepared for pasteurisation.

Pasteurisation of Red Dragon Fruit Juice

Pasteurisation was conducted at 60°C and 80°C for 30 s and 60 s, following Valliere & Harkins (2020) with minor modifications. Four hundred millilitres of red dragon fruit juice were placed in a pre-sterilised 500 mL beaker covered with aluminium foil. The juice

sample was heated to the desired temperature in the water bath (Memmert, New York, US) and rapidly cooled in an ice-water bath before storage at 4°C.

Microbiological Analysis

Total Plate Count

The amount of 25 mL of red dragon fruit juice was added to 225 mL of BPW, and this dilution was referred to as 10^{-1}. Serial dilutions were performed until 10^{-5}. Spread plates were prepared using 0.1 mL aliquots of these dilutions on PCA and incubated at 37°C in an incubator for 24 h. The colonies that had grown on the plate were counted, and CFU per mL were calculated. The average mean number of CFU per mL was calculated using Equation 1.

Yeast and Mold Count

A volume of 25 mL of red dragon fruit juice was mixed with 225 mL of BPW, constituting an initial 10^{-1} dilution. Serial dilutions up to 10^{-5} were performed, and 0.1 mL aliquots of these dilutions were spread on DRBC agar. Next, the plates were incubated at 25°C for 5 days in an incubator, and the number of CFU per mL was calculated using Equation 1.

$$\frac{CFU}{mL} = \frac{Number\ of\ Colonies\ Counted}{Dilution\ \times\ Volume\ of\ sample\ plated\ in\ mL} \quad [1]$$

Physicochemical Analysis

Colour

A colourimeter (Konica Minolta CM-5, Singapore) was calibrated with white and black standards to analyse the juice sample's colour using CIELAB colour values: L* (brightness to darkness), a* (green to red), and b* (blue to yellow). Measurements were taken in triplicate, and equations were applied to determine chroma (C*), hue angle (h), and colour difference (Kong et al., 2020).

$$\text{Chroma, } C^* = \sqrt{a^{*2} + b^{*2}} \quad [2]$$

$$\text{Hue angle, } h^\circ = \tan^{-1}\frac{b^*}{a^*} \quad [3]$$

$$\text{Colour difference, } \Delta E, = \sqrt{\Delta L^{*2} + \Delta a^{*2} + \Delta b^{*2}} \quad [4]$$

pH

The pH of the fruit juice samples was determined using a pH meter (Mettler Toledo, Darmstadt, Germany) calibrated using solutions with different pH values of 4.6, 7.2, and 9.2. The pH meter was immersed in the juice sample, and the reading was recorded. Three replicates were taken for each sample.

Total Soluble Solids (TSS)

The TSS in the fruit juice samples was measured using a digital refractometer (Hanna Instruments, Johor Bharu, Malaysia). Before the test, the instrument was calibrated by placing a few drops of distilled water on the detector. Approximately one drop of fruit juice was dripped onto the detector, and the reading was recorded. Three replicates were taken for each sample.

Titratable Acidity (TA)

An amount of 5 mL dragon fruit juice samples was diluted to 50 mL of distilled water and titrated against 0.1 M NaOH to a pink endpoint using phenolphthalein as an indicator. Before that, 0.1 M NaOH was prepared by dissolving 0.4 g in 100 mL water, whereas 1% phenolphthalein was made by diluting 1 g in 100 mL of 95% ethanol. Total TA was calculated using Equation 5, as described by Kong et al. (2020).

$$TA(\%) = \frac{N\ x\ V_1 \times Eq.Wt}{V_2 \times 10} \quad [5]$$

where N is the NaOH normality, V_1 is the NaOH volume (in mL), V_2 is the sample volume (in ml), and Eq. Wt. is the equivalent weight of citric acid (64.04g/mol).

Vitamin C Analysis

The vitamin C content of red dragon fruit juices was analysed using the redox titration method described by Satpathy et al. (2020) with minor modifications, including standardisation using an ascorbic acid solution.

Preparation of Iodine Solution

A solution with a concentration of 0.005 mol/L was prepared. An amount of 2 g of potassium iodide and 1.3 g of iodine were weighed and added to a 100 mL beaker. Distilled water (5 mL) was added, and the mixture was swirled for a few minutes until the iodine was completely dissolved. The iodine solution was then transferred to a 1 L volumetric flask, ensuring all traces of the solution were rinsed into the volumetric flask using distilled water. Then, the solution was made up to the 1 L mark with distilled water.

Preparation of Starch Indicator

A solution with a concentration of 0.5% was prepared. In a 100 mL conical flask, 0.25 g of soluble starch was weighed and added to 50 mL of boiled distilled water. The mixture was stirred to dissolve the starch and then cooled to room temperature before use.

Preparation of Ascorbic Acid Solution

An amount of 0.88 g of ascorbic acid was weighed in a 100 mL beaker and added to a 1 L volumetric flask to make up 1 L with the addition of distilled water. The remaining solids in the beaker and funnel were rinsed using small portions of distilled water to ensure all the ascorbic acid was transferred into the volumetric flask.

Titration

A 20 mL sample solution was pipetted into a 250 mL conical flask, followed by 150 mL of distilled water and 1 mL of starch indicator. The sample was titrated with a 0.005 mol/L iodine solution until a lasting purple colour indicated the endpoint. This process was repeated three times with additional sample aliquots. The volume of iodine used was recorded, and the vitamin C content (mg/100 mL) in the juice sample was calculated based on the moles of iodine reacting.

$$\text{Ascorbic acid} + I_2 \rightarrow 2\ I^- + \text{Dehydroascorbic acid}$$

Statistical Analysis

The experimental data was analysed through one-way analysis of variance (ANOVA) utilising Statistical Package for Social Sciences (SPSS) software version 28.0 (IBM Corporation, Endicott, NY, USA). This analysis aims to assess the significance of variations of microbiological, physicochemical, and vitamin C analysis for unpasteurised and pasteurised samples. The significance level for statistical significance was 95% confidence ($p < 0.05$). All experimental data were presented in duplicate or triplicate as mean ± standard deviation. Post hoc comparisons were performed using Tukey's test to identify and compare the statistical differences within the research study.

RESULTS AND DISCUSSION

Microbiological Analysis

Table 1 shows the effect of different pasteurisation temperatures and times on the microbial quality of red dragon fruit juice. TPC decreased significantly ($p < 0.05$) to 3.89 and 3.75 CFU/mL at 60°C for 30 s and 60 s, respectively, indicating that a longer exposure time at 60°C leads to greater microbial reduction. Notably, a significant reduction was achieved

Table 1
Effect of different pasteurisation temperatures and time on the microbiological quality of dragon fruit juice

	Pasteurisation (temperature, time)				
	Unpasteurised	**60 °C, 30 s**	**60 °C, 60 s**	**80 °C, 30 s**	**80 °C, 60 s**
TPC (log CFU/mL)	6.00 ± 0.18^{a}	3.89 ± 0.27^{b}	3.75 ± 0.14^{c}	3.72 ± 0.18^{c}	3.56 ± 0.35^{d}
YMC (log CFU/mL)	3.48 ± 0.23^{a}	$< LOD^{b}$	$< LOD^{b}$	$< LOD^{b}$	$< LOD^{b}$

Note. TPC = Total plate count, YMC = Yeast and mold count. Values expressed as means ± standard deviations, Different letters within a row denote a significant difference ($p < 0.05$), $n = 2$, LOD means the limit of detection where the count of the colonies formed is less than 1

even at the shorter exposure time of 30 s, suggesting that lower temperatures for shorter durations can still effectively reduce microbial load. No significant difference was observed between 60°C (for 30 s and 60 s) and 80°C (30 s). However, pasteurisation at 80°C for 60 s resulted in the lowest microbial load, demonstrating the combined effect of higher temperature and longer exposure. Mandha et al. (2023) state that higher temperatures enhance microbial inactivation due to enzyme denaturation and cell membrane disruption.

Microorganisms in fresh fruit juice can originate from environmental sources like contaminated water, soil, or animals during harvesting and cross-contamination during processing. Soil bacteria and fungi may adhere to fruit surfaces, transferring into the juice during extraction (Alegbeleye et al., 2022). The Food and Drug Administration (FDA) sets limits of 10^5 CFU/mL for TPC and 50 CFU/mL for YMC in fruit juice, and all pasteurised samples in this study met these standards, demonstrating effective microbial reduction regardless of temperature and time. These results align with previous research by Ferreira et al. (2022), where pasteurisation at 71°C for 30 s significantly reduced microbial populations in *Opuntia Ficus-Indica*. This research demonstrated that shorter pasteurisation is able to significantly extend the juices' shelf life by 22 days compared to non-pasteurised samples, highlighting the effectiveness of shorter pasteurisation times in microbial control. After pasteurisation, TPC for red, orange and white prickly pear juices was reduced to approximately 3.06, 3.02, and 3.04 log CFU/mL, respectively, with populations of *Enterobacteriaceae*, yeasts and moulds below detection limits, indicating high microbial safety. Unpasteurised samples showed 3.48 log CFU/mL of YMC, while all pasteurised samples had undetectable YMC. The fruit juice's high carbohydrate and nitrogen content supports yeast growth, but pasteurisation effectively kills these microorganisms. Yeast species such as *Saccharomyces cerevisiae* and *Zygosaccharomyces rouxii* are particularly vulnerable to heat pasteurisation, which reduces their populations below the detection limit of 2 log CFU/mL (Mandha et al., 2023).

Physicochemical Analysis

The effect of different pasteurisation temperatures and holding time on the physicochemical properties of red dragon fruit juice are presented in Table 2. Total acidity (TA) refers to the

amount of acid contained in a substance, and it can be observed that the acidity changes during pasteurisation. The unpasteurised juice maintained a TA of 0.12%, consistent with findings from Alim et al. (2023). TA remained stable for most pasteurised samples compared to unpasteurised ones except for those treated at 80°C for 60 s. Besides, TSS describe the concentration of all soluble compounds in a solution, predominantly sugars. TSS also stayed consistent between 10.4 and 10.6 °Brix across pasteurisation conditions. The pH was unchanged for unpasteurised and 60°C pasteurised samples, but the lowest was recorded at 80°C for 60 s. Pasteurisation did not significantly alter TA and TSS, aligning with previous findings by Mandha et al. (2023), but did significantly affect colour and pH. In addition, pasteurisation increased L*, a*, b*, h°, and C values, indicating brighter and more intense juice colour, especially at 80°C for 60 s. In this case, no ΔE value is provided for the unpasteurised juice sample because it serves as the reference point. The colour differences in the other samples are measured relative to this unprocessed state.

According to Food Regulation 1985 (235), the acidity of fruit juice should not exceed 3.5% w/v. In this study, all fresh and pasteurised samples remain below this regulatory threshold, which confirms their acceptability for consumption. The acidity decreases slightly as the pasteurisation temperature increases, reaching its lowest point (0.08%) at 80°C for 60 s. Generally, fruit juices have TA within the range of 0.3% to 1.5% depending on the fruit type, like ripeness, with lower values typically associated with less acidic fruits, including red dragon fruit (Vern et al., 2023). Pasteurisation reduces acidity by eliminating bacteria that produce acids as byproducts during fermentation. Fruit juices can naturally undergo acetic acid fermentation due to the presence of microorganisms such

Table 2
Effect of different pasteurisation temperature and time on the physicochemical properties of red dragon fruit juice

	Pasteurisation (temperature, time)				
	Unpasteurised	**60 °C, 30 s**	**60 °C, 60 s**	**80 °C, 30 s**	**80 °C, 60 s**
TA (%)	0.12 ± 0.02^{a}	0.11 ± 0.01^{a}	0.10 ± 0.01^{a}	0.11 ± 0.01^{a}	0.08 ± 0.01^{b}
pH	5.05 ± 0.01^{a}	5.03 ± 0.01^{a}	5.01 ± 0.01^{a}	4.70 ± 0.02^{b}	4.50 ± 0.01^{b}
TSS (°Brix)	10.60 ± 0.10^{a}	10.40 ± 0.03^{a}	10.60 ± 0.03^{a}	10.50 ± 0.01^{a}	10.60 ± 0.03^{a}
L*	13.50 ± 0.15^{a}	13.08 ± 0.02^{bc}	13.43 ± 0.03^{a}	15.77 ± 0.02^{bd}	16.02 ± 0.01^{bd}
a*	43.28 ± 0.01^{a}	43.49 ± 0.01^{b}	43.96 ± 0.01^{c}	45.87 ± 0.01^{d}	46.15 ± 0.01^{e}
b*	21.44 ± 0.01^{a}	21.72 ± 0.01^{b}	22.44 ± 0.01^{c}	27.14 ± 0.01^{d}	27.53 ± 0.01^{e}
h°	25.83 ± 0.10^{a}	26.53 ± 0.01^{b}	27.04 ± 0.01^{c}	30.07 ± 0.02^{d}	30.27 ± 0.01^{e}
C	49.20 ± 0.10^{a}	48.61 ± 0.02^{b}	49.36 ± 0.02^{c}	54.16 ± 0.02^{d}	54.60 ± 0.01^{e}
ΔE	-	0.94 ± 0.01^{a}	1.05 ± 0.02^{a}	6.66 ± 0.01^{b}	7.18 ± 0.01^{c}

Note. Values expressed as means ± standard deviations, Different letters within a row denote a significant difference ($p < 0.05$), $n = 3$, TA = Titratable acidity, TSS = Total soluble solids, L* = Lightness, a* = Redness, b* = Yellowness, H° = Hue angle, C = Chroma, ΔE = Colour difference

as *Acetobacter* species. These bacteria can convert the sugars in the juice into acetic acid and other byproducts, increasing acidity. Natural fermentation involves native bacteria fermenting raw materials without artificial inoculation. It is supported by Sourri et al. (2022), who reported that *Acetobacter* species, such as *Acetobacter pasteurianus* and *Acetobacter aceti*, are commonly found on fruit surfaces and are heat sensitive. However, this process can also lead to the growth of spoilage and pathogenic bacteria, making fermentation unpredictable. Consequently, pasteurisation effectively eliminates these acid-producing microbes by applying heat that denatures proteins and disrupts cell membranes, thus preventing spoilage and maintaining the quality of the juice (Saud et al., 2024).

Small changes in °Brix suggest that pasteurisation does not significantly affect the solute as sugar level generally remains stable under typical pasteurisation conditions (Nicklas et al., 2015). The TSS observed (10.6 °Brix) differs from the reported 12 °Brix due to variations in fruit ripeness of dragon fruits used as mature and ripened fruit have higher TSS in the juice, thus not influenced by pasteurisation (Yıkmış, 2020). The starch stored in the fruit is converted into sugars like glucose and fructose upon ripening, increasing the fruit's sweetness and achieving higher TSS in the juice.

The pH of red dragon fruit juice (5.05) aligns with previous findings from Arivalagan et al. (2021) that mentioned the pH of dragon fruit juice is slightly acidic, between 4.8 and 5.40. According to Kong et al. (2020), the significant decrease in pH of the high temperature pasteurised sample might be due to the higher dissociation of citric acid, which is abundant in red dragon fruit. The release of H^+ ions in the dissociation process at higher temperatures contributes to the acidity of the solution, resulting in a lower pH (Angonese et al., 2021).

Higher pasteurisation temperatures and durations increase L* values, indicating a lighter juice colour, likely due to pigment degradation. The highest L* value was observed at 80°C for 60 s, showing a significant change from the unpasteurised sample. The a* value reflects redness, which has increased slightly with temperature but remained minimal compared to unpasteurised samples. Similarly, b* values rise with temperature, indicating yellowing, which may result from chemical changes during pasteurisation. Pasteurisation degrades betanin, leading to a shift in colour from red to yellow.

Dragon fruit's vibrant red colour comes from betalains, particularly betacyanin, which degrades with heat (Liaotrakoon, 2013). Betacyanin content drops significantly with higher temperatures, from 80% at 50°C to 32% at 90°C. Heating above 80°C causes more pronounced colour changes and higher betacyanin loss. Besides, the hue angle (h°), which indicates the dominant colour tone, shifts from red to purple at higher temperatures. The result aligns with Wong and Siow (2015), who found greater betacyanin retention at lower temperatures, at 65°C than 85°C. Chroma values representing colour intensity also increase with higher temperatures. According to Kong et al. (2020), ΔE values can be categorised as not noticeable (0–0.5), slightly noticeable (0.5–1.5), noticeable (1.5–3.0),

clearly visible (3.0–6.0) and significant (6.0–12.0). The increase in ΔE values at higher temperatures indicates significant colour changes, while pasteurisation at 60°C results in minimal colour change, not exceeding 1.05. These findings are consistent with those of Moo-Huchin et al. (2017), who reported increased colour degradation in watermelon juice with higher pasteurisation temperatures due to carotenoid oxidation. Dragon fruit, which contains a relatively low concentration of carotenoids (0.86 mg/100 mL), shows similar trends as those obtained in this study. The results are also supported by Kong et al. (2020), who observed a significant decrease in the L* value in pomegranate juice after being heated at 95°C, the 30s.

Vitamin C Content Analysis

The effect of temperature and time on vitamin C in pasteurised and unpasteurised red dragon fruit juice is recorded in Table 3. Pasteurisation at 60°C for 30 s results in a significant decrease in vitamin C concentration, followed by an increase in the pasteurisation duration (60 s), which has resulted in a further decline to 33.9 mg/100 mL ($p < 0.05$). It indicates that mild vitamin C degradation. Higher temperatures often accelerate degradation in which pasteurisation at 80°C for a shorter duration of 30 s caused a more significant decrease in vitamin C content extending the time to 60 s at 80°C results in a further decline to 30.82 mg/100 mL, demonstrating more substantial degradation due to the combined effects of higher temperature and longer duration.

Fresh dragon fruit juice contains 37.4 mg/100 mL of vitamin C, higher than the 33 mg/100 mL reported by Liaotrakoon (2013). This variation is attributed to different ripeness levels of the fruit used. Ernest et al. (2017) state that vitamin C concentration decreases as fruit maturity increases. However, pasteurisation reduces vitamin C content because ascorbic acid is heat-sensitive. It is consistent with findings by Tchuenchieu et al. (2018), who observed that pasteurisation adversely affects vitamin C in orange juice. The degradation follows a first-order kinetic pattern, suggesting that temperature influences ascorbic acid breakdown during thermal processing.

Table 3
Effect of different pasteurisation temperature and time on vitamin C concentration

	Pasteurisation (temperature, time)				
	Unpasteurised	**60°C, 30 s**	**60°C, 60 s**	**80°C, 30 s**	**80°C, 60 s**
Vitamin C concentration (mg/100 mL)	37.40 ± 0.10^{a}	34.80 ± 0.01^{b}	33.90 ± 0.01^{c}	31.26 ± 0.05^{d}	30.82 ± 0.02^{e}

Note. Values expressed as means ± standard deviations; Different letters within a row denote a significant difference ($p < 0.05$), $n = 3$

Unpasteurised samples have significantly higher vitamin C than pasteurised ones due to ascorbic acid's susceptibility to oxidation, particularly heat and oxygen (Liaotrakoon, 2013). Oxidation converts ascorbic acid into dehydroascorbic acid and other products, such as furfural, 2-furoic acid, and 3-hydroxy-2-pyrone. Furfural can polymerise with amino acids, leading to browning in ascorbic acid-containing juices (Yin et al., 2022). Mandha et al. (2023) found a rapid decline in vitamin C in watermelon and mango juices with extended pasteurisation at 80°C. Similarly, Klopotek et al. (2005) reported a 35% reduction in vitamin C in strawberry juice after high-temperature pasteurisation at 85°C. Conversely, Giavoni et al. (2008) found that fresh orange pulp juice contains 17.63 mg/100 g of vitamin C, with no significant reduction after pasteurisation, likely due to due to the presence of solid parts where juices with the highest pulp concentration containing the highest level of vitamin C.

The microbiological quality of red dragon fruit juice is effectively enhanced through pasteurisation at 60°C for 60 s, as evidenced by a significant reduction in TPC to 3.75, which is almost the same with a higher pasteurisation temperature. However, extended time is crucial as 60°C for 30 s results in a higher TPC of 3.89 ($p < 0.05$). The physicochemical properties remain stable, with TA at 0.10%, indicating no adverse effect on acidity compared to the unpasteurised sample. Importantly, this pasteurisation condition avoids the significant decrease in pH observed at a higher temperature (80°C), thus maintaining the juice's desirable flavour profile (Ghorai, 2023). Vitamin C slightly degrades to 33.9 mg/100 mL, but colour preservation is effective. Therefore, pasteurisation at 60°C for 60 s ensured microbial quality, preserved physicochemical properties and minimised vitamin C degradation.

Effect of Storage on Microbial Quality

Table 4 shows the effectiveness of cold storage for pasteurised and unpasteurised red dragon fruit juices. After one week, the unpasteurised sample had a higher TPC and YMC than the initial week. In the following weeks, the unpasteurised sample's microbial counts increased significantly compared to pasteurised juice, reaching an uncountable range for TPC and a high value for yeasts and moulds by Week 4. Meanwhile, the pasteurised juice had a minimal increase for TPC, but YMC remained consistently below the detectable level of 2 log CFU/mL. A high TPC value indicates a shorter shelf life for the juice, as it may contain many bacteria that could lead to spoilage. Some spoilage organisms can survive pasteurisation, posing a risk of product spoilage during storage. Yeast and mould could grow in dragon fruit juice even at a low pH due to its acidophilic nature (Jerry & Bright, 2019). Spoilage bacteria and YMC found on the surface of fruits would be harmful if consumed without any treatment (Mengistu et al., 2022).

The pasteurised samples have shown a slight increase in TPC and maintained a consistently low YMC throughout the 4-week storage period. Pasteurisation kills most psychotropic bacteria, but some species and strains survive at refrigeration temperatures less than 7°C. However, the TPC is minimal and does not exceed the permitted level compared to before and during one month of storage. Thus, proper maintenance of refrigeration temperature after pasteurisation aids in ensuring the shelf life of juice is protected throughout storage until it reaches consumers.

The result is in line with a previous finding by Ma et al. (2020), who demonstrated that unpasteurised watermelon juice deteriorated rapidly due to microbial growth during storage. According to Mandha et al. (2023), pasteurisation effectively preserved a good microbial quality in watermelon juice throughout the storage period. However, the unpasteurised juice showed a gradual increase in TPC, reaching 8.33 log CFU/mL in the second week, which is higher than 6.05 log CFU/mL in this study. It might be due to the higher pH value of watermelon juice than dragon fruit juice, which limits microbial growth in more acidic environments. Additionally, Choo et al. (2022) reported that the microbial counts of pasteurised noni juice remained within acceptable levels throughout the 8-week storage period in refrigerated (4°C). This finding supports the suitability of refrigerated storage conditions in preserving the microbiological integrity of pasteurised noni juice.

Table 4
Microbiological analysis of unpasteurised and pasteurised (60°C, 60 s) red dragon fruit juice during storage at 4°C

	Microbiological analysis (log CFU/mL)	
	TPC	**YMC**
Unpasteurised		
Week 0	6.00 ± 0.18^{aA}	3.48 ± 0.23^{aA}
Week 1	6.03 ± 0.20^{aA}	4.28 ± 0.28^{bA}
Week 2	6.05 ± 0.15^{aA}	4.38 ± 0.23^{bA}
Week 3	$TNTC^{bA}$	5.32 ± 0.34^{cA}
Week 4	$TNTC^{bA}$	5.58 ± 0.73^{dA}
Pasteurised		
Week 0	3.75 ± 0.14^{aB}	$< LOD^{aB}$
Week 1	3.77 ± 0.25^{aB}	$< LOD^{aB}$
Week 2	3.79 ± 0.47^{bB}	$< LOD^{aB}$
Week 3	3.83 ± 0.32^{cB}	$< LOD^{aB}$
Week 4	3.86 ± 0.23^{dB}	$< LOD^{aB}$

Note. Values expressed as means ± standard deviations, Small letters within a column denote a significant difference ($p < 0.05$) within the same treatment group (either pasteurised or unpasteurised) across different storage weeks, $n = 3$, Capital letters within a column denote a significant difference ($p < 0.05$) between different treatment groups (pasteurised and unpasteurised) within the same storage week, $n = 3$, TNTC means too numerous to count, where the count of the colonies formed is > 300, LOD means the limit of detection, where the count of the colonies form is < 1

Effect of Storage on Physicochemical Properties

Table 5 presents the physicochemical properties of unpasteurised and pasteurised (60°C for 60 s) red dragon fruit juice samples for 4 weeks of cold storage. After titration, TA was determined by observing the colour changes in the dragon fruit juice sample. TA in the unpasteurised sample steadily increases, reaching 0.38%, while the pasteurised sample shows a more controlled increase, reaching 0.20%. Both samples' pH fluctuated, decreasing to 4.64 at week 1 and gradually increasing until week 4. TSS remained relatively stable in both samples. Colour parameters (L*, a*, b*, h°, C) demonstrate a darkening trend, which is more noticeable in the pasteurised sample. Hence, pasteurisation had no notable impact on the pH and TSS of dragon fruit juice compared to unpasteurised samples, but a significant difference can be observed for colour parameters. These findings align with the previous research on watermelon juice enriched with L-citrulline by Tarazona-Díaz et al. (2017).

Additionally, the sudden increase of pH and TA after week 1 in this study is similar to the previous research by Adedokun et al. (2022) on the storage stability of black plum, baobab, and pineapple juice blends. In that study, the authors found that the pH remained stable during the initial two weeks at 4°C. However, a slight pH reduction occurred from week 2 to week 4 due to biological processes within the juice samples.

TA of the unpasteurised dragon juice increased drastically from 0.17% to 0.27% after one week. It may be due to the growth of microorganisms in unpasteurised juice, which have contributed to forming organic acids such as lactic acid bacteria via metabolic processes. Additionally, yeasts and other microorganisms capable of fermenting sugars could increase the production of organic acids (Aneja et al., 2014). However, the TA has resulted in non-significant changes in the later weeks due to the sugars in the dragon fruit juice, which microorganisms may have utilised during the initial phase, reducing the acid production rate. It is supported by a previous finding by Sandle (2016), who stated that the nutrient requirements vary widely among microorganisms, in which most derive energy by metabolising simple sugars like fructose.

For the pasteurised sample, there was a slight increase in the TA, from 0.10 to 0.15%, possibly due to a lower microorganism count than in the unpasteurised sample. The finding is similar to Unluturk and Atilgan (2015), who identified a drastic increment in TA of untreated white grape juice compared to pasteurised juice. Besides, the pasteurised samples maintained a constant TA (0.15% to 0.20 %) from week 1 to week 4 due to slowed enzymatic reactions in the juice, which indicates that oxidative enzymes have a significant enzymatic activity in the pulp of dragon fruit. The activity of enzymes such as polyphenol oxidase (PPO) and peroxidase (POD) in fruit juices is influenced by the concentration of oxygen present in the environment. Changes in the fruit juice's flavour components, which might affect the juice's acidity, can also result from browning reactions facilitated by PPO

Table 5
Physicochemical analysis of unpasteurised and pasteurised (60°C, 60 s) red dragon fruit juice during storage at 4°C

	TA (%)	pH	TSS (°Brix)	L*	a*	b*	h°	C	ΔE
Unpasteurized									
Week 0	0.17 ± 0.02^{aA}	5.05 ± 0.01^{aA}	10.6 ± 0.1^{aA}	13.5 ± 0.15^{aA}	43.28 ± 0.01^{aA}	21.44 ± 0.01^{aA}	25.83 ± 0.10^{aA}	49.20 ± 0.10^{aA}	-
Week 1	0.27 ± 0.10^{bA}	4.64 ± 0.01^{bA}	11.1 ± 0.03^{bA}	4.92 ± 0.01^{bA}	25.02 ± 0.01^{bA}	7.82 ± 0.01^{bA}	17.36 ± 0.01^{bA}	26.21 ± 0.01^{bA}	-
Week 2	0.32 ± 0.26^{cA}	4.91 ± 0.10^{cA}	11.1 ± 0.03^{bA}	5.15 ± 0.04^{cA}	29.29 ± 0.04^{cA}	8.83 ± 0.01^{cA}	16.78 ± 0.26^{cA}	30.59 ± 0.17^{cA}	-
Week 3	0.33 ± 0.36^{cA}	4.93 ± 0.04^{cA}	11.1 ± 0.03^{bA}	5.15 ± 0.03^{cA}	29.65 ± 0.29^{cA}	8.86 ± 0.26^{cA}	16.64 ± 0.01^{cA}	30.95 ± 0.04^{cA}	-
Week 4	0.38 ± 0.10^{dA}	4.98 ± 0.02^{dA}	11.0 ± 0.02^{bA}	5.92 ± 0.02^{dA}	32.64 ± 0.02^{dA}	10.23 ± 0.01^{dA}	17.40 ± 0.01^{dA}	34.21 ± 0.03^{dA}	-
Pasteurized									
Week 0	0.10 ± 0.01^{aB}	5.01 ± 0.01^{aB}	10.6 ± 0.03^{a}	13.43 ± 0.03^{aA}	43.96 ± 0.01^{aA}	22.44 ± 0.01^{aB}	27.04 ± 0.01^{aB}	49.36 ± 0.02^{aB}	1.05 ± 0.02
Week 1	0.15 ± 0.20^{bB}	4.64 ± 0.01^{bB}	11.0 ± 0.02^{bA}	6.48 ± 0.02^{bB}	32.09 ± 0.01^{bB}	10.28 ± 0.01^{bB}	17.76 ± 0.01^{bB}	33.70 ± 0.01^{bB}	7.65 ± 0.04
Week 2	0.17 ± 0.10^{bB}	4.86 ± 0.01^{cB}	11.0 ± 0.03^{bA}	6.73 ± 0.02^{cB}	34.16 ± 0.01^{cB}	11.59 ± 0.26^{cB}	18.74 ± 0.36^{cB}	36.07 ± 0.01^{cB}	5.50 ± 0.03
Week 3	0.19 ± 0.10^{cB}	4.92 ± 0.01^{dB}	10.9 ± 0.02^{cA}	6.97 ± 0.02^{dB}	34.68 ± 0.01^{cB}	12.02 ± 0.10^{dB}	19.12 ± 0.10^{dB}	36.70 ± 0.26^{dB}	6.52 ± 0.10
Week 4	0.20 ± 0.10^{cB}	4.99 ± 0.02^{eB}	10.9 ± 0.03^{cA}	6.44 ± 0.01^{eB}	33.47 ± 0.02^{dB}	11.1 ± 0.36^{eB}	18.35 ± 0.10^{eB}	35.26 ± 0.36^{eB}	1.31 ± 0.10

Note. Values expressed as means ± standard deviations; Small letters within a column denote a significant difference ($p < 0.05$) within the same treatment group (either pasteurised or unpasteurised) across different storage weeks, n = 3, Capital letters within a column denote a significant difference ($p < 0.05$) between different treatment groups (pasteurised and unpasteurised) within the same storage week, $n = 3$, TA = Titratable acidity, TSS = total soluble solids, L* = Lightness, a* = Redness, b* = Yellowness, H° = Hue angle, C = Chroma, ΔE = Colour difference

and POD enzymes. A study by Shaik and Chakraborty (2023) mentioned that the enzyme activity remains below 10% when the treated lime juice is stored at temperatures of 4°C. Thus, cold storage is efficient in maintaining the acidity of pasteurised fruit juice.

The pH of unpasteurised and pasteurised samples decreased from 5.05 and 5.01, respectively, to 4.64 in week 1. Acids found naturally in fruit juice, such as citric and malic acids, can be degraded. Oxidation of citric and malic acids can form intermediate compounds such as oxalic acid and oxaloacetic acid. These reactions might include enzymatic or chemical activities that degrade bigger acid molecules into simpler ones, reducing pH (Jerry & Bright, 2019). However, for both samples, a slight increase in pH can be detected from week 1 to week 4. It might be due to the effectiveness of cold storage, which avoids further chemical reactions that could turn the juice highly acidic and affect its sensory characteristics of sweetness and sourness. TSS increased slightly from 10.6 to 11.1 and 11.0 for unpasteurised and pasteurised samples at week 1 because of the conversion of carbohydrates to simple sugars (Mandha et al., 2023). During cold storage, the TSS for both samples showed only a slight change; the overall values ranged from 10.9 to 11.01. Cold storage will inhibit enzymatic activity, which could increase the solid content in the juice. Storage temperature can impact the rate of enzymatic and chemical reactions. Higher temperatures may accelerate these reactions, leading to a more rapid increase in TSS (Babarinde et al., 2019). This finding is similar to Wang et al. (2022), who reported that the TSS increased initially due to starch hydrolysis and then decreased after the starch had been completely digested.

The drastic drop in colour values for unpasteurised and pasteurised samples at week 1 compared to initial values is due to the cold storage that slowed down or temporarily inhibited enzymatic and chemical reactions responsible for colour development or stability. Enzymatic browning reactions due to PPO and POD enzymes, oxidation or other chemical processes contributing to colour changes are typically temperature dependent. Lower temperatures can slow these reactions, reducing colour intensity (Wibowo et al., 2015). Furthermore, unpasteurised and pasteurised samples exhibited noticeable changes in their colour characteristics over the four weeks. The L* values showed a consistent increase in both samples, indicating that the colour of the juice became lighter. Similarly, the a* and b* values were consistently increased in unpasteurised and pasteurised samples.

Despite variations in the hue angle (h°) values, no consistent trend was observed over the four weeks, suggesting fluctuations in the dominant wavelength of colour without a distinct shift for unpasteurised. It might be due to a growing trend in the microbial count, especially psychrotrophic bacteria, which causes chemical changes that lead to improper colour degradation (Hwang et al., 2022). In addition, chroma values increased over the four weeks for unpasteurised and pasteurised samples, indicating an increment in colour saturation. For L*, a*, b*, h° and C values, there was a sudden decrease at week 4 for pasteurised samples from three weeks of gradual increase. Dragon fruit consists of enzymes,

including polyphenol oxidase, which can catalyse enzymatic browning reactions. Even though pasteurisation is intended to deactivate enzymes, residual enzymatic activity may still exist. This remaining activity may eventually result in browning (Zhu et al., 2019).

For the first week, pasteurised samples showed the highest colour difference (7.65), and there was only a slight change at week 4 (1.34). Lee and Coates (2003) observed an increase in the b* value after thermal processing of orange juice at 90°C for 30 s. Similarly, Xu et al. (2015) found that thermal processing at 110°C for 8.6 s increased the yellowness of an orange juice blend, while Igual et al. (2014) discovered an increase in the b* value of grapefruit juice after heat treatment at 80°C. These findings support that the higher the temperature, the greater the changes in the colour parameters of the fruit juice. Moreover, chemical changes, including enzymatic reactions, influence the colour change of the juice during storage. Thus, pasteurisation leads to a noticeable alteration in colour, yet maintaining a lower temperature lessens this effect and preserves the vibrant colour of the juice.

Effect of Storage on Vitamin C Concentration

Table 6 shows the vitamin C content of unpasteurised and pasteurised samples at cold storage. Initially, the unpasteurised sample had a significantly higher vitamin C concentration of 37.4 mg/100 mL. However, the vitamin C concentration decreased significantly ($p < 0.05$) over the four-week storage period. This decline can be due to the natural sensitivity of vitamin C to numerous environmental variables, such as air, light, and temperature (Ajibola et al., 2009). Factors such as oxygen exposure during handling and storage contribute to the breakdown of vitamin C in fruit juices, resulting in a progressive drop in concentration (Mieszczakowska-Frąc et al., 2021). There is a significant difference ($p < 0.05$) among unpasteurised and pasteurised samples, especially during week 4. Both samples resulted in a declining trend for vitamin C content. This result is similar to findings by Mgaya-Kilima et al. (2015) and Alim et al. (2023), who concluded that vitamin C degradation during storage is one of the most essential factors affecting the quality of the juice.

Vitamin C concentration in the pasteurised sample also decreased across the four weeks, starting in Week 0 at 33.9 mg/100 mL. Despite being heat treated at 60°C, 60 s the pasteurised sample showed a similar trend of vitamin C breakdown as unpasteurised sample. This decline can be due to persistent oxidative reactions even after pasteurisation (Hernandez et al., 2006). Although pasteurisation helps to reduce the activity of enzymes that degrade vitamin C, it does not eliminate the impact of oxygen exposure and other variables that contribute to the deterioration of this sensitive nutrient during long periods of storage. It is supported by Tiencheu et al. (2021), who found a decrease in vitamin C after 1 month of storage at the refrigerating temperature for pawpaw, pineapple, and watermelon

Table 6
Vitamin C analysis of unpasteurised and pasteurised (60 °C, 60 s) red dragon fruit juice during storage at 4°C

	Vitamin C concentration (mg/100 mL)
Unpasteurised	
Week 0	37.4 ± 0.10^{aA}
Week 1	28.3 ± 0.01^{bA}
Week 2	25.0 ± 0.10^{cA}
Week 3	22.9 ± 0.10^{dA}
Week 4	19.8 ± 0.26^{eA}
Pasteurised	
Week 0	33.9 ± 0.01^{aB}
Week 1	28.1 ± 0.26^{bB}
Week 2	22.0 ± 0.06^{cB}
Week 3	20.7 ± 0.10^{dB}
Week 4	17.8 ± 0.26^{eB}

Note. Values expressed as means ± standard deviations; Small letters within a column denote a significant difference ($p < 0.05$) within the same treatment group (either pasteurised or unpasteurised) across different storage weeks, $n = 3$, Capital letters within a column denote a significant difference ($p < 0.05$) between different treatment groups (pasteurised and unpasteurised) within the same storage week, $n = 3$

juices. Due to the unstable nature of vitamin C, the decrease in vitamin C is identified in juices with increased storage duration because of oxidation during storage.

In Week 4, the unpasteurised sample's vitamin C content dropped to 19.8 mg/100 mL, whereas the pasteurised sample's concentration decreased to 17.8 mg/100 mL. This finding is similar to Wurlitzer et al. (2019), who found that vitamin C in tropical fruit juice was degraded during storage with a considerable loss of 30% to 40% from its initial concentration. In addition, Mandha et al. (2023) found that cold storage had an adverse impact on vitamin C in mango juice by reducing it from 61.1 to 33.9 mg/100 mL due to the presence of oxygen, which led to oxidation. Despite the drop in both samples, the pasteurised sample's vitamin C concentration is close to the unpasteurised sample. This implies that although pasteurisation reduced the vitamin C content of red dragon fruit juice, it still contributes to an acceptable range for consumers' daily intake. According to the US FDA, the daily value for vitamin C is set at 90 mg to support immune function and overall health. In comparison, the Ministry of Health Malaysia (MOH) recommends a reference nutrient intake of 70 mg for maintaining adequate vitamin C levels in adults. Pasteurised juice retains a significant quantity of vitamin C (17.8 mg) even after week 4, making it efficient for consumption as it provides 19.7% of the daily value of vitamin C and 25.4% of the reference nutrient intake of vitamin C as recommended by the FDA and MOH respectively.

CONCLUSION

The study revealed that pasteurisation significantly impacted red dragon fruit juice's microbiological, physicochemical, and vitamin C properties. Both high (80°C) and low (60°C) temperature pasteurisation effectively reduced microbial counts, especially at 60-second durations. Physicochemical analysis showed no significant effects on total acidity (TA) and total soluble solids (TSS) but noticeable changes in colour and pH, particularly at 80°C, where pigment degradation occurred. Vitamin C content decreased with higher temperatures and longer pasteurisation times due to heat sensitivity. Unpasteurised juice saw rapid microbial growth over four weeks of storage, while pasteurised juice maintained acceptable bacterial counts. Pasteurisation did not significantly affect pH and TSS but affected colour throughout storage. Both unpasteurised and pasteurised juices experienced a decline in vitamin C content over time, with unpasteurised juice showing more significant losses due to enzymatic and oxidative degradation. Thus, the study determined that pasteurisation at 60°C for 60 s balances microbiological quality and has minimal impact on physicochemical characteristics and vitamin C concentration.

ACKNOWLEDGEMENTS

The authors extend their gratitude to Assoc. Prof. Dr. Cheng Lai Hoong for her valuable guidance and expertise in vitamin C analysis, particularly for suggesting key modifications. They also thank the laboratory assistants of the Food Technology Division, School of Industrial Technology, USM, for their assistance in preparing the necessary chemical reagents and equipment and for their support throughout the research.

REFERENCES

Ağçam, E., Akyıldız, A., & Dündar, B. (2018). Thermal pasteurization and microbial inactivation of fruit juices. In G. Rajauria & B. K. Tiwari (Eds.), *Fruit juices* (pp. 309–339). Academic Press. https://doi.org/10.1016/B978-0-12-802230-6.00017-5

Adedokun, T. O., Matemu, A., Höglinger, O., Mlyuka, E., & Adedeji, A. (2022). Evaluation of functional attributes and storage stability of novel juice blends from baobab, pineapple, and black-plum fruits. *Heliyon*, *8*(5), e09340. https://doi.org/10.1016/j.heliyon.2022.e09340

Ahmad, M., Sinchaipanit, P., & Twichatwitayakul, R. (2015). Kinetics of ascorbic acid degradation and quality changes in guava juice during refrigerated storage. *Journal of Food and Nutrition Research*, *3*(8), 550–557. https://doi.org/10.12691/jfnr-3-8-10

Ajibola, V. O., Babatunde, O. A., & Suleiman, S. (2009). The effect of storage method on the vitamin C content in some tropical fruit juices. *Trends in Applied Sciences Research, 4*(2), 79–84. https://doi.org/10.3923/tasr.2009.79.84

Alegbeleye, O., Odeyemi, O. A., Strateva, M., & Stratev, D. (2022). Microbial spoilage of vegetables, fruits and cereals. *Applied Food Research*, *2*(1), 100122. https://doi.org/10.1016/j.afres.2022.100122

Alim, M. A., Karim, A., Shohan, M. A. R., Sarker, S. C., Khan, T., Mondal, S., Esrafil, M., Linkon, K. M. M. R., Rahman, M. N., Akther, F., & Begum, R. (2023). Study on stability of antioxidant activity of fresh, pasteurized, and commercial fruit juice during refrigerated storage. *Food and Humanity*, *1*, 1117–1124. https://doi.org/10.1016/j.foohum.2023.09.008

Aneja, K. R., Dhiman, R., Aggarwal, N. K., & Aneja, A. (2014). Emerging preservation techniques for controlling spoilage and pathogenic microorganisms in fruit juices. *International Journal of Microbiology*, *2014*(1), 758942. https://doi.org/10.1155/2014/758942

Angonese, M., Motta, G. E., Silva de Farias, N., Molognoni, L., Daguer, H., Brugnerotto, P., de Oliveira Costa, A. C., & Olivera Müller, C. M. (2021). Organic dragon fruits (*Hylocereus undatus* and *Hylocereus polyrhizus*) grown at the same edaphoclimatic conditions: Comparison of phenolic and organic acids profiles and antioxidant activities. *LWT*, *149*, Article 111924. https://doi.org/10.1016/j.lwt.2021.111924

Arivalagan, M., Karunakaran, G., Roy, T. K., Dinsha, M., Sindhu, B. C., Shilpashree, V. M., Satisha, G. C., & Shivashankara, K. S. (2021). Biochemical and nutritional characterization of dragon fruit (*Hylocereus* species). *Food Chemistry*, *353*, Article 129426. https://doi.org/10.1016/j.foodchem.2021.129426

Babarinde, G. O., Olatunde, S. J., & Adebiyi-Olabode, A. (2019). Quality attributes and phytochemical properties of fresh juice produced from selected mango varieties. *Ceylon Journal of Science*, *48*(1), 31-36. https://doi.org/10.4038/cjs.v48i1.7585

Choo, Y. X., Teh, L. K., & Tan, C. X. (2022). Effects of sonication and thermal pasteurization on the nutritional, antioxidant, and microbial properties of noni juice. *Molecules*, *28*(1), 313. https://doi.org/10.3390/molecules28010313

Ernest, E., Onyeka, O., Obuagu, A. C., & Onu, R. O. (2017). Comparative assessment of the effect of ripening stage on the vitamin C contents of selected fruits grown within Nsukka Axis of Enugu State. *International Journal of Environment, Agriculture and Biotechnology*, *2*(2), 712–714. https://doi.org/10.22161/ijeab/2.2.19

Ferreira, R. M., Amaral, R. A., Silva, A. M. S., Cardoso, S. M., & Saraiva, J. A. (2022). Effect of high-pressure and thermal pasteurization on microbial and physico-chemical properties of *Opuntia ficus-indica* juices. *Beverages*, *8*(4), 84. https://doi.org/10.3390/beverages8040084

Ghorai, D. (2023). A comprehensive review of dragon fruit (*Hylocereus* spp.): Botanical attributes, nutritional value, health benefits, and culinary applications. *The Pharma Innovation Journal*, *12*(8), 1578–1584

Giavoni, M., Villanueva-Suárez, M. J., De la Peña-Armada, R., Garcia-Alonso, A., & Mateos-Aparicio, I. (2022). Pasteurization modifies the sensorial attributes and nutritional profile of orange pulp by-product. *Foods*, *11*(13), 1973. https://doi.org/10.3390/foods11131973

Harivainda, K. V., Rebecca, O. P. S., & Chandran, S. (2008). Study of optimal temperature, pH, and stability of dragon fruit (*Hylocereus polyrhizus*) peel for use as a potential natural colorant. *Pakistan Journal of Biological Sciences*, *11*(18), 2259–2263. https://doi.org/10.3923/pjbs.2008.2259.2263

Hwang, S. H., Lee, J., Nam, T. G., Koo, M., & Cho, Y. S. (2022). Changes in physicochemical properties and bacterial communities in aged Korean native cattle beef during cold storage. *Food Science and Nutrition*, *10*(8), 2590–2600. https://doi.org/10.1002/fsn3.2864

Igual, M., Contreras, C., Camacho, M. M., & Martínez-Navarrete, N. (2014). Effect of thermal treatment and storage conditions on the physical and sensory properties of grapefruit juice. *Food and Bioprocess Technology*, *7*(1), 191–203. https://doi.org/10.1007/s11947-013-1088-6

Jalgaonkar, K., Mahawar, M. K., Bibwe, B., & Kannaujia, P. (2022). Postharvest profile, processing, and waste utilization of dragon fruit (*Hylocereus* spp.): A review. *Food Reviews International*, *38*(4), 733–759. https://doi.org/10.1080/87559129.2020.1742152

Jerry, A.-A., & Bright, Q. (2019). Effect of storage temperature on the physicochemical, nutritional, and microbiological quality of pasteurized soursop (*Annona muricata* L.) juice. *African Journal of Food Science*, *13*(2), 38–47. https://doi.org/10.5897/ajfs2018.1767

Klopotek, Y., Otto, K., & Böhm, V. (2005). Processing strawberries to different products alters contents of vitamin C, total phenolics, total anthocyanins, and antioxidant capacity. *Journal of Agricultural and Food Chemistry*, *53*(14), 5640–5646. https://doi.org/10.1021/jf047947v

Kong, T. Y., Hasnan, N. Z. N., Abdul Ghani, N. H., Basha, R. K., & Aziz, N. A. (2020). Effect of different pasteurization temperatures on physicochemical properties, bioactive compounds, antioxidant activity, and microbiological qualities of reconstituted pomegranate juice (RPJ). *Food Research*, *4*(S5), 157–164. https://doi.org/10.26656/fr.2017.4(S6).057

Lee, H. S., & Coates, G. A. (2003). Effect of thermal pasteurization on Valencia orange juice color and pigments. *LWT - Food Science and Technology*, *36*(1), 153–156. https://doi.org/10.1016/S0023-6438(02)00087-7

Liaotrakoon, W. (2013). Characterization of dragon fruit (*Hylocereus* spp.) components with valorization potential [Doctoral dissertation, Ghent University]. CORE. https://core.ac.uk/download/pdf/55814526.pdf

Ma, T., Wang, J., Wang, H., Lan, T., Liu, R., Gao, T., Yang, W., Zhou, Y., Ge, Q., Fang, Y., & Sun, X. (2020). Is overnight fresh juice drinkable? The shelf-life prediction of non-industrial fresh watermelon juice based on the nutritional quality, microbial safety quality, and sensory quality. *Food & Nutrition Research*, *64*, 4237 https://doi.org/10.29219/fnr.v64.4327

Mandha, J., Shumoy, H., Matemu, A. O., & Raes, K. (2023). Characterization of fruit juices and effect of pasteurization and storage conditions on their microbial, physicochemical, and nutritional quality. *Food Bioscience*, *51*, 102335. https://doi.org/10.1016/j.fbio.2022.102335

Mengistu, D. A., Belami, D. D., Tefera, A. A., & Alemeshet Asefa, Y. (2022). Bacteriological quality and public health risk of ready-to-eat foods in developing countries: Systematic review and meta-analysis. *Microbiology Insights*, *15*, https://doi.org/10.1177/11786361221113916

Mgaya-Kilima, B., Remberg, S. F., Chove, B. E., & Wicklund, T. (2015). Physicochemical and antioxidant properties of roselle-mango juice blends: Effects of packaging material, storage temperature, and time. *Food Science and Nutrition*, *3*(2), 100–109. https://doi.org/10.1002/fsn3.174

Mieszczakowska-Frąc, M., Celejewska, K., & Płocharski, W. (2021). Impact of innovative technologies on the content of vitamin C and its bioavailability from processed fruit and vegetable products. *Antioxidants*, *10*(1), 54. https://doi.org/10.3390/antiox10010054

Ministry of Health Malaysia (2005). *Recommended nutrient intakes for Malaysia: A report of the technical working group on nutritional guidelines*. National Coordinating Committee on Food and Nutrition. https://www.moh.gov.my/moh/images/gallery/rni/insert.pdf

Moo-Huchin, V. M., Cuevas-Glory, L., Sauri-Duch, E., Mai, C. J., González-Aguilar, G. A., Moo-Huchin, M., Ortiz-Vázquez, E., & Betancur-Ancona, D. (2017). Carotenoid composition and antioxidant activity of extracts from tropical fruits. *Chiang Mai Journal of Science*, *44*(2), 605-616.

Myer, P. R., Parker, K. R., Kanach, A. T., Zhu, T., Morgan, M. T., & Applegate, B. M. (2016). The effect of a novel low temperature-short time (LTST) process to extend the shelf-life of fluid milk. *SpringerPlus*, *5*, 660. https://doi.org/10.1186/s40064-016-2250-1

Nguyen, N. (2020). The marketing for Vietnamese dragon fruit. *Archives of Business Research, 8*(5), 221–226. https://doi.org/10.14738/abr.85.8299

Nicklas, T. A., O'Neil, C. E., & Fulgoni, V. L., III. (2015). Replacing 100% fruit juice with whole fruit results in a trade-off of nutrients in the diets of children. *Current Nutrition & Food Science*, *11*(4), 267–273. https://doi.org/10.2174/1573401311666150618192703

Petruzzi, L., Campaniello, D., Speranza, B., Corbo, M. R., Sinigaglia, M., & Bevilacqua, A. (2017). Thermal treatments for fruit and vegetable juices and beverages: A literature overview. *Comprehensive Reviews in Food Science and Food Safety*, *16*(4), 668–691. https://doi.org/10.1111/1541-4337.12270

Rabie, M. A., Soliman, A. Z., Diaconeasa, Z. S., & Constantin, B. (2014). Effect of pasteurization and shelf life on the physicochemical properties of physalis (*Physalis peruviana*) juice. *Journal of Food Processing and Preservation*, *39*(6), 1051–1060. https://doi.org/10.1111/jfpp.12320

Saikia, S., Mahnot, N. K., & Mahanta, C. L. (2016). A comparative study on the effect of conventional thermal pasteurization, microwave, and ultrasound treatments on the antioxidant activity of five fruit juices. *Food Science and Technology International*, *22*(4), 288–301. https://doi.org/10.1177/1082013215596466

Sandle, T. (2016). Microbiological challenges to the pharmaceuticals and healthcare. In *Pharmaceutical Microbiology* (pp. 281–294). Woodhead Publishing. https://doi.org/10.1016/B978-0-08-100022-9.00022-0

Satpathy, L., Pradhan, N., Dash, D., Baral, P. P., & Parida, S. (2020). Quantitative determination of vitamin C concentration of common edible food sources by redox titration using iodine solution. *Letters in Applied NanoBioScience*, *10*(3), 2361–2369. https://doi.org/10.33263/lianbs103.23612369

Saud, S., Xiaojuan, T., & Fahad, S. (2024). The consequences of fermentation metabolism on the qualitative qualities and biological activity of fermented fruit and vegetable juices. *Food Chemistry: X*, *21*, 101209. https://doi.org/10.1016/j.fochx.2024.101209

Shaik, L., & Chakraborty, S. (2023). Effect of different storage conditions on the quality attributes of sweet lime juice subjected to pulsed light and thermal pasteurization. *Sustainable Food Technology*, *1*(5), 722–737. https://doi.org/10.1039/D3FB00023K

Sourri, P., Tassou, C. C., Nychas, G. J. E., & Panagou, E. Z. (2022). Fruit juice spoilage by *Alicyclobacillus*: Detection and control methods—A comprehensive review. *Foods, 11*(5), 747. https://doi.org/10.3390/foods11050747

Susilo, B., Sutan, S. M., Hendrawan, Y., & Damayanti, R. (2021). Improving quality of dragon fruit (*Hylocereus costaricensis*) syrup by processing with double jacket vacuum evaporator. *IOP Conference Series: Earth and Environmental Science*, *924*, 012012. https://doi.org/10.1088/1755-1315/924/1/012012

Tarazona-Díaz, M. P., Martínez-Sánchez, A., & Aguayo, E. (2017). Preservation of bioactive compounds and quality parameters of watermelon juice enriched with l-citrulline through short thermal treatment. *Journal of Food Quality*, *2017*(1), 3283054. https://doi.org/10.1155/2017/3283054

Tchuenchieu, A., Essia Ngang, J., Servais, M., Dermience, M., Sado Kamdem, S., Etoa, F., & Sindic, M. (2018). Effect of low thermal pasteurization in combination with carvacrol on color, antioxidant capacity, phenolic, and vitamin C contents of fruit juices. *Food Science & Nutrition*, *6*(4), 736–746. https://doi.org/10.1002/fsn3.611

Tiencheu, B., Nji, D. N., Achidi, A. U., Egbe, A. C., Tenyang, N., Tiepma Ngongang, E. F., Djikeng, F. T., & Fossi, B. T. (2021). Nutritional, sensory, physicochemical, phytochemical, microbiological, and shelf-life studies of natural fruit juice formulated from orange (*Citrus sinensis*), lemon (*Citrus limon*), honey, and ginger (*Zingiber officinale*). *Heliyon*, *7*(6), e07177. https://doi.org/10.1016/j.heliyon.2021.e07177

Unluturk, S., & Atilgan, M. R. (2015). Microbial safety and shelf life of UV-C treated freshly squeezed white grape juice. *Journal of Food Science*, *80*(8), M1831-M1841 https://doi.org/10.1111/1750-3841.12952

Valliere, B., & Harkins, S. (2020). A preliminary evaluation to establish bath pasteurization guidelines for hard cider. *Beverages*, *6*(2), 24. https://doi.org/10.3390/beverages6020024

Vern, W., Lejaniya, A., & Pui, L. (2023). Determination of preservatives and physicochemical properties of fruit juice-based beverages. *Carpathian Journal of Food Science and Technology*, *15*(1), 232–246. https://doi.org/10.34302/crpjfst/2023.15.1.17

Wang, H., Yuan, J., Chen, L., Ban, Z., Zheng, Y., Jiang, Y., Jiang, Y., & Li, X. (2022). Effects of fruit storage temperature and time on cloud stability of not from concentrated apple juice. *Foods*, *11*(17), 2568. https://doi.org/10.3390/foods11172568

Wibowo, S., Grauwet, T., Gedefa, G. B., Hendrickx, M., & Van Loey, A. (2015). Quality changes of pasteurized mango juice during storage. Part II: Kinetic modelling of the shelf-life markers. *Food Research International*, *78*, 410–423. https://doi.org/10.1016/j.foodres.2015.09.001

Wong, Y. M., & Siow, L. F. (2015). Effects of heat, pH, antioxidant, agitation, and light on betacyanin stability using red-fleshed dragon fruit (*Hylocereus polyrhizus*) juice and concentrate as models. *Journal of Food Science and Technology*, *52*(5), 3086–3092. https://doi.org/10.1007/s13197-014-1362-2

Wurlitzer, N. J., Dionísio, A. P., Lima, J. R., Garruti, D. dos S., Silva Araújo, I. M. da, da Rocha, R. F. J., & Maia, J. L. (2019). Tropical fruit juice: Effect of thermal treatment and storage time on sensory and functional properties. *Journal of Food Science and Technology*, *56*(12), 5184–5193. https://doi.org/10.1007/s13197-019-03987-0

Xu, Z., Lin, T., Wang, Y., & Liao, X. (2015). Quality assurance in pepper and orange juice blend treated by high pressure processing and high temperature short time. *Innovative Food Science and Emerging Technologies*, *31*, 28–36. https://doi.org/10.1016/j.ifset.2015.08.001

Yıkmış, S. (2020). Sensory, physicochemical, microbiological, and bioactive properties of red watermelon juice and yellow watermelon juice after ultrasound treatment. *Journal of Food Measurement and Characterization*, *14*(3), 1417–1426. https://doi.org/10.1007/s11694-020-00391-7

Yin, X., Chen, K., Cheng, H., Chen, X., Feng, S., Song, Y., & Liang, L. (2022). Chemical stability of ascorbic acid integrated into commercial products: A review on bioactivity and delivery technology. *Antioxidants*, *11*(1), 153. https://doi.org/10.3390/antiox11010153

Zhu, D., Shen, Y., Xu, L., Cao, X., Lv, C., & Li, J. (2019). Browning and flavour changing of cloudy apple juice during accelerated storage. *IOP Conference Series: Materials Science and Engineering*, *611*(1), 012061. https://doi.org/10.1088/1757-899X/611/1/012061

Pertanika J. Trop. Agric. Sci. 48 (3): 837 - 850 (2025)

PERTANIKA JOURNALS

TROPICAL AGRICULTURAL SCIENCE

Journal homepage: http://www.pertanika.upm.edu.my/

Enhancing Single-cell Protein Produced by *Aspergillus terreus* UniMAP AA-1 from Palm-pressed Fiber via Response Surface Methodology

Khadijah Hanim Abdul Rahman[1,2]*, Siti Jamilah Hanim Mohd Yusof[1,2] and Naresh Sandrasekaran[3]

[1]*Faculty of Chemical Engineering and Technology, Universiti Malaysia Perlis, Kompleks Pusat Pengajian Jejawi 3, 02600 Arau, Perlis, Malaysia*

[2]*Centre of Excellence for Biomass Utilization, Universiti Malaysia Perlis, Kompleks Pusat Pengajian Jejawi 3, 02600 Arau, Perlis, Malaysia*

[3]*Opteraz Sdn Bhd, PTD 53718, Jalan Teknologi 3, Kawasan Perindustrian Mengkibol, 86000 Kluang, Johor, Malaysia*

ABSTRACT

The increased demand for aquaculture has led to significant implications for fish feed supply since its cost contributes to most of the operational cost. The primary protein source in feed ingredients comes from fish meal (FM). However, increasing FM prices and overfishing concerns substantially challenge its sustainable production. Alternatively, single-cell protein (SCP) derived from microbial biomass has demonstrated efficacy as a protein substitute. This study enhanced microbial protein production of *Aspergillus terreus* UniMAP AA-1 cultivated on palm-pressed fiber (PPF) through the response surface methodology (RSM) approach. Screening of media compositions comprising potassium dihydrogen phosphate (KH_2PO_4), ammonium nitrate (NH_4NO_3), sodium chloride (NaCl), magnesium sulfate heptahydrate ($MgSO_4.7H_2O$), ferrous sulfate heptahydrate ($FeSO_4.7H_2O$), copper (II) sulfate pentahydrate ($CuSO_4.5H_2O$), and zinc sulfate heptahydrate ($ZnSO_4.7H_2O$) was conducted using the Plackett-Burman design (PBD). The Central Composite Rotatable Design (CCRD) approach was further used to optimize the significant parameters influencing SCP production. Screening by the PBD signifies that NH_4NO_3 and $MgSO_4.7H_2O$ are significant factors enhancing SCP production, with the highest SCP produced of 551 mg/L. Subsequently, optimization by CCRD revealed that the optimum concentration for NH_4NO_3 and $MgSO_4.7H_2O$ were 0.85% and 0.05% (w/v). This optimization strategy has increased the SCP

ARTICLE INFO

Article history:
Received: 05 August 2024
Accepted: 11 November 2024
Published: 16 May 2025

DOI: https://doi.org/10.47836/pjtas.48.3.10

E-mail addresses:
khadijahhanim@unimap.edu.my (Khadijah Hanim Abdul Rahman)
jamilahhanim@unimap.edu.my (Siti Jamilah Hanim Mohd Yusof)
nareshnash92@gmail.com (Naresh Sandrasekaran)
*Corresponding author

production to 673 mg/L, 22% higher than those obtained earlier. The data gathered in this study may be used for scale-up production of SCP from PPF by *A. terreus* UniMAP AA-1.

Keywords: Central Composite Rotatable Design, fish feed application, media composition optimization, palm-pressed fiber, Plackett-Burman Design, single-cell protein, solid-state fermentation

INTRODUCTION

The aquaculture industry is one of the fastest-growing food sectors globally, driven by the increasing demand for fish and shellfish on a global scale. The aquaculture sector has grown at an average yearly rate of 8.9% since 1970 (Huang & Nitin, 2019). The surge in demand has led to significant implications for fish feed supply. Feed costs typically account for 30%–70% of total operational costs, significantly impacting investment profitability (Bratosin et al., 2021). The primary protein source in feed ingredients is fish meal (FM). However, the increasing costs for FM and overfishing concerns substantially challenge its sustainable production. FM production is expected to struggle to meet global demand by 2050 (Bratosin et al., 2021). Therefore, exploring alternative protein sources is crucial, as they have the potential to be substitutes for fish meals. One promising alternative is a single-cell protein (SCP) derived from microbial biomass, which has demonstrated efficacy as a protein substitute for fish and soybeans. SCP is obtained from cultured cells and can be isolated as dried cells or purified protein. Various microorganisms can produce it, including bacteria, fungi, and algae. Microbial protein is cost-effective and offers better nutritional value than other protein sources. Its rapid growth rate also enables large-scale production (Bajić et al., 2023).

Oil palm holds significant importance in Malaysia's agricultural landscape alongside rubber, cocoa, rice, and coconut (Jafri et al., 2021). The oil palm plantations covered 5.67 million hectares as of 2022, producing 1.04 million tons (MT) of palm kernel oil and about 15.72 MT of palm oil (Malaysian Oil Palm Council [MPOC], 2024). The oil palm tree's biomass makes up 90% of its mass, with palm oil making up only 10% of this biomass (Jafri et al., 2021). Oil palm biomass refers to residues from the industry's replanting, pruning, and milling activities. Among these residues, palm-pressed fiber (PPF) emerges as a promising substrate for SCP production. PPF is made of a mixture of mesocarp fiber, crushed kernel, kernel shell, and debris extracted from the mesocarp of oil palm fruits after the oil is extracted (Neoh et al., 2011). Rich in cellulose and hemicellulose, PPF offers an ideal carbon source for fungi to produce SCP, thereby serving as a valuable ingredient in feed ingredients (Amara & El-Baky, 2023).

Optimizing the composition of the culture medium is essential for enhancing biomass accumulation and producing desired products. However, each element requires the appropriate concentration, ratios, and chemical forms to provide optimal growth conditions

(Bentahar & Deschênes, 2022). Fermentation medium optimization frequently involves either the one-factor-at-a-time (OFAT) or more advanced statistical optimization techniques. Although OFAT is simple, it can be expensive and time-consuming due to the multiple tests required to reach conclusions. Furthermore, OFAT overlooks the interactions among different factors under investigation.

On the contrary, statistical optimization methods offer advantages like nutrient balancing, enriching essential components, and eliminating unnecessary ones while considering factor interactions. These approaches also reduce the number of experiments needed, thus reducing costs and enhancing the production process's efficiency (Guo et al., 2019). Response surface methodology (RSM), Plackett-Burman design (PBD), and factorial design are common methods for achieving statistical optimization, which produces ideal results like increased cell proliferation or volumetric production. Thus, RSM, a robust mathematical tool, allows for the efficient testing of multiple process variables, reducing the number of trials required to identify significant components impacting microbial processes (Choi et al., 2021). Therefore, this study aims to investigate the performance of PPF as a substrate for SCP generation by *Aspergillus terreus* UniMAP AA-1. The PBD approach was selected to screen the most significant media components. Through the central composite rotatable design (CCRD), RSM was employed to further optimize the parameters that affect SCP production.

MATERIALS AND METHODS

Collection of Raw Materials and Preparation of Substrate

The PPF used in this study was provided by Norstar Palm Oil Mill Sdn. Bhd. in Kuala Ketil, Kedah (5°34′09.3″N 100°42′01.8″E). Dust, sand, and other contaminants were eliminated from the PPF by rinsing it with tap water, followed by drying at 60°C for 24 hours in the oven. Then, it was ground and sieved into 500 µm particle size before being kept in a dry container prior to further use.

Pretreatment of Substrate

About 1 L of 5% (w/v) NaOH (Merck, Germany) was used to treat 50 g of dried PPF. The substrate mixture was then incubated according to Rahman et al. (2021). Following the draining of the NaOH solution, the substrate was cleaned with dH_2O until the pH reached a neutral level and oven-dried at 60°C.

Inoculum Preparation

A. terreus UniMAP AA-1 (Gunny & Arbain, 2012) was obtained from the culture collection of the Faculty of Chemical Engineering and Technology, Universiti Malaysia Perlis. The

culture was cultivated for 7 days at 30°C on potato dextrose agar (PDA) (HiMedia, India). About 30 ml of sterilized dH_2O was added to the 7-day-old spores. After rubbing, the spores were filtered through Whatman Grade No. 1 filter paper, and the spore was adjusted to the concentration of 10^7 CFU/ml using a hemocytometer (De la Cruz-Quiroz et al., 2019). The filtrate was kept at 4°C before usage.

Growth Media Preparation and Solid-state Fermentation

A 250 ml conical flask was filled with approximately 6 g of substrate. About 50% moisture content was achieved by adding 6 ml of solution to the substrate, consisting of 20% inoculum and 80% growth media solution. The composition of the media solution was varied by altering the concentration of seven media components which include potassium dihydrogen phosphate (KH_2PO_4; Bendosen, Malaysia), ammonium nitrate (NH_4NO_3; HmbG, Germany), sodium chloride (NaCl; HmbG, Germany), magnesium sulfate heptahydrate ($MgSO_4.7H_2O$; HmbG, Germany), ferrous sulfate heptahydrate ($FeSO_4.7H_2O$; HmbG, Germany), copper (II) sulfate pentahydrate ($CuSO_4.5H_2O$; Bendosen, Malaysia), and zinc sulfate heptahydrate ($ZnSO_4.7H_2O$; HmbG, Germany) based on the experimental design. The mixture was thoroughly mixed prior to incubation at 30°C for 5 days (Rahman et al., 2021).

Identification of Significant Media Compositions Using Plackett-Burman Design (PBD)

The screening was conducted using the PBD (Design Expert v12). The design can decrease the number of experiments required to achieve goals efficiently. The first-order model in Equation 1 served as the basis for the Plackett-Burman experimental design:

$$Y = ß_0 + \sum ß_i X_i \quad [1]$$

where, Y is the SCP production, mg/L, $ß_0$ is the model intercept, and $ß_i$ is the variable estimates. A significant factor contributing to SCP production is denoted by a confidence level greater than 95%. A total of 12 runs were generated, which included seven media components. The experimental runs were replicated three times, and the response was the average of triplicates. The range used for each component is depicted in Table 1.

Table 1
Plackett-Burman Design of different media compositions and levels

Factor	Term	Unit	Level	
			-1	+1
NH_4NO_3	A	% (w/v)	0.30	0.70
KH_2PO_4	B	% (w/v)	0.15	0.35
NaCl	C	% (w/v)	0.00	0.20
$MgSO_4.7H_2O$	D	% (w/v)	0.10	0.20
$FeSO_4.7H_2O$	E	% (w/v)	0.00	0.20
$ZnSO_4.7H_2O$	F	% (w/v)	0.00	0.20
$CuSO_4.5H_2O$	G	% (w/v)	0.00	0.20

Optimization of Media Components by Central Composite Rotatable Design (CCRD)

The optimization was conducted using the CCRD (Design Expert v12). The significant media components identified by PBD were selected as variables in the CCRD. They were NH_4NO_3 and $MgSO_4.7H_2O$, and the levels were set, as shown in Table 2.

As indicated by the PBD, the $FeSO_4.7H_2O$, KH_2PO_4, NaCl, $CuSO_4.5H_2O$, and $ZnSO_4.7H_2O$ concentrations were kept at their optimal levels. About 13 runs were performed, including 5 duplicates at the center points. The analysis was done in triplicates. According to Equation 2, a second-order polynomial response surface approach was fitted using the experimental data in the statistical package Design Expert v12 (StatEase Inc. Minneapolis, USA):

$$Y = ß_0 + ß_1X_1 + ß_2X_2 + ß_{11}X^2_1 + ß_{22}X^2_2 + ß_{12}X_1X_2 \quad [2]$$

where, Y is the SCP (mg/L), $ß_0$ is the intercept, $ß_1$ and $ß_2$ are the linear coefficients, $ß_{11}$ and $ß_{22}$ are the squared coefficients, and $ß_{12}$ is the interaction of coefficients.

Protein Recovery and Determination

The fermentation sample was dried for 24 hr at 60°C. The dried samples were ground using a mortar and pestle to obtain a smaller and smoother substrate. In a centrifuge tube, 0.5 g of the dried sample and 25 ml of 1 N NaOH were mixed and soaked for 24 hours at room temperature. Subsequently, the mixture was centrifuged for 10 min at 10,062 *g* and the supernatant was kept at 4°C (Rahman et al., 2021). Protein concentration was determined using the Lowry method.

Total Reducing Sugar Content

In a test tube, 1 ml of 3,5-dinitrosalicylic acid (DNS) reagent and 1 ml of sample supernatant were mixed. The mixture was incubated for 10 min in an 80°C water bath and then cooled under running water. Absorbance was measured by a UV spectrophotometer (Thermo Fisher Scientific, USA) at a wavelength of 540 nm (Rahman et al., 2021).

Table 2
The factors and levels applied for Central Composite Rotatable Design (CCRD)

Factor	Unit	Level				
		$-\alpha$	−1	0	+1	α
NH_4NO_3	% (w/v)	0.64	0.70	0.85	1.00	1.06
$MgSO_4.7H_2O$	% (w/v)	0.00	0.00	0.05	0.10	0.12

RESULTS AND DISCUSSION

Screening of Media Compositions by Plackett-Burman Design (PBD)

PBD is a tool used to screen the effects of process variables on yield. This tool can reduce the number of experiments needed in the subsequent optimization study using RSM. The effects of different media compositions on SCP production were determined by performing 12 runs given by the PBD (Table 3). The highest protein concentration was obtained in run 2, with 551 mg/L, while the lowest was obtained in run 3, with 90 mg/L.

The PBD generates a regression equation that predicts the factors influencing the response, such as SCP production. This equation, expressed through the coefficient of R^2, showed a value of 0.9376 for SCP, confirming the design's significance in predicting variable effects on *A. terreus* UniMAP AA-1's SCP production. An analysis of variance (ANOVA) using Fisher's *F*-test and *F*-value further validated the model's significance (Table 4). The significance of the model is indicated by its *F*-value of 8.58, which has a 2.76% probability of happening owing to random variation. The *p*-value is useful for determining each coefficient's significance and identifying interaction patterns between variables. A smaller *p*-value (p-value < 0.05) signifies greater coefficient significance. In this study, only three parameters—NH_4NO_3, $MgSO_4.7H_2O$, and $FeSO_4.7H_2O$—showed significant model terms, as detailed in Table 4.

The main effects (*t*-value) of the analyzed factors on SCP production are graphically illustrated in Figure 1. The *t*-value with a large magnitude indicates the high significance

Table 3
The Placket-Burman experimental runs and resulting single-cell protein (SCP) of A. terreus *UniMAP AA-1 cultivated on palm-pressed fiber*

Run	A	B	C	D	E	F	G	SCP (mg/L)
1	0.7	0.35	0.2	0.1	0.0	0.0	0.2	452
2	0.7	0.35	0.0	0.1	0.0	0.2	0.0	551
3	0.3	0.35	0.0	0.2	0.2	0.0	0.2	90
4	0.7	0.15	0.0	0.1	0.2	0.0	0.2	393
5	0.3	0.35	0.2	0.2	0.0	0.0	0.0	250
6	0.3	0.15	0.2	0.1	0.2	0.2	0.0	291
7	0.7	0.15	0.2	0.2	0.0	0.2	0.2	364
8	0.3	0.35	0.2	0.1	0.2	0.2	0.2	273
9	0.7	0.15	0.2	0.2	0.2	0.0	0.0	312
10	0.3	0.15	0.0	0.2	0.0	0.2	0.2	345
11	0.3	0.15	0.0	0.1	0.0	0.0	0.0	338
12	0.7	0.35	0.0	0.2	0.2	0.2	0.0	381

Note. Variables listed in % (w/v): A = NH_4NO_3, B = KH_2PO_4, C = NaCl, D = $MgSO_4.7H_2O$, E = $FeSO_4.7H_2O$, F = $ZnSO_4.7H_2O$, G = $CuSO_4.5H_2O$

Table 4
Statistical analysis of Plackett-Burman design for each variable

Variable	*df*	*F*-value	*p*-value	Confidence level (%)
Model	7	8.58	0.0276	97.24
NH_4NO_3	1	28.53	0.0059	99.41
KH_2PO_4	1	0.081	0.7907	20.93
NaCl	1	0.926	0.3904	60.96
$MgSO_4.7H_2O$	1	11.76	0.0265	97.36
$FeSO_4.7H_2O$	1	11.93	0.0260	97.40
$ZnSO_4.7H_2O$	1	5.21	0.0846	91.54
$CuSO_4.5H_2O$	1	1.61	0.2727	72.73

Note. Highlighted in grey is the significant model term (*p*-value <0.05)

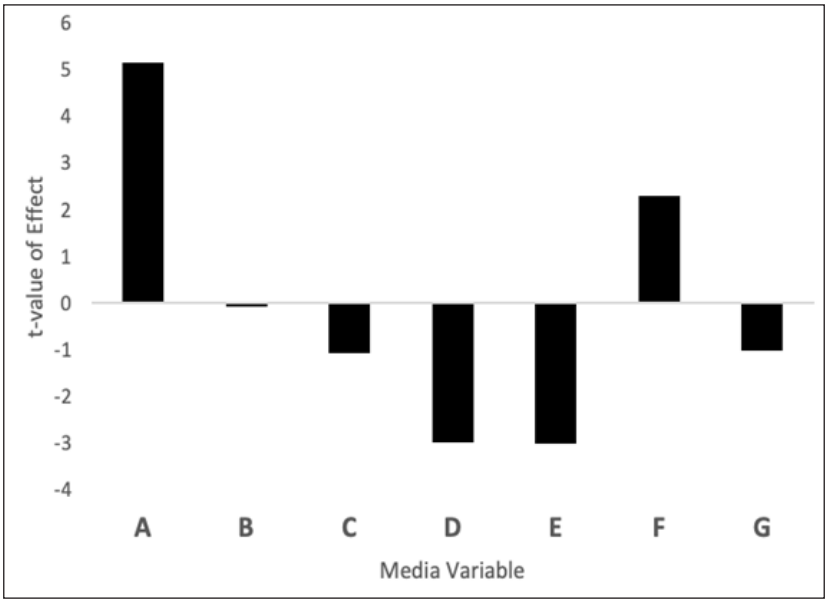

Figure 1. Main effects of media compositions for single-cell protein production

Note. A = NH_4NO_3, B = KH_2PO_4, C = NaCl, D = $MgSO_4.7H_2O$, E = $FeSO_4.7H_2O$, F = $ZnSO_4.7H_2O$, G = $CuSO_4.5H_2O$

of the equivalent coefficient. Based on Figure 1, the most significant factor is NH_4NO_3, and the positive value indicates that by increasing the parameter concentration, the production of SCP will be enhanced. Besides that, $MgSO_4.7H_2O$ and $FeSO_4.7H_2O$ are the other two significant factors that affect SCP production. The *t*-values of these factors are negative values, indicating that they are needed at lower concentrations for an enhanced production of SCP.

Nitrogen sources are an essential nutrient component for microbial growth and building blocks of protein. Organic or inorganic sources can supply nitrogen. Ammonium is the preferred nitrogen source because it promotes faster growth compared to other nitrogen sources available (Chen et al., 2022; Chutrakul et al., 2022; Jiang et al., 2019; Martin-Jézéquel et al., 2015). In this study, nitrogen in the form of NH_4NO_3 was added to the media, and the PBD identified this compound as the most significant compound for protein production at a concentration of 0.7% (w/v). An optimum amount of nitrogen source is vital for mycelium growth due to the formation of metabolic by-products (Nguyen et al., 2023). Akintomide and Antai (2012) also observed the effect of inorganic nitrogen supplementation on SCP production. They investigated how various inorganic nitrogen sources affected the development of microorganisms and discovered that adding $(NH_4)_2SO_4$ to *Saccharomyces cerevisiae* (21.3%) and *Aspergillus niger* (16.78%) resulted in the highest crude protein yields (Akintomide & Antai, 2012).

Moreover, supplementing a nitrogen source in the form of NH_4 can stimulate mycelial growth in fungi, as Dulay et al. (2020) reported, consequently enhancing both biomass and protein yields simultaneously. On the contrary, although $MgSO_4.7H_2O$ and $FeSO_4.7H_2O$ played significant roles in SCP production, their amount is needed in small amounts as they are the trace elements for fungi growth. The elevated concentrations of Mg^{2+} and Fe^{2+} are known to cause cell growth inhibition, leading to lagging of doubling time (Chen et al., 2022; Nepal & Kumar, 2020). Zięba et al. (2021) reported that the most significant decrease in *Plurotus djamor* productivity was observed when the media was supplemented with the highest Mg concentration of 4200 mg. The finding in this study was further corroborated by Prakash et al. (2015), who cultivated *Fusarium venenatum* in combination with jaggery water, date extract, and mineral salts (KH_2PO_4, K_2HPO_4, and $MgSO_4$). They observed that the highest protein concentration (4.9 g/L) was obtained at a low level (50 mg/L) of $MgSO_4$ (Prakash et al., 2015). The observed results suggested that although Mg^{2+} and nitrogen are essential elements in organisms, excess quantities may hamper protein production (Nepal & Kumar, 2020; Nguyen et al., 2023).

Optimization of Single-Cell Protein (SCP) Production by Response Surface Method (RSM) using Central Composite Rotatable Design (CCRD)

The significant parameters in the Plackett-Burman analysis were used to optimize SCP production by *A. terreus* UniMAP AA-1. The concentration of NH_4NO_3 and $MgSO_4.7H_2O$ were only considered parameters for optimization (Table 2), while $FeSO_4.7H_2O$ was not added in the media as suggested by PBD. The CCRD of the Design Expert software suggested a total of 13 runs, including five replicates at the center points, as shown in Table 5. Other parameters, such as KH_2PO_4, NaCl, $ZnSO_4.7H_2O$, and $CuSO_4.7H_2O$, were included in the growth medium at the concentration suggested optimum by Plackett-

Burman analysis. These trace elements are necessary to maintain *A. terreus* growth while increasing SCP production.

The ANOVA results (Table 6) reveal that the model is significant, with a *p*-value of 0.0004. As a result, only 0.04% of the models are insignificant due to noise. Although parameters A (NH_4NO_3), B ($MgSO_4.7H_2O$), and the interaction between AB are not significant (*p*-value > 0.05), they are still considered in the model because the higher order term, A^2, a quadratic term of NH_4NO_3, is significant with a value of less than 0.0001 because the model was built on a hierarchy. However, B^2 is insignificant and hence removed from the equation. It demonstrates that A^2 operates as a limiting factor, with a minor change in value affecting the protein concentration. In contrast to pure error, the lack of fitness is not significant, and noise has a 15.70% probability of being the source of a large lack of fit *F*-value. The model fits the data well (Elsayed & Ahmed Abdelwahed, 2020). A regression analysis was performed utilizing coded values from data estimates, as stated by Equation 3:

$$\text{SCP (mg/L)} = 639.18 + (10.78 \times NH_4NO_3) + (8.77 \times MgSO_4.\ 7H_2O) + (1.5\ NH_4NO_3 \times MgSO_4.\ 7H_2O) - (77.62 \times NH_4NO_3^2) \quad [3]$$

A quadratic model with an R^2 value of 0.9015 was proposed, indicating that the experimental variables analyzed accounted for 90.15% of the overall variation in the SCP.

Table 5
The predicted and experimental values of single-cell protein after parameters optimization by Central Composite Rotatable Design

Run	A = NH_4NO_3	B = $MgSO_4.\ 7H_2O$	Single-cell protein (mg/L)	
			Experimental	Predicted
1	0.70	0.00	553	533.43
2	0.70	0.10	576	554.45
3	0.85	0.05	673	647.02
4	1.00	0.10	591	579.01
5	0.85	0.05	663	647.02
6	0.85	0.05	635	647.02
7	1.00	0.00	562	551.99
8	0.85	0.00	597	620.83
9	0.85	0.05	640	647.02
10	1.06	0.05	497	506.02
11	0.64	0.05	453	475.54
12	0.85	0.12	616	635.65
13	0.85	0.05	636	647.02

Table 6
Analysis of variance for a quadratic model of single-cell protein production

Source	Sum of squares	df	Mean Square	F-value	p-value
Model	44459.21	4	11114.80	18.31	4.00×10^{-4}
A- NH_4NO_3	929.35	1	929.35	1.53	0.25
B- $MgSO_4.7H_2O$	536.83	1	536.83	0.88	0.37
AB	9.00	1	9.00	0.01	0.91
A^2	42580.21	1	42580.21	70.16	$<1.00\times10^{-4}$
Residual	4855.56	8	606.94		
Lack of Fit	3638.36	4	909.59	2.99	0.16
Pure Error	1217.20	4	304.30		
Cor Total	49314.77	1			

The graph model is graphically constructed from the regression model to determine the best value of SCP production. It demonstrates the interaction effect of NH_4NO_3 and $MgSO_4.7H_2O$ on SCP formation (Figure 2). The study reveals that the model has a quadratic elliptical response surface. The production of SCP increased in the orange-red circular region, as depicted in Figure 2, where the concentration of $MgSO_4.7H_2O$ ranged from 0.02% (w/v) to 0.1% (w/v), and the concentration of NH_4NO_3 ranged from 0.8% (w/v) to 0.9% (w/v). The figure also shows that $MgSO_4.7H_2O$ is close to 0.05% (w/v) and that NH_4NO_3 concentration is at 0.86% (w/v) for optimal SCP production.

In this study, the growth of *A. terreus* UniMAP AA-1 on optimized PPF media resulted in a significant increase in biomass and protein after five days of fermentation. Utilizing

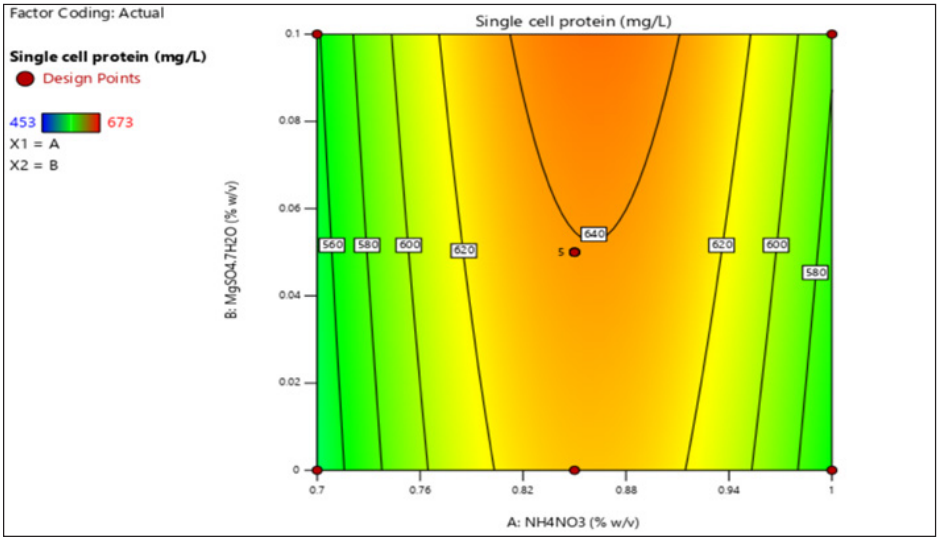

Figure 2. Contour plot for the interaction of NH_4NO_3 and $MgSO_4.7H_2O$ in response to protein concentration

the RSM approach, protein production for SCP was enhanced by 22%, rising from 551 mg/L with PBD to 673 mg/L with CCRD. In comparison, a similar enhancement in biomass production was observed by Choi et al. (2021) through PBD and CCD (RSM) studies utilizing *Lactobacillus plantarum* 200655. A total biomass concentration of 3.845 g/L was achieved in an optimal medium comprising of 31.29 g/L maltose, 30.27 g/L yeast extract, 39.43 g/L soytone, 5 g/L sodium acetate, 2 g/L K_2HPO_4, 1 g/L Tween 80, 0.1 g/L $MgSO_4 \cdot 7H_2O$, and 0.05 g/L $MnSO_4 \cdot H_2O$. It represents a 1.58-fold increase compared to the PBD medium (2.429 g/L; Choi et al., 2021). The maximum mycelial protein content of 2.11% was obtained by Tang et al. (2022) using an optimized fermentation medium designed with the Box-Behnken design to extract more mycelial soluble protein from *Ophiocordyceps sinensis*. The medium contained 20% beef broth, 0.10% peptone, 2% glucose, 0.15% yeast extract, 0.20% KH_2PO_4, and 0.02% $MgSO_4$ (Tang et al., 2022). Although media composition requirements vary among different organisms, these studies illustrate that employing the RSM approach for optimization can effectively increase protein production in microbes.

Validation of Optimum Process Condition

In the present study, the optimal amount of NH_4NO_3 to produce the utmost protein concentration is 0.86% (w/v), while $MgSO_4.7H_2O$ is 0.1% (w/v). The validation run was performed three times. The parameters were set within a range, whereas SCP production was set to the highest level. According to Table 7, the actual reading is within the predicted range, with a mean value of 650.3 mg/L and a standard deviation of 1.26. The predicted and actual values have a minimal standard deviation and are in good agreement. Hence, the model can be considered valid.

Table 7
Comparison of the predicted and experimental values of SCP production for model validation

Replicate	NH_4NO_3 (% w/v)	$MgSO_4.7H_2O$ (% w/v)	SCP concentration (mg/L)		Percentage error (%)	Standard deviation
			Predicted value	Actual value		
1	0.86	0.10	648.4	665	2.55	1.26
2	0.86	0.10	648.4	649	0.09	
3	0.86	0.10	648.4	637	1.76	

SCP Production and Glucose Utilization by *A. terreus* UniMAP AA-1 on Optimized Media

The performance of the optimized media was evaluated over a 7-day fermentation period at 30°C. The results are depicted in Figure 3. Generally, the trends in SCP generation and

glucose utilization are similar in which it was increasing from day 1, reaching peak values, and declining towards the end of the fermentation period. Day 3 yielded the highest glucose concentration of 365.3 mg/L. In contrast, day 5 produced the highest protein concentration of 648 mg/L (Figure 3). Since *A. terreus* UniMAP AA-1 hydrolyzes cellulose to sugar, a greater concentration of glucose at the start of the fermentation process is observed. During fermentation, the fungi's consumption of these sugars promotes biomass formation and growth, which raises the amount of protein. After five days of fermentation, the protein content increased from 162 mg/L to 648 mg/L, a 4-fold increase. Hence, PPF has been demonstrated to be an invaluable substrate for the cultivation of *A. terreus* UniMAP AA-1 and is promising to produce SCP for various potential applications.

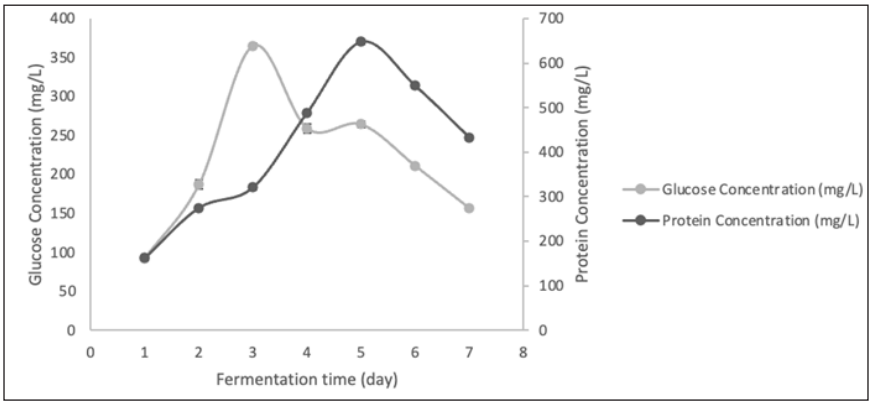

Figure 3. The single-cell protein profile and reducing sugar consumption of *Aspergillus terreus* UniMAP AA-1

CONCLUSION

In this study, SCP has been produced through the solid-state fermentation of *A. terreus* UniMAP AA-1 on PPF. $MgSO_4.7H_2O$, $FeSO_4.7H_2O$, and NH_4NO_3 were the variables that had a major impact on SCP formation. The CCRD approach optimization revealed that the optimized values for NH_4NO_3 and $MgSO_4.7H_2O$ were 0.85 and 0.05% (w/v). However, $FeSO_4.7H_2O$ was not added to the production media according to the PBD results. The highest SCP detected was 673 mg/L, which corresponds to a 22% rise in protein compared to screening findings. The large-scale production of SCP from PPF is possible with the application of these optimization data.

ACKNOWLEDGMENTS

The authors thank Universiti Malaysia Perlis for funding this project under the Short-term Grant (STG, Grant No. 9001-00308) and express their gratitude to Ms Yuvenesswari Vijayakumaran for her technical support during the project's implementation.

REFERENCES

Akintomide, M. J., & Antai, S. P. (2012). Inorganic nitrogen supplementation and micro-fungal fermentation of white yam peels (flour) into single cell protein. *Journal of Microbiology, Biotechnology and Food Sciences*, *2*(3), 820-832.

Amara, A. A., & El-Baky, N. A. (2023). Fungi as a source of edible proteins and animal feed. *Journal of Fungi*, *9*(1), 73. https://doi.org/10.3390/jof9010073

Bajić, B., Vučurović, D., Vasić, Đ., Jevtić-Mučibabić, R., & Dodić, S. (2023). Biotechnological production of sustainable microbial proteins from agro-industrial residues and by-products. *Foods*, *12*(1), 107. https://doi.org/10.3390/foods12010107

Bentahar, J., & Deschênes, J. S. (2022). Media optimization design towards maximizing biomass production of *Tetradesmus obliquus* under mixotrophic conditions. *Bioresource Technology Reports*, *17*, 100885. https://doi.org/10.1016/j.biteb.2021.100885

Bratosin, B. C., Darjan, S., & Vodnar, D. C. (2021). Single cell protein: A potential substitute in human and animal nutrition. *Sustainability*, *13*(16), 9284. https://doi.org/10.3390/su13169284

Chen, J., Lan, X., Jia, R., Hu, L., & Wang, Y. (2022). Response Surface Methodology (RSM) mediated optimization of medium components for mycelial growth and metabolites production of *Streptomyces alfalfae* XN-04. *Microorganisms*, *10*(9), 1854. https://doi.org/10.3390/microorganisms10091854

Choi, G. H., Lee, N. K., & Paik, H. D. (2021). Optimization of medium composition for biomass production of *Lactobacillus plantarum* 200655 using Response Surface Methodology. *Journal of Microbiology and Biotechnology*, *31*(5), 717–725. https://doi.org/10.4014/jmb.2103.03018

Chutrakul, C., Panchanawaporn, S., Vorapreeda, T., Jeennor, S., Anantayanon, J., & Laoteng, K. (2022). The exploring functional role of ammonium transporters of *Aspergillus oryzae* in Nitrogen metabolism: Challenges towards cell biomass production. *International journal of molecular sciences*, *23*(14), 7567. https://doi.org/10.3390/ijms23147567

De la Cruz-Quiroz, R., Roussos, S., Tranier, M. T., Rodríguez-Herrera, R., Ramírez-Guzmán, N., & Aguilar, C. N. (2019). Fungal spores production by solid-state fermentation under hydric stress conditions. *Journal of BioProcess and Chemical Technology*, *11*(21), 7-12.

Dulay, R. M., Cabrera, E. C., Kalaw, S., Reyes, R., & Hou, C. T. (2020). Nutritional requirements for mycelial growth of three Lentinus species from the Philippines. *Biocatalysis and agricultural biotechnology*, *23*, 101506. https://doi.org/10.1016/j.bcab.2020.101506

Elsayed, E. A., & Ahmed Abdelwahed, N. (2020). Medium optimization by response surface methodology for improved cholesterol oxidase production by a newly isolated *Streptomyces rochei* NAM-19 strain. *BioMed Research International*, *2020*, 1870807. https://doi.org/10.1155/2020/1870807

Gunny, A. A. N., & Arbain, D. (2012). *Aspergillus terreus* UniMAP AA-1: A newly isolated extracellular glucose oxidase-producing strain. *World Applied Sciences Journal*, *17*(1), 86–90.

Guo, F., Li, X., Zhao, J., Li, G., Gao, P., & Han, X. (2019). Optimizing culture conditions by statistical approach to enhance production of pectinase from *Bacillus sp*. Y1. *BioMed Research International*, *2019*(1), 8146948. https://doi.org/10.1155/2019/8146948

Huang, K., & Nitin, N. (2019). Edible bacteriophage based antimicrobial coating on fish feed for enhanced treatment of bacterial infections in aquaculture industry. *Aquaculture*, *502*, 18–25. https://doi.org/10.1016/j.aquaculture.2018.12.026

Jafri, N. H. S., Jimat, D. N., Azmin, N. F. M., Sulaiman, S., & Nor, Y. A. (2021). The potential of biomass waste in Malaysian palm oil industry: A case study of Boustead Plantation Berhad. *IOP conference series: Materials science and engineering*, *1192*, 012028. https://doi.org/10.1088/1757-899x/1192/1/012028

Jiang, J., Zhao, J., Duan, W., Tian, S., Wang, X., Zhuang, H., Fu, J., & Kang, Z. (2019). TaAMT23a, a wheat AMT2-type ammonium transporter, facilitates the infection of stripe rust fungus on wheat. *BMC plant biology*, *19*(1), 239. https://doi.org/10.1186/s12870-019-1841-8

Malaysian Oil Palm Council. (2024). *Industry overview*. https://www.mpoc.org.my/industry-overview/.

Martin-Jézéquel, V., Calu, G., Candela, L., Amzil, Z., Jauffrais, T., Séchet, V., & Weigel, P. (2015). Effects of organic and inorganic nitrogen on the growth and production of domoic acid by pseudo-nitzschia multiseries and *P. Australis* (Bacillariophyceae) in culture. *Marine Drugs*, *13*(12), 7067–7086. https://doi.org/10.3390/md13127055

Neoh, B. K., Thang, Y. M., Zain, M. Z. M., & Junaidi, A. (2011). Palm pressed fibre oil: A new opportunity for premium hardstock? *International Food Research Journal*, *18*(2), 769-773.

Nepal, S., & Kumar, P. (2020). Growth, cell division, and gene expression of *Escherichia coli* at elevated concentrations of magnesium sulfate: Implications for habitability of Europa and Mars. *Microorganisms*, *8*(5), 637. https://doi.org/10.3390/microorganisms8050637

Nguyen, L. T., Van Le, V., Nguyen, B. T. T., Nguyen, H. T. T., Tran, A. D., & Ngo, N. X. (2023). Optimization of mycelial growth and cultivation of wild *Ganoderma sinense*. *BioTechnologia*, *104*(1), 65–74. https://doi.org/10.5114/bta.2023.125087

Prakash P., Karthick Raja, N. S., & Swetha, S. (2015). Design of medium components for the enhanced production of mycoprotein by *Fusarium venenatum* using Plackett Burman model. *Research Journal of Pharmaceutical, Biological and Chemical Sciences*, *6*(1), 1251–1255.

Rahman, K. H. A., Ariffin, N. A., & Abdul Rahim, A. (2021). Production of bioprotein from oil palm fronds by *Aspergillus terreus* strain UniMAP AA-1. *IOP conference series: Earth and environmental science*, *765*, 012023. https://doi.org/10.1088/1755-1315/765/1/012023

Tang, C. Y., Wang, J., Liu, X., Chen, J. B., Liang, J., Wang, T., Simpson, W. R., Li, Y. L., & Li, X. Z. (2022). Medium optimization for high mycelial soluble protein content of *Ophiocordyceps sinensis* using Response Surface Methodology. *Frontiers in Microbiology*, *13*, 1055055. https://doi.org/10.3389/fmicb.2022.1055055

Zięba, P., Sękara, A., Bernaś, E., Krakowska, A., Sułkowska-Ziaja, K., Kunicki, E., Suchanek, M., & Muszyńska, B. (2021). Supplementation with magnesium salts-a strategy to increase nutraceutical value of *Pleurotus djamor* fruiting bodies. *Molecules (Basel, Switzerland)*, *26*(11), 3273. https://doi.org/10.3390/molecules26113273

Pertanika J. Trop. Agric. Sci. 48 (3): 851 - 866 (2025)

PERTANIKA JOURNALS

TROPICAL AGRICULTURAL SCIENCE

Journal homepage: http://www.pertanika.upm.edu.my/

Viruses Infecting Garlic in Indonesia: Incidence and its Transmission to Shallot and Spring Onion

Dhayanti Makyorukty[1], Sari Nurulita[1], Diny Dinarti[2] and Sri Hendrastuti Hidayat[1]*

[1]*Department of Plant Protection, Faculty of Agriculture, IPB University, 16680 Bogor, Indonesia*
[2]*Department of Agronomy and Horticulture, Faculty of Agriculture, IPB University, 16680 Bogor, Indonesia*

ABSTRACT

Garlic (*Allium sativum*) is an important horticultural crop globally and in Indonesia. Its production faces significant challenges due to diseases caused by viral infections. Therefore, this study aimed to determine the distribution of garlic viruses across cultivation areas in Indonesia and analyze the potential for transmission to shallot (*Allium cepa var. agregatum*) and spring onion (*Allium fistulosum* L.). In the process, garlic leaves and bulbs samples were collected from several growing areas in West Nusa Tenggara, Central Java, West Java, and East Java. Onion yellow dwarf virus (OYDV), leek yellow stripe virus (LYSV), garlic common latent virus (GCLV), and shallot latent virus (SLV) were detected by reverse transcription-polymerase chain reaction method using specific primers. The results showed that mixed infections of several viruses were more common than the single form. The average frequency of viral infection in order from the highest was LYSV (75.15%), OYDV (64.95%), SLV (36.47%), and GCLV (26.66%). Single isolates of LYSV, OYDV, GCLV, and SLV were selected for the transmission experiment in the screen house, and each was inoculated mechanically to shallot (cultivars Sanren F1 and Lokananta) and spring onion (cultivar Blaze F1). All viruses were successfully transmitted to shallot, but only LYSV, OYDV, and SLV could be mechanically transmitted to spring onion. The infection of shallot and spring onion significantly affected the number of bulbs but had no considerable effect on plant height, leaf number, and bulb diameter.

ARTICLE INFO

Article history:
Received: 29 August 2024
Accepted: 13 November 2024
Published: 16 May 2025

DOI: https://doi.org/10.47836/pjtas.48.3.11

E-mail addresses:
dhayantimakyorukty@apps.ipb.ac.id (Dhayanti Makyorukty)
sarinurulita@apps.ipb.ac.id (Sari Nurulita)
dinyagh@apps.ipb.ac.id (Diny Dinarti)
srihendrastuti@apps.ipb.ac.id (Sri Hendrastuti Hidayat)
* Corresponding author

Keywords: Frequency of infection, mechanical inoculation, mixed-infection, reverse transcription PCR, virus transmission

INTRODUCTION

Garlic (*Allium sativum*) is a horticultural crop cultivated in the highlands. Its main producing areas in Indonesia are Central Java, West Nusa Tenggara, and East Java.

e-ISSN: 2231-8542

In the country, garlic production has been unable to meet domestic market demand. Hence, the consumption relies on imports. A limitation in the cultivation of this crop is the availability of good seed bulbs free from pathogens, particularly viruses. The main viruses infecting garlic belong to the genera *Potyvirus, Carlavirus,* and *Allexivirus* (Katis et al., 2012). Symptoms of the infection include yellow mosaic, green mosaic, yellow-striped, green-striped, curly, and notched upper surface of leaves. Viruses in garlic can be transmitted through insect vectors (aphids), contaminated plant material, and mechanical transmission (Mang et al., 2022).

Virus infection is systemic, affecting the entire plant body, including the bulbs used as planting material (Bhusal et al., 2021). Bulbs from infected plants in the previous planting season, reused as seed materials tend to be a source of disease. Furthermore, Bagi et al. (2012) explained that virus infection caused a 21.5% decrease in bulb weight. Hidayat et al. (2023) and Nurulita et al. (2024) reported four main viruses infecting garlic plants in Indonesia, namely onion yellow dwarf virus (OYDV), leek yellow stripe virus (LYSV), garlic common latent virus (GCLV), and shallot latent virus (SLV). These infections are referred to as "Garlic viral complex" because single infections are rare (Cremer et al., 2021; Majumder & Baranwal, 2014).

Wulandari et al. (2016) detected OYDV, SLV, and GCLV in shallots, signifying virus transmission among Allium species. Plants in the same genus often share genetic similarities, facilitating susceptibility to the same viruses. Additionally, only specific genetic variants (genotypes) can infect certain host genotypes in virus species. PRSV-P infects papaya and cucurbits, while PRSV-W exclusively infects cucurbits (Tripathi et al., 2008). These cases explain the complex interactions between viruses and the hosts, driven by genetic factors (McLeish et al., 2019).

In Indonesia, garlic is typically cultivated in an intercropping system with spring onion (*Allium fistulosum* L.) or shallot (*Allium cepa var. agregatum*), as observed in Karanganyar Central Java, and Bandung West Java (Rahmawati & Jamhari, 2019). The cropping pattern increases the risk of virus transmission due to the overlapping host range (Kadwati & Hidayat, 2015; Taglienti et al., 2018). This study determines the distribution of garlic viruses across cultivation areas in Indonesia and analyzes the potential for transmission to shallot and spring onion.

METHODS

Sampling Methods

Samples were collected from the main garlic-producing areas in Indonesia to determine the spread of the virus. The study locations consisted of 3 fields in West Nusa Tenggara (Sembalun: 8°23'53.16"S, 116°32'49.2"E), 1 in West Java (Ciwidey: 7°06'51.6"S, 107°26'24.1"E), 2 in Central Java (Tawangmangu: 7°39'40.8"S, 111°06'28.6"E), and 4 in

East Java (Ngantang: 7°52'34.8"S, 112°22'40.5"E; Junrejo: 7°53'07.7"S, 112°33'16.3"E; Pacet: 7°40'55.9"S, 112°32'28.4"E).

This study determined five sampling blocks diagonally in fields, each with a minimum area of 800 m^2. The total area of the sampling blocks is 5/9 of the field area. Leaf samples were collected from symptomatic plants showing symptoms such as twisted or wrinkled, yellow mosaic, green mosaic, yellow stripes, green stripes, and curly (Bhusal et al., 2021; Cremer et al., 2021). Furthermore, ten symptomatic leaves from each block were combined into a composite sample for virus detection. Additional seed bulb samples sourced from the previous planting season were collected from village storage warehouses during visits to the production sites. A total of 35 bulbs were sampled from each warehouse.

Virus Detection and Identification

Leaf samples from the field were used directly for detection, while the bulbs were grown in water media until leaves appeared. The detection stage was preceded by total ribonucleic acid (RNA) xtraction using the CTAB method (Doyle, 1991). Subsequently, RNA was used as a template in the amplification of the target viruses (LYSV, OYDV, GCLV, and SLV), applying a one-step reverse transcriptase-polymerase chain reaction (RT-PCR) method described by Nurulita et al. (2024). The process started with cDNA synthesis at 45°C for 60 min and pre-denaturation at 94°C for 1 min. It was followed by 35 cycles consisting of denaturation at 94°C for 30 sec, annealing at 50°C for 30 sec, extension at 72°C for 1 min, and a final elongation at 72°C for 10 min.

Specific primers for LYSV and SLV (Haque & Hattori, 2017), OYDV (Sumi et al., 2001), and GCLV (Parrano et al., 2012) were adopted. RT-PCR premix comprised of 12.5 µl Dreamtaq Green master mix (2×) (Thermo Scientific), 1 µl 0.1 M DTT (Smobio, Taiwan), 0.5 µl RNAse inhibitor (Bioline London, UK), 0.25 µl RT enzyme (200 U/µl) (Smobio, Taiwan), 2 µl template RNA, 2 µl each of 10 µM forward and reverse primers, and 4.75 µl nuclease-free water. Amplification results were visualized using gel electrophoresis. Selected amplified DNA fragments were sent to 1st BASE Malaysia to obtain virus sequences using the Sanger sequencing method. Finally, sequence analysis was performed using BioEdit 7.7 (Hall, 1999), MEGA 11 (Tamura et al., 2021), and SDTV1.3 (Muhire et al., 2014).

Transmission of Garlic-origin Viruses

The LYSV, OYDV, GCLV, and SLV isolates used for the mechanical transmission experiment were obtained from a single infection and confirmed by sequencing to ensure identity. The plant materials used in the study were true seeds of shallot cv. Lokanata and cv. Sanren F1 (East-West Seed Indonesia), as well as spring onion cv. Blaze F1 (East-West Seed Indonesia). Initial virus detection was conducted 21 days after sowing (DAS) to

ensure the test plants were virus-free before transplantation into polybags at 35 DAS. The garlic-origin virus was transmitted by mechanical inoculation, where sap (exudate) from the inoculum source plants was applied to the test plants at 2 weeks post-transplanting (WPT). The sap was made by grinding the infected leaf in a mortar with 10,000 µl of cold 0.01 M phosphate buffer at pH 7 containing 1% mercaptoethanol, following the method of (Nurviani et al., 2016). Carborundum 600 mesh was sprinkled on the leaves of the test plants before the application. Subsequently, it was allowed to sit for 3 min until the sap dried, and the leaves were rinsed with distilled water to remove any residual carborundum. The inoculation was conducted simultaneously for all test plants.

The experiment was arranged using a two-factor, completely randomized design. The first and second factors were plant cultivar (TSS cv. Lokanata, TSS cv. Sanren F1, and spring onion cv. Blaze F1) and virus type (LYSV, OYDV, GCLV, SLV, and without virus inoculation as healthy control), respectively. This study experimented with control conditions in a screen house. All test plants were grown in polybags using a 1:1 mixture of soil and compost as a planting medium. The experimental design consisted of 3 replications for treatments. It was important to acknowledge that each replication had ten plants/treatments. The parameters observed were disease incidence, incubation period, plant height, number of leaves, and number and diameter of bulbs. Data were then analyzed using ANOVA followed by Tukey's test of 5%.

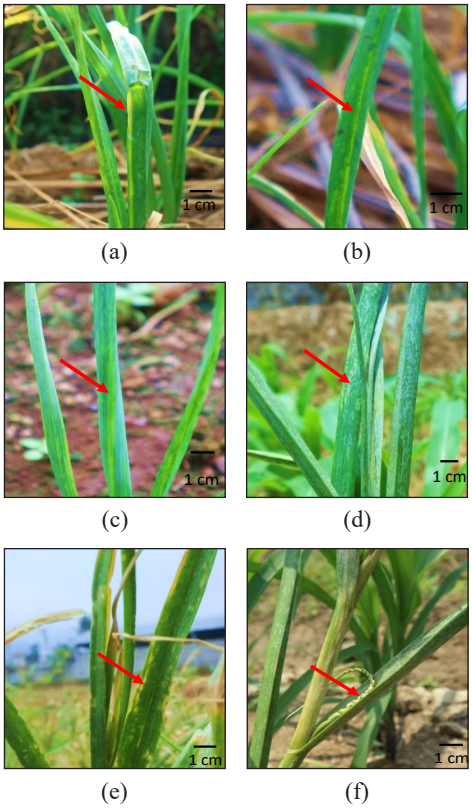

Figure 1. Symptoms of virus infection discovered in the field include: (a) yellow stripes and wrinkles; (b) yellow stripes; (c) green stripes; (d) green mosaic; (e) yellow mosaic; and (f) a curly leaf
Note. The red arrows signify the intended symptoms

RESULTS

Disease Symptoms and Virus Incidence

Virus infections were identified by symptoms in the fields, such as twisted or wrinkled leaves, yellow stripes, green stripes, green mosaic, yellow mosaic, and curly leaves, as shown in Figure 1. The dominant type in each field varied, as detailed in Table 1. Symptoms were also observed in young leaves growing out of the bulb samples but were less varied than those from the field (Figure 2).

Table 1
Symptoms of virus infection found on garlic plants in the field

Symptoms	Site					
	Tawangmangu	Ngantang	Pacet	Junrejo	Ciwidey	Sembalun
Twisted leaf	+	-	-	-	-	-
Striped, green on the leaf	-	-	-	+	+	+
Striped, yellow on the leaf	-	-	-	+	-	-
Leaf curling	+	-	-	-	-	-
Green mosaic on leaf	+	+	-	-	+	+
Yellow mosaic on leaf	-	-	+	-	-	-

(a) (b) (c)

Figure 2. Abnormal growth of garlic bulbs: (a) green stripe; (b) leaflet malformation; and (c) leaf curl
Note. The red arrows signify the intended symptoms

Virus infections were detected in all field samples collected from several garlic-growing areas (Figure 3). The average frequency of infection in order from the highest was LYSV (75.15%), OYDV (64.95%), SLV (36.47%), and GCLV (26.66%). All four target viruses from Tawangmangu, Ngantang, Pacet, Junrejo, and Ciwidey were present in each garlic cultivar. In samples from Sembalun, only LYSV and OYDV were consistently detected, while GCLV and SLV were exclusive to cv. Sangga Sembalun and cv. Lumbu Kuning, respectively. Based on the planting location, virus distribution varied in the same cultivar, as shown in Figure 3. For instance, all four viruses were detected on cv. Lumbu Putih from Tawangmangu, while only two were detected on cv Lumbu Putih from Sembalun. A similar pattern was observed for cv. Lumbu Hijau, with four viruses identified in Pacet and 2 in Sembalun.

The results showed that mixed infection was more common than the single-virus counterpart. As detailed in Figure 4, mixed infection of three viruses, particularly LYSV + OYDV + SLV, was mostly observed in leaf samples. In contrast, single and double infections, with the highest frequencies by LYSV and LYSV + SLV, respectively, were observed from bulb samples. It was important to acknowledge that the number and diversity

of viruses detected from leaf samples were more complex. Mixed infection of four viruses in leaf and bulb samples was low, while double infection of GCLV + SLV was absent in both samples.

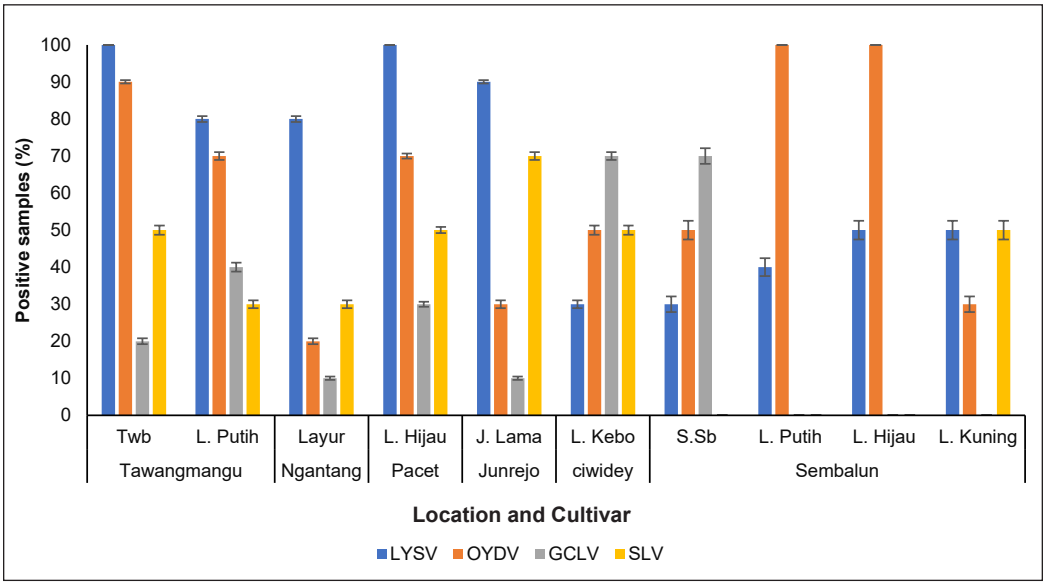

Figure 3. Frequency of virus infection on garlic cultivars planted in West Java (Ciwidey), Central Java (Tawangmangu), East Java (Ngantang, Pacet, and Junrejo) and West Nusa Tenggara (Sembalun)
Note. Garlic cultivars were Tawangmangu Baru (Twb), Lumbu Putih (L. Putih), Lumbu Hijau (L. Hijau), Jawa Lama (J. Lama), Lumbu Kebo (L. Kebo), Sangga Sembalun (S.Sb), Lumbu Kuning (L. Kuning). The viruses identified were Leek yellow stripe virus (LYSV), Onion yellow dwarf virus (OYDV), Garlic common latent virus (GCLV), Shallot latent virus (SLV). The error bars in the figures represent the standard deviation

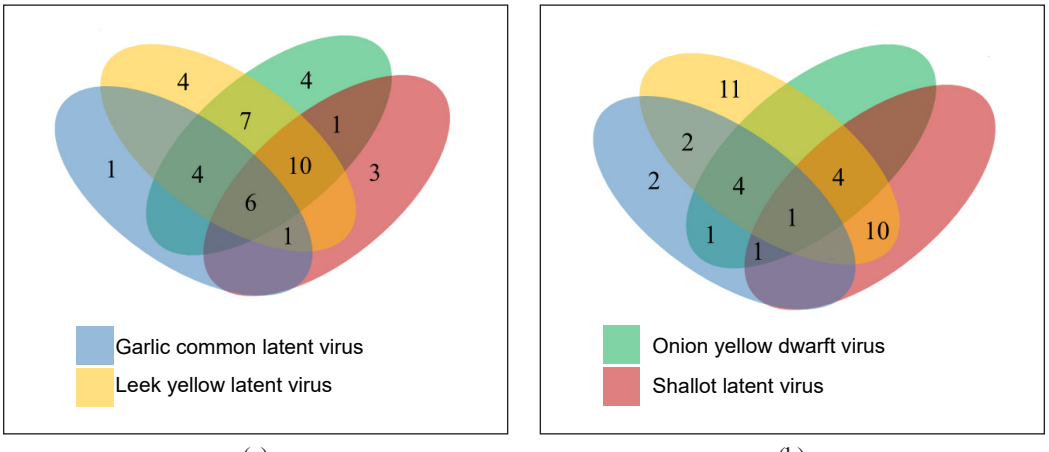

(a) (b)

Figure 4. Venn diagram of garlic virus mixed infection on: (a) leaf : and (b) bulb samples
Note. The numbers in the figure represent the positive samples infected with the virus based on RT-PCR detection

Identity of Garlic Virus Isolates

Single LYSV, OYDV, and SLV infection were detected in shoots of bulbs from cv. Layur (East Java), cv. Sangga Sembalun (West Nusa Tenggara), and cv. Layur (East Java), respectively. GCLV infection was discovered in field samples of cv. Lumbu Kebo (West Java). The isolates of LYSV, OYDV, GCLV, and SLV shared the highest identity with the isolates from China (homology 98.43%; GenBank MN059534.1), China (homology 93.06%; GenBank MN059637.1), Argentina (homology 95.91%; GenBank KJ124847.1), and Australia (homology 90.90%; GenBank JF320811.1), respectively, as shown in Figure 5. The sequences of these isolates have been deposited in the GenBank with accession numbers LC831819.1, LC831799.1, LC831600.1, and LC831613.1, respectively.

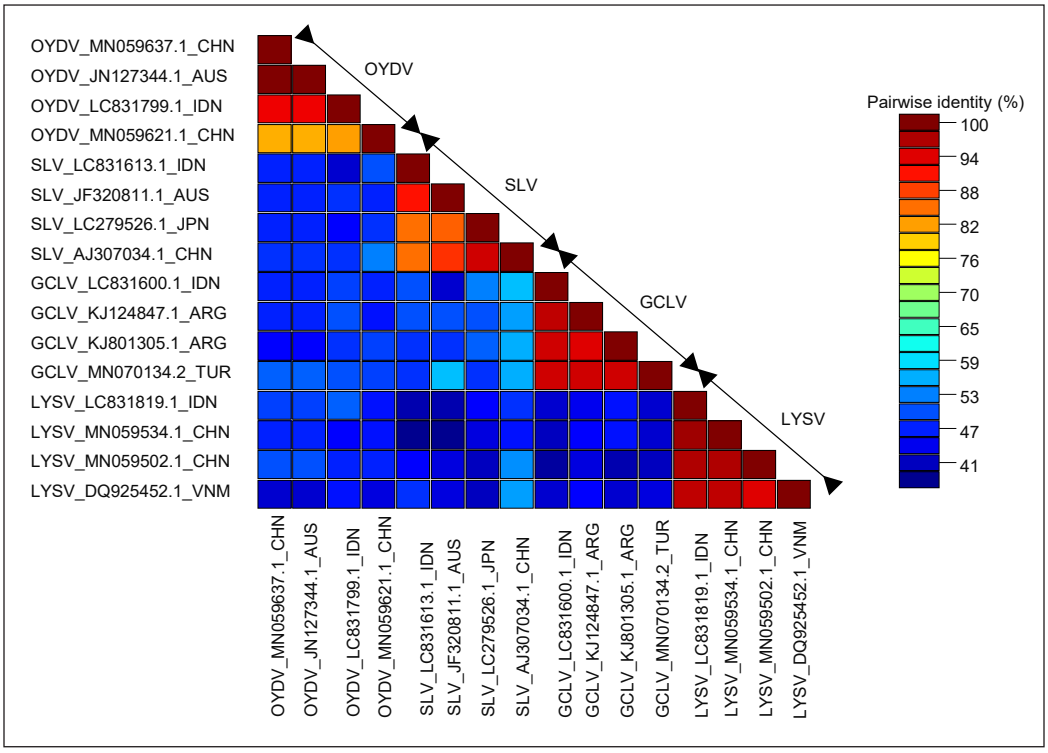

Figure 5. Pairwise alignment of garlic virus isolates with the Genbank database
Note. The isolates from this study are the blue-coded accession numbers (LC831799.1, LC831613.1, LC831600.1, and LC831819.1). The black-coded accession numbers are isolated from Genbank

Incidence of Virus Transmission from Garlic to Shallot and Spring Onion

Transmission studies of viruses originating from garlic successfully confirmed that shallot and spring onion are included in the host range. Shallot and spring onion showed symptoms after being inoculated with target viruses, except for GCLV. However, confirmation by

RT-PCR method proved that all plants were positively infected. Infection of GCLV was confirmed on cv. Lokananta and cv. Sanren F1 but not on cv. Blaze F1.

The highest disease incidence was 42 days after inoculation (DAI), discovered on cv. Blaze F1 and infected by LYSV (76.66%). SLV, OYDV, and LYSV followed it on 'Lokananta' (76.66%), cv. Lokananta (70%), and cv. Lokananta (63.33%). There was no significant difference in virus incidence among the 4 treatments, as shown in Figure 6. The incidence increased from the beginning of inoculation until 35 DAI and remained constant. However, the exception was observed for SLV and OYDV inoculation on cv. Blaze F1, which experienced a decrease starting from 27 and 33 DAI, respectively. The reduction in disease incidence in both treatments was 42.68% and 49.96%. It was important to acknowledge that spring onion cv. Blaze F1 inoculated with SLV or OYDV experienced a decrease in disease severity.

The experiment shows that OYDV and SLV originating from garlic only caused light green stripes and wrinkles on the leaves until 42 DAI, as detailed in Figure 7. Furthermore, twisted leaves and yellow mosaic appeared at 72 DAI on cv. Sanren F1 inoculated with OYDV, as presented in Figure 8. It signified differences in the symptoms that arise from the response of shallot and garlic plants.

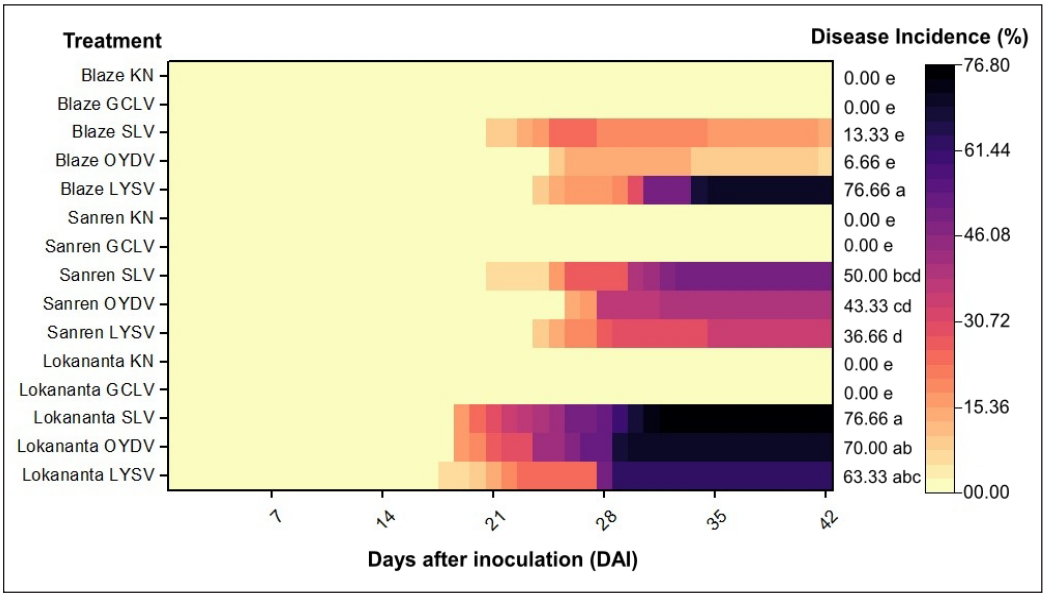

Figure 6. Heat map of the incubation period (days after inoculation) and incidence of virus infection based on symptoms appearance in test plants (%)

Note. The numbers on the right side of the diagram signify the incidence of symptoms at 42 DAI (days after inoculation). Meanwhile, the letter after the number showed that there was no significant difference between treatments based on Tukey's 5% test. The treatments on the left side of the diagram signify a combination of cultivar (cv. Blaze F1, cv. Sanren F1, cv. Lokananta) and virus (GCLV, SLV, OYDV, LYSV), KN: treatment without virus inoculation

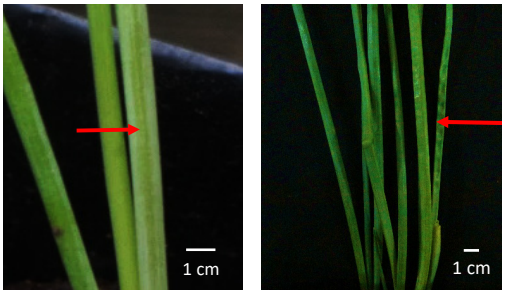

(a) (b)

Figure 7. Symptoms of OYDV and SLV on cv. Lokananta and cv. Blaze F1: (a) green stripes at 18 DAI; and (b) wrinkled leaves at 42 DAI
Note. The red arrows represent the intended symptoms

(a) (b)

Figure 8. Symptoms of OYDV on cv. Sanren F1 at 72 DAI: (a) twisted leaves; and (b) yellow mosaic
Note. The red arrows show the intended symptoms

Effect of Virus Transmission from Garlic on Agronomic Characters

Garlic virus infection did not affect plant height and number of leaves, except for SLV on cv. Blaze F1 and OYDV on cv. Sanren F1, as shown in Figures 9 and 10. However, genetic factors influence this condition more, as cv. Blaze F1 is a spring onion and cv. Sanren F1 is a shallot. In contrast to plant height and number of leaves, a significant effect was observed on the number of bulbs, as detailed in Figure 11. It was particularly

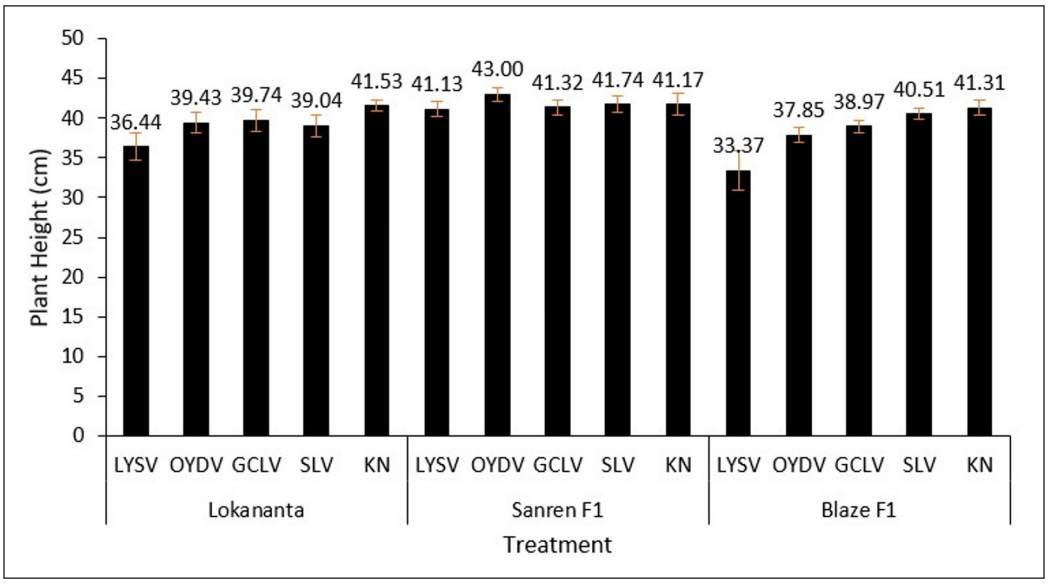

Figure 9. Average plant height of shallot (cv. Lokananta and cv. Sanren F1) and spring onion (cv. Blaze F1) given the inoculation of LYSV, OYDV, GCLV, and SLV
Note. KN = Treatment without virus inoculation. The numbers at the top of the diagram represent the average treatment values, while the error bars in the figures represent the standard deviation

for SLV, LYSV, and OYDV infections on cv. Sanren F1, as well as LYSV infection on cv. Lokananta. Despite the difference in the number of bulbs, the diameter was not affected. The study also shows that the effect of virus infection on yield reduction was different between the cultivars. For example, cv. Sanren F1 appeared to be more affected by the number of bulbs than cv. Lokananta.

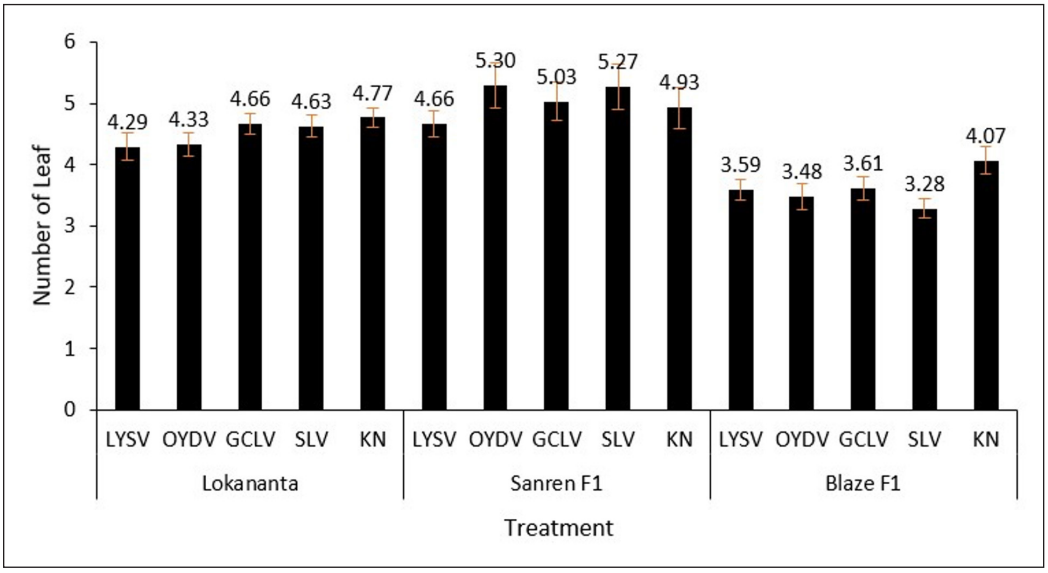

Figure 10. Average number of leaf of shallots (cv. Lokananta and cv. Sanren F1) and spring onion (cv. Blaze F1) given the inoculation of LYSV, OYDV, GCLV, and SLV
Note. KN = Treatment without virus inoculation. The numbers at the top of the diagram represent the average treatment values, while the error bars represent the standard deviation

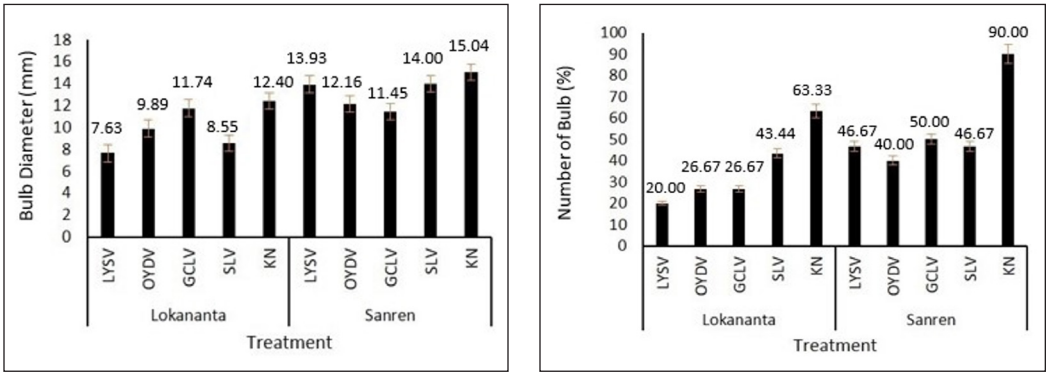

(a) (b)

Figure 11. Average of bulb diameter (mm) (a) and the number of bulb (%) (b) of shallot (cv. Lokananta and cv. Sanren F1) given the inoculation of LYSV, OYDV, GCLV, and SLV
Note. KN = treatment without virus inoculation. The numbers at the top of the diagram represent the average treatment values, while the error bars represent the standard deviation

DISCUSSION

Identifying 50 symptomatic plants in an 800 m^2 field presented no challenge during sampling. It signified the high prevalence of garlic virus infection in Indonesia. Variations in symptoms observed across locations were influenced by interaction between the host plant, virus, and environment. A single virus can present different symptoms in the same plant, while distinct viruses can produce similar symptoms in the same plant (Kumar et al., 2012). Mosaic symptoms in garlic are often associated with mixed infections of several viruses, specifically members of the genera *Potyvirus, Carlavirus,* and *Allexivirus* (Chen et al., 2001; Tsuneyoshi et al., 1998).

Symptom variations are evident across field locations, leaf samples, and young shoots grown from bulbs. This variation may relate to the infection process and disease development. Viruses detected from bulbs are carried over from a previous harvest, while those in leaves arise from various sources, including primary infections on seed bulbs (Bhusal et al., 2021) and transmission through contact between plants (Coutts & Jones, 2015) or insect vectors (Mang et al., 2020). The detection of viruses in bulbs confirmed the ability to infect all plant parts, including planting material (Bhusal et al., 2021). Potyvirus and carlavirus can spread through the help of aphid vectors in a non-persistent manner (Mang et al., 2022). Another reason for the complexity of the symptoms observed in the field is that the plants sampled were in the final vegetative phase. Meanwhile, the bulb samples were obtained from plants two weeks after planting. Paudel and Sanfacon (2018) explained that the virus accumulated to higher levels later in life. This factor leads to the more pronounced symptoms observed in the late stages of plant development.

Virus detection is essential to verify that the symptoms observed are caused by viral infection. According to this study, viruses infecting garlic have spread across the cultivation areas in Indonesia. The detection results do not clearly indicate whether garlic viruses are specific to certain locations or cultivars. Inconsistency originated when comparing viruses infecting with garlic from the same area and those infecting specific cultivars. For example, a cultivar may harbor different virus combinations, while a single location may yield varying results across cultivars. The current results suggest that viruses are not associated with specific locations or cultivars.

The data obtained explains that LYSV and OYDV are the two most dominant viruses compared to others. Using seed bulbs from previous planting seasons is a key factor in the extensive spread of infections. This practice increases the tendency of virus-carrying bulbs to serve as primary inoculum, spreading diseases in fields (Khan et al., 2017). Reducing sources of inoculum in the field can be achieved by producing pathogen-free seed bulbs and implementing a controlled seed certification system.

Based on RT-PCR detection, viruses infecting garlic are more frequently detected in the form of mixed infections. Kadwati and Hidayat (2015) previously reported mixed infections

of two or three viruses in samples from Indonesia. Abraham et al. (2019) stated that mixed infections caused most viral infections in Ethiopia (65.7%). In this study, a combination of GCLV and SLV was not observed. The same results were reported by Kadwati and Hidayat (2015) in that the viruses were not discovered in local garlic samples from Bandung.

Infection of a virus may cause detrimental effects to the presence of another. The most common interference is attributed to the activation of the host cell defense response by a primary virus infection. It facilitates the prevention of subsequent infection by a secondary virus (Alves-Junior et al., 2009; Singhal et al., 2021). Furthermore, the reduced rate of viral multiplication in mixed infections may be due to competition for host cell resources. Generally, closely related virus strains do not invade the same cells in their hosts. This condition is known as the phenomenon of spatial exclusion or spatial separation between viruses (Singhal et al., 2021). GCLV, SLV, and other carlaviruses often cause latent infections without symptoms. Acknowledging that co-infections can worsen symptoms and greatly impact crop yield and quality (Katis et al., 2012; Santosa & Ertunc, 2021).

Studies confirmed that shallots cv. Lokananta and cv. Sanren F1 are susceptible to LYSV, OYDV, GCLV, and SLV, while cv. Blaze F1 was only infected by LYSV, OYDV, and SLV. The virus inoculation procedure conducted in this study was performed only once. It implied that the lack of positive detection of GCLV could be attributed to the need for multiple inoculations. There have been no studies addressing cv. Blaze F1's resistance to the virus.

Based on the incidence analysis, not all viruses that were inoculated displayed symptoms. For example, the results of GCLV inoculation in 'cv. Lokananta and cv. Sanren F1 showed no symptoms despite being detected as positive. Asymptomatic virus infection, as evidenced by GCLV, may result from the tolerance response of the host plant. Tolerant plants are generally able to suppress virus replication. It ensures that the virus titer decreases and inhibits cytopathic or harmful effects on the host (Takahashi et al., 2019; Zhang et al., 2018).

Spring onion cv. Blaze F1 inoculated with SLV or OYDV was subjected to a recovery process after several days, signifying a decrease in disease severity. A factor contributing to reducing disease incidence is the recovery process from the plant's resistance response and its interaction with the environment. Trebicki (2020) explained that the compatibility of the virus and the host plant and its interaction with the environment had positive, negative, or neutral effects on disease development and severity. Given the differences between the host isolates being transmitted from garlic to spring onion, this mechanism can possibly occur. The transmission also showed mild symptoms, unlike those observed in garlic infected with the virus. The symptoms observed from OYDV and SLV inoculations were primarily green stripes and wrinkling on the leaf. It is important to acknowledge that severe viral infections can lead to stunting or leaf malformation (Nurulita et al., 2024).

Garlic virus infection in shallot and spring onion did not affect plant height and number of leaves. It is with the exception of SLV on cv. Blaze F1 and OYDV on cv. Sanren F1, which influenced leaf number due to genetic factors. In contrast to plant height and number of leaves, a significant effect was observed on the number of bulbs. The need for proper development of the material caused the reduction in bulbs. The equatorial diameter should reach twice the diameter of the bulb neck to meet the criteria of good quality (Sullivan et al., 2021). In this study, many bulbs did not meet this criterion and had to be eliminated. The condition signified that the virus did not reduce the bulb size during the initial infection. As explained by Cafrune et al. (2006), the infection of Allexivirus in the first season did not lead to a significant yield reduction but was significantly decreased in the next planting season. This study also shows that the effects of virus infection are different among the different cultivars. Cultivar Sanren F1 appeared to be more affected by the number of bulbs than cv. Lokananta.

CONCLUSION

The incidence of garlic virus infection was widely spread in Indonesia. Infection of LYSV, OYDV, SLV, and GCLV was detected from leaf and bulb samples. This signified that seed bulbs played an important role as the primary source of disease inoculum. All four viruses were transmitted to shallot, but only LYSV, OYDV, and SLV were mechanically transmitted to spring onion. Therefore, virus-free seed bulbs were recommended to suppress the spread of the virus in the field.

ACKNOWLEDGMENTS

The authors are grateful to Lembaga Pengelola Dana Pendidikan (Indonesia Endowment Fund for Education) under the Ministry of Finance of Indonesia for providing scholarships. This study was partially funded by ACIAR Project SLAM/2018/145 and Regular Fundamental Research grant (PFR) No: 22029/IT3.D10/PT.01.03/P/B/2024.

REFERENCES

Abraham, A. D., Kidanemariam, D. B., & Holton, T. A. (2019). Molecular identification, incidence and phylogenetic analysis of seven viruses infecting garlic in Ethiopia. *European Journal of Plant Pathology*, *155*, 181-191. http://doi.org/10.1007/s10658-019-01760-9

Alves-Júnior, M., Alfenas-Zerbini, P., Andrade, E. C., Esposito, D. A., Silva, F. N., da Cruz, A. C. F., Ventrella, M.C., Otoni, W.C., & Zerbini, F. M. (2009). Synergism and negative interference during co-infection of tomato and *Nicotiana benthamiana* with two bipartite begomoviruses. *Virology*, *387*(2), 257-266. https://doi.org/10.1016/j.virol.2009.01.046

Bagi, F., Stojscaron, V., Budakov, D., El Swaeh, S. M. A., & Gvozdanovi-Varga, J. (2012). Effect of *Onion yellow dwarf virus* (OYDV) on yield components of fall garlic (*Allium sativum* L.) in Serbia. *African Journal of Agricultural Research*, *7*(15), 2386-2390. https://doi.org/10.5897/AJAR11.1772

Bhusal, H., Shemesh-Mayer, E., Forer, I., Kryukov, L., Peters, R., & Kamenetsky-Goldstein, R. (2021). Bulbils in garlic inflorescence: Development and virus translocation. *Scientia Horticulturae*, *285*, 110146. https://doi.org/10.1016/j.scienta.2021.110146

Cafrune, E. E., Perotto, M. C., & Conci, V. C. (2006). Effect of two Allexivirus isolates on garlic yield. *Plant disease*, *90*(7), 898-904. https://doi.org/10.1094/PD-90-0898

Chen, J., Chen, J., & Adams, M. J. (2001). Molecular characterisation of a complex mixture of viruses in garlic with mosaic symptoms in China. *Archives of virology*, *146*, 1841-1853. https://doi.org/10.1007/s007050170037

Coutts, B. A., & Jones, R. A. C. (2015). Potato virus Y: Contact transmission, stability, inactivation, and infection sources. *Plant Disease*, 99(3), 387-394. https://doi.org/10.1094/PDIS-07-14-0674-RE

Cremer, J., Campbell, P., Steele, V., Persley, D., Thomas, J., Harper, S., & Gambley, C. (2021). Detection and distribution of viruses infecting garlic crops in Australia. *Plants*, *10*(5), 1-14. https://doi.org/10.3390/plants10051013

Doyle, J. (1991). DNA protocols for plants. In G. M. Hewitt, A. W. B. Johnston & J. P. W. Young (Eds.), *Molecular techniques in taxonomy* (pp. 283–293). Springer eBooks. https://doi.org/10.1007/978-3-642-83962-7_18

Hall, T. A. (1999). BioEdit: A user-friendly biological sequence alignment editor and analysis program for Windows 95/98/NT. *Nucleic Acids Symposium Series*, *41*(2), 95–98. https://doi.org/10.14601/phytopathol_mediterr-14998u1.29

Haque, M. S., & Hattori, K. (2017). Detection of viruses of Bangladeshi and Japanese garlic and their elimination through root meristem culture. *Progressive Agriculture*, *28*(2), 55-63. https://doi.org/10.3329/pa.v28i2.33465

Hidayat, S. H., Yulianingsih, R., Dinarti, D., & Nurulita, S. (2023). Incidence of main viruses infecting local garlic in Java, Indonesia. *Jurnal Hama dan Penyakit Tumbuhan Tropika*, *23*(2), 7-15. https://doi.org/10.23960/jhptt.2237-15

Kadwati, K., & Hidayat, S. H. (2015). Deteksi virus utama bawang merah dan bawang putih dari daerah Jawa Barat dan Jawa Tengah [Detection of main viruses infecting shallot and garlic in West and Central Java]. *Jurnal Fitopatologi Indonesia*, *11*(4), 121-127. https://doi.org/10.14692/jfi.11.4.121

Katis, N. I., Maliogka, V. I, Dovas, C. I. (2012). Viruses of the Genus Allium in the mediterranean region. *Advances in Virus Research*, *84*, 163-208. https://doi.org/10.1016/B978-0-12-394314-9.00005-1

Khan, N., Chaudhary, M. F., Abbasi, A. M., Khan, S. A., Nazir, A., & Shah, G. M. (2017). Development of an efficient callus derived regeneration system for garlic (Allium sativum L.) from root explant. *Journal of Plant Breeding and Agriculture*, *1*(1), 1-12.

Kumar, P., Dhawan, P., & Mehra, R. (2012). Symptoms and losses caused by *Onion yellow dwarf virus* and *Iris yellow spot virus* diseases of onion crop in Northern India. *Journal of Mycology and Plant Pathology*, *42*(1), 153–160.

Majumder, S., & Baranwal, V. K. (2014). Simultaneous detection of four garlic viruses by multiplex reverse transcription PCR and their distribution in Indian garlic accessions. *Journal of Virological Methods*, *202*, 34-38. https://doi.org/10.1016/j.jviromet.2014.02.019

Mang, S. M., Altieri, L., Candido, V., Miccolis, V., & Camele, I. (2022). Garlic (*Allium* spp.) Viruses: detection, distribution and remediation attempts in a European garlic collection. *Notulae Botanicae Horti Agrobotanici Cluj-Napoca*, *50*(3), 12779. https://doi.org/10.15835/nbha50312779

McLeish, M. J., Fraile, A., & García-Arenal, F. (2019). Evolution of plant–virus interactions: host range and virus emergence. *Current Opinion in Virology*, *34*, 50–55. https://doi.org/10.1016/j.coviro.2018.12.003

Muhire, B. M., Varsani, A., & Martin, D. P. (2014). SDT: A virus classification tool based on pairwise sequence alignment and identity calculation. *PloS one*, *9*(9), e108277. https://doi.org/10.1371/journal.pone.0108277

Nurulita, S., Mawarni, S., & Hidayat, S. H. (2024). Identification of garlic viruses associated with seed bulbs and consumption bulbs from several locations in Indonesia. *HAYATI Journal of Biosciences*, *31*(4), 733-743. https://doi.org/10.4308/hjb.31.4.733-743

Nurviani, N., Sulandari, S., Somowiyarjo, S., & Subandiyah, S. (2016). Deteksi virus terbawa umbi benih pada bawang merah kultivar Biru Bantul [Detection of seed bulb viruses on Shallot Cultivar Biru Bantul]. *Jurnal Fitopatologi Indonesia*, *12*(5), 185-190. https://doi.org/10.14692/jfi.12.5.185

Parrano, L., Afunian, M., Pagliaccia, D., Douhan, G., & Vidalakis, G. (2012). Characterization of viruses associated with garlic plants propagated from different reproductive tissues from Italy and other geographic regions. *Phytopathologia Mediterranea*, *51*(3), 549-565.

Paudel, D. B., & Sanfaçon, H. (2018). Exploring the diversity of mechanisms associated with plant tolerance to virus infection. *Frontier Plant Science*, *2*(9), 1575. https://doi.org/10.3389/fpls.2018.01575

Rahmawati, F., & Jamhari, N. (2019). Efisiensi teknis usaha tani bawang putih pola tumpang sari di Kabupaten Karanganyar, Provinsi Jawa Tengah [Technical efficiency of garlic farming with intercropping pattern in Karanganyar Regency, Central Java Province]. *Jurnal Agro Ekonomi*, *36*(2), 135-147. https://doi.org/10.21082/jae.v36n2.2018.135-147

Santosa, A. I., & Ertunc, F. (2021). Phylogenetic and diversity analyses of Garlic common latent virus based on the TGB and CP gene sequence. *Plant Protection Science*, *57*(3), 179–187. https://doi.org/10.17221/149/2020-PPS

Singhal, P., Nabi, S. U., Yadav, M. K., & Dubey, A. (2021). Mixed infection of plant viruses: Diagnostics, interactions and impact on host. *Journal of Plant Diseases and Protection*, *128*(2), 353-368. https://doi.org/10.1007/s41348-020-00384-0

Sullivan, D. M., Brown, B. D., Shock, C. C., Horneck, D. A., Stevens, R. G., Pelter, G. Q., & Feibert, E. B. G. (2001). *Nutrient management for onions in the Pacific Northwest.* Pacific Northwest Publications. https://extension.oregonstate.edu/sites/extd8/files/documents/pnw546.pdf

Sumi, S. I., Tsuneyoshi, T., Suzuki, A., & Ayabe, M. (2001). Development and establishment of practical tissue culture methods for production of virus-free garlic seed bulbs, a novel field cultivation system and convenient methods for detecting garlic infecting viruses. *Plant Biotechnology*, *18*(3), 179-190. https://doi.org/10.5511/plantbiotechnology.18.179

Taglienti, A., Tiberini, A., Manglli, A., Rea, R., Paoletti, S., Taviani, P., & Tomassoli, L. (2018). Molecular identification of allexiviruses in a complex mixture of garlic viruses in Latium (central Italy). *European Journal of Plant Pathology*, *150*, 797-801. https://doi.org/10.1007/s10658-017-1315-5

Takahashi, H., Fukuhara, T., Kitazawa, H., & Kormelink, R. (2019). Virus latency and the impact on plants. *Frontiers in Microbiology*, *10*, 2764. https://doi.org/10.3389/fmicb.2019.02764

Tamura, K., Stecher, G., & Kumar, S. (2021). MEGA11: Molecular evolutionary genetics analysis version 11. *Molecular Biology and Evolution, 38*(7), 3022-3027. https://doi.org/10.1093/molbev/msab120

Trebicki, P. (2020). Climate change and plant virus epidemiology. *Virus research*, *286*, 198059. https://doi.org/10.1016/j.virusres.2020.198059

Tripathi, S., Suzuki, J.Y., Ferreira, S.A, Gonsalves, D. (2008). Papaya ringspot virus-P: Characteristics, pathogenicity, sequence variability and control. *Molecular Plant Pathology*, *9*(3), 269-280. https://doi.org/10.1111/j.1364-3703.2008.00467.x.

Tsuneyoshi, T., Matsumi, T., Natsuaki, K. T., & Sumi, S. (1998). Nucleotide sequence analysis of virus isolates indicates the presence of three potyvirus species in Allium plants. *Archives of Virology*, *143*, 97-113. https://doi.org/10.1007/s007050050271

Wulandari, A. W., Hidayat, S. H., & Sobir, S. (2016). Deteksi virus pada bawang merah (*Allium cepa var. ascalonicum*) dengan metode dot immuno binding assay [Detection of Shallot Viruses (*Allium cepa var. ascalonicum*) by Dot Immuno Binding Assay]. *Jurnal Hortikultura*, *25*(4), 350-356. https://doi.org/10.21082/jhort.v25n4.2015.p350-356

Zhang, Y. Z., Shi, M., & Holmes, E. C. (2018). Using metagenomics to characterize an expanding virosphere. *Cell*, *172*(6), 1168-1172. https://doi.org/10.1016/j.cell.2018.02.043

Pertanika J. Trop. Agric. Sci. 48 (3): 867 - 877 (2025)

PERTANIKA JOURNALS

TROPICAL AGRICULTURAL SCIENCE

Journal homepage: http://www.pertanika.upm.edu.my/

Short Communication

Effect of N, N-Dimethylglycine (DMG) Supplementation on Haematological Parameters and Frequency of CD4+ and CD8+ T Cells in Cats Post-vaccination

Syahir Aiman Shahril Agus[1], Nurul Afiqah Shamsul-Bahri[1], Juliana Syafinaz[1], Muhammad Farris Mohd Sadali[1], Hazilawati Hamzah[1] and Farina Mustaffa-Kamal[1,2]*

[1]*Faculty of Veterinary Medicine, Universiti Putra Malaysia, 43400 Serdang, Selangor, Malaysia*
[2]*Institute of Bioscience, Universiti Putra Malaysia, 43400 Serdang, Selangor, Malaysia*

ABSTRACT

N, N-Dimethylglycine (DMG) is a commonly used nutraceutical in veterinary medicine, which is claimed to have immunomodulating properties. This novel study investigated the effect of DMG supplementation on feline haematological parameters and the percentages of CD4+ and CD8+ T cells after vaccination with a single-dose commercial core vaccine. A total of twelve neutered cats were divided into control (n=6) and treatment groups (n=6) and received one dose of feline core vaccine at day 0. The treatment group then received oral DMG supplementation (125 mg/mL) twice daily for 14 days. Blood samples were collected on days 0 and 15 for haematological, differential cell count, and T cell phenotyping analysis. Haematological analysis revealed no significant difference between the control and treatment groups after 14 days of the experiment. At post-treatment, the neutrophil percentage of the treatment group was significantly lower (p=0.0238) compared to the control group, while the lymphocyte percentage of the treatment group was significantly higher (p=0.013) compared to the control group. The reduction in neutrophil percentage could be due to bromelain, an anti-inflammatory enzyme, while an increase in lymphocyte percentage could be attributed to an increase in B cell or NK cell subsets instead of T cells. Future research is warranted to investigate the effects of DMG on B cells and natural killer cell activation and to explore the long-term effects of DMG supplementation on feline immune health.

Keywords: Dimethylglycine, feline, haematological parameters, immunomodulation

ARTICLE INFO

Article history:
Received: 30 August 2024
Accepted: 15 November 2024
Published: 16 May 2025

DOI: https://doi.org/10.47836/pjtas.48.3.12

E-mail addresses:
200749@student.upm.edu.my (Syahir Aiman Shahril Agus)
nurulafiqah_12@yahoo.com (Nurul Afiqah Shamsul-Bahri)
julianasyafinaz@gmail.com (Juliana Syafinaz)
farrissadali98@gmail.com (Muhammad Farris Mohd Sadali)
hazilawati@upm.edu.my (Hazilawati Hamzah)
farina@upm.edu.my (Farina Mustaffa-Kamal)
* Corresponding author

e-ISSN: 2231-8542

INTRODUCTION

Nutraceuticals can be defined as food products or components of food that are postulated to be beneficial for human and animal health (Hayek et al., 2004). An example of a nutraceutical that is commonly used in veterinary medicine is N, N-Dimethylglycine (DMG). DMG is a naturally occurring tertiary amino acid and a by-product of the metabolism of choline (Cupp, 2003). DMG is claimed by its proponents to be able to support the production of both lymphocytes and antibodies via the OKT4 epitope that activates T-cells or by the inhibition of T-suppressor cells, thereby enhancing both cell-mediated and humoral immunity (Reap & Lawson, 1990). Correlating to that claim, human subjects given DMG orally exhibited a four times increase in antibody titres against pneumococcal vaccine antigen after vaccination with pneumococcal vaccine compared to human subjects in the control group (Graber et al., 1981). Similarly, in a study done on rabbits, animals supplemented with DMG showed a four times increase of neutralising antibodies titre towards influenza antigen post-vaccination with a killed influenza virus vaccine (Reap & Lawson, 1990). Interestingly, in contrast, DMG failed to exhibit its immunomodulating capabilities in a cat study as it shows that cats treated with DMG showed a lower titre of virus-neutralising antibodies against feline herpesvirus-1 when compared to the control group (Weisrs, 1992). In the same study, the feline lymphocyte blastogenic response towards T cell mitogens was assessed *ex vivo*, and no significant difference in T cell proliferation was observed between feline lymphocytes treated with DMG and those treated with control. It was postulated that the difference in the outcome could be due to species variability or suboptimal dose of DMG; however, to the author's knowledge, there were no other feline studies. Therefore, given the widespread promotion and usage of DMG by veterinarians and the limited data on its immunomodulating or immunoadjuvant effects in cats, this current study aims to evaluate the impact of DMG supplementation on haematological parameters as well as the percentages of CD4+ and CD8+ T cells in cats' post-vaccination. The results will provide updated insights that will potentially assist veterinarians in making informed decisions regarding DMG's immunomodulatory properties.

MATERIALS AND METHODS

Animals and Study Design

This study was approved by the Universiti Putra Malaysia Institutional Animal Care and Use Committee (UPM IACUC) with approval number U032/2023. The study was conducted at an animal shelter, and 12 healthy neutered cats of both genders (male; $n = 5$, female; $n = 7$) were recruited for this study. Two weeks before the start of the study, recruited cats were given ectoparasite control and dewormed (Inovet, Belgium) at a dosage of 1 tab/10 kg of body weight. All the cats were conditioned in the same room they had been in before

the start of the study. Food in the form of kibbles and water was provided *ad libitum* throughout the study. Since this study aims to evaluate the immune response of the cats, only neutered cats were included in this study to minimise any hormone-related effects (Hellard et al., 2013). The cats (n=12) were randomly assigned to two groups, control and treatment, consisting of six cats per group. All cats were physically examined for clinical signs and tested negative for FeLV/FIV prior to vaccination. At day 0, both groups were administered a single dose of Purevax® Feline 4 Vaccine (Boehringer Ingelheim, Germany) containing modified live feline viral rhinotracheitis, feline calicivirus, feline panleukopenia virus and *Chlamydia psittaci* subcutaneously. Cats in the treatment group (n=6) were then orally supplemented with N, N–Dimethylglycine (DMG) in the liquid form (VetriDMG 125 mg/ml, VetriSciences, Vermont, USA) at a manufacturer's recommended dosage of 0.5 mL twice a day daily (BID) for 14 days. All 12 cats were monitored for 14 days post-vaccination and DMG supplementation for adverse reaction signs.

Sample Collection

All cats were subjected to blood sampling on days 0 (pre-treatment) and 15 (post-treatment) for haematological parameters, CD4 and CD8 T-cell phenotyping analysis. Approximately 3 mL of blood samples from the cats in both groups were collected and transferred into 3 mL tubes containing ethylenediaminetetraacetic acid (EDTA) anticoagulant. The samples were then placed in a cool box and transported to the lab for processing. Samples were processed within 24 hours, starting with haematological analysis, followed by peripheral blood mononuclear cell isolation and flow cytometric analysis.

Haematological Analysis

Haematological parameters such as haematocrit (HCT), red blood cells (RBC), white blood cells (WBC), haemoglobin (HGB), and platelet (PLT) counts were determined using Celltac Alpha VET MEK-6550K Haematological Analyser (Nihon Kohden, Japan). A thin blood smear was performed on all blood samples and stained with modified Wright's stain. A differential white blood cell count was carried out on each stained blood smear, whereby 100 cells were counted per slide to determine the percentages of neutrophils, lymphocytes, monocytes, eosinophils, and basophils.

CD4 and CD8 Phenotyping from PBMC Using Flow Cytometry

Peripheral blood mononuclear cell (PBMC) isolation was performed using a previously published protocol (Megat et al., 2022). Upon isolation, the PBMC pellet was resuspended and adjusted to a concentration of 2×10^6 cells/mL for flow cytometric analysis. Briefly, 2×10^6 cells/mL of PBMC were washed with 1 ml of buffer containing 2% FBS and 0.5 mM EDTA prior to antibody staining. Mouse anti-feline CD4-FITC (clone 34F4; Southern

Biotech, USA) and mouse anti-feline CD8-PE (clone: fCD8; Southern Biotech, USA) of 1 µL each were added to the cells and incubated at 4°C for 30 minutes in the dark. The cells were washed again with staining buffer containing 2% FBS and 2M EDTA, resuspended in 200 µL of 1% paraformaldehyde, and stored at 4°C for up to 72 hours before flow analysis. Data were acquired using BD FACSCanto (BD Biosciences, USA) for 50,000 events and analysed using BD FACSDiva software (BD Biosciences, USA). Compensation was carried out using fluorochrome minus one (FMO) CD4+ and FMO CD8+ controls. The positive CD4+ and CD8+ T lymphocyte population was determined by gating a similar population of unstained cells.

Statistical Analysis

All data were presented as median (M) and standard deviation (SD) except for haematological parameters where median and interquartile range (IQR) were used. As the data were not normally distributed, non-parametric tests were used using GraphPad Prism 9 software (GraphPad Software Inc., USA) to compare differences within (Wilcoxon matched pairs test) and between groups (Mann-Whitney test) at different time points. $p \leq 0.05$ was considered statistically significant, and for the Wilcoxon matched pairs test, Spearman's correlation coefficient (rs) was indicated if the result was statistically significant.

RESULTS

Haematological Parameters and Differential White Blood Cell Percentage

There were no significant differences in RBC, HCT, HGB, PLT, and WBC values between the control and treatment groups at post-treatment (Table 1). However, within each group,

Table 1
The effect of N, N-Dimethylglycine Supplementation on haematological parameters

Parameters	Time point	Control Group (*n*=6)	Treatment Group (*n*=6)
Red blood cells (RBC) (10^{12}/L)	D0	9.56 (9.99–8.62)	10.50 (10.83–9.49)
	D15	9.02 (9.45–8.64)	9.01 (10.75–8.27)
Haematocrit (HCT) (%)	D0	42.50 (44.50–40.10)	45.50 (47.53–41.13)
	D15	39.80 (41.10–39.25)	39.70 (47.40–34.73)
Haemoglobin (HGB) (g/dL)	D0	139.00 (146.75–133.75)	145.00 (156.00–131.25)
	D15	135.00 (137.00–131.75)	134.00 (159.25–117.00)
Platelet (PLT) (10^9/L)	D0	226.00 (323.50–184.00)	171.50 (195.50–96.00)
	D15	265.00 (334.50–207.50)	135.50 (210.25–122.25)
White blood cells (WBC) (10^9/L)	D0	12.150 (20.55–10.45)	11.90 (17.48–10.65)
	D15	14.05 (20.83–9.30)	18.30 (23.98–14.68)

Note. Data is presented as median (IQR). Haematological parameters were obtained at pre-treatment (day 0) and post-treatment (day 15) of the study

the cats exhibited a decrease in RBC, HCT, and HGB and increased in WBC numbers. Nevertheless, all these haematological changes were not statistically significant ($p \geq 0.05$). It is also important to note that most of the values for haematological parameters of both groups for both day 0 and day 15 were within the normal reference range or slightly above the upper normal limits (RBC value for treatment group on day 0; median: 10.50 x 10^{12}/L [IQR: 10.83–9.49], and HCT value for treatment group on day 0; median: 45.5 [IQR: 47.53–41.13]). However, the values for PLT for both groups on both day 0 and day 15 were below the reference range (Latimer, 2011; Weiss & Wardrop, 2010).

At post-treatment, values for parameters such as monocyte and eosinophil did not differ significantly between the control and treatment groups (Figure 1). Basophils were not detected in both cohorts at the two different time points (data not shown). Interestingly, cats in the treatment group exhibited significantly lower neutrophil percentage ($p = 0.024$; $M = 60.67$, $SD = 4.63$) compared to the control group ($M = 67.50$, $SD = 4.93$) at post-treatment. Conversely, cats in the treatment group exhibited significantly higher lymphocyte percentage ($p = 0.013$; $M = 33.83$, $SD = 4.49$) compared to the control group ($M = 25.50$,

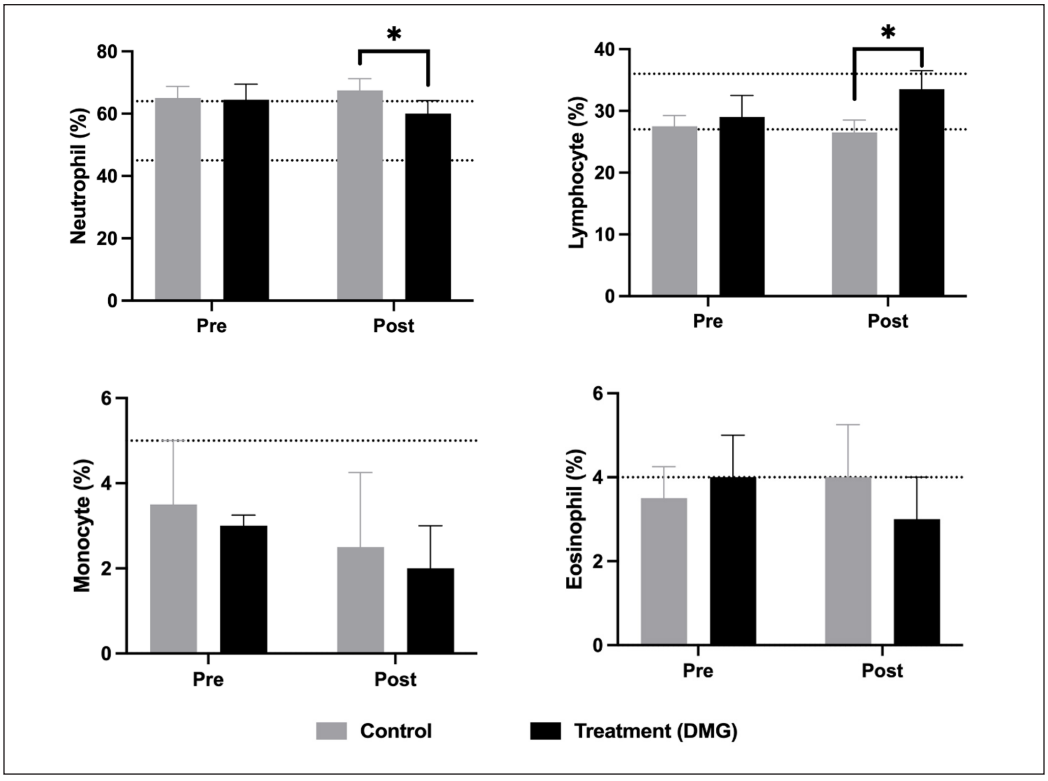

Figure 1. Effect of N, N-Dimethylglycine supplementation on differential white blood cell percentages. Data was analysed using a non-parametric Mann-Whitney test to determine significant differences between groups at day 15 (*) and a Wilcoxon matched pairs test to determine significant differences within groups at day 0 versus day 14. $p \leq 0.05$ is considered to be statistically significant

SD = 3.94). As shown in Figure 1, except for the lymphocyte percentage of the control group post-treatment, all the values for differential white blood cell percentage parameters of both pre-and post-treatment are within the normal reference range or slightly above the upper normal limit.

CD4+, CD8+ T Cells Phenotypic Analysis

Figure 2 presents all results and statistical analyses of differences between the control and treatment groups regarding lymphocyte subsets (CD4+ T cell percentage, CD8+ T cell percentage, and CD4+ to CD8+ ratio). The Wilcoxon matched pairs test indicated that cats in the control group exhibited a significant increase in CD4+ T cell percentage from day 0 ($p = 0.03$; *rs*: -0.086; *M*: 16.75 *SD*: 8.00) to post-treatment (*M*: 29.90, *SD*: 8.063).

In contrast, cats in the treatment group showed a decrease in CD4+ T cell percentage from pre- to post-treatment, albeit non significantly. Due to this, the control group had a significantly higher mean CD4+ T cell percentage post-treatment than the treatment group (p: 0.0022; $M = 29.90$, $SD = 8.063$ vs $M = 6.933$, $SD = 3.681$). As for CD8+ T cell percentage, both groups exhibited a non-significant ($p \geq 0.05$) decrease from pre- to post-treatment, although the decrease in CD8+ T cell mean percentage was prominent in the treatment group. Lastly, the control group showed a slight increase in the mean CD4:CD8 ratio post-treatment, as determined by the reference range, represented by the dotted line (Byrne et al., 2000). Conversely, the treatment group exhibited a non-significant reduction of the CD4:CD8 ratio from pre- to post-treatment. It is important to

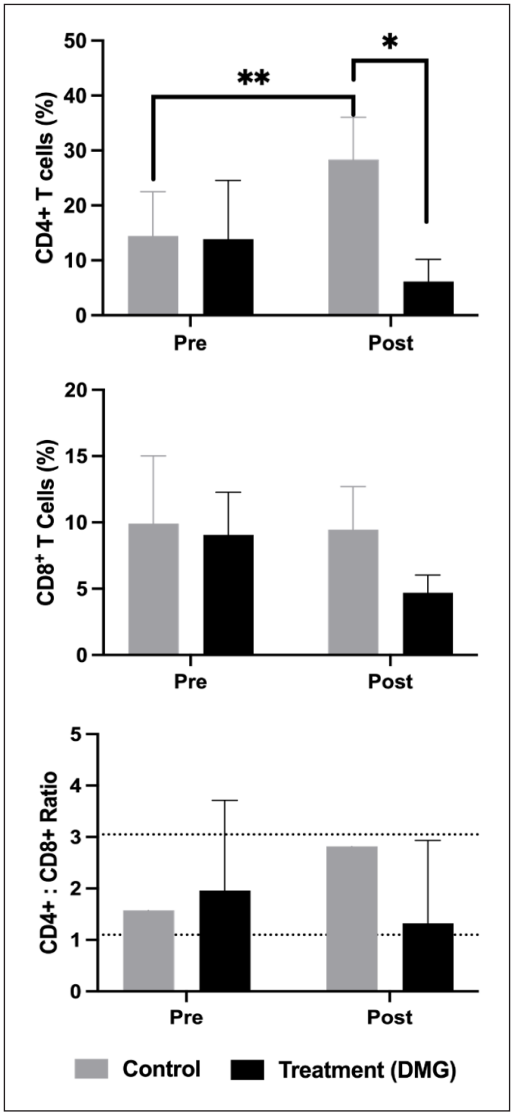

Figure 2. Effect of N, N-Dimethylglycine supplementation on Lymphocyte Subsets (CD4+ and CD8+ T cell). Data was analysed using a non-parametric Mann-Whitney test to determine the significant differences between groups at day 15 (*) and a Wilcoxon matched pairs test (**) for within-group analysis at day 0 versus day 15. $p \leq 0.05$ is considered to be statistically significant

note that, as seen in Figure 2, the CD4:CD8 ratios of both groups on day 0 and day 15 were within the normal range.

DISCUSSION

The impacts of oral supplementation of various nutraceuticals on the immune response towards infectious diseases and their influence on vaccine response are still being studied in various animal species (Mayer et al., 2019; Mohamed et al., 2019). In the context of DMG, studies pertaining to the relationship between DMG supplementation and its effects on the immune response to this day are still relatively scarce and infinitesimal, especially for the feline species. As noted earlier, the only study that investigated the effects of DMG supplementation on the immune response of cats was conducted back in the early 90s (Weiss, 1992). As a result of this, further explanations regarding the DMG's mechanism in affecting the feline immune system can only be extrapolated from earlier research conducted on other species, such as poultry (Kalmar et al., 2012), and a model of human keratinocyte (Lendvai et al., 2023). This study focused on the effects of DMG supplementation on haematological parameters (complete blood count including differential white cell count) and lymphocyte subset**.** The results showed there were no significant differences between pre-treatment (Day 0) and post-treatment (Day 15) for both groups of cats for RBC, HCT, HGB, PLT, and WBC (Table 1). Additionally, both groups' RBC, HCT, HGB, and WBC values were within the normal range or slightly above the upper normal limit. The RBC and HCT values were slightly high on Day 0 for the treatment group, most probably due to haemoconcentration. This could be due to dehydration prior to the start of the study, as the RBC and HCT values were normalised at the end of the study. This is unsurprising as the cats were from an animal shelter, and according to Miller and Zawistowski (2015), many shelters must work within tight budgets, often opting for the most affordable food options or depending on donations to meet their needs.

Hence, the cats' nutrition and hydration status would probably not be optimal. Considering these findings, we can extrapolate based on our study that short-term supplementation of DMG does not affect the normal values of haematological parameters. This finding supports the claims of the manufacturer, whereby it is claimed that DMG does not cause any side effects (Weiss, 1992). Clinically, throughout the entire study, cats that received daily bi-supplementation of DMG also did not exhibit any abnormal clinical signs and behaviours. Indeed, studies have shown that supplementation of DMG was proven to be safe when consumed in large doses and for long-term duration (Kalmar et al., 2012). For instance, chickens that were supplemented with DMG in the form of dimethylglycine sodium salt (Na-DMG) at a dosage of 10 g/kg for 39 days did not cause significant alteration to the liver enzyme activities such as aspartate aminotransferase activity or impaired their broiler performance parameters (Kalmar et al., 2012).

Although no side effects were observed, post-mortem examination, and a toxicity study could only rule out any toxicity effects. As for the PLT values, both groups showed lower PLT values compared to the reference range on both day 0 and day 15. One possible explanation for this is due to a 12–24 24-hour interval between sample collection and processing, of which a significant decrease in apparent platelet count could occur if sample processing were delayed (Hardy et al., 2020). However, the treatment group had a significantly lower neutrophil percentage and significantly higher lymphocyte percentage compared to the control group. There are a few possible explanations for the lower neutrophil percentage of the treatment group. First, the decrease in neutrophils in the treatment group may signify DMG's ability to reduce the ongoing inflammatory process in the cats. It is common knowledge that increased neutrophil count may signify an ongoing inflammatory process. In the context of our study, immunisation or vaccination could cause the recruitment and mobilisation of neutrophils from blood vessels to the site of the vaccination leading to an inflammatory process (Wang et al., 2022).

However, the reduced neutrophil count was not observed in the control group that also received vaccination. When studied in models of human keratinocytes, mimicking inflammatory diseases such as contact dermatitis, dimethylglycine exerts robust anti-inflammatory as well as antioxidant properties (Lendvai et al., 2023). Therefore, the reduction in neutrophils in the treatment group may also signify the anti-inflammatory properties of bromelain, which is present in DMG supplements at a concentration of 2 mg/mL. Bromelain is an enzyme extracted from pineapples and is considered an alternative to non-steroidal anti-inflammatory drugs (Rathnavelu et al., 2016). Bromelain has been shown to have anti-inflammatory properties in various *in vivo* and *in vitro* studies (Pavan et al., 2012). Although the vaccine would cause an increase in lymphoproliferative effects due to T and B cell activations (Vojtek et al., 2021), the control group that received vaccination did not show a significant increase in their lymphocyte percentage compared to the treatment group.

The significant increase in the treatment group can be attributed to the synergistic effects of both the vaccine and DMG (Graber et al., 1981; Vojtek et al., 2021). Interestingly, in contrast, in the cat study of Weiss (1992), the supplementation of DMG did not result in a lymphoproliferative effect towards T cell mitogens. However, the lymphoproliferative effect was not tested in our study. In several studies done in the past, DMG has been shown to have lymphoproliferative properties when studied in *in vitro* and *in vivo* (Graber et al., 1981; Reap & Lawson, 1990). One of the proposed mechanisms is inhibiting T-suppressor cells and enhancing the T-cell presentation of the OKT4 antigen (Real & Lawson, 1990). However, in this study, DMG appears to have no significant impact on the percentages of CD4+ and CD8+ T cells.

Moreover, there was a significant reduction in CD4+ after the DMG supplementation, which could also be due to the effects of bromelain in the DMG supplementation (Secor et al., 2009). Treatment of lymphocytes with bromelain *in vitro* caused a reduction in the activation of CD4+ T cells and lowered the expression of CD25 in a mouse study. We speculate that the lymphocyte increase upon DMG supplementation might cause an increase in other lymphocyte subsets, such as B cells and natural killer cells. However, these subsets were not measured in the current study. Hence, based on our results, we can extrapolate that DMG supplementation does not significantly affect the percentages of CD4+ and CD8+ T cells. In addition, the study only evaluated the effects of DMG supplementation for 14 days. It is possible that long-term supplementation could produce a pronounced effect on the immune system parameters, which was seen in the human study where subjects were supplemented with DMG for 10 weeks (Graber et al., 1981). As for the long-term supplementation duration, we suggest extending the study to 40 days or longer, similar to the previous DMG study done in cats and broiler chickens (Weiss, 1992; Kalmar et al., 2012).

CONCLUSION

Cats supplemented with DMG displayed lower neutrophils and higher lymphocytes compared to the control group, suggesting potential anti-inflammatory and lymphoproliferative effects. However, DMG did not significantly influence the percentages of CD4+ and CD8+ T cells. Therefore, a comprehensive and longer longitudinal study is warranted to look at the effect of DMG in B cell and NK cell activations and long-term supplementation in cats to fully understand DMG's immunomodulatory properties.

ACKNOWLEDGEMENTS

We thank Mr. Yong for allowing us to conduct the study at their animal shelter. We would also like to extend our gratitude to Ms Amrina Mohd Amin of the Haematology Laboratory of the Faculty of Medicine and Health Sciences, UPM, for their assistance throughout the flow cytometric analysis. This research was supported by the Ministry of Education (MOE), Malaysia, through the Fundamental Research Grant Scheme (FRGS) [project number: 01-01-18-1991FR; reference number: FRGS/1/2018/STG03/UPM/02/15].

REFERENCES

Byrne, K. M., Kim, H. W., Chew, B. P., Reinhart, G. A., & Hayek, M. G. (2000). A standardized gating technique for the generation of flow cytometry data for normal canine and normal feline blood lymphocytes. *Veterinary Immunology and Immunopathology*, *73*(2), 167-182. https://doi.org/10.1016/S0165-2427(99)00163-4

Cupp, M. J. (2003). Patients' understanding of herbal product "suggested use" and "disclaimer" statements. *Annals of Pharmacotherapy*, *37*(7-8), 1148. https://doi.org/10.1345/aph.1D065

Graber, C. D., Goust, J. M., Glassman, A. D., Kendall, R., & Loadholt, C. B. (1981). Immunomodulating properties of dimethylglycine in humans. *Journal of Infectious Disease*, *143*(1), 101-105. https://doi.org/10.1093/infdis/143.1.101

Hardy, M., Lessire, S., Kasikci, S., Baudar, J., Guldenpfennig, M., Collard, A., Dogné, J.-M., Chatelain, B., Jacqmin, H., Lecompte, T., & Mullier, F. (2020). Effects of time-interval since blood draw and of anticoagulation on platelet testing (count, indices and impedance aggregometry): A systematic study with blood from healthy volunteers. *Journal of Clinical Medicine*, *9*(8), 2515.

Hayek, M. G., Massimino, S. P., & Ceddia, M. A. (2004). Modulation of immune response through nutraceutical interventions: Implications for canine and feline health. *Veterinary Clinics of North America: Small Animal Practice*, *34*(1), 229-247. https://doi.org/10.1016/j.cvsm.2003.09.002

Hellard, E., Fouchet, D., Rey, B., Mouchet, A., Poulet, H., & Pontier, D. (2013). Differential association between circulating testosterone and infection risk by several viruses in natural cat populations: a behavioural-mediated effect? *Parasitology*, *140*(4), 521–529. https://doi:10.1017/S0031182012001862

Kalmar, I. D., Verstegen, M. W., Maenner, K., Zentek, J., Meulemans, G., & Janssens, G. P. (2012). Tolerance and safety evaluation of N,N-dimethylglycine, a naturally occurring organic compound, as a feed additive in broiler diets. *British Journal of Nutrition*, *107*(11), 1635-1644. https://doi.org/10.1017/S0007114511004752

Latimer, K. S. (2011). *Duncan and Prasse's veterinary laboratory medicine: Clinical pathology* (5th ed.). Wiley-Blackwell. https://doi.org/10.1111/vcp.12042

Lendvai, A., Beke, G., Hollosi, E., Becker, M., Volker, J. M., Schulze Zur Wiesche, E., Bacsi, A., Biro, T., & Mihaly, J. (2023). N,N-Dimethylglycine sodium salt exerts marked anti-inflammatory effects in various dermatitis models and activates human epidermal keratinocytes by increasing proliferation, migration, and growth factor release. *International Journal of Molecular Science*s, *24*(14), 11264. https://doi.org/10.3390/ijms241411264

Mayer, J., Williams, R., Kleine, S., He, B., Meichner, T., & Gogal, R. M., Jr. (2019). Immunomodulatory effects of dietary IMUNO-2865 in mice, pre-and post-vaccine challenge with parainfluenza virus 5. *International Immunopharmacology*, *76*, 105846. https://doi.org/10.1016/j.intimp.2019.105846

Megat, M. K. M. H., Selvarajah, G. T., Omar, A. R., & Mustaffa-Kamal, F. (2022). Expression of Toll-like receptors 3, 7, 9 and cytokines in feline infectious peritonitis virus-infected CRFK cells and feline peripheral monocytes. *Journal of Veterinary Science*, *23*(2). https://doi.org/10.4142/jvs.21225

Miller, Lila, and Stephen Zawistowski. 2015. *Animal behavior for shelter veterinarians and staff*. Wiley-Blackwell. https://doi.org/10.1017/S0962728600007764

Mohamed, N. E., Sharawi, S. S., Omar, R. E.-S., El-Habbaa, A. S., & Saad-Allah, E. T. (2019). The effect of some immunomodulators like Propolis and Immulant® against live Newcastle disease virus vaccination on broiler chickens, Egypt. *Benha Veterinary Medical Journal*, *36*(2), 90-99. https://doi.org/10.21608/bvmj.2019.12742.1010

Pavan, R., Jain, S., Shraddha, & Kumar, A. (2012). Properties and therapeutic application of bromelain: A review. *Biotechnology Research International*, *2012*(1), 976203. https://doi.org/10.1155/2012/976203

Rathnavelu, V., Alitheen, N. B., Sohila, S., Kanagesan, S., & Ramesh, R. (2016). Potential role of bromelain in clinical and therapeutic applications. *Biomedical reports*, *5*(3), 283–288. https://doi.org/10.3892/br.2016.720

Reap, E. A., & Lawson, J. W. (1990). Stimulation of the immune response by dimethylglycine, a nontoxic metabolite. *Journal of Laboratory Clinical Medicine*, *115*(4), 481-486.

Secor, E. R., Jr., Singh, A., Guernsey, L. A., McNamara, J. T., Zhan, L., Maulik, N., & Thrall, R. S. (2009). Bromelain treatment reduces CD25 expression on activated CD4+ T cells in vitro. *International Immunopharmacology*, *9*(3), 340-346. https://doi.org/10.1016/j.intimp.2008.12.012

Vojtek, B., Mojzisova, J., Kulichova, L., Smrco, P., & Drazovska, M. (2021). Effects of dietary nucleotides and cationic peptides on vaccination response in cats. *Veterinární Medicína*, *66*(1), 17-23. http://dx.doi.org/10.17221/35/2020-VETMED

Wang, Y., Qu, K., Lu, W., Zhao, P., Wang, Z., Cui, C., Liu, Y., Yang, M., Yu, Y., & Wang, L. (2022). Neutrophils recruited to immunization sites initiating vaccine-induced antibody responses by locally expressing BAFF. *iScience*, *25*(6), 104453. https://doi.org/10.1016/j.isci.2022.104453

Weiss, D. J., & Wardrop, K. J. (2010). *Schalm's veterinary hematology* (6th ed.). Wiley-Blackwell. https://doi.org/10.1002/9781119500537

Weiss, R. C. (1992). Immunologic responses in healthy random-source cats fed N,N-dimethylglycine-supplemented diets. *American Journal of Veterinary Research*, *53*(5), 829-833.

Pertanika J. Trop. Agric. Sci. 48 (3): 879 - 910 (2025)

PERTANIKA JOURNALS

TROPICAL AGRICULTURAL SCIENCE

Journal homepage: http://www.pertanika.upm.edu.my/

Assessment of *Avicennia* Species Using Leaf Morphology and Nuclear Ribosomal Internal Transcribed Spacer DNA Barcode

Jeffry Syazana[1], Zakaria Muta Harah[1,2]*, Ramaiya Devi Shiamala[3], Esa Yuzine[1,2,5] and Bujang Japar Sidik[4]

[1]Department of Aquaculture, Faculty of Agriculture, Universiti Putra Malaysia, 43000 Serdang, Selangor, Malaysia

[2]International Institute of Aquaculture and Aquatic Sciences, Universiti Putra Malaysia, 71050 Port Dickson, Negeri Sembilan, Malaysia

[3]Department of Crop Science, Faculty of Agricultural and Forestry Sciences, Universiti Putra Malaysia Bintulu Sarawak Campus, 97008 Bintulu, Sarawak, Malaysia

[4]No. 8 Jalan Sri Hartamas 18, Taman Sri Hartamas, 50480 Kuala Lumpur, Federal Territory, Malaysia

[5]Department of Aquaculture, Faculty of Fisheries and Marine, Universitas Airlangga, Campus C Jalan Mulyorejo, Surabaya 60115 East Java, Indonesia

ABSTRACT

The mangrove genus *Avicennia*, found in tropical and temperate regions, plays a crucial role in providing critical services such as habitat, shoreline stabilisation, and carbon sequestration. Given their ecological and economic significance, expanding knowledge by revising species recognition is essential for validating morphological characteristics and overlapping traits. This study reassessed *Avicennia* species using morphological and genetic analysis. Samples were collected from Pulau Bagan Pinang, Pulau Burong, Pulau Kamat, Pulau Merambong, and Sungai Kemasik, Peninsular Malaysia. Mature leaves were assessed for their morphological traits, whereas young leaves were used to extract DNA for internal transcribed spacer (ITS) sequences. Statistical and phylogenetic analyses were conducted to evaluate leaf morphology variations and genetic divergence. Leaf morphology and size ($p < 0.05$) varied significantly among *Avicennia* species across study sites. *Avicennia alba* and *A. rumphiana* from the islands exhibited shorter, narrower, and thicker leaves than Sungai Kemasik. *Avicennia marina* displayed consistent leaf sizes. Leaf hierarchical relationships showed three to four phenetic groups, with separations at Euclidean distances of 25.0 (length), 18.0 (width), and 25.0 (thickness). Phylogenetics of *Avicennia* revealed four clades with strong bootstrap supports (83-100%). The guanine-cytosine (%GC) content was consistent, ranging from 63.5% to 64.6%. *Avicennia rumphiana*

ARTICLE INFO

Article history:
Received: 25 September 2024
Accepted: 15 November 2024
Published: 16 May 2025

DOI: https://doi.org/10.47836/pjtas.48.3.13

E-mail addresses:
gs62983@student.upm.edu.my (Jeffry Syazana)
muta@upm.edu.my (Zakaria Muta Harah)
shiamala@upm.edu.my (Ramaiya Devi Shiamala)
yuzine@upm.edu.my (bin Esa Yuzine)
japar@upm.edu.my (Bujang Japar Sidik)
* Corresponding author

displayed high intraspecific genetic variation (1.57%) and distinctness from other species, supported by morphological and genetic data. This integrated approach is crucial for species identification and effective biodiversity assessments.

Keywords: *Avicennia*, genetic, internal transcribed spacer (ITS), leaf morphology, leaf morphometric, mangroves

INTRODUCTION

The mangrove genus *Avicennia* L., locally known as Api-api, is monotypic and distributed across tropical and temperate regions (Tomlinson, 1986; Kavitha et al., 2010). Historically, the taxonomy of *Avicennia* has undergone several revisions, reflecting both morphological and genetic evidence that shaped the current classification (Thatoi et al., 2016). Based on the consensus in phylogenetic evolution, the latest updated checklist confirms that the genus *Avicennia* includes eight species: *Avicennia alba* Blume, *A. balanophora* Stapf & Moldenke., *A. bicolor* Standl., *A. germinans* (L.) L., *A. integra* N.C. Duke., *A. marina* (Forssk.) Vierh., *A. officinalis* L. and *A. schaueriana* Stapf & Leechm. ex Moldenke. The presence of species variance is in *A. alba*, *A. bicolor*, *A. germinans*, *A. marina*, *A. officinalis,* and *A. schaueriana* (Hassler, 2024). This genus is found across a range that extends from East Africa through the Indo-Malayan region to Australia and New Caledonia.

According to the botanical reports (Duke, 1991; Tomlinson, 2016; Watson, 1928), five *Avicennia* species (*Avicennia alba*, *A. officinalis*, *A, rumphiana*, *A. integra*, and *A. marina*) are confined to the area of Indo-western Pacific region. In contrast, the latest Catalogue of Life (Hassler, 2024) list recognises *A. rumphiana* as a variety of *A. marina*, according to Ridley (1923) and Bakhuizen (1921). Moldenke (1990) proposed that the morphological characteristics (for example, pale green leaf undersurface) distinguished *A. marina* var. *rumphiana* as a valid variety. However, as Duke (1991) noted, Moldenke formally made his new combination with *A. marina* but curiously never offered the correction in subsequent writings, preferring to use the Bakhuizen van den Brink name, leaving the change unresolved and controversial. Subsequent advances in phylogenetic research have been revisited to better understand the species relationships and introgressive hybridisation (Mori et al., 2015). Huang et al. (2014) found that *A. rumphiana* is genetically distinct from *A. marina*, and Li et al. (2016) still referred to *A. rumphiana* as a distinct species.

Classically, the method based on morphological characters was a traditional technique to name the species (Vy et al., 2017). Taxonomists also often depended on flowers to identify species (Borg & Schönenberger, 2011; Nadia et al., 2012). However, this approach is challenging when flowers are unavailable during non-flowering seasons. Consequently, researchers have explored alternative methods, such as using leaf morphology for species identification. For example, Duke (2012) used leaf morphology to identify specimens of

Avicennia. Leaf morphology is useful for field identification because it varies widely and is easy to observe in studies such as phytosociology, which needs to identify every tree, even when flowers and fruits are absent (Nascimento et al., 2021). In addition, Said and Ehsan (2010) emphasised that leaf characteristics such as shape, edge, colour, and base are important for distinguishing *Avicennia* species and classifying intraspecies variations. Studies by Abou Seedo et al. (2018), Farooqui and Dangi (2018), and Sabdanawaty et al. (2021) have effectively used leaf morphology for this purpose. However, relying only on morphological characteristics can be challenging, as environmental factors often influence them (Thatoi et al., 2016), including soil salinity and the seasonality of the local climate. Some species have evolved different leaf adaptations based on geographical location, leading to further confusion in species identification (Thatoi et al., 2016).

In recent years, there have been increasing efforts made by several authors, for example, Rani et al. (2018) and Ruang-areerate et al. (2022), on identification using various approaches among mangroves species, including *Avicennia* based on DNA barcoding (Bhadalkar et al., 2014). DNA barcoding is a technique that employs short, variable, and standardised DNA sequences to assess and classify species (Said & Bahnasy, 2023). Subsequently, molecular markers were utilised for various applications, from gene localisation to the genetic enhancement of plant varieties (Karuppaiya et al., 2020). The molecular markers used are Restriction Fragment Length Polymorphism (RFLP), Random Amplified Polymorphic DNA (RAPD), Amplified Fragment Length Polymorphism (AFLP), Simple Sequence Repeat (SSR), Sequence Tagged Site (STS), and Single Nucleotide Polymorphism (SNP) (Bhadalkar et al., 2014). Internal transcribed spacer (ITS) has been described as a primer for identifying mangrove plant species using leaves due to its effectiveness as a DNA barcode marker (Chen et al., 2015). Bast et al. (2016) noted that ITS regions are easily amplified even from small DNA samples, have moderate length (under 700 bp), and exhibit significant variation among closely related species. The evolution rate of ITS is appropriate at the species and generic levels, as it is phylogenetically explainable for phylogenetic reconstruction and flanked by highly conserved sequences within genera, making polymerase chain reaction (PCR) amplification and sequencing straightforward (Maguire & Saenger, 2000).

Since taxonomic confusion may arise from variations in morphology characteristics, the genetic approach was used as an important tool in this present study for species identification works. Although Tomlinson (2016) rarely used leaf shape in his identification key, he noted that it could be a distinguishing feature for some *Avicennia* species. He investigated the range of variation in leaf shape within each species. Therefore, this study reassessed *Avicennia* species using leaf morphology and genetic analysis of ITS sequences. Our findings are anticipated to enhance the accuracy of *Avicennia* species identification, contributing to more effective field observations and biodiversity assessments.

MATERIALS AND METHODS

Sampling Sites

The sample collection covered five mangrove sites in Peninsular Malaysia (Figure 1a). Pulau Bagan Pinang (2° 30' 28.29" N, 101° 49' 35.19" E) (Figure 1b) and Pulau Burong (2° 32' 46.58" N, 101° 47' 10.15" E) (Figure 1c), are mangrove islands located in the coastal areas of Port Dickson, Negeri Sembilan. Along the coast area of Pulau Kamat (2° 20' 50.83" N, 102° 2' 19.16" E) (Figure 1d) is in Teluk Gong, Malacca. These three islands are situated within the Strait of Malacca. Further south, Pulau Merambong (1° 18' 54.69" N, 103° 36' 36.58" E) (Figure 1e) is in Johor, directly exposed to marine conditions of the Johor Strait. Sungai Kemasik, an estuary located at Kemasik, Terengganu (4° 25' 6.17" N, 103° 27' 15.08" E) (Figure 1f), is influenced by a combination of saltwater from the South China Sea and freshwater inflow.

Plant Materials

For morphometric analysis, thirty mature leaves of *Avicennia* species were randomly collected from three individual trees, depending on their presence within the above mangrove sites. These leaf samples were placed in zip-lock plastic bags and transferred to the Aquatic Botany Laboratory, Department of Aquaculture, Universiti Putra Malaysia, for further leaf morphological analysis. The leaf morphological traits considered for physiognomic study are qualitative (leaf shape, margin, tip, base, upper surface, under surface, and colour) and quantitative (leaf length, width, and thickness). Five to eight young leaves were collected and placed in zip-lock plastic bags with silica gels for DNA analysis.

Figure 1. (a) Sample collection at different sites; (b) Pulau Bagan Pinang; (c) Pulau Burong; (d) Pulau Kamat; (e) Pulau Merambong; and (f) Sungai Kemasikw
Source: Google Earth

DNA Extraction

The dried leaf samples were crushed and ground in a mortar to obtain fine powder. Approximately 25 mg of powder from each sample was transferred to a 1.5 µL Eppendorf tube. The total genomic DNA was extracted using a commercially available kit, DNeasy® Plant Mini Kit (Qiagen, Germany) derived from the manufacturer's instructions. Buffer API (400 µL) and RNase A (4 µL) were added to the 25 mg powder sample, vortexed, and incubated at 65°C for 15 minutes. After cooling, Buffer P3 (130 µL) was added, mixed, and incubated for 4 minutes on ice, followed by 1 minute at room temperature. After cooling, Buffer P3 (130 µL) was added, mixed, and incubated for 4 minutes on ice, followed by 1 minute at room temperature. The lysate was centrifuged, transferred to a QIAshredder column and centrifuged again. The flow-through was mixed with Buffer AW1 and processed through a DNeasy Mini spin column, followed by centrifugation. Buffer AW2 (500 µL) was added and centrifuged. Genomic DNA was eluted with Buffer AE (100 µL), incubated for 5 minutes, and centrifuged. The eluted DNA was quantified on a 0.6% agarose gel (1st BASE, Singapore) and visualised using runVIEW Gel Imager (Cleaver Scientific Ltd., UK) to obtain high-quality DNA.

Polymerase Chain Reaction (PCR) and Sequencing

The complete internal transcribed spacer (ITS) regions (including ITS-1, 5.8S rRNA gene, and ITS-2) were amplified using both universal primers (Integrated DNA Technologies, Singapore) of ITS-1 (forward: 5'-TCC GTA GGT GAA CCT GCG G-3') and ITS-4 (reverse: 5'- TCC TCC GCT TAT TGA TAT GC-3'). The amplification followed DreamTaq Green PCR Master Mix (2X) (Thermo Fisher Scientific™, USA) standard protocol with several modifications in the reaction mixture volume. The 35 µL reaction mixture contained 5 µL of template DNA, 16.5 µL of DreamTaq Green PCR Master Mix (2X), 1 µL of each primer, and 10.5 µL of nuclease-free water. The double-stranded fragments were employed with 35 cycles of the polymerase chain reaction (PCR; 94°C for 5 min; 94°C for 1 min, 53.3°C for 30 s, 72°C for 2 min; and final extension at 72°C for 10 min) in T100™ Thermal Cycler (Bio-Rad, Germany).

PCR products were verified through electrophoresis on 1% agarose gels, stained with Midori Green (Nippon Genetics Europe GmbH, Germany), and visualised under UV light. The size of the DNA fragments was determined using a GeneRuler 1 kb plus DNA ladder (Thermo Fisher Scientific™, USA) that had been premixed with a 6x loading buffer (1st BASE, Singapore). Gel electrophoresis was performed in TAE (Tris-Acetate-EDTA) buffer (1st BASE, Singapore) for 45 min at 87 V. Both forward and reverse strands were then sequenced bidirectionally using the Sanger method at 1st BASE Ltd., Malaysia.

Statistical Analysis

Quantitative data on leaf length, width, and thickness were subjected to statistical analysis using SPSS Statistics version 26 for Windows (IBM Corp., Armonk, NY, USA). Differences in mean values were compared using one-way ANOVA followed by Duncan's post hoc test at the $p < 0.05$ level (Zar, 2010).

The leaf morphometric variations among *Avicennia* species were determined from leaf length, width, and thickness means. A hierarchical cluster analysis was performed using Agglomerative hierarchical clustering (AHC), which was applied to the normalised data set by Ward's method, using Euclidean distances as a measure of dissimilarity. The dendrogram was generated in Microsoft Excel using the statistical software of XLSTAT 2021 (Addinsoft, Paris, France).

Clustering and Phylogenetic Analysis

PCR products with high-quality scores (> 20) were filtered and selected using FinchTV 1.4 (Geospiza, Seattle, USA; http://www.geospiza.com/finchtv) for sequence alignment analysis. Consensus sequences were assembled into contigs with BioEdit software, version 7.1.9 (Ibis Biosciences, USA; http://www.mbio.ncsu.edu/BioEdit/bioedit.html), and used for phylogenetic reconstruction (Hall, 1999). Twenty-seven ITS sequences of *Avicennia* from this study (Nos. 1 to 27), 28 sequences from other locations (Nos. 28 to 53), and two outgroups *Sonneratia* (Nos. 54 to 55) as shown in Table 1 were aligned using CLUSTALW version 1.83 (EMBL-EBI, Cambridge, UK) (Larkin et al., 2007). Sequences from other locations were retrieved from the National Centre for Biotechnology Information (NCBI; http://www.ncbi.nlm.nih.gov/blast).

Phylogenetic analyses were performed using Maximum Likelihood (ML) in MEGA11 software (Tamura et al., 2021). Tamura 3-parameter model with gamma distributions (T92+G) was selected as the best-fitting substitution model. Model selection for ITS sequences identified the Tamura 3-parameter model with gamma distribution (T92+G) as the best fit using Akaike Information Criterion (AIC), Bayesian Information Criterion (BIC), and divergence estimation criterion (Kalyaanamoorthy et al. 2017). The analyses employed the bootstrapping method with 1000 replications using default parameters. A monophyletic clade comprising multiple individuals and exhibiting a bootstrap value greater than 60% in phylogenetic trees indicated successful species identification (Meier et al., 2006). Sequence divergence and pairwise distance estimations were also analysed in MEGA11 for their resolution inference. The guanine-cytosine (%GC) content was calculated for the ITS sequences of each species. The formula to calculate the %GC content, according to Altschul et al. (1990), is shown below.

$$\%\text{GC content} = \left(\frac{\text{Number of G bases} + \text{Number of C bases}}{\text{Total number of bases}}\right) \times 100\%$$

Table 1
List of Avicennia *species used in the molecular analysis in this study, including the length of its base pair sequences*

No.	Species	Geographic distributions	Accession number	ITS length (bp)
		Present study		
1.	*Avicennia alba*	Pulau Bagan Pinang	MY050304.1	695
2.	*Avicennia alba*	Pulau Bagan Pinang	MY050304.2	695
3.	*Avicennia alba*	Pulau Bagan Pinang	MY050304.3	695
4.	*Avicennia alba*	Pulau Burong	MY050304.10	695
5.	*Avicennia alba*	Sungai Kemasik	MY110307.1	695
6.	*Avicennia alba*	Sungai Kemasik	MY110307.2	695
7.	*Avicennia alba*	Sungai Kemasik	MY110307.3	695
8.	*Avicennia alba*	Pulau Merambong	MY010207.9	695
9.	*Avicennia alba*	Pulau Merambong	MY010207.10	695
10.	*Avicennia alba*	Pulau Merambong	MY010207.11	695
11.	*Avicennia alba*	Pulau Kamat	MY040310.1	695
12.	*Avicennia alba*	Pulau Kamat	MY040310.2	695
13.	*Avicennia marina*	Pulau Bagan Pinang	MY050304.4	694
14.	*Avicennia marina*	Pulau Bagan Pinang	MY050304.5	694
15.	*Avicennia marina*	Pulau Bagan Pinang	MY050304.6	694
16.	*Avicennia marina*	Pulau Burong	MY050304.11	694
17.	*Avicennia marina*	Pulau Burong	MY050304.12	694
18.	*Avicennia marina*	Pulau Burong	MY050304.13	694
19.	*Avicennia marina*	Pulau Merambong	MY010207.12	694
20.	*Avicennia marina*	Pulau Merambong	MY010207.13	694
21.	*Avicennia marina*	Pulau Merambong	MY010207.14	694
22.	*Avicennia rumphiana*	Pulau Merambong	MY010207.15	695
23.	*Avicennia rumphiana*	Pulau Merambong	MY010207.16	695
24.	*Avicennia rumphiana*	Pulau Merambong	MY010207.17	695
25.	*Avicennia rumphiana*	Sungai Kemasik	MY110307.4	695
26.	*Avicennia rumphiana*	Sungai Kemasik	MY110307.5	695
27.	*Avicennia rumphiana*	Sungai Kemasik	MY110307.6	695
		Other locations		
28.	*Avicennia alba*	India	MH243935.1	688
29.	*Avicennia. alba*	United States	EF540977.1	653
30.	*Avicennia alba*	Vietnam	MG880036.1	570
31.	*Avicennia alba*	Vietnam	MG880030.1	570
32.	*Avicennia alba*	China	KX641594.1	666
33.	*Avicennia marina*	India	MH243938.1	689
34.	*Avicennia marina*	United States	EF540978.1	652
35.	*Avicennia marina*	Saudi Arabia	MK027295.1	640
36.	*Avicennia marina*	United Kingdom	MN883387.1	647

Table 1 (*continue)*

No.	Species	Geographic distributions	Accession number	ITS length (bp)
37.	*Avicennia marina*	Thailand	KT004470.1	468
38.	*Avicennia marina*	China	MF063712.1	549
39.	*Avicennia marina* subsp. *australasica*	United States	AF365978.1	671
40.	*Avicennia marina* subsp. *australasica*	China	KX641591.1	666
41.	*Avicennia marina* subsp. *eucalyptifolia*	China	KX641592.1	666
42.	*Avicennia marina* subsp. *marina*	China	KX641593.1	666
43.	*Avicennia marina* var. *rumphiana*	China	KX641595.1	666
44.	*Avicennia bicolor*	United States	EF540989.1	652
45.	*Avicennia germinans*	United States	EF540985.1	652
46.	*Avicennia germinans*	China	KX641596.1	667
47.	*Avicennia germinans*	Brazil	AB861217.1	648
48.	*Avicennia officinalis*	India	MH243949.1	688
49.	*Avicennia officinalis*	India	KJ784553.1	669
50.	*Avicennia officinalis*	China	KX641597.1	665
51.	*Avicennia officinalis*	Vietnam	MG880054.1	569
52.	*Avicennia schaueriana*	United States	EF540986.1	652
53.	*Avicennia schaueriana*	Brazil	AB861406.1	646
54.	*Sonneratia alba*	China	KJ511914.1	626
55.	*Sonneratia caseolaris*	China	AF420219.1	631

RESULTS

Leaf Morphology and Morphometric Variation Among *Avicennia* Species

Leaf shapes among *Avicennia* species vary, even within the same species at different locations (Figure 2). *Avicennia alba* leaves from Pulau Bagan Pinang, Pulau Burong, Pulau Kamat, and Pulau Merambong are lanceolate with sharply pointed apices (Figure 2a). In contrast, *A. alba* leaves from Sungai Kemasik are elliptic (Figure 2b) or obovate (Figure 2c), with acute to nearly rounded apices. *Avicennia marina* leaves from Pulau Bagan Pinang, Pulau Burong, and Pulau Merambong exhibit variations, including leaf curling and blade shapes that range from elliptic with acute (Figure 2d) to cuspidate (Figure 2e) apices and ovate shapes with obtuse apices (Figure 2f). *Avicennia rumphiana* leaves from Pulau Merambong and Sungai Kemasik (Figure 2g-i) are elliptic to oblong with acute to rounded apices. Additional details on morphological and morphometric differences for each individual species are provided in Tables 2–4.

Leaf size and thickness vary among *Avicennia* species, with statistical analysis (one-way ANOVA) showing significant differences in the five collection sites ($p < 0.05$) (Tables 2-4). *Avicennia alba* on the islands of Pulau Bagan Pinang, Pulau Burong, Pulau Kamat, and Pulau Merambong had shorter leaf lengths, narrower widths, and thicker leaves compared

to those along the open coast riverine of Sungai Kemasik (Table 2). *Avicennia marina* showed slight variation, with leaf sizes and thickness similar to those of the islands (Pulau Bagan Pinang, Pulau Burong and Pulau Merambong) (Table 3). *Avicennia rumphiana* from Pulau Merambong had shorter leaf lengths, narrower widths, and thicker leaves than those growing along Sungai Kemasik (Table 4).

Based on a dendrogram, the hierarchical clustering (HC) analysis classified the 27 *Avicennia* samples into three major clusters (Figure 3, Table 5), with a Euclidean distance of 47.5%. Cluster 1 consisted of both *A. alba* and *A. marina*, encompassing most samples. Cluster 2 was exclusively comprised of *A. alba*, characterised by the longest leaf lengths among all samples, ranging from 8.66 cm to 9.13 cm. Cluster 3 represented *A. marina* and *A. rumphiana* mixed. These results highlight the variation in leaf morphometrics among *Avicennia* species, which could lead to overlapping species classifications when considering samples from different study sites, with *A. alba* displaying the longest leaf lengths.

Phylogenetic Position of *Avicennia* Species Based on ITS Sequences

The *Avicennia* species were classified into four strongly supported clades (Clades 1 to 4), with bootstrap supports ranging from 83% to 100%, yielded in the most suitable sequence alignment using Maximum Likelihood (ML) analysis (Figure 4). All *Avicennia* accessions occupied separate topological positions, indicating no overlap

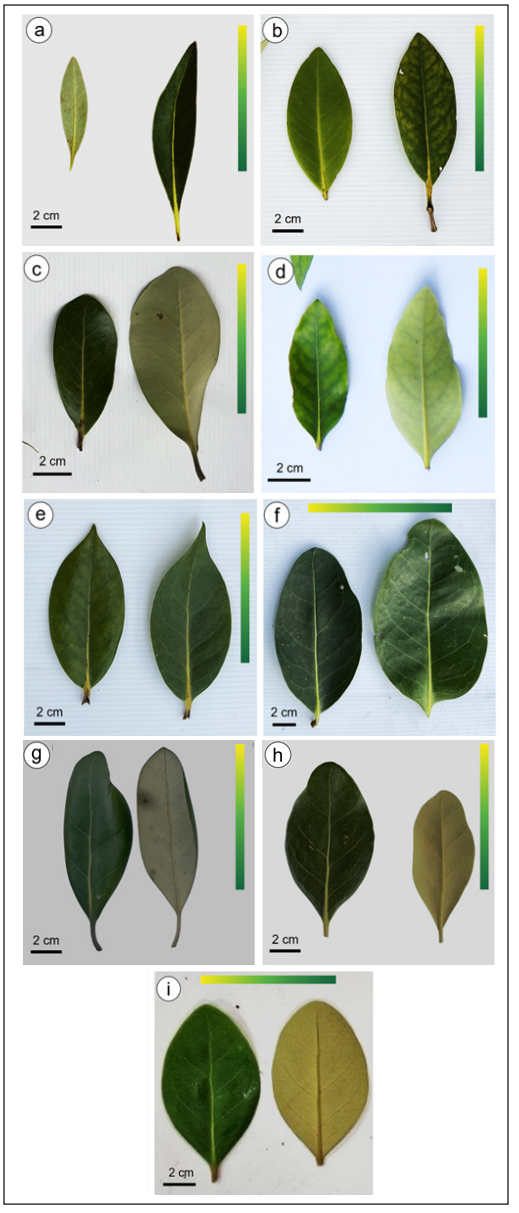

Figure 2. Leaf morphology variability of *Avicennia* species. (a) Lanceolate shape with sharply pointed apex; (b) elliptic shape with acute apex; (c) obovate shape with almost rounded apex of *Avicennia alba*; (d) Elliptic shape with acute to e) cuspidate apex; (f) ovate shape with obtuse apex of *A. marina*; and (g) oblong shape with acute apex, (h) elliptic shape with acute to (i) rounded apex of *A. rumphiana*. The scale bar (2 cm) indicates measurements, and the colour bar represents leaf colour variation from dark green to yellowish green

Table 2
Morphological leaf characteristics and ANOVA results (mean ± standard deviation and ranges) from morphometric measurements of Avicennia alba *in different sites*

	Morphology						Morphometric		
Study sites	**Blade shape**	**Margin**	**Apex**	**Base**	**Upper surface**	**Under surface**	**Length (cm)**	**Width (cm)**	**Thickness (mm)**
Pulau Bagan Pinang									
MY050304.1	Lanceolate	Entire	Sharply pointed	Acute	Smooth dark green	Smooth silvery grey	7.95±1.06^{def} (6.0-9.8)	2.85±0.62^{ab} (1.5-4.0)	0.42±0.05^{b} (0.36-0.50)
MY050304.2	Lanceolate	Entire	Sharply pointed	Acute	Smooth dark green	Smooth silvery grey	7.76±1.27^{def} (6.0-11.0)	2.57±0.61^{bc} (1.4-3.9)	0.42±0.05^{b} (0.36-0.50)
MY050304.3	Lanceolate	Entire	Sharply pointed	Acute	Smooth dark green	Smooth silvery grey	7.99±1.44^{cde} (6.0-10.8)	2.58±0.55^{bc} (1.4-3.4)	0.42±0.06^{b} (0.36-0.54)
Pulau Burong									
MY050304.10	Lanceolate	Entire	Sharply pointed	Acute	Smooth dark green	Smooth silvery grey	8.39±1.23^{bcd} (6.0-11.0)	2.54±0.63^{c} (1.5-4.0)	0.51±0.02^{a} (0.45-0.55)
Pulau Kamat									
MY040310.1	Lanceolate	Entire	Sharply pointed	Acute	Smooth dark green	Smooth silvery grey	7.72±1.15^{def} (6.0-10.2)	2.49±0.58^{c} (2.0-5.0)	0.52±0.07^{a} (0.42-0.76)
MY040310.2	Lanceolate	Entire	Sharply pointed	Acute	Smooth dark green	Smooth silvery grey	7.77±1.16^{def} (6.0-10.2)	2.46±0.58^{c} (2.0-5.0)	0.51±0.05^{a} (0.42-0.70)
Pulau Merambong									
MY010207.9	Lanceolate	Entire	Sharply pointed	Acute	Smooth dark green	Smooth silvery grey	7.32±0.91^{ef} (5.7-9.0)	2.40±0.45^{cd} (1.7-3.1)	0.39±0.13^{bc} (0.24-0.75)
MY010207.10	Lanceolate	Entire	Sharply pointed	Acute	Smooth dark green	Smooth silvery grey	7.24±0.73^{f} (5.0-8.6)	1.90±0.24^{e} (1.2-2.4)	0.37±0.09^{cd} (0.20-0.54)
MY010207.11	Lanceolate	Entire	Sharply pointed	Acute	Smooth dark green	Smooth silvery grey	7.39±0.88^{ef} (5.6-9.3)	2.16±0.41^{de} (1.4-3.0)	0.34±0.07^{d} (0.22-0.46)
Sungai Kemasik									
MY110307.1	Elliptic	Entire	Acute	Acute	Smooth dark green	Smooth silvery grey	8.66±1.51^{abc} (7.0–11.2)	3.02±0.41^{a} (2.1–4.0)	0.23±0.04^{e} (0.18–0.33)

Table 2 *(continue)*

	Morphology						Morphometric		
Study sites	**Blade shape**	**Margin**	**Apex**	**Base**	**Upper surface**	**Under surface**	**Length (cm)**	**Width (cm)**	**Thickness (mm)**
MY110307.2	Elliptic and obovate	Entire	Acute and almost rounded	Acute	Smooth dark green	Smooth silvery grey	8.71±1.55^{ab} (6.0–11.9)	3.00±0.61^{a} (2.0-4.0)	0.23±0.05^{e} (0.13–0.31)
MY110307.3	Elliptic	Entire	Acute and sharply pointed	Acute	Smooth dark green	Smooth silvery grey	9.13±1.84^{a} (5.0–11.7)	3.03±0.65^{a} (2.0–4.5)	0.23±0.04^{e} (0.18–0.31)
						df	11	11	11
						MS	10.82	3.68	0.35
						F	6.77	12.48	79.06
						p-value	0.000	0.001	0.001

Note. The varying superscript alphabet in the same column demonstrates the contrast at $p < 0.05$ (ANOVA Duncan's post hoc test)

Table 3
Morphological leaf characteristics and ANOVA results (mean ± standard deviation and ranges) from morphometric measurements of Avicennia marina *in different sites*

	Morphology						Morphometric		
Study sites	**Blade shape**	**Margin**	**Apex**	**Base**	**Upper surface**	**Under surface**	**Length (cm)**	**Width (cm)**	**Thickness (mm)**
Pulau Bagan Pinang									
MY050304.4	Elliptic, curling	Entire	Acute	Acute	Smooth, green	Smooth, pale green	7.14±0.93^{ab} (4.0–8.9)	3.28±0.57^{a} (2.0–4.1)	0.43±0.11^{a} (0.28–0.56)
MY050304.5	Elliptic, curling	Entire	Acute, obtuse, cuspidate	Acute	Smooth, green	Smooth, pale green	7.52±1.26^{a} (4.5–10.0)	3.51±0.85^{a} (2.0–5.0)	0.46±0.09^{a} (0.28–0.56)
MY050304.6	Elliptic, curling	Entire	Acute, obtuse	Acute	Smooth, green	Smooth, pale green	7.60±1.32^{a} (4.9–9.8)	3.52±0.64^{a} (2.0–4.6)	0.43±0.10^{a} (0.28–0.56)
Pulau Burong									
MY050304.11	Elliptic, curling	Entire	Acute	Acute	Smooth, green	Smooth, pale green	7.35±0.93^{a} (5.6–9.0)	2.66±0.35^{c} (2.0–3.2)	0.35±0.04^{b} (0.25–0.40)

Table 3 *(continue)*

Study sites	Morphology						Morphometric		
	Blade shape	Margin	Apex	Base	Upper surface	Under surface	Length (cm)	Width (cm)	Thickness (mm)
MY050304.12	Elliptic, curling	Entire	Acute, obtuse	Acute	Smooth, green	Smooth, pale green	7.14±1.10^{ab} (4.5–9.1)	2.45±0.44^{c} (1.6–3.1)	0.32±0.05^{b} (0.22–0.40)
MY050304.13	Elliptic, curling	Entire	Acute, obtuse	Acute	Smooth, green	Smooth, pale green	7.04±0.95^{ab} (4.5–9.0)	2.71±0.37^{bc} (1.9–3.6)	0.30±0.05^{bc} (0.23–0.40)
Pulau Merambong									
MY010207.12	Elliptic, curling	Entire	Acute	Acute	Smooth, green	Smooth, pale green	7.06±0.81^{ab} (5.7–8.9)	2.97±0.56^{b} (2.0–4.0)	0.27±0.05^{c} (0.19–0.38)
MY010207.13	Elliptic, curling	Entire	Acute	Acute	Smooth, green	Smooth, pale green	6.60±0.89^{b} (5.0–8.9)	2.64±0.56^{c} (1.8–4.0)	0.27±0.04^{c} (0.20–0.34
MY010207.14	Elliptic and ovate, curling	Entire	Acute, obtuse	Acute	Smooth, dark green	Smooth, pale green	6.61±0.80^{b} (5.0–8.9)	3.57±0.64^{a} (2.0–3.3)	0.27±0.10^{c} (0.19–0.56)
						df	8	8	8
						MS	3.67	5.83	0.17
						F	3.57	17.83	39.06
						p-value	0.000	0.000	0.000

Note. The varying superscript alphabet in the same column demonstrates the contrast at $p < 0.05$ (ANOVA Duncan's post hoc test)

Table 4
Morphological leaf characteristics and ANOVA results (mean ± standard deviation and ranges) from morphometric measurements of Avicennia rumphiana *in different sites*

Study sites	Morphology						Morphometric		
	Blade shape	Margin	Apex	Base	Upper surface	Under surface	Length (cm)	Width (cm)	Thickness (mm)
Pulau Merambong									
MY010207.15	Elliptic	Entire	Acute, rounded	Acute, rounded	Smooth, green	Densely pubescent, yellow-green	7.18±0.64^{bc} (5.7–8.6)	3.13±0.45^{b} (2.0–4.0)	0.28±0.04^{a} (0.20–0.34)

Table 4 *(continue)*

	Morphology						Morphometric		
Study sites	**Blade shape**	**Margin**	**Apex**	**Base**	**Upper surface**	**Under surface**	**Length (cm)**	**Width (cm)**	**Thickness (mm)**
MY010207.16	Elliptic and oblong	Entire	Rounded	Acute, rounded	Smooth, dark green	Densely pubescent, yellow-green	7.14±0.71^{c} (5.0–8.0)	3.22±0.53^{b} (2.0–4.3)	0.28±0.04^{a} (0.20–0.34)
MY010207.17	Elliptic and oblong	Entire	Rounded	Acute, rounded	Smooth, dark green	Densely pubescent, yellow-green	7.13±0.66^{c} (5.7–8.0)	3.06±0.45^{b} (2.0–4.0)	0.28±0.04^{a} (0.18–0.34)
Sungai Kemasik									
MY110307.4	Elliptic	Entire	Acute, rounded	Acute, rounded	Smooth, green	Densely pubescent, yellow-green	7.74±0.66^{a} (6.0–9.0)	4.20±0.35^{a} (3.0–5.0)	0.21±0.07^{b} (0.09–0.34)
MY110307.5	Elliptic	Entire	Acute, rounded	Acute, rounded	Smooth, dark green	Densely pubescent, yellow-green	7.66±0.44^{a} (6.7–8.2)	4.28±0.34^{a} (3.8–5.0)	0.21±0.03^{b} (0.10–0.29)
MY110307.6	Elliptic	Entire	Acute, rounded	Acute, rounded	Smooth, dark green	Densely pubescent, yellow-green	7.48±0.46^{ab} (5.0–9.0)	4.32±0.34^{a} (4.0–5.0)	0.22±0.06^{b} (0.17–0.29)
						df	5	5	5
						MS	2.24	11.62	0.04
						F	6.21	66.76	21.78
						p-value	0.000	0.000	0.000

Note. The varying superscript alphabet in the same column demonstrates the contrast at $p < 0.05$ (ANOVA Duncan's post hoc test)

Table 5
Distribution of Avicennia *species based on leaf morphometrics in different clustering classes*

Clustering class	No. of species	Within-class variance	Minimum distance to the centroid	Average distance to the centroid	Maximum distance to the centroid	Species
1	13	0.292	0.214	0.464	0.933	*A. alba* and *A. marina*
2	3	0.067	0.124	0.198	0.297	*A. alba*
3	11	0.369	0.276	0.544	0.820	*A. marina* and *A. rumphiana*

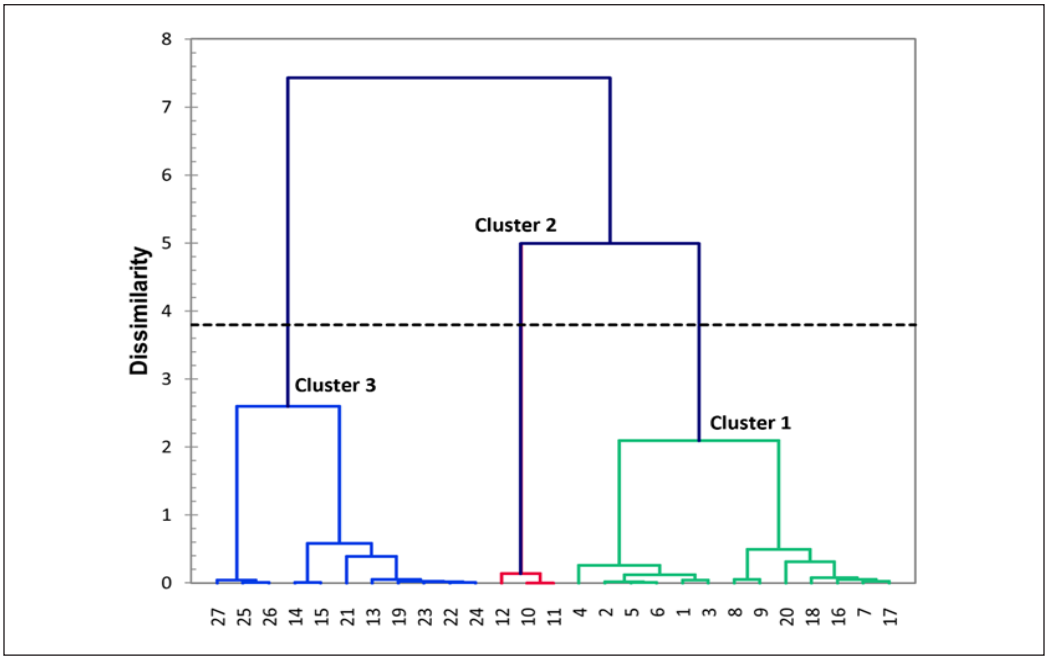

Figure 3. Dendrogram showing the classes of hierarchical clustering of the variability leaf morphometric (leaf lengths, widths and thickness) among 27 samples of *Avicennia* species

among species observed. In Clade 1, *A. alba* from this study was clustered with *A. alba* from other geographic distributions (Vietnam, India, China, and the United States of America supported by a high bootstrap value of 100%. Clade 2 was separated into two subclades supporting the 80% bootstrap. In this clade, *A. rumphiana* from this study formed a subclade with *A. marina* var. *rumphiana* from China with a 99% bootstrap value, whereas *A. officinalis* from other geographic distributions fell outside these subclades with an 80% bootstrap value. Clade 3 consisted of *A. marina* accessions with a moderately strong BS value of 83. Eleven subclades based on species similarities were formed in Clade 3, including *A. marina* and *A. marina* subsp. *australasica, A. marina* subsp. *marina* and *A. marina* subsp. *eucalyptifolia.* Only two subclades were clustered in the same group. In contrast, other accessions were well segregated into separated subclades based on their genetic sequences' dissimilarity, supported by BS values ranging from 61% to 95%. Clade 4 comprised three *Avicennia* accessions*:* (1) *A. bicolor*, (2) *A. germinans* and (3) *A. schaueriana*, which were retrieved from GenBank, with a bootstrap value of 99%.

Table 6 presents the final alignment of 27 nrITS sequences from *Avicennia* species with total nucleotides ranging from 643 to 695. The percentage of guanine-cytosine (%GC) content for *A. alba* ranges from 63.6% to 64.2% (695 base pairs). For *A. marina*, the %GC content ranges from 64.2% to 64.6% (694). Meanwhile, *A. rumphiana* exhibits a varied %GC content ranging from 63.5% to 64.6% across the 643 to 695 nucleotides.

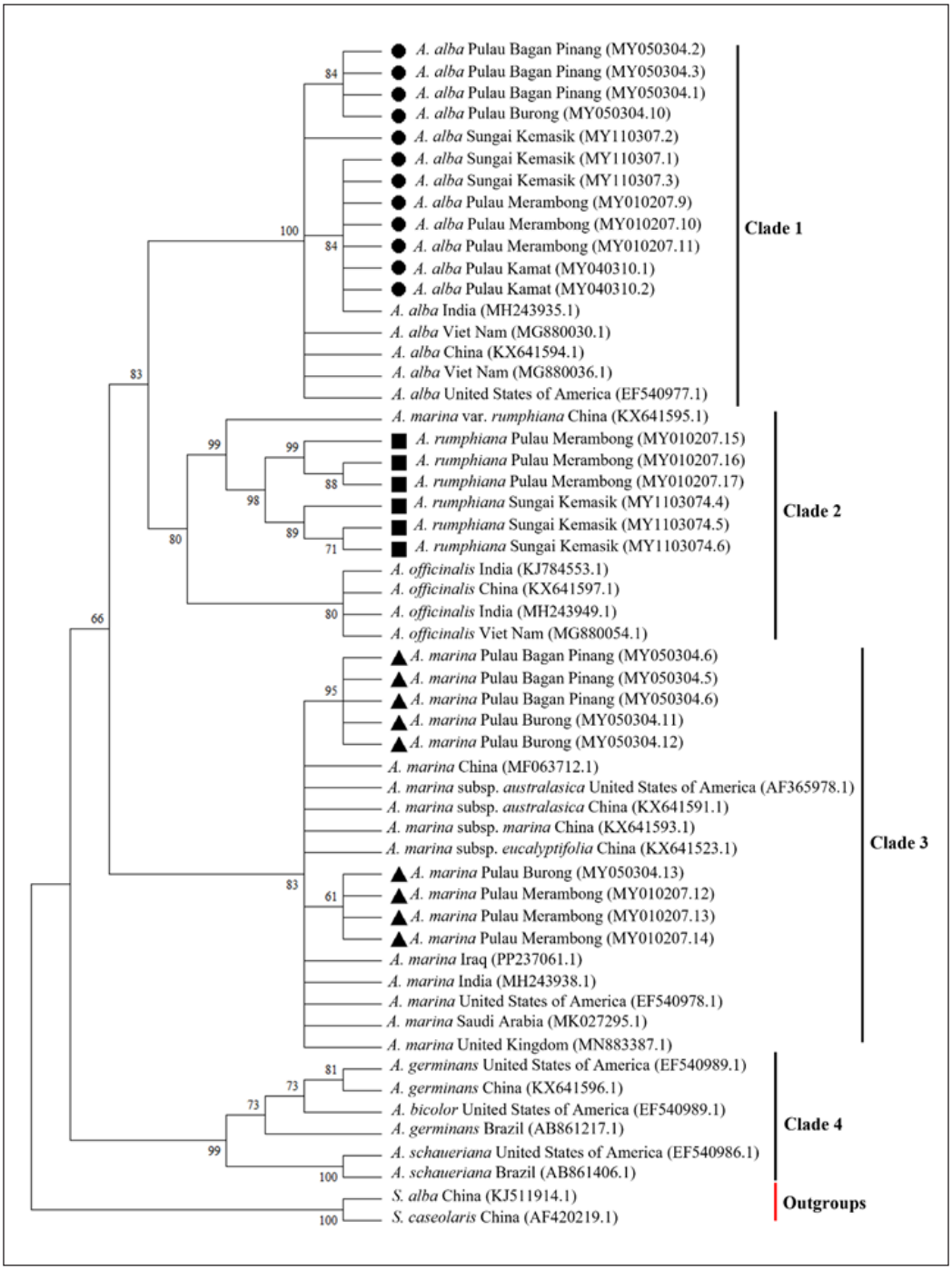

Figure 4. Phylogenetic tree of *Avicennia* species inferred from Maximum Likelihood (ML) analysis using 696 base pairs (bp) of 55 nucleotide sequences nrDNA ITS1, 5.8S rDNA, and ITS2. Bootstrap support values above 60% are shown on branches

Note. Shapes on the nodes of the phylogenetic tree indicated accessions obtained from this study

Table 6
Nucleotide composition (%) of the sequenced Avicennia *species from different sites*

Sites, species and accession number	Nucleotide composition (%)				Total number of nucleotides
	T(U)	C	A	G	
Pulau Bagan Pinang					
A. alba (MY050304.1)	16.0	33.2	20.4	30.4	695
A. alba (MY050304.2)	16.0	33.2	20.4	30.4	695
A. alba (MY050304.3)	16.0	33.2	20.4	30.4	695
Pulau Burong					
A. alba (MY050304.10)	16.0	33.2	20.4	30.4	695
Pulau Kamat					
A. alba (MY040310.1)	15.8	33.2	20.0	30.9	695
A. alba (MY040310.2)	15.8	33.2	20.0	30.9	695
Pulau Merambong					
A. alba (MY010207.9)	15.8	33.2	20.0	30.9	695
A. alba (MY010207.10)	15.8	33.2	20.0	30.9	695
A. alba (MY010207.11)	15.8	33.2	20.0	30.9	695
Sungai Kemasik					
A. alba (MY110307.1)	15.8	33.2	20.0	30.9	695
A. alba (MY110307.2)	15.8	33.2	20.3	30.6	695
A. alba (MY110307.3)	15.8	33.2	20.0	30.9	695
Pulau Bagan Pinang					
A. marina (MY050304.4)	16.3	33.1	19.5	31.1	694
A. marina (MY050304.5)	16.3	33.1	19.5	31.1	694
A. marina (MY050304.6)	16.3	33.1	19.5	31.1	694
Pulau Burong					
A. marina (MY050304.11)	16.3	33.1	19.5	31.1	694
A. marina (MY050304.12)	16.3	33.1	19.5	31.1	694
A. marina (MY050304.13)	16.0	33.1	19.3	31.4	694
Pulau Merambong					
A. marina (MY010207.12)	16.0	33.1	19.3	31.4	694
A. marina (MY010207.13)	16.0	33.1	19.3	31.4	694
A. marina (MY010207.14)	16.0	33.1	19.3	31.4	694
Pulau Merambong					
A. rumphiana (MY010207.15)	15.6	34.1	19.8	30.6	643
A. rumphiana (MY010207.16)	15.3	33.3	21.0	30.4	694
A. rumphiana (MY010207.17)	15.3	33.4	21.2	30.2	695
Sungai Kemasik					
A. rumphiana (MY110307.4)	15.4	33.4	20.9	30.4	695
A. rumphiana (MY110307.5)	15.4	33.4	20.9	30.4	695
A. rumphiana (MY110307.6)	15.4	33.4	20.9	30.4	695

Note. T = Thymine, C = Cytosine, A = Adenine, G = Guanine. The nucleotide composition (%) was analyzed using MEGA11

ITS Sequence Similarity Between *Avicennia* Species

The evolutionary divergence and pairwise distances of ITS sequences among species of *Avicennia* are detailed in Supplementary Tables 1, 2 and 3. *Avicennia alba* from various locations, including India, Vietnam, China, and the United States, are identical or exhibit 99.4% ITS sequence similarity (4-bp difference) (Supplementary Table 1). In Clade 3, *A. marina* exhibits a high sequence 99.2%–100% similarity (5-6-bp difference) in the ITS region with *A. marina* from other locations (Supplementary Table 2). In Clade 2, *A. rumphiana* from Pulau Merambong and Sungai Kemasik exhibit high ITS sequence 99%–100% similarity (7-bp difference) (Supplementary Table 3). *Avicennia rumphiana* and *A. marina* var. *rumphiana* share ITS sequences of 98.9% similarities (7-8-bp difference). However, *A. rumphiana* and *A. officinalis* show relatively lower ITS sequence 96.4%–96.7% similarity 22–25-bp difference). Thus, within this clade, the ITS sequences of *A. marina* var. *rumphiana* accession from China (KX641595.1) are similar to the *A. rumphiana* sequences in the present study.

The molecular distances between (interspecific variation) and within (intraspecific variation) species were analysed using the Tamura 3-parameter model (Table 7). Interspecific variation showed variation ranging from 3.56% to 6.61%. The value of the closest molecular distance (3.56%) was between *Avicennia alba* and *A. marina*, while the furthest is between *A. alba* and *A. rumphiana*. The intraspecific variation within *A. rumphiana* (1.57%) was the highest, while *A. alba* (0.29%) and *A. marina* (0.24%) share similarly low variation.

Table 7
Estimates of average evolutionary divergence over sequence pairs between species (interspecific variation) and within species (intraspecific variation)

Clades	**Interspecific variation**			**Intraspecific variation (%)**
	A. alba	*A. marina*	*A. rumphiana*	
A. alba		3.56%	6.61%	0.29%
A. marina	0.0356		6.50%	0.24%
A. rumphiana	0.0661	0.0650		1.57%

DISCUSSION

Variation in Leaf Morphology and Morphometric

The present study represents six leaf morphological characteristics (Tables 2–4) for consideration in identifying different species of *Avicennia*. Due to divergent evolution, *Avicennia* species exhibit varied taxonomic descriptions (Thatoi et al., 2016). Krauss et al. (2023) have previously reported that environmental conditions play a significant

role in shaping the leaf morphology variation of mangroves, including species within the *Avicennia*, as they adapt to the ecological challenges of mangrove habitats.

Studies in Malaysia by Rahman et al. (2023) at the mangrove estuarine wetland of Setiu in Terengganu and by Cheah (2016) at the riverine Linting wetlands describe *A. alba* leaves as having a silvery-grey or white colouration with a silvery upper surface, consistent with the findings of this study. *Avicennia alba* is also distinguished from other *Avicennia* species by their narrow and lanceolate leaves (An et al., 2022). These descriptions align with the characteristics of *A. alba* observed on the islands of Pulau Bagan Pinang, Pulau Burong, Pulau Merambong, and Pulau Kamat. Such leaf trait differences along the estuary of Sungai Kemasik are difficult to apply due to variations in individual trees, particularly in leaf blade shape and apex shape characteristics. In this context, the *A. alba* leaves from Sungai Kemasik exhibit a contrasting leaf shape, being elliptic to ovate with almost rounded and acute apex shapes instead of the sharply pointed characteristics observed in leaves from the islands.

However, previous studies have also described a range of leaf shape characteristics such as broadly elliptical leaves along the coastal areas of Northern Mindanao, Philippines (Osing et al., 2019), lanceolate at the estuary of East Kalimantan, Indonesia (Saptiani et al., 2018), and ovate at the sea fringe of Kien Giang, Vietnam (Duke, 2012). Hence, the leaf blade and apex shape were the leaf characteristics that further divided *A. alba* into two primary groups within the species in this study. It should be noted that the *A. alba* considered in the present study were exposed to different environmental conditions. Thus, the differences between the leaf characteristics observed would have been mainly due to the interaction with the particular environment of the location. This suggestion of leaf within *A. alba* differed and required comparable studies in different environmental conditions globally.

The leaf characteristics of *A. marina* have been extensively documented in previous studies. Leaves have been described as elliptical at the eastern coasts of Thailand (Huang et al., 2014) and on sheltered shores of Malaysia (Shin et al., 2015), ovate along the coastal areas of Indonesia (Noor et al., 2012), and occasionally lanceolate at the sea fringe of Kien Giang, Vietnam (Duke, 2012). They have also detailed the apex shape of *A. marina* as acute, obtuse, almost rounded, slightly acuminate, or variably pointed. These descriptions are consistent in this study's different sampling sites for *A. marina*, where both elliptic and ovate leaf shapes were reported, particularly in Pulau Merambong. The elliptic shape was consistently observed in other study sites (Pulau Bagan Pinang, Pulau Burong and Pulau Merambong). The elliptic and ovate shape of *A. marina* aligns more closely with the descriptions found in previous studies, particularly in Malaysia, Thailand and Indonesia, while the lanceolate shape is less frequently reported. It is important to differentiate *A. marina* from *A. alba* found in Sungai Kemasik, as their leaf characteristics can overlap,

potentially leading to confusion. Thus, a key identifier for *A. marina* is the presence of leaves with curled margins. The leaf feature differentiates it from *A. alba*. Win et al. (2021) and Primavera (2004) also described that the leaf blades range from flat to curly.

Further, the comparative assessment shows that the leaf of *A. rumphiana* can easily be distinguished from *A. alba* and *A. marina*, notably the presence of powdery hairs on *A. rumphiana* hairy undersurface leaves, a trait absent in the characteristics of the other two species. This characteristic was also identified in previous morphology assessments by Prakashamani et al. (2019) and Mariano et al. (2019). *Avicennia rumphiana,* primarily found in Pulau Merambong and Sungai Kemasik, was classified as vulnerable by the International Union for Conservation of Nature (IUCN, 2024). Previously, *A. rumphiana* was identified as *A. lanata*, with its distribution ranging from Peninsular Malaysia and the Philippines to New Guinea (Giesen et al., 2007). Blade shapes of *A. rumphiana* observed at Pulau Merambong and Sungai Kemasik include elliptic, oblong and obovate with both acute and rounded apexes. In the present study, the leaf morphology of *A. rumphiana* showed only slight distinctions compared to reports from other regions. The leaf blades in this study were elliptic to ovate with acute bases, aligning with descriptions of *A. rumphiana* along the east coast of Peninsular Malaysia (Shin et al., 2015), the mangrove estuarine areas of Setiu wetlands in Terengganu (Rahman et al., 2023), and in the Panay Islands, Philippines (Primavera et al., 2004).

However, this differs slightly from *A. rumphiana* in the Zamboanga del Sur coastal areas of the Philippines (Mariano et al., 2019) and at the sea fringe of Kien Giang, Vietnam (Duke, 2015), which described the species with elliptic to ovate leaves characterised by a rounded base. Primavera et al. (2004), Mariano et al. (2019) and Chan et al. (2022), along with the present study, reported a yellowish-green leaf undersurface covered with dense hairs. In contrast, Huang et al. (2014) reported a russet, tomentose, nearly brown undersurface on the eastern coasts of Thailand, while Duke (2012) noted similar characteristics at the sea fringe of Kien Giang, Vietnam. These variations highlight the distinct leaf characteristics of *A. rumphiana* species, reflecting their variability that may be attributed to geographic distribution or local environmental conditions.

Moreover, the dark green colouration on the upper surface and the presence of dense powdery hairs undersurface were noted as common traits in these studies. *Avicenna rumphiana* is often misidentified as *A. officinalis* due to their similarities in hairy leaves, as described by Selvam and Karunagaran (2004). However, as outlined by Primavera et al. (2004), *A. officinalis* exhibits shiny and glossy upper surface leaves, contrasting with the dull dark green surface of *A. rumphiana*, a similarity noted in the leaf surface observation of *A. rumphiana* in this study as well. Additional distinctions observed in various studies include those by Primavera et al. (2004), who highlighted differences such as the yellowish-to-russet tomentose undersurface of *A. rumphiana* leaves, as opposed to the yellowish-green

undersurfaces of *A. officinalis* (Cheah, 2016). Therefore, in morphological comparison, *A. rumphiana* demonstrates morphological similarities consistent with previous studies.

Leaf characteristics, including length, width, thickness, perimeter, area, and mass, are crucial indicators of mangrove health, productivity, and overall condition (Dookie et al., 2023). These measurements serve as a basis for calculating additional leaf parameters, including leaf-specific area, leaf mass per area, density, relative water content, and sclerophylly indices (Liu et al., 2017). Primavera et al. (2004) summarised the leaf descriptions of the mangroves in the Philippines based on the leaf length and width. One-way ANOVA and Duncan's post hoc tests indicated significant differences ($p < 0.05$) in all leaf parameters among *Avicennia* species, indicating leaf size variation within the genus. According to Duncan's post hoc analysis, it is suggested that the leaf width of *A. alba* may reach widths of up to 4.0 cm, potentially overlapping with the broader leaf widths observed in *A. marina*. This similarity in leaf width between the two species could lead to confusion during field identification. Despite variations observed within species, particularly in leaf width between island populations and those near Sungai Kemasik, the range of width measurements for *A. alba* leaves remains consistent with previous studies. Primavera et al. (2004) reported widths ranging from 2 to 5 cm, while Duke (2012) noted widths between 2.0 and 4.6 cm.

Similarly, the average length and width of *A. marina* closely match Duke's (1990) findings, ranging from 7.3 to 8.2 cm in length and 5 to 8 cm in width. Saenger and Brooks (2008) and Ahmed et al. (2022) also reported similar widths, ranging from 1.9 to 4.3 cm. Our measurements for *A. rumphiana* also fall within the ranges identified by Primavera et al. (2004) and Mariano et al. (2019). Several studies, including those by Barhoumi et al. (2021), Mollick et al. (2021), and Alam and Hossain (2023), utilise leaf measurements to assess responses to various environmental factors, such as soil and water salinity in mangroves rather than for species identification. Therefore, this study highlights the need for further research on leaf measurements to distinguish between different species.

Genetic Diversity Within the *Avicennia* Species

A common problem in identifying the *Avicennia* species is the variation in morphology and divergence within the genus (Nguyen et al., 2014). This variability makes species identification based on morphology challenging, especially outside the flowering season. Genetic methods offer a more reliable approach, particularly internal transcribed spacer (ITS). ITS are advantageous due to their easy amplification from small DNA quantities and moderate size (below 700 bp), which facilitates amplification and sequencing of high-degree variation even among closely related species (Bast et al., 2016). This study uses the ITS locus to represent Malaysia's *Avicennia* species' first DNA barcode-based biodiversity assessment. The genetic structure of Malaysian *Avicennia* has been examined

using nuclear microsatellites (Wee et al., 2013, 2020) and chloroplast sequences (Triest et al., 2021). A clear East-West genetic division has been identified in *A. marina* and *A. alba* Peninsular Malaysian populations based on microsatellite markers (Wee et al., 2020; Triest et al., 2021). All *Avicennia* accessions in this study were separated into four distinct clades, each supported by high bootstrap (BS) values. Our findings align with those of Li et al. (2016), who observed that *A. marina* and *A. officinalis* form distinct clusters separate from *A. rumphiana* and *A. alba*. Similarly, Saddhe et al. (2017) demonstrated the genetic distinctness of *A. alba* from *A. marina* and *A. officinalis* or *A. integra*. Our findings, where *A. alba*, further support this genetic separation. *Avicennia alba* formed a separate clade from other *Avicennia* species with a BS value of 83.

In Clade 2, *A. marina* var. *rumphiana* from China and *A. rumphiana* in this study show genetic association but with varying support, forming a cluster with *A. officinalis*. *Avicennia rumphiana*'s taxonomic history often leads to confusion with *A. marina* var. *rumphiana* and *A. lanata* (Duke, 1991). Ridley (1923) and Moldenke (1960) initially treated *A. lanata* and *A. marina* var. *rumphiana* as separate species. However, Duke (1991) later found their descriptions identical, recognising *A. rumphiana* as distinct and categorising *A. lanata* and *A. marina* var. *rumphiana* as synonyms. Despite this, the Catalogue of Life (Hassler, 2024) still recognises *A. rumphiana* as an accepted variety of *A. marina* (*A. marina* var. *rumphiana*) and noted its distribution in Southeast Asia, including Malaysia. However, we follow the taxonomy of *A. rumphiana* H. Hallier (*A. lanata*) as per Tomlinson (1986), Duke (1991) and Japar Sidik (1994), distinguishing it from *A. marina* var. *rumphiana*. This distinction is based on our morphological details of the leaves, which align with the botanical descriptions of *A. rumphiana* provided by Duke (1991) and Giesen et al. (2007).

These descriptions characterise the leaves as ovate or elliptic, dark green above, and covered with dense, fawn-coloured, velvety hairs on the undersurface. Our ITS sequencing has proven essential in assessing genetic relationships, revealing significant divergence between *A. rumphiana* and *A. marina*, as indicated by their grouping in separate clades (Clade 2 and Clade 3). The molecular evidence obtained from our analysis complements morphological descriptions, enhancing our understanding of the evolutionary relationships among these species and supporting the rationale for the recognition of *A. rumphiana* as a separate entity.

Guanine-cytosine (%GC) content determines genetic and species diversity (Liu et al., 2023). We observed consistent %GC content within *Avicennia*, ranging from 63.5% to 64.6%. Given the widespread use of ITS as a marker in plant systematics, our finding of consistent %GC content in *Avicennia* significantly contributes to our evolutionary model. It suggests similar genomic stability and nucleotide composition among the species.

Genetic pairwise distance is the standard measurement of genetic heterogeneity and the raw material for evolutionary change (Ellegren & Galtier, 2016). In our analysis, the

pairwise distance between *A. alba* clade sequences was the smallest (0.006), followed by *A. marina* (0.008), while *A. rumphiana* sequences exhibited the greatest distance (0.010). Literature suggests it typically shows 0–3 bp differences within a species (Lidén et al., 1995; Sun et al., 1994) and more than 3 bp differences between species (Sun et al., 1994). Our nucleotide differences (0.6%–1% sequence dissimilarity; 4–7-bp difference) support this hypothesis. Despite being collected from different sites, no evidence of hybridisation among taxa was found based on pairwise distance. This finding is consistent with Duke (1992), who also noted the absence of hybrids in *Avicennia* compared to other widely distributed mangrove genera. The pairwise distance among *A. alba* in this study ranged from 0.000 to 0.006 (4-bp difference), consistent with Rani et al. (2021), who reported a pairwise distance of 0.007 between *A. alba* from Sajnekhali, Sundarbans Delta and Kerala, India, indicating the coexist evolution. Both *A. alba* and *A. marina* had a slight intraspecific variation of 0.29 and 0.24%, respectively.

Avicennia rumphiana forms a distinct subclade within Clade 2 with a strong bootstrap support value of 99. However, this species has notable genetic diversity, as evidenced by a significant pairwise distance of 0.010 among individuals (1% sequence dissimilarity; 7-bp difference). Their intraspecific variation was also found to be high, at 1.57%. *Avicennia rumphiana* accession MY010207.17 from Pulau Merambong exhibits notably lower ITS sequence (99.3% sequence similarity; 5-base pair difference) compared to the other two accessions from the same location (MY010207.15 and MY010207.16). In contrast, it (MY010207.17) shares a higher ITS sequence (99.7% sequence similarity; 2-bp difference) with accessions from Sungai Kemasik. Distinct differences in leaf morphological traits further indicate this diversity. For instance, morphologically, there are differences between *A. rumphiana* accessions from Pulau Merambong, particularly MY010207.16 and MY010207.17, and those from Sungai Kemasik. The former displayed darker green leaves and differences in apex shapes (rounded), whereas the latter had lighter green leaves with acute to rounded apex shapes.

Although the classification remains genetically controversial, this study has resolved it using leaf morphological characteristics. The variability in genetic distance observed in *A. rumphiana* aligns with the differences in leaf morphology, demonstrating a clear relationship between genetic diversity and leaf characteristics. Therefore, by referencing botanical descriptions, we have placed the taxon under the species name *A. rumphiana*, as accepted in this study. These sequences were compared with those of *A. marina* var. *rumphiana*, *A. officinalis*, and other *Avicennia* species available in NCBI GenBank to determine their taxonomic positions.

As indicated by pairwise distance, genetic diversity within the *A. marina* was low (0.000-0.008), which aligns with findings reported by Malekmohammadi et al. (2022) using ITS. Similarly, using microsatellite markers, low genetic variation was observed

in *A. marina* populations in northern Australia (Maguire et al., 2002) and along the east coast of India (Zolgharnein et al., 2002), on Zifaf and Sajid islands in Vietnam (Giang et al., 2003). However, these previous studies assessed the genetic diversity of *A. marina* using microsatellite markers, which differs from the approach employed in this study, which utilised ITS.

CONCLUSION

The present study reassessed and confirmed *Avicennia* species identification and provided an overview of individuals' morphological and genetic variation. Morphological analysis revealed significant differences in six leaf characteristics and three morphometric traits ($p < 0.05$) of *Avicennia* leaf morphology. This study also utilised ITS sequences to better understand relationships within *Avicennia*. The ITS sequences of 27 *Avicennia* accessions and 26 accessions from other locations revealed four distinct clades (BS = 83-100). The consistent %GC content within *Avicennia* also indicates the level of genomic stability and nucleotide composition among the species. Despite significant divergence found in pairwise genetic distance among *Avicennia* accessions in Clade 2, the recognition of *A. rumphiana*'s taxonomic position is resolved based on evidence involving morphology, confirming its acceptance as a distinct species in this study. Leaf morphological differences further support the phylogenetic position that separates *A. rumphiana* from *A. marina* and *A. officinalis*. Therefore, our findings show that leaf morphological and genetic analyses are reliable for determining relationships in *Avicennia* and can contribute to refining species classifications and updating mangrove species records. These advances are crucial for effective biodiversity assessments.

ACKNOWLEDGEMENTS

This work was funded by Universiti Putra Malaysia under Geran Putra Inisiatif Siswazah (GP-IPS) (9713900) and Country Garden Pacificview Sdn. Bhd. The funders had no role in study design, data collection and analysis, decision to publish, or preparation of the manuscript. The authors thank the Department of Aquaculture, Faculty of Agriculture, Universiti Putra Malaysia, for providing the necessary facilities to conduct this research.

REFERENCES

Abou Seedo, K., Abido, M. S., Salih, A., & Abahussain, A. (2018). Morphophysiological traits of gray mangrove (*Avicennia marina* (Forsk.) Vierh.) at different levels of soil salinity. *International Journal of Forestry Research*, *2018*, 7404907. https://doi.org/10.1155/2018/7404907

Ahmed, M., Nazim, K., & Khan, M. U. (2022). Mangrove ecosystem with changing climate: A review. *International Journal of Biology and Biotechnology*, *19*(1), 77-88.

Alam, M. R., & Hossain, M. (2023). Salinity and parent-of-origins affect leaf neogenesis of *Avicennia officinalis* L. in the Sundarbans, Bangladesh. *Khulna University Studies*, *20*(2), 29-37. https://doi.org/10.53808/KUS.2023.20.02.966-ls

Altschul, S. F., Gish, W., Miller, W., Myers, E. W., & Lipman, D. J. (1990). Basic local alignment search tool. *Journal of Molecular Biology*, *215*, 403-410. https://doi.org/10.1016/S0022-2836(05)80360-2

An, D. T., Thanh, D. T. N., Ngot, P. V., & Anh, H. N. V. (2022). Antibacterial activity of ethanol extract and decoction from *Avicennia alba* Blume growing in the Can Gio Mangrove Biosphere Reserve, Vietnam. *GSC Biological and Pharmaceutical Sciences*, *21*(1), 152-159. https://doi.org/10.30574/gscbps.2022.21.1.0342

Bakhuizen van den Brink, R. C. (1921). *Revisio generis Avicenniae* [Revision of the genus *Avicennia*]. *Bulletin du Jardin Botanique de Buitenzorg*, *33*, 199-226.

Barhoumi, Z., Hussain, A. A., & Atia, A. (2021). Physiological response of *Avicennia marina* to salinity and recovery. *Russian Journal of Plant Physiology*, *68*, 696-707. https://doi.org/10.1134/S1021443721040026

Bast, F., John, A. A., & Bhushan, S. (2016). Molecular assessment of invasive Carrageenophyte *Kappaphycus alvarezii* from India based on ITS-1 sequences. *Webbia*, *71*(2), 287–292. https://doi.org/10.1080/00837792.2016.1221187

Bhadalkar, A., Vyas, B., & Bhatt, S. (2014). Molecular characterization of mangrove plants: A review. *Life Sciences Leaflets*, *50*, 148–158. https://petsd.org/ojs/index.php/lifesciencesleaflets/article/view/662/579

Borg, A. J., & Schönenberger, J. (2011). Comparative floral development and structure of the black mangrove genus *Avicennia* L. and related taxa in the Acanthaceae. *International Journal of Plant Sciences*, *172*(3), 330-344. https://doi.org/10.1086/658159

Chan, E. W. C., Lim, W. Y., Wong, C. W., & Ng, Y. K. (2022). Some notable bioactivities of *Rhizophora apiculata* and *Sonneratia alba*. *ISME/GLOMIS Electronic Journal*, *20*(4), 23-26.

Cheah, D. (2016). *Guidebook to the biodiversity of Linting wetlands.* Wetlands International Malaysia. https://malaysia.wetlands.org/publication/guidebook-to-the-biodiversity-of-linting-wetlands/

Chen, Y., Hou, Y., Guo, Z., Wang, W., Zhong, C., Zhou, R., & Shi, S. (2015). Applications of multiple nuclear genes to the molecular phylogeny, population genetics and hybrid identification in the mangrove genus *Rhizophora*. *PLoS ONE*, *10*(12), e0145058. https://doi.org/10.1371/journal.pone.0145058

Dookie, S., Jaikishun, S., & Ansari, A. A. (2023). *Avicennia germinans* leaf traits in degraded, restored, and natural mangrove ecosystems of Guyana. *Plant-Environment Interactions*, *4*, 324-341. https://doi.org/10.1002/pei3.10126

Duke, N. C. (1990). Morphological variation in the mangrove genus *Avicennia* in Australasia: Systematic and ecological considerations. *Australian Systematic Botany*, *3*, 221-239. https://doi.org/10.1071/SB9900221

Duke, N. C. (1991). A systematic revision of the mangrove genus *Avicennia* (Avicenniaceae) in Australasia. *Australian Systematic Botany*, *4*, 299-324. https://doi.org/10.1071/SB9910299

Duke, N. C. (1992). Mangrove floristics and biogeography. In A. I. Robertson & D. M. Alongi (Eds.), *Tropical mangrove ecosystems* (pp. 63-100). American Geophysical Union.

Duke, N. C. (2012). *Mangroves of the Kien Giang Biosphere Reserve Vietnam.* In S. Brown, S. Simpson, C. V. Cuong & H. Woerner (Eds.), Deutsche Gesellschaft fur Internationale Zusammenarbeit (GIZ) GmbH. https://www.scribd.com/document/348601498/mangrovebook-en-web-pdf

Ellegren, H., & Galtier, N. (2016). Determinants of genetic diversity. *Nature Reviews Genetics*, *17*, 422-433. https://doi.org/10.1038/nrg.2016.58

Farooqui, N. U., & Dangi, C. B. S. (2018). Distribution and morphological adaptations of *Avicennia marina* in the Sundarbans. *Biosciences Biotechnology Research Asia*, *15*(1), 229-234. https://doi.org/10.13005/bbra/2626

Giang, L. H., Hong, P. N., Tuan, M. S., & Harada, K. (2003). Genetic variation of *Avicennia marina* (Forsk.) Vierh. (Avicenniaceae) in Vietnam revealed by microsatellite and AFLP markers. *Genes and Genetic Systems*, *78*, 399-407. https://doi.org/10.1266/ggs.78.399

Giesen, W., Wulffraat, S., Zieren, M., & Scholten, L. (2007). *Mangrove guidebook for Southeast Asia*. FAO Regional Office for Asia and the Pacific. https://www.cabidigitallibrary.org/doi/full/10.5555/20083307268

Hall, T. A. (1999). BioEdit: A user-friendly biological sequence alignment editor and analysis program for Windows 95/98/NT. *Nucleic Acids Symposium Series*, *41*, 95-98.

Hassler, M. (2024). *Synonymic checklists of the vascular plants of the world*. Catalogue of Life. https://www.catalogueoflife.org/data/taxon/36PY

Huang, L., Li, X., Huang, Y., Shi, S., & Zhou, R. (2014). Molecular evidence for natural hybridization in the mangrove genus *Avicennia*. *Pakistani Journal of Botany*, *46*(5), 1577-1584.

International Union for Conservation of Nature. (2024). *Search results: Avicennia species*. https://www.iucnredlist.org/search?taxonomies=124139&searchType=species

Japar Sidik, B. (1994). Mangrove plant resources in the ASEAN region. In C. Wilkinson, S. Sudara & L. M. Chou (Eds.), *Proceedings of the Third ASEAN-Australia symposium on living coastal resources: Vol. 1. Status reviews* (pp. 123-138). Chulalongkorn University.

Kalyaanamoorthy, S., Minh, B. Q., Wong, T. K. F., von Haeseler, A., & Jermiin, L. S. (2017). ModelFinder: Fast model selection for accurate phylogenetic estimates. *Nature Methods*, *14*, 587-589. https://doi.org/10.1038/nmeth.4285

Karuppaiya, M., Balamurugan, S., Sivakumar, K., & Kathiresan, K. (2020). Mangrove diversity assessment by molecular markers. In S.-K. Kim (Ed.), *Encyclopedia of marine biotechnology* (pp. 2191-2210). Wiley. https://doi.org/10.1002/9781119143802.ch99

Kavitha, K., Usha, B., George, S., Venkataraman, G., & Parida, A. (2010). Molecular characterization of a salt-inducible monodehydroascorbate reductase from the halophyte *Avicennia marina*. *International Journal of Plant Sciences*, *171*(5), 457-465. https://doi.org/10.1086/651946

Krauss, K. W., Whelan, K. R. T., Kennedy, J. P., Friess, D. A., Rogers, C. S., Stewart, H. A., Grimes, K. W., Trench, C. A., Ogurcak, D. E., Toline, C. A., Ball, L. C., & Form, A. S. (2023). Framework for facilitating mangrove recovery after hurricanes on Caribbean islands. *Restoration Ecology*, *31*(7), e13885. https://doi.org/10.1111/rec.13885

Larkin, M. A., Blackshields, G., Brown, N. P., Chenna, R., McGettigan, P. A., McWilliam, H., Valentin, F., Wallace, I. M., Wilm, A., Lopez, R., Thompson, J. D., Gibson, T. J., & Higgins, D. G. (2007). Clustal W and Clustal X version 2.0. *Bioinformatics*, *23*(21), 2947-2948. https://doi.org/10.1093/bioinformatics/btm404

Li, X., Duke, N. C., Yang, Y., Huang, L., Zhu, Y., Zhang, Z., Zhou, R., Zhong, C., Huang, Y., & Shi, S. (2016). Re-evaluation of phylogenetic relationships among species of the mangrove genus *Avicennia* from Indo-West Pacific based on multilocus analyses. *PLoS ONE*, *11*(10), e0164453. https://doi.org/10.1371/journal.pone.0164453

Lidén, M., Fukuhara, T., & Axberg, T. (1995). Phylogeny of *Corydalis*: ITS and morphology. In U. Jensen & J. W. Kadereit (Eds.), *Systematics and evolution of the Ranunculiflorae: Vol. 9. Plant systematics and evolution supplement 9* (pp. 183–188). Springer. https://doi.org/10.1007/978-3-7091-6612-3_17

Liu, M., Wang, Z., Li, S., Lü, X., Wang, X., & Han, X. (2017). Changes in specific leaf area of dominant plants in temperate grasslands along a 2500-km transect in northern China. *Scientific Reports, 7*, 10780. https://doi.org/10.1038/s41598-017-11133-z

Liu, Y., Liang, N., Xian, Q., & Zhang, W. (2023). GC heterogeneity reveals sequence-structures evolution of angiosperm ITS2. *BMC Plant Biology*, *23*, 608. https://doi.org/10.1186/s12870-023-04634-9

Maguire, T. L., & Saenger, P. (2000). The taxonomic relationships within the genus *Excoecaria* L. (Euphorbiaceae) based on leaf morphology and rDNA sequence data. *Wetlands Ecology and Management*, *8*, 19-28. https://doi.org/10.1023/A:1008407009397

Maguire, T. L., Peakall, R., & Saenger, P. (2002). Comparative analysis of genetic diversity in the mangrove species *Avicennia marina* (Forsk.) Vierh. (Avicenniaceae) detected by AFLPs and SSRs. *Theoretical and Applied Genetics*, *104*, 388-398. https://doi.org/10.1007/s001220100724

Malekmohammadi, L., Sheidai M., Ghahremaninejad, F., Danehkar, A., & Koohdar, F. (2022). *Avicennia* genus molecular phylogeny and barcoding: A multiple approach. *Caryologia*, *75*(4), 3-13. https://doi.org/10.36253/caryologia-1592

Mariano, H. G., Dagoc, F. L. S., Espra, A. S., & Amparado, Jr., R. F. (2019). Mangrove diversity, taxonomic classification, and morphological characteristics of natural and reforested mangrove forests in selected municipalities of Zamboanga Del Sur, Mindanao Island, Philippines. *Journal of Biodiversity Environmental Sciences*, *15*(4), 86-99.

Meier, R., Shiyang, K., Vaidya, G., & Ng, P. K. L. (2006). DNA barcoding and taxonomy in Diptera: A tale of high intraspecific variability and low identification success. *Systematic Biology*, *55*(5), 715-728. https://doi.org/10.1080/10635150600969864

Moldenke, H. N. (1960). Materials towards a monograph of the genus *Avicennia*. I, II, & III. *Phytologia*, *7*(3-5), 123-193. https://doi.org/10.5962/bhl.part.5041

Mollick, A. S., Sultana, R., Azad, M. S., & Khan, M. N. I. (2021). Leaf morphological plasticity in three dominant tree species in the Sundarbans mangrove forest of Bangladesh in different salinity zones. *Wetlands Ecology and Management*, *29*, 265-279. https://doi.org/10.1007/s11273-020-09782-5

Mori, G. M., Zucchi, M. I., Sampaio, I., & Souza, A. P. (2015). Species distribution and introgressive hybridization of two *Avicennia* species from the Western Hemisphere unveiled by phylogeographic patterns. *BMC Evolutionary Biology*, *15*, 61. https://doi.org/10.1186/s12862-015-0343-z

Nadia, T. D. L., De Menezes, N. L., & Machado, I. C. (2012). Floral traits and reproduction of *Avicennia schaueriana* Moldenke (Acanthaceae): A generalist pollination system in the Lamiales. *Plant Species Biology*, *28*, 70-80. https://doi.org/10.1111/j.1442-1984.2011.00361.x

Nascimento, M. G. P., Mayo, S. J., & de Andrade, I. M. (2021). Distinguishing the Brazilian mangrove species *Avicennia germinans* and *A. schaueriana* (Acanthaceae) by elliptic fourier analysis of leaf shape. *Feddes Repertorium*, *132*(2), 77-107. https://doi.org/10.1002/fedr.202000025

Nguyen, L. T., Schmidt, H. A., von Haeseler, A., & Minh, B. Q. (2014). IQ-TREE: A fast and effective stochastic algorithm for estimating maximum-likelihood phylogenies. *Molecular Biology and Evolution*, *32*(1), 268-274. https://doi.org/10.1093/molbev/msu300

Noor, Y. R., Khazali, M., & Suryadiputra, I. N. N. (2012). *Panduan pengenalan mangrove di Indonesia* [Guide to introduction of mangroves in Indonesia]. Wetlands International – Indonesia Programme. http://www.mangrovesforthefuture.org/assets/Repository/Documents/Panduan-Mangrove-Reprint-3.pdf

Osing, P. K. A. S., Jondonero, M. A. P., Suson, P. D., Guihawan, J. Q., & Amparado Jr, R. F. (2019). Species composition and diversity in a natural and reforested mangrove forests in Panguil Bay, Mindanao, Philippines. *Journal of Biodiversity Environmental Sciences*, *15*(3), 88-102.

Prakashamani, G., Srivani, A., & Mohan, G. K. (2019). A review on *Avicennia officinalis*. *International Journal of Pharmacy and Biological Sciencess-IJPBS™*, *9*(1), 553-557.

Primavera, J. H., Sadaba, R. B., Lebata, M. J. H. L., & Altamirano, J. P. (2004). *Handbook of mangroves in the Philippines-Panay*. Aquaculture Department, Southeast Asian Fisheries Development Center. https://repository.seafdec.org.ph/handle/10862/3053

Rahman, A. F. M. A., Islam, M. A., Idris, M. H., Bhuiyan, M. K. A., Chowdhury, M. M., Abualreesh, M. H., & Mustafa Kamal, A. H. (2023). Species diversity and assemblage of mangroves at Setiu Wetland, Terengganu, Malaysia. *Borneo Journal of Resource Science and Technology*, *13*(1), 173-190. https://doi.org/10.33736/BJRST.5109.2023

Rani, A., Jugale, S., & Bast, F. (2021). DNA barcode-based phylogenetic assessment of selected mangroves from Sundarbans delta and Kerala. *Proceedings of the Indian National Science Academy*, *87*, 148-155. https://doi.org/10.1007/s43538-021-00021-w

Rani, V., Sreelekshmi, S., Asha, C. V., & Nandan, S. B. (2018). Forest structure and community composition of Cochin mangroves, South-West coast of India. *Proceedings of the National Academy of Sciences India Section B: Biological Sciences*, *88*, 111-119. https://doi.org/10.1007/s40011-016-0738-7

Ridley, H. N. (1923). *The flora of the Malay Peninsula*. Reeve and Co. https://doi.org/10.2307/4115416

Ruang-areerate, P., Yoocha, T., Kongkachana, W., Phetchawang, P., Maknual, C., Meepol, W., Jiumjamrassil, D., Pootakham, W., & Tangphatsornruang, S. (2022). Comparative analysis and phylogenetic relationships of *Ceriops* species (Rhizophoraceae) and *Avicennia lanata* (Acanthaceae): Insight into the chloroplast genome evolution between middle and seaward zones of mangrove forests. *Biology*, *11*, 383. https://doi.org/10.3390/biology11030383

Sabdanawaty, F. P., Purnomo., & Daryono, B. S. (2021). Species diversity and phenetic relationship among accessions of api-api (*Avicennia* spp.) in Java based on morphological characters and ISSR markers. *Biodiversitas Journal of Biological Diversity*, *22*(1), 193-198. https://doi.org/10.13057/biodiv/d220125

Saddhe, A. A., Jamdade, R. A., & Kumar, K. (2017). Evaluation of multilocus marker efficacy for delineating mangrove species of West Coast India. *PLoS ONE*, *12*(8), e0183245. https://doi.org/10.1371/journal.pone.0183245

Saenger, P., & Brooks, L. (2008). Phenotypic leaf variation in *Avicennia marina* in tropical Australia: Can discrete subpopulations be recognised in the field? *Australian Journal of Botany*, *56*, 487-492. https://doi.org/10.1071/BT07124

Said, E. M., & Bahnasy, M. I. (2023). Identification of Egyptian mangrove species based on DNA barcoding. *Asian Journal of Agricultural and Horticultural Research*, *10*(4), 131-145. https://doi.org/10.9734/AJAHR/2023/v10i4254

Said, W. M., & Ehsan, N. O. M. (2010). Morphological and molecular evidences among four heteroforms of *Avicennia marina* (Forssk) Vierh. *Journal of American Science*, *6*(11), 843-856.

Saptiani, G., Asikin, A. N., Ardhani, F., & Hardi, E. H. (2018). Mangrove plants species from Delta Mahakam, Indonesia with antimicrobial potency. *Biodiversitas Journal of Biological Diversity*, *19*(2), 516-521. https://doi.org/10.13057/biodiv/d190220

Selvam, V., & Karunagaran, V. M. (2004). *Ecology and biology of mangroves orientation guide*. M. S. Swaminathan Research Foundation. https://scholar.google.com/scholar?hl=en&as_sdt=0%2C5&q=Ecology+and+Biology+of+Mangroves%3A+Orientation+Guide&btnG=

Shin, L. S., Muhamad, A., & Tong, J. (2015). *Mangrove guidebook for Malaysia*. Wetlands International Malaysia. https://malaysia.wetlands.org/publication/mangrove-guidebook-for-malaysia/

Sun, Y., Skinner, D. Z., Liang, G. H., & Hulbert, S. H. (1994). Phylogenetic analysis of Sorghum and related taxa using internal transcribed spacers of nuclear ribosomal DNA. *Theoretical and Applied Genetics*, *89*, 26-32. https://doi.org/10.1007/BF00226978

Tamura, K., Stecher, G., & Kumar, S. (2021). MEGA11: Molecular evolutionary genetics analysis version 11. *Molecular Biology and Evolution*, *38*(7), 3022-3027. https://doi.org/10.1093/molbev/msab120

Thatoi, H., Samantaray, D., & Das, S. K. (2016). The genus *Avicennia*, a pioneer group of dominant mangrove plant species with potential medicinal values: A review. *Frontiers in Life Science*, *9*(4), 267-291. https://doi.org/10.1080/21553769.2016.1235619

Tomlinson, P. B. (1986). *The botany of mangroves*. Cambridge University Press.

Tomlinson, P. B. (2016). *The botany of mangroves* (2nd ed.). Cambridge University Press. https://doi.org/10.1017/CBO9781139946575

Triest, L., Satyanarayana, B., Delange, O., Sarker, K. K., Sierens, T., & Dahdouh-Guebas, F. (2021). Barrier to gene flow of grey mangrove *Avicennia marina* populations in the Malay Peninsula as revealed from nuclear microsatellites and chloroplast haplotypes. *Frontiers in Conservation Science*, *2*, 727819. https://doi.org/10.3389/fcosc.2021.727819

Vy, N. X., Thuy, N. N. N., Hieu, N. T., & Doc, L. Q. (2017). DNA barcoding of the true mangrove plants, a selection of genetic markers. *Journal of Marine Science and Technology*, *17*(4A), 311-321.

Wee, A. K. S., Noreen, A. M. E., Ono, J., Takayama, K., Kumar, P. P., Tan, H. T. W., Saleh, M. N., Kajita, T., & Webb, E. L. (2020). Genetic structures across a biogeographical barrier reflect dispersal potential of

four Southeast Asian mangrove plant species. *Journal of Biogeography*, *47*(6), 1258-1271. https://doi.org/10.1111/jbi.13813

Wee, A. K. S., Takayama, K., Kajita, T., & Webb, E. L. (2013). Microsatellite loci for *Avicennia alba* (Acanthaceae), *Sonneratia alba* (Lythraceae) and *Rhizophora mucronata* (Rhizophoraceae). *Journal of Tropical Forest Science*, *25*(1), 131-136.

Win, S., & Win, T. Z. N. (2021). Vegetative structure and zonal distribution of true mangroves in Shwe-Thaung-Yan coastal areas, Myanmar. *Journal of Aquaculture & Marine Biology*, *10*(1), 33-39. https://doi.org/10.15406/jamb.2021.10.00305

Zar, H. J. (2010). *Biostatistical analysis* (5th ed.). Prentice Hall. https://dl.acm.org/doi/10.5555/1203271

Zolgharnein, H., Kamyab, M., Keyvanshokooh, S., Ghasemi, A., & Nabavi, S.M.B. (2010). Genetic diversity of *Avicennia marina* (Forsk.) Vierh. populations in the Persian Gulf by microsatellite markers. *Journal of Fisheries and Aquatic Science*, 5(3), 223-229. https://doi.org/10.3923/jfas.2010.223.229

APPENDIX

Supplementary Table 1
Evolutionary divergence and pairwise distances among Avicennia *species*

		1	2	3	4	5	6	7	8	9	10	11	12	13
1	*A. alba* PBP (MY050304.2)													
2	*A. alba* PBP (MY050304.3)	0.000												
3	*A. alba* PBP (MY050304.1)	0.000	0.000											
4	*A. alba* PB (MY050304.10)	0.000	0.000	0.000										
5	*A. alba* SKEM (MY110307.1)	0.006	0.006	0.006	0.006									
6	*A. alba* SKEM (MY110307.2)	0.003	0.003	0.003	0.003	0.003								
7	*A. alba* SKEM (MY110307.3)	0.006	0.006	0.006	0.006	0.000	0.003							
8	*A. alba* PM (MY010207.9)	0.006	0.006	0.006	0.006	0.000	0.003	0.000						
9	*A. alba* PM (MY010207.10)	0.006	0.006	0.006	0.006	0.000	0.003	0.000	0.000					
10	*A. alba* PM (MY010207.11)	0.006	0.006	0.006	0.006	0.000	0.003	0.000	0.000	0.000				
11	*A. alba* PKA (MY040310.1)	0.006	0.006	0.006	0.006	0.000	0.003	0.000	0.000	0.000	0.000			
12	*A. alba* PKA (MY040310.2)	0.006	0.006	0.006	0.006	0.000	0.003	0.000	0.000	0.000	0.000	0.000		
13	*A. marina* PBP (MY050304.4)	0.037	0.037	0.037	0.037	0.036	0.037	0.036	0.036	0.036	0.036	0.036	0.036	0.027
14	*A. marina* PBP (MY050304.5)	0.037	0.037	0.037	0.037	0.036	0.037	0.036	0.036	0.036	0.036	0.036	0.036	0.027
15	*A. marina* PBP (MY050304.6)	0.037	0.037	0.037	0.037	0.036	0.037	0.036	0.036	0.036	0.036	0.036	0.036	0.027
16	*A. marina* PB (MY050304.11)	0.037	0.037	0.037	0.037	0.036	0.037	0.036	0.036	0.036	0.036	0.036	0.036	0.027
17	*A. marina* PB (MY050304.12)	0.037	0.037	0.037	0.037	0.036	0.037	0.036	0.036	0.036	0.036	0.036	0.036	0.027
18	*A. marina* PB (MY050304.13)	0.039	0.039	0.039	0.039	0.033	0.036	0.033	0.033	0.033	0.033	0.033	0.033	0.027
19	*A. marina* PM (MY010207.12)	0.039	0.039	0.039	0.039	0.033	0.036	0.033	0.033	0.033	0.033	0.033	0.033	0.027
20	*A. marina* PM (MY010207.13)	0.039	0.039	0.039	0.039	0.033	0.036	0.033	0.033	0.033	0.033	0.033	0.033	0.027
21	*A. marina* PM (MY010207.14)	0.039	0.039	0.039	0.039	0.033	0.036	0.033	0.033	0.033	0.033	0.033	0.033	0.027
22	*A. marina* var. *rumphiana* China (KX641595.1)	0.022	0.022	0.022	0.022	0.020	0.020	0.020	0.020	0.020	0.020	0.020	0.020	0.020
23	*A. rumphiana* PM (MY010207.15)	0.067	0.067	0.067	0.067	0.064	0.064	0.064	0.064	0.064	0.064	0.064	0.064	0.055
24	*A. rumphiana* PM (MY010207.16)	0.068	0.068	0.068	0.068	0.070	0.068	0.070	0.070	0.070	0.070	0.070	0.070	0.055

Supplementary Table 1 *(continue)*

		1	2	3	4	5	6	7	8	9	10	11	12	13
25	*A. rumphiana* PM (MY010207.17)	0.068	0.068	0.068	0.068	0.070	0.068	0.070	0.070	0.070	0.070	0.070	0.070	0.055
26	*A. rumphiana* SKEM (MY110307.4)	0.063	0.063	0.063	0.063	0.060	0.060	0.060	0.060	0.060	0.060	0.060	0.060	0.054
27	*A. rumphiana* SKEM (MY110307.5)	0.063	0.063	0.063	0.063	0.060	0.060	0.060	0.060	0.060	0.060	0.060	0.060	0.054
28	*A. rumphiana* SKEM (MY110307.6)	0.063	0.063	0.063	0.063	0.060	0.060	0.060	0.060	0.060	0.060	0.060	0.060	0.054
29	*A. officinalis* India (MH243949.1)	0.024	0.024	0.024	0.024	0.022	0.022	0.022	0.022	0.022	0.022	0.022	0.022	0.022
30	*A. officinalis* China (KX641597.1)	0.024	0.024	0.024	0.024	0.022	0.022	0.022	0.022	0.022	0.022	0.022	0.022	0.022
31	*A. officinalis* VietNam (MG880054.1)	0.025	0.025	0.025	0.025	0.024	0.024	0.024	0.024	0.024	0.024	0.024	0.024	0.024
32	*A. officinalis* India (KJ784553.1)	0.024	0.024	0.024	0.024	0.022	0.022	0.022	0.022	0.022	0.022	0.022	0.022	0.022

Note. PBP = Pulau Bagan Pinang, PB = Pulau Burong, PKA = Pulau Kamat, PM = Pulau Merambong, SKEM = Sungai Kemasik

Supplementary Table 2
Evolutionary divergence and pairwise distances among Avicennia *species*

		1	2	3	4	5	6	7	8	9
1	*A. marina* PBP (MY050304.4)									
2	*A. marina* PBP (MY050304.5)	0.000								
3	*A. marina* PBP (MY050304.6)	0.000	0.000							
4	*A. marina* PB (MY050304.11)	0.000	0.000	0.000						
5	*A. marina* PB (MY050304.12)	0.000	0.000	0.000	0.000					
6	*A. marina* PB (MY050304.13)	0.004	0.004	0.004	0.004	0.004				
7	*A. marina* PM (MY010207.12)	0.004	0.004	0.004	0.004	0.004	0.000			
8	*A. marina* PM (MY010207.13)	0.004	0.004	0.004	0.004	0.004	0.000	0.000		
9	*A. marina* PM (MY010207.14)	0.004	0.004	0.004	0.004	0.004	0.000	0.000	0.000	
10	*A. marina* var. *rumphiana* China (KX641595.1)	0.021	0.021	0.021	0.021	0.021	0.021	0.021	0.021	0.021
11	*A. rumphiana* PM (MY010207.15)	0.067	0.067	0.067	0.067	0.067	0.065	0.065	0.065	0.065
12	*A. rumphiana* PM (MY010207.16)	0.070	0.070	0.070	0.070	0.070	0.070	0.070	0.070	0.070
13	*A. rumphiana* PM (MY010207.17)	0.070	0.070	0.070	0.070	0.070	0.070	0.070	0.070	0.070

Supplementary Table 2 *(continue)*

		1	2	3	4	5	6	7	8	9
14	*A. rumphiana* SKEM (MY110307.4)	0.064	0.064	0.064	0.064	0.064	0.062	0.062	0.062	0.062
15	*A. rumphiana* SKEM (MY110307.5)	0.064	0.064	0.064	0.064	0.064	0.062	0.062	0.062	0.062
16	*A. rumphiana* SKEM (MY110307.6)	0.064	0.064	0.064	0.064	0.064	0.062	0.062	0.062	0.062
17	*A. officinalis* India (MH243949.1)	0.025	0.025	0.025	0.025	0.025	0.025	0.025	0.025	0.025
18	*A. officinalis* China (KX641597.1)	0.025	0.025	0.025	0.025	0.025	0.025	0.025	0.025	0.025
19	*A. officinalis* VietNam (MG880054.1)	0.027	0.027	0.027	0.027	0.027	0.027	0.027	0.027	0.027
20	*A. officinalis* India (KJ784553.1)	0.025	0.025	0.025	0.025	0.025	0.025	0.025	0.025	0.025

Note. PBP = Pulau Bagan Pinang, PB = Pulau Burong, PKA = Pulau Kamat, PM = Pulau Merambong, SKEM = Sungai Kemasik

Supplementary Table 3
Evolutionary divergence and pairwise distances among Avicennia *species*

		1	2	3	4	5	6	7	8	9	10	11
1	*A. marina* var. *rumphiana* China (KX641595.1)											
2	*A. rumphiana* PM (MY010207.15)	0.011										
3	*A. rumphiana* PM (MY010207.16)	0.011	0.007									
4	*A. rumphiana* PM (MY010207.17)	0.011	0.007	0.000								
5	*A. rumphiana* SKEM (MY110307.4)	0.011	0.003	0.010	0.010							
6	*A. rumphiana* SKEM (MY110307.5)	0.011	0.003	0.010	0.010	0.000						
7	*A. rumphiana* SKEM (MY110307.6)	0.011	0.003	0.010	0.010	0.000	0.000					
8	*A. officinalis* India (MH243949.1)	0.011	0.035	0.035	0.035	0.033	0.033	0.033				
9	*A. officinalis* China (KX641597.1)	0.011	0.035	0.035	0.035	0.033	0.033	0.033	0.000			
10	*A. officinalis* VietNam (MG880054.1)	0.013	0.036	0.036	0.036	0.035	0.035	0.035	0.001	0.001		
11	*A. officinalis* India (KJ784553.1)	0.011	0.035	0.035	0.035	0.033	0.033	0.033	0.000	0.000	0.001	

Note. PM = Pulau Merambong, SKEM = Sungai Kemasik

Pertanika J. Trop. Agric. Sci. 48 (3): 911 -928 (2025)

PERTANIKA JOURNALS

TROPICAL AGRICULTURAL SCIENCE

Journal homepage: http://www.pertanika.upm.edu.my/

Toxicity Assessment of Ethanolic *Moringa oleifera* Leaf Extract (MOLE) Using Zebrafish (*Danio rerio*) Model

Intan Nurzulaikha Abdul Zahid[1], Seri Narti Edayu Sarchio[1]*, Nur Liyana Daud[1], Suhaili Shamsi[2] and Elysha Nur Ismail[1]

[1]Department of Biomedical Science, Faculty of Medicine and Health Sciences, Universiti Putra Malaysia, 43400 Serdang, Selangor, Malaysia
[2]Department of Biochemistry, Faculty of Biotechnology and Biomolecular, Universiti Putra Malaysia, 43400 Serdang, Selangor, Malaysia

ABSTRACT

Moringa oleifera, locally known as 'Kelor' in Malay, is a medicinal plant valued in Malaysia and other countries for its therapeutic bioactive compounds and health benefits, including anticancer and anti-inflammatory properties. However, the toxicity profile of ethanolic *M. oleifera* leaf extract (MOLE) has not been well explored. This study aims to assess the toxicity profile of MOLE using a zebrafish (*Danio rerio*) model. Zebrafish embryos were subjected to MOLE ($n \geq 15$; 24 h post-fertilisation [hpf]) at a concentration of 5-1000 µg/mL, and the survival rate, hatching rate, heart rate, and morphological development of zebrafish embryos were monitored daily for up to 72 h. Embryo media was used as a control. MOLE treatment was shown to be safe at concentrations ≤ 400 µg/mL with LC_{50} values of 1186 ±7 µg/mL, 560.1 ±7 µg/mL, and 445.1 ± 7 µg/mL at 24, 48, and 72 h post-treatment, respectively. A significant mortality rate and low heartbeat were recorded in embryos exposed to > 800 µg/mL across the three-time points. MOLE did not affect the hatching rate. A significant difference in embryos treated with > 800 µg/mL at 72 h post-treatment was not attributable to MOLE effects, as the embryos had died before hatching. Scoliosis was predominantly observed in embryos subjected to MOLE concentrations ranging from 25 to 200 µg/mL. The present data demonstrated that MOLE exhibited concentration- and time-dependent toxicities. Further studies are needed to identify the effective concentrations of MOLE for therapeutic application in *in vitro* and *in vivo* models.

Keywords: *Moringa oleifera*, toxicity, zebrafish embryo

ARTICLE INFO

Article history:
Received: 23 September 2024
Accepted: 20 November 2024
Published: 16 May 2025

DOI: https://doi.org/10.47836/pjtas.48.3.14

E-mail addresses:
intan.nurzulaikha123@gmail.com (Intan Nurzulaikha Abdul Zahid)
serinarti@upm.edu.my (Seri Narti Edayu Sarchio)
nurliyanadaudd@gmail.com (Nur Liyana Daud)
sh_suhaili@upm.edu.my (Suhaili Shamsi)
elysha@upm.edu.my (Elysha Nur Ismail)
* Corresponding author

e-ISSN: 2231-8542

INTRODUCTION

Recently, in pharmaceutical research, there has been a surge in public interest in exploring medicinal plants for their bioactive compounds, which may offer various health benefits that improve human health. *Moringa oleifera*, locally known as 'Kelor,' has garnered significant attention in the industry due to extensive research on its nutritional, phytochemical, and pharmacological properties. *M. oleifera* has been recognised as a 'Miracle Tree' and 'Superfood'. Its leaves contain high concentrations of essential vitamins, minerals, and antioxidants. Studies have demonstrated that *M. oleifera* contains higher concentrations of vitamin C than oranges and greater potassium levels than bananas (Rockwood et al., 2013). Furthermore, it exhibits a higher proportion of polyunsaturated fatty acids compared to saturated fatty acids (Cervera-Chiner et al., 2024). These properties provide substantial health benefits, including overcoming malnutrition and exhibiting anti-inflammatory, antioxidant and anticancer effects (Leone et al., 2015). One of the 13 members of the genus Moringa is *M. oleifera,* and it belongs to the family Moringaceae. It is indigenous to South Asia and was initially discovered in northeast Pakistan, extending to northern West Bengal and India (Azlan et al., 2022). It is usually cultivated in subtropical and tropical areas (Milla et al., 2021).

Previous studies have indicated that plants used in traditional medicine may present risks if consumed inappropriately, contradicting their perceived safety (Başaran et al., 2022; Ekor, 2014; Shamsi et al., 2021). It is frequently attributed to a lack of scientific evaluation and regulation, rendering them potentially less safe than prescription drugs, which have been associated with severe adverse effects such as congestive, allergic reactions, heart failure, renal failure, and liver toxicity (Lorenzo et al., 2015; Posadzki et al., 2013). *Moringa oleifera*, though widely used in traditional medicine and dietary supplements, lacks comprehensive toxicological data. This study aims to fill this gap by evaluating the potential toxicity of ethanolic *M. oleifera* leaf extract (MOLE), ensuring it can be used safely at various doses. Testing on zebrafish embryos allows for an initial assessment of developmental toxicity, helping to identify safe concentration levels and prevent potential health risks associated with overconsumption or high-dose exposure.

Several studies have investigated the cytotoxic effects of ethanolic MOLE in various cell lines. In one of the studies, the fibroblast cells derived from chicken embryos were exposed to ethanolic MOLE at concentrations ranging from 0.02 to 400 µg/mL. The results showed significant cytotoxicity at concentrations > 200 µg/mL but were safe at < 50 µg/mL. The same study also reported that the 50% cytotoxic concentration (CC_{50}) was 100 µg/mL (Ashraf et al., 2017). In another study, the cytotoxic effects of ethanolic MOLE on the human cervical carcinoma cell line (HeLa cells) were compared with callus extract using the MTT assay (Jafarain et al., 2014). It was noted that both MOLE and callus extracts showed a significant decrease in cell viability at concentrations of 100 to

500 µg/mL and 1000 to 3000 µg/mL, respectively, in a concentration-dependent manner. Notably, ethanolic MOLE exhibited higher cytotoxicity compared to the callus extract, as indicated by a lower 50% inhibitory concentration (IC_{50}) (Jafarain et al., 2014). Despite the therapeutic benefits of medicinal plants, the prolonged use of *M. oleifera* may be toxic. In rats, extended consumption of ethanolic MOLE at doses of 200 and 400 mg/kg per body weight resulted in dose-dependent weight gain and elevated serum alanine transaminase (ALT), aspartate transaminase (AST), blood urea nitrogen (BUN), and creatinine levels, indicating liver and kidney damage. These findings suggest chronic MOLE supplementation could induce hepatic and renal injuries (Oyagbemi et al., 2013). It highlights the importance of understanding the potential toxic effects of both short- and long-term use of medicinal plants. Thus, comprehensive toxicity studies on medicinal plants and their preparations are essential to ensure their safety for human consumption.

Moreover, *in vivo* models have been used to study the toxicity profile of MOLE. Administration of 70% ethanol-extracted *M. oleifera* leaves at a concentration of 150 mg/mL intraperitoneally to albino rats and rabbits every 5-min interval until mortality was reached resulted in lethal doses of acute toxicity (Osman et al., 2015). Histopathological examination revealed significant damage to the kidney, heart, and liver, including renal tubule degeneration, cardiac muscle haemorrhage, and hepatic cell necrosis. It suggests that fluid accumulation leads to cell swelling and rupture, indicating minimal toxicity of MOLE when administered in concentrated doses over a short period in rodents (Osman et al., 2015). Nevertheless, a comprehensive toxicity profile of ethanolic MOLE using zebrafish embryos as an *in vivo* model has not yet been reported.

Zebrafish (*Danio rerio*) serves as a valuable toxicity model, offering real-time, *in vivo* studies to evaluate the potential risks to human health associated with naturally occurring compounds (Abdullah et al., 2022; Bambino & Chu, 2017). This model has been extensively utilised in toxicity studies due to its numerous advantages, particularly in terms of technical and economic aspects, compared to other vertebrate models such as rodents. One key advantage is their small size, which makes them both cost-effective and technically easier to manage. Additionally, zebrafish exhibit high fecundity, producing many embryos per mating session. The transparency of embryos facilitates detailed imaging and observation of developmental processes (Rothenbücher et al., 2019). Moreover, the zebrafish genome exhibits approximately 70% similarity to the human genome compared to the human reference genome. This similarity shows the potential of using zebrafish to enhance our understanding of the precise roles of genes in human diseases, spanning both rare and common conditions (Howe et al., 2013). The Fish Embryo Toxicity (FET) test, which employs zebrafish, is widely recognised for its application in pre-screening drugs and diseases, including the evaluation of lethal concentrations for 50% of the population (LC_{50}). The zebrafish embryo model bridges the gap between the *in vitro* and *in vivo*

methods, providing essential insights before conducting biocompatibility and toxicity assessments in living organisms, thus diminishing the necessity for animal experimentation (Rothenbücher et al., 2019).

In this study, MOLE was assessed for its toxicity during zebrafish embryogenesis. While MOLE is recognised for its beneficial properties, including anticancer (Jafarain et al., 2014), anti-inflammatory (Arulselvan et al., 2016), and antibacterial (Farooq & Koul, 2020) activities, its toxic effects, particularly during the critical embryogenesis period, remain largely unexplored. Therefore, this study aims to evaluate the toxicity and teratogenicity of MOLE during zebrafish embryogenesis.

MATERIALS AND METHODS

Plant Sample Collection and Identification

Fresh leaves of the *M. oleifera* plant were acquired from Bukit Katil, Malacca. The plant was sent to the Institute of Bioscience (IBS) UPM to authenticate its species. The voucher number obtained was KM 0088/23.

Preparation and Extraction of *Moringa oleifera* Leaves

The extraction of *M. oleifera* leaves was conducted according to the method described by Ismail et al. (2020). Approximately 500 g of *M. oleifera* leaves were washed, air-dried to a constant weight, and then ground into powder at room temperature. For the maceration process, 80% (v/v) ethanol (Chemiz, Malaysia) was used to extract the powdered plant material over 72 h. The resulting crude ethanol extract was filtered through Whatman No. 1 filter paper (GE Healthcare, Singapore). The filtrate was then evaporated using a rotary evaporator (BUCHI Rotavapor R-200, Buchi Corporation, Switzerland), dried, and stored in an airtight container at 4°C until needed. This extraction process was repeated three times. The plant extraction yield obtained was 20.78%. The percentage yield of the extract was calculated using the equation below:

$$\text{Percentage of yield (\%)} = \frac{\text{Weight of concentrated extract (g)}}{\text{Weight of dried plan sample (g)}} \times 100\% \qquad [1]$$

Phytochemical Identification Using Liquid Chromatography Analysis

The sample was dissolved in methanol (1 mg/mL) (Fisher Scientific, UK) and filtered through a 0.22 µm PTFE membrane filter (Phenomenex, USA) prior to analysis to identify the phytochemicals contained in the *M. oleifera* leaf extract (MOLE). The sample was analysed using a Liquid Chromatography–Mass Spectrometry (LC-MS) system consisting of a Q Exactive Focus mass spectrometer with Ultimate 3000 photodiode array detector, Rapid Separation (RS) column compartment, RS pump and RS autosampler (Thermo

Scientific, USA). A Hypersil Gold Dim (1.9 µm) column was used throughout (100 mm × 2.1 mm), and for mobile phase elution, a gradient of two solvents denoted as 'A' and 'B' was employed. 'A' was 0.1% of aqueous formic acid, whereas 'B' was 0.1% formic acid in acetonitrile with a 400 µL/min flow rate. The initial condition consists of 95% of 'A' and 5% of 'B', with a linear gradient increase from 5 to 100% of 'B' at 30–34 minutes of elution time, and the analysis was conducted at the initial solvent ratio until 38 min of elution time. A mass spectrometer with an electrospray ion source was set to positive and negative ionisation modes using data-dependent automatic switching between the MS and MS/MS acquisition modes. The system was controlled using Xcalibur software (Vijayalakshmi et al., 2015).

Zebrafish Embryo Toxicity Testing

Zebrafish embryos were purchased from the AAALAC-accredited Zebrafish Satellite Animal Facility, Animal Experimental Unit, Faculty of Medicine, Universiti Malaya.

Briefly, 4 h post-fertilisation (hpf) healthy embryos were transferred into 96-well culture plates (TPP, Switzerland), one embryo in 200 µL of embryo medium (E3 media [Zebrafish Satellite Animal Facility, Malaysia]) (5 mM NaCl, 0.17 mM KCl, 0.33 mM $CaCl_2$, 0.33 mM $MgSO_4$, and 0.1% (*w*/*v*) methylene blue) per well and acclimatised at 28°C for 24 h in a 12-h light-12-h dark (LD) cycle. The following day, any dead or unfertilised embryos were removed, and fresh embryo media was added in place of the old one. The viable embryos were exposed to eight different MOLE concentrations (5-1000 µg/mL) for 72 h at 28°C in a semi-static environment (24 hpf to 96 hpf). Using an inverted microscope equipped with a camera (Leica, Germany), several toxicological endpoints, such as survival rate, heart rate, hatching rate, and morphological development, were monitored and recorded at 24-hour intervals. The treatment solutions were changed daily, and E3 media was used as a control (Ghafor et al., 2020; Mohamad Shariff et al., 2020; Shamsi et al., 2022).

The mortality of the embryos was indicated by the presence of coagulation and the absence of a heartbeat to assess the survival rate. The survival rate was determined by counting the number of live embryos or larvae at each observation point. Dead embryos were denoted as "1," while surviving embryos were labelled as "0". A similar approach was employed for the hatching rate observation. Heart rate was determined by observing heartbeats over a 15-second interval and then extrapolating the count to 60 seconds to establish the average beats per minute (bpm) (Shamsi et al., 2020). Additionally, to assess the impact of MOLE toxicity on embryos, their morphological development was examined at 24 h, 48 h, and 72 h post-treatment, including the presence of body axis curvature, yolk sac oedema, pericardial oedema, and scoliosis. The dead embryos were extracted daily during the observation period to prevent contamination. Three independent experiments were performed for each treatment group ($n \geq 10$ embryos per exposure group).

Statistical Analysis

One-way Analysis of Variance (ANOVA), a statistical hypothesis test, was performed with Dunnett post-hoc test comparison where indicated. The statistical significance of the results was defined by a $p \leq 0.05$. The data were analysed using GraphPad Prism version 10.2.3 statistical analysis software (GraphPad Software, USA). All experiments were independently repeated three times. Data was presented as mean ± standard error of the mean (SEM). A *p*-value of less than 0.05 was considered to be statistically significant.

RESULTS AND DISCUSSION

Phytochemicals Composition of MOLE

An LC-MS analysis was conducted using both positive and negative ionisation MS/MS modes to investigate the phytochemical composition of the ethanolic MOLE. Ethanolic extracts efficiently solubilise a wide range of bioactive compounds, facilitating thorough toxicity evaluation while maintaining the pharmacological attributes of the plant (Lee et al., 2024). The data were compared and validated using online databases, PubChem, and previously published studies. Table 1 lists some of the principal phytochemicals detected in MOLE, which may have influenced the extract's pharmacological activities and toxicity profile. These phytochemical compounds are well-documented for their diverse properties, such as antioxidant activity, which interferes with the cell cycle, induces apoptosis, and decreases oxidative stress (Shukla & Gupta, 2010). For example, alkaloids, notably cepharanthine, may possess significant antioxidant properties that facilitate the scavenging and prevention of radical formation, thereby safeguarding deoxyribonucleic acid (DNA) from damage induced by endogenously generated radicals during oxidative metabolism.

A study reported that cepharanthine exhibits potent anti-inflammatory activity by diminishing the expression of the NF-κB transcription factor. This effect is achieved by inhibiting the IκB kinase (IKK) pathway and reducing pro-inflammatory cytokines such as TNF-α and IL-1β (Bailly, 2019). In the IKK pathway, IκB normally inhibits cytoplasmic NF-κB. However, upon LPS stimulation, IκB is phosphorylated, allowing NF-κB to translocate into the nucleus and activate pro-inflammatory genes. Cepharanthine interrupted this process by inhibiting LPS-induced IκB phosphorylation, thereby blocking NF-κB activation. As a result, the secretion of cytokines and nitric oxide (NOx) is reduced, demonstrating its anti-inflammatory mechanism (Kudo et al., 2011). In addition, flavonoids exhibit anti-inflammatory properties by inhibiting NF-κB activation, exerting anti-inflammatory effects, and preventing lipid oxidation (Milla et al., 2021). The terpenoid derivative, emmotin A, was also detected in MOLE. Emmotin A is an anti-neuroinflammatory agent that showed strong binding interactions with AChE, BChE, α-glucosidase, α-amylase, and tyrosinase in an *in silico* molecular docking study, indicating its ability to maintain ACh levels and suppress neuroinflammation (Saleem et al., 2020).

Table 1
List of major phytochemicals in MOLE and its potential activity

Name of compound	Molecular formula	Class of bioactive compound	Potential activity	Ion (+/-)	Reference
Cepharanthine	$C_{37}H_{38}N_2O_6$	Alkaloids	Antioxidant, anti-inflammatory	[M+H]+	Bailly (2019)
Apigenin 5-glucoside	$C_{21}H_{20}O_{10}$	Flavonoids	Antioxidant, anti-mutagenic and anti-inflammatory properties	[M+H]+	Shukla & Gupta (2010)
Quercetin 3-(6"-malonylgalactoside)	$C_{24}H_{22}O_{15}$	Flavonoids	Anti-inflammatory, anticancer, cardioprotective, anti-tumour, anti-viral, anti-diabetic, antihypertensive, gastroprotective effects	[M+H]+	Milla et al. (2021)
Emmotin A	$C_{16}H_{22}O_4$	Terpenoid	Anti-neuroinflammatory	[M+H]+	Ngu et al. (2022)
3,4-dihydroxyphenylethanol-elenolic acid (3,4-DHPEA-EA)	$C_{19}H_{22}O_8$	Phenolic compounds	Antioxidant, antihypertensive, antibacterial	[M+H]-	Segade et al. (2016), Bisignano et al. (2014)
Trans-Stilbene	$C_{14}H_{12}$	Phenolic compounds	Antioxidant, cardioprotective, cancer chemopreventive, anti-inflammatory, anti-diabetic, antibacterial	[M+H]-	Treml & Šmejkal (2016)
Monocrotaline	$C_{16}H_{23}NO_6$	Pyrrolizidine alkaloid (PA) family of plant toxins	Induce developmental toxicity, hepatotoxicity, pulmonary lesions, and cancer	[M+H]-	Luo et al. (2019), Chen et al. (2010), Louisse et al. (2019), Sakamoto et al. (2017)

The negative ionisation results of aMS/MS revealed several bioactive compounds, including 3,4-dihydroxyphenylethanol-elenolic acid (3,4-DHPEA-EA). This isomer of oleuropein aglycone acts as an antioxidant, protecting cells from oxidative damage through radical scavenging, metal ion chelation, and induction of antioxidant enzymes. Additionally, 3,4-DHPEA-EA has antihypertensive activity and is a major component of virgin olive oil consumed to regulate blood pressure (Segade et al., 2016). It also shows antibacterial properties and is effective against gram-positive bacteria such as staphylococci,

suggesting its potential as a natural antimicrobial for treating bacterial skin infections (Bisignano et al., 2014). Additionally, trans-stilbene has been identified and is renowned for its antioxidant properties. In a lipoperoxidation inhibition assay, which measures the ability of a compound to prevent the oxidative degradation of lipids, trans-stilbene emerged as the most active compound (Treml & Šmejkal, 2016). Its other pharmacological properties include cardio-protection, cancer chemoprevention, anti-inflammatory effects, anti-diabetes, and antibacterial activity. Monocrotaline (MCT) was detected in the extract. It is an 11-membered macrocyclic diester classified as a pyrrolizidine alkaloid (PA), a plant toxin. Ingestion of MCT can severely affect humans, causing developmental toxicity, hepatotoxicity, pulmonary lesions, and cancer (Chen et al., 2010; Louisse et al., 2019; Luo et al., 2019). Consequently, MCT has been utilised in toxicity studies to induce pulmonary hypertension, aiding research on chronic pulmonary vascular diseases in humans. For example, a study showed that rats can experience significant and gradual lung damage from even small amounts of MCT (Sakamoto et al., 2017).

Survival Rate of Zebrafish Embryos Treated with MOLE

In the present study, the toxicity effects of MOLE were determined using a zebrafish embryo model as it is known to provide real-time *in vivo* studies to address possible health risks to humans resulting from naturally occurring compounds (Bambino & Chu, 2017). The survival rate of zebrafish embryos exposed to different concentrations of MOLE (5-1000 µg/mL), as observed at 24 h, 48 h, and 72 h post-treatment, is shown in Figure 1A-C. The lethal concentration for the embryos (LC_{50}) values of MOLE in zebrafish embryos exposure for 24 h to 72 h post-treatment are also presented in Table 2. The concentration range of MOLE

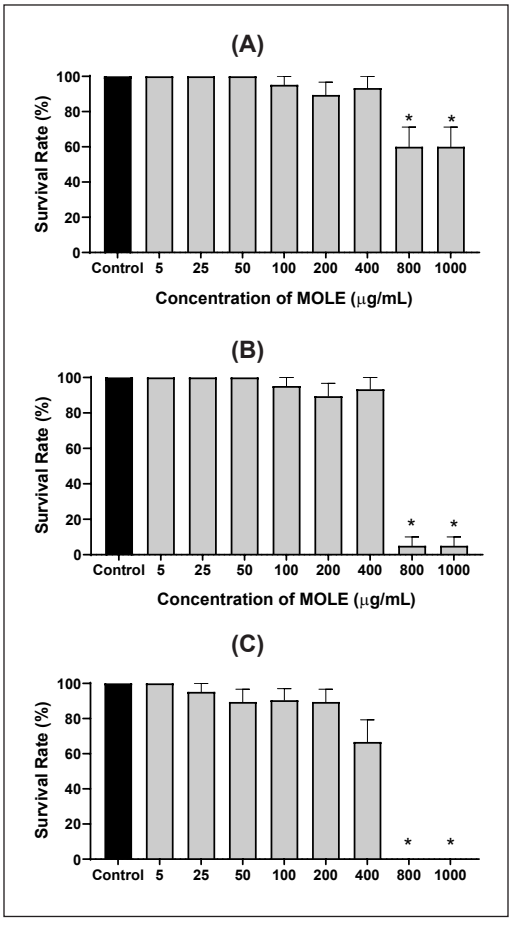

Figure 1. The effects of different concentrations of MOLE (5-1000 µg/mL) on survival of zebrafish (*Danio rerio*) at (A) 24 h, (B) 48 h, and (C) 72 h post-exposure ($n \geq 15$). Embryo media was used as control. Data were shown as mean ± SEM
Note. Significant difference to control is denoted by "*" (One-way ANOVA, followed by a post hoc test: Dunnet $p \leq 0.05$)

used in this study was determined based on previous findings indicating that embryos treated with aqueous ethanolic extract of MOLE exhibited better embryogenesis development compared to those treated with aqueous methanolic extract at equivalent concentrations (Mohamad Shariff et al., 2020).

Table 2
LC_{50} values of MOLE following its exposure to zebrafish embryos from 24 h to 72 h post-treatment

Time of exposure (post-treatment, hr)	LC_{50} of MOLE (µg/mL)
24	1186.0 ± 7
48	560.1 ± 7
72	445.1 ± 7

Survival analysis revealed that embryo survivability decreased with increasing MOLE concentrations in a time-dependent manner. A lower survival rate was recorded as the concentration of MOLE and the exposure times increased. Embryos treated with concentrations < 400 µg/mL of MOLE showed good survival rates over time, with > 80% of embryos surviving up to 48 h post-treatment before slightly declining at 72 h post-treatment (Figure 1). Although treatment with 400 µg/mL of MOLE caused a reduction in the survival rate to approximately 70% at 72 h post-treatment, it was not statistically significant. It was still comparable to the control group (Figure 1C). In contrast, the survival rate of zebrafish embryos treated with a higher concentration of MOLE (> 800 µg/mL) progressively decreased over the exposure period, from approximately 60% at 24 h post-treatment (Figure 1A) to less than 10% at 48h post-treatment (Figure 1B). By 72 h post-treatment, none of the zebrafish embryos in this group survived the study (Figure 7C). As expected, all embryos in the control group (E3 media) maintained 100% survival throughout the study.

This finding indicates that higher concentrations and prolonged exposure to MOLE significantly compromised the survivability of embryos. It is possible that MOLE is taken up by zebrafish embryos through the skin and gills in the early stages of embryo development (Sakeh et al., 2020). Furthermore, these results suggested that the ability of the surrounding compounds to penetrate the embryo became greater as the time of exposure lengthened, leading to its toxicity. It could be explained by the fact that the protective layer surrounding the embryo, called the chorion, which is present in the early stages of development, changes with age. Previous research has indicated that changes in the protein composition of the chorion could result in the expansion or enlargement of chorion pore channels, enabling a higher entry of external substances (Ali et al., 2017).

Hatching Rate of Zebrafish Embryos Treated with MOLE

The hatching rate is a critical stage during embryogenesis and an important parameter in toxicity studies. A zebrafish embryo is considered to have hatched once its body has completely emerged from the chorion (David et al., 2016), and it would usually begin at 48 h post-fertilisation (hpf) under normal conditions (Chen et al., 2018). In the present study, the

hatching rate of zebrafish embryos did not show significant differences when exposed to various concentrations of MOLE at any of the monitored time points (Figure 2), with all embryos showing comparable hatching rates to the control group. However, a significant difference in hatching rate was observed in embryos treated with > 800 µg/mL of MOLE at 96 hpf (Figure 2C). This reduction was not due to delayed hatching from the MOLE treatment but was attributed to high mortality rates at higher concentrations. Most embryos treated with 800 and 1000 µg/mL of MOLE died at 72 hpf (48 h post-treatment) (Figure 1B), explaining the similar hatching rates observed at both 72 hpf and hpf (Figure 1B-C). These findings show that MOLE did not affect the hatching rate at any time point or tested concentration.

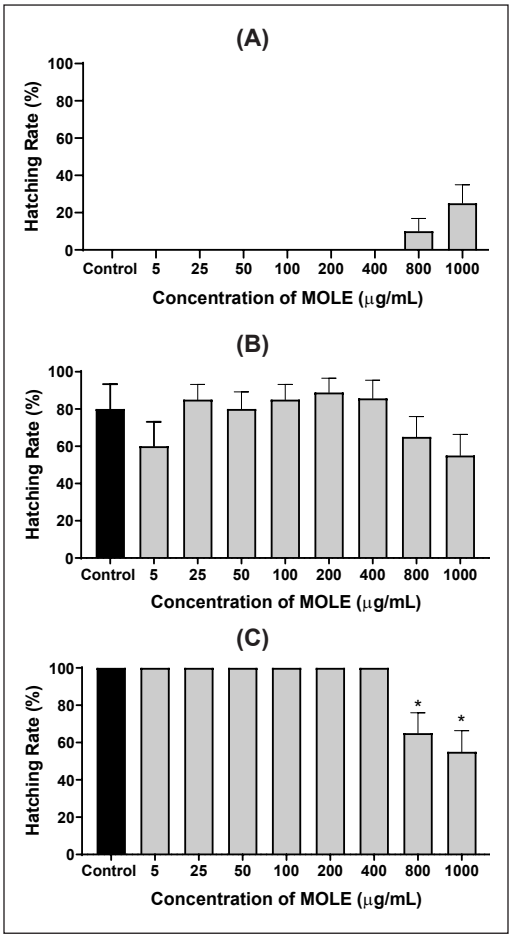

Figure 2. The effects of different concentrations of MOLE (5-1000 µg/mL) on the hatching rate of zebrafish (*Danio rerio*) at (A) 48 h, (B) 72 h and (C) 96 h post-fertilisation (hpf) ($n \geq 15$). Embryo media was used as a control

Note. Significant difference to control is denoted by "*" (One-way ANOVA, followed by a post hoc test: Dunnet $p \leq 0.05$)

Heart Rate of Zebrafish Embryos Treated with MOLE

The heart is the first organ to form and operate in zebrafish development. Zebrafish hearts have a transparency property that allows for single-cell resolution visualisation, making them a perfect subject for monitoring toxicity. Zebrafish embryos have a heart rate of 120–180 beats per minute (bpm) (Chahardehi et al., 2020; Ghafor et al., 2020).

The heart rates of the zebrafish embryos treated with different concentrations of MOLE are shown in Figure 3. There were no significant differences in the heart rate of zebrafish embryos treated with MOLE concentrations ≤ 400 µg/mL compared to the control group at all time points, as all rates fell within the normal range of between 120 and 180 bpm. At 72 h post-treatment, the heart rate of the 100 µg/mL concentration group appeared slightly above the normal range (>180 bpm). However, the difference was not statistically significant and comparable to the control group. The increase in heart rate could be due

to various factors, such as a response to sudden changes in temperature. A previous study has reported that a sudden decrease in temperature from 28°C to 18°C caused a 48% reduction in the heart rate of zebrafish (Lee et al., 2016).

In addition, abnormalities in the heart rate of zebrafish embryos might also result from exposure to compounds that influence sodium and potassium channels, particularly ATP-sensitive potassium (K_{ATP}) channels. For example, ouabain, which is a cardiac glycoside usually derived from *Stropanthus gratus*, primarily inhibits the Na^+/K^+-ATPase pump, leading to a disruption in the balance of sodium and potassium ions across the cell membrane (Rajanathan et al., 2023). These channels play crucial roles in heart rate control and adaptation to metabolic changes. Disruption of K_{ATP} channels through genetic manipulation or exposure to external compounds can lead to heart rate dysregulation (Aziz et al., 2018). Elevated heart rates can strain heart muscles, which could eventually cause damage to zebrafish hearts. Similar to other observations, higher concentrations of MOLE (> 800 µg/mL) significantly affected the heart rate of the treated embryos (Figure 3). A decrease in heart rate was noted at 24 h post-treatment, which gradually declined as exposure time increased. By the end of the observation period (72 h post-treatment), all embryos at these higher concentrations exhibited no heart rate, leading to mortality (Figure 3C). These findings suggest that MOLE may be harmful at higher doses that induce cardiac arrhythmia and embryonic bradycardia, which in turn causes severe hypoxia and foetal distress, contributing to the fatality observed in Figure 1 (Manjunatha et al., 2018).

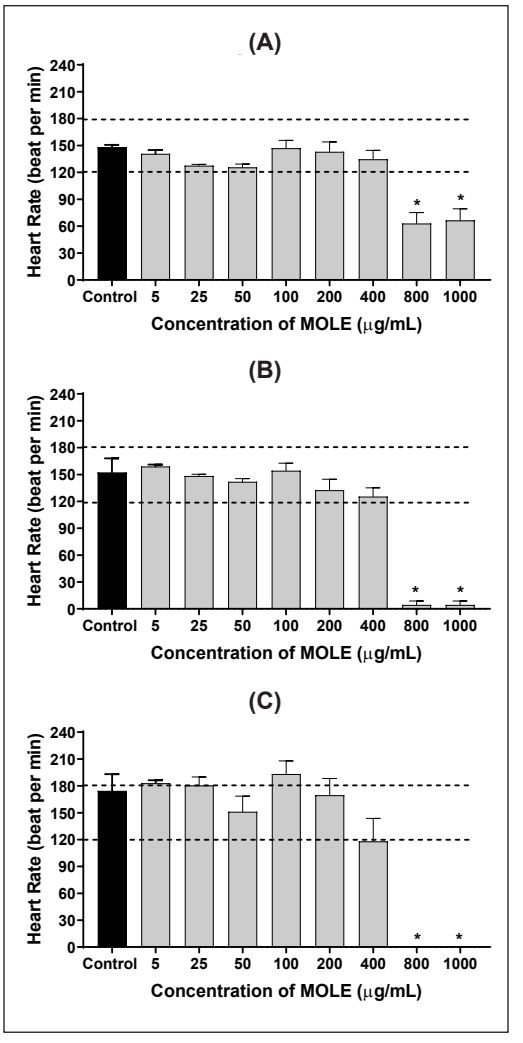

Figure 3. Heartbeats of zebrafish embryos in the presence of different concentrations of MOLE (5-1000 µg/mL) at (A) 24 h, (B) 48 h and (C) 72 h post-treatment ($n \geq 15$). Embryo media was used as control. Significant difference to control is denoted by "*" (One-way ANOVA, followed by a post hoc test: Dunnet $p \leq 0.05$). Dashed lines (---) represent the range of a normal heart rate for zebrafish embryos (120–180 beats per minute)

Morphological Assessments of Zebrafish Embryos Treated with MOLE

In the present study, the toxicity effects of MOLE were also assessed morphologically daily for up to 96 h post-treatment. The deformities or malformations detected in this study included scoliosis (S), pericardial oedema (PE), yolk sac oedema (YSE) and body axis curvature (BAC) (Figure 4). Scoliosis, which is the lateral curvature of the spine, was the only abnormality observed in embryos treated with 25 to 200 µg/mL of MOLE (Table 3), which might be caused by oxidative damage (Heredia-García et al., 2021). This oxidative damage may play a role in the development and progression of scoliosis, as elevated oxidative stress has been reported to lead to apoptosis and disrupt muscle tissue formation, potentially contributing to the pathological changes seen in patients with Idiopathic Scoliosis (IS). In zebrafish models, oxidative stress has been linked to muscle degeneration and spinal deformities, suggesting a possible mechanism by which oxidative damage influences scoliosis (Li et al., 2019). Interestingly, no other abnormalities were observed at this concentration range.

In contrast, pericardial oedema, yolk sac oedema, and body axis curvature were collectively observed in embryos treated with higher concentrations of MOLE (> 800 µg/mL). The formation of pericardial oedema during embryogenesis is most likely due to the weakening of the embryo chorion layer following exposure to the treatments, which allows a greater intake of MOLE and induces toxic effects on zebrafish over time (Ali et al.,

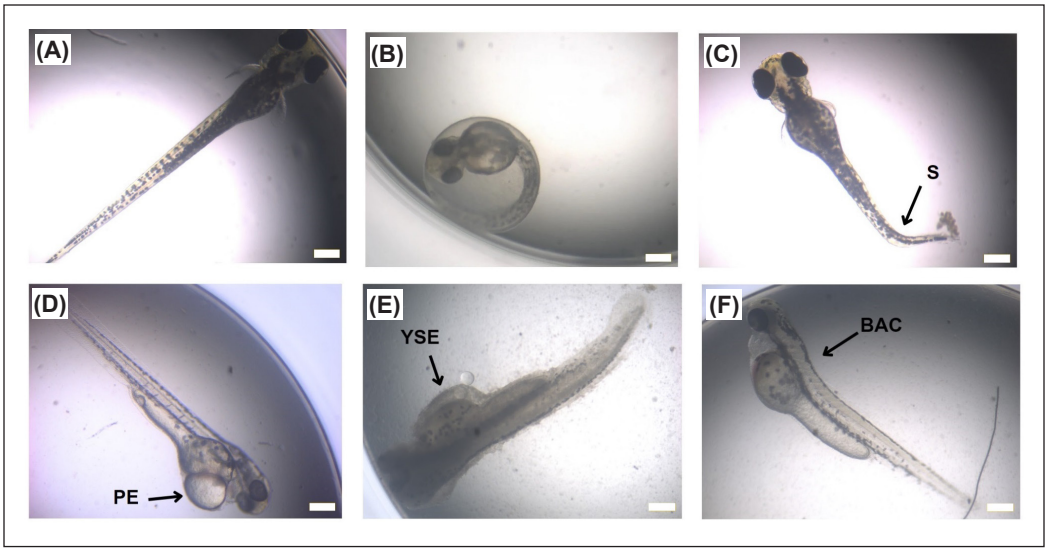

Figure 4. Microscope images showing the incidence of malformations in zebrafish embryos, as indicated by a black arrow. (A) Normal hatched zebrafish, (B) Normal zebrafish embryo, (C) Zebrafish with scoliosis, (D) Zebrafish with pericardial oedema, (E) Zebrafish with yolk sac oedema, (F) Zebrafish with body axis curvature *Note*. S = Scoliosis, PE = Pericardial oedema, YSE = Yolk sac oedema, BAC = Body axis curvature. Scale = 250 µm

2017). The yolk sac plays an important role in embryogenesis and normally stores nutrients. Impairment of the yolk sac, such as yolk sac oedema observed at higher concentrations, could impair nutrient absorption by the embryo, resulting in malnourished embryos that may eventually perish. Meanwhile, body axis curvature formations are potentially caused by chorion formation failure, which disrupts somite development and subsequently induces malformation in the body axis (Syahbirin et al., 2017).

Table 3
Malformation incidences in zebrafish embryos treated with different concentrations of MOLE at 24 to 72 h post-treatment

MOLE Concentration (µg/mL)	Malformation incidence (%)			
	Scoliosis (S)	Pericardial oedema (PE)	Yolk sac oedema (YSE)	Body axis curvature (BAC)
Control	0	0	0	0
5	0	0	0	0
25	14	0	0	0
50	15	0	0	0
100	35	0	0	0
200	52	0	0	0
400	0	0	0	0
800	25	8	33	50
1000	8	0	41	50

CONCLUSION

Moringa oleifera is rich in bioactive compounds with potential health benefits, particularly from its leaves. The toxicity assessment of ethanolic *M. oleifera* leaf extract (MOLE) on zebrafish embryos in this study revealed concentration- and time-dependent toxic effects on survivability, changes in heart rate and malformations during embryogenesis. Consequently, MOLE is considered safe at up to 400 µg/mL concentrations, as higher concentrations result in significant toxic effects. These findings indirectly highlight the effectiveness of the zebrafish embryo model in providing comprehensive toxicity profiles of medicinal plants, compared to other settings such as cell lines and rodents. Further toxicity assessments of MOLE are essential for comprehensive understanding and safe implementation as a human herbal therapeutic agent.

ACKNOWLEDGEMENTS

This research was funded by the Universiti Putra Malaysia Putra Grant (GP-IPS/2024/9813900). The authors gratefully acknowledge the support and technical assistance of the Cell Signalling Laboratory facilities in the Faculty of Medicine and Health

Sciences, Universiti Putra Malaysia, the AAALAC-accredited Zebrafish Satellite Animal Facility, Animal Experimental Unit, Faculty of Medicine, Universiti Malaya, and Monash University Malaysia Proteomics and Metabolomics Platform (MUMPMP), Jeffrey Cheah School of Medicine and Health Sciences, Monash University Malaysia.

REFERENCES

Abdullah, S. N. S., Subramaniam, K. A., Muhamad Zamani, Z. H., Sarchio, S. N. E., Yasin, F. M., & Shamsi, S. (2022). Biocompatibility study of curcumin-loaded Pluronic F127 nanoformulation (NanoCUR) against the embryonic development of zebrafish (*Danio rerio*). *Molecules*, *27*(14), 4493. https://doi.org/10.3390/molecules27144493

Ali, M. K., Saber, S. P., Taite, D. R., Emadi, S., & Irving, R. (2017). The protective layer of zebrafish embryo changes continuously with advancing age of embryo development (AGED). *Journal of Toxicology and Pharmacology*, *1*(009).

Arulselvan, P., Tan, W. S., Gothai, S., Muniandy, K., Fakurazi, S., Esa, N. M., Alarfaj, A. A., & Kumar, S. S. (2016). Anti-inflammatory potential of ethyl acetate fraction of *Moringa oleifera* in downregulating the NF-κB signaling pathway in lipopolysaccharide-stimulated macrophages. *Molecules (Basel, Switzerland)*, *21*(11), 1452. https://doi.org/10.3390/molecules21111452

Ashraf, M., Alam, S. S., Fatima, M., Altaf, I., Khan, F. & Afzal, A. (2017). Comparative anti-influenza potential of *Moringa oleifera* leaves and amantadine *in vitro*. *Pakistan Postgraduate Medical Journal*, *28*, 127–131. https://doi.org/10.51642/ppmj.v28i4.66

Aziz, Q., Li, Y., Yang, P., Hu, D., Palmer, C., Wang, P., & Logantha, S. J. R. J. (2018). ATP-sensitive potassium channels in the sinoatrial node contribute to heart rate control and adaptation to hypoxia. *Journal of Biological Chemistry*, *293*(23), 8912-8921. https://doi.org/10.1074/jbc.RA118.002775

Azlan, U. K., Mediani, A., Rohani, E. R., Tong, X., Han, R., Misnan, N. M., Jam, F. A., Bunawan, H., Sarian, M. N., & Hamezah, H. S. (2022). A comprehensive review with updated future perspectives on the ethnomedicinal and pharmacological aspects of *Moringa oleifera*. *Molecules*, *27*(18), 5765. https://doi.org/10.3390/molecules27185765

Bailly, C. (2019). Cepharanthine: An update of its mode of action, pharmacological properties and medical applications. *Phytomedicine*, *62*, 152956–152956. https://doi.org/10.1016/j.phymed.2019.152956

Bambino, K., & Chu, J. (2017). Zebrafish in toxicology and environmental health. *Current Topics in Developmental Biology/Current Topics in Developmental Biology*, *124*, 331–367. https://doi.org/10.1016/bs.ctdb.2016.10.007

Başaran, N., Paslı, D., & Başaran, A. A. (2022). Unpredictable adverse effects of herbal products. *Food and Chemical Toxicology*, *159*, 112762. https://doi.org/10.1016/j.fct.2021.112762

Bisignano, C., Filocamo, A., Ginestra, G., Giofrè, S. V., Navarra, M., Romeo, R., & Mandalari, G. (2014). 3,4-DHPEA-EA from *Olea europaea* L. is effective against standard and clinical isolates of *Staphylococcus sp*. *Annals of Clinical Microbiology and Antimicrobials*, *13*, 24. https://doi.org/10.1186/1476-0711-13-24

Cervera-Chiner, L., Pageo, S., Juan-Borrás, M., García-Mares, F. J., Castelló, M. L., & Ortolá, M. D. (2024). Fatty acid profile and physicochemical properties of *Moringa oleifera* seed oil extracted at different temperatures. *Foods (Basel, Switzerland)*, *13*(17), 2733. https://doi.org/10.3390/foods13172733

Chahardehi, A. M., Arsad, H., & Lim, V. (2020). Zebrafish as a successful animal model for screening toxicity of medicinal plants. *Plants*, *9*(10), 1345. https://doi.org/10.3390/plants9101345

Chen, L., Xu, M., Gong, Z., Zonyane, S., Xu, S. & Makunga, N. P. (2018). Comparative cardio and developmental toxicity induced by the popular medicinal extract of *Sutherlandia frutescens* (L.) R.Br. detected using a zebrafish Tuebingen embryo model. *BMC Complementary and Alternative Medicine*, *18*, 273. https://doi.org/10.1186/s12906-018-2303-9

Chen, T., Mei, N., & Fu, P. P. (2010). Genotoxicity of pyrrolizidine alkaloids. *Journal of Applied Toxicology: An International Journal*, *30*(3), 183-196. https://doi.org/10.1002/jat.1504

David, C. R. S., Angeles, A., Angoluan, R. C., Santos, J. P. E., David, E. S., & Dulay, R. M. R. (2016). *Moringa oleifera* (Malunggay) water extracts exhibit embryo-toxic and teratogenic activity in zebrafish (*Danio rerio*) embryo model. *Der Pharma Letters*, *8*, 163–168.

Ekor, M. (2014). The growing use of herbal medicines: Issues relating to adverse reactions and challenges in monitoring safety. *Frontiers in pharmacology*, *4*, 177. https://doi.org/10.3389/fphar.2013.00177

Farooq, B., & Koul, B. (2020). Comparative analysis of the antioxidant, antibacterial and plant growth promoting potential of five Indian varieties of *Moringa oleifera* L. *South African Journal of Botany*, *129*, 47-55. https://doi.org/10.1016/j.sajb.2018.12.014

Ghafor, A. A. A. H., Elias, N., Shamsi, S., Yasin, F. M., & Sarchio, S. N. E. (2020). Toxicity assessment of gallic acid loaded graphene oxide (GAGO) nano-formulation in zebrafish (*Danio rerio*) embryos. *Pertanika Journal of Science & Technology*, *28*(1), 311-326.

Gupta, S., Jain, R., Kachhwaha, S., & Kothari, S. L. (2018). Nutritional and medicinal applications of *Moringa oleifera* Lam.—Review of current status and future possibilities. *Journal of Herbal Medicine*, *11*, 1-11, https://doi.org/10.1016/j.hermed.2017.07.003

Heredia-García, G., Gómez Oliván, L. M., Elizalde-Velázquez, G. A., Cardoso-Vera, J. D., Orozco-Hernández, J. M., Rosales-Pérez, K. E., García-Medina, S., Islas-Flores, H., Galar-Martínez, M., & Dublán-García, O. (2021). *Developmental alterations and oxidative damage induced by environmentally relevant concentrations of bisphenol A in zebrafish embryos (Danio rerio).* Social Science Research Network. https://ssrn.com/abstract=3970772

Howe, K., Clark, M. D., Torroja, C. F., Torrance, J., Berthelot, C., Muffato, M., Collins, J. E., Humphray, S., McLaren, K., Matthews, L., McLaren, S., Sealy, I., Caccamo, M., Churcher, C., Scott, C., Barrett, J. C., Koch, R., Rauch, G.-J., White, S., ... Stemple, D. L. (2013). The zebrafish reference genome sequence and its relationship to the human genome. *Nature*, *496*(7446), 498-503. https://doi.org/10.1038/nature12111

Ismail, E. N., Jantan, I., Vidyadaran, S., Jamal J. A. & Azmi, N. (2020). *Phyllanthus amarus* prevents LPS-mediated BV2 microglial activation via MyD88 and NF-κB signaling pathways. *BMC Complementary Medicine and Therapies*, *20*, 202. https://doi.org/10.1186/s12906-020-02961-0

Jafarain, A., Asghari, G., & Ghassami, E. (2014). Evaluation of cytotoxicity of *Moringa oleifera* Lam. callus and leaf extracts on Hela cells. *Advanced Biomedical Research*, *3*, 194. https://doi.org/10.4103/2277-9175.140668

Kudo, K., Hagiwara, S., Hasegawa, A., Kusaka, J., Koga, H., & Noguchi, T. (2011). Cepharanthine exerts anti-inflammatory effects via NF-κB inhibition in a LPS-induced rat model of systemic inflammation. *Journal of Surgical Research*, *171*(1), 199-204. https://doi.org/10.1016/j.jss.2010.01.007

Lee, J. E., Jayakody, J. T. M., Kim, J. Il, Jeong, J. W., Choi, K. M., Kim, T. S., Seo, C., Azimi, I., Hyun, J. M., & Ryu, B. M. (2024). The influence of solvent choice on the extraction of bioactive compounds from Asteraceae: A comparative review. *Foods*, *13*(19), 3151. https://doi.org/10.3390/FOODS13193151/S1

Lee, L., Genge, C. E., Cua, M., Sheng, X., Rayani, K., Beg, M. F., Sarunic, M. V., & Tibbits, G. F. (2016). Functional assessment of cardiac responses of adult zebrafish (*Danio rerio*) to acute and chronic temperature change using high-resolution echocardiography. *PLOS ONE, 11*(1), e0145163. https://doi.org/10.1371/journal.pone.0149741

Leone, A., Spada, A., Battezzati, A., Schiraldi, A., Aristil, J., & Bertoli, S. (2015). Cultivation, genetic, ethnopharmacology, phytochemistry and pharmacology of *Moringa oleifera* leaves: An overview. *International Journal of Molecular Sciences*, *16*(6), 12791-12835. https://doi.org/10.3390/ijms160612791

Li, J., Tang, M., Yang, G., Wang, L., Gao, Q., & Zhang, H. (2019). Muscle injury associated elevated oxidative stress and abnormal myogenesis in patients with idiopathic scoliosis. *International Journal of Biological Sciences*, *15*(12), 2584–2595. https://doi.org/10.7150/ijbs.33340

Lorenzo, C. D., Ceschi, A., Kupferschmidt, H., Lüde, S., Nascimento, E.D.S., Santos, A.D., Colombo, F., Frigerio, G., Nørby, K., Plumb, J., Finglas, P., & Restani, P. (2015). Adverse effects of plant food supplements and botanical preparations: A systematic review with critical evaluation of causality. *British journal of clinical pharmacology*, *79*(4), 578–592. https://doi.org/10.1111/bcp.12519

Louisse, J., Rijkers, D., Stoopen, G., Jansen Holleboom, W., Delagrange, M., Molthof, E., Mulder, P. P. J., Hoogenboom, R. L. A. P., Audebert, M., & Peijnenburg, A. A. C. M. (2019). Determination of genotoxic potencies of pyrrolizidine alkaloids in HepaRG cells using the γH2AX assay. *Food and Chemical Toxicology*, *128*, 171-180. https://doi.org/10.1016/j.fct.2019.05.040

Luo, J., Yang, X., Qiu, S., Li, X., Xiang, E., Fang, Y., Wang, Y., Zhang, L., Wang, H., Zheng, J., & Guo, Y. (2019). Sex difference in monocrotaline-induced developmental toxicity and fetal hepatotoxicity in rats. *Toxicology*, *418*, 32-40. https://doi.org/10.1016/j.tox.2019.02.014

Manjunatha, B., Park, S. H., Kim, K., Kundapur, R. R., & Lee, S. J. (2018). *In vivo* toxicity evaluation of pristine graphene in developing zebrafish (*Danio rerio*) embryos. *Environmental Science and Pollution Research*, *25*(13), 12821-12829. https://doi.org/10.1007/s11356-018-1484-1

Milla, P. G., Peñalver, R., & Nieto, G. (2021). Health benefits of uses and applications of *Moringa oleifera* in bakery products. *Plants*, *10*(2), 318. https://doi.org/10.3390/plants10020318

Mohamad Shariff, N. F. S., Singgampalam, T., Ng, C. H., & Kue, C. S. (2020), Antioxidant activity and zebrafish teratogenicity of hydroalcoholic *Moringa oleifera* L. leaf extracts. *British Food Journal*, *122*(10), 3129-3137. https://doi.org/10.1108/BFJ-02-2020-0113

Ngu, E. L., Tan, C. Y., Lai, N. J.Y., Wong, K. H., Lim, S. H., Ming, L. C., Tan, K. O., Phang, S. M., & Yow, Y. Y. (2022). *Spirulina platensis* suppressed iNOS and proinflammatory cytokines in lipopolysaccharide-induced BV2 microglia. *Metabolites*, *12*(11), 1147. https://doi.org/10.3390/metabo12111147

Osman, H. M., Shayoub, M. E., Babiker, E. M., Faiza, A. O., Ahmed, M. E. M., Osman, B., Elhassan, A. M., & Taha, K. K. (2015). Assessment of acute toxicity and LD50 of *Moringa oleifera* ethanolic leaf extract in albino rats and rabbits. *Journal of Medical and Biological Science Research*, *1*(4), 38-43.

Oyagbemi, A. A., Omobowale, T. O., Azeez I. O., Abiola J. O., Adedokun, R. A., Nottidge, H. O. (2013). Toxicological evaluations of methanolic extract of *Moringa oleifera* leaves in liver and kidney of male Wistar rats. *Journal of Basic and Clinical Physiology and Pharmacology*, *24*(4), 307-12. https://doi.org/10.1515/jbcpp-2012-0061

Posadzki, P., Watson, L. K., & Ernst, E. (2013). Adverse effects of herbal medicines: An overview of systematic reviews. *Clinical Medicine*, *13*(1), 7–12. https://doi.org/10.7861/clinmedicine.13-1-7

Rajanathan, R., Pedersen, T. M., Guldbrandsen, H. O., Olesen, L. F., Thomsen, M. B., Bøtker, H. E., & Matchkov, V. V. (2023). Augmented ouabain-induced vascular response reduces cardiac efficiency in mice with migraine-associated mutation in the Na^+, K^+-ATPase α_2-isoform. *Biomedicines*, *11*(2), 344. https://doi.org/10.3390/biomedicines11020344

Rockwood, J. L., Anderson, B. G., & Casamatta, D. A. (2013). Potential uses of *Moringa oleifera* and an examination of antibiotic efficacy conferred by *M. oleifera* seed and leaf extracts using crude extraction techniques available to under-served indigenous populations. *International Journal of Phytothearpy Research*, *3*(2), 61–71.

Rothenbücher, T. S.P., Ledin, J., Gibbs, D., Engqvist, H., Persson, C. & Hulsart-Billström, G. (2019). Zebrafish embryo as a replacement model for initial biocompatibility studies of biomaterials and drug delivery systems. *Acta Biomaterialia*, *100*(235-243). https://doi.org/10.1016/j.actbio.2019.09.038.

Sakamoto, S., Nagamitsu, R., Yusakul, G., Miyamoto, T., Tanaka, H., & Morimoto, S. (2017). Ultrasensitive immunoassay for monocrotaline using monoclonal antibody produced by N, N'-carbonyldiimidazole mediated hapten-carrier protein conjugates. *Talanta*, *168*, 67-72. https://doi.org/10.1016/j.talanta.2017.03.028

Sakeh, N. M., Razip, N. N. M., Ma'in, F. I. M., Bahari, M. N. A., Latif, N., Akhtar, M. N., Yusof, Z. N. B., & Ahmad S. (2020). Melanogenic inhibition and toxicity assessment of flavokawain A and B on B16/F10 melanoma cells and zebrafish (*Danio rerio*). *Molecules*, *25*(15), 3403. https://doi.org/10.3390/molecules25153403

Saleem, H., Sarfraz, M., Khan, K. M., Anwar, M. A., Zengin, G., Ahmad, I., Khan, S. U., Mahomoodally, M. F., & Ahemad, N. (2020). UHPLC-MS phytochemical profiling, biological propensities and in-silico studies of *Alhagi maurorum* roots: A medicinal herb with multifunctional properties. *Drug development and industrial pharmacy*, *46*(5), 861-868. https://doi.org/10.1080/03639045.2020.1762199

Segade, M., Bermejo, R., Silva, A., Paiva-Martins, F., Gil-Longo, J., & Campos-Toimil, M. (2016). Involvement of endothelium in the vasorelaxant effects of 3,4-DHPEA-EA and 3,4-DHPEA-EDA, two major functional bioactives in olive oil. *Journal of Functional Foods, 23*, 637-646, https://doi.org/10.1016/j.jff.2016.03.024

Shamsi, S., Abdul Ghafor, A. A. H., Norjoshukrudin, N. H., Ng, I. M. J., Abdullah, S. N. S., Sarchio, S. N. E., Yasin, F. M., Abd Gani, S., & Mohd Desa, M. N. (2022). Stability, toxicity, and antibacterial potential of gallic acid-loaded graphene oxide (GAGO) against methicillin-resistant *Staphylococcus aureus* (MRSA) strains. *International Journal of Nanomedicine*, *17*, 5781–5807. https://doi.org/10.2147/IJN.S369373

Shamsi, S., Alagan, A. A., Sarchio, S. N. E., & Yasin, F. M. (2020). Synthesis, characterization, and toxicity assessment of pluronic F127-functionalized graphene oxide on the embryonic development of zebrafish (*Danio rerio*). *International Journal of Nanomedicine*, *15*, 8311–8329. https://doi.org/10.2147/IJN.S271159

Shamsi, S., Zainudin, F. S., & Othman, A. N. (2021). Effects of different extraction solvents on the toxicity of *Piper sarmentosum* leaf extract in zebrafish (*Danio rerio*) embryos. *Malaysian Journal of Biochemistry & Molecular Biology*, *24*(3), 127-142. https://doi.org/10.2147/IJN.S369373

Shukla, S., & Gupta, S. (2010). Apigenin: A promising molecule for cancer prevention. *Pharmaceutical Research*, *27*(5), 962-978. https://doi.org/10.1007/s11095-010-0089-7

Syahbirin, G., Mumuh, N., & Mohamad, K. (2017). Curcuminoid and toxicity levels of ethanol extract of Javanese ginger (*Curcuma xanthorriza*) on brine shrimp (*Artemia salina*) larvae and zebrafish (*Danio rerio*) embryos. *Asian Journal of Pharmaceutical and Clinical Research*, *10*(4), 169-173. http://doi.org/10.22159/ajpcr.2017.v10i4.16429

Treml, J., & Šmejkal, K. (2016). Flavonoids as potent scavengers of hydroxyl radicals. *Comprehensive Reviews in Food Science and Food Safety*, *15*(4), 720-738. https://doi.org/10.1111/1541-4337.12204

Vijayalakshmi, M., Kiruthika, R., Bharathi, K., & Kandasamy, R. (2015). Phytochemical screening by LC-MS analysis and *in vitro* anti-inflammatory activity of *Marselia quadrifolia* plant extract. *International Journal of Pharmaceutical Sciences and Research, 8*(9), 148-157.

Pertanika J. Trop. Agric. Sci. 48 (3): 929 - 948 (2025)

PERTANIKA JOURNALS

TROPICAL AGRICULTURAL SCIENCE

Journal homepage: http://www.pertanika.upm.edu.my/

Effects of Silicon and Multimolig-M Fertilizer on the Morphological Characteristics, Growth, and Yield of the VTNA6 Rice in Vietnam

Hien Huu Nguyen[1]*, Minh Xuan Tran[1] and Thanh Cong Nguyen[2]

[1]School of Agriculture and Natural Resources, Vinh University, 182 Le Duan, Vinh City 43108, Vietnam
[2]Cyber School, Vinh University, 182 Le Duan, Vinh City 43108, Vietnam

ABSTRACT

Multimolig-M and silicon are essential fertilisers that enhance crop growth and yield. Silicon provides structural and protective benefits, while Multimolig-M supplies crucial micronutrients for metabolic functions, improving yield and quality. This study aims to evaluate the effects of silicon and Multimolig-M on the morphological characteristics, growth, and yield of the VTNA6 rice variety in Nghe An Province, Central Vietnam. The experiments were conducted using a randomised complete block design (RCBD) with three replications. Three levels of Multimolig-M (M_1: 360 ml/ha; M_2: 420 ml/ha; M_3: 480 ml/ha) and silicon (Si_1: 120 kg/ha; Si_2: 160 kg/ha; Si_3: 200 kg/ha) were applied. The results indicated significant improvements in flag leaf length, flag leaf width, panicle length, plant height, number of leaves, number of tillers, and number of effective tillers applying fertilisers. The treatment combination of 420 ml/ha Multimolig-M and 200 kg/ha silicon (M_2Si_3) produced the highest theoretical yield of 10.32 tons/ha and a net yield of 7.93 tons/ha, suggesting a synergistic effect of the two fertilisers. These findings highlight the positive impact of combining 420 ml/ha Multimolig-M with 200 kg/ha silicon on optimising yield and growth characteristics for VTNA6 rice, making it a recommended approach for enhancing rice productivity under local conditions in Nghe An.

Keywords: Multimolig-M fertiliser, morphological characteristics, plant growth, silicon fertiliser, VTNA6 rice yield

ARTICLE INFO

Article history:
Received: 15 September 2024
Accepted: 09 December 2024
Published: 16 May 2025

DOI: https://doi.org/10.47836/pjtas.48.3.15

E-mail addresses:
hiennh@vinhuni.edu.vn (Hien Huu Nguyen)
minhtx@vinhuni.edu.vn (Minh Xuan Tran)
thanhnc@vinhuni.edu.vn (Thanh Cong Nguyen)
* Corresponding author

INTRODUCTION

Rice (*Oryza sativa* L.) is an essential food source for over half of the global population. It ranks among the five most widely cultivated crops worldwide, alongside maise, wheat, cassava, and potatoes (Mohidem et al., 2022). Originating in tropical and subtropical regions of Southeast Asia and Africa, rice supplies vital nutrients and

e-ISSN: 2231-8542

calories to billions across continents, including Asia, Africa, the Americas, Australia, and Europe (Baltazar & De Datta, 2023).

In Vietnam, rice plays a crucial role in the agricultural sector and rural livelihoods (Tran, 2019), especially in regions like Nghe An Province, where challenging climatic and soil conditions affect rice productivity (Hạnh et al., 2020). High-yielding rice varieties, such as VTNA6, have contributed significantly to production increases, yet they encounter nutrient deficiency challenges that impact yield and quality (Đoàn et al., 2022). Effective nutrient management tailored to local conditions is essential to fully realise these varieties' growth and yield potential.

Nutrient application plays a key role in determining rice growth, morphology, and yield. Silicon (Si), for example, is well-documented for its beneficial effects on rice, fortifying leaves, stems, and roots to enhance growth and resilience (Meena et al., 2014). Research indicates that rice plants can absorb significant silicon, typically 230 to 470 kg/ha (Abdullah et al., 2021). Adequate silicon levels in rice plants lead to more upright leaves, which enhances sunlight absorption and improves photosynthetic capacity (Kheyri, 2022). Additionally, silicon-enriched leaves exhibit increased resistance to rice blast disease, while stronger stems reduce lodging, thereby decreasing the incidence of empty and shrivelled grains (Sheykhzadeh et al., 2022). Moreover, the application of silicon has been shown to reduce the prevalence of various diseases, such as brown spot disease, neck blast, sheath blight, leaf blight, and root nematodes, ultimately improving both the quality and yield of rice (Ma & Yamaji, 2006). However, rice response to silicon varies with environmental conditions and nutrient interactions.

Sustainable agriculture has increasingly been recognised as a crucial aspect of modern farming practices (Amrutha et al., 2022). Biofertilisers have become a promising approach for sustainable rice production, mitigating pollution (Pallarés et al., 2021) while significantly enhancing crop yields (Nosheen et al., 2021). Biofertilisers complement chemical fertilisers and serve as environmentally friendly supplements that promote healthy plant growth, making them a valuable resource for sustainable agriculture (Thomas & Singh, 2019). Multimolig-M is a biofertiliser that enhances soil quality and plant nutrition in organic agriculture. It can be applied to the soil to enhance its structure, nutrient uptake, and moisture retention, as well as to plant leaves to facilitate the rapid absorption of essential nutrients, including nitrogen (N), phosphorus (P), potassium (K), calcium (Ca), magnesium (Mg), sulfur (S), copper (Cu), iron (Fe), zinc (Zn), manganese (Mn), boron (B), and molybdenum (Mo). It enhances plant strength and reduces the reliance on traditional fertilisers and pesticides. Multimolig-M can increase crop yields by 10-40%, improve product quality, lower production costs by 30-50%, and is environmentally friendly (Đỗ, 2018).

Despite the established benefits of silicon and micronutrient fertilisers, limited research exists on their combined effects on the VTNA6 rice variety in Nghe An Province. This

study aims to fill this gap by evaluating the synergistic effects of silicon and Multimolig-M fertiliser on the VTNA6 rice variety. The findings are expected to provide valuable insights into optimising fertilisation strategies for improved rice production in Vietnam.

The objectives of this study are to (1) determine the effects of different levels of silicon and Multimolig-M fertiliser on the morphological traits, growth and yield of VTNA6 rice and (2) provide recommendations for effective fertiliser management practices in rice cultivation to enhance productivity and sustainability in Nghe An Province.

MATERIALS AND METHODS

Treatments and Experimental Design

The field experiments were conducted during the winter-spring season from December 2023 to May 2024 at the agricultural research station of the School of Agriculture and Natural Resources, Vinh University, located in Dien Chau district, Nghe An province, Central Vietnam (105.30-105.45°N, 18.20-19.50°E). Soil properties of the experimental site are shown in Table 1. The average temperature, rainfall and humidity during the experiments were 21.3°C, 91.7 mm and 84%, respectively (Figure 1). This study focused on the VTNA6 hybrid rice variety developed by the Nghe An Agricultural Materials Joint Stock Company (Ministry of Agriculture and Rural Development [MARD], 2018). Multimolig-M fertilizer is imported from Russia by UBB Trading and Service Co., Ltd., Dong Son silicon fertilizer is produced by Limex Vietnam Co., Ltd., Que Lam manure (cow dung) is manufactured by Que Lam Group, Vietnam, and Van Dien chemical fertilizer (N, P_2O_5, K_2O) is produced by Van Dien Fused Magnesium Phosphate Fertilizer Joint Stock Company, Vietnam.

The experiments were arranged as randomised complete block designs (RCBD) with three replications. The area of each plot was 25 m^2 (5 × 5 m). The rice was planted in rows of 13 × 20 cm spacing with one plant per cluster. Three levels of Multimolig-M (M_1: 360 ml/ha; M_2: 420 ml/ha; M_3: 480 ml/

Table 1
Soil properties of the experimental site

Properties	Values
pH (1: 2.5 soil water suspension)	5.20
ECe (mS/cm)	0.31
Organic carbon (%)	0.70
Total N (%)	0.13
Available P (mg/kg)	26.50
Exchangeable K (mg/kg)	90.50
Exchangeable Mg (mg/kg)	90.90
Available S (mg/kg)	62.30
DTPA-extractable Zn (mg/kg)	2.20
DTPA-extractable Mn (mg/kg)	63.30
Available B (mg/kg)	0.38
Available Si - $CaCl_2$ (mg/kg)	36.50
Soil Texture	
Sand (%)	62.00
Silt (%)	24.00
Clay (%)	14.00
Soil classification	Sandy loam

Note. Ece = Electrical conductivity at saturation point, N = nitrogen, P = phosphorus, K = potassium, Ca = calcium, Mg = magnesium, S = sulfur, Cu = copper, Zn = zinc, Mn = manganese, B = boron, Si = silicon, DTPA = diethylenetriaminepentaacetic acid

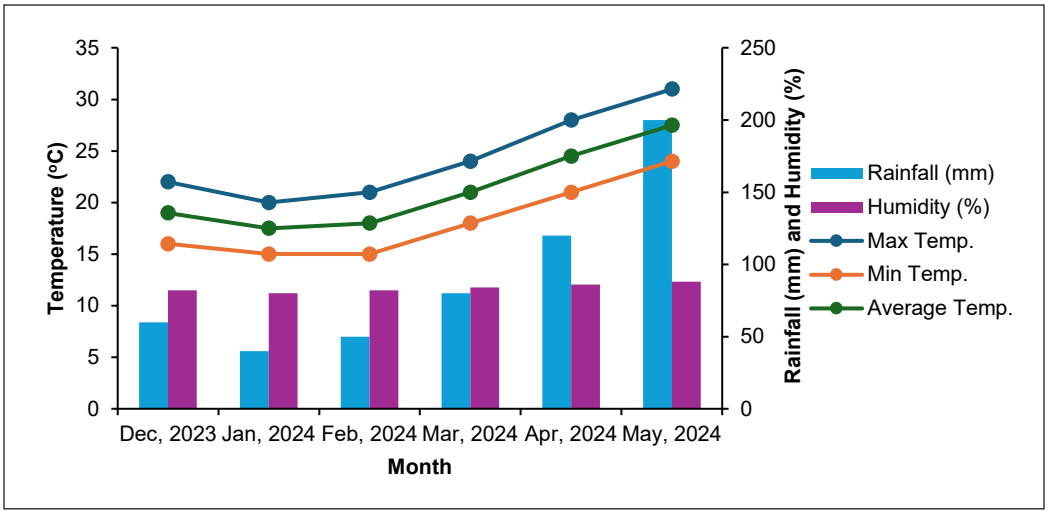

Figure 1. Temperature, rainfall and humidity variations during the experiment

ha) and silicon (Si_1: 120 kg/ha; Si_2: 160 kg/ha; Si_3: 200 kg/ha) fertilisers were used in this experiment. A total of 9 experimental units were involved in the study (Table 2).

Table 2
Fertiliser rates for each treatment

Treatment	Multimolig-M (ml/ha)	Silicon (kg/ha)
M_1Si_1	360	120
M_1Si_2	360	160
M_1Si_3	360	200
M_2Si_1	420	120
M_2Si_2	420	160
M_2Si_3	420	200
M_3Si_1	480	120
M_3Si_2	480	160
M_3Si_3	480	200

Note. M_1Si_1 is the control treatment, which represents the amount of fertiliser farmers are currently using

Multimolig-M and silicon are commercial fertilisers with a composition provided by the manufacturer as follows: 10.5% organic matter, 0.25% humic acid, 2% total nitrogen, 192 ppm calcium, 0.02% available phosphorus, 0.11% potassium, 1.88% sulphur, 2370 ppm magnesium, 3570 ppm iron, 590 ppm copper, 1000 ppm zinc, 2770 ppm manganese, and 892 ppm boron; pH (in water) is 5.5, with 400 ppm cobalt and 800 ppm molybdenum. The silicon fertiliser contains a minimum of 45% total silicon, at least 25% available silica (SiO_2), more than 10% available iron (Fe_2O_3), and more than 5% available magnesium (MgO). Multimolig-M, a liquid fertiliser with a concentration of 1 ml per 1 litre, was prepared and applied three times during the tillering, panicle initiation, and heading stages. Silicon fertiliser was applied as a basal dressing once before transplanting.

The experiment was conducted on a base fertiliser application used by local farmers, which included 10 tons of manure (cow dung), 50 kg N, 40 kg P_2O_5, and 40 kg K_2O per hectare. The basic fertiliser applications were 100 % manure, 100 % P_2O_5 and 30% N. The

remaining fertiliser was applied twice to the top dressing. The first top dressing application was during the tillering with 50% K_2O and 40% N, and the second was at panicle initiation with 50% K_2O and 30% N.

Data Collection

Ten plants in each plot were randomly selected to record agronomic traits. These agronomic traits included morphological characteristics (heading duration, panicle exertion, culm strength, leaf senescence, flag leaf length, flag leaf width, panicle length); growth parameters (plant height, number of leaves, number of tillers, and number of effective tillers) and yield components and yield (number of effective panicles per square meter, number of grains per panicle, number of filled grains per panicle, weight of 1000 grains, theoretical yield, and net yield).

The agronomic traits were monitored under normal field conditions. Visual assessment methods were conducted by observing the entire experimental plot, individual plants, or plant parts. Quantitative indicators were measured on sample plants. Monitoring occurred 15, 30, 45, and 60 days after transplanting (DAT) and at harvest (125 DAT).

Statistical Analysis

The data were subjected to an analysis of variance (ANOVA) in an RCBD design that contained nine treatments and three replicates per treatment. Duncan's multiple range tests performed the mean separation at the 5% significance level. The correlations between silicon and Multimolig-M fertiliser agronomic traits on the VTNA6 rice were analysed after Pearson's test evaluated the data's normality.

RESULTS AND DISCUSSION

Morphological Characteristics

The research findings indicate that the interaction between Multimolig-M fertiliser and silicon significantly influences the morphological characteristics of the VTNA6 rice (Table 3). Specifically, applying Multimolig-M at level M_2 in combination with varying levels of silicon results in a concentrated heading duration of no more than three days and ensures complete panicle exertion. Culm strength is significantly enhanced when Multimolig-M levels are combined with silicon levels Si_2 and Si_3, thereby reducing lodging risk. Leaf senescence, however, remains unaffected by these treatments.

Multimolig-M fertiliser and silicon combination affect the length and width of flag leaves and the length of panicles (Table 3). The treatment combination M_3Si_3 resulted in the greatest flag leaf length (36.40 cm) and width (1.86 cm), with statistically significant differences ($p<0.05$) compared to other treatments. However, it did not show statistically

Table 3
Effects of silicon and Multimolig-M fertiliser on the morphological characteristics of the VTNA6 rice in Nghe An Province, Central Vietnam

Treatment	Heading duration	Panicle exertion	Culm strength	Leaf senescence	Flag leaf length	Flag leaf width	Panicle length
M_1Si_1	5	1	5	1	33.32^{d}	1.23^{c}	23.44^{b}
M_1Si_2	1	1	1	1	34.05^{cd}	1.30^{de}	23.65^{b}
M_1Si_3	1	1	1	1	34.96^{bc}	1.42^{cde}	25.02^{ab}
M_2Si_1	1	1	5	1	34.01^{cd}	1.43^{cde}	24.76^{b}
M_2Si_2	1	1	1	1	35.02^{bc}	1.52^{cd}	24.94^{b}
M_2Si_3	1	1	1	1	36.06^{ab}	1.60^{bc}	27.50^{a}
M_3Si_1	5	5	5	1	34.63^{c}	1.60^{bc}	22.54^{b}
M_3Si_2	5	5	1	1	35.93^{ab}	1.76^{ab}	22.90^{b}
M_3Si_3	5	5	1	1	36.40^{a}	1.86^{a}	23.21^{b}
$LSD_{0.05}$	-	-	-	-	1.23	0.24	2.85
CV (%)	-	-	-	-	1.00	4.60	2.71

Note. Different letters within the columns denote significant differences ($p \leq 0.05$). The scoring criteria are as follows: (1) Heading duration: score 1 = concentrated (no more than 3 days), score 5 = intermediate (4–7 days), score 9 = extended (more than 7 days), (2) Panicle exertion: score 1 = complete exertion, score 5 = exertion just at the panicle neck, score 9 = partial exertion, (3) Culm strength: score 1 = strong (plants do not lodge), score 5 = intermediate (most plants are leaning), score 9 = weak (most plants lodge completely), (4) Leaf senescence: score 1 = late (leaves remain naturally green), score 5 = intermediate (leaves turn yellow), score 9 = early (all leaves turn yellow or die)

significant differences ($p<0.05$) compared to the M_3Si_2 and M_2Si_3 treatments. Regarding panicle length, the M_2Si_3 treatment achieved the longest panicle length (27.50 cm), also showing statistically significant differences ($p<0.05$) compared to other treatments, except for the M_1S_3 treatment. These findings confirm that the levels of Multimolig-M and silicon fertilisers, as well as their combinations, have a pronounced impact on the morphological characteristics of the VTNA6 rice.

Silicon plays an essential role in regulating the morphology of rice plants, particularly in the development of key structures such as leaves, stems, and roots. Silicon is absorbed and primarily accumulates in the outer parts of the plant, such as the flag leaf and the epidermis of the stem, enhancing rigidity and improving resilience against adverse conditions such as drought and pests (Mandloi et al., 2024; Snehalatha et al., 2023). Due to silicon, the flag leaf's thicker and more robust structure allows for optimised photosynthesis by keeping the leaf upright, thereby improving light absorption and photosynthetic efficiency (Ahmed et al., 2024). Studies have shown that rice varieties with larger flag leaf areas and smaller leaf angles exhibit higher photosynthetic efficiency and greater dry matter accumulation, which positively impacts yield (Wang et al., 2023). Silicon also reinforces the mechanical strength of rice stems, minimising lodging—a factor that often negatively impacts grain yield and quality (Yusob et al., 2023). A sturdier stem facilitates more efficient water and

nutrient transport from the roots to the leaves and grains, promoting uniform development and higher yield (Snehalatha et al., 2023).

Multimolig-M, rich in micronutrients like Zn, Fe, and Mn, supports the balanced development of plant organs. These elements are crucial in forming enzymes that regulate cell division and elongation, impacting leaf and stem size. The observed increase in leaf length and width in this study may be attributed to the micronutrient supplementation from Multimolig-M, which optimises leaf surface area for photosynthesis. Additionally, Multimolig-M can improve the rice root system, enhancing water and nutrient uptake from the soil. It positively influences overall growth and plant morphology, including the number and size of tillers. The increase in productive tillers contributes to a higher number of rice panicles, resulting in a noticeable yield improvement. As indicated in the study, the combination of silicon and Multimolig-M led to an increase in flag leaf length and panicle length, demonstrating a synergistic effect in enhancing critical morphological traits of rice plants.

Number of Leaves on Main Stem

The application of Multimolig-M and silicon fertilisers significantly influenced the leaf count on the main stem of the VTNA6 rice variety (Table 4). The study found that the leaf count increased notably with higher levels of Multimolig-M fertiliser and increased silicon content. The greatest effect was observed in the M_3Si_3 treatment, with statistically significant differences ($p<0.05$) compared to other treatments. However, it did not show statistically significant differences ($p<0.05$) compared to the M_2Si_3 and M_3Si_2 treatments at harvest. It suggests combining Multimolig-M and silicon fertilisers

Table 4
Effects of silicon and Multimolig-M fertiliser on the number of leaves of the VTNA6 rice in Nghe An Province, Central Vietnam

Treatment	15 DAT	30 DAT	45 DAT	60 DAT	At harvest (125 DAT)
M_1Si_1	5.40^{c}	7.57^{b}	10.47^{c}	12.63^{c}	13.10^{c}
M_1Si_2	5.63^{abc}	8.37^{a}	11.13^{abc}	13.27^{bc}	13.97^{b}
M_1Si_3	5.90^{a}	8.63^{a}	11.50^{ab}	13.63^{ab}	14.47^{b}
M_2Si_1	5.47^{bc}	8.30^{a}	11.20^{abc}	13.43^{ab}	14.17^{b}
M_2Si_2	5.63^{abc}	8.57^{a}	11.47^{ab}	13.63^{ab}	14.43^{b}
M_2Si_3	5.83^{ab}	8.70^{a}	11.67^{ab}	13.87^{ab}	14.63^{ab}
M_3Si_1	5.43^{bc}	8.37^{a}	11.27^{ab}	13.50^{ab}	14.33^{b}
M_3Si_2	5.60^{abc}	8.60^{a}	11.60^{ab}	13.80^{ab}	14.70^{ab}
M_3Si_3	5.83^{ab}	8.80^{a}	11.87^{a}	14.17^{a}	15.40^{a}
$LSD_{0.05}$	0.41	0.61	0.78	0.75	0.79
CV (%)	2.17	1.75	1.35	1.48	1.67

Note. Different letters within the columns denote significant differences ($p\leq0.05$)

can enhance leaf production in the VTNA6 rice, potentially leading to improved growth and yield outcomes.

The growth and development of leaves, particularly the flag leaf, are crucial for determining the yield of rice crops as they influence the duration of flowering and seed formation (Kalaignan, 2024). Leaves are essential for photosynthesis, providing nutrients necessary for plant activity, and their physiological efficiency directly affects grain filling and yield potential (Rădoi et al., 2022). The use of biofertilisers and silicon has been found to significantly influence the leaf count of rice, promoting better leaf development and increasing the number of leaves, which ultimately enhances crop productivity and quality (Elekhtyar & Al-Huqail, 2023). Biofertilisers have been found to promote leaf growth. At the same time, silicon treatments, such as potassium silicate, positively affect leaf count, resulting in a higher leaf count compared to control groups (Ning et al., 2022).

Number of Tillers per Hill

The number of tillers per hill in the VTNA6 rice variety did not show statistically significant differences ($p<0.05$) between treatments from 15 to 60 DAT (Table 5). At harvest, the application of M_2Si_3 resulted in the highest number of effective tillers (5.80 tillers), demonstrating a significant difference ($p<0.05$) relative to other treatments, except for M_2Si_2. The effective tiller rate (%) tended to decrease when the amount of Multimolig-M was increased to 480 ml/ha. The effective tiller rate was highest with M_2Si_3, but there was no significant difference between M_2Si_3 and other treatments.

This study's findings demonstrate that silicon and Multimolig-M fertilisers positively impact the number of tillers per hill in VTNA6 rice, especially as the plants progress through different growth stages, from early tillering to maturity. These effects align with earlier studies highlighting the role of silicon in enhancing tillering and overall plant robustness and the complementary role of micronutrient-enriched fertilisers in promoting balanced growth. Pati et al. (2016) established that silicon application improves tiller numbers and plant structure, contributing to enhanced yield attributes. Specifically, treatments M_2Si_3 and M_3Si_3, with the highest silicon concentrations, produced more tillers and maintained these gains through later growth stages, showing silicon's role in supporting sustained tillering and plant stability. Silicon's known ability to reinforce cell walls and enhance resistance to environmental stress likely contributed to the increased tiller count and stability against lodging (Ma & Yamaji, 2006).

The addition of Multimolig-M enhanced tillering, particularly in combination with silicon, where M_2 and M_3 levels resulted in improved tiller production rates. Micronutrients such as zinc, manganese, and iron are vital in enzymatic and cellular functions essential for plant growth and nutrient uptake (Snehalatha et al., 2023). These micronutrients likely facilitated stronger root systems and enhanced leaf expansion,

contributing to a more effective tillering process and increased nutrient uptake efficiency (Gabasawa & Yusuf, 2013).

Treatments with higher combined levels of silicon and Multimolig-M (notably M_2Si_3 and M_3Si_3) showed synergistic effects on tiller production. This synergistic effect aligns with findings from Monika and Malhotra (2022), who reported similar interactions where combined nutrient management strategies led to optimal tillering and yield outcomes. Biofertilisers combined with reduced chemical fertilisers significantly increase the number of effective tillers, resulting in higher grain yields. This effect is observed when biofertilisers use 50% to 75% of the recommended chemical fertiliser doses (Ghimire et al., 2021; Hindarwati et al., 2023). Furthermore, the combined application of silicon and biofertilisers has been found to improve soil physiochemical properties, increase available silicon content, and alter the soil microbiota structure, leading to an increase in the number of tillers per plant (Mallano et al., 2022).

Table 5
Effects of silicon and Multimolig-M fertiliser on the number of tillers per hill of the VTNA6 rice in Nghe An Province, Central Vietnam

Treatment	15 DAT	30 DAT	45 DAT	60 DAT	At harvest (125 DAT)	Effective tiller rate (%)
M_1Si_1	2.07^{a}	5.73^{a}	9.10^{a}	9.20^{a}	4.43^{bc}	48.23^{ab}
M_1Si_2	2.17^{a}	5.80^{a}	9.23^{a}	9.27^{a}	4.60^{bc}	49.12^{ab}
M_1Si_3	2.40^{a}	6.03^{a}	9.50^{a}	9.67^{a}	4.83^{bc}	50.00^{ab}
M_2Si_1	2.10^{a}	5.90^{a}	9.33^{a}	9.50^{a}	5.07^{bc}	53.35^{a}
M_2Si_2	2.23^{a}	6.03^{a}	9.60^{a}	9.80^{a}	5.17^{ab}	52.75^{a}
M_2Si_3	2.43^{a}	6.27^{a}	10.00^{a}	10.23^{a}	5.80^{a}	56.73^{a}
M_3Si_1	2.13^{a}	6.00^{a}	9.90^{a}	10.37^{a}	4.33^{c}	41.81^{b}
M_3Si_2	2.30^{a}	6.23^{a}	10.13^{a}	10.53^{a}	4.47^{bc}	42.43^{b}
M_3Si_3	2.47^{a}	6.50^{a}	10.43^{a}	10.77^{a}	4.70^{bc}	43.71^{b}
$LSD_{0.05}$	0.48	0.79	1.45	1.02	0.82	8.58
CV (%)	6.55	4.96	5.05	5.07	6.38	5.61

Note. Different letters within the columns indicate significant differences ($p \leq 0.05$)

Plant Height

Table 6 demonstrates a clear trend where increasing levels of Multimolig-M and silicon fertilisers lead to higher rice plant heights. The M_3Si_3 treatment produced the tallest plant height, with statistically significant differences ($p<0.05$) compared to other treatments, except for the M_2Si_3 and M_3Si_2 treatments. This result is consistent with findings from Chen et al. (2011) on silicon's role in enhancing cell wall structure, leading to steady growth that results in higher plant height as the crop matures. Pati et al. (2016) showed that silicon supports plant rigidity and improves nutrient absorption, increasing plant height and robust

Table 6
Effects of silicon and Multimolig-M fertiliser on the plant height of the VTNA6 rice in Nghe An Province, Central Vietnam

Treatment	15 DAT	30 DAT	45 DAT	60 DAT	At harvest (125 DAT)
M_1Si_1	24.50[a]	46.52[c]	64.53[d]	81.11[d]	121.89[e]
M_1Si_2	26.08[a]	48.57[bc]	66.69[bcd]	83.58[cd]	124.56[de]
M_1Si_3	27.27[a]	50.29[ab]	68.52[abc]	85.12[bc]	125.25[cde]
M_2Si_1	24.91[a]	47.93[bc]	66.26[cd]	83.49[cd]	124.72[de]
M_2Si_2	26.17[a]	49.29[abc]	67.72[abcd]	85.37[bc]	127.23[bcd]
M_2Si_3	27.34[a]	51.20[ab]	69.72a[b]	87.40[ab]	128.63[abc]
M_3Si_1	24.98[a]	48.00[bc]	66.61[bcd]	84.50[bcd]	126.04[bcd]
M_3Si_2	26.44[a]	50.25[ab]	68.96[abc]	86.98[abc]	128.99[ab]
M_3Si_3	27.52[a]	52.34[a]	71.23[a]	89.85[a]	131.74[a]
$LSD_{0.05}$	3.68	3.68	3.68	3.68	3.68
CV (%)	3.86	2.04	3.49	2.18	2.80

Note. Different letters within the columns indicate significant differences ($p \leq 0.05$)

growth. Barus et al. (2023) and Setiawati et al. (2023) reported increased rice plant height using PGPR biofertilisers in saline soils, particularly in early growth stages. Ning et al. (2022) also found that combining biochar with silicon-rich fertilisers significantly enhanced the leaves' silicon accumulation, potentially influencing rice plant height.

Yield Components and Yield

Number of Effective Panicle per m²

Multimolig-M and silicon fertilisers significantly influenced the number of effective panicles per m² in the VTNA6 rice (Table 7). Applying M_2Si_3 resulted in the highest number of effective panicles (261 panicles/m²), significantly different ($p<0.05$) from other fertiliser levels.

Integrating silicon and biofertilisers significantly increased the number of effective panicles per m². Sheikhani et al. (2014) reported that biofertilisers and varying silicon rates improved grain yield, tiller number, and panicle number per square meter, with the highest results observed at a silicon application rate of 450 kg/ha combined with biofertiliser seed treatment. Another study demonstrated that the combination of silicon (600 kg/ha) and biofertilisers (10 tons/ha) significantly increased the number of tillers, which directly improved the number of effective panicles and overall grain yield (Naher et al., 2016).

Number of Grains per Panicle

Application of M_2Si_3 resulted in the highest grains per panicle (191.71), but there was no statistically significant difference between the treatments. Integrating silicon and biofertilisers has significantly enhanced the number of grains per panicle (Naher et al.,

2016). Islam et al. (2012) found that using *Azospirillum* biofertiliser strains combined with silicon significantly increased the number of grains per panicle, increasing grain yield. Similarly, Bhuiyan et al. (2006) showed that combining the recommended N-P_2O_5 – K_2O (5.5 - 2.75 - 2.4 kg $10a^{-1}$) with biofertilisers (500 kg/ha) produced growth and yield components, including the number of grains per panicle, comparable to N-P_2O_5 – K_2O (11 – 5.5 – 4.8 kg $10a^{-1}$) application. Additionally, Cuong et al. (2017) reported that when applied during the reproductive growth stage with biofertilisers, silicon fertilisers significantly improved the number of grains per panicle and overall yield.

Number of Filled Grains per Panicle

The levels of Multimolig-M and silicon fertilisers affected the number of filled grains per panicle in the VTNA6 rice. The number of filled grains per panicle ranged from 144.09 to 164.29, with the M_2Si_3 combination yielding the highest and M_3Si_1 the lowest. However, no statistically significant differences were found between the treatments. Ghimire et al. (2021) showed that combining silicon with biofertilisers, specifically Azolla and NPK, resulted in the highest number of filled grains per panicle at 114.30. Additionally, Sheikhani et al. (2014) demonstrated that silicon fertilisation at 450 kg/ha, combined with biofertiliser seed treatment (*Azospirillum* spp. and *Azotobacter* spp.), significantly increased the number of filled grains per panicle.

Weight of 1,000 Grains

Applying 420 ml Multimolig-M per ha (M_3) in combination with different silicon levels resulted in the highest 1000-grain weight, but there was no significant difference compared to other fertiliser levels. However, the application of M_2Si_3 resulted in the highest grain weight (24.07 g), while the M_3Si_1 combination had the lowest (22.73 g).

The application of silicon fertilisers significantly enhances the 1000-grain weight of rice. Higher doses of silicon (up to 400 kg/ha SiO_2), when combined with standard fertiliser practices, have demonstrated notable improvements in grain weight (Pati et al., 2016). Additionally, biofertilisers used with reduced chemical fertilisers further increase the 1000-grain weight. Optimal results have been achieved with a 50% reduction in nitrogen and phosphorus fertilisers, supplemented with biofertilisers (Hapsoh et al., 2023; Noraida & Hisyamuddin, 2021). Sheikhani et al. (2014) found that while silicon application and biofertiliser independently significantly affected the 1000-grain weight, the interaction between silicon rate and biofertiliser application was not statistically significant.

Theoretical and Net Yield

When 420 ml of Multimolig-M per hectare was applied with different silicon levels, theoretical and net yields increased. Application of M_2Si_3 achieved the highest yields

for both theoretical (10.32 tons/ha) and net (7.93 tons/ha), significantly surpassing other combinations.

Cuong et al. (2017) demonstrated that applying silicon-based fertiliser at an optimal dose of 329 kg/ha, along with standard fertiliser practices, can significantly boost rice yield and enhance nutrient uptake in the tropical zone of Vietnam. Pati et al. (2016) found that silicon fertilisation using diatomaceous earth at 600 kg/ha, combined with standard fertiliser practices, increased rice grain and straw yields. Bhuiyan et al. (2006) reported that a combined treatment of half the recommended fertiliser (HRF) and 500 kg/ha biofertiliser had similar effects on the growth and yield of rice as the full recommended fertiliser (RF). Moreover, Noraida and Hisyamuddin (2021) showed that a combination of 50% biofertiliser with 50% chemical fertiliser produced better growth and yield in rice. Integrating biofertilisers and silicon fertilisers leads to significant yield improvements, as silicon application enhances the effectiveness of biofertilisers, resulting in better nutrient uptake and higher grain yield (Sheikhani et al., 2014).

Silicon plays an essential role in improving soil structure and health. When added to soil, silicon enhances water retention, loosens soil texture, and boosts crop productivity by supporting microbial communities and reducing harmful heavy metal accumulation (Wang et al., 2020). Combining silicon with biochar also aids carbon storage and improves soil durability (Huang et al., 2020). For sustainable use, long-term research on silicon's effects on soil is necessary, as Si accumulation may alter soil properties and affect nutrient availability for plants (Szulc et al., 2016). Additionally, Multimolig-M provides essential micronutrients such as zinc, manganese, and iron that are critical for rice growth; however, excessive use of these micronutrients can lead to toxic buildup in soil, potentially harming crops and soil microorganisms. Therefore, controlling Multimolig-M application rates is vital to maintaining soil health and preventing harmful accumulation, contributing to a balanced soil ecosystem (Zhao et al., 2022).

The use of silicon in agriculture can indirectly help reduce greenhouse gas emissions. Silicon enhances drought and disease resistance in rice plants, reducing the need for pesticides and chemical fertilisers, which are significant sources of greenhouse gas emissions. Research shows that silicon helps rice improve drought tolerance by enhancing photosynthesis and regulating nutrient absorption under dry conditions, supporting plant health and growth (Chen et al., 2011). Additionally, silicon can improve carbon sequestration in rice roots, reducing atmospheric CO_2 emissions (Zhao et al., 2019).

Silicon also strengthens the disease resistance of plants, reducing the need for pesticides. Studies have shown that silicon can partially substitute for pesticides by boosting rice resistance to common diseases, thereby lowering the use of agricultural chemicals (Datnoff et al., 2001). However, Multimolig-M may contribute to greenhouse gas emissions if the plants do not fully absorb micronutrients and undergo chemical transformations in the soil.

Some micronutrients may engage in soil reactions that produce N_2O or CO_2, gases with a strong greenhouse effect. Therefore, optimising the dosage and application techniques of Multimolig-M is essential to minimising greenhouse gas emissions in rice cultivation (Zhang et al., 2021). The use of silicon fertiliser and Multimolig-M can potentially improve rice yields. It may bring environmental benefits, such as reducing the need for chemical fertilisers and enhancing plant resilience to adverse conditions. However, strict control measures are necessary to prevent negative impacts on soil health and greenhouse gas emissions. Long-term studies and sustainable management practices will help maximise these fertilisers' benefits while protecting the environment.

Table 7
Effects of silicon and Multimolig-M fertiliser on the yield components and yield of the VTNA6 rice in Nghe An Province, Central Vietnam

Treatment	No. of effective panicle/m²	No. of grains/ panicles	No. of filled grains/ panicles	1000-grain weight (g)	Theoretical yield (tons/ha)	Net yield (tons/ha)
M_1Si_1	199.50^{bc}	177.57^{a}	145.61^{a}	22.73^{a}	6.60^{b}	5.58^{ab}
M_1Si_2	207.00^{bc}	179.28^{a}	147.91^{a}	23.10^{a}	7.08^{b}	6.07^{ab}
M_1Si_3	217.50^{bc}	178.78^{a}	148.39^{a}	23.23^{a}	7.52^{b}	6.36^{ab}
M_2Si_1	228.00^{bc}	182.93^{a}	153.66^{a}	24.00^{a}	8.42^{ab}	6.88^{ab}
M_2Si_2	232.50^{ab}	188.10^{a}	159.89^{a}	24.03^{a}	8.94^{ab}	7.36^{ab}
M_2Si_3	262.00^{a}	191.71^{a}	164.29^{a}	24.07^{a}	10.32^{a}	7.93^{a}
M_3Si_1	195.00^{c}	169.52^{a}	144.09^{a}	22.73^{a}	6.39^{b}	4.93^{b}
M_3Si_2	201.00^{bc}	173.88^{a}	146.06^{a}	22.97^{a}	6.74^{b}	6.01^{ab}
M_3Si_3	211.50^{bc}	172.76^{a}	146.85^{a}	23.07^{a}	7.16^{b}	6.24^{ab}
$LSD_{0.05}$	36.85	44.07	40.47	1.71	2.73	2.77
CV (%)	4.38	5.47	5.44	1.93	7.97	7.36

Note. Different letters within the columns indicate significant differences ($p \leq 0.05$)

Correlation Matrix Between Agronomic Traits

The correlations between agronomic traits of silicon and Multimolig-M fertiliser on the VTNA6 rice are shown in Table 8. The plant height, number of leaves per plant, and panicle length were positively correlated with the net yield. However, these three correlation coefficients were not statistically significant. The theoretical and net yield was positively correlated with effective tiller rate, panicle length, number of effective panicles per m², number of grains per panicle, number of filled grains per panicle, and 1000-grain weight. The correlations indicated that these six traits were the best indicators of yield and contributed more to yield than other agronomic traits. Therefore, the application of silicon and Multimolig-M fertiliser for rice in Nghe An Province should be selected based on these traits. The effective tiller ratio showed a significant correlation with theoretical yield (r =

Table 8
Correlation coefficients between agronomic traits of silicon and Multimolig-M fertiliser on the VTNA6 rice

Traits	Plant height (cm)	No. of leaves/ plant	Effective tiller rate (%)	Panicle length (cm)	No. of effective panicle/m²	No. of grains/ panicles	No. of filled grains/ panicles	1000-grain weight (g)	Theoretical yield (tons/ha)	Net yield (tons/ha)
Plant height	1									
No. of leaves/plant	0.86**	1								
Effective tiller rate	-0.25	-0.23	1							
Panicle length	0.08	0.09	0.86**	1						
No. of effective panicle	0.27	0.22	0.84**	0.92**	1					
No. of grains/panicles	-0.05	-0.15	0.94**	0.82**	0.89**	1				
No. of filled grains/ panicles	0.22	0.13	0.82**	0.82**	0.96**	0.94**	1			
1000-grain weight	0.20	0.24	0.83**	0.73*	0.87**	0.83**	0.85**	1		
Theoretical yield	0.26	0.20	0.84**	0.89**	0.99**	0.88*	0.94**	0.89**	1	
Net yield	0.37	0.20	0.67*	0.65*	0.78*	0.79*	0.77*	0.78*	0.75*	1

Note. *$p<0.05$; **$p<0.01$

0.84**) and net yield (r = 0.67*), consistent with findings by Rahman et al. (2014) and Oladosu et al. (2018), who noted that the effective tiller number directly influences yield and is an important factor in yield prediction. Panicle length also exhibited a significant positive correlation with theoretical yield (r = 0.89**) and net yield (r = 0.65*), indicating that longer panicles typically have higher numbers and weights of grains. Sharma et al. (2012) and Gudepu et al. (2022) also reported a positive relationship between panicle length and rice yield. Furthermore, the number of grains and filled grains per panicle were highly correlated with both theoretical and net yield, with values of (r = 0.88*) and (r = 0.79*), respectively. These traits are crucial for yield prediction, as the number of filled grains determines the harvested grain weight. This result aligns with the studies of Sharma et al. (2012) and Oladosu et al. (2018), where the number of grains and filled grain ratio were considered key factors affecting yield. The 1000-grain weight strongly correlated with theoretical yield (r = 0.89**) and net yield (r = 0.78*). Gudepu et al. (2022) and Kafi et al. (2021) showed the contribution of the 1000-grain weight to higher yield.

CONCLUSION

The study demonstrates that the combined application of silicon and Multimolig-M fertilisers significantly enhances the morphological characteristics, growth parameters, and yield of the VTNA6 rice variety in Nghe An Province, Vietnam. Although the M_2Si_3 treatment (420 ml/ha Multimolig-M and 200 kg/ha silicon) produced the highest theoretical and net yields (10.32 and 7.93 tons/ha, respectively), it was not consistently superior in all measured traits. Other treatments, particularly those with similar levels of Multimolig-M and silicon, such as M_2Si_2 and M_3Si_3, also showed positive effects, indicating that multiple combinations of these fertilisers can effectively improve rice productivity under local conditions.

These findings underscore the flexibility in fertiliser management practices, allowing for tailored combinations that suit specific growth requirements and environmental conditions. Integrating silicon and Multimolig-M fertilisers offers a sustainable approach to rice production, enhancing yield while potentially reducing reliance on chemical fertilisers. Further studies are recommended to explore long-term impacts and the economic feasibility of these practices across different rice varieties and agroecological zones in Vietnam and similar regions.

ACKNOWLEDGMENTS

The authors are grateful to the School of Agriculture and Natural Resources, Vinh University staff for using their laboratory equipment.

REFERENCES

Abdullah, E., Misran, A., Yaapar, N., Rafii, M., & Ramli, A. (2021). The potential of silicon in improving rice yield, grain quality, and minimising chalkiness: A review. *Pertanika Journal of Tropical Agricultural Science*, *44*(3), 655-672. https://doi.org/10.47836/pjtas.44.3.09

Ahmed, T., Guo, J., Noman, M., Lv, L., Manzoor, N., Qi, X., & Li, B. (2024). Metagenomic and biochemical analyses reveal the potential of silicon to alleviate arsenic toxicity in rice (*Oryza sativa* L.). *Environmental Pollution*, *345*, 123537. https://doi.org/10.1016/j.envpol.2024.123537

Amrutha, E. A., Manju, R. V., Viji, M. M., Roy, S., Jacob, J., Swapna, A., & Meera, A. V. (2022). The influence of biofertilizers on growth and yield of rice (*Oryza sativa* L.). *Biological Forum – An International Journal*, *14*(4A), 23-28.

Baltazar, A. M., & De Datta, S. K. (2023). Rice and rice-based cropping systems. In *Weed science and weed management in rice and cereal-based cropping systems* (pp. 125-182). John Wiley. https://doi.org/10.1002/9781119737582.ch4

Barus, J., Endriani, Tambunan, R. D., Soraya, & Herdiansyah, E. (2023). The effectiveness of biosilica and liquid organic fertilizer application on growth and yields of lowland rice. *IOP conference series: Earth and environmental science*, *1172*, 012008. IOP Publishing. https://doi.org/10.1088/1755-1315/1172/1/012008

Bhuiyan, M. K. I., Rico, C. M., Mintah, L. O., Kim, M. K., Shon, T. K., Chung, I. K., & Lee, S. C. (2006). Effects of biofertilizer on growth and yield of rice. *The Korean Journal of Crop Science*, *51*(4), 282-286.

Chen, W., Yao, X., Cai, K., & Chen, J. (2011). Silicon alleviates drought stress of rice plants by improving plant water status, photosynthesis and mineral nutrient absorption. *Biological Trace Element Research*, *142*, 67-76. https://doi.org/10.1007/s12011-010-8742-x.

Cuong, T. X., Ullah, H., Datta, A., & Hanh, T. C. (2017). Effects of silicon-based fertilizer on growth, yield and nutrient uptake of rice in tropical zone of Vietnam. *Rice Science*, *24*(5), 283-290. https://doi.org/10.1016/j.rsci.2017.06.002

Datnoff, L., Seebold, K., & Correa-V, F. (2001). The use of silicon for integrated disease management: reducing fungicide applications and enhancing host plant resistance. *Studies in Plant Science*, *8*, 171-184. https://doi.org/10.1016/S0928-3420(01)80014-8

Đỗ H. (2018, March 29). Phân bón Multimolig-M phụng sự cho nông nghiệp sạch [Multimolig-M fertilizer serves clean agriculture]. *Vietnam Agriculture News*. https://nongnghiep.vn/phan-bon-multimolig-m-phung-su-cho-nong-nghiep-sach-d215604.html

Đoàn, V. S., Hoàng, M. T., Nguyễn, T. H., Nguyễn, T. H., & Võ, T. M. T. (2022). Nghiên cứu, ứng dụng kỹ thuật chiếu xạ gamma, nguồn Co-60 có hoạt độ 236 Ci, trong tạo nguồn vật liệu khởi đầu cho chọn tạo giống lúa [Research and application of 60 Co gamma irradiation with the source active at 236 Ci to create initial materials for rice breeding]. *Tạp chí Nông nghiệp và Phát triển nông thôn Việt Nam*, *23*, 3-10.

Elekhtyar, N. M., & Al-Huqail, A. A. (2023). Influence of chemical, organic, and biological silicon fertilization on physiological studies of Egyptian japonica green super rice (*Oryza sativa* L.). *Sustainability*, *15*(17), 12968. https://doi.org/10.3390/su151712968

Gabasawa, A., & Yusuf, A. (2013). Biological nitrogen fixation of some groundnuts as affected by genotype and applied phosphorus at Samaru, northern Guinea Savannah of Nigeria. *Bayero Journal of Pure and Applied Sciences*, *5*, 132-135. https://doi.org/10.4314/BAJOPAS.V5I2.26

Ghimire, A., Nainawasti, A., Shah, T. B., & Dhakal, S. (2021). Effect of different biofertilizers on yield of spring rice (*Oryza Sativa* L.) cv. Hardinath-1 in Rajapur Municipality, Bardiya. *SAARC Journal of Agriculture*, *19*(1), 57-69. https://doi.org/10.3329/sja.v19i1.54778

Gudepu, S., Chennamadhavuni, D., & Katragadda, S. (2022). Variability and association studies for yield and yield contributing traits in long grain rice (Oryza sativa L.). *Oryza-An International Journal on Rice*, *4*, 409-417. https://doi.org/10.35709/ory.2022.59.4.3

Hạnh, T. T, Cường, P. V., & Nhung, V. T. (2020). Đánh giá ảnh hưởng của lượng phân bón và lượng hạt giống gieo thẳng đến sinh trưởng, phát triển, năng suất giống lúa cực ngắn ngày DCG72 tại Nghệ An [Effects of applying different fertilizer doses and direct seeding rates on the growth, development and yield of early maturity rice variety DCG72 in Nghe An Province]. *Tạp chí Khoa học Nông nghiệp Việt Nam*, *18*(4), 239-247.

Hapsoh, Dini, I. R., Wawan, Rifai, M., & Khoiruddin, F. (2023). Combination of inorganic and bio-organic fertilizer on growth and production of Paddy rice (*Oryza sativa* L.). *IOP conference series: Earth and environmental science*, *1241*, 012036. https://doi.org/10.1088/1755-1315/1241/1/012036

Hindarwati, Y., Minarsih, S., Praptana, R. H., Supriyo, A., & Romdon, A. S. (2023). The effect of biofertilizer on increasing upland rice yield in rainfed rice field in Boyolali. *IOP conference series: Earth and environmental science*, *1230*, 012138. https://doi.org/10.1088/1755-1315/1230/1/012138

Huang, C., Wang, L., Gong, X., Huang, Z., Zhou, M., Li, J., Wu, J., Chang, S., & Jiang, P. (2020). Silicon fertilizer and biochar effects on plant and soil PhytOC concentration and soil PhytOC stability and fractionation in subtropical bamboo plantations. *The Science of the Total Environment*, *715*, 136846. https://doi.org/10.1016/j.scitotenv.2020.136846.

Islam, M. Z., Sattar, M., Ashrafuzzaman, M., & Uddin, M. (2012). Improvement of yield potential of rice through combined application of biofertilizer and chemical nitrogen. *African Journal of Microbiology Research*, *6*, 745-750. https://doi.org/10.5897/AJMR11.859

Kafi, S., Abiodun, E., Bunmi, O., & Kyung-Ho, K. (2021). Correlation coefficient and path analyses of yield and yield related traits of Korean double haploid rice for germplasm improvement in Nigeria. *American Journal of Agriculture and Forestry, 9*(3), 114-121. https://doi.org/10.11648/j.ajaf.20210903.13.

Kalaignan, K. (2024). Flag leaf recorded more photosynthetic rate in rice. *International Journal of Current Microbiology and Applied Sciences*, *13*(3), 248-251. https://doi.org/10.20546/ijcmas.2024.1303.023

Kheyri, N. (2022). Effect of silicon and nanosilicon application on rice yield and quality. In H. Etesami, A. H. Al Saeedi, H. El-Ramady, M. Fujita, M. Pessarakli & M. A. Hossain (Eds.), *Silicon and Nano-silicon in Environmental Stress Management and Crop Quality Improvement* (pp. 297-307). Academic Press. https://doi.org/10.1016/B978-0-323-91225-9.00019-4

Ma, J. F., & Yamaji, N. (2006). Silicon uptake and accumulation in higher plants. *Trends in Plant Science*, *11*(8), 392-397. https://doi.org/10.1016/j.tplants.2006.06.007

Mallano, A. I., Zhao, X., Wang, H., Jiang, G., Sun, B., & Huang, C. (2022). Divergent taxonomic responses of below-ground microbial communities to silicate fertilizer and biofertilizer amendments in two rice ecotypes. *Frontiers in Agronomy*, *4*, 1071890. https://doi.org/10.3389/fagro.2022.1071890

Mandloi, S., Kumar, A., Surya, M., Reddy, P., Singh, R., & Tripathi, S.K. (2024). Influence of silicon on leaf blast of rice (*Pyricularia grisea*) and their relationship on morph physiological and yield parameters under drought stress. *Ecology, Environment And Conservation*, *30*(May Suppl. Issue), S386-S398. https://doi.org/10.53550/eec.2024.v30i03s.067

Meena, V. D., Dotaniya, M. L., Coumar, V., Rajendiran, S., Ajay, Kundu, S., & Rao, A. S. (2014). A case for silicon fertilization to improve crop yields in tropical soils. *Proceedings of the National Academy of Sciences, India Section B: Biological Sciences*, *84*(3), 505-518. https://doi.org/10.1007/s40011-013-0270-y

Ministry of Agriculture and Rural Development. (2018). *Quyết định về việc công nhận chính thức giống cây trồng nông nghiệp mới* [Decision on the official recognition of a new agricultural crop variety]. https://asisov.org.vn/quyet-dinh-cong-nhan-giong-cay-trong/quyet-dinh-cong-nhan-chinh-thuc-giong-lua-vat-tu-na6-685.html

Mohidem, N. A., Hashim, N., Shamsudin, R., & Man, H. C.(2022). Rice for food security: Revisiting its production, diversity, rice milling process and nutrient content. *Agriculture*, *12*(6), 741. https://doi.org/10.3390/agriculture12060741

Monika, M., & Malhotra, C. (2022). Silicon fertilization in paddy field. *International Journal of Health Sciences*, *6*(S1), 3161-3167. https://doi.org/10.53730/ijhs.v6nS1.5356

Naher, U., Panhwar, Q., Othman, R., Ismail, M., & Zulkarami, B. (2016). Biofertilizer as a supplement of chemical fertilizer for yield maximization of rice. *Journal of Agriculture Food and Development*, *2*, 16-22. https://doi.org/10.30635/2415-0142.2016.02.3

Ning, C., Liu, R., Kuang, X., Chen, H., Tian, J., & Cai, K. (2022). Nitrogen fertilizer reduction combined with biochar application maintain the yield and nitrogen supply of rice but improve the nitrogen use efficiency. *Agronomy*, *12*, 3039. https://doi.org/10.3390/agronomy12123039

Noraida, M. R., & Hisyamuddin, M. R. (2021). The effect of different rate of biofertilizer on the growth performance and yield of rice. *IOP conference series: Earth and environmental science*, *757*, 012050. IOP Publishing. https://doi.org/10.1088/1755-1315/757/1/012050

Nosheen, S., Ajmal, I., & Song, Y. (2021). Microbes as biofertilizers, a potential approach for sustainable crop production. *Sustainability*, *13*(4), 1868. https://doi.org/10.3390/su13041868

Oladosu, Y., Rafii, M., Magaji, U., Abdullah, N., Miah, G., Chukwu, S., Hussin, G., Ramli, A., & Kareem, I. (2018). Genotypic and phenotypic relationship among yield components in rice under tropical conditions. *BioMed Research International*, *2018*, 8936767. https://doi.org/10.1155/2018/8936767.

Pallarés, M. I., Álvarez, C., Cantón, F. M. G., Moncayo, C. R., Martínez, P. A., Heredia, F. P. M., & Mariscal, V. (2021). Sustaining rice production through biofertilization with N2-Fixing Cyanobacteria. *Applied Sciences*, *11*(10), 4628. https://doi.org/10.3390/app11104628

Pati, S., Pal, B., Badole, S., Hazra, G. C., & Mandal, B. (2016). Effect of silicon fertilization on growth, yield, and nutrient uptake of rice. *Communications in Soil Science and Plant Analysis*, *47*(3), 284-290. https://doi.org/10.1080/00103624.2015.1122797

Rădoi, D. M., Bonciu, E., Păunescu, G., Roșculete, C. A., & Roșculete, E. (2022). A brief review on the influence of flag leaf on cereals production. *Annals of the University of Craiova - Agriculture, Montanology, Cadastre Series*, *52*(1), 320-327. https://doi.org/10.52846/aamc.v52i1.1351

Rahman, M., Hossain, M., Chowdhury, I., Matin, M., & Mehraj, H. (2014). Variability study of advanced fine rice with correlation, path co-efficient analysis of yield and yield contributing characters. *International Journal of Applied Sciences and Biotechnology*, *2*, 364-370. https://doi.org/10.3126/IJASBT.V2I3.11069

Setiawati, M. R., Kurnia, S. N., Nurhopipah, P., Ramdhani, A., Suryatmana, P., Herdiyantoro, D., Simarmata, T., & Fitriatin, B. N. (2023). Effect of biofertilizer and amelioran briquette on rice growth in saline soil. *Jurnal Agroekoteknologi*, *15*(1), 1-15. https://doi.org/10.33512/jur.agroekotetek.v15i1.19763

Sharma, R., Singh, D., Kaushik, R., & Pandey, D. (2012). Correlation and path analysis for grain yield and its component traits in rice. *Oryza-An International Journal on Rice*, *49*, 215-218.

Sheikhani, A. R., Aminpanah, H., & Firouzi, S. (2014). Effects of inoculation method of plant growth-promoting rhizobacteria and silicon rate on rice grain yield. *Thai Journal of Agricultural Science*, *47*, 227-234.

Sheykhzadeh, M., Mobasser, H., Petrodi, E., & Rezvani, M. (2022). Silicon and zinc improves grain yield and nutrient status in rice when supplied during the different growth stages. *Romanian Agricultural Research*, *39*, 371-383. https://doi.org/10.59665/rar3934

Snehalatha, D., Bharghavi, J., Raghuveer, P., Rao, B., Srikanth, C. V., Kumar, S., & Thatikunta, R. (2023). Silicon improved water stress tolerance in rice genotypes. *International Journal of Environment and Climate Change*, *13*(9), 2056-2068. https://doi.org/10.9734/ijecc/2023/v13i92437

Szulc, W., Rutkowska, B., Hoch, M., Spychaj-Fabisiak, E., & Murawska, B. (2016). Exchangeable silicon content of soil in a long-term fertilization experiment. *Plant Soil and Environment*, *61*, 458-461. https://doi.org/10.17221/438/2015-PSE.

Thomas, L., & Singh, I. (2019). Microbial biofertilizers: Types and applications. In B. Giri, R. Prasad, Q. S. Wu & A. Varma (Eds.), *Biofertilizers for Sustainable Agriculture and Environment* (pp. 1-19). Springer, Cham. https://doi.org/10.1007/978-3-030-18933-4_1

Tran, D. T. (2019). *Technical efficiency, technical change and return to scale of rice, maize and agricultural production in Vietnam* [Doctoral dissertation, University of Göttingen]. Göttingen. http://doi.org/10.53846/goediss-8069

Wang, B., Chu, C., Wei, H., Zhang, L., Ahmad, Z., Wu, S., & Xie, B. (2020). Ameliorative effects of silicon fertilizer on soil bacterial community and pakchoi (Brassica chinensis L.) grown on soil contaminated with multiple heavy metals. *Environmental pollution*, *267*, 115411. https://doi.org/10.1016/j.envpol.2020.115411

Wang, N., Wang, X., Qian, Y., Bai, D., Bao, Y., Zhao, X., Xu, P., Li, K., Li, J., Li, K., Zhang, D., & Shi, Y. (2023). Genome-wide association analysis of rice leaf traits. *Agronomy*, *13*(11), 2687. https://doi.org/10.3390/agronomy13112687

Yusob, S. M., Haruna, A. O., Omar, L., Kueh, R., Heng, J., & Kamaruzaman, R. (2023). 5. Inorganic and natural silicon sources as soil amendment on growth of local aromatic rice variety. *Journal of Tropical Plant Physiology*, *15*(1), 24-36. https://doi.org/10.56999/jtpp.2023.15.1.27

Zhang, X., Zhou, S., Bi, J., Sun, H., Wang, C., & Zhang, J. (2021). Drought-resistance rice variety with water-saving management reduces greenhouse gas emissions from paddies while maintaining rice yields. *Agriculture, Ecosystems & Environment*, *320*, 107592. https://doi.org/10.1016/J.AGEE.2021.107592

Zhao, D. D., Zhang, P. B., Bocharnikova, E. A., Matichenkov, V. V., Khomyakov, D. M., & Pakhnenko, E. P. (2019). Estimated carbon sequestration by rice roots as affected by silicon fertilizers. *Moscow University Soil Science Bulletin*, *74*, 105-110. https://doi.org/10.3103/S0147687419030025

Zhao, K., Yang, Y., Zhang, L., Zhang, J., Zhou, Y., Huang, H., Luo, S., & Luo, L. (2022). Silicon-based additive on heavy metal remediation in soils: Toxicological effects, remediation techniques, and perspectives. *Environmental Research*, *205*, 112244. https://doi.org/10.1016/j.envres.2021.112244

Pertanika J. Trop. Agric. Sci. 48 (3): 949 - 971 (2025)

PERTANIKA JOURNALS

TROPICAL AGRICULTURAL SCIENCE

Journal homepage: http://www.pertanika.upm.edu.my/

Review Article

Unraveling the Biology of *Spodoptera frugiperda* (Lepidoptera: Noctuidae) and its Biocontrol Potential Using Entomopathogenic Nematodes: A Review

Siti Noor Aishikin Abdul-Hamid[1,2], Wan Nurashikin-Khairuddin[2], Razean Haireen Mohd. Razali[3] and Johari Jalinas[1]*

[1]Applied Entomology Laboratory, Center for Insect Systematics, Department of Biological Sciences and Biotechnology, Faculty of Science and Technology, Universiti Kebangsaan Malaysia (UKM), Bangi 43600, Malaysia
[2]Biological Control Program, Agro-biodiversity and Environmental Research Center, Malaysian Agricultural Research and Development Institute (MARDI), Serdang 43400, Malaysia
[3]Pests and Diseases Program, Industrial Crops Research Center, Malaysian Agricultural Research and Development Institute (MARDI), Serdang 43400, Malaysia

ABSTRACT

The fall armyworm (FAW), *Spodoptera frugiperda*, is a polyphagous pest that infest various plants. This highly invasive pest is native to the American continent and has spread rapidly over 100 countries worldwide. Its rapid spread and ability to cause severe damage to various crops, especially maize, pose a significant threat to food security, particularly in developing countries. Curative control using chemical insecticides is the primary choice in most countries, especially in Africa and Asia. However, dependence on chemical insecticides can have adverse effects on the environment and humans and can lead to the development of resistance to these pests. Therefore, various efforts have been made to develop effective, low-risk, and cost-efficient biocontrol measures. Entomopathogenic nematodes (EPNs) are a viable and potential choice for the biological control of this pest. This review compiles information on FAW, EPNs, and their developmental stages, focusing specifically on the pathogenicity of EPNs against FAW. This contributes to Integrated Pest Management (IPM) strategies addressing FAW infestations, which have caused severe maize crop losses in Malaysia since their detection in 2019. The potential for locally adapted EPN formulations tailored to Malaysia's climate ensures their practical application in the field.

ARTICLE INFO

Article history:
Received: 09 September 2024
Accepted: 23 December 2024
Published: 16 May 2025

DOI: https://doi.org/10.47836/pjtas.48.3.16

Keywords: Biological control, Entomopathogenic nematodes (EPNs), Integrated Pest Management (IPM), invasive species, *Spodoptera frugiperda*

E-mail addresses:
P108595@siswa.ukm.my (Siti Noor Aishikin Abdul-Hamid)
wannurashikin93@gmail.com (Wan Nurashikin-Khairuddin)
aireenmr@mardi.gov.my (Razean Haireen Mohd Razali)
johari_j@ukm.edu.my (Johari Jalinas)
* Corresponding author

e-ISSN: 2231-8542

INTRODUCTION

The fall armyworm (FAW), *Spodoptera frugiperda* J.E. Smith (Lepidoptera: Noctuidae), is an invasive pest threatening global crop production systems. This pest can cause up to a 70% reduction in maize yield when crops are attacked early (Hruska, 2019). FAW infestations cause significant damage to other crops, such as cotton, rice, soybeans, tomatoes, potatoes, onions, beans, cabbages, sorghum, and a few pasture grass species (Day et al., 2017). *Spodoptera frugiperda* was first reported in Malaysia in 2019 (International Plant Protection Convention [IPPC], 2019; Jamil, Saranum, Saleh-Hudin et al., 2021). Since then, FAW infestations have caused severe damage, with 50%–100% crop loss in maize fields in Malaysia (Department of Agriculture [DOA], 2021; Jamil, Saranum, Mat et al., 2021).

Various preventive and curative approaches are being implemented to combat FAW attacks on maize crops, particularly regular monitoring, pheromone traps, ultraviolet (UV) light traps, agro-ecological methods, and the application of chemical and biopesticides (DOA, 2021). Curative control using chemical insecticides remains the primary choice for farmers. Reliance on chemical insecticides can adversely affect the environment and humans and increase the risk of FAW developing resistance to these chemicals (Guo et al., 2020). Entomopathogenic nematodes (EPNs) function similarly to entomopathogenic fungi and bacteria in reducing or replacing chemical insecticides (Cuthbertson & Audsley, 2016). Several studies have evaluated the pathogenicity of EPNs as potential biological control agents against FAW in laboratory and field environments. Therefore, this manuscript discusses the biology of FAW and EPNs pathogenicity against it.

TAXONOMY, ORIGIN, AND DISTRIBUTION OF THE FALL ARMYWORM (FAW), SPODOPTERA FRUGIPERDA

The fall armyworm (FAW) was initially named *Phalaena frugiperda* by Smith and Abbot in 1797. It was later known as *Laphygma frugiperda* (Luginbill, 1928) and, since 1958, has been referred to as *Spodoptera frugiperda* (European and Mediterranean Plant Protection Organization [EPPO], 2024). There are two strains of *S. frugiperda*: corn and rice (Food and Agriculture Organization of the United Nations & Plant Protection Division [FAO & PPD], 2020). Both strains have similar morphology but differ in pheromone composition, mating behaviors, and host plant selection (Dumas et al., 2015; FAO & PPD, 2020). The corn strain of *S. frugiperda* prefers maize, cotton, and sorghum as host plants, whereas the rice strain prefers rice and pasture grasses (Dumas et al., 2015). The two strains can be differentiated using molecular markers, specifically polymorphism in the mitochondrial cytochrome oxidase 1 (CO1) gene (Ke & Pashley, 1992; Nagoshi et al., 2012).

Spodoptera frugiperda originates from tropical and subtropical regions of the United States (Luginbill, 1928; Rwomushana, 2019; Sparks, 1979). *Spodoptera frugiperda* has spread to almost every part of the world except Europe and Antarctica (EPPO, 2024;

Rwomushana, 2019). It was first recorded in Central and West Africa in early 2016 (Goergen et al., 2016). By 2017, *S. frugiperda* had spread to all sub-Saharan African countries except Lesotho (Food and Agriculture Organization of the United Nations [FAO], 2017). In 2018, it was first found in the districts of Shivamogga and Navanagere in Karnataka, India (Ganiger et al., 2018; Sharanabasappa et al., 2018; Shylesha et al., 2018). The following year, *S. frugiperda* was recorded in Bangladesh, Myanmar, Sri Lanka, Thailand, Vietnam, Indonesia, China, and Malaysia (Lamsal et al., 2020). Morphological and molecular identification confirmed that pest samples from maize fields in Chuping, Perlis (near the Malaysia-Thailand border) were *S. frugiperda* (IPPC, 2019). By early 2020, *S. frugiperda* had been detected in all states of Malaysia (Jamil et al., 2021b).

BIOLOGY OF FALL ARMYWORM (FAW), SPODOPTERA FRUGIPERDA

The ability of *S. frugiperda* to migrate and cause repeated attacks in both native and new areas is facilitated by various biological traits such as strong flight capability, polyphagous feeding habits, high fecundity, and significant ecological resilience (FAO & PPD, 2020; Montezano et al., 2018). *Spodoptera frugiperda* has no diapause mechanism and cannot survive in winter in northern parts of America, prompting migration to the warmer southern regions (Rose et al., 1975). Low temperatures reduce flight speed and wingbeat frequency, and the flight performance of *S. frugiperda* moths is abysmal at 10°C (Ge et al., 2021). Nocturnal in nature, *S. frugiperda* moths can fly up to 100 km overnight (Assefa & Ayalew, 2019; Johnson, 1987; Sparks, 1979). Ge et al. (2021) found that 84% of *S. frugiperda* moths flew more than 40 km, covering a total distance of 163.58 km over five days. *Spodoptera frugiperda* undergoes complete metamorphosis, transitioning through egg, larval, pupal, and adult stages. The development of S. *frugiperda* depends on the larval food source, as in Table 1 and Table 2.

Tables 1 and 2 comprehensively compare various parameters related to the biology and development of *S. frugiperda* (fall armyworm) across different host plants and conditions. These parameters include fecundity, egg incubation, larval and pupal periods, adult emergence, and longevity. The data is derived from multiple studies conducted in different countries. The highest fecundity is observed on an artificial corn-based diet (1746.3 eggs/female), while the lowest is recorded on sorghum (106.44 eggs/female). However, the absence of data on several parameters for this diet (pupation percentage, adult emergence) leaves gaps in fully understanding its effects. Among natural plants, maize variants (fodder maize, field maize, sweet maize) generally support higher fecundity and faster development compared to other crops like sorghum and rice, which suggests that maize could be a more suitable host for *S. frugiperda*. The larval period ranges from 10.83 days on sweet maize to 21.28 days on sunn hemp, indicating that the host plant choice significantly affects the time required for larval development. Pupal periods also vary, with some values not provided

(No data, ND) for several plants. However, available data shows the shortest pupal period on rice leaves (7.03 days for males) and the longest on corn var. NK 6410 (7.98 days for males). The total life cycle period spans from 24.58 days on corn var. Macho F1 to 48.61 days on rice leaves, reflecting the host plant's impact on the overall development speed of *S. frugiperda*. The data in Tables 1 and 2 underscores the significant effect of host plants on the biological traits of *S. frugiperda*. This variability is crucial for understanding the pest's adaptability and developing targeted management strategies.

DAMAGE AND LOSSES DUE TO FAW LARVAE INFESTATION IN MAIZE FIELD

Larvae of *S. frugiperda*, particularly from the third to the sixth instar, have caused more than 70% damage to corn crops (Assefa & Ayalew, 2019). *Spodoptera frugiperda* attacks reported in maize fields in Nicaragua, Central America, have resulted in yield losses ranging from 15% to 73%, with an attack rate of 55% to 100% (Hruska & Gould, 1997). Fall armyworm (FAW) larvae attacks in Ghana, Zambia, and Cameroon have caused crop yield losses ranging from 0.3 to 20.5 million tons, valued at US$0.1 to 6.2 billion (Day et al., 2017). In Malaysia, *S. frugiperda* infestations have caused severe attacks (100%) in maize fields in Changlun, Kedah, severely damaging all parts of the corn plants (Jamil, Saranum, Saleh-Hudin et al., 2021). Maize fields affected by *S. frugiperda* attacks covered an area of 246.35 hectares, with an infestation severity percentage ranging from 50% to 100% (IPPC, 2019).

CONTROL AND MANAGEMENT OF FALL ARMYWORM (FAW), SPODOPTERA FRUGIPERDA

Regular monitoring and early detection are vital in managing and controlling infestations of *S. frugiperda* to prevent economic damage to crops (Assefa & Ayalew, 2019). For infestations with less than 5% of seedlings or 20% of corn plants under 30 days old, curative control using chemical insecticides is recommended (EPPO, 2024). The economic threshold level (ETL) for this pest in hybrid maize and sorghum crops is 1.8-2.5 larvae/10 plants and 1-2 larvae/plant, respectively (Jaramillo-Barrios et al., 2020; Pitre, 1985). Meanwhile, the economic injury level (EIL) on maize is 14%, 21%, 23%, 26%, and 50% infestation by *S. frugiperda* at 2, 3, 4, 5, and 6 weeks after crop germination (Evans & Stansly, 1990).

Chemical insecticides are the primary method to control *S. frugiperda* larvae in the Americas and Africa (Otim et al., 2021). Commonly used active ingredients include Emamectin benzoate, Chlorantraniliprole, Spinetoram, Diamides, Avermectin, Spinosad, and Indoxacarb (Bird et al., 2022; Otim et al., 2021; Sarkowi & Mokhtar, 2021). Reliance on chemical control strategies on a global scale for several decades has led to resistance in *S. frugiperda* to at least 29 active ingredients across six mode-of-action groups (Bird et al.,

Table 1
Development performance of Spodoptera frugiperda *based on host plant*

Plant/ Parameter	Egg Incubation period (days)	Larval period (days)	Pupal period (days)	Oviposition period (days)	Adult longevity (days)		Total life cycle period (days)		Country	Reference
					M	F	M	F		
Pearl millet	2 ± 0.43	16.93 ± 0.61	7.61 ± 0.38	1.20 ± 0.03	4.31 ± 0.05	6.80 ± 0.06	30.85 ± 0.46	33.34 ± 0.52	India	Bankar and Bhamare (2023a)
Sugar cane	2.52 ± 0.30	19.17 ± 0.51	8.49 ± 0.42	1.36 ± 0.04	4.18 ± 0.09	5.86 ± 0.04	34.36 ± 0.80	36.04 ± 0.51		
Fodder maize	2.17 ± 0.00	ND	9.05 ± 0.21	4.25 ± 0.75	7.00 ± 0.05	7.00 ± 0.41	ND	ND	Egypt	Mohamed et al. (2023)
Corncobs	2.51 ± 0.00	NE	7.76 ± 0.28	5.00 ± 0.55	8.50 ± 0.29	10.00 ± 0.41	NE	NE		
Maize leaves	2.66 ± 0.57	16.65 ± 0.61	ND	ND	16.13 ± 1.02	16.89 ± 0.55	43.79 ± 0.99	44.55 ± 0.59	Indonesia	Maharani et al. (2021)
Rice leaves	3.00 ± 0.00	20.32 ± 0.68	ND	ND	16.71 ± 0.93	18.94 ± 1.50	43.79 ± 0.99	48.61 ± 0.55		
Sorghum	2.26 ± 0.21	15.93 ± 0.94	7.99 ± 0.24	1.14 ± 0.05	5.13 ± 0.07	6.34 ± 0.03	31.31 ± 0.77	32.52 ± 0.44	India	Bankar & Bhamare (2023b)
Maize	2 ± 0.33	12.58 ± 0.75	6.74 ± 0.44	1.88 ± 0.04	6.29 ± 0.09	8.46 ± 0.03	27.61 ± 0.60	29.78 ± 0.66		
Maize leaves	3-4	16.6 ± 0.82	9.2 ± 1.64	2.8 ± 0.27	10.4 ± 0.41	12.4 ± 0.54	36.2 ± 1.25	38.2 ± 1.35	India	Aarthi-Helen et al. (2021)
Traditional corn (Tinigib)	ND	14.07 ± 0.44	8.09 ± 0.26	3.80 ± 0.38a	8.93 ± 1.14	10.13 ± 1.02	25.31 ± 0.57		Philippines	Agravante et al. (2023)
Corn var. Macho F1	ND	13.52 ± 0.36	8.02 ± 0.33	3.78 ± 0.25	9.07 ± 0.43	9.98 ± 0.49	24.58 ± 0.44			
Corn var. NK 6410	ND	13.60 ± 0.44	7.98 ± 0.29	4.00 ± 0.33	9.20 ± 0.38	10.40 ± 0.86	24.66 ± 0.33			
Rice var. RC 226	ND	14.41 ± 0.19	8.81 ± 0.57	2.80 ± 0.69	8.80 ± 0.77	9.80 ± 0.70	26.45 ± 0.62			
OPV Corn	ND	14.49 ± 0.39	8.65 ± 0.35	3.33 ± 0.24	9.13 ± 0.69	10.40 ± 0.60	26.36 ± 0.47			
Napier grass	2.00 ± 0.00	16.74 (F) 21.16 (M)	7.26 ± 0.08 8.71 ± 0.09	8.20 ± 0.46	12.55 ± 0.82	14.40 ± 0.88	26.90 ± 0.21	25.13 ± 0.21	Taiwan	Chen et al. (2023)
Natal grass	2.00 ± 0.00	21.18 (F) 20.95 (M)	7.03 ± 0.06 8.02 ± 0.06	6.17 ± 0.40	8.67 ± 0.42	9.41 ± 0.39	27.26 ± 0.16	26.11 ± 0.17		
Sunn hemp	2.00 ± 0.00	19.85 (F) 21.28 (M)	6.96 ± 0.07 7.93 ± 0.06	6.78 ± 0.57	10.31 ± 0.57	11.78 ± 0.56	25.41 ± 0.24	24.00 ± 0.18		
Field maize	2.00 ± 0.00	11.28 ± 0.05	7.93 ± 0.09	3.33 ± 0.33	4.82 ± 0.46	5.64 ± 0.44	28.26 ± 0.39	27.96 ± 0.41	Thailand	Hong et al. (2022)
Sweet maize	2.03 ± 0.02	10.83 ± 0.14	7.57 ± 0.09	3.00 ± 0.58	4.71 ± 0.42	6.13 ± 0.35	26.90 ± 0.37	27.42 ± 0.36		

Table 1 *(continue)*

Plant/ Parameter	Egg Incubation period (days)	Larval period (days)	Pupal period (days)	Oviposition period (days)	Adult longevity (days)		Total life cycle period (days)		Country	Reference
					M	F	M	F		
Waxy maize	2.02 ± 0.01	11.15 ± 0.15	8.24 ± 0.09	4.00 ± 0.00	4.53 ± 0.52	5.35 ± 0.43	28.61 ± 0.30	28.21 ± 0.38		
Artificial corn-based diet	ND	15.3 ± 0.15	11.3 ± 0.20	ND	ND	ND	ND	ND	Brazil	Pinto et al. (2019)

Note. M = Male, F = Female, ND = No Data

Table 2
Reproductive performance of Spodoptera frugiperda *based on host plant*

Plant/Parameter	Larval weight (g)	Pupal weight (g)	Pupation (%)	Adult emergence (%)	M: F ratio	Country	Reference
Pearl millet	ND	ND	71 ± 1.06	86 ± 0.50	1:1.26	India	Bankar and Bhamare
Sugar cane	ND	ND	85 ± 0.74	87 ± 0.37	1:1.19		(2023a)
Fodder maize	0.34 ± 0.008	0.16 ± 0.004	ND	ND	3: 5	Egypt	Mohamed et al. (2023)
Corncobs	0.41 ± 0.01	0.20 ± 0.005	ND	ND	8:13		
Maize leaves	ND	ND	ND	ND	1.03:1	Indonesia	Maharani et al. (2021)
Rice leaves	ND	ND	ND	ND	1.04:1		
Sorghum	ND	ND	91±1.17	91±0.69	1:1.31	India	Bankar and Bhamare
Maize	ND	ND	88±0.84	92±0.49	1:1.20		(2023b)
Traditional corn (Tinigib)	ND	ND	ND	94.00 ± 8.40	50:50	Philippines	Agravante et al. (2023)
Corn var. Macho F1	ND	ND	ND	100 ± 0.00	60:40		
Corn var. NK 6410	ND	ND	ND	100 ± 0.00	36:64		
Rice var. RC 226	ND	ND	ND	88.00 ± 10.95	48:52		
OPV Corn	ND	ND	ND	94.67 ± 8.69	51:49		
Field maize	ND	ND	89.06	ND	7.25: 6.5	Thailand	Hong et al. (2022)
Sweet maize	ND	ND	85.71	ND	7.25: 7.75		
Waxy maize	ND	ND	92.31	ND	8: 9.75		
Artificial corn-based diet	ND	0.259 ± 0.003	89.3 ± 7.59	ND	0.55 ± 0.07	Brazil	Pinto et al. (2019)

Note. M = Male, F = Female, ND = No Data

2022). Within Integrated Pest Management (IPM), chemical insecticides are considered a last resort to curb crop pest infestations (Day et al., 2017).

Biological control, mainly using microbes such as bacteria, fungi, viruses, and entomopathogenic nematodes, has also been employed to manage *S. frugiperda* infestations (Guo et al., 2020). *Bacillus thuringiensis* causes 61%–87% larval mortality in the field and 100% in the laboratory (Liu et al., 2019). Spraying *nucleopolyhedrovirus (NPV)* in maize fields has resulted in 93.4% larval mortality of *S. frugiperda* (Cruz et al., 1997). Using a combination of viruses, such as *S. frugiperda multiple nucleopolyhedroviruses (SfMNPV)* and *S. frugiperda granulovirus (SfGV),* can enhance virus efficacy and help delay resistance evolution (Hussain et al., 2021). The use of entomopathogenic fungi such as *Beauveria bassiana* and *Metarhizium anisopliae* has been reported to cause 64.3% and 67.8% larval mortality of *S. frugiperda* in the laboratory (Ramanujam et al., 2020).

ENTOMOPATHOGENIC NEMATODES (EPN) AND THEIR SYMBIOTIC BACTERIA

Entomopathogenic nematodes (EPNs) are a group of nematodes that infect and kill insects. Entomopathogenic nematodes (EPNs) reside in the soil and are obligate parasites from the Phylum Nematoda (Gozel & Gozel, 2016). The first EPN, identified as *Aplectana kraussei* (now known as *Steinernema kraussei*), was described by Steiner in 1923 (Poinar & Grewal, 2012). Steinernematidae comprises two genera, *Steinernema* (with more than 50 species) and *Neosteinernema* (one species: *Neosteinernema longicurvicauda*). The family Heterorhabditidae is monotypic, containing only one genus, *Heterorhabditis*, with one species, *Heterorhabditis bacteriophora* (Gozel & Gozel, 2016; Stock & Blair, 2008). Poinar (1976) described the first Heterorhabditis in 1976. Hunt and Nguyen (2016) reported that by the end of 2015, 95 species of *Steinernema* and 16 species of *Heterorhabditis* had been identified. Entomopathogenic nematode (EPN) species identification is based on morphological and morphometric data comparisons and cross-breeding tests (Gaugler, 2002). Diagnostic methods like Polymerase Chain Reaction (PCR), PCR-RFLP, and Random Amplified Polymorphic DNA (RAPD) are employed to identify EPN species based on dioxyribonucleic acid (DNA) sequence comparisons (Caoili et al., 2018; Stock & Blair, 2008). Two families are widely used as effective biological control agents for managing pests above and below the soil: Steinernematidae and Heterorhabditidae (Kaya et al., 2006; Vashisth et al., 2015).

Entomopathogenic nematodes (EPNs) are capable of infecting and thriving within a wide range of insects, completing their life cycle in species from orders such as Lepidoptera, Coleoptera, Orthoptera, Diptera, Thysanoptera, and Siphonaptera (Půža & Mráček 2010). The life cycle of EPNs begins with the third stage, infective juvenile (IJ), which is free-living in the soil, capable of infecting the target host, and the only stage found outside the

host. Entomopathogenic nematodes (EPNs) in the soil detect target hosts by responding to carbon dioxide, vibrations, chemical signals/stimuli, or sensing the physical structure of the insect's integument (Gaugler, 2002). The life cycle of EPN is shown in Figure 1. Entomopathogenic nematodes (EPNs) are associated with symbiotic bacteria from the family Enterobacteriaceae. Steinernematidae is associated with symbiotic bacteria from the genus *Xenorhabdus*, while Heterorhabditidae is associated with symbiotic bacteria from the genus *Photorhabdus* (Gozel & Gozel, 2016; Vashisth et al., 2013). Symbiotic bacteria, *Xenorhabdus* and *Photorhabdus*, kill the insect host quickly, create a suitable environment for EPN reproduction, produce antibiotics and secondary metabolites that inhibit the growth of other microorganisms, and convert host tissue into food (Forst & Nealson, 1996). In exchange, EPNs provide protection and access to the host insect's hemolymph (Vashisth et al., 2013).

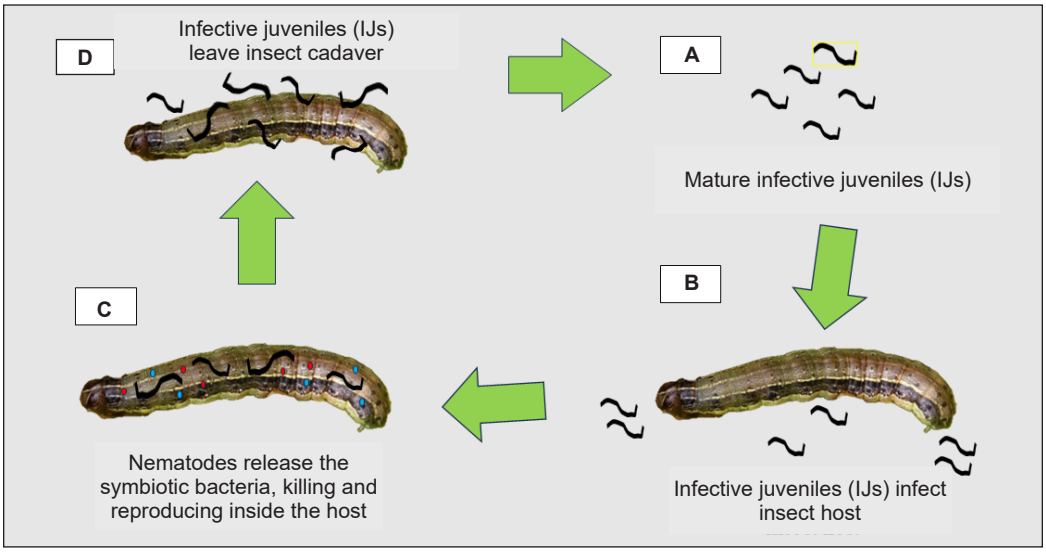

Figure 1. Illustration of the life cycle of entomopathogenic nematodes on insect host. (A) Mature infective juveniles (IJ3) find a host in the soil. (B) Infective juveniles (IJs) enter the host via the mouth, anus, and spiracle opening. (C-D) Infective juveniles (IJs) infect and release symbiotic bacteria to elude the host immune system and kill the host. Both species (nematode and symbiotic bacteria) reproduce using the cadaver's nutrients; when the nutrients are impoverished, the two creatures recombine and enter the soil to restart the cycle

BIOLOGICAL CONTROL OF FALL ARMYWORM (FAW), SPODOPTERA FRUGIPERDA USING ENTOMOPATHOGENIC NEMATODES (EPN)

Researchers from different countries have conducted various studies on the pathogenicity of entomopathogenic nematodes against *S. frugiperda* (Guo et al., 2020). Rodríguez-Zamora (2019) reported that the entomopathogenic nematode (EPN), *Heterorhabditis bacteriophora*, caused 65% mortality in *S. frugiperda* larvae in the laboratory within 48

hours. *Heterorhabditis bacteriophora* also caused 92% and 80% mortality in pre-pupae and pupae of *S. frugiperda*, respectively (Alonso & Mejia, 2018). Meka et al. (2020) stated that the highest larval mortality of *S. frugiperda*, 100%, occurred when infected with *Steinernema glaseri* at a concentration of 2000 IJs/plate, followed by 95% at 1000 IJs/plate after 96 hours of inoculation. Due to the high pathogenicity of insect hosts, various EPN species have been studied for their potential as biological control agents against *S. frugiperda* (Table 3).

The studies presented in Table 3 are a comprehensive summary of various studies investigating the effectiveness of different entomopathogenic nematode (EPN) species against the fall armyworm (FAW), *Spodoptera frugiperda*, under various conditions, including laboratories, fields, greenhouses, and across different countries. A variety of EPN species, such as *Steinernema sp.*, *Heterorhabditis indica*, *S. carpocapsae*, and others, were tested against different developmental stages of FAW larvae (third instar, sixth instar, pre-pupae, and pupae). The concentrations of EPNs used in these studies varied significantly, ranging from as low as five infective juveniles (IJs) per larva to as high as 50,000 IJs per plant in field trials. The duration of exposure also differed across studies, from as short as 14 hours to as long as 25 days. The results indicate that the effectiveness of EPNs in causing mortality in FAW larvae is highly dependent on the EPN species, concentration, and environmental conditions. For instance, *Steinernema sp*. and *Heterorhabditis sp*. showed a mortality rate of 100% in certain laboratory conditions. Studies with combinations of EPNs and other biocontrol agents, like *Metarhizium anisopliae* or insecticides, demonstrated varying levels of success, highlighting the potential for integrated pest management approaches.

Species of entomopathogenic nematodes (EPNs) outperform others under certain conditions due to biological, ecological, and environmental factors. Based on the provided data (Table 3), the key reasons are symbiotic bacteria efficacy, host stage suitability, application techniques, synergistic combinations, and speed of host mortality. Entomopathogenic nematodes (EPNs) are closely associated with specific symbiotic bacteria, such as *Photorhabdus* in *Heterorhabditis* and *Xenorhabdus* in *Steinernema*. The virulence of these bacteria varies, affecting the speed and efficiency of killing the host insect (Owuama, 2001). Different EPN species more effectively target specific developmental stages of the FAW. For instance, *Steinernema carpocapsae* showed 100% mortality in second and third-instar larvae, whereas higher doses of *Heterorhabditis bacteriophora* were required for similar effects on pre-pupae and pupae. The concentration of infective juveniles (IJs) and delivery methods significantly impact outcomes. Higher concentrations, such as 2000 IJs per plate for *Steinernema glaseri*, result in more excellent mortality rates than lower doses. Moreover, species like *S. carpocapsae* are known for rapid action due to their ambush strategy, while others, like *H. bacteriophora*, adopt a more cruising approach, affecting their performance under specific conditions (Stock & Blair, 2008).

Overall, the studies summarized in Table 3 illustrate the potential of EPNs as biocontrol agents against FAW, with varying degrees of success influenced by multiple factors. The data suggest that laboratory conditions often yield higher mortality rates, while field applications may require combination treatments and further optimization to achieve consistent results. The table also underscores the global research interest in EPNs, with studies conducted across different continents emphasizing the universal challenge posed by FAW and the widespread efforts to manage this pest.

ENTOMOPATHOGENIC NEMATODES (EPN) AS BIOPESTICIDES AND THEIR APPLICATION IN INTEGRATED PEST MANAGEMENT (IPM)

Countries that have commercialized EPN as biopesticides include Sanoplant (Switzerland), Helix (Canada), ORTHO Biosafe USA (United States), Koppert (Netherlands), and BASF (Germany). Entomopathogenic nematode (EPN) can be stored and produced in large quantities *in vivo* and *in vitro* (Shapiro-Ilan et al., 2012). At least 13 species of Steinernematidae and Heterorhabditidae have been commercialized for pest control (Shapiro-Ilan et al., 2016). In the laboratory, EPN can be inoculated onto insect hosts using Petri dishes and filter papers with a minimum concentration of EPN before being transferred to White Traps for *in vivo* collection (Shapiro-Ilan et al., 2012). However, mass production of EPN can be carried out *in vitro* using solid or liquid culture media (McMullen & Stock, 2014). The *in vitro* liquid method is the most cost-effective way to produce nematodes, followed by the *in vitro* solid method. In contrast, the *in vivo* method is the least economical. While *in vitro* techniques allow for large-scale, affordable production ideal for treating vast field areas to control crop pests, the *in vivo* method is more costly. It produces nematodes in smaller quantities, making it better suited for nursery soil treatments or small plots (Askary & Ahmad, 2017).

Mass production of EPN allows for the creation of biopesticide products. EPN formulation occurs when the active ingredient (EPN) combines several materials, such as sunscreens, additives, and carriers. Entomopathogenic nematode (EPN) biopesticides can be produced as aqueous solutions, synthetic sponges, gels, and clay powders to facilitate storage and transportation (Cruz-Martínez et al., 2017). Since EPNs are sensitive to ultraviolet (UV) radiation, EPN sprays should be done in the late afternoon (Negrisoli et al., 2010).

Entomopathogenic nematodes (EPNs) are critical components of integrated pest management (IPM) systems and have practical applications in managing fall armyworms (FAW) and other agricultural pests. These essential applications include EPNs being an eco-friendly replacement for chemical insecticides; they fit the IPM principle of minimizing chemical inputs while maintaining effective pest control (Day, 2017). Combining EPNs with biopesticides such as *Metarhizium anisopliae* or *Bacillus thuringiensis* (Bt) could increase

Table 3
Studies on the pathogenicity of entomopathogenic nematodes against the fall armyworm, Spodoptera frugiperda

EPN species	Condition	FAW stage	Concentration	Duration	Result (% Mortality)	Symbiotic bacteria	Country	Reference
Steinernema sp. *Heterorhabditis indica*	Laboratory	100 third instar larvae	0, 50, 100, 200 and 400 IJ/ml per larvae	14 h	• 100% (200IJ) • 75% (400IJ)	ND	Brazil	Garcia et al. (2008)
H. indica, *S. carpocapsae* *S. glaseri*	Laboratory	11 200 third instar larvae	100IJ/container + Half dose insecticides	4 d	• 88%–90% • 94%–98% • 98%–100%.	ND	Brazil	Negrisoli et al. (2010)
H. indica	Field	Maize	250IJ/ cm2 + Luferon/ Chlorpyrifos	2 y	• 62.5% (Year 1) and 57.5% (Year 2)—Combination of *H. indica* and lufenuron (0.15 L/ha)			
S. arenarium *Heterorhabditis sp.* RSC02	Laboratory	80 fourth or fifth instar larvae	0, 100, 250, and 500 IJ/ml per larvae	72 h	• 80% and 100% • 85% and 97.6%	ND	Brazil	Andaló et al. (2010)
S. arenarium *Heterorhabditis* sp. RSC02	Glasshouse	40 fourth or fifth instar larvae	200IJ/container	96 h	• 75% • 87.5%			
Heterorhabditis sp. (2) *Steinernema* sp.	Laboratory	200-fifth instar larva	100 and 300µl IJ per larva	120 h	• 70%–80% • 28%–56%	• *Photorhabdus luminescens* subsp. *Laumondii* • *Xenorhabdus szen- tirmaii*	Brazil	Salvadori et al. (2012)
H. amazonensis RSC2 *S. arenarium* A11	Laboratory	20 larvae	500 IJ/10 ml per larva	6 d	• 100% • 100%	ND	Brazil	Andaló et al. (2012)
S. diaprepesi	Laboratory	45 sixth instar larvae	0, 50, and 100 IJ/0.5 ml per larva	6 d	93% (50 IJ) and 100% (100 IJ)	ND	Argentina	Caccia et al. (2014)

Table 3 *(continue)*

EPN species	Condition	FAW stage	Concentration	Duration	Result (% Mortality)	Symbiotic bacteria	Country	Reference
H.bacteriophora	Field	1 larva per corn cob	250 EPN/plant	5d	• 100% (*H. bacteriophora* + *Metarhizium anisopliae*) • 93.33% (*H. bacteriophora* + *M. anisopliae* + Chlorpyrifos)	ND	Costa Rica	Bissiwu & Pérez (2016)
H. indica	Laboratory	60 sixth instar larvae	200 IJ/ml per larva and 1–104 CFU/ larva (symbiotic bacteria	72h	Symbiotic bacterial extracts (intra- and extracellular) caused 10% and 93% larval mortality	*Photorhabdus luminescens subsp. akhurstii* SL0708	Colombia	Salazar-Gutiérrez et al. (2017)
S. carpocapsae	Laboratory	60 larvae	200µl/larva	96h	90% within 72h (*S. carpocapsae* + chlorantraniliprole or spinetoram at high doses	ND	Puerto Rico, USA	Viteri et al. (2018)
H. bacteriophora	Laboratory	240 pre-pupae and pupae	1000, 3000 and 5000 EPN/ml	72h	• 75%, 87% and 92% (pre-pupae) • 55%, 70% and 80% (Pupae)	ND	Peru	Alonso & Mejia (2018)
	Glasshouse	80 pre-pupa and pupa		120h	• 68%, 70% and 78% (pre-pupae) • 48%, 53% and 62% (pupae)			
S. carpocapsae (strain SK27)	Laboratory	24 sixth instar larvae	150 IJ/150µl per larva	48h	100%	*Xenorhabdus nematophila*	France	Huot et al. (2019)

Table 3 *(continue)*

EPN species	Condition	FAW stage	Concentration	Duration	Result (% Mortality)	Symbiotic bacteria	Country	Reference
H. bacteriophora *H. indica*	Laboratory	125 second instar larvae	0, 20, 40, 80 and 170 IJ/larva	5d	• 65% in 48h (40IJ), LC_{50}= 32 IJ/ml • 65% in 48 (170IJ), LC_{50}= 42 IJ/ml	*Photorhabdus luminescens*	Nicaragua	Rodríguez-Zamora (2019)
H. indica *H. bacteriophora,* *Heterorhabditis sp.* *S. carpocapsae* *S. arenarium* *S. longicaudum*	Laboratory	All larva stages pupae	250 IJ/ml, 600 IJ/5ml and 25 IJ/ cm^2	5d	100% (*H. indica* and *S. carpocapsae)* against first and second instar larvae	ND	South Korea	Acharya et al. (2020)
S. glaseri	Laboratory	All larva stages	0, 250, 500, 1000 and 2000 IJ/Petri dish	96j	• 100% (2000IJ) • 95% (1000IJ)	ND	India	Meka et al. (2020)
Steinermatidae sp. (Kepahiang) *Steinermatidae sp.* (Bengkulu)	Laboratory	15 third instar larvae	0 IJ/ml, 200 IJ/ml, 400 IJ/ 2ml, 600 IJ/3ml per larva	5d	• 60%, 80% and 100% (LC_{50}=163.5 IJ/ml) • 46.6%, 73.3% and 93.3% (LC_{50}= 186.5 IJ/ml)	ND	Indonesia	Hade et al. (2020)
H. ruandica *Steinernema sp.* *S. carpocapsae*	Laboratory	24 second, third, and six instar larvae for each treatment	5, 10, 25, 125 IJ/400µl per larva	7d	*S. carpocapsae* from Rwanda caused 100% rapid mortality in second and third-instar larvae and 75% in sixth-instar larvae.	ND	Rwanda	Fallet et al. (2022)
H. indica	Laboratory	Third, fourth, and fifth instar larvae	10, 20, 40, 60, 80, 100, 120, 140, and 160 IJs/larva	96h	100% (160IJs/larva)	ND	India	Shinde et al. (2023)

Table 3 *(continue)*

EPN species	Condition	FAW stage	Concentration	Duration	Result (% Mortality)	Symbiotic bacteria	Country	Reference
S. carpocapsae	Field	Maize	200, 400, and 500 IJs per treatment	25d and 40d	*S. carpocapsae* @ 500 IJs significantly reduced the larval population and leaf damage score	ND	India	Ratnakala et al. (2023)
H. bacteriophora	Laboratory	Third and fifth instar larvae	60, 120, 250, 500, 1000, 2000 and 5000 IJs/ml	48h	78.33% to 100%	ND	China	Chen et al. (2023)
	Glasshouse	Third instar larvae	5000, 10,000 and 20,000 IJs/500ml	72h	51.56% at 48h and 68.72% at 72h (2000 IJs)			
	Field	Maize	10,000/25,000/ 50,000 IJs per plant	14d	43.18% (10,000/plant), 51.20% (25,000/plant), 25.17% (50,000/plant) after 48h			
S. carpocapsae *H. indica*	Laboratory	Second to sixth instar larvae	150, 300, 600, 1200 and 2400 IJs/ larvae/ml	188h	• 100% after 48-72h • 100% after 96h	ND	Egypt	Mohamed and Shairra (2023)
H. indica *S. abbasi*	Laboratory	Fifth instar larva	200IJ/150µl/plates	48h	• 100% • 100%	ND	Philippines	Duza et al. (2024)
S. carpocapsae	Field	Maize	1,500 EPN/ml / 3,000 EPN per plan	7d and 14d	Decreased larvae infestation by about 50%	ND	Rwanda	Fallet et al. (2024)
H. alii.	Laboratory	Third, fourth, fifth and sixth larval instars	100, 250, and 500 IJs/ml	72h	100% for all tested instar larvae	ND	Egypt	Shamseldean et al. (2024)
S. aciari	Laboratory	Third and sixth instar larvae	40, 60, 80, 100 IJ/ larva	96h	52%, 68%, 88% and 92% (third instar larvae)	ND	China	Sun et al. (2024)

Note. ND = No data

mortality rates and broaden the pest control spectrum (Bissiwu, 2016). Entomopathogenic nematodes (EPNs) can also be applied alongside cultural control practices like pheromone traps or crop rotation, creating a multi-layered pest management strategy. EPNs are effective against various FAW life stages, including larvae, pre-pupae, and pupae (Table 3). This capability makes them versatile IPM components capable of reducing pest populations at multiple points in their lifecycle. Unlike chemical insecticides, EPNs do not induce resistance in pests. This characteristic makes them valuable in IPM, which aims to sustain long-term pest suppression without escalating resistance risks. Entomopathogenic nematodes (EPNs) can be applied using standard agricultural equipment, either as soil treatments or foliar sprays, making them easy to integrate into existing farming practices (Shapiro-Ilan et al., 2012).

CONCLUSION

Based on the review of various articles, thesis, and books regarding the pathogenicity of EPNs and their symbiotic bacteria against the fall armyworm (FAW), *S. frugiperda*, there is potential for EPN (either local isolates or imported) to be developed as effective biological control agents in Malaysia. This manuscript highlights significant gaps and underexplored aspects in applying EPNs as biocontrol agents for managing FAW *Spodoptera frugiperda* in Malaysia and beyond. The key contributions are field-level efficacy, environmental constraints, local adaptation, and EPN formulations. The need for extensive field-based studies on EPN pathogenicity against FAW is identified. Environmental factors like UV radiation, soil composition, and moisture levels can significantly affect EPN efficacy. Developing formulations or application strategies to overcome these challenges is crucial. Moreover, research on identifying and testing local EPNs is essential as local EPN isolates in Malaysia suggest that locally adapted species may perform better in Malaysia's environment.

Using EPNs as biological control agents in Malaysia will significantly affect the country's agricultural landscape and policy frameworks. Potential impacts and considerations include reducing chemical dependency, increasing food sustainability, and improving yield protection. Although biopesticides' initial costs may be higher than traditional pesticides, long-term savings through reduced pest resistance and ecosystem restoration can make EPNs economically viable. Nevertheless, promoting EPN-based products could spur local industries into biopesticide manufacturing, reducing reliance on imports and creating jobs. Besides, research into native species can optimize efficacy and reduce dependency on imported strains. Expanding field-level research will demonstrate EPN's effectiveness to farmers, increasing adoption rates. Policies promoting the adoption of EPNs, such as subsidies for biopesticides or incentives for sustainable practices, could accelerate their integration into pest management strategies. Training and awareness

programs that educate farmers about EPNs, including their benefits and application methods, are critical to overcoming resistance to adopting new practices. Adopting EPNs in Malaysia could revolutionize pest management practices, enhance sustainability, and reduce reliance on chemical solutions. These benefits align with national priorities, including environmental conservation, agricultural productivity, and food security, while fostering innovation and policy evolution in the agricultural sector.

Therefore, future research should prioritize formulating EPNs, IPM approaches, combining biocontrol measures with sustainable agricultural practices to enhance efficiency and minimize environmental impact. Government agencies and local and international organizations also play a role in providing knowledge and advisory services. Policies such as providing biopesticide subsidies to farmers should be established to encourage the use of biopesticides.

ACKNOWLEDGEMENTS

We thank the Ministry of Higher Education Malaysia and Universiti Kebangsaan Malaysia (UKM) for sponsoring the FRGS/1/2019/STG03/UKM/02/8 research grant.

REFERENCES

Aarthi-Helen, P., Tamboli, N., Kulkarni, S., More, S., & Kumbhar, J. (2021). Biology of fall armyworm *Spodoptera frugiperda* (J.E. Smith) on maize under laboratory conditions. *Journal of Entomology and Zoology Studies*, *9*(3), 125-127.

Acharya, R., Hwang, H. S., Mostafiz, M. M., Yu, Y. S., & Lee, K. Y. (2020). Susceptibility of various developmental stages of the fall armyworm, *Spodoptera frugiperda* to entomopathogenic nematodes. *Insects*, *11*, 868. https://doi.org/10.3390/insects11120868

Agravante, A. S., Alviar, K. B., Ramirez, A. H. M., & Yap, S. A. (2023). Biology of *Spodoptera frugiperda* (J.E. Smith) (Lepidoptera: Noctuidae) on rice and different corn varieties. *Philipp Agric Scientist*, *106*(1), 1-6. https://doi.org/10.62550/JZ118021

Alonso, A. A. A., & Mejia, M. R. N. (2018). *Efecto de tres concentraciones de Heterorhabditis bacteriophora Poinar en la mortalidad de prepupas y pupas de Spodoptera frugiperda en laboratorio e invernadero* [Effect of three concentrations of *Heterorhabditis bacteriophora* Poinar on the mortality of pre-pupae and pupae of *Spodoptera frugiperda* in the laboratory and greenhouse]. [Professional Degree's thesis, Universidad Nacional De Trujillo]. Semantic Scholar. https://www.semanticscholar.org/author/A.-Alonso/37712761?q=Spodoptera frugiperda&sort=influence

Andaló, V., Santos, V., Moreira, G. F., Moreira, C. C., & Junior, A. M. (2010). Evaluation of entomopathogenic nematodes under laboratory and greenhouse conditions for the control of *Spodoptera frugiperda*. *Ciencia Rural*, *40*(9), 1860-1866. https://doi.org/10.1590/s0103-84782010005000151

Andaló, V., Santos, V., Moreira, G. F., Moreira, C. C., Freire, M., & Moino, A. (2012). Movement of *Heterorhabditis amazonensis* and *Steinernema arenarium* in search of corn fall armyworm larvae in artificial conditions. *Scientia Agricola*, *69*(3), 226-230. https://doi.org/10.1590/S0103-90162012000300008

Askary, T. H. & Ahmad, M. J. (2017). Entomopathogenic nematodes: Mass production, formulation and application. In M. M. M. Abd-Elgawad, T. H. Askary & J. Coupland (Eds.), *Biocontrol agents: Entomopathogenic and slug parasitic nematodes* (pp. 261-286). CABI Publishing.

Assefa, F., & Ayalew, D. (2019). Status of fall armyworm (*Spodoptera frugiperda*), biology and control measures on maize crop in Ethiopia: A review. *International Journal of Entomological Research*, *5*, 1641902. https://doi.org/https://doi.org/10.1080/23311932.2019.1641902

Bankar, D. R., & Bhamare, V. K. (2023a). Biology and life-fecundity table of invasive fall armyworm, *Spodoptera frugiperda* (J.E. Smith) on maize and sorghum. *Indian Journal of Ecology*, *50*(6), 2055-2060. https://doi.org/10.55362/IJE/2023/4174

Bankar, D. R., & Bhamare, V. K. (2023b). Comparative biology, life tables, and intrinsic rate of increase of *Spodoptera frugiperda* (J. E. Smith) reared on pearl millet and sugarcane. *Journal of Entomological Research*, *47*, 866-870.

Bird, L., Miles, M., Quade, A., & Spafford, H. (2022). Insecticide resistance in Australian *Spodoptera frugiperda* (J.E. Smith) and development of testing procedures for resistance surveillance. *Plos One*, *17*(2), e0263677. https://doi.org/10.1371/journal.pone.0263677

Bissiwu, P., & Pérez, M. J. (2016). Control efficacy of *Spodoptera frugiperda* using the entomopathogens *Heterorhabditis bacteriophora* and *Metarhizium anisopliae* with insecticide mixtures in corn. [Degree's thesis, EARTH University]. Repositorio EARTH. https://repositorio.earth.ac.cr/handle/UEARTH/588

Caccia, M. G., Del Valle, E., Doucet, M. E., & Lax, P. (2014). Susceptibility of *Spodoptera frugiperda* and *Helicoverpa gelotopoeon* (Lepidoptera: Noctuidae) to the entomopathogenic nematode *Steinernema diaprepesi* (Rhabditida: Steinernematidae) under laboratory conditions. *Chilean Journal of Agricultural Research*, *74*(1), 123-126. doi:10.4067/S0718-58392014000100019

Caoili, B. L., Latina, R. A., Sandoval, R. F. C., & Orajay, J. I. (2018). Molecular identification of entomopathogenic nematode isolates from the Philippines and their biological control potential against Lepidopteran pests of corn. *Journal of Nematology*, *50*(2), 99-110. https://doi.org/10.21307/jofnem-2018-024

Chen, W. H., Itza, B., Kafle, L., & Chang, T. Y. (2023). Life table study of fall armyworm (*Spodoptera frugiperda*) (Lepidoptera: Noctuidae) on three host plants under laboratory conditions. *Insects*, *14*, 329. https://doi.org/https://doi.org/10.3390/ insects14040329

Chen, Y., Long, H., Jin, T., Peng, Z., Sun, Y., & Feng, T. (2023). Potential of entomopathogenic nematode HbSD as a candidate biocontrol agent against *Spodoptera frugiperda*. *Insects*, *14*, 2. https://doi.org/https://doi.org/ 10.3390/insects14010002

Cruz, I., Figueiredo, M. L., Valicente, F. H., & Oliveira, A. C. (1997) Application rate trials with a nuclear polyhedrosis virus to control *Spodoptera frugiperda* (Smith) on maize. *Anais da Sociedade Entomolo´gica do Brasil*, *26*, 145-152. https://doi.org/10.1590/S0301-80591997000100019

Cruz-Martínez, H., Ruiz-Vega, J., Matadamas-Ortíz, P. T., Cortés-Martínez, C. I., & Rosas-Diaz, J. (2017). Formulation of entomopathogenic nematodes for crop pest control: A review. *Plant Protection Science*, *53*(1), 15-24. https://doi.org/10.17221/35/2016-PPS

Cuthbertson, A. G. S., & Audsley, N. (2016). Further screening of entomopathogenic fungi and nematodes as control agents for *Drosophila suzukii*. *Insects*, *7*, 24. https://doi.org/10.3390/insects7020024

Day, R., Abrahams, P., Bateman, M., Beale, T., Clottey, V., Cock, M., & Witt, A. (2017). Fall armyworm: Impacts and implications for Africa. *Outlooks on Pest Management*, *28*(5), 196-201. https://doi.org/10.1564/v28_oct_02

Department of Agriculture. (2021). *Pelan tindakan kawalan ulat ratus fall armyworm (FAW)* [Action plan for controlling fall armyworm (FAW)]. DOA Malaysia. https://www.doa.gov.my/doa/resources/aktiviti_sumber/sumber_awam/penerbitan/buku/pelan_tindakan_kawalan_ulat_ratus_faw.pdf

Dumas, P., Legeai, F., Lemaitre, C., Scaon, E., Orsucci, M., Labadie, K., & D'Alençon, E. (2015). *Spodoptera frugiperda* (Lepidoptera: Noctuidae) host-plant variants: Two host strains or two distinct species? *Genetica*, *143*, 305-316. https://doi.org/10.1007/s10709-015-9829-2

Duza, G. M., Latina, R. A., Yap, S. A., Dalisay, T. U., Pinili, M. S., & Caoili, B. L. (2024). Virulence of Philippine entomopathogenic nematode isolates against strains of fall armyworm, *Spodoptera frugiperda* (J.E. Smith) (Lepidoptera: Noctuidae). *Journal of Plant Diseases and Protection*, *131*, 459-464. https://doi.org/10.1007/s41348-024-00877-2

European and Mediterranean Plant Protection Organization. (2024). *Spodoptera frugiperda*: *EPPO datasheets on pests recommended for regulation*. https://gd.eppo.int/taxon/LAPHFR

Evans, D. C. & Stansly, P. A. (1990). Weekly economic injury levels for fall armyworm (Lepidoptera: Noctuidae) infestation of corn in lowland Ecuador. *Journal of Economic Entomology*, *83*(6), 2452-2454. https://doi.org/10.1093/jee/83.6.2452

Fallet, P., Bazagwira, D., Guanet, J. M., Bustos-segura, C., Karangwa, P., Mukundwa, I. P., Kajuga, J., Degen, T., Toepfer, S., & Turlings, T. C. J. (2022). Laboratory and field trials reveal the potential of a gel formulation of entomopathogenic nematodes for the biological control of fall armyworm caterpillars (*Spodoptera frugiperda*). *Biological Control*, *176*, 105086. https://doi.org/https://doi.org/10.1016/j.biocontrol.2022.105086

Fallet, P., Bazagwira, D., Ruzzante, L., Ingabire, G., Levivier, S., Bustos-Segura, C., Kajuga, J., Toepfer, S., & Turlings, T. C. J. (2024). Entomopathogenic nematodes as an effective and sustainable alternative to control the fall armyworm in Africa. *PNAS Nexus*, *3*, 122. https://doi.org/10.1093/pnasnexus/pgae122

Food and Agriculture Organization of the United Nations. (2017). *FAO advisory note on fall armyworm (FAW) in Africa*. https://openknowledge.fao.org/handle/20.500.14283/i7470en

Food and Agriculture Organization of the United Nations & Plant Protection Division. (2020). *Manual on integrated fall armyworm management*. https://doi.org/10.4060/ca9688en

Forst, S., & Nealson, K. (1996). Molecular biology of the symbiotic-pathogenic bacteria *Xenorhabdus spp.* and *Photorhabdus spp. Microbiological Reviews*, *60*(1), 21-43. https://doi.org/10.1128/mr.60.1.21-43.1996

Ganiger, P. C., Yeshwanth, H. M., Muralimohan, K., Vinay, N., Kumar, A. R. V., & Chandrashekara, K. (2018). Occurrence of the new invasive pest, fall armyworm, *Spodoptera frugiperda* (J. E. Smith) (Lepidoptera: Noctuidae), in the maize fields of Karnataka, India. *Current Science*, *115*(4), 621-623. https://doi.org/10.18520/cs/v115/i4/621-623

Garcia, L. C., Raetano, C. G., & Leite, L. G. (2008). Application technology for the entomopathogenic nematodes *Heterorhabditis indica* and *Steinernema sp.* (Rhabditida: Heterorhabditidae and Steinernematidae) to control *Spodoptera frugiperda* (Smith) (Lepidoptera: Noctuidae) in corn. *Neotropical Entomology*, *37*(3), 305-311. https://doi.org/10.1590/S1519-566X2008000300010

Gaugler, R. (Ed.) (2002). *Entomopathogenic nematology*. CABI Publishing. https://www.cabidigitallibrary.org/doi/book/10.1079/9780851995670.0000

Ge, S. S., He, L., He, W., Yan, R., Wyckhuys, K. A. G., & Wu, K.M. (2021). Laboratory-based flight performance of the fall armyworm, *Spodoptera frugiperda*. *Journal of Integrative Agriculture*, *20*(3), 707-714. https://doi.org/10.1016/S2095-3119(20)63166-5

Goergen, G., Kumar, P. L., Sankung, S. B., Togola, A., & Tamò, M. (2016). First report of outbreaks of the fall armyworm *Spodoptera frugiperda* (J. E. Smith) (Lepidoptera: Noctuidae), a new alien invasive pest in West and Central Africa. *PLoS ONE*, *11*(10), e0165632. https://doi.org/10.1371/journal.pone.0165632

Gozel, U., & Gozel, C. (2016). Entomopathogenic nematodes in pest Management. In H. Gill & Goyal (Eds.), *Integrated pest management (IPM): Environmentally sound pest management* (pp. 55-69). IntechOpen. http://doi.org/10.5772/63894

Guo, J., Wu, S., Zhang, F., Huang, C., He, K., Babendreier, D., & Wang, Z. (2020). Prospects for microbial control of the fall armyworm *Spodoptera frugiperda*: A review. *BioControl*, *65*, 647-662. https://doi.org/10.1007/s10526-020-10031-0

Hade, W. S., Djamilah, & Priyatiningsih. (2020). Entomopatogen nematode exploration and virulency against *Spodoptera frugiperda* J.E Smith. *Agritropica: Journal of Agricultural Science*, *3*(2), 70-81. https://doi.org/10.31186/Jagritropica.3.2.70-81

Hong, S., Titayavan, M., Intanon, S., & Thepkusol, P. (2022). Biology and life-table parameters of fall armyworm, *Spodoptera frugiperda* on three maize cultivars grown in Thailand. *Chiang Mai University Journal of Natural Sciences*, *21*(1), e2022001.

Hruska, A. J., & Gould, F. (1997). Fall armyworm (Lepidoptera: Noctuidae) and *Diatraea lineolata* (Lepidoptera: Pyralidae): Impact of larval population level and temporal occurrence on maize yield in Nicaragua. *Journal of Economic Entomology*, *90*(2), 611-622. https://doi.org/10.1093/jee/90.2.611

Hruska, A. J. (2019). Fall armyworm (*Spodoptera frugiperda*) management by smallholders. *CAB Reviews*, *14*(043), 1-11. https://doi.org/10.1079/PAVSNNR201914043

Hunt, D. J., & Nguyen, K. B. (2016). *Advances in entomopathogenic nematode taxonomy and phylogeny*. Brill Leiden-Boston. https://doi.org/10.1163/9789004285347

Huot, L., George, S., Girard, P. A., Severac, D., Nègre, N., & Duvic, B. (2019). *Spodoptera frugiperda* transcriptional response to infestation by *Steinernema carpocapsae*. *Scientific Reports*, *9*, 12879. https://doi.org/10.1038/s41598-019-49410-8

Hussain, A. G., Wennmann, J. T., Goergen, G., Bryon, A., & Ros, V. I. D. (2021). Viruses of the fall armyworm *Spodoptera frugiperda*: A review with prospects for biological control. *Viruses*, *13*, 2220. https://doi.org/10.3390/v13112220

International Plant Protection Convention. (2019). *Report on new pest: Fall armyworm in Malaysia*. www.ippc.int/static/media/files/pestreport/2019/12/06/2.1_VI_Report_FAW_.pd

Jamil, S. Z., Saranum, M. M., Saleh-Hudin, L. J., & Wan-Ali, W. K. A. (2021). First incidence of the invasive fall armyworm, *Spodoptera frugiperda* (J.E. Smith, 1797) attacking maize in Malaysia. *BioInvasions Records*, *10*(1), 81-90. https://doi.org/10.3391/bir.2021. 10.1.10

Jamil, S. Z., Saranum, M. M., Mat, M., Saleh-Huddin, L. J., Muhammad-Rapidi, M. Z., Mohd-Nor, M. F., & Keshavla, J. P. (2021). Field status, damage symptoms, and potential natural enemies of the invasive fall armyworm, *Spodoptera frugiperda* (J.E Smith) in Malaysia. *Serangga*, *26*(2), 226-244.

Jaramillo-Barrios, C. I., Varón-Devia, E. H., & Monje-Andrade, B. (2020). Economic injury level and action thresholds for *Spodoptera frugiperda* (J.E. Smith) (Lepidoptera: Noctuidae) in maize crops. *Revista Facultad Nacional de Agronomia Medellin*, *73*(1), 9065-9076. https://doi.org/10.15446/rfnam.v73n1.78824

Johnson, S. J. (1987). Migration and the life history strategy of the fall armyworm, *Spodoptera frugiperda* in the western hemisphere. *International Journal of Tropical Insect Science*, *8*(4-5–6), 543-549. https://doi.org/10.1017/s1742758400022591

Kaya, H. K., Aguillera, M. M., Alumai, A., Choo, H. Y., de la Torre, M., Fodor, A., & Ehlers, R. U. (2006). Status of entomopathogenic nematodes and their symbiotic bacteria from selected countries or regions of the world. *Biological Control*, *38*, 134-155.

Ke, L. D., & Pashley, D. P. (1992). Characterization of fall armyworm mitochondrial DNA (Lepidoptera: Noctuidae). *Archives of Insect Biochemistry and Physiology*, *21*, 263-269. https://doi.org/10.1002/arch.940210403

Lamsal, S., Sibi, S., & Yadav, S. (2020). Fall armyworm in South Asia: Threat and management. *Asian Journal of Advances in Agricultural Research*, *13*(3), 21-34. https://doi.org/10.9734/AJAAR/2020/v13i330106

Liu, H. M., Hu, X., Wang, Y. L., Yang, P. Y., Shu, C. L., Zhu, X. M., Zhang, J., Sun, G. Z., Zhang, X. M., & Li, Q. (2019). Screening for *Bacillus thuringiensis* strains with high toxicity against *Spodoptera frugiperda*. *Chinese Journal of Biological Control*, *35*, 721-728.

Luginbill, P. (1928). The fall armyworm. *USDA Technical Bulletin*, (34), 1-92.

Maharani, Y., Puspitaningrum, D., Istifadah, N., Hidayat, S., & Ismail, A. (2021). Biology and life table of fall armyworm, *Spodoptera frugiperda* (J.E. Smith) (Lepidoptera: Noctuidae) on maize and rice. *Serangga*, *26*(4), 161-174.

McMullen, J. G., & Stock, S. P. (2014). *In vivo* and *in vitro* rearing of entomopathogenic nematodes (Steinernematidae and Heterorhabditidae). *Journal of Visualized Experiments*, *91*, e52096. https://doi.org/10.3791/52096

Meka, M., Anita, B., Vetrivelkalai, P., & Muthukrishnan, N. (2020). Infectivity of entomopathogenic nematode, *Steinernema glaseri* on fall armyworm (FAW), *Spodoptera frugiperda* (Smith, 1797) in Maize (*Zea mays*). *Journal of Entomology and Zoology Studies*, *8*(6), 1023-1028. https://doi.org/10.22271/j.ento.2020.v8.i6n.7971

Mohamed, H. O., Dahi, H. F., Awad, A. A., Gamil, W. E., & Fahmy, B. F. (2023). Damage symptoms, development, and reproductive performance of the fall armyworm, *Spodoptera frugiperda* (J.E. Smith) (Lepidoptera: Noctuidae) on fodder maize and cob. *Academia Biology*, *1*(1), 1-9. https://doi.org/10.20935/AcadBiol6073.

Mohamed, H. O., & Shairra, S. A. (2023). Pathogenicity of entomopathogenic nematodes against the new invasive fall armyworm, *Spodoptera frugiperda* (J. E. Smith) (Lepidoptera: Noctuidae). *Egyptian Journal of Biological Pest Control*, *33*, 24. https://doi.org/https://doi.org/10.1186/s41938-023-00669-0

Montezano, D. G., Specht, A., Sosa-Gómez, D. R., Roque-Specht, V. F., Sousa-Silva, J. C., de Paula-Moraes, S. V., Peterson J. A., & Hunt, T. (2018). Host plants of *Spodoptera frugiperda* (Lepidoptera: Noctuidae) in the Americas. *African Entomology*, *26*(2), 286-300. https://doi.org/10.4001/003.026.0286

Nagoshi, R. N., Gabriela Murúa, M., Hay-Roe, M., Laura Juárez, M., Willink, E., & Meagher, R. L. (2012). Genetic characterization of fall armyworm (Lepidoptera: Noctuidae) host strains in Argentina. *Journal of Economic Entomology*, *105*(2), 418-428. https://doi.org/10.1603/EC11332

Negrisoli, A. S., Garcia, M. S., Barbosa-Negrisoli, C. R. C., Bernardi, D., & Silva, A. D. (2010). Efficacy of entomopathogenic nematodes (Nematoda: Rhabditida) and insecticide mixtures to control *Spodoptera frugiperda* (Smith, 1797) (Lepidoptera: Noctuidae) in corn crops. *Crop Protection*, *29*(7), 677-683. https://doi.org/10.1016/j.cropro.2010.02.002

Otim, M. H., Fiaboe, K. K. M., Akello, J., Barnabas, M., Obonyom, A. T., Bruce, A. Y., Opio, W. A., Chinwada, P., Hailu, G., & Paparu, P. (2021). Managing a transboundary pest: The fall armyworm on maize in Africa. In V. D. C. Shields (Ed.), *Moth and caterpillars* (pp. 1-26). IntechOpen. https://doi.org/10.5772/intechopen.96637

Owuama, C. I. (2001). Entomopathogenic symbiotic bacteria, *Xenorhabdu*s and *Photorhabdus* of nematodes. *World Journal of Microbiology & Biotechnology*, *17*, 505-515. https://doi.org/10.1023/A:1011916021378

Pinto, J. R. L., Torres, A. F., Truzi, C. C., Vieira, N. F., Vacari, A. M., & De Bortoli, S. A. (2019). Artificial corn-based diet for rearing *Spodoptera frugiperda* (Lepidoptera: Noctuidae). *Journal of Insect Science*, *19*(4), 1-8. https://doi.org/10.1093/jisesa/iez052

Pitre, H. N. (1985). Insect problems on sorghum in the USA. In *Proceedings of the International Sorghum Entomology Workshop, 15-21 July 1984.* ICRISAT. https://oar.icrisat.org/478/1/RA_00088.pdf

Poinar, G. O. (1976). Description and biology of a new insect parasitic Rhabditoid, *Heterorhabditis bacteriophora* n. gen., n. sp. (Rhabditida; Heterorhabditidae n. fam.). *Nematologica*, *21*, 463-470. https://doi.org/10.1163/187529275X00239

Poinar, G. O. & Grewal, P. S. (2012). History of entomopathogenic nematology. *Journal of Nematology*, *44*(2), 153-161.

Půža, V., & Mráček, Z. (2010). Does scavenging extend the host range of entomopathogenic nematodes (Nematoda: Steinernematidae)? *Journal of Invertebrate Pathology*, *104*(1), 1–3. https://doi.org/10.1016/j.jip.2010.01.002

Ramanujam, B., Poornesha, B., & Shylesha, A. N. (2020). Effect of entomopathogenic fungi against invasive pest *Spodoptera frugiperda* (J. E. Smith) (Lepidoptera: Noctuidae) in maize. *Egyptian Journal of Biological Pest Control*, *30*, 100. https://doi.org/10.1186/s41938-020-00291-4

Ratnakala, B., Kalleshwaraswamy, C. M., Rajkumar, M., Deshmukh, S. S., Mallikarjuna, H. B., & Narasimhaiah, L. (2023). Field evaluation of whorl application of sand mixed entomopathogenic nematodes for the management of invasive fall armyworm, *Spodoptera frugiperda* (J. E. Smith) (Lepidoptera: Noctuidae) in sweet corn. *Egyptian Journal of Biological Pest Control*, *33*, 58. https://doi.org/10.1186/s41938-023-00706-y

Rodríguez-Zamora, M. J. (2019). *Caracterización de aislados nativos de nematodos entomopatógenos y uso potencial contra Spodoptera frugiperda* [Characterization of native isolates of entomopathogenic nematodes and their potential use against *Spodoptera frugiperda*]. [Master's thesis, Universidad Nacional Agraria]. Repositorio Institucional. https://repositorio.una.edu.ni/id/eprint/3830

Rose, A. H., Silversides, R. H., & Lindquist, O. H. (1975). Migration flight by an aphid, *Rhopalosiphum maidis* (Hemiptera: Aphididae), and a noctuid, *Spodoptera frugiperda* (Lepidoptera: Noctuidae). *The Canadian Entomologist*, *107*, 567-576.

Rwomushana, I. (2019). Invasive species compendium datasheet report for *Spodoptera frugiperda* (fall armyworm). CABI Digital Library. https://doi.org/10.1079/cabicompendium.29810

Salazar-Gutiérrez, J. D., Castelblanco, A., Rodríguez-Bocanegra, M. X., Teran, W., & Sáenz-Aponte, A. (2017). *Photorhabdus luminescens subsp. akhurstii* SL0708 pathogenicity in *Spodoptera frugiperda* (Lepidoptera: Noctuidae) and *Galleria mellonella* (Lepidoptera: Pyralidae). *Journal of Asia-Pacific Entomology*, *20*, 1112-1121.

Salvadori, J. D. M., Defferrari, M. S., Ligabue-Braun, R., Yamazaki Lau, E., Salvadori, J. R., & Carlini, C. R. (2012). Characterization of entomopathogenic nematodes and symbiotic bacteria active against *Spodoptera frugiperda* (Lepidoptera: Noctuidae) and contribution of bacterial urease to the insecticidal effect. *Biological Control*, *63*, 253-263. https://doi.org/10.1016/j.biocontrol.2012.08.002

Sarkowi, F. N., & Mokhtar, A. S. (2021). The fall armyworm (FAW) *Spodoptera frugiperda*: A review on biology, life history, invasion, dispersion and control. *Outlooks on Pest Management*, *32*(1), 27-32. https://doi.org/10.1564/v32_feb_07

Shamseldean, M. S. M., Abo-Shady, N. M., El-Awady, M. A. M., & Heikal, M. N. (2024). *Heterorhabditis alii n. sp*. (Nematoda: Heterorhabditidae), a novel entomopathogenic nematode from Egypt used against the fall armyworm, *Spodoptera frugiperda* (Smith 1797) (Lepidoptera: Noctuidae). *Egyptian Journal of Biological Pest Control*, *34*, 13. https://doi.org/10.1186/s41938-024-00778-4

Shapiro-Ilan, D. I., Han, R., & Dolinksi, C. (2012). Entomopathogenic nematode production and application technology. *Journal of Nematology*, *44*(2), 206-217.

Shapiro-Ilan, D. I., Morales-Ramos, J. A., & Rojas, M. G. (2016). *In vivo* production of entomopathogenic nematodes. In T. R. Glare & M. E. Moran-Diez (Eds.), *Microbial-based biopesticides: Methods and protocols, methods in molecular biology* (pp. 137-158). Springer Science + Business Media. https://doi.org/10.1007/978-1-4939-6367-6_11

Sharanabasappa, Kalleshwaraswamy, C. M., Asokan, R., Swamy, H. M. M., Maruthi, M. S., Pavithra, H. B., & Goergen, G. (2018). First report of the fall armyworm, *Spodoptera frugiperda* (J.E. Smith) (Lepidoptera: Noctuidae), an alien invasive pest on maize in India. *Pest Management in Horticultural Ecosystems*, *24*(1), 23-29.

Shinde, S. P., Biradar, V. K., Ingole, D. B., Lavhe, N. V, & Pragati, R. (2023). Potential of the entomopathogenic nematode, *Heterorhabditis indica* in managing the S*podoptera frugiperda. Scientist*, *22*(2), 48-55. https://doi.org/10.5281/zenodo.7633276

Shylesha, A. N., Jalali, S. K., Gupta, A., Varshney, R., Venkatesan, T., Shetty, P., Ojha, R., Ganiger, P. C., Navik, O., Subaharan, K., Bakthavatsalam, N., & Ballal, C. R. (2018). Studies on new invasive pest *Spodoptera frugiperda* (J. E. Smith) (Lepidoptera: Noctuidae) and its natural enemies. *Journal of Biological Control*, *32*(3), 1-7. https://doi.org/10.18311/jbc/2018/21707

Sparks, A. N. (1979). A review of the biology of the fall armyworm. *The Florida Entomologist*, *62*(2), 82-87. https://doi.org/https://doi.org/10.2307/3494083

Stock, S. P., & Blair, H. G. (2008). Entomopathogenic nematodes and their bacterial symbionts: The inside out of a mutualistic association. *SYMBIOSIS*, *46*, 65-75.

Sun, J., Fanf, M., Zuo, J., Wang, A., Tang, H., Wang, L., & Ruan, W. (2024). Identification of entomopathogenic nematodes in Hainan Province, China, and their efficacy against *Spodoptera frugiperda* (J. E. Smith) (Lepidoptera: Noctuidae). *Crop Protection*, *184*, 106838. https://doi.org/10.1016/j.cropro.2024.106838

Vashisth, S., Chandel, Y. S., & Chandel, R. S. (2015). Distribution and occurrence of entomopathogenic nematodes in Himachal Pradesh. *Journal of Entomological Research*, *39*(1), 71-76.

Vashisth, S., Chandel, Y. S., & Sharma, P. (2013). Entompathogenic nematodes: A review. *Agricultural Reviews*, *34*(3), 163-175. https://doi.org/10.5958/j.0976-0741.34.3.001

Viteri, D. M., Linares, A. M., & Flores, L. (2018). Use of the entomopathogenic nematode *Steinernema carpocapsae* in combination with low-toxicity insecticides to control fall armyworm (Lepidoptera: Noctuidae) larvae. *Florida Entomologist*, *101*(2), 327-329. https://doi.org/10.1653/024.101.0228

Pertanika J. Trop. Agric. Sci. 48 (3): 973 - 990 (2025)

PERTANIKA JOURNALS

TROPICAL AGRICULTURAL SCIENCE

Journal homepage: http://www.pertanika.upm.edu.my/

Impact of Silicon-enriched Fertilizer on Basal Stem Rot Disease in Palm Species Caused by *Ganoderma boninense*

Nurul Jamaludin Mayzaitul-Azwa[1]*, Nur Muhamad Tajudin Shuhada[2], Mohamed Musa Hanafi[3] and Nurul Huda[4]

[1]*Crop Production Program, Faculty of Sustainable Agriculture, Universiti Malaysia Sabah, Locked Bag No. 3, 90509, Sandakan, Sabah, Malaysia*
[2]*Department of Plant Science, Kulliyyah of Science, International Islamic University Malaysia (IIUM), Kuantan, 25200, Pahang, Malaysia*
[3]*Department of Land Management, Faculty of Agriculture, Universiti Putra Malaysia, 43400 UPM Serdang, Selangor, Malaysia*
[4]*Postgraduate School, Universitas Brawijaya, Malang 65145, East Java, Indonesia*

ABSTRACT

Silicon (Si) is the second most abundant element that encourages plant growth, particularly in higher plants. This research maximizes Si's stress-tolerance benefits for plants. Therefore, this study aimed to evaluate the impact of silicon-enriched fertilizer in reducing the impact of Basal Stem Rot (BSR) disease in palm species, suggesting a potential sustainable solution to this critical agricultural challenge. The study utilized the root-sitting technique on three-month-old palm seedlings grown under controlled nursery conditions. The T1 and T2 seedlings were untreated with silicon-enriched fertilizer. In contrast, the T3 seedlings were treated with 500g of silicon-enriched fertilizer. The T2 and T3 seedlings were further challenged with *G. boninense* PER 17 using the rubber woodblocks (RWBs) sitting technique during the nursery trial (10 months). Results revealed that disease incidence (DI) in oil palm (50.0%) and betel nut palm (44.4%) for T3 seedlings was significantly lower ($p \leq 0.05$) compared to T2 seedlings, both of which had a DI of 94.4%. The BSR DI in T3 seedlings was reduced by 52.63% in oil palm and 67.35% in betel nut palm. These findings suggest that treatment T3 offers protection against *G. boninense* infection in both palm species. The results demonstrated that treatment T3, involving silicon-enriched fertilizer, significantly reduced the progression of BSR disease in palm seedlings, highlighting its effectiveness as a disease management strategy.

Keywords: Basal stem rot, betel nut palm, *Ganoderma boninense*, oil palm, silicon

ARTICLE INFO

Article history:
Received: 19 November 2024
Accepted: 30 December 2024
Published: 16 May 2025

DOI: https://doi.org/10.47836/pjtas.48.3.18

E-mail addresses:
mayzaitulazwa@ums.edu.my (Nurul Jamaludin Mayzaitul-Azwa)
nurshuhada@iium.edu.my (Nur Muhamad Tajudin Shuhada)
mmhanafi@upm.edu.my (Mohamed Musa Hanafi)
drnurulhuda@ub.ac.id (Nurul Huda)
* Corresponding author

e-ISSN: 2231-8542

INTRODUCTION

Basal stem rot (BSR) is a major disease affecting various palm species, particularly oil palm (*Elaeis guineensis*), in Southeast Asia and other tropical areas. The pathogen responsible, *Ganoderma boninense*, causes significant financial damage by leading to stem deterioration, lower fruit production, and, ultimately, the death of affected trees (Abubakar et al., 2022). Traditional strategies for managing this disease, such as chemical and cultural interventions, have had limited effectiveness, highlighting the need for more sustainable and successful solutions (Khoo & Chong, 2024).

Although not classified as an essential nutrient, silicon (Si) has gained attention for its positive role in enhancing a plant's resilience to various biotic and abiotic challenges. Research has demonstrated that fertilizers containing Si can strengthen plant defenses by increasing cell wall thickness, enhancing systemic resistance, and decreasing infections caused by fungal pathogens (Etesami et al., 2020). Numerous studies have explored the effects of Si on BSR in oil palms; further research is needed to address key gaps. Si has been widely shown to reduce diseases in various crops. However, its specific mechanisms and effectiveness against BSR caused by *G. boninense* in palm species, particularly in betel nut palm, remain underexplored. This lack of knowledge is critical because the betel nut palm may respond differently to Si compared to oil palm due to species-specific physiological and biochemical differences. Additionally, understanding Si's role across multiple palm species can provide broader insights into its potential as a sustainable disease management strategy. Recent investigations have highlighted Si as a valuable component for strengthening plant defenses against a variety of diseases (Debona et al., 2017). Fertilizers enriched with silicon have demonstrated effectiveness in reducing disease severity across numerous crops by fortifying cell walls, initiating biochemical defense responses, and enhancing overall plant vigor (Sarma et al., 2024).

The precise impact of Si on combating *G. boninense* in palm species remains underexplored. This study focuses on oil palm (*Elaeis guineensis* Jacq.) and betel nut palm (*Areca catechu*) because of their economic importance and vulnerability to BSR. Although the betel nut palm is not as extensively studied regarding BSR, its susceptibility to *Ganoderma* infections makes it a relevant subject for examining disease management strategies. This research concentrates on these two palm species to investigate both a globally important crop and a less frequently studied species, aiming to provide a wider understanding of controlling *G. boninense* across various palm types. Consequently, this study focuses on evaluating the extent to which Si mitigates the severity of the BSR disease.

MATERIALS AND METHODS

Study Site, Plant Materials and Growth Conditions

The study was conducted at an outdoor nursery in Ladang 2 (3°00'86.9"N, 101°70'44.7"E) at Universiti Putra Malaysia, Serdang, Selangor. This study used two palm species: the oil palm (*Elaeis guineensis* Jacq.) and the betel nut palm (*Areca catechu*). 3-month-old oil palm seedlings were collected from Federal Land Development Authority (FELDA) Agricultural Services, Sungai Tekam, Jerantut, Pahang, while 3-month-old betel nut palm seedlings were obtained from Kuala Pilah, Negeri Sembilan. All seedlings were implanted in black polybags (38 cm high × 46 cm in diameter) filled with soil from the 'Munchong' series. Soil for the study was sourced from the Universiti Putra Experimental Farm in Puchong, Selangor, and combined with organic compost from the Federal Land Consolidation and Rehabilitation Authority (FELCRA) in Seberang Perak, Malaysia. A mixture ratio of 3 parts soil to 1 part compost was used. The research site had a 30°C to 36°C temperature range, with relative humidity between 60% and 80%. During the experiment, seedlings were irrigated twice daily and fertilized monthly. Fertilizer application and routine operations were conducted in accordance with standard, approved nursery practices (Fairhurst et al., 2019). Control seedlings received NPK Blue fertilizer (12: 12: 17: 2 + TE) (YaraMila, Malaysia), while seedlings were treated with fertilizer enriched with silicon (6: 6: 8: 2 + Si) (Sigma-Aldrich, United States of America) (Table 1).

Table 1
Characteristics of fertilizer enriched with silicon

Selected features	Unit	Value
Potential of hydrogen	-	5.23
Total Carbon	%	7.37
Total Nitrogen	%	6.25
Phosphorus oxide	%	6.56
Potassium oxide	%	8.54
Calcium oxide	%	9.77
Magnesium oxide	%	1.98
Silicone oxide	%	4.06
Available Copper	mg/kg	3.12
Available Iron	mg/kg	53.62
Available Zinc	mg/kg	5.66
Available Manganese	mg/kg	597.88

Maintenance of *Ganoderma boninense* PER 71 Isolates

The *G. boninense* PER 71 isolate was obtained from the Malaysian Palm Oil Board (MPOB), Bangi, Selangor. This strain was subcultured onto Potato Dextrose Agar (PDA) (Oxoid, USA) and maintained at room temperature of 28°C for 7 to 8 days (Surendran et al., 2021).

Preparation of Rubber Wood Blocks

Following the guidelines by Idris et al. (2006), 108 rubber wood blocks (RWBs) were made from fresh *Hevea brasiliensis* wood, each with dimensions of 6.0 cm by 6.0 cm by

6.0 cm. Each RWB was washed under running water and placed in a double-layered, heat-resistant polypropylene bag measuring 10.0 cm × 32.0 cm. The sample was autoclaved at 103.4 kPa and 121°C for 30 min. Following sterilization, 100 mL of molten malt extract agar (MEA) (Oxoid, USA) was added to each bag to provide supplementary nutrients for the growth of *G. boninense*. The bags were knotted with raffia string and autoclaved again in the mentioned circumstances. After sterilization, the bags were turned 360° to ensure the rubber wood blocks were completely coated with the MEA before they solidified. The preparation of *G. boninense* inoculum on RWBs involved placing a small piece from a 7- to 9-day-old pure culture of *G. boninense*, grown on PDA and obtained using a 10 mm in diameter core borer, onto the surface of each autoclaved RWB. This process was performed in a laminar flow hood to prevent contamination, and the bags were immediately sealed with a rubber band. The inoculated RWBs were then incubated in a dark cabinet at 27±2°C for approximately 10 to 12 weeks until fully colonized by the *G. boninense* mycelium.

Artificial Inoculation of Palm Seedlings Using Rubber Wood Blocks Infected with *G. boninense PER 71*

The inoculation procedure followed the method described by Idris et al. (2006). A nursery study was conducted using 18 blocks in a randomized complete block design (RCBD) with 3 sub-replications. Seedlings in T1 (negative control) were planted in polybags without *G. boninense* infection. In treatments T2 and T3, the seedlings were placed directly on the RWBs, ensuring their roots were in contact with the *G. boninense*-infected inoculum. After placement, the seedlings were covered with topsoil according to their respective treatments (Table 2). Seedlings were treated with silicon-enriched fertilizer and artificially infected with *G. boninense* over 10 months through the application of 10 doses, each consisting of 50 g per month. This process resulted in 500 g of silicon-enriched fertilizer per seedling, with rubber wood blocks (RWBs) serving as the inoculation medium.

Table 2
Treatments for basal stem rot in oil palm and betel nut palm seedlings

Treatment	Description
T1	Seedlings without treatment or infection (negative control).
T2	Seedlings left untreated but exposed to artificial infection with *G. boninense* (positive control).
T3	Seedlings were given silicon-enriched fertilizer and artificially infected with *G. boninense* (10 doses, 50 g per month, totaling 500 g per seedling).

Disease Incidence

The progression of disease in palm seedlings was tracked bi-monthly using a quantitative indicator known as disease incidence (DI), which reflects the number of seedlings exhibiting

visible symptoms, such as yellowing or necrosis of leaves, with or without white fungal growth or the presence of fruiting bodies. The DI was calculated using the equation formulated by Priwiratama et al. (2020):

$$\text{Disease incidence } (\%) = \left[\left(\frac{\text{Seedlings infested number}}{\text{Total number of seedlings assessed}}\right) \times 100\right]$$

A curve depicting disease progression was derived from the disease incidence measurements. A decrease in disease incidence compared to the control would suggest higher treatment efficacy in disease management. The progression of the disease was evaluated using the area under the disease progress curve (AUDPC), as described by Kamu et al. (2021).

$$\text{The area under the disease progress curve} = \sum_{i}^{n-1}\left[\left(\frac{Y_i - Y_{i+1}}{2}\right)(t_{i+1} - t_i)\right]$$

Where, n = assessment time number, Y = disease incidence and t = time.

Kamu et al. (2021) obtained the curve slopes by transforming the DI data using the monomolecular model (Monit).

Disease Severity Index

The progression of BSR disease in palm seedlings was evaluated using the disease severity index (DSI), which measures the total area or extent of disease in plant tissue (Rakib et al., 2015). The DSI was determined based on the seedlings' external and internal symptoms. The foliar disease severity index (DSFI) was assessed using a scale from 0 to 5, reflecting the severity of leaf symptoms (Table 3). *Ganoderma* selective medium (GSM) was used to confirm the presence of *G. boninense* in the palm tissue (Idris et al., 2006; Rees et al., 2009).

Table 3
Disease severity index of foliar

Disease class	Associated signs and symptoms of infection
0	A healthy plant with vibrant green leaves and no signs of fungal growth anywhere on the plant.
1	1–3 yellowing leaves, with no fungal growth observed on any part of the plant.
2	Presence of fungal growth, with or without yellowing leaves.
3	More than three yellowing leaves, along with dead or necrotic leaves, with or without fungal growth on the plant.
4	At least 50% of the leaves show severe yellowing or necrosis, with or without fungal growth.
5	The plant is dead, with or without visible fungal growth.

Note. Adapted from Rakib et al. (2015)

After the experiment (10 months after artificial infection with *G. boninense* PER 71), the palm seedlings were destructively sampled by carefully uprooting, longitudinally sectioning, and visually examining them for internal symptoms. The bole (DSIB) and roots (DSIR) disease severity index were evaluated according to a disease classification scale ranging from 0 to 4, as outlined in Table 4.

Table 4
Disease severity index of bole and disease severity index of root at oil palm and betel nut palm

Class	Associated signs and symptoms of infection
0	0% (healthy bole or root tissues)
1	Up to 25% (decay in bole or root tissues)
2	25–50% (decay in bole or root tissues)
3	51–75% (decay in bole or root tissues)
4	More than 75% (decay in bole or root tissues)
5	100% (complete decay of bole or root tissues)

Note. Adapted from Rakib et al. (2015)

The DSIF, DSIB, and DSIR were calculated using the following formulas revised from Rakib et al. (2015):

$$\text{Disease severity index of foliar / bole / root} = \left(\frac{\sum (\text{Disease class} \times \text{Number of seedlings for each disease class})}{\sum (\text{Total number of replicates} \times 5)}\right) \times 100$$

Where five is the constant indicating the highest assessment class. The number of seedlings that died due to BSR should be recorded regularly, typically throughout 6 to 12 months, depending on the growth stage of the seedlings.

Dead Seedlings

Dead seedlings were recognized by complete necrosis, defoliation, and stem collapse (Noor Azmi, 2020). A severity index can be assigned based on visual scoring of symptoms, ranging from healthy (0) to dead (5), following established disease rating scales (Rakib et al., 2015).

$$\text{Dead seedlings (\%)} = \left(\frac{\text{Number of Dead Seedlings}}{\text{Total Number of Seedlings}} \times 100\right)$$

Re-isolation of the pathogen from the decayed basal stem tissues was essential to confirm that the seedlings died due to *G. boninese*. The infected tissues were cultured on *Ganoderma* selective media (GSM) to isolate and identify *G. boninense* under a microscope based on its characteristic morphology (Idris et al., 2020).

Measurements by SEM and TEM

The measurement of silica bodies and their deposition were carried out using scanning electron microscopy (SEM) and transmission electron microscopy (TEM), following the

method described by Zhang et al. (2013). Fresh root samples were cut into 21 cm³ sections for SEM observation (S-4000, Hitachi Co. Ltd., Japan) and 21 mm³ sections for TEM (HT7800 RuliTEM, Hitachi High-Tech, Japan). Images captured under both microscopes revealed silica bodies (SB) and silica layers (SL) in the root tissues.

Statistical Analysis

Statistical analysis was performed using one-way analysis of variance (ANOVA). Any significant difference was further analyzed using the least significant difference (LSD) post-hoc analysis at $p \leq 0.05$. All statistical analysis was performed using the Statistical Analysis System (SAS) 9.2 software.

RESULTS

Disease Incidence

A notable difference in treatment interactions was observed over time, with statistical significance at $p \leq 0.05$. The disease index (DI), determined by leaf symptoms, was substantially lower in the T3 group treated with silicon-enriched fertilizer compared to the T2 seedlings (Figure 1). A reduced DI value indicated disease suppression. No DI was found for T3 seedlings at four months. This indicated that the seedlings in treatment T3 had gradually reduced the development of BSR disease symptoms. Disease symptoms in the seedlings treated with T3 began to appear six months after inoculation with *G.*

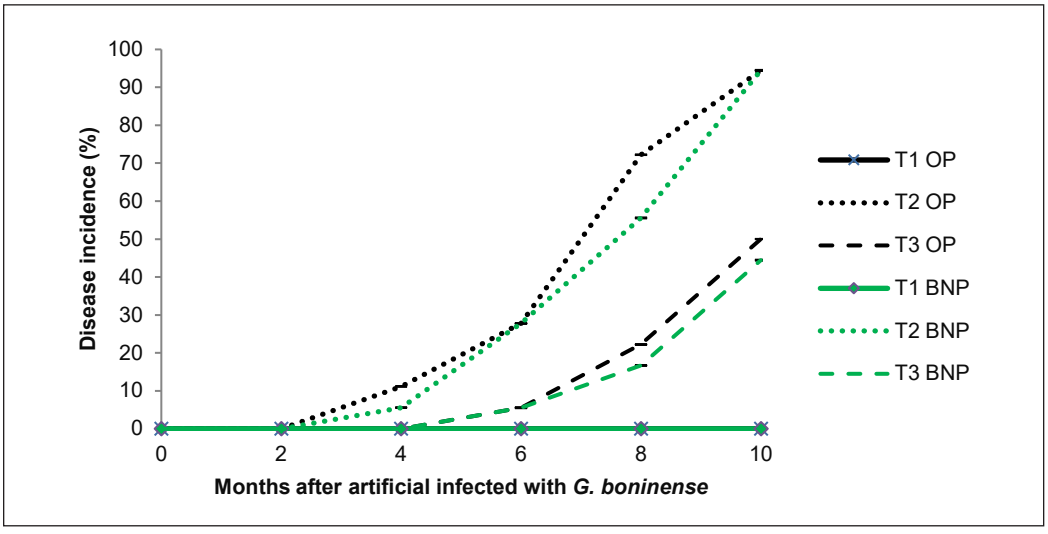

Figure 1. The incidence of basal stem rot occurrence in oil palm and betel nut palm seedlings for ten months following artificial inoculation with *G. boninense*

Note. OP = oil palm and BNP = betel nut palm. Data are presented as means ± standard error, with statistical analysis using the least significant difference test ($p \leq 0.05$)

boninense. The disease symptoms in oil palm seedlings gradually increased thereafter, with a DI of 50.00% at ten months of observation. In contrast, the disease symptoms in betel nut palms gradually increased subsequently, with a DI of 44.44% at ten months of observation. The findings indicated that the use of silicon-enriched fertilizer offered an effective degree of disease management. Symptoms of the disease appeared much earlier in T2-treated seedlings, starting four months post-infection with *G. boninense*. As anticipated, after ten months of evaluation, the untreated control group (T2) of oil palm and betel nut palm seedlings exhibited the highest disease incidence (DI) of 94.44%. However, while the foliar symptoms were evident, they did not reveal the extent of damage affecting the roots and bole region.

Area Under Disease Progress Curve and Disease Reduction

The disease incidence (DI) of oil palm and betel nut palm seedlings was analyzed using the area under the disease progress curve (AUDPC) to evaluate the severity of the disease in each treatment (Table 5). The AUDPC offers a quantitative measure of disease intensity over time, facilitating comparisons between different disease management approaches. The calculation was made using the DI derived from the classification of leaf symptoms. In treatment, T3, oil palm and betel nut palm seedlings treated with silicon-enriched fertilizer showed a marked reduction in AUDPC, with values of 150.00 unit² and 88.89 unit², respectively, ten months post-infection with *G. boninense.* Based on the AUDPC, it was clear that treatment T3 was the most effective in slowing the progression of BSR disease. As anticipated, disease reduction was significantly higher in treatment T3 for both palm seedlings, with decreases of 52.62% in oil palm and 67.35% in betel nut palm. The highest AUDPC values were observed in the T2 treatment, with oil palm seedlings showing 316.66 unit² and betel nut palm 272.22 unit², indicating greater susceptibility to the disease.

Table 5
The area under disease progress curve and disease reduction of oil palm and betel nut palm seedlings at 10 months following artificial inoculation with G. boninense *PER 71*

	Oil palm seedlings			**Betel nut palm seedlings**		
Treatment	T1	T2	T3	T1	T2	T3
Area Under Disease Progress Curve (unit²)	0.00	316.66	150.00	0.00	272.22	88.89
Disease Reduction (%)	-	-	52.63	-	-	67.35

Disease Severity Index of Foliar

Significant differences existed between the treatment interaction and month at $p \leq 0.05$. For oil palm and betel nut palm seedlings, the DSI, derived from observable leaf symptoms, was considerably lower in the T3 seedlings treated with silicon-enriched fertilizer (Figure

2). A lower disease severity index of foliar (DSIF) indicated success in suppressing the onset of BSR disease infection development in oil palm seedlings. There was a total absence of symptoms in treatment T3 at four months. However, the disease progression in oil palm and betel nut palm seedlings gradually increased with a DSIF of 37.50% and 52.78%, respectively, at ten months of observation. The percentage of DSIF recorded in treatment T3 for both seedlings was significantly lower than the T2 seedlings. Visible disease symptoms in the T2 seedlings emerged as early as four months into the study. By the tenth month, T2 seedlings of oil palm and betel nut palm recorded external DSFI values of 86.11% and 87.50%, respectively.

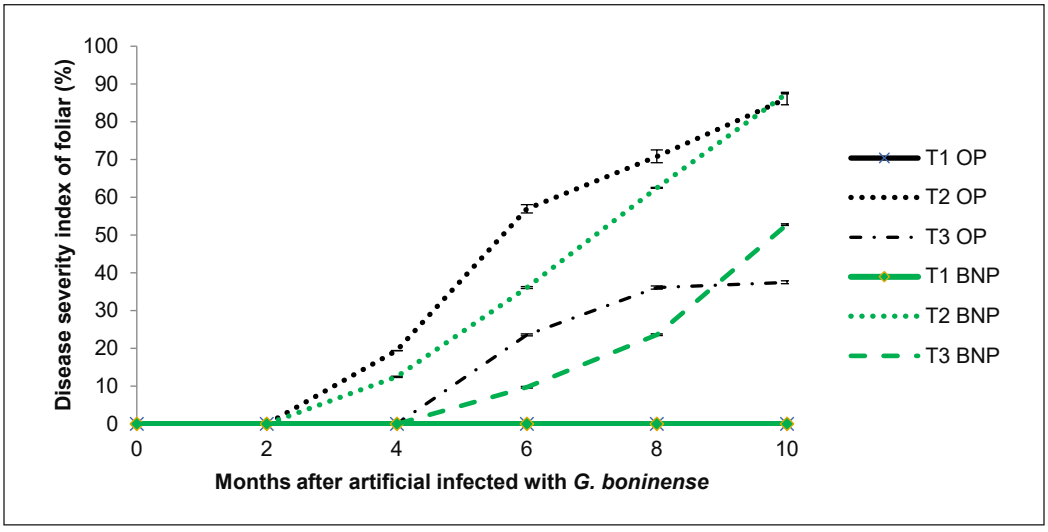

Figure 2. Foliar disease severity index of oil palm and betel nut palm seedlings ten months after artificial inoculation with *G. boninense*
Note. OP = oil palm and BNP = betel nut palm. Data are presented as means ± standard error, with statistical analysis using the least significant difference test ($p \leq 0.05$)

Bole and Root Disease Severity Index

There was a statistically significant difference ($p \leq 0.05$) between treatments T1 and T2 concerning the disease severity indices for the bole (DSIB) and roots (DSIR) (Figure 3). Treatment T2 in oil palm and betel nut palm seedlings exhibited the highest disease severity index of roots (DSIR), with 38.89% and 70.83% of the primary roots showing brown discoloration, compared to 20.83% and 30.56% in treatment T3 seedlings, respectively (Figures 4A and 4B). When evaluating bole decay and disease severity, it was found that using silicon-enriched fertilizer in T3 treatment led to the lowest disease severity index of the bole (DSIB) in oil palm seedlings, recorded at 6.94%. This was significantly lower than the 26.39% DSIB observed in the treatment T2 seedlings. The same trend was

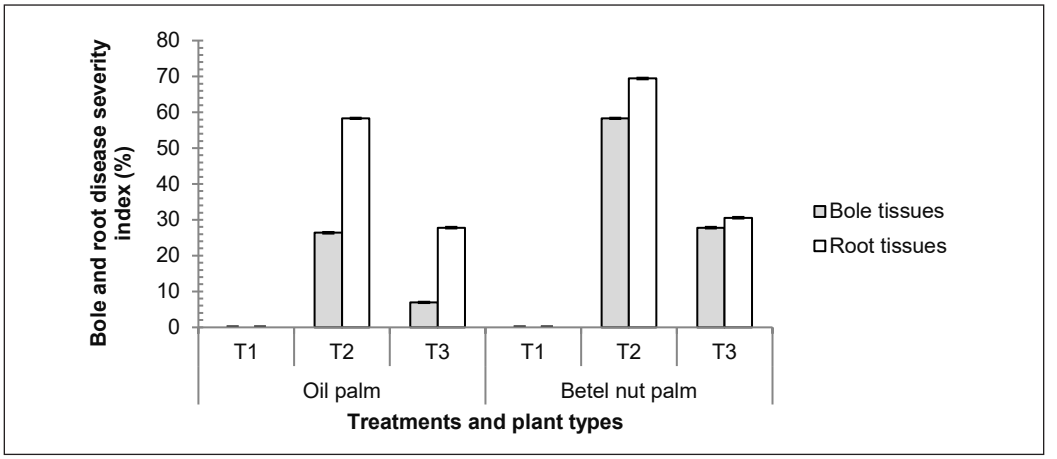

Figure 3. Bole and root disease severity index of oil palm seedlings ten months after artificial inoculation with *G. boninense*
Note. OP = oil palm and BNP = betel nut palm. Data are presented as means ± standard error, with statistical analysis using the least significant difference test ($p \leq 0.05$)

also recorded in betel nut palm seedlings for treatment T3 (27.78%) compared to treatment T2 (66.67%). Brown lesions, characterized by an irregular, darker zone, were observed in longitudinal sections of the infected boles (Figures 4C and 4D). The results suggest that treatment T3 effectively hindered the penetration and dissemination of *G. boninense* within the vascular tissues of the seedlings.

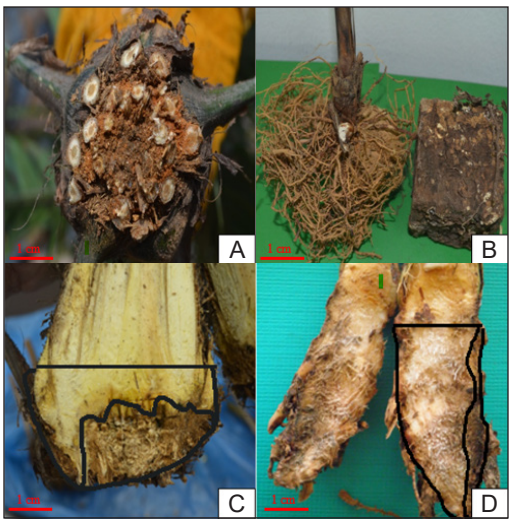

Figure 4. Decay of primary roots and bole resulting from *G. boninense* infection. (A) Primary roots of oil palm, (B) primary roots of betel nut palm, (C) bole of oil palm, and (D) bole of betel nut palm. The black lines in Figures 4C and 4D depict the area decay of primary roots and the bole

Dead Seedlings

For both oil palm and betel nut palm seedlings, there was a notable difference ($p \leq 0.05$) in the count of dead seedlings (DS) between treatments T1 and T2 (Figure 5). Silicon-enriched fertilizer was deemed effective in controlling BSR infection, as it significantly reduced the number of DS in both oil palm and betel nut palm seedlings. Ten months after being artificially infected with *G. boninense*, the DS in the T3 seedlings of oil palm and betel nut palms in treatment were 11.11 and 5.56%, respectively. In contrast, treatment T2 for oil palm seedlings showed a DS

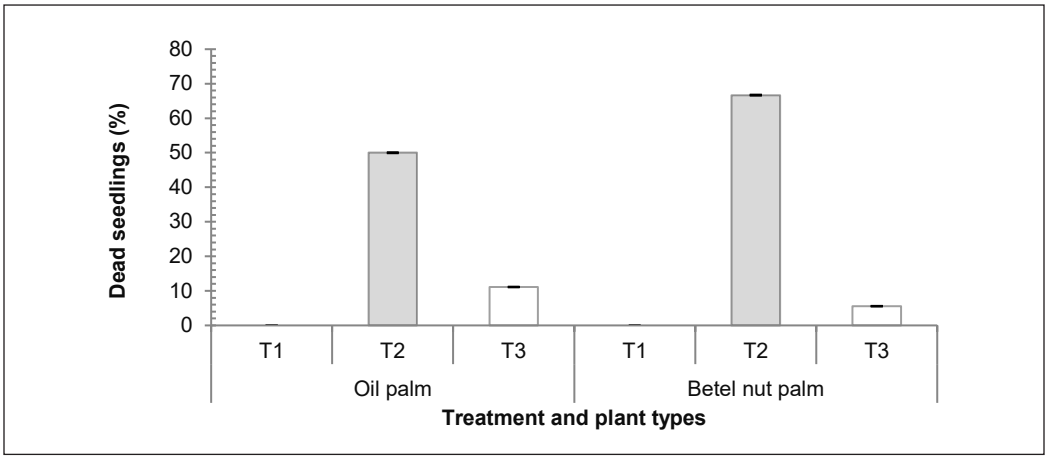

Figure 5. Mortality of oil palm and betel nut palm seedlings due to *G. boninense* infection, measured ten months after inoculation

Note. The different colours represent different treatments. OP = oil palm and BNP = betel nut palm. Data are presented as means ± standard error, with statistical analysis using the least significant difference test ($p \leq 0.05$)

of 50.00% at ten months after artificial infection with *G. boninense*. However, treatment T2 seedlings showed a DS of 66.67% at ten months after artificial infection with *G. boninense.*

Measurement by SEM and TEM

The Scanning Electron Microscope (SEM) images from this analysis showed that silicon accumulated as silica bodies in the plants' roots (Figure 6). A dense silicon layer was also observed in the plant roots' endodermal cell wall diagram (Figure 7).

DISCUSSION

This research evaluated the effectiveness of silicon-enriched fertilizer on palm seedlings exposed to *G. boninense* PER 71, the pathogen responsible for BSR. Lower disease incidence (DI), area under the disease progress curve (AUDPC), disease severity indices for foliar (DSIF), root (DSIR), and bole (DSIB), as well as fewer dead seedlings (DS) and higher disease reduction (DR) in T3-treated seedlings compared to the T2 positive control, highlight that fertilization with nutrient enhancement is a key cultural management strategy for controlling *Ganoderma* infections in palm seedlings. Consistent with the findings of this research, Rebitanim et al. (2020) also reported a 77.78% decrease in BSR disease incidence in seedlings treated with GanoCare®, a fertilizer containing beneficial elements, with a notable reduction in dead seedlings to 6.67%, in contrast to 93.33% in untreated samples. Therefore, it is necessary to maintain nutrient availability in palm seedlings with fertilizers. This study demonstrated that nutrient supplementation with silicon-enriched

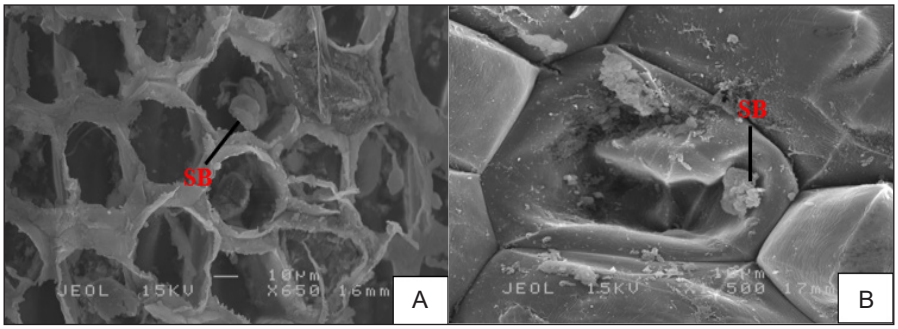

Figure 6. Silica bodies deposition in palm roots. Betel nut palm (A) and oil palm (B). Silica bodies are detected by scanning electron microscopy energy. Magnification = 10 µm × 600 (A) and 10 µm × 1,500 (B).
Note. SB = Silica bodies

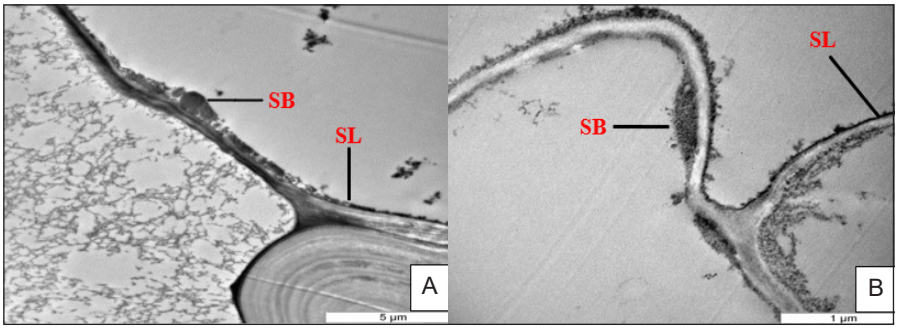

Figure 7. Si deposition in endodermis of palm roots cell wall. Betel nut palm (A) and oil palm (B). The blackened area represents the location of Si deposition. Silica is detected by transmission electron microscopy. Magnification A= 5 µm and B = 1 µm
Note. SB = Silica bodies; SL = silica layer

fertilizer enhanced the resistance of oil palm seedlings to the physical damage caused by *G. boninense*, as well as in betel nut palm seedlings. It is well-documented that silicon-enriched fertilizers contain advantageous elements that effectively lower infection rates. Recent research continues to support the use of silicon-based fertilizers in boosting plant health and disease resistance (Ma, 2021; Ning et al., 2014). Silicon is vital in strengthening plant structure, reinforcing cell walls, and triggering various defense mechanisms against biotic stress factors. This has been particularly noted in crops such as rice, wheat, and oil palm, where silicon application has been associated with better resistance against fungal infections and other pathogens.

This study's findings revealed a significant link between silicon-enriched fertilizer use and silicification initiation in the roots of palm seedlings treated with this fertilizer. Elevated silicon concentrations in the root tissues improved resistance to *G. boninense*. Two primary theories explain silicon's role in plant resistance: It creates a physical barrier to hinder fungal entry and enhances physiological defenses through biochemical

processes (Brunings et al., 2021; Ranjan et al., 2021). An amplified number of silicified bulliform cells in the root epidermis cell walls is suggested to be a physical barrier, preventing *G. boninense* penetration. This barrier is related to lignin-carbohydrate complexes bound to silicon in the epidermal cell wall (Carré-Missio et al., 2021; Lux et al., 2020). Liang et al. (2015) further supported this physical barrier concept by showing that silicon-organic molecule complexes in the epidermal cell walls enhance plant resistance to fungal degradation enzymes. A higher disease reduction (DR) percentage in palms supplemented with silicon-enriched fertilizer suggests that sufficient silicon content slows disease progression by strengthening the cell wall, making it more resistant when *G. boninense* attempts to invade. The creation of a-Si cuticle double layer is a physical barrier to restrict pathogen penetration, as revealed in various research, including novel findings on Si deposition in epidermal cells (Kim et al., 2002; Ma & Yamaji, 2006). These observations are consistent with SEM and TEM analysis, which identified a silicon layer on the outer cell wall of root epidermal cells in palm seedlings that received silicon-enriched fertilizer treatment. The Si-cuticle layer may act as a physical barrier that reduces NH_4-N volatilization from leaf surfaces, thereby suppressing potential nutrient sources for pathogens (Bhardwaj et al., 2023).

The second theory posits that disease suppression is related to the stimulation and buildup of defense mechanisms, such as phenolics and phytoalexins, which are closely tied to the activity of P-R genes (Boudet, 2000; Del Río et al., 2001). This hypothesis is supported by Rodrigues et al. (2003), who found that silicon application in rice led to the buildup of osmophilic materials in epidermal cells, thereby increasing resistance to the fungus *M. grisea*. Si can impede fungal hyphae penetration by promoting the buildup of an antifungal chemical, flavonoid, which can damage fungal cell walls (Alvarez & Datnoff, 2001; Brescht et al., 2004). This study demonstrates that *G. boninense* effectively infects palm seedlings through artificial inoculation using a placement method, where infection mainly happens when healthy palm roots encounter fungal inoculum-containing debris. Further, it was predicted that *G. boninense* would infect the root cell wall by making holes through all cell wall layers. This indicated simultaneous wood deterioration with the infection-producing enzymes that can break down cell wall layers. Recent studies have confirmed that different *Ganoderma* species cause concurrent degradation of plant cell walls. Comparable wood decay patterns have been observed in *Laurelia Filipina* and date palm wood infected by *G. colosseum* (Adaskaveg et al., 1991; Agosin, 1990). This degradation is primarily due to the critical function of carbohydrate-active enzymes (CAZymes), especially cell wall degrading enzymes (CWDEs), which are essential for *Ganoderma* species to break down lignin and cellulose, enabling pathogen infiltration (Ramzi et al., 2019).

Initial findings showed that adding silicon-enriched fertilizer enhanced the synthesis and deposition of silicon in root cell walls, leading to an increase in silicification. Cell wall destruction occurred in discrete areas with elevated lignin content, including the central lamella region. Effective silicification requires high concentrations of silicon cells and bodies in the middle lamella and cell wall corners, which are crucial regions for this process (He et al., 2013; Ma et al., 2006). Recent studies have shown that silicon accumulates in the intracellular spaces (ICS) between the cortical cells of *Molinia caerulea* (purple moor grass) roots, confirming its role in enhancing plant structural defenses (He et al., 2013; Ma et al., 2006). These findings reveal that Si is concentrated in essential locations like the ICS, reinforcing the plant's tolerance to environmental challenges.

Applying silicon-enriched fertilizer appears to be an effective method for managing BSR disease caused by *G. boninense*, comparable to fungicides, with the added potential of lowering the number of fungicide treatments or reducing the necessary active ingredient quantities (Fabricio et al., 2005). Additionally, the organic content in the specially formulated fertilizer provides several benefits, including improving soil structure, increasing soil pH, and boosting nutrient absorption in palm seedlings. These effects help minimize the likelihood of *G. boninense* adhering to the root cell wall, thus promoting the general health of the palm seedlings. The findings indicate that silicon-enriched fertilizer enhanced disease resistance, improved nutrient availability, and correct imbalances of key elements affecting palm growth and resilience against disease. Therefore, it will impact infection and pathogen sporulation.

Research findings confirmed the presence and accumulation of silica bodies in palm roots and a thick double layer of silicon in the cuticle of the endodermal cell walls in palm roots. These results were similarly supported by earlier research, which showed that Si deposition in the roots was a unique multifunctional plant component that worked as the soil environment's frontline (Lux et al., 2020). The unique attributes of this organ highlight certain features, like its cooperative interaction with soil microorganisms and specific morphological traits absent in other parts of the plant, such as Casparian bands in the endodermis and exodermis (Lux et al., 2020).

The study showed that applying Si-enriched fertilizer (treatment T3) altered root cell wall structure, thus increasing cell wall extensibility and improving plant resilience. The buildup of silicon in palm roots increases disease resistance by fortifying cell walls through crosslinking mechanisms like lignification (Currie & Perry, 2009). However, silica deposition is more energy-efficient than lignification, offering a cost-effective method for improving mechanical rigidity (Kumar et al., 2017). Despite these advantages, the precise interaction between silicification and lignification in roots is still not fully understood. Previous investigations by Gopal et al. (2005) demonstrated that coconut palms (*Cocos nucifera*) infected by root wilt phytoplasma altered the rhizosphere by

secreting chemicals that promoted beneficial microorganisms, including nitrogen-fixers, silicate solubilizers, and actinomycetes. This reduced harmful microorganisms and boosted silicon intake, boosting palm growth and production. The results indicate that silicon-enriched fertilizer (treatment T3) increased disease tolerance, reducing infection and pathogen sporulation.

CONCLUSION

The study demonstrates that silicon-enriched fertilizer (T3) substantially lowers the risk of *G. boninense* infection in palm seedlings by enhancing their disease resistance. Research indicates that silicon-enriched fertilizer (T3) can serve as a powerful tool for disease management, significantly reducing DI ($p \leq 0.05$) by 52.63% in oil palm and 67.35% in betel nut palm while delaying the onset of BSR. This fertilizer contains beneficial elements such as silicon (Si), which may influence the ultrastructure of palm roots and shoots by thickening cell walls. Silicon strengthens these structures, creating a physical barrier that limits the penetration of *G. boninense* hyphae. Additionally, it may stimulate the production of antifungal compounds that degrade fungal cell walls. As a result, these changes in root structure effectively restrict fungal movement toward the stem, thereby delaying the development of BSR and demonstrating increased tolerance in Si-treated plants.

Further research is essential to uncover the mechanisms involved in silicon (Si) uptake, translocation, and accumulation across various plant species. Investigating the expression and localization of Si transporter genes is particularly recommended to better understand genotypic differences in Si accumulation. Additionally, one of the least understood areas is how Si influences plants under combined stress conditions. Plants are subjected to multiple stressors in natural environments, including extreme temperatures, water scarcity, and salinity. Exploring these processes should be a key focus of future studies to enhance knowledge of plant adaptation to adverse conditions. Practical field trials of Si application in economically significant crops are also recommended to evaluate its real-world benefits.

Although the precise functions of Si in plants remain unclear, evidence suggests it plays a beneficial role, particularly in enhancing resistance to fungal pathogens. However, this hypothesis has yet to be definitively proven, as quantitative data supporting the mechanical barrier hypothesis is still lacking. Addressing this gap is critical for developing effective agricultural strategies. Recent studies have demonstrated the role of silicon-enriched fertilizers in promoting growth in both oil palm and betel nut palm species. However, these studies often face limitations in observing long-term effects, highlighting the need for extended research periods. Future applications of Si fertilizers are likely to contribute to greater biomass accumulation, including increased grain yields. A genetic approach could provide valuable insights into the mechanisms of Si action in palms, further

advancing our understanding. Moreover, evaluating the potential of Si fertilizers to reduce agricultural costs while delivering environmental benefits is vital. Developing optimized management practices for Si applications should be a priority for future research, ensuring its effectiveness and sustainability in agriculture.

ACKNOWLEDGMENTS

The authors are incredibly grateful to Universiti Putra Malaysia (UPM) and the Malaysian Palm Oil Board (MPOB) for supporting this research study. Furthermore, we would like to thank the Ex-Director of the Biology Division (Allahyarham Haji Dr. Idris Bin Abu Seman) and the management of MPOB generally for the support and comments in conducting this research. Also, thanks to all involved Plant Pathology and Biosecurity (PPB) Unit staff, MPOB, for their assistance in destructive sampling, help, and cooperation during this study.

REFERENCES

Abubakar, A., Ishak, M. Y., Bakar, A. A., & Uddin, M. K. (2022). *Ganoderma boninense* basal stem rot induced by climate change and its effect on oil palm. *Environmental Sustainability*, *5*, 289–303. https://doi.org/10.1007/s42398-022-00244-7

Adaskaveg, J. E., Gilberston, R. L., & Blanchette, R. A. (1991). Comparative studies of delignification caused by *Ganoderma* species. *Applied and Environmental Microbiology*, *56*(6), 1932–1943. https://doi.org/10.1128/aem.56.6.1932-1943.1990

Agosin, E., Blanchette, R. A., Silva, H. A., Lapierre, C., Cease, K. R., Ibach, R. E., Abad, A. R., & Muga, P. (1990). Characterisation of *palo podrigo*, a natural process of delignification in wood. *Applied and Environmental Microbiology*, *56*(1), 65–74. https://doi.org/10.1128/aem.56.1.65-74.1990

Alvarez, J., & Datnoff, L. E. (2001). The economic potential of silicon for integrated management and sustainable rice production. *Crop Protection*, *20*(1), 43–48. https://doi.org/10.1016/S0261-2194(00)00051-X

Bhardwaj, S., Sharma, D., & Singh, S. (2023). Physiological and molecular insights into the role of silicon in improving plant performance under abiotic stresses. *Plant and Soil, 486*, 25–43. https://doi.org/10.1007/s11104-022-053954

Boudet, A. M. (2000). Lignins and lignification: Selected issues. *Plant Physiology and Biochemistry*, *38*(1–2), 81–96. https://doi.org/10.1016/S0981-9428(00)00166-2

Brescht, M. O., Datnoff, L. E., Kucharek, T. A., & Nagata, R. T. (2004). Influence of silicon and chlorothalonil on the suppression of grey leaf spot and increased plant growth in St. Augustine grass. *Plant Disease*, *88*(4), 338–344. https://doi.org/10.1094/PDIS.2004.88.4.338

Brunings, A. M. (2021). Differential gene expression of rice in response to silicon and rice blast fungus. *Annals of Applied Biology*, *155*(2), 161–170. https://doi.org/10.1111/aab.2021.00347.x

Carré-Missio, V. (2021). *Silicon-mediated host defense mechanisms in plants against pathogens*. SpringerLink. https://doi.org/10.1007/s00299-021-02765-3

Currie, H. A., & Perry, C. C. (2009). Chemical evidence for intrinsic 'Si' within *Equisetum* cell walls. *Phytochemistry*, *70*(17–18), 2089–2095. https://doi.org/10.1016/j.phytochem.2009.07.039

Debona, D., Rodrigues, F. A., & Datnoff, L. E. (2017). Silicon's role in abiotic and biotic plant stresses. *Annual Review of Phytopathology, 55*, 85–107. https://doi.org/10.1146/annurev-phyto-080516-035312

Del Río, J. A. (2001). Tyloses formation and changes in phenolic compounds in grapevine roots infected with *Phaeomoniella chlamydospora* and *Phaeoacremonium* species. *Phytopathologia Mediterranea*, *40*(3), 394–399.

Etesami, H., Jeong, B. R., & Glick, B. R. (2020). Silicon-induced plant resistance against pathogens: Mechanisms and future prospects. *Plant Pathology Journal*, *36*(1), 1–10. https://doi.org/10.5423/PPJ.OA.06.2019.0127

Fabricio, A. R., & Lawrence, E. D. (2005). Silicon and rice disease management. *Fitopatologia Brasileira, 30*(5), 457–468. http://doi.org/10.1590/S0100-41582005000500001

Fairhurst, T., Griffiths, W., & Rankine, I. (2019*). TCCL field handbooks. Oil palm – nursery*. TCCL Publications.

Gopal, M., Gupta, A., & Nair, R. (2005). Variations in hosting beneficial plant-associated microorganisms by root (wilt)-diseased and field-tolerant coconut palms of West Coast tall variety. *Current Science Journal*, *59*(12), 1922–1927.

He, C., Ma, J., & Wang, L. (2013). Silicon-mediated amelioration of aluminum toxicity in higher plants: A review. *Journal of Plant Physiology*, *170*(12), 1189–1194. https://doi.org/10.1016/j.jplph.2013.03.009

Idris, A. S., Ismail, S., & Arif, A. M. (2020). Disease management of basal stem rot in oil palm using integrated approaches. *Journal of Plant Protection Research*, *60*(1), 1–10.

Idris, A. S., Kushairi, A., Ariffin, D., & Basri, M. W. (2006). *Techniques for inoculation of oil palm germinated seeds with Ganoderma*. http://tot.mpob.gov.my/tt-no-314-technique-for-inoculation-of-oil-palm-germinated-seeds-with-ganoderma/

Kamu, A., Phin, C. K., Idris, A. S., Gabda, D., & Mun, H. C. (2021). Estimating the yield loss of oil palm due to *Ganoderma* basal stem rot disease by using Bayesian model averaging. *Journal of Oil Palm Research*, *33*(1), 46-55. https://doi.org/10.21894/jopr.2020.0061

Khoo, Y. W., & Chong, K. P. (2024) Corrigendum: *Ganoderma boninense*: General characteristics of pathogenicity and methods of control. *Frontiers of Plant Science*, *15*, 1360323. https://doi.org/10.3389/fpls.2024.1360323

Kim, Y. H. (2002). Role of silicon in suppressing fungal diseases in plants. *Plant Pathology, 51*(2), 178–185.

Kumar, S., Milstein, Y., Brami, Y., Elbaum, M., & Elbaum, R. (2017). Mechanism of silica deposition in sorghum silica cells. *New Phytologist*, *213*(2), 791–798. https://doi.org/10.1111/nph.14173

Liang, Y. C., Sun, W., Si, J., & Romheld, V. (2015). Silicon-mediated enhancement of plant resistance to disease. *Plant Pathology Journal*, *31*(1), 12–21. https://doi.org/10.5423/PPJ.RW.09.2014.0089

Lux, A., Lukačová, Z., Vaculík, M., Švubová, R., Kohanová, J., Soukup, M., Martinka, M., & Bokor, B. (2020). Silicification of root tissues. *Plants*, *9*(1), 111. https://doi.org/10.3390/plants9010111

Ma, J. F. (2021). Role of silicon in enhancing the resistance of plants to biotic and abiotic stresses. *Soil Science and Plant Nutrition*, *67*(1), 11–18. https://doi.org/10.1080/00380768.2021.10408447

Ma, J. F., & Yamaji, N. (2006). Silicon uptake and accumulation in higher plants. *Journal of Experimental Botany*, *57*(8), 1255–1261. https://doi.org/10.1093/jxb/erj073

Ning, D. F. (2014). Effects of slag-based silicon fertilizer on rice growth and brown-spot resistance. *PLoS One*, *9*(7), e102681. https://doi.org/10.1371/journal.pone.0102681

Noor Azmi, A. N., Bejo, S. K., Jahari, M., Muharam, F. M., Yule, I., & Husin, N. A. (2020). Early detection of *Ganoderma boninense* in oil palm seedlings using support vector machines. *Remote Sensing*, *12*(23), 3920. https://doi.org/10.3390/rs12233920

Priwiratama, H., Prasetyo, A. E., & Susanto, A. (2020). Incidence of basal stem rot disease of oil palm in converted planting areas and control treatments *IOP Conference Series: Earth and Environmental Science*, *468*, 012036. https://doi.org/10.1088/1755-1315/468/1/012036

Rakib, M. R. M., Bong, C. F. J., Khairulmazmi, A., & Idris, A. S. (2015). Aggressiveness of *Ganoderma boninense* and *G. zonatum* isolated from upper and basal stem rot of oil palm (*Elaeis guineensis*) in Malaysia. *Journal of Oil Palm Research*, *27*, 229–240.

Ramzi, A. B., Che Me, M. L., Ruslan, U. S., Baharum, S. N., & Nor Muhammad, N. A. (2019). Insight into plant cell wall degradation and pathogenesis of *Ganoderma boninense* via comparative genome analysis. *PeerJ*, *7*, e8065. https://doi.org/10.7717/peerj.8065

Ranjan, A. (2021). Silicon-mediated abiotic and biotic stress mitigation in plants. *Plant Physiology and Biochemistry*, *163*, 15–25. https://doi.org/10.1016/j.plaphy.2021.03.044

Rebitanim, N. A., Hanafi, M. M., Idris, A. S., Abdullah, S. N. A., Mohidin, H., & Rebitanim, N. Z. (2020). GanoCare® improves oil palm growth and resistance against *Ganoderma* basal stem rot disease in nursery and field trials. *Biomed Research International*, *2020*, 3063710. https://doi.org/10.1155/2020/3063710

Rees, R. W., Flood, J., Hasan, Y., Potter, U., & Cooper, R. M. (2009). Basal stem rot of oil palm (*Elaeis guineensis*): Mode of root infection and lower stem invasion by *Ganoderma boninense*. *Plant Pathology*, *61*(4), 877–887. https://doi.org/10.1111/j.1365-3059.2009.02100.x

Rodrigues, F. A., Vale, F. X. R., Datnoff, L. E., Prabhu, A. S., & Korndörfer, G. H. (2003). Effect of rice growth stages and silicon on sheath blight development. *Phytopathology, 93*(3), 256–261. https://doi.org/10.1094/PHYTO.2003.93.3.256

Sarma, R., Patel, N., & Gomez, L. (2024). Role of silicon-enriched fertilizers in plant disease resistance and vigor. *Journal of Agricultural Sciences*, *112*(3), 245–259. https://doi.org/10.1234/jas.2024.11203

Surendran, A., Siddiqui, Y., Ahmad, K., & Fernanda, R. (2021). Deciphering the physicochemical and microscopical changes in *Ganoderma boninense*-infected oil palm woodblocks under the influence of phenolic compounds. *Plants*, *10*(9), 1797. https://doi.org/10.3390/plants10091797

Zhang, C., Wang, L., Zhang, W., & Zhang, F. (2013). Do lignification and silicification of the cell wall precede silicon deposition in the silica cell of the rice (*Oryza sativa* L.) leaf epidermis? *Plant Soil*, *372*, 137–149. https://doi.org/10.1007/s11104-013-1723-z

Pertanika J. Trop. Agric. Sci. 48 (3): 991 - 1017 (2025)

PERTANIKA JOURNALS

TROPICAL AGRICULTURAL SCIENCE

Journal homepage: http://www.pertanika.upm.edu.my/

Parent Material, Elemental Composition, and Pedogenic Processes in Ophiolitic Soils in Eastern Taiwan

Marvin Decenilla Cascante, Cho Yin Wu, Chia Yu Yang, Hui Zhen Hum and Zeng Yei Hseu*

Department of Agricultural Chemistry, National Taiwan University, Taipei 10617, Taiwan

ABSTRACT

The ophiolite complex in Chishang, Eastern Taiwan, exhibits a wide variety of soil parent materials, resulting in notable variations in elemental composition and pedological properties. This study characterized soils from four pedons along a toposequence, focusing on mineral composition, micromorphology, general properties, and elemental composition. A mass balance model quantified the mobility of clay, along with major and trace elements. The soils predominantly comprised chlorites, feldspars, quartz, micas, and calcite, with higher silica (Si) concentrations followed by Al. Some of the studied soils had elevated Ca/Mg ratios (≥ 1.0), indicating a primary derivation from sedimentary parent material, such as mudstone. However, concentrations of Cr (71.2 to 105.0 mg kg^{-1}), Ni (43.2 mg kg^{-1}), and Co (20.3 to 27.9 mg kg^{-1}) were notably lower than those reported in other global studies on ophiolite complexes. A significant and positive correlation occurred between Fe- and Al-oxides and Cr, Ni, and Co. The poor correlations between these trace metals and other soil properties (pH, organic carbon, Ca/Mg ratio, rare earth elements) suggest that these factors had limited influence on Cr, Ni, and Co concentrations. The strong ($p < 0.01$) correlations among trace metals indicate a genetic linkage formed during soil development rather than anthropogenic activities. Additionally, trace metal enrichment in surface soils, as evidenced by the increase of clay and Fe/Al oxides, implies that these components provide crucial adsorption sites for Cr, Ni, and Co.

Keywords: Mass balance, mudstone, ophiolitic soils, pedogenesis, trace metals

ARTICLE INFO

Article history:
Received: 04 October 2024
Accepted: 23 December 2024
Published: 16 May 2025

DOI: https://doi.org/10.47836/pjtas.48.3.19

E-mail addresses:
marvin.cascante@vsu.edu.ph (Marvin Decenilla Cascante)
d08623001@ntu.edu.tw (Cho Yin Wu)
d10623003@ntu.edu.tw (Chia Yu Yang)
d11623003@ntu.edu.tw (Hui Zhen Hum)
zyhseu@ntu.edu.tw (Zheng Yei Hseu)
* Corresponding author

INTRODUCTION

Ophiolites originate from the oceanic crust and upper mantle and are primarily emplaced along continental margins through complex tectonic processes. These geological formations are characterized by their association with significant tectonic movements, often observed in regions with

active plate boundaries. Soils derived from ophiolites are relatively rare on the Earth's surface, mainly found near tectonic plate boundaries such as those in the circum-Pacific region and the Mediterranean (DiPietro, 2013; Dilek & Furnes, 2014). Despite their limited distribution, soils in ophiolite complexes are of great scientific interest because they offer valuable insights into the sources of detrital materials, geodynamic processes, and soil formation scenarios (Bédard et al., 2019; Gawlick & Missoni, 2019; Robertson et al., 2020). For instance, the elemental composition of soils within the ophiolite complex in eastern Taiwan, which originated from marine sediments during the convergence of the Eurasian continental and Philippine oceanic plates, was significantly influenced by pedogenic processes, topographic position, and the composition of the parent material (Cheng et al., 2009). The concept of parent material, referring to the original rock types from which the components of an ophiolite are derived, is central to understanding these soils' chemical and mineralogical properties.

Soils from ophiolite complexes typically exhibit considerable variation in the geochemical concentrations of trace metals. For example, in the soils of the Zhob Valley in Pakistan, the total concentrations of chromium (Cr; 588–1929 mg kg^{-1}), nickel (Ni; 665–1725 mg kg^{-1}), and cobalt (Co; 2.5–14.5 mg kg^{-1}) were several times higher than those found in benchmark soils, where Cr, Ni, and Co concentrations were 34.8 mg kg^{-1}, 541 mg kg^{-1}, and 1.2 mg kg^{-1}, respectively (Ullah & Muhammad, 2020). In addition, serpentinites, which form a significant part of ophiolites, are primarily composed of serpentine minerals such as antigorite, lizardite, and chrysotile, along with other minerals like talc, calcite, brucite, chlorite, magnetite, and chromite (Hseu et al., 2018; Yang et al., 2022). Besides their high concentrations of Cr, Ni, and Co, soils from ophiolitic complexes often exhibit low calcium (Ca) to magnesium (Mg) ratios and reduced levels of essential macronutrients, including nitrogen (N), phosphorus (P), and potassium (K). These characteristics contribute to the development of unique flora and distinct soil properties, which can significantly affect local ecosystems (Hseu et al., 2018; Merrot et al., 2021; Tazikeh et al., 2018; Yang et al., 2022). The low Ca/Mg ratio, coupled with the high trace metal concentrations, presents significant challenges to agricultural productivity in these regions (Hseu et al., 2018).

The origin and landscape of soils within ophiolite complexes are closely linked to their marine sedimentary origins, leading to distinct variations in elemental composition and pedological characteristics. Hseu et al. (2007) reported that the concentrations of Cr and Ni in soils derived from serpentinites were five to ten times higher than those in soils derived from mixed mudstones in an ophiolite complex in Eastern Taiwan. The finding underscores the critical role of parent material in determining the geochemical composition of soils derived from sedimentary sources and the behavior of these elements under various environmental conditions (Tazikeh et al., 2018). In addition to the parent material, various soil properties, including pH, the presence of iron (Fe) oxides (Fe_2O_3), Fe sulfides, Fe-

bearing clay minerals, manganese (Mn), and organic matter (OM) play significant roles in controlling the distribution of trace metals in terrestrial environments (Bolaños-Benitez et al., 2021; Merrot et al., 2021; Rinklebe & Shaneen, 2017). At low pH, Cr is reduced and adsorbed onto the surfaces of OM and Fe oxides, forming highly stable and less mobile Cr (III) species (Baralkiewicz & Siepak, 1999).

However, Mn acts as a critical oxidant, forming the toxic and carcinogenic Cr (VI) species at high pH (Hseu, 2018; Merrot et al., 2021; Morrison et al., 2015). Similarly, the solubility and mobility of Ni and Co increase with decreasing soil pH, with Ni (II) and Co (II) being the more stable species under varying pH levels and oxidation-reduction conditions (Ma & Hooda, 2010). The mass balance model has determined the geochemical behaviors of trace metals in soils (da Silva et al., 2020; Ito et al., 2021; Wu et al., 2024). This model accounts for the addition, removal, and redistribution of elements within a soil profile relative to its parent material, making it a critical tool for understanding the fate of trace metals during soil formation and evolution (Chadwick et al., 1990; Hum et al., 2024; Wu et al., 2023). In addition to trace metals, mass balance models have been widely applied to major elements, providing insights into the interactions of these components within the soil system (da Silva et al., 2020; Ito et al., 2021; Hum et al., 2024; Wu et al., 2023; Wu et al., 2024).

Despite the importance of the mass balance approach, limited studies have specifically applied it to investigate the mobility and distribution of Cr, Ni, Co, and other major elements during soil formation, particularly in soils derived from sedimentary parent materials, such as those found in ophiolitic complexes. Applying mass balance models provides a valuable approach for evaluating the behavior of trace metals and major elements in ophiolitic soils, allowing quantification of the rate of gains and losses of elements throughout the soil profile, thereby revealing the processes that influence their distribution and mobility. These rates were measured relative to the immobile element, such as titanium (Ti), which remains stable and provides a reference point during weathering (Chapman & Horn, 1968; Egli et al., 2008; Harnois, 1988; Hum et al., 2024; Wu et al., 2023). This approach offers critical insights into mechanisms such as leaching, which removes soluble metal forms; adsorption onto clay minerals; complexation with various inorganic ligands; and secondary mineral formation that can immobilize metals under certain conditions (Chadwick et al., 1990; da Silva et al., 2020; Hum et al., 2024; Ito et al., 2021; Wu et al., 2023).

Studies on soils from ophiolite complexes have advanced significantly, with a focus on the environmental impact of trace metals and their elemental composition. These studies have highlighted the dual role of these soils: They can be relevant for agriculture yet pose undeniable threats to environmental sustainability due to their unique chemical properties (Hseu, 2018; Morrison et al., 2015; Yang et al., 2022). Understanding the geochemical background concentrations and distribution of major and trace elements in ophiolitic soils

is essential for effective pedological and environmental assessments, providing valuable information for land management and conservation efforts (Hseu et al., 2018). This study was conducted (1) to identify and characterize the parent materials of ophiolitic soils from Eastern Taiwan, (2) to analyze the elemental composition of these soils, (3) to explore the relationships between trace metals and pedogenic factors, and (4) to assess the mobility of soil components in these complex and dynamic environments.

MATERIALS AND METHODS

Site Description and Sampling

The study area was located in the ophiolite complex that belongs to the Miocene-aged Lichi Formation in the township of Chishang, Taiwan (Figure 1) (Ho, 1988). Four soil pedons along the south-facing gradient transect were selected from the summit (CP1), upper backslope (CP2), lower backslope (CP3), and foot slope (CP4) with elevation ranges from 290 to 343 m above sea level (Table 1). The climate condition of the study site is tropical humid, with massive rainfall and tropical cyclones from May to September. The mean annual air temperature is 22.5 °C, and the average rainfall is 1800 mm. The soil moisture and

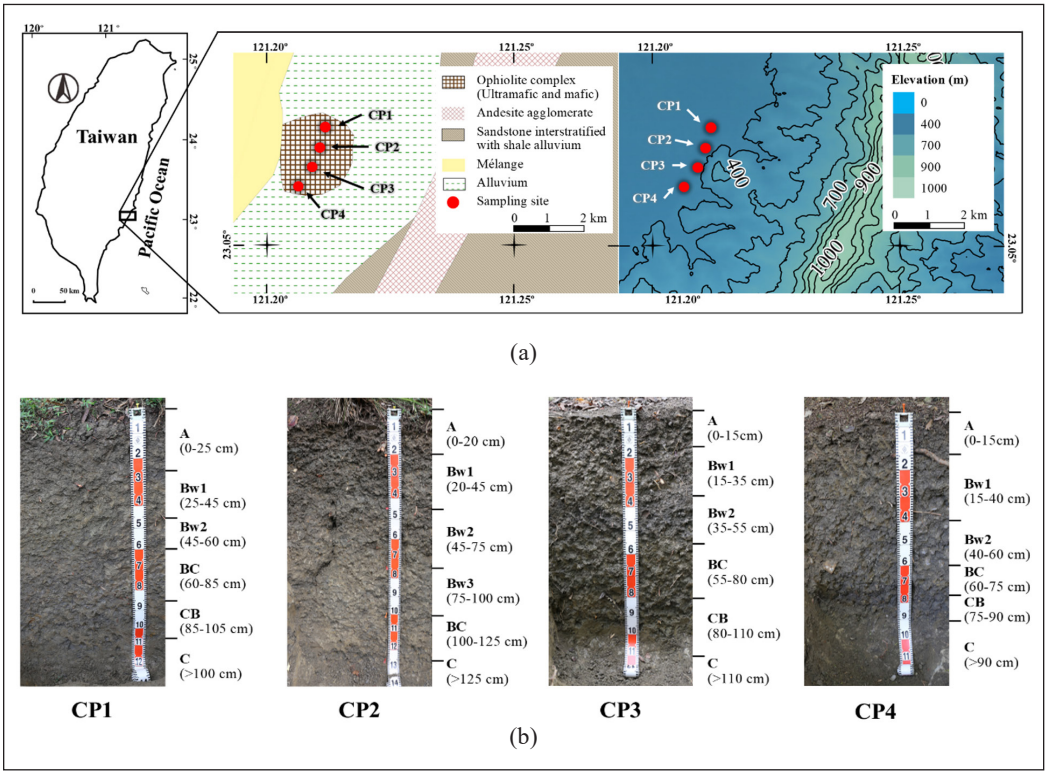

Figure 1. (a) Location of the studied soils and their geological and topographic map; and (b) studied pedons (CP1-summit, CP2-upper backslope, CP3-lower backslope, and CP4-footslope)

Table 1
Geographic information and classification of the studied pedons

Pedon	Location	Elevation m	Slope %	Landscape Position	Soil Classification[1]
CP1	N 23° 04' 16.82", E 121° 13' 21.64"	343	15	Summit	Typic Dystrudept
CP2	N 23° 04' 11.95", E 121° 13' 16.34"	322	15	Upper backslope	Typic Dystrudept
CP3	N 23° 04' 10.05", E 121° 13' 14.72"	310	10	Lower backslope	Typic Dystrudept
CP4	N 23° 04' 09.21", E 121° 13' 11.04"	290	5	Foot slope	Typic Dystrudept

Note. [1] Soil Taxonomy (Soil Survey Staff, 2022)

temperature regimes are udic and hyperthermic, respectively. The vegetation is dominated by tropical deciduous trees (*Annonaceae* sp.), exotic trees (*Leucaena leucocephala*), and perennial grasses (*Oplismenus hirtellus*, *Carex obnupta*, *Cortaderia jubata*, and *Saccharum spontaneum*). The field morphological description was determined according to the protocol suggested by the U.S. Soil Survey Manual (Soil Science Division Staff, 2017). The soil samples were collected according to genetic horizons, air-dried, and gently crushed to pass a 2-mm sieve for laboratory analyses.

Characterization of the Studied Soil

The bulk density (Bd) was measured using the core method (Blake & Hartge, 1986). The pH was measured using a mixture of soil and deionized water (1:1, w/v) with a glass electrode (McLean, 1982). The Walkley-Black wet oxidation method was used to determine the organic carbon (OC) content (Nelson & Sommers, 1982). Cation exchange capacity (CEC) and base saturation (BS) percentage were determined by the ammonium acetate method (pH 7.0) (Rhoades, 1982). The particle-size distribution of the soil samples was determined using the pipette method (Gee & Bauder, 1986). Dithionite-citrate-bicarbonate (DCB) extraction was used to determine the dissolved crystalline and noncrystalline Fe- and Al-oxides (Mehra & Jackson, 2013).

The total concentrations of silicon dioxide (SiO_2), aluminum oxide (Al_2O_3), Fe_2O_3, potassium oxide (K_2O), calcium oxide (CaO), magnesium oxide (MgO), sodium oxide (Na_2O), manganese oxide (MnO), and titanium dioxide (TiO_2) were determined after the following pretreatment of the sample procedure: A soil sample of 0.6 g (<75 μm) was combined with 6.0 g of flux composed of 49.75% $Li_2B_4O_7$, 49.75% $LiBO_2$, and 0.50% LiBr in a Pt-Au crucible. The mixture was fused using a fusion instrument (Claisse M4, Malvern Panalytical, UK) for 13 min with a liquefied petroleum gas and air flame. After fusion, the clear melt was poured into a 32 mm Pt-Au mold and cooled to room temperature. The uniform fused glass disk was used to determine major elements using a wavelength-dispersive X-ray fluorescence spectrometer (WDXRF; Axios^{mAX} Advanced WDXRF, Malvern Panalytical, UK).

The total concentrations of trace elements (Cr, Ni, and Co) were measured following digestion with a mixture of HF- HNO_3-HCl, as outlined in the U.S. Environmental Protection Agency's protocol (method 3052; U.S. Environmental Protection Agency, 2021). The digestion process was associated with a microwave oven system (Speedwave Entry, Berghof, Germany) at a gradual temperature increase of 180 ℃ in 10 min and further sustained at the same temperature and time. The concentration of all major and trace elements in the extraction and digestion solutions was quantified using inductively coupled plasma optical emission spectroscopy (ICP-OES; Optima 2100DV, PerkinElmer, Waltham, USA).

Mineralogical and Micromorphological Analyses

The powdered sand fractions (0.05–2 mm) by the pipette method were used for the mineral composition determination of the parent materials using X-ray diffraction (XRD, MiniFlex 600 Powder Diffractometer, Rigaku, Japan). The XRD patterns of the samples were obtained from 0º to 70º 2θ at a scanning rate of 10º 2θ min^{-1}. Furthermore, micromorphological characteristics and primary minerals were identified on thin sections of soil with a polarized light microscope (DM2700 M, Leica, Germany).

Elemental Mass Balance Calculation

The elemental mass balance approach was applied to estimate the gain and loss of the clay fractions, major elements (Si, Al, Fe, Ca, and Mg), and trace metals (Cr, Ni, and Co) in the studied pedons. The mass variation of the target element (j) was compared with the relative immobile index element (i) with the consideration of soil volume changes during soil development. Strain [ε], which stands for the volume change, was calculated based on the following equation (Brimhall & Dietrich, 1987; Brimhall et al., 1992; Chadwick et al., 1990):

$$\varepsilon_{i,w} = (\rho_p C_{i,p} / \rho_w C_{i,w}) - 1 \qquad [1]$$

where subscripts *p* and *w* represent the parent material and the weathered soil, respectively. ρ stands for Bd, while *C* refers to target and index element concentration. ε was employed to get the mobility of the target element (j) in the soils. The mass transfer coefficient ($\tau_{j,w}$) was calculated, followed by the equation below:

$$\tau_{j,w} = ((\rho_w C_{j,w} / \rho_p C_{j,p})(\varepsilon_{i,w}+1)) - 1 \qquad [2]$$

where the positive value indicates the net gain of the target element (j) related to the parent material while the negative value represents the net loss, in Equations 1 and 2, C horizons in the studied pedons were regarded as the parent material, and Ti was employed as the immobile index element in the calculations.

Quality Assurance and Control and Statistical Analysis

A standard reference material, SRM 2709a (San Joaquin Soil) from the National Institute of Standards and Technology (NIST), USA, was also digested and analyzed using the U.S. Environmental Protection Agency (2021). The recoveries of the trace metals were as follows: Cr, 104%; Ni, 89.6%; Co, 94.60%. Additionally, a certified reference material, BCR-2 (Columbia River Basalt) from the United States Geological Survey, was also analyzed using WDXRF. The recoveries of targeted elements from the BCR-2 were as follows: Si, 99.6%; Ti, 100%; Al, 100%; Fe, 99.9%; Mn, 101%; Mg, 99.6%; Ca, 100%; Na, 110%; and K, 101%. For every 10 sample sets, a blank and spiked procedure was performed for interference assessment and contamination check.

Statistical software R (version 4.1.0) was used to perform Pearson's correlation coefficient (r) analysis for the linear correlation among soil properties. The statistical significance levels are as follows: $*p < 0.05$, $**p < 0.01$, and $***p < 0.001$.

RESULTS AND DISCUSSION

Parent Material and Micromorphology

This study utilized XRD to identify the primary minerals present in the sand fractions of ophiolitic soil. That is, chlorites were identified by peaks at 1.44, 0.72, 0.48, 0.46, and 0.15 nm; feldspars were characterized by peaks at 0.64, 0.43, 0.39, and 0.38 nm; quartz was indicated by peaks at 0.25, 0.18, and 0.17 nm; micas were identified from peaks at 1.00, 0.33, and 0.20 nm; and calcite was observed from peaks at 0.23 and 0.17 nm (Figure 2). The abovementioned minerals suggested a complex mineralogical composition that deviates from the typical ophiolite parent materials. Ophiolites were generally expected to be composed mainly of minerals such as serpentinized amphibole, pyroxene, and accessory olivine, which reflect the soils developed, particularly those that have not undergone extensive weathering (Dilek & Furnes, 2014; Külah et al., 2014). However, the dominance of chlorites, feldspars, quartz, micas, and calcite in the studied soils indicated that they were predominantly derived from other parent materials rather than serpentinites. Instead, the mineralogy of these soils suggested a significant influence from marine sediments, particularly mudstones, which were known to contribute to the mineral diversity found in ophiolitic soil profiles (Hseu et al., 2007; Külah et al., 2014). Additionally, no slickensides or visible cracks, typically characteristic of soils derived from fine-textured marine sediments, were observed in the field, and this corresponded with the absence of smectite in the XRD results. Furthermore, the relatively lower number of peaks and peak intensities for serpentine (0.72 and 0.22 nm), chrysotile (0.36 and 0.15 nm), and talc (1.0, 0.31 and 0.25 nm) suggested that these minerals were present in smaller quantities than expected. However, kaolinite appears to be identified by the peaks at 0.72 nm and 0.36 nm in the XRD spectra, which are characteristic of soils derived from fine-grained marine sediments.

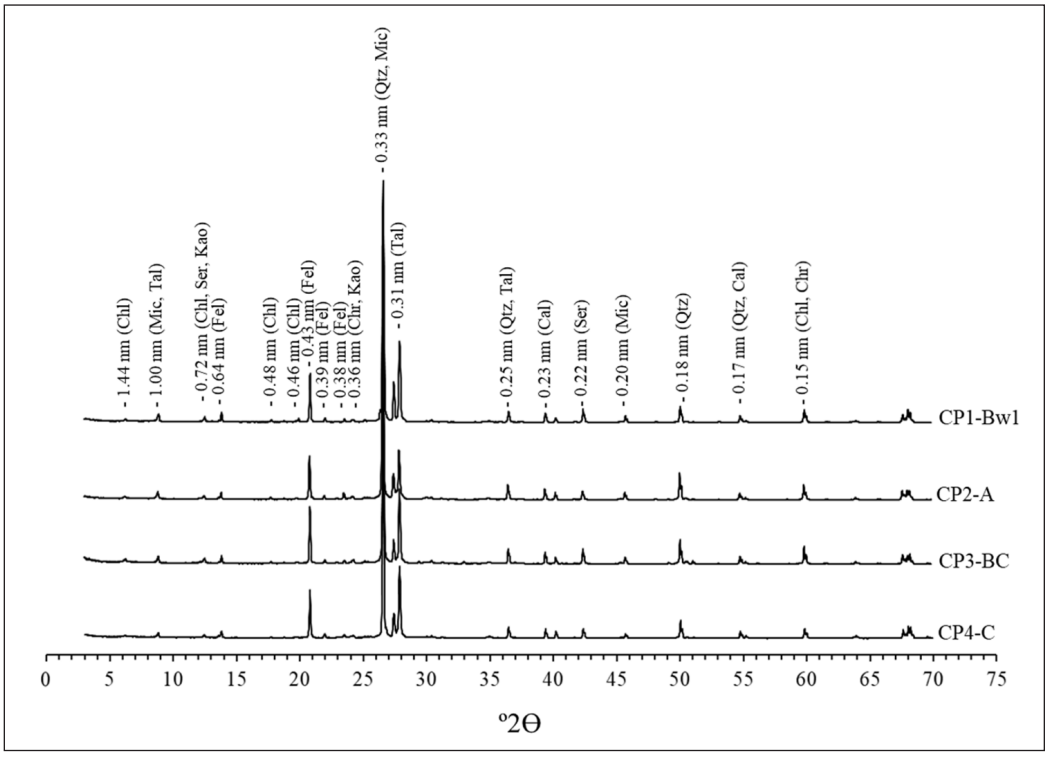

Figure 2. X-ray diffraction pattern of the sand fractions in ophiolite soils (CP1-Bw1, CP2-A, CP3-BC, and CP4-C). Chl = chlorite, Fel = feldspar, Qtz = quartz, Mic = micas, Ser = serpentine, Chr = chrysotile, Tal = talc, Kao = kaolinite

This observation is consistent with the findings of Hseu et al. (2007). Moreover, talc could also potentially overlap with mica near 1.00 nm. This indicated that the soils had been less influenced by serpentinites than one might anticipate, implying a more complex geological history involving altering the original ophiolitic materials during their formation. This alteration reflects the broader geological processes and environmental conditions that have impacted the ophiolite complex over time.

Plane-polarized light (PPL) and cross-polarized light (XPL) microscopy images verified the presence of minerals previously identified by XRD. Under PPL, chlorite was recognized by its colorless to pale green appearance, showcasing its pleochroic behavior as it changed intensity with the rotation of the microscope stage. When viewed under XPL, chlorite displayed striking blue interference colors, which is characteristic of this mineral (Figure 3a). Feldspar, which is a significant rock-forming mineral commonly found in ultramafic and sedimentary parent materials (Verrecchia & Trombino, 2021), was identified by its distinctive features. Under PPL, feldspar exhibited a tabular parallel habit with a cloudy color; under XPL, it showed a distinctive polysynthetic twinning pattern with interference colors ranging from gray to white (Figure 3a). Quartz was identified by

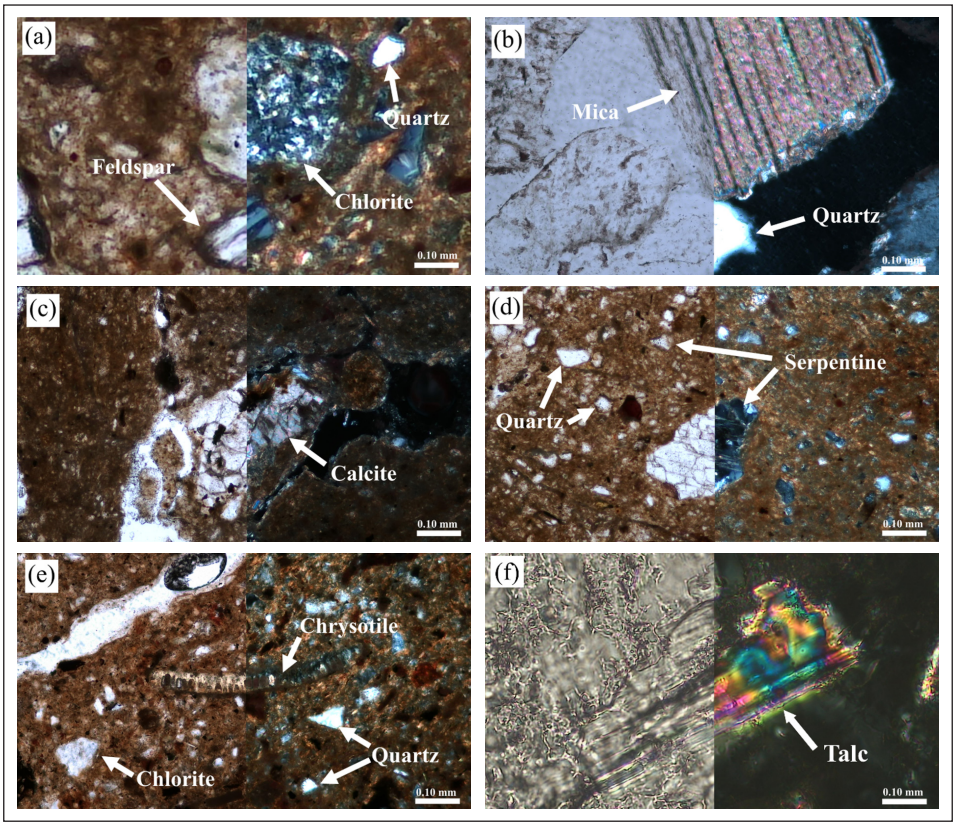

Figure 3. Photomicrographs of the thin section (left, plane polarized; right, cross-polarized light) showing: (a) chlorite, feldspar and quartz in Bw2 horizon of CP2 pedon; (b) quartz and micas from CB horizon of CP3 pedon; (c) calcite in Bw2 horizon of CP2 pedon; (d) quartz and serpentine in CB horizon of CP4 pedon; € chlorite, chrysotile, and quartz in A horizon of CP1 pedon; (f) and talc in Bw1 horizon of CP3 pedon

detrital grains that appeared colorless or white under both PPL and XPL. These grains were observed consistently across multiple photos (Figures 3a, 3b, 3d, and 3e), reinforcing the identification of quartz by the XRD. The presence of micas group minerals was indicated by laminar grains that showed brown to brownish-green colors with white to gray bands under PPL. Under XPL, these grains exhibited bright colors ranging from pink to green to blue (Figure 3b). This range of interference colors is typical for mica minerals and helps identify them. Calcite was identified by an aggregate of white grains with pink to gray borders under PPL. When observed under XPL, calcite displayed high-order interference colors, which are indicative of its high birefringence (Figure 3c). The identification of the primary minerals in the thin sections using polarized light microscopy was based on the mineralogical criteria described by Deer et al. (2013).

The thin sections also revealed the presence of serpentine, chrysotile, and talc. Serpentine minerals were identified by their platy texture, which appeared white under PPL

and showed gray to yellow interference colors under XPL. Chrysotile, a fibrous variety of serpentine, appeared with a parallel fibrous texture that was white in PPL and displayed gray to yellow colors under XPL (Figures 3d and 3e). Furthermore, the presence of talc was indicated by a flaky aggregate with an irregular bladed texture that appeared colorless with hints of very pale green under PPL. Under XPL, this aggregate displayed high third-order interference colors.

The detailed observations under PPL and XPL offer a comprehensive and conclusive verification of the mineral composition in the ophiolitic soils, providing nuanced insights that strongly corroborate the findings from XRD. The presence of tectosilicates such as feldspar and quartz, as well as phyllosilicate minerals like chlorite, serpentine group minerals, and micas, matches the expected outcomes. This evidence suggested that the parent materials of these soils were lithified, fine-grained sediment particles that weathered from various minerals and rocks, which underwent chemical alteration during tectonic movements (Macquaker et al., 1997; Lazar et al., 2015). Serpentine group minerals are generally not found in soils derived from sedimentary parent materials, particularly mudstone, due to their specific formation conditions (Perri et al., 2021). Their presence in the studied ophiolitic soils indicated a significant tectonic event and reflected the incorporation of primary minerals from serpentinites.

Soil Physical and Chemical Characteristics

Table 2 provides a detailed overview of the selected soil characteristics across the studied ophiolitic soil pedons. The particle size distribution in these pedons showed no distinct variation, with the clay fraction consistently dominating. Specifically, the clay content ranged from 45.0% to 62.5%, surpassing the sand fraction, which varied between 2.5% and 40.0%. This trend was evident across all pedons, with the highest clay content observed in the lower backslope pedon (CP3) and the lowest in the foot slope pedon (CP4). The study further revealed that soil Bd tended to be lower in the surface horizons across all pedons compared to the subsurface horizons, indicative of the higher OM content (Jiménez-Ballesta et al., 2024). The soil pH values across the pedons were found to be slightly to moderately acidic, ranging from 6.1 to 6.9. Notably, these pH values remained consistent with increasing depth, suggesting a relatively uniform distribution of acidity throughout the soil profiles.

In terms of organic carbon (OC) content, the surface horizons exhibited relatively higher levels, ranging from 5.0% to 5.8%. The higher OC content in the surface horizons was attributed to the accumulation of OM, which is often deposited from plant litter and other organic inputs at the soil surface (Jiménez-Ballesta et al., 2024). Conversely, the OC content decreased with soil depth, ranging from 3.6% to 2.0% in the subsurface horizons. A notable observation was the consistently higher levels of exchangeable Ca compared

to Mg, K, and Na across all pedons. Exchangeable Ca ranged from 3.62 to 10.6 cmol(+) kg^{-1}, while Mg levels were lower, ranging from 0.45 to 1.12 cmol(+) kg^{-1}. The finding was somewhat unexpected, as soils developed in ophiolitic complex typically exhibit higher Mg levels than Ca (Hseu, 2018; Yang et al., 2022). The higher Ca levels in the studied soils suggested that they were primarily derived from sedimentary materials, namely calcite, which have a different elemental composition than ultramafic rocks. The CEC values in the studied pedons ranged from 14.5 to 27.3 cmol(+) kg^{-1}. The highest CEC value was recorded in the summit pedon (CP1), while the lowest was observed in the upper backslope pedon (CP2). The BS percentage in the studied soils ranged from 17.1% to 82.2%. Higher BS values were observed in the C horizons of all pedons, which was attributed to the leaching and accumulation of basic cations from the surface and subsurface soils into these deeper layers, highlighting the dynamic nature of nutrient cycling and soil development within the ophiolitic landscape.

The study also determined the contents of DCB extractable Fe_d and Al_d, which ranged from 65.5 to 96.3 g kg^{-1} and 5.04 to 11.8 g kg^{-1}, respectively (Table 2). Elevated concentrations of Fe_d and Al_d were particularly noticeable in the B horizons, where the accumulation of free Fe and Al oxides was more pronounced. The accumulation was likely due to the processes of weathering and leaching that preferentially concentrated these oxides in the subsurface horizons. Based on the observed soil characteristics, including the well-structured development in the mineral subsurface horizons (Bw) and the presence of low basic cations, the four studied pedons were classified as Typic Dystrudepts according to the Soil Survey Staff (2022)(Table 1).

Total Content of Major and Trace Elements

The total contents of major and trace elements in the studied pedons (CP1 to CP4) within the ophiolite complex are detailed in Table 3. Results showed that SiO_2 across the four pedons showed irregular fluctuations throughout the soil horizons, ranging from 65.8% to 53.2 %. Similarly, the concentrations of Al_2O_3 and Fe_2O_3 also exhibited vertical variations, with Al ranging from 16.8% to 13.5% and Fe from 6.59% to 4.52%. Notably, slightly higher levels of Al_2O_3 and Fe_2O_3 were observed in the CP2 pedon (located on the upper backslope) and the CP3 pedon (situated on the lower backslope). This was consistent with their topographic positions, which were typically zones of deposition where these elements could be accumulated. Moreover, results showed noticeably elevated concentrations of Al_2O_3 (15.1% to 16.8%) and Fe_2O_3 (5.41% to 6.45%) in B horizons, indicating the accumulation of the element during soil formation. In contrast, other selected elements, such as K_2O (2.36% to 2.89%), Na_2O (0.96% to 1.78%), MgO (1.51% to 2.31%), CaO (0.56% to 2.60%), and MnO (0.05% to 0.10%), were present in lower concentrations compared to SiO_2, Al_2O_3, and Fe_2O_3 across all pedons (Table 3). The elemental composition of the studied ophiolitic

Table 2
Selected properties of the studied pedons

Pedon	Depth	Horizon	Sand	Clay	Bd[1]	pH	OC[2]	Exchangeable bases				CEC[3]	BS[4]	Fe_d[5]	Al_d[5]
								K	Na	Ca	Mg				
	cm		%		g cm^{-3}		%	cmol (+) kg^{-1}					%	g kg^{-1}	
CP1	0-25	A	17	50	1.4	6.3	4.97	0.20	0.02	3.91	0.60	27.3	17	78.4	10.7
	25-45	Bw1	12	55	1.4	6.5	2.87	0.11	0.01	3.70	0.74	23.5	19	87.8	10.9
	45-60	Bw2	10	55	1.5	6.8	2.54	0.11	0.01	4.10	0.82	20.6	24	78.4	9.97
	60-85	BC	12	52	1.6	6.6	2.08	0.11	0.04	3.93	0.85	19.7	25	76.1	8.75
	85-105	CB	30	45	1.6	6.8	1.86	0.12	0.09	6.62	0.90	16.4	47	75.9	7.30
	>105	C	18	50	1.7	6.8	2.57	0.15	0.25	5.66	1.12	17.6	41	65.5	6.30
CP2	0-20	A	10	55	1.5	6.6	4.99	0.22	0.05	6.69	0.60	24.4	31	75.1	7.78
	20-45	Bw1	2.0	63	1.4	6.8	3.42	0.15	0.01	5.74	0.61	18.0	36	86.2	6.76
	45-75	Bw2	15	58	1.5	6.6	3.08	0.13	0.02	6.64	0.77	17.8	43	84.2	6.18
	75-100	Bw3	2	60	1.7	6.6	3.13	0.12	0.03	8.83	0.87	17.7	56	85.8	6.84
	100-125	BC	25	47	1.6	6.1	2.77	0.14	0.05	9.79	1.04	14.9	74	80.7	5.70
	>125	C	15	45	1.7	6.6	3.16	0.14	0.06	10.6	1.11	14.5	82	85.5	5.04
CP3	0-15	A	12	53	1.3	6.6	4.79	0.13	0.01	3.74	0.53	23.5	19	93.4	9.80
	15-35	Bw1	17	58	1.4	6.9	2.80	0.10	0.01	3.95	0.57	22.4	21	93.2	10.8
	35-55	Bw2	18	58	1.4	6.9	3.10	0.08	0.01	3.62	0.53	24.8	17	94.7	11.3
	55-80	BC	15	60	1.5	6.7	3.19	0.09	0.01	4.72	0.73	22.9	24	96.3	11.8
	80-110	CB	28	58	1.4	6.7	2.77	0.10	0.05	5.28	0.68	20.5	30	91.9	10.1
	>110	C	13	60	1.5	6.7	2.74	0.10	0.02	6.93	0.71	19.4	40	91.6	10.9
CP4	0-15	A	38	45	1.2	6.3	5.43	0.13	0.01	4.41	0.45	24.2	21	77.1	8.60
	15-40	Bw1	30	50	1.6	6.5	2.95	0.17	0.02	5.29	0.54	20.3	30	85.6	9.81
	40-60	Bw2	40	45	1.4	6.3	2.89	0.08	0.02	4.23	0.61	20.3	24	85.9	9.40
	60-75	BC	25	55	1.5	6.6	2.92	0.07	0.02	4.47	0.69	20.4	26	87.4	9.54
	75-90	CB	33	50	1.3	6.8	1.31	0.07	0.02	4.31	0.62	20.5	24	85.7	9.84
	>90	C	30	48	1.4	6.7	1.93	0.07	0.03	4.61	0.64	19.5	27	86.0	10.1

Note. [1] Bulk density. [2] Organic carbon. [3] Cation exchange capacity. [4] Base saturation. [5] DCB-extractable

soils did not align with the characteristics of the typical soils found in ophiolite complexes, which were known for their low SiO_2 content (<45%) and relatively high Fe_2O_3 content. The low SiO_2 and high Fe_2O_3 content were inherited from the mafic and ultramafic parent materials (serpentinites), which are rich in Mg- and Fe- silicates (Hseu et al., 2007; Yang et al., 2022). However, the relatively high SiO_2 (>45%) and Al_2O_3 contents observed in the studied soils were indicative of their derivation from fine-grained sedimentary rocks, such as mudstone (Macquaker et al., 1997; Perri et al., 2021).

These rocks were primarily composed of clay minerals and silt-sized particles, which contained significant amounts of aluminosilicate minerals, including feldspars and micas. The presence of these minerals was confirmed through XRD analysis and cross-polarized light microscopy (Table 3; Figures 2 and 3).

Regarding the Ca/Mg ratio, the results revealed lower values in CP1, CP3, and CP4 pedons, all showing a ratio of less than or equal to 1.0 (Table 3). This outcome was likely influenced by the formation of carbonates, such as calcite, which developed after the parent materials in the ophiolite complex were formed (Dandar et al., 2023). Consequently, Ca tended to be depleted in the soils during weathering under a tropical humid climate (Nesbitt & Young, 1982; Harnois, 1988; Jiménez-Ballesta et al., 2022). In contrast, the subsurface horizons of the CP2 pedon exhibited a higher concentration of Ca compared to the total Mg concentration, which resulted in a Ca/Mg ratio exceeding 1.0. This elevated ratio in CP2, in comparison to the other pedons, was significantly influenced by the presence of feldspar and carbonate minerals (Nesbitt & Young, 1982). This was further supported by mineral micromorphology observed through polarized light microscopy, which indicated these minerals' contributions to the increased Ca levels in the CP2 pedon (Figures 2, 3a, and 3d). The intricate and diverse composition of the ophiolite complex created a unique mineralogical structure, which significantly contributed to the specific characteristics and behavior of this element. This relationship between the complexity of the mineral composition and the properties of the elements underscores the importance of the geological context in determining the distribution, concentration, and chemical behavior of the element within the ophiolite complex.

Ophiolitic soils are commonly enriched with trace metals, such as Cr, Ni, and Co, due to the presence of ultramafic rocks in the ophiolite complex (Kierczak et al., 2007; Oze et al., 2004; Kierczak et al., 2016; Hseu et al., 2018). Nevertheless, the formation of ophiolite complexes typically involved the accretion of sedimentary cover and other crustal layers, which led to lower concentrations of Cr, Ni, and Co in soils derived from these sedimentary parent materials (Kierczak et al., 2016; Hseu et al., 2018). In the studied ophiolitic soils, the concentrations of trace metals exhibited variations that ranged from 71.2 to 105.0 mg kg^{-1} for Cr, 23.6 to 43.2 mg kg^{-1} for Ni, and 20.3 to 27.9 mg kg^{-1} for Co (Table 3). Interestingly, the levels of Cr, Ni, and Co were slightly elevated in the CP3 pedon compared

Table 3
Total contents of major and trace elements of the studied pedons

Pedon	Depth	Horizon	SiO_2	Al_2O_3	Fe_2O_3	K_2O	Na_2O	CaO	MgO	MnO	Co	Cr	Ni	Ca/Mg
	cm					%						mg kg^{-1}		
CP1	0-25	A	57.9	15.5	5.54	2.63	1.34	0.68	1.7	0.07	23.0	84.2	30.8	0.40
	25–45	Bw1	60.5	16.2	5.84	2.65	1.35	0.58	1.84	0.06	24.3	95.1	35.3	0.31
	45–60	Bw2	61.3	16.0	5.72	2.66	1.36	0.58	1.88	0.06	23.6	90.2	32.4	0.31
	60–85	BC	65.8	13.5	4.52	2.36	1.78	1.24	1.76	0.05	25.5	92.3	35.9	0.70
	85–105	CB	61.1	16.0	5.98	2.76	1.27	0.70	2.05	0.08	21.2	75.5	26.8	0.34
	>105	C	62.4	14.9	5.30	2.60	1.56	1.36	2.11	0.07	23.9	85.0	30.8	0.65
CP2	0–20	A	56.5	16.3	6.06	2.77	1.06	0.71	1.98	0.09	25.7	94.2	38.1	0.36
	20–45	Bw1	56.1	16.7	6.45	2.89	1.01	1.89	2.24	0.10	26.7	100	37.5	0.84
	45–75	Bw2	57.2	16.3	6.28	2.76	1.06	1.98	2.26	0.09	25.8	95.6	33.6	0.88
	75–100	Bw3	57.0	16.5	6.33	2.78	1.14	1.97	2.28	0.09	26.5	97.2	36.4	0.87
	100–125	BC	59.2	15.5	5.88	2.6	1.19	2.25	2.25	0.09	25.3	91.9	32.2	1.00
	>125	C	58.7	15.2	5.90	2.56	1.17	2.60	2.31	0.09	23.7	86.5	30.3	1.13
CP3	0–15	A	59.3	15.6	5.82	2.52	1.17	0.77	1.73	0.09	25.9	96.8	36.5	0.45
	15–35	Bw1	60.1	16.1	6.05	2.51	1.17	0.56	1.73	0.09	25.2	93.7	35.7	0.32
	35–55	Bw2	58.8	16.1	6.09	2.53	1.14	0.58	1.77	0.09	25.2	95.5	35.8	0.33
	55–80	BC	53.2	16.2	6.22	2.55	0.96	0.67	1.90	0.09	27.9	105	43.2	0.36
	80–110	CB	57.9	16.6	6.21	2.65	1.10	0.74	1.90	0.08	26.4	103	40.6	0.39
	>110	C	56.1	16.8	6.59	2.72	1.08	1.61	2.10	0.10	26.6	103	41.3	0.77
CP4	0–15	A	60.8	14.2	5.16	2.39	1.41	0.73	1.51	0.08	23.8	84.1	31.3	0.48
	15–40	Bw1	62.8	15.1	5.43	2.49	1.40	0.56	1.61	0.07	22.6	79.5	28.9	0.35
	40–60	Bw2	62.8	15.1	5.41	2.48	1.40	0.59	1.59	0.08	20.2	71.2	26.6	0.37
	60–75	BC	63.9	14.9	5.28	2.44	1.45	0.61	1.55	0.08	23.7	85.2	30.8	0.39
	75–90	CB	64.0	14.7	5.15	2.41	1.46	0.59	1.52	0.07	23.7	83.2	30.6	0.39
	>90	C	64.3	14.9	5.22	2.43	1.49	0.57	1.55	0.07	21.5	75.1	27.7	0.37

to the CP1, CP2, and CP4 pedons, which were situated in the lower backslope positions, respectively. Backslope areas were often considered zones of accumulation where eroded materials from upper slopes were deposited, leading to higher trace metal concentrations (Zhang et al., 2020). This observation was further supported by the fact that these higher concentrations of Cr, Ni, and Co in CP3 pedon corresponded with the elevated levels of DCB extractable Al and Fe in the same pedons, indicating the significant role of Fe- and Al-oxides in influencing the distribution of trace metals in the environment (Rinklebe & Shaheen, 2017; Merrot et al., 2021) (Tables 2 and 3).

The concentrations of Cr, Ni, and Co in the studied pedons (CP1 to CP4) were notably higher than the world soil averages of 59.5 mg kg^{-1} for Cr, 29.0 mg kg^{-1} for Ni, and 11.3 mg kg^{-1} for Co (Kabata-Pendias, 2011), suggesting that these heavy metals accumulated during soil formation. However, when considering the implications for agricultural practices, the Cr, Ni, and Co levels in these soils were below the contamination control thresholds set for Taiwan, which were 175 mg kg^{-1} for Cr and 130 mg kg^{-1} for Ni, with no specific permissible limit for Co. The presence of minerals such as chlorite, serpentine, and chrysotile in the studied pedons (Figures 2, 3a, 3d, and 3e) further supported the idea that these elements were primarily of geogenic origin (Kierczak et al., 2007; Caillaud et al., 2009).

The trace metal levels found in this study were significantly lower than those reported in previous research, which was also conducted on ophiolite complexes in eastern Taiwan. For instance, Hseu et al. (2007) reported Cr concentrations (400 to 3,100 mg kg^{-1}) that were as far as thirty times higher, and Ni concentrations (400 to 5,800 mg kg^{-1}) were up to over a hundred times greater than those observed in this study. Similarly, Yang et al. (2022) reported that the Cr and Ni total concentrations ranged from 1,880 to 3,854 mg kg^{-1} and 2,355 to 4,994 mg kg^{-1}, respectively. This discrepancy underscores the variability in trace metal concentrations across different ophiolite complexes, likely due to the fact that the studied soils are being partially derived from other parent materials as indicated by the higher Si content, the elevated concentration Al over Fe, and the limited presence of primary minerals responsible for the high concentration of trace metals. There was no data for the concentration of Co in the mentioned studies in Taiwan, but Kierczak (2016) reported that the total concentration of the element in Poland ranged from 83 to 168 mg kg^{-1}, much higher than the studied ophiolitic soils.

Relationships Between Soil Properties, Major Elements, and Trace Metals

The geochemical characteristics of trace metals in ophiolitic soils were analyzed using Pearson's correlation to investigate their relationships with basic soil properties, major elements, and trace metals to better comprehend their solubility and mobility (Table 4). No significant correlation was observed between soil pH and the concentrations of Cr, Ni, and Co in the ophiolitic soils (Table 4). Even though higher concentrations of trace metals

were observed in CP2 and CP3 pedons, the soil pH values remained relatively consistent across different horizons and pedons (Tables 2 and 3). The studied ophiolitic soils were classified as Inceptisols, which exhibit comparable acidic to moderate pH values, causing the lack of relationships between soil pH and the trace metals. As these soils continue to develop, the influence of pedogenic processes on trace metal distribution is expected to become more pronounced.

Generally, besides pH, OC and Fe/Al-oxides were also the critical factors that influence the oxidation states and solubility of these trace metals, affecting their distribution and mobility (Hseu et al., 2018; Wang et al., 2020; Xu et al., 2020). OC generally provides retention sites and controls the movement of absorbed trace metals in soils (Wang et al., 2020). However, in this study, no significant correlations were found between OC and the concentrations of Cr, Ni, and Co, suggesting that the distribution of these trace metals may be influenced by factors other than OC (Table 4). The highest concentrations of trace metals were observed in the BC horizon of pedon CP3, with values of 105 mg kg^{-1} for Cr, 43.2 mg kg^{-1} for Ni, and 27.9 mg kg^{-1} for Co. In contrast, the lowest values were recorded in the Bw2 horizon (71.2 mg kg^{-1} for Cr, 20.2 mg kg^{-1} for Co) and the C horizon (27.7 mg kg^{-1} for Ni) of the CP4 pedon. Interestingly, both the highest (5.43% OC) and lowest (1.31% OC) levels of OC were found in the CP4 pedon, highlighting the variability in OC distribution across different soil horizons. The observed differences in the distributions of Cr, Ni, Co, and OC were likely associated with the strong affinity of these trace metals for Fe and Al oxides, which incorporate them into the mineral matrix rather than associating them with OM (Hseu et al., 2018; Wang et al., 2020; Xu et al., 2020).

The strong positive correlation between Fe_t and Al_t with Cr_t ($p < 0.01$) and the positive correlations of these total elements with Ni_t and Co_t ($p < 0.05$) indicated a significant influence of the parent material and the geochemical affinity between these trace metals and the Fe and Al oxides present in the soils. The considerably elevated concentrations of total Al and Fe and the DCB-extractable Fe in the B horizons (79.7 to 88.3 g kg^{-1} Fe_t; 37.8 to 45.1 g kg^{-1} Al_t; 78.4 to 94.7 g kg^{-1} Fe_d; Tables 2 and 3) strengthen the relationships of these elements with Cr, Ni, and Co. The high surface areas and reactive sites of Fe and Al oxides facilitate the adsorption of trace metals, leading to their co-precipitation with Cr, Ni, and Co (Bolaños-Benitez et al., 2021; Cornell & Schwertmann, 2003; Merrot et al., 2021). Pedogenic metal oxides, particularly Fe and Al oxides, were considered important sinks for trace metals in soils (Hseu, 2018). Moreover, the slightly to moderately acidic conditions of the studied soils (pH 6.06 to 6.88) likely played a role in the formation of these oxides (Schwertmann et al., 2000), as their pH-dependent solubility affects the availability of trace metals in the soil solution, leading to their accumulation in association with Fe and Al oxides (Table 2) (Bolaños-Benitez et al., 2021; Merrot et al., 2021). Among the trace metals studied, only Ni showed a positive correlation with Fe_d ($p < 0.05$) in the

Table 4
Pearson's correlation matrix among selected soil properties, selected total major elements, and total trace metals in the studied soil samples (n=24)

	pH	OC	Fe_d	Al_d	Si_t	Al_t	Fe_t	Cr_t	Ni_t	Co_t	Ca/Mg
pH											
OC	-0.43*										
Fe_d	0.21	-0.04									
Al_d	0.21	0.01	0.52*								
Si_t	0.02	-0.48*	-0.32	0.10							
Al_t	0.25	0.11	0.39	0.01	-0.77***						
Fe_t	0.19	0.19	0.42*	-0.15	-0.86***	0.95***					
Cr_t	0.23	0.22	0.40	0.06	-0.69***	0.56**	0.60**				
Ni_t	0.26	0.25	0.43*	0.23	-0.66***	0.50*	0.51*	0.95***			
Co_t	0.21	0.23	0.34	-0.03	-0.65***	0.43*	0.50*	0.97***	0.93***		
Ca/Mg	-0.26	-0.01	-0.19	-0.84***	-0.22	-0.02	0.18	0.21	0.01	0.29	

Note. Fe_d: Fe DCB-extractable; Al_d: Al DCB-extractable. Si_t: total SiO_2; Al_t: total Al_2O_3; Fe_t: total Fe_2O_3; Cr_t: total Cr; Ni_t: total Ni; Co_t: total Co. *, **, and *** Significant at $p < 0.05$, 0.01, and 0.001

DCB extractable fraction, further emphasizing the role of free Fe oxides in influencing Ni distribution.

The Ca/Mg ratio is another important indicator that provides insights into the geological history and processes influencing the formation and evolution of ophiolites. This ratio is particularly useful in understanding the enrichment and depletion of basic cations through hydrothermal alteration processes (Miyashiro et al., 1969; Coleman & Keith, 1971; Hseu et al., 2018). The interactions between oceanic fluids and primary minerals during these processes can lead to the enrichment and incorporation of trace metals into the mineral structure (Naldrett & Lehmann, 1988; Grieco et al., 2004). As ophiolitic parent materials weather, they release major elements and trace metals, which become incorporated into the developing soil (Hseu et al., 2018). As soil development progresses, Ca is recycled by plants, while Mg is lost due to its solubility in the soil environment, which also affects the concentrations of Cr and Ni (Hseu, 2018). However, in this study, no significant correlations were observed between the Ca/Mg ratio and the concentrations of Cr, Ni, and Co in the ophiolitic soils (Figure 5), suggesting that the behavior of Ca and Mg during pedogenesis may have an indirect impact on trace metal concentrations rather than a direct one.

The study also revealed strong positive and significant correlations among Cr_t, Ni_t, and Co_t ($p < 0.001$), indicating that these trace metals were concurrently released during the weathering of the ophiolitic parent material and were not significantly influenced by non-geogenic sources. In typical ophiolitic environments, where ultramafic rocks are the dominant source of soil development, Ni is often found in the structures of minerals located in octahedral layers, such as lizardite, antigorite, chrysotile, and other phyllosilicate

minerals, including those in the chlorite group. These minerals can be easily released during soil formation (Hseu et al., 2007; Kierczak et al., 2016). Cr and Co, on the other hand, are primarily sourced from chromite, a key mineral in ultramafic rocks, and are often enriched by magnetite (Oze et al., 2004; Kierczak et al., 2016; Hseu, 2018; Hseu et al., 2018; Yang et al., 2022). The weathering of the abovementioned minerals has a significant impact on the proportions of Cr, Ni, and Co in sediment-derived ophiolitic soils, such as those derived from mudstone. For instance, Garver et al. (1996) reported that elevated concentrations of trace metals in soils suggest the presence of ultramafic rocks in the sediment source region. While the origin of trace metals is often determined using background concentrations, world average elemental equivalence, and Earth's crust composition, the significant correlations between these trace metals and their abundance in ophiolitic soils also provide valuable provenance information, as they reflect the lithological characteristics of their parent materials (Tables 3 and 4) (Gonnelli & Renella, 2012; Kabata-Pendias, 2011).

Mobility of Soil Components

The enrichments and depletion factors of clay, along with elements like Si, Al, Fe, Ca, Mg, and trace metals, were carefully analyzed to understand the long-term weathering rates of soils. The mass transfer coefficient (τ) of clay increased significantly at the surface of the studied pedons, especially for the CP1 (summit; $Clay_{\tau}$ = 0.24) and CP2 (upper backslope; $Clay_{\tau}$ = 0.23) pedons, where the stability of the landscape allowed for intense chemical weathering over time, leading to the gradual build-up of clay, suggesting that the landscape has remained stable enough to favor clay accumulation. In contrast, in CP3 to CP4 pedons (lower backslope to the footslope; CP3, $Clay_{\tau}$ = 0.09; CP4, $Clay_{\tau}$ = 0.10), in consideration of the increasing slope, the enrichment of clay might be mainly due to erosion and deposition processes. These processes have moved clay particles from higher areas to lower ones, resulting in sediment accumulation and a corresponding increase in clay content in these pedons. In terms of the subsurface horizons, both pedons CP1 and CP2 generally had similar increases in clay content ($Clay_{\tau}$ = 0.00 to 0.02), suggesting the constant accumulation of clay particles. CP3 pedon ($Clay_{\tau}$ = -0.01 to 0.02), however, generally showed no significant gains or losses in the subsurface horizons, indicating a balance between erosion and deposition. On the other hand, CP4 pedon ($Clay_{\tau}$ = -0.19 to 0.04) experienced a noticeable loss of clay in the subsurface layers, which is likely due to water percolation that leaches clay particles away, leaving behind coarser materials (Table 2).

Similar patterns were observed for the major elements Si, Al, and Fe, which correlated with the clay content, indicating that the behavior of these major elements appears to be interrelated, likely due to the influence of soil formation processes, particularly the translocation of secondary clay minerals within the soil profiles (Tonkha et al., 2021). The accumulation of major elements in the surface horizon in CP1 to CP4 pedons (Si_{τ} = 0.10 to

0.21; Al_{τ} = 0.09 to 0.21; Fe_{τ} = 0.09 to 0.20) is probably due to the higher concentration of fine particles, while the losses of these elements in the subsurface horizons, especially in CP4 pedon (Si_{τ} = -0.18 to 0.04; Al_{τ} = -0.19 to 0.04; Fe_{τ} = -0.19 to 0.04), may be attributed to coarser or less uniform textures (Macquaker et al., 1997; Tonkha et al., 2021). CP1 (Ca_{τ} = 0.00 to 0.15; Mg_{τ} = 0.00 to 0.18), CP2 (Ca_{τ} = 0.00 to 0.11; Mg_{τ} = 0.00 to 0.16), CP3 (Ca_{τ} = 0.00 to 0.05; Mg_{τ} = 0.00 to 0.08) pedons, and the surface soils of CP4 (Ca_{τ} = 0.14; Mg_{τ} = 0.10) exhibited no net gain and loss to positive mass fluxes for Ca and Mg (Figure 4). Typically, in ophiolitic soils, the behavior of these basic cations changes as soil development progresses. Mg is often leached out through the breakdown of Mg-silicate minerals and high-activity clay minerals, while Ca tends to be recycled by plants (Hseu, 2018; Yang et al., 2022). However, in this study, both Ca and Mg showed comparable mass fluxes, which is consistent with the intermediate stage of soil development observed in the studied ophiolitic soils (Table 1).

The selected trace metals in the ophiolitic soils exhibited similar mass flux patterns, indicating consistent geochemical behavior and uniformity in the source material (Figure 5). Notable positive mass fluxes were observed in surface and upper subsurface soils from pedons CP1 (Cr_{τ} = 0.14 to 0.24; Ni_{τ} = 0.14 to 0.25; Co_{τ} = 0.13 to 0.24) and CP2 (Cr_{τ} = 0.04 to 0.20; Ni_{τ} = 0.04 to 0.23; Co_{τ} = 0.04 to 0.20), as well as in the surface soils of pedons CP3 (Cr_{τ} = 0.11; Ni_{τ} = 0.10; Co_{τ} = 0.11) and CP4 (Cr_{τ} = 0.14; Ni_{τ} = 0.14; Co_{τ} = 0.14), suggesting an enrichment of these metals in the upper soil layers. Conversely, the subsurface horizons of pedon CP4 displayed negative mass fluxes, indicating a loss of trace metals in the soils from low-elevation areas. The observed gains and losses of trace metals in the studied ophiolitic soils (CP1 to CP4 pedons) corresponded closely with the behavior of the major elements, such as Al, Fe, and clay. These elements are known to provide retention sites for trace metals, effectively controlling their mobility and availability within the soil matrix (Bolaños-Benitez et al., 2021; Cornell & Schwertmann, 2003; Merrot et al., 2021; Hseu et al., 2018; Wang et al., 2020).

Specifically, the positive correlations between trace metals and Fe and Al in the studied ophiolitic soils (Table 4), along with the substantially elevated concentrations of total and DCB extractable Al and Fe in B horizons (Tables 2 & 3) as mentioned above, reinforced the idea that these elements played a critical role in the accumulation of metals, particularly Cr, Ni, and Co. Although OC did not exhibit a direct positive correlation with the trace metals (Table 4), the high concentrations of OC in the surface soils still reflect the observed gains of trace metals in these horizons, which serves as binding agents that enhance trace metal retention (Wang et al., 2020; Table 2; Figure 5). Furthermore, the noticeable change in the mass flux of trace metals was observed only in pedon CP4, which exhibited a negative trend in the subsurface horizons, likely influenced by the higher proportion of coarse particles (25 to 40% sand; Table 2; Figure 5). Coarse-textured soils,

with their higher permeability, tend to promote the mobility and leaching of trace metals. Additionally, the elevated concentrations of trace metals in the surface soils of the studied pedons might be attributed to the higher OC content, which can bind trace metals and enhance their retention (Table 2).

The observed behavior of trace metals in these ophiolitic soils did not align with findings from previous studies, which suggested that trace metals tend to accumulate more at lower elevations due to longer water residence time (Chen & Torres, 2012; Liu et al., 2016). This discrepancy suggested that other soil components, such as texture and OM, may play a more significant role in determining trace metal distribution than elevation alone. Moreover, the behavior of clay content, major elements, and trace metals in the studied ophiolitic soils followed similar trends, reinforcing that the parent material and pedogenesis primarily influence these soil components. Furthermore, the consistency across these elements suggested that external factors, particularly anthropogenic inputs, did not significantly impact the observed patterns but rather reflected the intrinsic characteristics of the soil and its natural development over time.

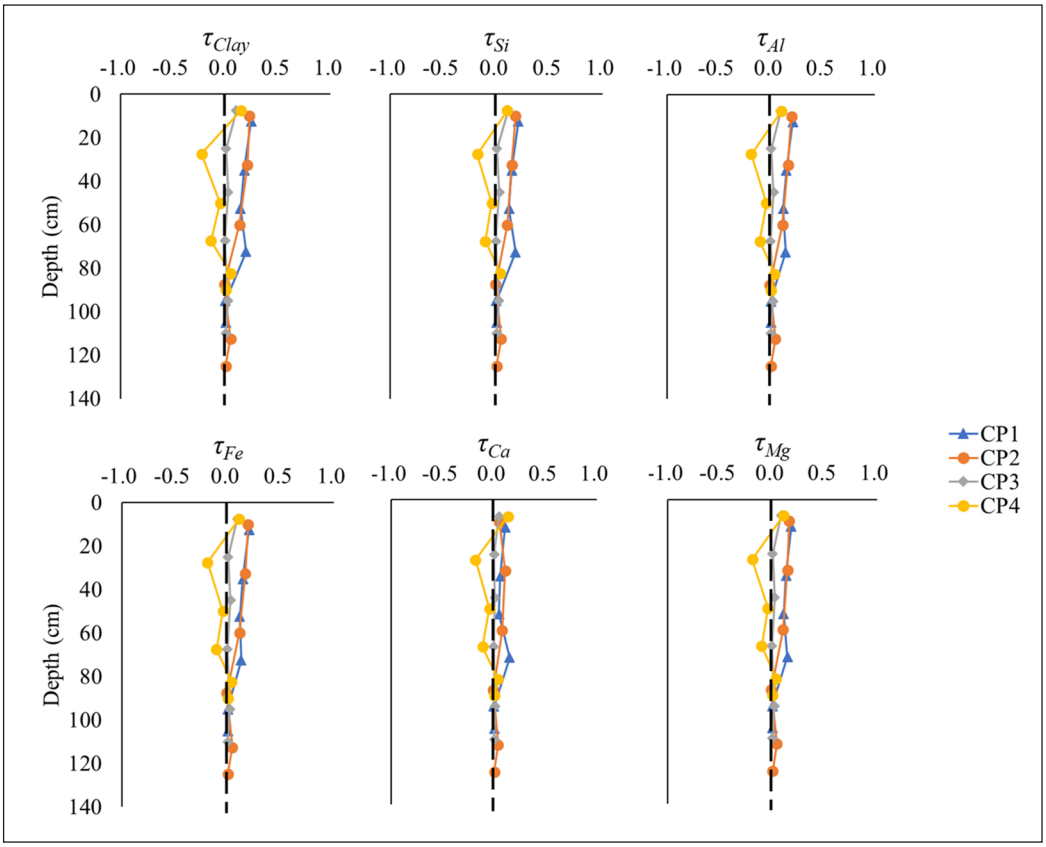

Figure 4. Mass transport coefficient (τ) of clay, Si, Al, Fe, Ca, and Mg with depth

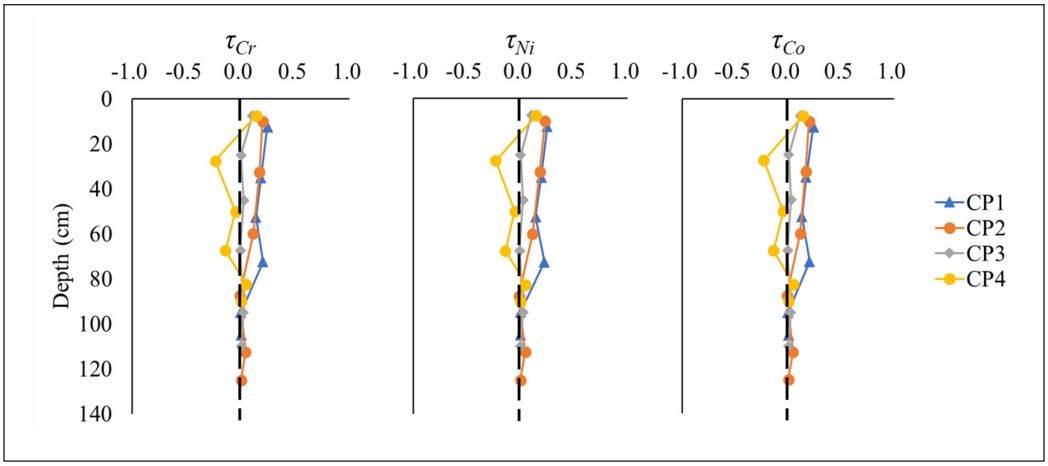

Figure 5. Mass transport coefficient (τ) of Cr, Ni, and Co with depth

CONCLUSION

The study provided a comprehensive understanding of their mineralogical and geochemical properties, highlighting the intricate relationships between soil formation processes and trace metal dynamics. The study identified key minerals such as chlorites, feldspars, and quartz, which reflect that the studied soils were not derived from typical ophiolite parent materials (serpentine) but rather mudstones. It also revealed that the concentrations of trace metals, including Cr, Ni, and Co, were influenced significantly by the presence of Fe and Al oxides. Moreover, the mobility and retention of trace metals in the studied pedons are closely linked to soil texture, suggesting that well-drained, coarse-textured soils may facilitate leaching. The accumulation of trace metals in CP1, CP2, and CP3 pedons (summit and upper backslope) rather than in CP4 (footslope) emphasized the need to consider local soil characteristics and environmental factors in understanding trace metal behavior. Additionally, the results emphasized the variability in trace metal concentrations across different pedons in the ophiolite complex, which was attributed to other parent materials and soil formation processes. Furthermore, the exploration of the relationships between trace metals and soil components highlighted the complex interactions that govern their mobility, emphasizing the need for a nuanced understanding of soil dynamics in these unique environments and providing valuable insights for future research and land management practices.

ACKNOWLEDGMENTS

The authors thank the National Science and Technology Council, Taiwan, for financially supporting this research under Grant No. MOST 111-2313-B-002-045-MY3. They would

also like to acknowledge the support of the Department of Science and Technology—Science Education Institute through the DOST-SEI Foreign Graduate Scholarships in Specialized Priority Fields in Science and Technology.

REFERENCES

Baralkiewicz, D., & Siepak, J. (1999). Chromium, nickel and cobalt in environmental samples and existing legal norms. *Polish Journal of Environmental Studies*, *8*(4), 201-208.

Bédard, É., Hébert, R., Guilmette, C., & Dostal, J. (2008). The supra-ophiolitic sedimentary cover of the Asbestos ophiolite, Québec, Canada: First geochemical evidence of transition from oceanic to continental sediment flux. *Lithos*, *105*(3–4), 239–252. https://doi.org/10.1016/j.lithos.2008.04.005

Blake, G. R., & Hartge, K. H. (1986). Bulk density. In A. K. Klute (Ed.), *Methods of soil analysis: Part 1, physical and mineralogical methods* (pp. 363–375). Academic Press. https://doi.org/10.2136/sssabookser5.1.2ed.c13

Bolaños-Benítez, V., Van Hullebusch, E., Birck, J., Garnier, J., Lens, P. N., Tharaud, M., Quantin, C., & Sivry, Y. (2021). Chromium mobility in ultramafic areas affected by mining activities in Barro Alto massif, Brazil: An isotopic study. *Chemical Geology*, *561*, 120000. https://doi.org/10.1016/j.chemgeo.2020.120000

Brimhall, G. H., & Dietrich, W. E. (1987). Constitutive mass balance relations between chemical composition, volume, density, porosity, and strain in metasomatic hydrochemical systems: Results on weathering and pedogenesis. *Geochimica Et Cosmochimica Acta*, *51*(3), 567–587. https://doi.org/10.1016/0016-7037(87)90070-6

Brimhall, G. H., Chadwick, O. A., Lewis, C. J., Compston, W., Williams, I. S., Danti, K. J., Dietrich, W. E., Power, M. E., Hendricks, D., & Bratt, J. (1992). Deformational mass transport and invasive processes in soil evolution. *Science*, *255*(5045), 695–702. https://doi.org/10.1126/science.255.5045.695

Caillaud, J., Proust, D., Philippe, S., Fontaine, C., & Fialin, M. (2009). Trace metals distribution from a serpentinite weathering at the scales of the weathering profile and its related weathering microsystems and clay minerals. *Geoderma*, *149*(3–4), 199–208. https://doi.org/10.1016/j.geoderma.2008.11.031

Chadwick, O. A., Brimhall, G. H., & Hendricks, D. M. (1990). From a black to a gray box — A mass balance interpretation of pedogenesis. *Geomorphology*, *3*(3–4), 369–390. https://doi.org/10.1016/0169-555x(90)90012-f

Chapman, S. L., & Horn, M. E. (1968). Parent material uniformity and origin of silty soils in northwest arkansas based on zirconium-titanium contents. *Soil Science Society of America Journal*, *32*(2), 265-271. https://doi.org/10.2136/sssaj1968.03615995003200020030x

Chen, S., & Torres, R. (2012). Effects of geomorphology on the distribution of metal abundance in salt marsh sediment. *Estuaries and Coasts*, *35*(4), 1018–1027. https://doi.org/10.1007/s12237-012-9494-y

Cheng, C., Jien, S., Tsai, H., Chang, Y., Chen, Y., & Hseu, Z. (2009). Geochemical element differentiation in serpentine soils from the Ophiolite Complexes, eastern Taiwan. *Soil Science*, *174*(5), 283–291. https://doi.org/10.1097/ss.0b013e3181a4bf68

Coleman, R. G., & Keith, T. E. (1971). A chemical study of serpentinization--Burro Mountain, California. *Journal of Petrology*, *12*(2), 311–328. https://doi.org/10.1093/petrology/12.2.311

Cornell, R. M., & Schwertmann, U. (2003). *The iron oxides: structure, properties, reactions, occurrences and uses* (2nd ed.). Wiley. http://doi.org/10.1002/3527602097

Da Silva, Y. J. A. B., Nascimento, C. W. A. D., Biondi, C. M., Van Straaten, P., Da Silva, Y. J. A. B., De Souza, V. S., De Araújo, J. D. C. T., Alcantara, V. C., Da Silva, F. L., & Da Silva, R. J. A. B. (2020). Concentrations of major and trace elements in soil profiles developed over granites across a climosequence in northeastern Brazil. *Catena*, *193*, 104641. https://doi.org/10.1016/j.catena.2020.104641

Dandar, O., Okamoto, A., Uno, M., & Tsuchiya, N. (2023). Mantle hydration initiated by Ca metasomatism in a subduction zone: An example from the Chandman meta-peridotite, western Mongolia. *Lithos*, *452–453*, 107212. https://doi.org/10.1016/j.lithos.2023.107212

Deer, W. A., Howie, R. A., & Zussman, J. (2013). *An introduction to the rock-forming minerals* (3rd ed.). Berforts Information Press. https://doi.org/10.1180/dhz

Dilek, Y., & Furnes, H. (2014). Ophiolites and their origins. *Elements*, *10*(2), 93–100. https://doi.org/10.2113/gselements.10.2.93

DiPietro, J. A. (2013). Keys to the interpretation of Geological history. In J. A. DiPietro (Ed.), *Landscape evolution in the United States: An introduction to the geography, geology, and natural history* (pp. 327–344). Elsevier. https://doi.org/10.1016/b978-0-12-397799-1.00020-8

Egli, M., Mirabella, A., & Sartori, G. (2008). The role of climate and vegetation in weathering and clay mineral formation in late Quaternary soils of the Swiss and Italian Alps. *Geomorphology*, *102*(3–4), 307–324. https://doi.org/10.1016/j.geomorph.2008.04.001

Garver, J. I., Royce, P. R., & Smick, T. A. (1996). Chromium and nickel in shale of the taconic foreland: A case study for the provenance of fine-grained sediments with an ultramafic source. *Journal of Sedimentary Research*, *66*(1), 100–106. https://doi.org/10.1306/d42682c5-2b26-11d7-8648000102c1865d

Gawlick, H., & Missoni, S. (2019). Middle-late Jurassic sedimentary mélange formation related to ophiolite obduction in the Alpine-Carpathian-Dinaridic Mountain Range. *Gondwana Research*, *74*, 144–172. https://doi.org/10.1016/j.gr.2019.03.003

Gee, G. W., & Bauder, J. W. (1986). Particle-size analysis. In A. K. Klute (Ed.), *Methods of soil analysis: Part 1, physical and mineralogical methods* (pp. 383–411). Academic Press. https://doi.org/10.2136/sssabookser5.1.2ed.c15

Gonnelli, C., & Renella, G. (2012). Chromium and nickel. In B. J. Alloway (Ed.), *Heavy metals in soils: Trace metals and metalloids in soils and their bioavailability* (pp. 313–333). Springer. https://doi.org/10.1007/978-94-007-4470-7_11

Grieco, G., Ferrario, A., & Mathez, E. A. (2004). The effect of metasomatism on the Cr-PGE mineralization in the Finero Complex, Ivrea Zone, Southern Alps. *Ore Geology Reviews*, *24*(3–4), 299–314. https://doi.org/10.1016/j.oregeorev.2003.05.004

Harnois, L. (1988). The CIW index: A new chemical index of weathering. *Sedimentary Geology*, *55*(3–4), 319–322. https://doi.org/10.1016/0037-0738(88)90137-6

Ho, C. (1988). *An introduction to the geology of Taiwan: Explanatory text of the geologic map of Taiwan*. Central Geological Survey, Ministry of Economic Affairs. http://ci.nii.ac.jp/ncid/BA17266618

Hseu, Z. Y. (2018). Element enrichment in serpentine soils. In Z. Y. Hseu (Ed.), *Biogeochemistry of serpentine soils* (pp. 61–90). Nova Science Publisher. https://doi.org/10.1201/9781315154664-8

Hseu, Z. Y., Tsai, H., Hsi, H. C., & Chen, Y. C. (2007). Weathering sequences of clay minerals in soils along a serpentinitic toposequence. *Clays and Clay Minerals*, *55*(4), 389–401. https://doi.org/10.1346/ccmn.2007.0550407

Hseu, Z., Zehetner, F., Fujii, K., Watanabe, T., & Nakao, A. (2018). Geochemical fractionation of chromium and nickel in serpentine soil profiles along a temperate to tropical climate gradient. *Geoderma*, *327*, 97–106. https://doi.org/10.1016/j.geoderma.2018.04.030

Hum, H. Z., Huang, W., & Hseu, Z. (2024). Pedogenic characterization of rare earth elements in humid subtropical soils on volcanic plateaus. *Catena*, *244*, 108256. https://doi.org/10.1016/j.catena.2024.108256

Ito, A., Otake, T., Maulana, A., Sanematsu, K., Sufriadin, N., & Sato, T. (2021). Geochemical constraints on the mobilization of Ni and critical metals in laterite deposits, Sulawesi, Indonesia: A mass-balance approach. *Resource Geology*, *71*(3), 255–282. https://doi.org/10.1111/rge.12266

Jiménez-Ballesta, R., Bravo, S., García-Pradas, J., Pérez-de-los-Reyes, C., Amorós, J. A., & García-Navarro, F. J. (2022). Characteristics of vineyard soils derived from Plio-Quaternary landforms (raña or rañizo) in southern Europe. *European Journal of Soil Science*, *73*(4), e13291. https://doi.org/10.1111/ejss.13291

Jiménez-Ballesta, R., Bravo, S., Pérez-De-Los-Reyes, C., Amorós, J. A., Villena, J., & García-Navarro, F. J. (2024). Pedological formations on old mountain geomorphological surfaces of central Spain. *Heliyon*, *10*(1), e23852. https://doi.org/10.1016/j.heliyon.2023.e23852

Kabata-Pendias, A. (2011). *Trace elements in soils and plants* (4th ed.). CRC Press. https://doi.org/10.1201/b10158

Kierczak, J., Neel, C., Bril, H., & Puziewicz, J. (2007). Effect of mineralogy and pedoclimatic variations on Ni and Cr distribution in serpentine soils under temperate climate. *Geoderma*, *142*(1–2), 165–177. https://doi.org/10.1016/j.geoderma.2007.08.009

Kierczak, J., Pędziwiatr, A., Waroszewski, J., & Modelska, M. (2016). Mobility of Ni, Cr and Co in serpentine soils derived on various ultrabasic bedrocks under temperate climate. *Geoderma*, *268*, 78–91. https://doi.org/10.1016/j.geoderma.2016.01.025

Külah, T., Kadir, S., Gürel, A., Eren, M., & Önalgil, N. (2014). Mineralogy, geochemistry, and genesis of mudstones in the Upper Miocene Mustafapaşa member of the Ürgüp Formation in the Cappadocia region, central Anatolia, Turkey. *Clays and Clay Minerals*, *62*(4), 267–285. https://doi.org/10.1346/ccmn.2014.0620403

Lazar, O. R., Bohacs, K. M., Macquaker, J. H. S., Schieber, J., & Demko, T. M. (2015). Capturing key attributes of fine-grained sedimentary rocks in outcrops, cores, and thin sections: Nomenclature and description guidelines. *Journal of Sedimentary Research*, *85*(3), 230–246. https://doi.org/10.2110/jsr.2015.11

Liu, H., Xiong, Z., Jiang, X., Liu, G., & Liu, W. (2016). Heavy metal concentrations in riparian soils along the Han River, China: The importance of soil properties, topography and upland land use. *Ecological Engineering*, *97*, 545–552. https://doi.org/10.1016/j.ecoleng.2016.10.060

Ma, Y., & Hooda P. S. (2010). Chromium, nickel and cobalt. In P. S. Hooda (Ed.), *Trace elements in soils* (1st ed., pp. 461-479). Blackwell Publishing Ltd. http://doi.org/10.1002/9781444319477.ch19

Macquaker, J. H. S., Curtis, C. D., & Coleman, M. L. (1997). The role of iron in mudstone diagenesis: Comparison of Kimmeridge Clay Formation Mudstones from Onshore and Offshore (UKCS) Localities. *Journal of Sedimentary Research*, *67*(5), 871–878. https://doi.org/10.1306/d426865d-2b26-11d7-8648000102c1865d

Mclean, E. O. (1982). Soil pH and lime requirement. In A. L. Page (Ed.), *Methods of soil analysis: Part 2, chemical and microbiological properties* (2nd ed., pp. 199–224). Academic Press. https://doi.org/10.2134/agronmonogr9.2.2ed.c12

Mehra, O., & Jackson, M. (2013). Iron oxide removal from soils and clays by a dithionite–citrate system buffered with sodium bicarbonate. In E. Ingerson (Ed.), *Clays and clay minerals: Proceedings of the seventh national conference on clays and clay minerals* (pp. 317–327). Pergamon Press. https://doi.org/10.1016/b978-0-08-009235-5.50026-7

Merrot, P., Juillot, F., Pape, P. L., Lefebvre, P., Brest, J., Kieffer, I., Menguy, N., Viollier, E., Fernandez, J., Moreton, B., Radakovitch, O., & Morin, G. (2021). Comparative Cr and Mn speciation across a shore-to-reef gradient in lagoon sediments downstream of Cr-rich Ferralsols upon ultramafic rocks in New Caledonia. *Journal of Geochemical Exploration*, *229*, 106845. https://doi.org/10.1016/j.gexplo.2021.106845

Miyashiro, A., Shido, F., & Ewing, M. (1969). Composition and origin of serpentinites from the Mid-Atlantic Ridge near 24° and 30° North Latitude. *Contributions to Mineralogy and Petrology*, *23*(2), 117–127. https://doi.org/10.1007/bf00375173

Morrison, J. M., Goldhaber, M. B., Mills, C. T., Breit, G. N., Hooper, R. L., Holloway, J. M., Diehl, S. F., & Ranville, J. F. (2015). Weathering and transport of chromium and nickel from serpentinite in the Coast Range ophiolite to the Sacramento Valley, California, USA. *Applied Geochemistry*, *61*, 72–86. https://doi.org/10.1016/j.apgeochem.2015.05.018

Naldrett, A. J., & Lehmann, J. (1988). Spinel non-stoichiometry as the explanation for NI-, CU- and PGE-enriched sulphides in chromitites. In H. M. Prichard, P. J. Potts, J. F. W. Bowles & S. J. Cribb (Eds.), *Geo-Platinum 87* (pp. 93–109). Elsevier Science Publishers. https://doi.org/10.1007/978-94-009-1353-0_10

Nelson, D. W., & Sommers, L. E. (1982). Total carbon, organic carbon, and organic matter. In A. L. Page (Ed.), *Methods of soil analysis: Part 2, chemical and microbiological properties* (pp. 961-1010). Academic Press. https://doi.org/10.2134/agronmonogr9.2.2ed.c29

Nesbitt, H. W., & Young, G. M. (1982). Early Proterozoic climates and plate motions inferred from major element chemistry of lutites. *Nature*, *299*(5885), 715–717. https://doi.org/10.1038/299715a0

Oze, C., Fendorf, S., Bird, D. K., & Coleman, R. G. (2004). Chromium geochemistry in serpentinized ultramafic rocks and serpentine soils from the Franciscan complex of California. *American Journal of Science, 304*, 67–101. https://doi.org/10.2475/ajs.304.1.67

Perri, F., Milli, S., Campilongo, G., Tentori, D., & Critelli, S. (2021). The mudstone composition as reflected in the sedimentary evolution of a turbidite basin: The example of the Agnone Flysch (Molise, Italy). *Marine and Petroleum Geology*, *132*, 105241. https://doi.org/10.1016/j.marpetgeo.2021.105241

Rhoades, J. (1982). Cation exchange capacity. In A. L. Page (Ed.), *Methods of soil analysis: Part 2, chemical and microbiological properties* (2nd ed., pp. 149–157). Academic Press. https://doi.org/10.2134/agronmonogr9.2.2ed.c8

Rinklebe, J., & Shaheen, S. M. (2017). Redox chemistry of nickel in soils and sediments: A review. *Chemosphere*, *179*, 265–278. https://doi.org/10.1016/j.chemosphere.2017.02.153

Robertson, A. H., Palak, O., Tasli, K., & Dumitrica, P. (2020). Processes of clastic sedimentation associated with Late Cretaceous ophiolite emplacement in the SW segment of the Antalya Complex (S Turkey). *Sedimentary Geology*, *408*, 105718. https://doi.org/10.1016/j.sedgeo.2020.105718

Schwertmann, U., Friedl, J., Stanjek, H., & Schulze, D. G. (2000). The effect of Al on Fe Oxides. XIX. Formation of Al-Substituted Hematite from Ferrihydrite at 25°C and pH 4 To 7. *Clays and Clay Minerals*, *48*(2), 159–172. https://doi.org/10.1346/ccmn.2000.0480202

Soil Science Division Staff. (2017). Examination and description of soils profiles. In *Soil Survey Manual* (pp. 83-234). USDA-Soil Conservation Service.

Soil Survey Staff. (2022). Inceptisols. In *Keys to Soil Taxonomy* (pp. 207-246). USDA Natural Resources Conservation Service.

Tazikeh, H., Khormali, F., Amini, A., & Motlagh, M. B. (2018). Geochemistry of soils derived from selected sedimentary parent rocks in Kopet Dagh, North East Iran. *Journal of Geochemical Exploration*, *194*, 52–70. https://doi.org/10.1016/j.gexplo.2018.07.008

Tonkha, O., Butenko, A., Bykova, O., Kravchenko, Y., Pikovska, O., Kovalenko, V., Evpak, I., Masyk, I., & Zakharchenko, E. (2021). Spatial heterogeneity of soil silicon in Ukrainian phaozems and chernozems. *Journal of Ecological Engineering*, *22*(2), 111–119. https://doi.org/10.12911/22998993/130884

U. S. Environmental Protection Agency. (2021). *Method 3052 – Microwave assisted acid digestion of siliceous and organically based matrices.* https://www.epa.gov/sites/default/files/2015-12/documents/3052.pdf

Ullah, R., & Muhammad, S. (2020). Heavy metals contamination in soils and plants along with the mafic–ultramafic complex (Ophiolites), Baluchistan, Pakistan: Evaluation for the risk and phytoremediation potential. *Environmental Technology and Innovation*, *19*, 100931. https://doi.org/10.1016/j.eti.2020.100931

Verrecchia, E. P., & Trombino, L. (2021). *A visual atlas for soil micromorphologists*. Springer. https://doi.org/10.1007/978-3-030-67806-7

Wang, Y., Tsou, M., Liao, H., Hseu, Z., Dang, W., Hsi, H., & Chien, L. (2020). Influence of soil properties on the bioaccessibility of Cr and Ni in geologic serpentine and anthropogenically contaminated non-serpentine soils in Taiwan. *The Science of the Total Environment*, *714*, 136761. https://doi.org/10.1016/j.scitotenv.2020.136761

Wu, C., & Hseu, Z. (2023). Pedochemical behaviors of rare earth elements in soil profiles along a lithosequence in eastern Taiwan. *Catena*, *225*, 107047. https://doi.org/10.1016/j.catena.2023.107047

Wu, W., Guan, Y., Nel, W., & Xu, C. (2024). Heavy metal migration and Lithium isotope fractionation under extreme weathering of basalt on tropical Hainan Island, China. *Applied Geochemistry*, *175*, 106163. https://doi.org/10.1016/j.apgeochem.2024.106163

Xu, T., Nan, F., Jiang, X., Tang, Y., Zeng, Y., Zhang, W., & Shi, B. (2020). Effect of soil pH on the transport, fractionation, and oxidation of chromium (III). *Ecotoxicology and Environmental Safety*, *195*, 110459. https://doi.org/10.1016/j.ecoenv.2020.110459

Yang, C., Nguyen, D., Ngo, H., Navarrete, I., Nakao, A., Huang, S., & Hseu, Z. (2022). Increases in Ca/Mg ratios caused the increases in the mobile fractions of Cr and Ni in serpentinite-derived soils in humid Asia. *Catena*, *216*, 106418. https://doi.org/10.1016/j.catena.2022.106418

Zhang, Y., Zhang, X., Bi, Z., Yu, Y., Shi, P., Ren, L., & Shan, Z. (2020). The impact of land use changes and erosion process on heavy metal distribution in the hilly area of the Loess Plateau, China. *The Science of the Total Environment*, *718*, 137305. https://doi.org/10.1016/j.scitotenv.2020.137305

Pertanika J. Trop. Agric. Sci. 48 (3): 1019 - 1040 (2025)

PERTANIKA JOURNALS

TROPICAL AGRICULTURAL SCIENCE

Journal homepage: http://www.pertanika.upm.edu.my/

Brown Plant Hopper Resistance in Promising Doubled Haploid Rice Lines Selected by MGIDI and FAI-BLUP Index

Iswari Saraswati Dewi[1], Bambang Sapta Purwoko[2]*, Ratna Kartika Putri[2] and Iskandar Lubis[2]

[1]Research Organization of Agriculture and Food, National Research and Innovation Agency (BRIN), Kawasan Sains dan Teknologi (KST) Soekarno, Jl. Raya Jakarta - Bogor KM 46, Cibinong-Bogor, West Java 16911, Indonesia

[2]Department of Agronomy and Horticulture, Faculty of Agriculture, IPB University, Kampus IPB Dramaga, Bogor 16680, Indonesia

ABSTRACT

Rice (*Oryza sativa* L.) is the main source of calories for the world's population but faces challenges from climate change and pest infestations, particularly the brown planthopper (BPH) in Indonesia. This study assessed agronomic traits, yield components, and resistance to BPH in 16 rice genotypes, comprising 14 doubled-haploid (DH) lines and two commercial varieties (Ciherang and Inpari 18). Genotype selection involved the Multi-Trait Genotype–Ideotype Distance Index (MGIDI) and Factor Analytic Index-Based Best Linear Unbiased Prediction (FAI-BLUP). Genotype-by-trait (GT) biplots were also utilized to visualize genotype performance across various traits. The response of the DH lines to BPH was assessed using biotypes 1, 2, and 3. The MGIDI-selected genotypes, were M-5, M-7, and M-12, which yielded 9.0-, 8.9-, and 9.6- ton ha^{-1}, respectively. They significantly surpassed yield of the commercial checks. M-5 and M-7 were also selected in the FAI-BLUP, while M-12 was not due to the advantage of trait weighting in the MGIDI analysis. These lines aligned with the selection goals based on the rice ideotype, demonstrating ideal agronomic performance. The effectiveness of both MGIDI and FAI-BLUP in the selection has shown promising results, explaining 100% of the variance among traits and resulting in predicted genetic gains indicating improvements in most traits. Two promising DH lines (M-5 and M-7) showed moderate resistance to BPH biotype 1 and moderately susceptible to biotype 2 while susceptible to biotype 3. This variability highlights the challenge of using these lines in different environments with those two BPH biotypes.

Keywords: Agronomic trait, BPH, doubled-haploid, multivariate selection, selection index

ARTICLE INFO

Article history:
Received: 03 September 2024
Accepted: 30 December 2024
Published: 16 May 2025

DOI: https://doi.org/10.47836/pjtas.48.3.20

E-mail addresses:
iswari.dewi01@gmail.com (Iswari Saraswati Dewi)
bspurwoko@apps.ipb.ac.id (Bambang Sapta Purwoko)
ratnakputri@apps.ipb.ac.id (Ratna Kartika Putri)
iskandarlbs@yahoo.com (Iskandar Lubis)
* Corresponding author

e-ISSN: 2231-8542

INTRODUCTION

Rice (*Oryza sativa* L.) provides 20% of the calorie intake required by humans worldwide and exceeds 70% of human calorie requirements in several Asian countries (Zhao et al., 2020). Of the total global rice production, 90.6% is produced in Asia (Mohidem et al., 2022). The majority of rice consumers were also in Asia, where from 2018 to 2020, the per capita rice consumption reached 77 kg per year. Meanwhile, in Latin America, Africa, Europe, Oceania, and North America, the per capita rice consumption levels were 28.0 kg, 27.4 kg, 13.5 kg, and 6.3 kg per year, respectively (Rahman & Zhang, 2023). According to the Food and Agriculture Organization of the United Nation ([FAO], 2021), rice consumption in low-income Asian countries such as Indonesia is expected to increase from 122 kg per capita per year in 2020 to 129 kg by 2030, following previous trends. According to data released by the United States Department of Agriculture ([USDA], 2023), to meet global rice demand, rice production in 2024 is projected to increase by 8.1 million tons from the previous year, with an estimate of reaching 520.9 million tons of dry paddy rice. However, this projection may not be reached due to production constraints, one of which is global climate change.

The Asian continent is the region most vulnerable to the impacts of global climate change (Queiroz et al., 2021). These impacts include unpredictable pest and disease attacks (Iqbal et al., 2023; Nguyen et al., 2023), which limit agricultural activities and threaten food availability. In 2020, approximately 720 to 811 million people worldwide experienced hunger, mainly due to climate change, conflict, and economic slowdowns (FAO, IFAD, UNICEF, WFP, & WHO, 2021). Global climate change is also leading to increasing water scarcity and land degradation problems, adding complexity to crop production (Hermans & McLeman, 2021). The impact of climate change significantly reduces rice yields (Habib-ur-Rahman et al., 2022). Therefore, the primary focuses in developing superior rice varieties in these conditions are high yields, good quality, resistance to pests and diseases, and tolerance to environmental stress (Rezvi et al., 2023).

Doubled haploid (DH) rice lines derived from anther culture can be used to accelerate the development of new varieties (Hadianto et al., 2023). An efficient selection method using a novel approach for genotype selection and treatment recommendation based on information on multiple traits that overcome the fragility of classical linear indexes called multi-trait genotype–ideotype distance index (MGIDI) has been proposed by Olivoto & Nardino (2021). The lack of varieties resistant to various pests and diseases is one of the main obstacles to achieving high rice production (Fahad et al., 2019). The worsening conditions of climate change and global warming are increasing abiotic stress and affecting the biological processes of biotic factors like pests and diseases, including their development, reproduction, and survival rates, and their interactions with host plants (Wang et al., 2022). Plants respond differently to abiotic factors compared to biotic factors,

and most pests and diseases can co-evolve with the host plant, causing the host to remain vulnerable and increasing the potential for epidemics (Bhar et al., 2021). Therefore, developing hosts that are resistant to pests and diseases is considered a practical approach to addressing these challenges (Wang et al., 2021).

On average, 37% of global rice plantations experience yield loss due to pests and diseases every year. In particular, insects significantly limit high rice production (Rasool et al., 2020). The use of insecticides to control insects has reportedly led to an increase in secondary incidences, especially of the brown planthopper (BPH) (*Nilaparvata lugens*), and in the long term, has resulted in consistent resistance (Wu et al., 2018). The BPH, an important pest of rice plants, is widespread in tropical areas, especially in the Asia-Pacific region (Iamba & Dono, 2021). Peak BPH outbreaks in Indonesia occurred during La Nina in 2010 and 2011, affecting 137,481 hectares and 221,832 hectares, respectively, with estimated losses of around Indonesian Rupiah (IDR) 1,102 trillion in 2010 and IDR 1,740 trillion in 2011 (Baehaki & Mejaya, 2014). While the number of BPH attacks in Indonesia was lower in 2023, it is reported that the affected area increased by 1.4% from 6,068.2 hectares in 2022 to 8,511.53 hectares in 2023 (Forecasting Center for Plant Pest Organisms, 2023).

The severity of BPH attacks tends to increase under the conditions of global climate change (Ali et al., 2014). Continuous high temperatures caused by climate change affect the growth, fecundity, and reproductive fitness of the BPH. Such conditions may drive BPH migration to more suitable areas, potentially exacerbating damage in those environments (Yang et al., 2021). A study by Surmaini et al. (2024) models the impact of climate variability on the distribution of BPH in Indonesia, forecasting an increase in BPH-damaged areas from 2024 to 2060. Higher temperatures and rainfall during the dry season, especially linked to La Niña events, significantly influence BPH dynamics. Horgan et al. (2021) found that high temperatures reduce the effectiveness of anti-herbivore resistance in rice, affecting BPH distribution to suitable environments. The study also shows that resistant varieties lower adult survival at 20–25°C and nymph weight gain at 25°C, aligning with optimal temperatures for survival and development. Thereby enhancing rice production in changing climates.

Direct damage is caused by BPH-sucking plant fluids, leading to the drying and death of plants (hopper burn). Additionally, brown planthoppers are vectors that spread viruses, which cause extended yield losses and crop failure in rice plants (Jeevanandham et al., 2023). Therefore, it is important to develop high-yielding rice varieties with good agronomic performance and resistance to BPH in anticipation of the outburst of BPH attacks due to climate change. This research discussed the yield, important agronomic traits, and resistance of the DH rice lines to BPH.

MATERIAL AND METHODS

Yield Trial

Plant Material

A yield trial was conducted in Indramayu, West Java, in December 2023. The genetic material used in the yield trial was 14 DH rice lines (M-1 to M-14) and 2 check commercial varieties (M-15: Ciherang and M-16: Inpari 18), as listed in Table 1. Doubled haploid lines were obtained from anther culture of several F1s, specifically F1: Inpago 8 × IR8770514-11-B-SKI-12 (M-1 to M-3); F1: Inpago 8 × IR83140-B-11-B (M-4 to M-9); F1: B1111430D-MR-1-1-PN-3-MR-2-Si-3-PN × IR83140-B-11-B (M-10 to M-14).

Methods

The yield trial was arranged in a randomized complete block design (RCBD) with one factor, namely, the genotype, with 16 levels and three replications. The experimental unit was a plot measuring 4 m × 5 m, with a population density of 320 rice hills per plot. Maintenance included replanting, irrigation arrangements, fertilization, and pest and disease control. Harvesting occurred when 90% of the panicles in one plot were yellow.

Observation

Observations included agronomic traits and yield components, including vegetative (VPH) and generative plant heights (GPH), the number of vegetative tillers (NVT) and productive tillers per hill (NPT), the ages at flowering (FA) and harvest (HA), the number of filled (NFG) and unfilled grains (NUG), the weight of 1000 grains (W1000), and productivity (PRD). Observations were carried out on ten hills of sample plants per experimental unit.

Data Analysis

Genotype selection was performed based on simultaneous multiple traits selection using several approaches to compare the effectiveness of each selection method. The traits include all observed agronomic and yield component traits. The methods include the Multi-Trait Genotype–Ideotype Distance Index (MGIDI) (Olivoto & Nardino, 2021) and Factor Analytic Index-Based Best Linear Unbiased Prediction (FAI-BLUP) (Rocha et al., 2018). In addition, the Genotype by Trait (GT) biplot was utilized to visualize the relationships between genotypes and their performance across various traits. Analysis of variance (ANOVA) and posthoc LSD tests were conducted using SAS On Demand for Academics, while genotype selection analysis was performed using the metan R package (Olivoto & Lúcio, 2020). Genetic gains were compared using those analyses to determine

the most effective approaches for selecting genotypes based on multiple trait selection using MGIDI and FAI-BLUP. This comparison contributes to more informed decision-making in breeding programs to improve crop performance.

Multi-Trait Genotype–Ideotype Distance Index (MGID) in this study was conducted with a selection percentage of 30% across multiple traits. Consequently, genotypes with lower MGIDI closer to the ideotype were chosen. The MGIDI index theory revolves around four steps, which were rescaled of the traits to a uniform range of 0 to 100, factor analysis to address the correlation structure and reduce data dimensionality, planning the ideotype based on the known or desired trait values, and finally, calculating the distance between each genotype and the planned ideotype (Olivoto & Nardino, 2021). In this study, the rescaled traits considered the desired direction of selection (increase or decrease) aligned with breeding objectives. The traits designated as increasing include NVT, NPT, PL, NFG, W1000, and PRD. Productivity (PRD) was given a weighting of (+) 3, considering productivity is a crucial target trait in rice breeding programs. Meanwhile, traits designated for the decrease were VPH, GPH, FA, HA, and NUG. In the biplot genotype ranking results from the MGIDI, the selected genotypes are those closest to the cut point according to the selection pressure. Strength and weakness plots were then used to analyze the proportion of MGIDI values.

Factor Analytic Index-Based Best Linear Unbiased Prediction (FAI-BLUP) was also conducted with a selection percentage of 30%, assigning maximum and minimum values for traits based on their desirable and undesirable traits, in alignment with the rice New Plant Type (NPT) ideotype. This approach mirrors the methodology used in MGIDI. Specifically, traits such as NVT, NPT, PL, NFG, W1000, and PRD were designated as desirable for maximum values (undesirable for minimum values). Conversely, traits including VPH, GPH, FA, HA, and NUG were considered desirable for minimum values (undesirable for maximum values). The analysis utilized best linear unbiased prediction (BLUP) values to rank genotypes based on their performance, incorporating factor analysis to capture the correlation structure among traits. The ideotype was then designed using factorial scores adjusted to reflect the ideal trait values (Rocha et al., 2018). Subsequently, the spatial probability was estimated using the genotype-ideotype distance to facilitate the ranking of genotypes.

The GT biplot was one of the GGE biplot methods used to study genotype-trait interaction data (Shojaei et al., 2022). An analysis was carried out to explore the interactions between genotypes and their performance across the various evaluated traits. This analysis provided insights into how specific traits contributed to overall performance and highlighted genotypes that were consistently superior or exhibited particular strengths of traits. In biplot analysis based on traits, genotypes were considered as lines and traits as testers, enabling the visualization of genotype performance and ranking genotypes with each trait.

Brown Plant Hopper (BPH) Evaluation

Plant Material

The Brown plant hopper evaluation was conducted at the Indonesian Center for Rice Standard Testing (ICRIST) greenhouse in Sukamandi, West Java, Indonesia. The same genetic material as in the Yield Trial was used (Table 1), adding BPH checks (PTB33 and IR74 as resistant and TN-1 as susceptible checks). BPH biotypes 1, 2, and 3 were used in the resistance evaluation. BPH biotypes were grouped according to their virulency to differential varieties (Chaerani et al., 2021).

Table 1
List of DH lines and check varieties

No	Genotype	No	Genotype
1.	M-1	9.	M-9
2.	M-2	10.	M-10
3.	M-3	11.	M-11
4.	M-4	12.	M-12
5.	M-5	13.	M-13
6.	M-6	14.	M-14
7.	M-7	15.	M-15
8.	M-8	16.	M-16

Note. DH lines obtained from another culture of several F_1s crosses F_1: Inpago 8 × IR8770514-11-B-SKI-12 (M-1 to M-3); F_1: Inpago 8 × IR83140-B-11-B (M-4 to M-9); F_1: B1111430D-MR-1-1-PN-3-MR-2-Si-3-PN × IR83140-B-11-B (M-10 to M-14). Check varieties: M-15: Ciherang; M16: Inpari 18

Methods

Brown plant hopper biotypes were propagated on susceptible rice plants (IR 42) in insect-rearing cages. The maintenance involved fertilizing, watering, weeding, and collecting egg masses to obtain adult BPHs for multiplication. Egg-laying occurred 40–45 days after transplanting (DAT) by transferring 25 pairs of male and female planthoppers to new plants in mylar buckets for 48 hours, after which they were returned to the stock cage. The eggs were kept until evaluation. One week later, 2–3 instar planthoppers were harvested for resistance evaluation. Genotypes were sown in plastic boxes filled with NPK-treated soil, with each furrow containing 25 seeds based on the genotype being planted.

The experiment was conducted with three replications. At the age of seven days, the plants were infested with two or three BPH nymph instars, with a density of eight individuals per stem. Observations were conducted when the susceptible check variety showed 90% death by calculating the level of damage based on International Rice Research Institute Standard Evaluation System (IRRI SES) as presented in Table 2. The

Table 2
Response of rice plants to brown planthopper attack

Score	Damage	Category
0	No damage	Resistant (R)
1	Very slight damage	Resistant (R)
3	First and 2nd leaves of most plants partially yellowing	Moderately resistant (MR)
5	Pronounced yellowing and stunting, or about 10% to 25% of plants wilting or dead, and remaining plants severely stunted or dying	Moderately susceptible (MS)
7	More than half of the plants are dead	Susceptible (S)
9	All the plants are dead	Highly susceptible (HS)

Source: IRRI SES (2013)

collected data were analyzed descriptively to compare the resistance of each genotype to the BPH biotype.

RESULTS AND DISCUSSIONS

Agronomic Performance and Yields of Tested Genotypes

The agronomic traits and yields of the tested genotypes varied (Table 3). The tested DH lines exhibited some characteristics of a new plant type, characterized by the high number of grains per panicle, productive tillers, sturdy stems, early harvest, and moderate plant height. Plant height modulated susceptibility to lodging and photosynthetic efficiency, and it had a relationship with environmental factors and cultivation management, as modeled by Confalonieri et al. (2011). Plant height also contributed to the canopy characteristics of rice plants, which was an essential aspect of plant protection against pests and diseases (Jing et al., 2023). Therefore, plant height is a focus in developing superior varieties. Eight DH lines, M-3, M-5 to M-7, and M-10 to M-13 had plant heights in the 80–125 cm range, which was ideal and equivalent to the commercial variety Inpari 18 (99.7 cm). The other DH lines had plant heights above 125 cm, but their height was still similar to Ciherang.

The tested DH lines had sufficient productive tillers, ranging from 15 to 19 per hill. The DH lines with productive tillers equivalent to Ciherang and Inpari 18 were M-1 to M-8. A high number of productive tillers in rice plants significantly increases yields and production efficiency because more panicles could increase the grains per unit of land area and the total yield. A tiller behavior study found that more panicles in tillers produced higher yields (Srimathi & Subramanian, 2022). In addition, a study by Huang et al. (2020) revealed that around 85% of the variation in the total grain number was caused by the primary tiller grain yield, which was positively related to primary tiller panicles.

Plant age was another critical characteristic that was taken into account. Ideally, superior rice varieties mature between 105 and 124 days after sowing (DAS). Based on flowering and harvesting age observations, Inpari 18 had early flowering and harvesting ages of 74 DAS and 107 DAS, respectively. The M-4 line was identified as having a harvest age equivalent to Inpari 18, namely 107 DAS, with a flowering age close to 77 DAS. All the tested DH lines were classified as having early maturity, and some outperformed Ciherang (119 DAS).

A rice plant's yield is determined by the sink size, which includes the number of grains, the percentage of filled grains, and the weight of 1000 grains (Mai et al., 2021). A high weight of 1000 grains means that each grain of rice has a greater mass, indicating good yields if other factors are ideal. Nine of the tested DH lines, namely, M-3 and M-7 to M-14, had significantly higher numbers of filled grains than the two check varieties. Most DH lines showed 1000-grain weights in the 25–30 g range, with one line, M-12, having a significantly higher weight of 34 g for 1000 grains than the check varieties.

Table 3
Agronomic performance and yield of 16 rice genotypes

Genotype	VPH	GPH'	NVT	NPT	FA	HA	PL	NUG'	NFG	W1000	PRD
M-1	92.8	150.3	20.2	17.9	85.7	122.0	27.3	29.9	111.2	31.0	6.5
M-2	85.6	134.2	21.2	19.7	87.0	121.0	27.3	30.3	110.4	30.0	8.4
M-3	85.4	112.5	21.4	19.4	86.3	121.0	26.5	40.3	162.1	26.7	7.6
M-4	84.5	139.9	21.3	18.8	77.7	107.0	26.9	62.2	110.0	27.0	3.2
M-5	65.1	93.2	21.6	18.0	79.0	111.0	27.0	25.8	157.1	26.0	9.0
M-6	65.2	92.6	22.0	18.6	79.0	111.0	25.4	22.0	153.8	24.0	7.9
M-7	89.0	119.5	20.0	17.8	82.0	113.0	28.5	24.3	175.0	27.7	8.9
M-8	92.8	142.5	19.4	16.9	82.7	116.0	29.8	32.7	177.1	25.3	7.9
M-9	99.0	151.3	18.4	16.2	81.0	114.3	31.7	35.6	184.2	26.7	7.5
M-10	78.8	112.5	20.2	15.2	90.3	121.3	27.8	35.1	169.4	26.0	8.1
M-11	84.5	113.3	19.8	15.4	83.3	118.0	25.8	32.1	186.7	27.7	9.0
M-12	84.0	114.6	19.4	15.8	83.3	115.7	25.9	34.8	174.4	34.0	9.6
M-13	92.0	120.0	19.7	15.7	90.3	118.0	28.1	37.2	184.8	26.3	7.0
M-14	95.8	127.9	18.9	15.9	92.0	118.0	27.0	42.1	183.1	26.3	6.1
M-15	76.5	141.7	22.6	19.8	85.0	119.7	25.8	24.7	127.2	26.0	7.2
M-16	82.9	99.7	20.4	18.3	74.0	107.0	25.6	29.9	137.5	32.3	7.5
Average	84.6	122.9	20.4	17.5	83.7	115.9	27.3	33.7	156.5	27.7	7.6
Pr> F	<0.001**	0.0001**	<0.001**	<0.001**	<0.001**	<0.001**	<0.001**	0.0004**	<0.001**	<0.001**	<0.001**
CV (%)	2.1	2.6	3.1	5.8	1.8	0.4	2.2	6.2	7.9	3.1	8.0
LSD	2.9	31.6	1.0	1.7	1.65	0.78	1.0	11.8	20.5	1.4	1.0

Note. '= Data have been transformed using the logarithm (log[x]). *Pr> F*= Probability of *F* value in the ANOVA test, *CV*= Coefficient of variation (%), ** highly significant difference at α= 0.01, ns= not significantly different at α= 0.05, *LSD*= critical value of *LSD* test to determine the significance of the difference between the means at α= 0.05. VPH= vegetative plant height (cm), GPH= generative plant height (cm), NVT= number of vegetative tillers per hill, NPT= number of productive tillers per hill, FA= flowering age (day after sowing), HA= harvesting age (day after sowing), PL= panicle length (cm), NUG= total number of unfilled grains, NFG= number of filled grains, W1000= 1000-grain weight (g), PRD= productivity (t ha^{-1})

As one of the essential traits in evaluating the performance of genotypes, panicle length was studied in this research. The panicle lengths of the DH lines M-3, M-6, M-11, and M-12 were equivalent to those of the two check varieties. In comparison, the other DH lines had improved panicle lengths significantly longer than those of the two check varieties, ranging from 26.9 to 31.7 cm.

Productivity is the primary consideration because the ideal variety must produce high yields per unit land area. In general, the productivity of the tested DH lines varied. The rice lines M-2, M-5, M-7, M-11, and M-12 showed significantly higher productivity than Ciherang. Except for M-2 (equivalent to Inpari 18), these lines also exhibited significantly higher productivity than Inpari 18. Selection to identify potential high-yield DH lines with desirable ideotypes could be done using simultaneous multi-trait selection methods based on agronomic traits and yield components (Baraki et al., 2024; Olivoto & Nardino, 2021).

In this study, genotype selection was performed using the MGIDI described by Olivoto and Nardino (2021) and FAI-BLUP by Rocha et al. (2018). The Multi-Trait Genotype–Ideotype Distance Index (MGIDI) and the Factorial Analysis of Interaction Best Linear Unbiased Prediction (FAI-BLUP) explained 100% of the variance among the traits through the principal components PC1-PC11 (Table 4). There were slight differences in the proportions of variance explained by each principal component, which were negligible. Thus, the overall explanatory power of both methods remained comparable. This indicated that while specific components might capture varying amounts of variance, the methods effectively represented the underlying data structure across all traits, reflecting their robustness in genotype selection.

Table 4
Principal components, eigenvalues, and cumulative variance in MGIDI and FAI-BLUP

MGIDI			FAI-BLUP		
PC	**Eigenvalue**	**Cum. var (%)**	**PC**	**Eigenvalue**	**Cum. var (%)**
PC1	3.90	35.4	PC1	3.87	35.22
PC2	2.38	57.1	PC2	2.37	56.75
PC3	1.70	72.5	PC3	1.69	72.16
PC4	1.31	84.4	PC4	1.33	84.23
PC5	1.06	94.1	PC5	1.07	93.99
PC6	0.25	96.3	PC6	0.23	96.07
PC7	0.20	98.2	PC7	0.22	98.07
PC8	0.11	99.2	PC8	0.12	99.15
PC9	0.06	99.7	PC9	0.06	99.68
PC10	0.03	99.9	PC10	0.03	99.89
PC11	0.01	100.0	PC11	0.01	100.00

Note. PC= principal component, Cum.var= cumulative variance

In both MGIDI and FAI-BLUP analyses, the observed traits were grouped into five factors (FA), as shown in Table 5. The MGIDI index selected the genotypes M-7, M-5, M-12, M-16 (Inpari 18), and M-9 (Figure 1[a]). Among these selected genotypes, MGIDI shares three lines with the FAI-BLUP index, which were M-7, M-16, and M-5. The genotypes selected by FAI-BLUP were M-7, M-16, M-5, M-8, and M-6 (Figure 2). Based on the predicted genetic gain, MGIDI demonstrated superior performance compared to FAI-BLUP for traits expected to increase in value, such as panicle length, productivity, W1000, number of vegetative and productive tillers, and number of filled grains. This is evident from the higher total increase in predicted genetic gain values for these traits, as shown in Table 5. Conversely, for traits where the selection goal is to decrease, FAI-BLUP outperformed MGIDI, with a higher total decrease in predicted genetic gain across traits such as vegetative and generative plant height, number of unfilled grains, flowering age, and harvesting age.

Each trait remains important in developing the ideal rice genotype. Thus, both MGIDI and FAI-BLUP can be effectively used to select and provide options for breeders. The higher predicted genetic gain values for traits targeted for enhancement under MGIDI and FAI-BLUP emphasize their advantage in selecting genotypes that better meet breeding objectives. In the context of traits targeted for increase, the more positive total increase in predicted genetic gain, such as 11.48% in MGIDI compared to 4.22% in FAI-BLUP, indicates a stronger addition. Meanwhile, the more negative total decrease in predicted

Table 5
Factor analysis and predicted genetic gain for MGIDI and FAI-BLUP indexes

Trait	Factor analysis		Goal	Predicted genetic gain (%)	
	MGIDI	FAI-BLUP		MGIDI	FAI-BLUP
VPH	FA1	FA1	Decrease	-0.62	-5.61
GPH	FA1	FA1	Decrease	-0.07	-0.10
PL	FA1	FA1	Increase	0.46	-0.03
NUG	FA2	FA2	Decrease	-0.12	-0.19
PRD	FA2	FA2	Increase	0.91	0.64
FA	FA3	FA3	Decrease	-3.80	-4.32
HA	FA3	FA3	Decrease	-3.67	-4.27
W1000	FA4	FA4	Increase	1.65	-0.62
NVT	FA5	FA5	Increase	-0.45	0.26
NPT	FA5	FA5	Increase	-0.24	0.45
NFG	FA5	FA5	Increase	9.14	3.52
Total (Increase)				11.48	4.22
Total (Decrease)				-8.26	-14.49

Note. VPH= vegetative plant height, GPH= generative plant height, PL= panicle length, NUG= number of unfilled grains, PRD= productivity, FA= flowering age, HA= harvesting age, W1000= 1000-grain weight, NVT= number of vegetative tillers per hill, NPT= number of productive tillers per hill, NFG= number of filled grains

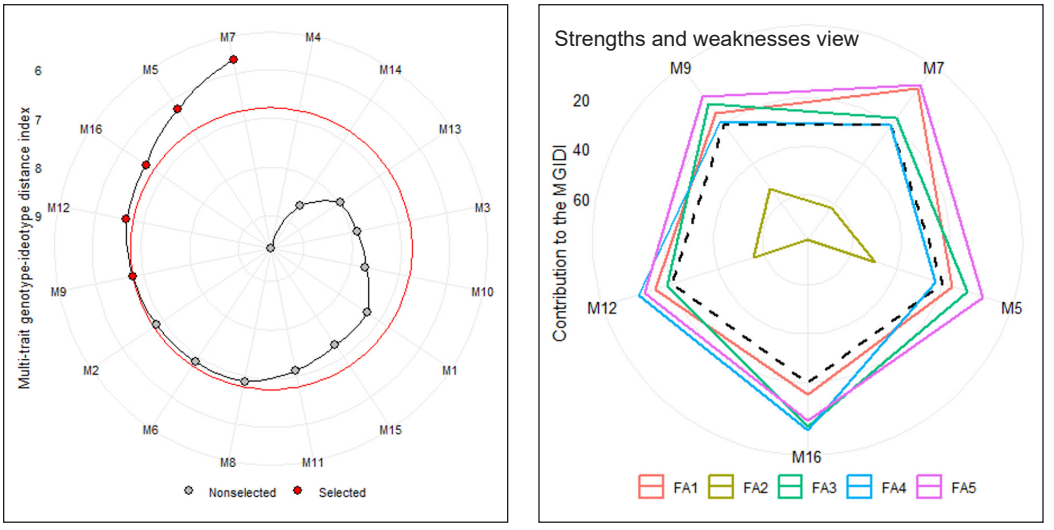

(a) (b)

Figure 1. (a) Genotype ranking in ascending order for the MGIDI index with a selection pressure of 30%; the selected genotypes were shown in red dot, and the circle represents the cutpoint according to the selection pressure. (b) The strengths and weaknesses of the selected genotype are shown in the proportion of each factor on the computed multi-trait genotype–ideotype distance index (MGIDI). The factor contributing the most to selection is represented by the polygon closest to the center of the MGIDI. Genotype strength in a specific factor is indicated by the outermost polygon nearest to the genotype. The closer the genotype is to the outer polygon of a factor, the stronger its performance for the traits grouped under that factor. The dashed line shows the theoretical value if all the factors had contributed equally. FA1= vegetative plant height, generative plant height, and panicle length, FA2= number of unfilled grains and productivity, FA3= flowering age and harvesting age, FA4= 1000 grain weight, FA5= number of vegetative tillers and productive tillers per hill and number of filled grains

genetic gain, such as -14.49% in FAI-BLUP compared to -8.26% in MGIDI, reflects a stronger reduction, aligning with the selection goal. These results further support the effectiveness of both methods in achieving breeding objectives.

When examining the differences, MGIDI showed a slightly higher predicted genetic gain than FAI-BLUP, with MGIDI being 1.02% higher than FAI. These results were consistent with Olivoto and Nardino (2021), which demonstrated that the performance of the MGIDI index in selecting superior genotypes based on multi-trait data surpassed that of classical indices,

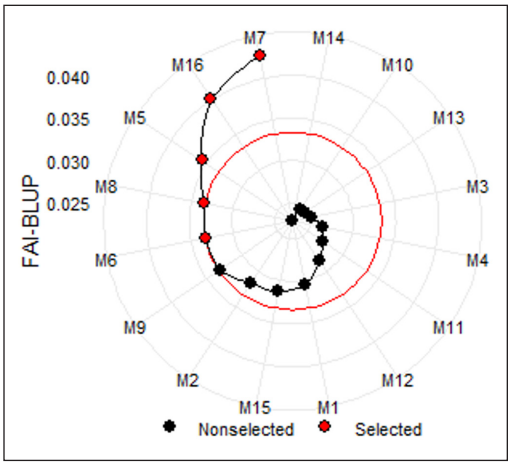

Figure 2. Genotype ranking based on the FAI-BLUP method with a selection percentage of 30%. The selected genotypes were highlighted with red dots, and the circle indicates the cut point corresponding to the selection pressure applied

including the Smith-Hazel (SH) index, a widely-used base linear phenotypic selection index, as well as modern methods like FAI-BLUP, thereby aiding practitioners in making more effective strategic decisions for multivariate selection in biological experiments. Various researchers have used MGIDI and revealed its effectiveness in selecting superior genotypes while simultaneously considering multiple traits (Al Mamun et al., 2024; Baraki et al., 2024; Klein et al., 2023; Mamun et al., 2022; Pallavi et al., 2024; Raj et al., 2024).

Multi-Trait Genotype–Ideotype Distance Index (MGIDI) is considered superior to FAI-BLUP for several reasons. First, in MGIDI, the breeder could lead the direction of selection for each trait by assigning 'h' (high) for traits intended to increase and 'l' (low) for traits intended to decrease (Olivoto et al., 2022; Debnath et al., 2024). Although FAI-BLUP can also specify the direction of selection by assigning "max" and "min" for traits that are desired to increase and decrease, MGIDI offered an additional advantage by allowing breeders to apply weightings to traits based on their economic importance or alignment with breeding goals. For example, in this study, a trait like productivity (PRD) was given higher weight than other traits to reflect its importance in the rice breeding program. In contrast, FAI-BLUP does not provide this option for weighting traits, which limits its customization for specific breeding priorities. This explained the two genotypes not selected by FAI-BLUP but selected by MGIDI, i.e., M-12 and M-9, due to their superior traits. The productivity trait was given a higher weight than other traits (+3) in the MGIDI analysis, so M-12 was selected due to its high productivity. As a result, this genotype performed better under the MGIDI index. M-9, due to its high number of filled grains, was selected following the predicted genetic gain for the goal of an increase in MGIDI. The number of filled grains had a predicted genetic gain of 9.14% compared to only 3.52% in FAI-BLUP.

Moreover, MGIDI offers a visualization of the strengths and weaknesses of each selected genotype through factor analysis (Figure 1[b]), which allows breeders to understand why certain genotypes were selected (Olivoto & Nardino, 2021). This visual representation could clarify specific traits that contributed to the genotypes' selection, providing deeper insights into their overall performance. FAI-BLUP, on the other hand, lacks this further visualization and only identifies which genotypes were selected. Therefore, MGIDI is a more powerful tool for breeders, as it allows customization through trait weighting and provides visual insights to support the selection process.

The selected genotypes by MGIDI were M-7, M-5, M-12, M-16 (Inpari 18), and M-9. In Figure 1(b), it can be seen that FA2 (NUG and PRD) made the largest contribution to the MGIDI. The strengths of these lines are as follows: M-5 is strong in PRD, FA, HA, VPH, and GPH; M-7 is strong in PRD, VPH, GPH, NFG, FA, HA, and W1000; M-12 demonstrates strength in PRD, W1000, NFG, VPH, GPH, FA, and HA; and M-9 is strong in NFG, HA, FA, and PL. M-16 (Inpari 18) is slightly weaker in FA1 (VPH, GPH, and PL). This finding aligns with the description of the Inpari 18 variety, known for its relatively shorter plant height, approximately ±93 cm (in this study, it measured 99.7 cm).

Biplot genotype by trait (GT) biplot type 3, also known as the "which-won-where" biplot, visualizes the interaction of traits with genotypes (Figure 3). The polygon formed connects the outer genotype (those with the most extended vectors from the center of the polygon) in all directions. Dashed lines drawn from the center of the polygon divide the traits into sections. The genotypes on the outer edges of the polygon indicate extreme performance in specific traits. In contrast, genotypes near the center of the polygon are generally more stable. Genotypes M5 and M6 are among the outer corner of the polygon and demonstrate good performance in specific traits, with M5 leaning towards PRD (evidenced by a PRD value of 9.0 t ha^{-1}) and M6 leaning towards NVT, indicated by its high value corresponding to their positions on the polygon. Genotype M-9 is another outer genotype in the area with PL, FA, HA, and VPH traits. Among these traits, M-9 is closest to PL, highlighting M-9's superiority in PL. Genotype M-12 is the outermost genotype closest to PRD (demonstrated by the highest PRD among all genotypes), followed by genotypes M-11 and M-7, which also exhibit high PRD and tend to be closer to the center of the polygon, indicating consistently average performance across all traits. These results do not precisely align with the strengths and weaknesses observed in MGIDI, as MGIDI considers various factors that may not be fully reflected in the two principal components (PC1 and PC2) of this biplot, which together explain approximately 57.1% of the total variance among traits.

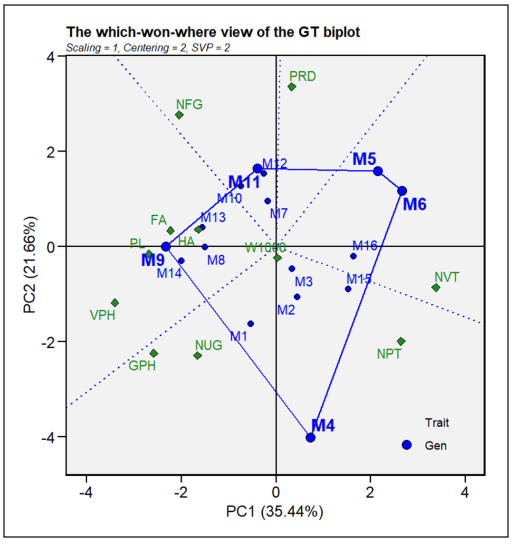

Figure 3. Which-won-where view of the genotype by trait biplot. Genotypes are labeled with blue circles, and traits with green diamonds. The biplot captures 57.1% of the total variance among traits, with PC1 accounting for 35.44% and PC2 for 21.66%. GT= genotype by trait, SVP= singular value partitioning, PC= principal component

Resistance of Tested Genotypes to Brown Planthoppers

Several DH lines (M-2 to M-9) demonstrated moderate resistance to biotype 1 brown planthopper (BPH) but exhibited varied responses to biotypes 2 and 3 (Figure 4). Specifically, resistance levels ranged from moderately resistant (M-2, M-3, and M-4) to moderately susceptible (M-5, M-6, M-7, M-8, and M-9) against biotype 2, and from moderately susceptible (M-2, M-3, and M-6) to susceptible against biotype 3. The tested DH lines mostly exhibited better resistance to BPH biotypes 1 and 2 than to biotype 3. This variation in resistance underscores the challenges of deploying these lines in diverse

environments where different biotypes may dominate. However, their ability to resist BPH biotypes 1 and 2 offers hope for protecting rice plants from BPH attacks. Lines with varying susceptibility require careful consideration, including thorough surveys to identify prevalent biotypes, which is essential for selecting suitable resistant varieties. In the future, farmers can reduce yield losses from BPH infestations and enhance overall productivity by using BPH-resistant varieties derived from the lines.

Varying resistance levels to brown planthopper (BPH) biotypes pose a significant challenge in developing durable resistant rice varieties (Baehaki & Mejaya, 2014). Those responses underscore the complex interactions between host plant genetics and BPH biotype characteristics. Zheng et al. (2021) note that resistance variations reflect the differing virulence of BPH among rice varieties, which depends on the specific resistance genes present in host plants. Currently, 70 BPH-resistant gene loci have been identified in rice, and 17 genes have been successfully cloned (Yan et al., 2023). Four BPH biotypes have been identified and correspond to specific resistance genes with the prefix *Bph/bph* genes. BPH biotype 1 could not infest plants with major resistance genes, while biotype 2 could infest plants with the Bph_1 gene.

Furthermore, the Bph_1 gene provides resistance to biotypes 1 and 3, the bph_2 gene offers resistance to biotypes 1 and 2, and Bph_3, bph_4, bph_8, and Bph_9 confer resistance to all four biotypes, whereas bph_5, Bph_6, and bph_7 provide resistance only to biotype 4 (Cheng et al., 2013). BPH biotypes 1 and 2 are common in East and Southeast Asia, biotype 3 originated from laboratory breeding, and biotype 4 is prevalent in the Indian subcontinent. BPH

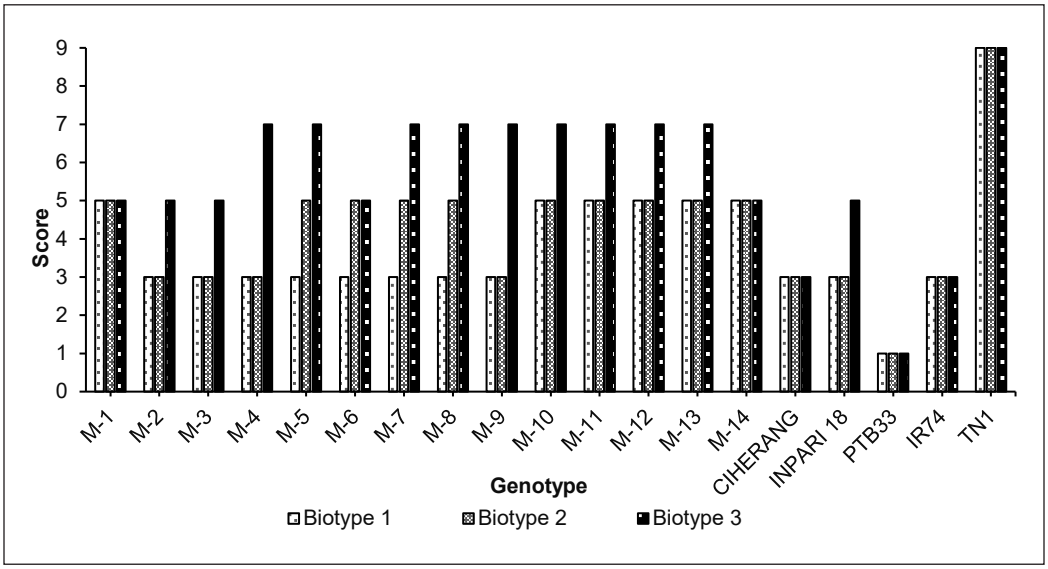

Figure 4. Bar diagram of resistant scoring on test genotypes to brown planthopper biotypes 1, 2, and 3. Score 0-1= resistant, 3= moderately resistant, 5= moderately susceptible, 7= susceptible, 9= highly susceptible. PTB33 and IR74= resistant check, TN1= susceptible check

distribution varies with environmental conditions and agricultural practices, as shown by Surmaini et al. (2024), who modeled BPH biotype distribution based on climate suitability, identifying regions in southern Indonesia as particularly favorable.

The TN-1 variety, serving as a susceptibility check for BPH, exhibited a high susceptibility to the three biotypes of BPHs (Figure 4). This aligns with the findings of Chaerani et al. (2021), who confirmed that TN1 lacks a single *Bph* (brown planthopper) gene, making it susceptible to all biotypes of BPHs. *Bph* is the gene for resistance to brown planthoppers. The resistance check, PTB33, is reported to have three Bph genes, BPH_2, BPH_{17}-*ptb*, and BPH_{32}, causing durable resistance (Nguyen et al., 2021). That aligns with the results of this study, as PTB33 showed resistance to all BPH biotypes tested. IR74 is reported to have the BPH_3 locus, which can overcome Biotype 3 (Jena & Kim, 2010). The evaluation results for IR74 showed moderate resistance to all biotypes and were equivalent to popular rice varieties such as Ciherang. Meanwhile, the commercial variety Inpari 18 showed moderate resistance to Biotypes 1 and 2 but was moderately susceptible to Biotype 3.

Selected DH Lines and Their Resistance to BPH

All DH lines significantly varied in agronomic traits and yield components, with several lines showing promising characteristics. The field performance of the four selected rice genotypes is shown in Figure 5. Three out of the four selected DH lines based on MGIDI significantly outperformed the commercial varieties Ciherang and Inpari 18 in terms of yield, with M-7, M-5, and M-12 yielding 8.9-, 9.0-, and 9.6- ton ha^{-1}, respectively. Among these, M-7 and M-5 were also selected by FAI-BLUP, highlighting their consistent performance across both selection methods. M-12, previously selected by MGIDI, was not chosen by FAI-BLUP, likely due to its higher productivity, which was weighted more heavily in the MGIDI analysis. These three DH lines demonstrated desirable agronomic traits, including ideal plant height (93.2–119.5 cm), a good number of productive tillers, and a high grain number per panicle (Table 3).

Particularly, M-5, M-7, and M-12 showed notable strength based on MGIDI strengths and weaknesses in traits such as PRD, FA, HA, VPH, GPH, NFG, and W1000, making them ideal candidates for future breeding programs focused on improving rice yield and performance (Figure 1[b]). Regarding brown planthopper (BPH) resistance, M-5 and M-7 showed moderate resistance to biotype 1 and moderate susceptibility to biotype 2, while the M-9 line demonstrated moderate resistance to both biotypes 1 and 2. In contrast, M-12 shows susceptibility to biotypes 1 and 2. However, all lines were susceptible to biotype 3 (Table 6). This suggests that although the lines exhibit some resistance, further breeding efforts are necessary to enhance resistance to all BPH biotypes, especially biotype 3. Utilizing suitable resistant varieties for the dominant BPH biotypes in a given environment

will help farmers reduce yield losses from brown planthopper (BPH) infestations and enhance overall productivity.

The response of the selected genotypes based on the MGIDI analysis was presented in Table 6, with the selection criteria aligned with the ideal ideotype based on the Rice New Plant Type, characterized by a high number of grains per panicle, productive tillers, early harvest, and moderate plant height, along with BPH resistance. Among these lines, M-5 and M-7 stand out for their superior yields, agronomic performance, and resistance to BPH, as well as their consistent selection in both MGIDI and FAI-BLUP analyses, which aligned with the breeding goals and ideal genotype traits, making them promising candidates for future varietal development. Genotype selection using MGIDI has proven slightly more effective than FAI-BLUP in identifying these superior lines, as it offers the ability to apply trait weighting. Additionally, the biplot genotype by trait (GTB) provided valuable insights into genotype performance. For future studies, it is recommended that additional multi-environment trials be conducted to confirm their stability and adaptability.

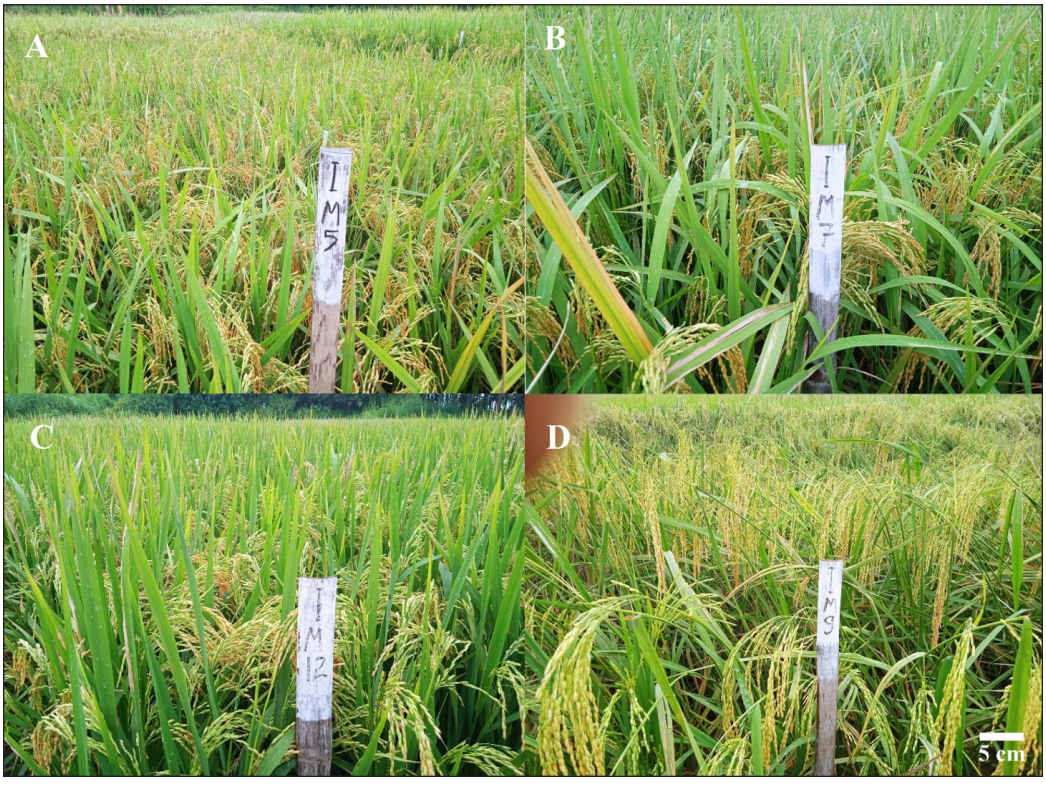

Figure 5. Field performance of four selected rice genotypes: (A) M-7, (B) M-5, (C) M-12, and (D) M-9 based on MGIDI. The photograph illustrates the agronomic appearance of the selected doubled-haploid lines in the field at the reproductive stage

Table 6
Agronomic traits, yield components, and BPH resistance of selected doubled-haploid lines based on MGIDI compared with check varieties

Traits	Doubled-haploid lines				Check variety	
	M-7	M-5	M-9	M-12	M-15	M-16
Agronomic Traits and Yield Components						
GPH	119.5	93.2	151.3	114.6	141.7	99.7
NPT	17.8	18.0	15.8	15.8	19.8	18.3
FA	82.0	79.0	82.0	83.3	85.0	74.0
HA	113.0	111.0	114.3	115.7	119.7	107.0
PL	28.5	27.0	31.7	25.9	25.8	25.6
NFG	175.5	157.1	184.2	174.4	127.2	137.5
NUG	24.3	25.8	35.6	34.8	24.7	29.9
W1000	27.7	26.0	26.7	34.0	26.0	32.3
PRD	8.9	9.0	7.5	9.6	7.2	7.5
Response to Brown Planthopper						
Biotype 1	MR	MR	MR	MS	MR	MR
Biotype 2	MS	MS	MR	MS	MR	MR
Biotype 3	S	S	S	S	MR	MS

Note. M-15= Ciherang, M-16= Inpari 18, GPH= generative plant height (cm), NPT= number of productive tillers per hill, FA= flowering age (days after sowing), HA= harvesting age (days after sowing), PL= panicle length (cm), NUG= total number of unfilled grains, NFG= the number of filled grains, W1000= 1000-grain weight (g), PRD= productivity (t ha^{-1}), MR= moderately resistant, MS= moderately susceptible, S= susceptible

CONCLUSION

The genotypes selected through the MGIDI index exhibited yields exceeding the commercial checks, with M-5, M-7, and M-12 yielding 9.0-, 8.9-, and 9.6- ton ha^{-1}, respectively. M-5 and M-7 were also selected in the FAI-BLUP analysis, while M-12 was not due to the advantage of weighting in the MGIDI analysis. These lines also demonstrate superior agronomic traits and yield components, including ideal plant height, a good number of productive tillers, a high filled grain number per panicle, and early maturity. The effectiveness of both MGIDI and FAI-BLUP in the selection has shown promising results, explaining 100% of the variance among traits and resulting in predicted genetic gains indicating improvements in most traits. The M-5 and M-7 lines show moderate resistance to BPH biotype 1 and moderate susceptibility to biotype 2, marking them as the most promising genotypes. Utilizing suitable resistant varieties based on the dominant BPH biotypes in the field will help farmers reduce yield losses and enhance productivity. However, conducting multi-environment trials to confirm the stability and adaptability of those lines, along with their resistance evaluation to other main rice diseases, is recommended to ensure robust performance across diverse environments.

ACKNOWLEDGMENTS

The authors acknowledge funding support for this research from the National Research and Innovation Agency (BRIN) and the Indonesia Endowment Funds for Education (LPDP) through the Riset dan Inovasi untuk Indonesia Maju (RIIM) Scheme, contract numbers 18/IV/KS/06/2022 and 4830/IT3.L1/PT.01.03/P/B/2022, and from Riset Aksi IPB, contract number 41079/IT3.D10/PT.01.03/P/B/2023. The authors also wish to thank the Indonesian Center for Rice Instrument Standard Testing (ICRIST), Sukamandi, for its assistance in brown plant hopper evaluation.

REFERENCES

Ali, M. P., Huang, D., Nachman, G., Ahmed, N., Begum, M. A., & Rabbi, M. F. (2014). Will climate change affect outbreak patterns of planthoppers in Bangladesh? *Plos One*, *9*(3), e91678. https://doi.org/10.1371/journal.pone.0091678

Al Mamun, S. A., Ivy, N. A., Khan, M. A. I., Rehana, S., Sultana, M. S., Adhikary, S. K., & Islam, M. M. (2024). Genotype selection from azide-induced rice mutants using multitrait genotype–ideotype distance index (MGIDI): Unveiling promising variants for yield improvement. *Advances in Agriculture*, *2024*(1), 5719580. https://doi.org/10.1155/2024/5719580

Baehaki, S. E., & Mejaya, I. M. (2014). Wereng cokelat sebagai hama global bernilai ekonomi tinggi dan strategi pengendaliannya [Brown planthopper as a high-economic-value global pest and its management strategies]. *Iptek Tanaman Pangan*, *9*(1), 1-2

Baraki, F., Gebregergis, Z., Belay, Y., Teame, G., Gebremedhin, Z., Berhe, M., Fisseha, D., Araya, G., & Gebregergs, G. (2024). Identification of adaptable sunflower (*Helianthus annuus* L.) genotypes using yield performance and multiple-traits index. *Heliyon*, *10*, e29405. https://doi.org/10.1016/j.heliyon.2024.e29405

Bhar, A., Chakraborty, A., & Roy, A. (2021). Plant responses to biotic stress: Old memories matter. *Plants*, *11*(1), 84. https://doi.org/10.3390/plants11010084

Chaerani, Dadang, A., Sutrisno, Husin, B. A., & Yunus, M. (2021). Virulence and SSR diversity of brown planthopper (*Nilaparvata lugens*) adapted on differential rice host varieties. *HAYATI Journal of Bioscience*, *28*(4), 293-303. https://doi.org/10.4308/hjb.28.4.293-303

Cheng, X., Zhu, L., & He, G. (2013). Towards understanding of molecular interactions between rice and the brown planthopper. *Molecular Plant*, *6*(3), 621-634. https://doi.org/10.1093/mp/sst030

Confalonieri, R., Bregaglio, S., Rosenmund, A. S., Acutis, M., & Savin, I. (2011). A model for simulating the height of rice plants. *European Journal of Agronomy*, *34*(1), 20-5. https://doi.org/10.1016/j.eja.2010.09.003

Debnath, P., Chakma, K., Bhuiyan, M. S. U., Reshma Thapa, R., Pan, R., & Akhter, D. (2024). A novel multi trait genotype ideotype distance index (MGIDI) for genotype selection in plant breeding: Application, prospects, and limitations. *Crop Design*, *3*, 100074. https://doi.org/10.1016/j.cropd.2024.100074

Fahad, S., Adnan, M., Noor, M., Arif, M., Alam, M., Khan, I. A., Ullah, H., Wahid, F., Mian, I. A., Jamal, Y., & Basir, A. (2019). Major constraints for global rice production. In M. Hasanuzzaman, M. Fujita, K

Nahar & J. K Biswas (Eds.), *Advances in rice research for abiotic stress tolerance* (pp. 1-22). Woodhead Publishing. https://doi.org/10.1016/B978-0-12-814332-2.00001-0

Forecasting Center for Plant Pest Organisms. (2023). *Laporan kinerja BBPOPT Tahun 2023* [BBPOPT performance report for 2023]. https://bbpopt.tanamanpangan.pertanian.go.id/informasi/laporan-kinerja-2023

Food and Agriculture Organization of the United Nation (2021). *The state of food security and nutrition in the world 2021: Transforming food systems for food security, improved nutrition, and affordable healthy diets for all.* https://doi.org/10.4060/cb4474en

Habib-ur-Rahman, M., Ahmad, A., Raza, A., Hasnain, M. U., Alharby, H. F., Alzahrani, Y. M., Bamagoos, A.A., Hakeem, K.R., Ahmad, S., Nasim, W., Ali, S., Mansour, F., & El Sabagh, A. (2022). Impact of climate change on agricultural production: Issues, challenges, and opportunities in Asia. *Frontiers in Plant Science*, *13*, 925548. https://doi.org/10.3389/fpls.2022.925548

Hadianto, W., Purwoko, B. S., Dewi, I. S., Suwarno, W. B., Hidayat, P., & Lubis, I. (2023). Agronomic performance, yield stability, and selection of doubled haploid rice lines in advanced yield trials. *AIMS Agriculture & Food*, *8*(4), 1010-1027. https://doi.org/10.3934/agrfood.2023054

Hermans, K., & McLeman, R. (2021). Climate change, drought, land degradation and migration: exploring the linkages. *Current Opinion in Environmental Sustainability*, *50*, 236-244. https://doi.org/10.1016/j.cosust.2021.04.013

Horgan, F. G., Arida, A., Ardestani, G., & Almazan, M. L. P. (2021). Elevated temperatures diminish the effects of a highly resistant rice variety on the brown planthopper. *Scientific Reports*, *11*(1), 262. https://doi.org/10.1038/s41598-020-80704-4

Huang, M., Shan, S., Cao, J., Fang, S., Tian, A., Liu, Y., Cao, F., Yin, X., & Zou, Y. (2020). Primary-tiller panicle number is critical to achieving high grain yields in machine-transplanted hybrid rice. *Scientific Reports*, *10*(1), 2811. https://doi.org/10.1038/s41598-020-59751-4

Iamba, K., & Dono, D. (2021). A review on brown planthopper (*Nilaparvata lugens* Stål), a major pest of rice in Asia and Pacific. *Asian Journal of Research in Crop Science*, *6*(4), 7-19. 10.9734/AJRCS/2021/v6i430122

International Rice Research Institute. (2013). *Standard evaluation system (SES) for Rice: 5th edition*. https://www.scribd.com/document/333585255/SES-5th-Edition

Iqbal, J., Yousaf, U., Asgher, A., Dilshad, R., Qamar, F. M., Bibi, S., Rehman, S. U., & Haroon, M. (2023). Sustainable rice production under biotic and abiotic stress challenges. In C. S. Prakash, S. Fiaz, M. A. Nadeem, F. Baloch & A. Qayyum (Eds.), *Sustainable agriculture in the era of the OMICs revolution* (pp. 241-268). Springer Cham. https://doi.org/10.1007/978-3-031-15568-0_11

Jeevanandham, N., Raman, R., Ramaiah, D., Senthilvel, V., Mookaiah, S., & Jegadeesan, R. (2023). Rice: *Nilaparvata lugens* Stal interaction—current status and future prospects of brown planthopper management. *Journal of Plant Diseases and Protection*, *130*(1), 125-141. https://doi.org/10.1007/s41348-022-00672-x

Jena, K. K., & Kim, S. M. (2010). Current status of brown planthopper (BPH) resistance and genetics. *Rice*, *3*, 161-171. https://doi.org/10.1007/s12284-010-9050-y

Jing, L., Wei, X., Song, Q., & Wang, F. (2023). Research on estimating rice canopy height and LAI Based on LiDAR Data. *Sensors*, *23*(19), 8334. https://doi.org/10.3390/s23198334

Klein, L. A., Marchioro, V. S., Toebe, M., Olivoto, T., Meira, D., Meier, C., Benin, G., Busatto, C.A., Garafini, D.C., Alberti, J.V., & Finatto, J. L. B. (2023). Selection of superior black oat lines using the MGIDI index. *Crop Breeding and Applied Biotechnology*, *23*(3), e45112332. https://doi.org/10.1590/1984-70332023v23n3a25

Mai, W., Abliz, B., & Xue, X. (2021). Increased number of spikelets per panicle is the main factor in higher yield of transplanted vs. Direct-seeded rice. *Agronomy*, *11*(12), 2479. https://doi.org/10.3390/agronomy11122479

Mamun, A. A., Islam, M. M. I., Adhikary, S. K., & Sultana, M. S. (2022). Resolution of genetic variability and selection of novel genotypes in EMS induced rice mutants based on quantitative traits through MGIDI. *International Journal of Agriculture and Biology*, *28*(2), 100-112. https://doi.org/10.17957/IJAB/15.1957

Mohidem, N. A., Hashim, N., Shamsudin, R., & Che Man, H. (2022). Rice for food security: Revisiting its production, diversity, rice milling process and nutrient content. *Agriculture*, *12*(6), 741. https://doi.org/10.3390/agriculture12060741

Nguyen, C. D., Zheng, S. H., Sanada-Morimura, S., Matsumura, M., Yasui, H., & Fujita, D. (2021). Substitution mapping and characterization of brown planthopper resistance genes from indica rice variety, 'PTB33' (*Oryza sativa* L.). *Breeding Science*, *71*(5), 497-509. https://doi.org/10.1270/jsbbs.21034

Nguyen, T. T., Grote, U., Neubacher, F., Do, M. H., & Paudel, G. P. (2023). Security risks from climate change and environmental degradation: Implications for sustainable land use transformation in the Global South. *Current Opinion in Environmental Sustainability*, *63*, 101322. https://doi.org/10.1016/j.cosust.2023.101322

Olivoto, T., Diel, M. I., Schmidt, D., & Lúcio A. D. (2022). MGIDI: A powerful tool to analyze plant multivariate data. *Plant Methods*, *18*, 121. https://doi.org/10.1186/s13007-022-00952-5

Olivoto, T., & Lúcio, A. D. C. (2020). Metan: An R package for multi-environment trial analysis. *Methods in Ecology and Evolution*, *11*(6), 783–789. https://doi.org/10.1111/2041-210X.13384

Olivoto, T., & Nardino, M. (2021). MGIDI: Toward an effective multivariate selection in biological experiments. *Bioinformatics*, *37*(10), 1383-1389. https://doi.org/10.1093/bioinformatics/btaa981

Pallavi, M., Prasad, B. M., Shanthi, P., Reddy, V. L. N., & Kumar, A. N. (2024). Multi trait genotype-ideotype distance index (MGIDI) for early seedling vigour and yield related traits to identify elite lines in rice (Oryza sativa L.). *Electronic Journal of Plant Breeding*, *15*(1), 120-131. https://doi.org/10.37992/2024.1501.020

Queiroz, C., Norström, A. V., Downing, A., Harmáčková, Z. V., De Coning, C., Adams, V., Bakarr, M., Baedeker, T., Chitate, A., Gaffney O., Gordon, L., Hainzelin, E., Howlett, D., Krampe, F., Loboguerrero, M.A., Nel, D., Okollet, C., Rebermark, M., Rockstrom, J. ... & Matthews, N. (2021). Investment in resilient food systems in the most vulnerable and fragile regions is critical. *Nature Food*, *2*(8), 546-551. https://doi.org/10.1038/s43016-021-00345-2

Rahman, A. R., & Zhang, J. (2023). Trends in rice research: 2030 and beyond. *Food and Energy Security*, *12*(2), e390. https://doi.org/10.1002/fes3.390

Raj, D. S., Patil, R. S., Patil, B. R., Nayak, S. N., & Pawar, K. N. (2024). Characterization of early maturing elite genotypes based on MTSI and MGIDI indexes: an illustration in upland cotton (*Gossypium hirsutum* L.). *Journal of Cotton Research*, *7*, 25. https://doi.org/10.1186/s42397-024-00187-w

Rasool, A., Akbar, F., Rehman, A., & Jabeen, H. (2020). Genetic engineering of rice for resistance to insect pests. In A. Roychoudhury (Eds.), *Rice research for quality improvement: genomics and genetic engineering: Volume 2: Nutrient biofortification and herbicide and biotic stress resistance in rice* (pp. 129-148). Springer Singapore. https://doi.org/10.1007/978-981-15-5337-0_7

Rezvi, H. U. A., Tahjib-Ul-Arif, M., Azim, M. A., Tumpa, T. A., Tipu, M. M. H., Najnine, F., Dawood, M., Skalicky, M., & Brestič, M. (2023). Rice and food security: Climate change implications and the future prospects for nutritional security. *Food and Energy Security*, *12*(1), e430. https://doi.org/10.1002/fes3.430

Rocha, J. R. do A. S. de C., Machado, J. C., & Carneiro, P. C. S. (2018). Multitrait index based on factor analysis and ideotype-design: proposal and application on elephant grass breeding for bioenergy. *GCB Bioenergy*, *10*(1), 52–60. https://doi.org/10.1111/gcbb.12443

Shojaei, S. H., Ansarifard, I., Mostafavi, K., Bihamta, M. R., & Zabet, M. (2022). GT biplot analysis for yield and related traits in some sunflower (*Helianthus annuus* L.) genotypes. *Journal of Agriculture and Food Research*, *10*, 100370. https://doi.org/10.1016/j.jafr.2022.100370

Srimathi, K., & Subramanian, E. (2022). Evaluation of tillering behaviour and yielding ability of different rice varieties under unpuddled conditions. *Current Journal of Applied Science and Technology*, *41*(28), 26-32. https://doi.org/ 10.9734/cjast/2022/v41i2831792

Surmaini, E., Sarvina, Y., Susanti, E., Widiarta, I. N., Misnawati, M., Suciantini, S., Fanggidae, Y. R., Rahmini, R., & Dewi, E. R. (2024). Climate change and the future distribution of Brown Planthopper in Indonesia: A projection study. *Journal of the Saudi Society of Agricultural Sciences*, *23*(2), 130-141. https://doi.org/10.1016/j.jssas.2023.10.002

United States Department of Agriculture. (2023). *Rice outlook: August 2023: Global rice trade forecast for 2023 and 2024 lowered based on export ban by India*. https://ers.usda.gov/sites/default/files/_laserfiche/outlooks/107164/RCS-23G.pdf?v=85172

Wang, B. X., Hof, A. R., & Ma, C. S. (2022). Impacts of climate change on crop production, pests and pathogens of wheat and rice. *Frontiers of Agricultural Science and Engineering*, *9*(1), 4-18. https://doi.org/10.15302/J-FASE-2021432

Wang, X., Jing, Z. H., He, C., Liu, Q. Y., Jia, H., Qi, J. Y., & Zhang, H. L. (2021). Breeding rice varieties provides an effective approach to improve productivity and yield sensitivity to climate resources. *European Journal of Agronomy*, *124*, 126239. https://doi.org/10.1016/j.eja.2021.126239

Wu, S. F., Zeng, B., Zheng, C., Mu, X. C., Zhang, Y., Hu, J., Zhang, S., Gao, C.F., & Shen, J. L. (2018). The evolution of insecticide resistance in the brown planthopper (*Nilaparvata lugens* Stal) of China in the period 2012–2016. *Scientific Reports*, *8*(1), 4586. https://doi.org/10.1038/s41598-018-22906-5

Yan, L., Luo, T., Huang, D., Wei, M., Ma, Z., Liu, C., Qin, Y., Zhou, X., Lu, Y., Li, R., Qin, G., & Zhang, Y. (2023). Recent advances in molecular mechanism and breeding utilization of brown planthopper resistance genes in rice: An integrated review. *International Journal of Molecular Sciences*, *24*(15), 12061. https://doi.org/10.3390/ijms241512061

Yang, L., Huang, L. F., Wang, W. L., Chen, E. H., Chen, H. S., & Jiang, J. J. (2021). Effects of temperature on growth and development of the brown planthopper, *Nilaparvata lugens* (Homoptera: Delphacidae). *Environmental Entomology*, *50*(1), 1-11. https://doi.org/10.1093/ee/nvaa144

Zhao, M., Lin, Y., & Chen, H. (2020). Improving nutritional quality of rice for human health. *Theoretical and Applied Genetics*, *133*, 1397-1413. https://doi.org/10.1007/s00122-019-03530-x

Zheng, X., Zhu, L., & He, G. (2021). Genetic and molecular understanding of host rice resistance and *Nilaparvata lugens* adaptation. *Current Opinion in Insect Science*, *45*, 14-20. https://doi.org/10.1016/j.cois.2020.11.005

Pertanika J. Trop. Agric. Sci. 48 (3): 1041 - 1053 (2025)

PERTANIKA JOURNALS

TROPICAL AGRICULTURAL SCIENCE

Journal homepage: http://www.pertanika.upm.edu.my/

Effects of Rainfall on Durian Productivity and Production Variability in Peninsular Malaysia

Aoi Eguchi[1]*, Noordyana Hassan[2, 3] and Shinya Numata[1]

[1]Graduate School of Urban Environmental Sciences, Tokyo Metropolitan University, Minami-Osawa 1-1, Hachioji, Tokyo 192-0397, Japan

[2]Geoscience and Digital Earth Centre (INSTeG), Research Institute of Sustainable Environment, Universiti Teknologi Malaysia, 81310 Johor Bahru, Johor, Malaysia

[3]Department of Geoinformatics, Faculty of Built Environment and Surveying, Universiti Teknologi Malaysia, 81310 Johor Bahru, Johor, Malaysia

ABSTRACT

Durian (*Durio zibethinus*) is a popular and economically valuable tropical fruit tree native to Southeast Asia. It is empirically known that weather conditions can affect spatio-temporal variations in durian production. However, few studies have investigated the influence of climatic and meteorological factors on durian production and variability. This study examined the spatio-temporal patterns of durian production in Peninsular Malaysia using published statistical data from different geographical scales (peninsular, state, and district). The effects of rainfall on durian production and yield were discussed. District-level durian production data for Peninsular Malaysia for six years (2015–2021, except 2019), published by the Malaysian Ministry of Agriculture and weather data from the World Weather Online were used for the analysis. Durian production and yield did not generally fluctuate across years at the peninsular scale but showed high variability among the years at the district level. There was a significant increase in rainfall in 2017, corresponding with a significantly lower yield. Therefore, these findings suggest that durian temporal productivity and production variability are influenced by extreme rainfall. Extreme rainfall could have reduced durian productivity by inhibiting flower bud induction and flowering, decreasing pollinator activity, and causing direct damage to the fruit and trees. However, the coefficient of variation was lower in districts with higher production, suggesting that artificial factors mitigated part of the variation in productivity because the effects of extreme weather could be mitigated by a well-managed plantation system in large farms.

Keywords: Extreme rainfall, phenology, production, tropical fruits, yield

ARTICLE INFO

Article history:
Received: 27 August 2024
Accepted: 08 October 2024
Published: 16 May 2025

DOI: https://doi.org/10.47836/pjtas.48.3.21

E-mail addresses:
aoi82e@gmail.com (Aoi Eguchi)
noordyana@utm.my (Noordyana Hassan)
nmt@tmu.ac.jp (Shinya Numata)
*Corresponding author

e-ISSN: 2231-8542

INTRODUCTION

Weather plays a significant role in tropical fruit production (Magdalita & Saludes, 2015; Ounlert & Sdoodee, 2015; Ramírez & Davenport, 2010). Due to climate change, many tropical regions have experienced longer and more intense heat waves over the past 40 years (Li, 2020). Moreover, there has been a notable trend in precipitation, with extreme precipitation events becoming more frequent and severe over the past 30 years (Ng et al., 2022). These climatic shifts render tropical ecosystems particularly vulnerable to climate changes, affecting the reproductive seasons of Southeast Asia's tropical rainforests (Numata et al., 2022). Therefore, it is crucial to identify the impact of weather on the productivity of tropical fruits.

Durian (*Durio zibethinus* L.) is a popular tropical fruit tree known as the “king of fruits." It is native to Southeast Asia and is mainly grown in Thailand, Malaysia, and Indonesia (Subhadrabandhu & Ketsa, 2001). It is an economically valuable fruit tree in Malaysia, accounting for 27.3% of total fruit production, 43.8% of total fruit area planted, and 78.0% of total fruit value (Department of Agriculture Malaysia, 2022). It is grown throughout Malaysia, with 150 registered varieties of durian (Department of Agriculture Malaysia, n.d.). Durian is harvested during two seasons in Peninsular Malaysia, from May to August and November to December (Lim & Luders, 1997). Geographic and temporal variations in durian production have been empirically demonstrated. For example, the variation between the maximum and minimum durian production in Peninsular Malaysia over 18 years (2000 to 2017) was shown to be about 2-fold (Ahmad et al., 2020). Durian production can be influenced by artificial factors such as irrigation, fertilization, pruning, artificial pollination, and pest and disease control, in addition to environmental factors, particularly climatic conditions, throughout the stages of flowering, fruiting, and harvesting (Ketsa et al., 2020; Salakpetch, 2005).

Dry periods are necessary for flower bud induction and flowering in durian, which influence productivity. The harvest season begins after the dry season in Peninsular Malaysia (Hoe & Palaniappan, 2013; Ketsa et al., 2020). Specifically, factors known to affect flower bud induction include at least 18 continuous days with daily precipitation of less than 1 mm (Zainab et al., 2002) and continuous dry periods of 7–14 days (Salakpetch, 2005). Weather conditions that affect flowering include a dry period of 10–14 days (Chandraparnik et al., 1992) and a dry season lasting 1–2 months (Yaacob & Subhadrabandhu, 1995). In addition, the wild durian species *Durio dulcis* and *Durio oxleyanus*, which are phylogenetically closely related to *D. zibethinus*, are known to synchronize with general flowering episodes observed in Southeast Asian rainforests at irregular intervals of several years (Fredriksson et al., 2006). Drought and low temperatures occurring on a seasonal scale of 2–3 months can explain the timing of large-scale synchronization of general flowering (Chen et al., 2018). Therefore, considering the close systematic relationship between durians and the two wild species (*D. dulcis* and *D. oxleyanus*) that exhibit synchronized flowering, the variability

in durian productivity may be influenced by prolonged dryness and low temperatures. Previous studies have established that a dry period and low temperatures serve as triggers for flower bud induction and flowering. However, the extent to which weather conditions impact durian productivity is still unclear. In particular, tropical rainfall is intermittent temporally and spatially (Martin et al., 2016; Trenberth et al., 2017). Therefore, conducting analyses at a finer scale is ideal for understanding the spatiotemporal effects of rainfall on durian production.

This study examined the spatio-temporal patterns of durian production in Peninsular Malaysia using durian statistical data published by the Department of Agriculture. The effects of rainfall on durian production and on yield were examined. For the analysis, we used datasets from different geographic scales, namely Peninsular Malaysia, states, and districts. The spatio-temporal variation in annual durian production at the district level in Peninsular Malaysia was analyzed, and its relationship with rainfall in the same year was evaluated.

MATERIALS AND METHODS

Study Area

Peninsular Malaysia is located between 1°E and 7°E and between 99°W and 105°W. It includes 85 districts in 11 states (Figure 1). The region is characterized by various types of forest, including montane (oak) forests, hill dipterocarp forests, lowland dipterocarp

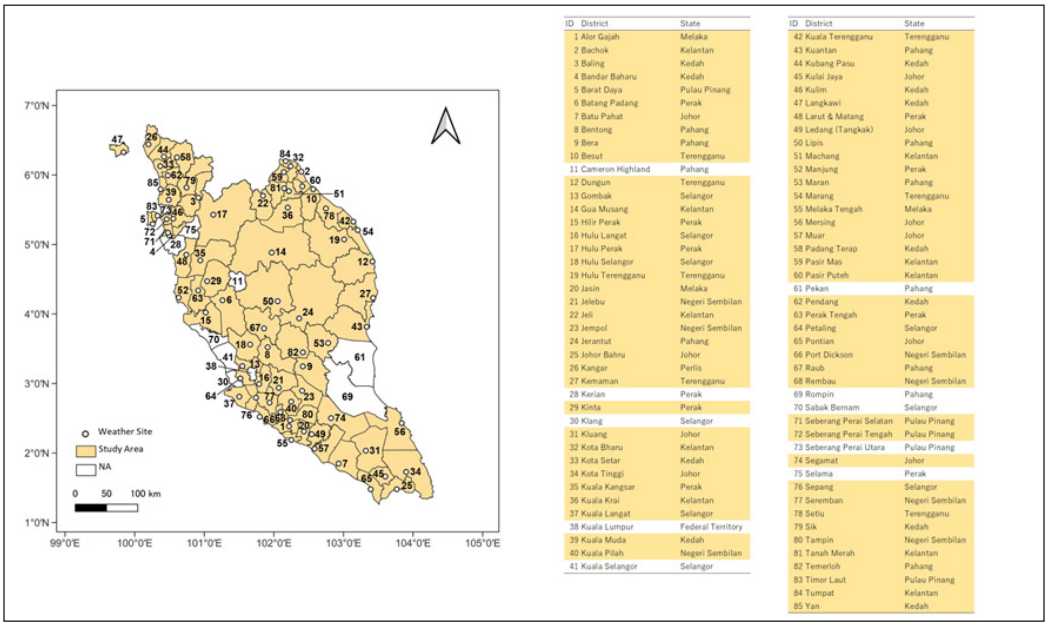

ID	District	State
1	Alor Gajah	Melaka
2	Bachok	Kelantan
3	Baling	Kedah
4	Bandar Baharu	Kedah
5	Barat Daya	Pulau Pinang
6	Batang Padang	Perak
7	Batu Pahat	Johor
8	Bentong	Pahang
9	Bera	Pahang
10	Besut	Terengganu
11	Cameron Highland	Pahang
12	Dungun	Terengganu
13	Gombak	Selangor
14	Gua Musang	Kelantan
15	Hilir Perak	Perak
16	Hulu Langat	Selangor
17	Hulu Perak	Perak
18	Hulu Selangor	Selangor
19	Hulu Terengganu	Terengganu
20	Jasin	Melaka
21	Jelebu	Negeri Sembilan
22	Jeli	Kelantan
23	Jempol	Negeri Sembilan
24	Jerantut	Pahang
25	Johor Bahru	Johor
26	Kangar	Perlis
27	Kemaman	Terengganu
28	Kerian	Perak
29	Kinta	Perak
30	Klang	Selangor
31	Kluang	Johor
32	Kota Bharu	Kelantan
33	Kota Setar	Kedah
34	Kota Tinggi	Johor
35	Kuala Kangsar	Perak
36	Kuala Krai	Kelantan
37	Kuala Langat	Selangor
38	Kuala Lumpur	Federal Territory
39	Kuala Muda	Kedah
40	Kuala Pilah	Negeri Sembilan
41	Kuala Selangor	Selangor

ID	District	State
42	Kuala Terengganu	Terengganu
43	Kuantan	Pahang
44	Kubang Pasu	Kedah
45	Kulai Jaya	Johor
46	Kulim	Kedah
47	Langkawi	Kedah
48	Larut & Matang	Perak
49	Ledang (Tangkak)	Johor
50	Lipis	Pahang
51	Machang	Kelantan
52	Manjung	Perak
53	Maran	Pahang
54	Marang	Terengganu
55	Melaka Tengah	Melaka
56	Mersing	Johor
57	Muar	Johor
58	Padang Terap	Kedah
59	Pasir Mas	Kelantan
60	Pasir Puteh	Kelantan
61	Pekan	Pahang
62	Pendang	Kedah
63	Perak Tengah	Perak
64	Petaling	Selangor
65	Pontian	Johor
66	Port Dickson	Negeri Sembilan
67	Raub	Pahang
68	Rembau	Negeri Sembilan
69	Rompin	Pahang
70	Sabak Bernam	Selangor
71	Seberang Perai Selatan	Pulau Pinang
72	Seberang Perai Tengah	Pulau Pinang
73	Seberang Perai Utara	Pulau Pinang
74	Segamat	Johor
75	Selama	Perak
76	Sepang	Selangor
77	Seremban	Negeri Sembilan
78	Setiu	Terengganu
79	Sik	Kedah
80	Tampin	Negeri Sembilan
81	Tanah Merah	Kelantan
82	Temerloh	Pahang
83	Timor Laut	Pulau Pinang
84	Tumpat	Kelantan
85	Yan	Kedah

Figure 1. Administrative division map of Peninsular Malaysia and the location of 75 districts and weather site used in this study

forests, mangroves, and peat swamps (Omar et al., 2017). In the Köppen world climate classification system, Peninsular Malaysia falls under a tropical rainforest climate (Af), characterized by high temperatures and humidity throughout the year. Temperatures range from 25°C–32°C and mean annual rainfall ranges from 2000 mm to 4000 mm (Suhaila & Jemain, 2007). Rainfall patterns in Peninsular Malaysia are affected by the north-east monsoon (NEM) from November to February and the south-west monsoon (SWM) from May to September (Mahmud et al., 2015). The timing of the wet and dry seasons varies according to geographical location. In eastern Peninsular Malaysia, the rainy season is during the northeast monsoon. In contrast, in the west, there are two rainy seasons per year: the inter-monsoon season from mid-March to May and October to November.

Durian Production Data

The genus *Durio* comprises approximately 30 species, but only *D. zibethinus* is cultivated for fruits on a large scale; therefore, this study focused on *D. zibethinus* (Lim, 1990). The annual production (mt) and planted area (ha) data for durian over six years (2015–2021, except for 2019 because the data was inaccessible) at three scales (Peninsular Malaysia, states, and districts) were obtained from the Department of Agriculture in Malaysia. This study used data from all 11 states and 75 districts in Peninsular Malaysia, excluding the ten districts with missing values: Cameron Highland, Pekan, Rompin, Kerian, Selama, Seberang Perai Utara, Klang, Kuala Selangor, Sabak Bernam, and Kuala Lumpur. According to the Department of Agriculture in Malaysia, the planted area covers all agricultural areas in Malaysia and was calculated using crop hectarage equivalent (CHE) methods. The CHE was obtained by dividing the number of trees planted on a particular lot by the recommended planting density per hectare of that particular crop. Production was estimated based on a crop production survey, potential yield, and farm records.

Weather Data

Daily rainfall (mm) and daily minimum temperature (°C) data were obtained from the World Weather Online (World Weather Online, 2023b) from 2015 to 2021, except for 2019, and the area covering 75 districts in 11 states, the same as the durian production data. Annual rainfall and minimum temperature data derived from daily rainfall and minimum temperature data were used in this study. World Weather Online provides historical weather forecast data for any geo-point by developing its own weather forecasting model using data from the World Meteorological Organization and other sources (World Weather Online, 2023a). Previous studies have also used these data (Gunthe et al., 2022; Ibekwe & Ukonu, 2019; Kamal et al., 2021). A previous study evaluated the accuracy of World Weather Online forecasts by comparing them with actual observations. It found a 70% correctness rate for rainfall forecasts for a one-day lead time in Kadoma, Zimbabwe (Terence et al., 2015).

Data Analysis

The yield (mt/ha) was calculated by dividing the production by the planted area. One-way analysis of variance (ANOVA) and Tukey's multiple comparison tests were performed to compare and clarify the temporal characteristics of each factor on durian production, yield, and rainfall for each year. The coefficients of variation (CV) of durian production and yield were calculated to evaluate the variability in the data relative to the mean at different spatial scales over six years at three scales: Peninsular Malaysia, state, and district. The six-year average for each district was taken as 100%, and the percentage difference from the average of each year's factors was calculated and mapped as an anomaly to visualize the spatial variation in production, yield, and rainfall. Spearman's rank correlation coefficients (r_s) between CV and 6-year mean production and between CV and 6-year mean yield at the district level were calculated to identify the characteristics of locations with high production variability.

Given that the harvest season in Peninsular Malaysia is from May to August and November to December and that it takes approximately three months for durian fruit to mature after flowering, the flowering periods would be from February to May and August to September (Lim & Luders, 1997; Subhadrabandhu & Ketsa, 2001). Since the flowering of tropical tree species is triggered by specific weather conditions a few weeks prior, it is likely that the weather conditions in the same year as the harvest influence durian flowering. Partial Spearman's rank correlation coefficients between production and rainfall and between yield and rainfall, excluding the influence of minimum temperature, were calculated to determine the spatial relationship between rainfall and production at the district level. All statistical analyses were performed using R ver. 4.2.2. All spatial analyses were conducted using a geographic information system QGIS 3.32.2.

RESULTS

Temporal Variability in Durian Production and Yield

Durian production and yield in Peninsular Malaysia from 2015 to 2021 (excluding 2019) displayed a relatively consistent trend, except for lower production and yield in 2017 (Figure 2a, 2b). One-way ANOVA showed no significant differences in the mean annual production from year to year ($p > 0.05$), whereas significant differences were observed in mean yield ($p < 0.05$). Tukey's multiple comparison tests showed that the mean yield was significantly lower in 2017 than in 2020 ($p < 0.05$) and 2021 ($p < 0.05$). Durian production and yield varied across different geographical scales and increased from the large (peninsular) to the small scale (district). The CV at the peninsular scale was 0.24 for production and 0.20 for yield. The mean CV was 0.40 for production, 0.32 for yield at the state level, 0.49 for production, and 0.41 for yield at the district level.

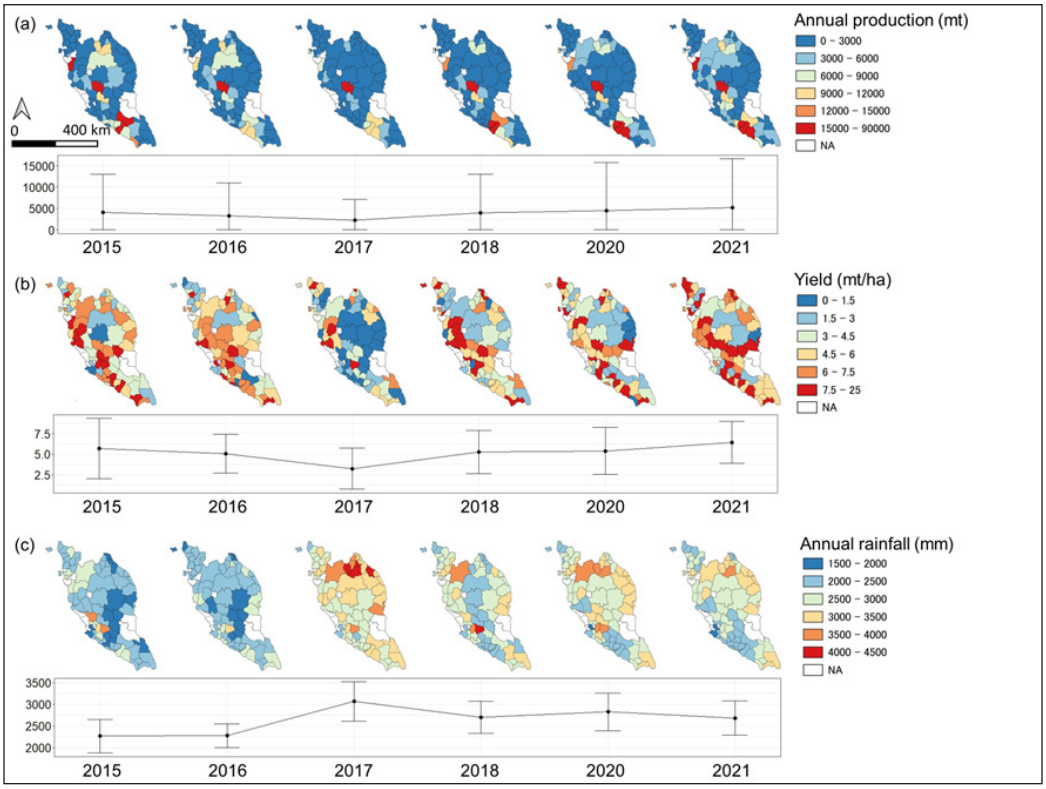

Figure 2. Geographical and temporal patterns of (a) annual production, (b) yield, and (c) annual rainfall at the district level in Peninsular Malaysia from 2015 to 2021, except for 2019. The graphs show the means (± SD)
Note. Legend of administrative divisions are shown in Figure 1

The annual production varied from 0.1 mt in Kuala Langat in 2015 to 85364.4 mt in Raub in 2021 (Figure 2a). Several districts (Raub, Ledang, Batu Pahat, and Muar) had high production; Raub had a large six-year mean production of 67977 mt, accounting for 23.3% of the total Peninsular Malaysia production. Production was consistently high in the southern part of the western coast of Peninsular Malaysia. The yield was highly uneven regionally, and the trends varied from year to year (Figure 2b). The yield ranged from 0.001 mt/ha in Kuala Langat in 2015 to 24.3 mt/ha in Jasin in 2015. It tended to be relatively high on the west coast of Peninsular Malaysia, particularly in 2015, 2020, and 2021, with relatively high yields in the southern part of the western coast of Peninsular Malaysia.

The results showed a significant negative correlation between the mean annual production and CV (r_s = -0.36, $p < 0.05$) and between the mean yield and CV (r_s = -0.30, $p < 0.05$). However, no significant relationship was observed between the annual production and yield.

Geographical Pattern of Temporal Variability in Durian Production and Yield Anomaly

The production and yield anomalies varied annually and geographically but showed low productivity throughout Peninsular Malaysia in 2017 (Figure 3a, 3b). The geographical pattern trends of production and yield in 2017 were similar, with declines, particularly in the central Peninsula. Specifically, in Peninsular Malaysia during that year, the mean annual production anomaly was -47.1%, with 92% of all districts showing a negative anomaly. Similarly, the mean yield anomaly for 2017 was -41.6% and 85.3% of all districts had a negative anomaly. From 2015 to 2016, the production and yield anomalies were higher in the central peninsula and lower in the coastal areas. Conversely, after 2018, especially in 2021, production anomalies were low in the central peninsula and high in the coastal areas.

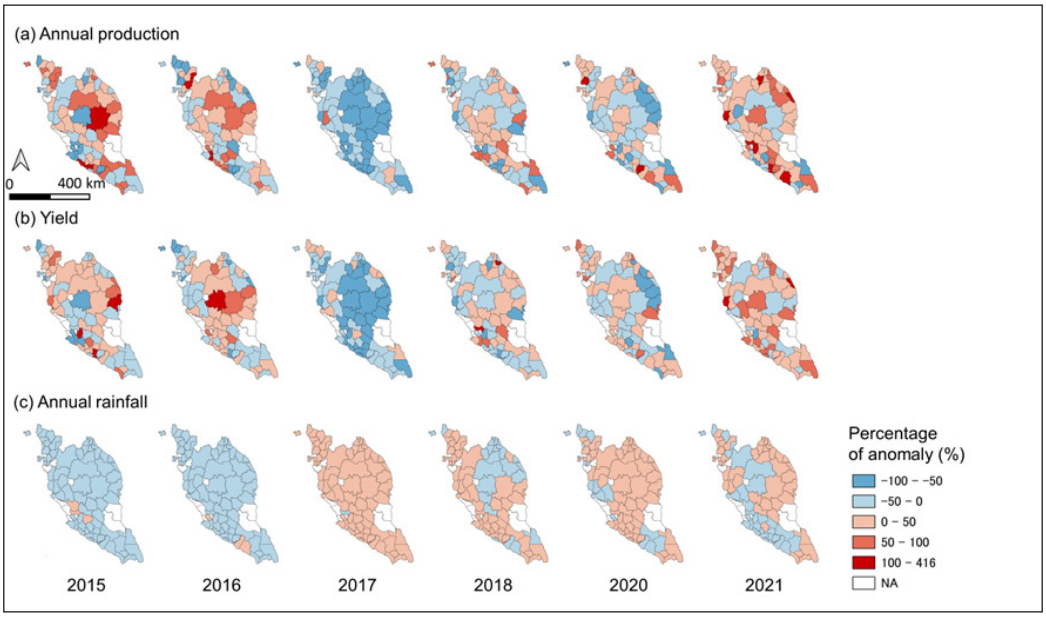

Figure 3. Spatial patterns of the percentage of anomalies for (a) annual production, (b) yield, and (c) annual rainfall at the district level in Peninsular Malaysia
Note. Legend of administrative divisions are shown in Figure 1

Temporal and Geographical Pattern of Annual Rainfall

The mean annual rainfall in 2017 was significantly higher ($p < 0.05$) than that in the other years in Peninsular Malaysia and was significantly lower in 2015 ($p < 0.05$) and 2016 ($p < 0.05$). The CV at the peninsular scale was 0.108, and the mean CV values were 0.114 and 0.130 on the state and district scales, respectively.

The annual rainfall ranged from 1531.8 mm in Kuala Pilah in 2016 to 4266.1 mm in Setiu in 2017 (mean 4266.1 mm). Rainfall was particularly low in the central Peninsula in 2015, 2016, and 2018 (Figure 2c). In 2018, 2020, and 2021, a trend of less rainfall in the southern part of the Peninsula's west coast and more rainfall in the northern part was observed.

Geographical Pattern of Temporal Variability in Rainfall Anomaly

Rainfall across Peninsular Malaysia was higher in 2017 and lower in 2015 and 2016 (Figure 3c). In 2017, rainfall anomalies were positive in all districts except for one, with a mean of 16.3%. Rainfall anomalies in 2015 and 2016 were negative in all but three districts, with mean values of 14.1% and 13.4%, respectively. The rainfall anomaly decreased in 2018 in the northern part of the east coast of Peninsular Malaysia and 2020 and 2021 on the western coast.

Spatial Relationship between Durian Production, Yield, and Rainfall

The partial Spearman's rank correlation results showed no significant correlations between production and rainfall or yield and rainfall (Table 1).

Table 1
Partial Spearman's rank correlation coefficients (r_s) between annual rainfall and annual production and between annual rainfall and yield

	Annual production		Yield	
Year	r_s	***p*-value**	r_s	***p*-value**
2015	0.07	0.53	0.09	0.43
2016	0.13	0.27	0.14	0.24
2017	0.10	0.42	0.03	0.81
2018	-0.05	0.70	0.03	0.81
2020	0.01	0.91	-0.05	0.67
2021	0.14	0.23	-0.09	0.43

DISCUSSION

This study found that higher-than-average rainfall may be the key to understanding the decline in durian productivity throughout Peninsular Malaysia. Durian production and yield were lower than average in 2017 when the level of rainfall throughout Peninsular Malaysia was significantly higher than average (Figure 2, 3). Therefore, it was concluded that durian temporal productivity and variability are influenced by extreme rainfall.

Extreme rainfall could have reduced durian productivity by suppressing durian flower bud induction and flowering, decreasing pollinator activity, and causing direct damage

to fruits and trees. First, extreme rainfall reduces the dry period required for flower bud induction and flowering (Chandraparnik et al., 1992; Zainab et al., 2002). An insufficient dry period may have reduced production by reducing flower bud induction and flowering rate. Second, bats, which are important durian pollinators in Malaysia (Low et al., 2021), have been noted to decrease their foraging activity during wet weather periods (Mohd-Azlan et al., 2010). Durian is self-incompatible, and artificial cross-pollination is recommended for commercial production. However, natural pollination is also used because artificial pollination requires ladders at night to pollinate the flowers on high branches, which is dangerous and labor-intensive (Honsho et al., 2007).

Therefore, when rainfall is high in farms where natural pollination occurs, the reduced bat activity results in inadequate pollination, which decreases production. Third, extreme rainfall and flooding have been shown to directly damage durian fruits. A positive correlation was found between rainfall and durian fruit loss (Nicolas et al., 2019). Extreme rainfall and flooding caused by Typhoon Damrey were reported throughout Penang, Kedah, and Perak in November 2017 (NASA Applied Sciences, 2017). Because one of the two durian harvesting seasons in a year is November–December (Lim & Luders, 1997), direct damage to the fruit by extreme rainfall and flooding may have contributed to the decline in production. The results suggest a potential increase in years with decreased durian production due to increased precipitation associated with abnormal weather patterns. Projections indicate an anticipated average precipitation increase of 10%–20% throughout the 21st century in the Indochina Peninsula (Tangang et al., 2020). Therefore, addressing extreme rainfall is crucial when considering variations in durian production.

Although a temporal correlation between productivity and extreme rainfall was observed, no spatial correlation was found (Table 1). This result suggests that changes in rainfall within the same location can affect productivity; however, the amount of rainfall in that specific location compared to other locations does not impact productivity. Therefore, the spatial distribution of productivity may be influenced by meteorological factors other than rainfall or human interventions, indicating the need for further research.

Several points should be noted regarding the durian statistical data used in this study. First, the statistical data were annual data with two harvest seasons combined in some areas, making it difficult to identify the timing of weather conditions that affect each harvest season. Second, because the statistical data was not variety-specific, it was impossible to discuss the differences in productivity and environmental responses among the varieties. Additionally, the differences in CVs at different scales may have occurred because of the weak spatial correlation between production and yield, which may have offset the observed range of variability in each district, resulting in a smaller assessment of the variability range at the state and peninsular levels. Although these limitations are unlikely to affect the conclusions of this study, more detailed analyses at wider spatiotemporal scales and

variety-specific data would provide a deeper understanding of the mechanisms by which extreme rainfall affects durian production.

The results also showed that highly productive areas exhibit low variability. In general, districts with high production have large farms, possibly for export, and may, therefore, have strict production management practices, such as fertilization and pest/vermin management (Datepumee et al., 2019; Thongkaew et al., 2021). Artificial pollination (Honsho et al., 2004) and soil moisture monitoring (Ramli et al., 2022) can reduce the negative effects of heavy rainfall. Therefore, extreme rainfall effects can be mitigated on large farms using a well-managed plantation system.

CONCLUSION

This study used durian statistical data to examine the spatio-temporal patterns of durian production in Peninsular Malaysia and discussed how rainfall affects durian production and yield. The results suggested that production and yield decreased in 2017 because of high annual rainfall. Therefore, it was concluded that extreme rainfall could significantly influence durian temporal productivity and variability. Two possible reasons exist for the weak correlation between durian productivity and rainfall. First, production and harvest control may partly mitigate the variations in productivity. Such artificial factors can obscure the spatial and temporal relationships between rainfall and durian productivity. In addition, the statistical data used in this study were not data by harvest period or variety, making it difficult to discuss the relationship between durian production and rainfall in terms of differences in productivity and environmental responses among varieties and to identify the timing of climatic conditions. It is necessary to consider the time lag in production data and investigate how extreme rainfall affects durian's reproductive processes to understand the mechanism by which extreme rainfall affects durian production.

ACKNOWLEDGEMENTS

This study was funded by the Japan Society for the Promotion of Science Grants-in-Aid for Scientific Research (KAKENHI), Grant Number 22J21299.

REFERENCES

Ahmad, A. A., Yusof, F., Mispan, M. R., Rasid, M. Z. A., & Nizar, M. M. M. (2020). Durian yield trends and distribution patterns in Peninsular Malaysia. *Pertanika Journal of Tropical Agricultural Science*, *43*(1), 47–64.

Chandraparnik, S., Hiranpradit, H., Punnachit, U., & Salakpetch, S. (1992). Paclobutrazol influences flower induction in durian, *Durio Zibethinus* Murr. *Acta Horticulturae*, *321*, 282–290. https://doi.org/10.17660/actahortic.1992.321.28

Chen, Y. Y., Satake, A., Sun, I. F., Kosugi, Y., Tani, M., Numata, S., Hubbell, S. P., Fletcher, C., Nur Supardi, M. N., & Wright, S. J. (2018). Species-specific flowering cues among general flowering Shorea species at the Pasoh Research Forest, Malaysia. *The Journal of Ecology*, *106*(2), 586–598. https://doi.org/10.1111/1365-2745.12836

Datepumee, N., Sukprasert, P., Jatuporn, C., Thongkaew, S. (2019). Factors affecting the production of export quality durians by farmers in Chanthaburi province, Thailand. *Journal of Sustainability Science and Management*, *14*(4), 94–105.

Department of Agriculture Malaysia (n.d.). *Varieties registered for national crop list*. Plant Variety Protection Malaysia. http://pvpbkkt.doa.gov.my/

Department of Agriculture Malaysia. (2022). *Fruit Crops Statistic 2021*. https://www.doa.gov.my/doa/resources/aktiviti_sumber/arkib/statistik_tanaman/2022/statistik_tanaman_buah_2021.pdf

Fredriksson, G. M., Wich, S. A., & Trisno. (2006). Frugivory in sun bears (*Helarctos malayanus*) is linked to El Niño-related fluctuations in fruiting phenology, East Kalimantan, Indonesia. *Biological Journal of the Linnean Society*, *89*(3), 489–508. https://doi.org/10.1111/j.1095-8312.2006.00688.x

Gunthe, S. S., Swain, B., Patra, S. S., & Amte, A. (2022). On the global trends and spread of the COVID-19 outbreak: Preliminary assessment of the potential relation between location-specific temperature and UV index. *Journal of Public Health*, *30*(1), 219–228. https://doi.org/10.1007/s10389-020-01279-y

Hoe, T. K., & Palaniappan, S. (2013). Performance of a durian germplasm collection in a Peninsular Malaysian fruit orchard. *Acta Horticulturae*, *975*, 127–137. https://doi.org/10.17660/ActaHortic.2013.975.13

Honsho, C., Somsri, S., Tetsumura, T., Yamashita, K., Yapwattanaphun, C., & Yonemori, K. (2007). Characterization of male reproductive organs in durian; anther dehiscence and pollen longevity. *Journal of the Japanese Society for Horticultural Science*, *76*(2), 120–124. https://doi.org/10.2503/jjshs.76.120

Honsho, C., Yonemori, K., Somsri, S., Subhadrabandhu, S., & Sugiura, A. (2004). Marked improvement of fruit set in Thai durian by artificial cross-pollination. *Scientia Horticulturae*, *101*(4), 399–406. https://doi.org/10.1016/j.scienta.2003.11.019

Ibekwe, P. U., & Ukonu, B. A. (2019). Impact of weather conditions on atopic dermatitis prevalence in Abuja, Nigeria. *Journal of the National Medical Association*, *111*(1), 88–93. https://doi.org/10.1016/j.jnma.2018.06.005

Kamal, A., Abidi, S. M. H., Mahfouz, A., Kadam, S., Rahman, A., Hassan, I. G., & Wang, L. L. (2021). Impact of urban morphology on urban microclimate and building energy loads. *Energy and Buildings*, *253*, 111499. https://doi.org/10.1016/j.enbuild.2021.111499

Ketsa, S., Wisutiamonkul, A., Palapol, Y., & Paull, R. E. (2020). The durian: Botany, horticulture, and utilization. *Horticultural Reviews*, *47*(4), 125–211. https://doi.org/10.1002/9781119625407.ch4

Li, X. X. (2020). Heat wave trends in Southeast Asia during 1979-2018: The impact of humidity. *The Science of the Total Environment*, *721*, 137664. https://doi.org/10.1016/j.scitotenv.2020.137664

Lim, T. K. (1990). *Durian: Diseases and disorders*. Tropical Press.

Lim, T. K., & Luders, L. (1997). *Boosting durian productivity*. Rural Industries Research and Development Corporation. https://daf.nt.gov.au/__data/assets/pdf_file/0018/227610/durian.pdf

Low, S. Y., Zulfemi, M. N. H., & Shukri, S. (2021). Small pteropodid bats are important pollinators of durian in Terengganu, Malaysia. *Pertanika Journal of Tropical Agricultural Science*, *44*(3), 583–597. https://doi.org/10.47836/pjtas.44.3.05

Magdalita, P. M., & Saludes, R. B. (2015). Influence of changing rainfall patterns on the yield of rambutan (*Nephelium lappaceum* L.) and selection of genotypes in known drought-tolerant fruit species for climate change adaptation. *Science Diliman*, *27*(1), 64–90.

Mahmud, M., Numata, S., Matsuyama, H., Hosaka, T., & Hashim, M. (2015). Assessment of effective seasonal downscaling of TRMM precipitation data in Peninsular Malaysia. *Remote Sensing*, *7*(4), 4092-4111. https://doi.org/10.3390/rs70404092

Martin, G. M., Klingaman, N. P., & Moise, A. F. (2016). Connecting spatial and temporal scales of tropical precipitation in observations and the MetUM-GA6. *Geoscientific Model Development Discussions*, *10*, 105-126. https://doi.org/10.5194/gmd-10-105-2017

Mohd-Azlan, J., Alek Tuen, A., & Abd Rahman, M. R. (2010). Preliminary assessment of activity pattern and diet of the lesser dog faced fruit bat *Cynopterus brachyotis* in a Dipterocarp Forest, Sarawak, Borneo. *Tropical Ecology*, *51*(2), 175–180.

NASA Applied Sciences (2017). *Typhoon Damrey 2017*. Retrieved December 25, 2023, from https://appliedsciences.nasa.gov/

Ng, C. Y., Wan Jaafar, W. Z., Mei, Y., Othman, F., Lai, S. H., & Liew, J. (2022). Assessing the changes of precipitation extremes in Peninsular Malaysia. *International Journal of Climatology*, *42*(15), 7914–7937. https://doi.org/10.1002/joc.7684

Nicolas, S. C. L., Abad, R. G., Tac-an, M. I. A., & Bayogan, E. R. V. (2019). Yield and harvest quality of thinned durian (*Durio Zibethinus* Murray CV. 'puyat'). *Journal of Science, Engineering and Technology*, *7*(1), 9–18. https://doi.org/10.61569/ffv7kt86

Numata, S., Yamaguchi, K., Shimizu, M., Sakurai, G., Morimoto, A., Alias, N., Noor Azman, N. Z., Hosaka, T., & Satake, A. (2022). Impacts of climate change on reproductive phenology in tropical rainforests of Southeast Asia. *Communications Biology*, *5*(1), 1–10. https://doi.org/10.1038/s42003-022-03245-8

Omar, H., Misman, M. A., & Kassim, A. R. (2017). Synergetic of PALSAR-2 and Sentinel-1A SAR polarimetry for retrieving aboveground biomass in dipterocarp forest of Malaysia. *Applied Sciences*, *7*(7), 675. https://doi.org/10.3390/app7070675

Ounlert, P., & Sdoodee, S. (2015). The effects of climatic variability on mangosteen flowering date in southern and eastern of Thailand. *Research Journal of Applied Sciences Engineering and Technology*, *11*(6), 617–622. https://doi.org/10.19026/rjaset.11.2021

Ramírez, F., & Davenport, T. L. (2010). Mango (*Mangifera indica* L.) flowering physiology. *Scientia Horticulturae*, *126*(2), 65–72. https://doi.org/10.1016/j.scienta.2010.06.024

Ramli, M. S. A., Abidin, M. S. Z., Hean, P. B., Rahman, M. A. A., Perumal, T., & Reba, M. N. (2022). Empirical based irrigation model using predicted soil moisture for durian plantation. *Control, Instrumentation and Mechatronics: Theory and Practice. Lecture Notes in Electrical Engineering*, *921*, 261-272. https://doi.org/10.1007/978-981-19-3923-5_23

Salakpetch, S. (2005). Durian (Durio zibethinus L.) flowering, fruit set and pruning. In M. A. Nagao (Ed.), *Proceedings of the Fifteenth Annual International Tropical Fruit Conference* (pp. 17-26). Hawaii Tropical Fruit Growers. https://www.cabidigitallibrary.org/doi/full/10.5555/20123109774

Subhadrabandhu, S., & Ketsa, S. (2001). *Durian: king of tropical fruit.* Daphne Brasell Associates.

Suhaila, J., & Jemain, A. A. (2007). Fitting daily rainfall amount in Malaysia using the normal transform distribution. *Journal of Applied Sciences*, *7*(14), 1880-1886. https://doi.org/10.3923/jas.2007.1880.1886

Tangang, F., Chung, J. X., Juneng, L., Supari, Salimun, E., Ngai, S. T., Jamaluddin, A. F., Mohd, M. S. F., Cruz, F., Narisma, G., Santisirisomboon, J., Ngo-Duc, T., Van Tan, P., Singhruck, P., Gunawan, D., Aldrian, E., Sopaheluwakan, A., Grigory, N., Remedio, A. R. C., … Kumar, P. (2020). Projected future changes in rainfall in Southeast Asia based on CORDEX–SEA multi-model simulations. *Climate Dynamics*, *55*(5–6), 1247–1267. https://doi.org/10.1007/s00382-020-05322-2

Terence, D. M., Emmanuel, M., Tichaona, Z., & Nation, M. (2015). Assessment of the reliability of world weather online forecasts for Kadoma community. *Journal of Earth Science & Climatic Change*, *6*(7), 291. https://doi.org/10.4172/2157-7617.1000291

Thongkaew, S., Jatuporn, C., Sukprasert, P., Rueangrit, P., & Tongchure, S. (2021). Factors affecting the durian production of farmers in the eastern region of Thailand. *International Journal of Agricultural Extension*, *9*(2), 285–293. https://doi.org/10.33687/ijae.009.02.3617

Trenberth, K. E., Zhang, Y., & Gehne, M. (2017). Intermittency in precipitation: Duration, frequency, intensity, and amounts using hourly data. *Journal of Hydrometeorology*, *18*(5), 1393–1412. https://doi.org/10.1175/JHM-D-16-0263.1

Wiangsamut, B., & Wiangsamut, M. E. (2022) Effects of paclobutrazol on flowering of juvenile durian trees cv. 'Monthong' and its costs and returns of production. *International Journal of Agriculture Technology*, *18*(5), 2315-2328.

World Weather Online. (2023a). *About world weather online*. https://www.worldweatheronline.com/aboutus.aspx

World Weather Online. (2023b). *Historical weather data*. https://www.worldweatheronline.com/hwd/

Yaacob, O., & Subhadrabandhu, S. (1995). *The production of economic fruits in South-East Asia*. Oxford University Press.

Zainab, R. S., Zainal Abidin, M., & Norzila, M. G. (2002, September 10-12). Performance of promising durian hybrids at MARDI Bukit Tangga. In *Proceedings of the 13th Malaysian Society of Plant Physiology Conference 2002* (pp. 191-196). Malaysian Society of Plant Physiology.

Pertanika J. Trop. Agric. Sci. 48 (3): 1055 - 1070 (2025)

PERTANIKA JOURNALS

TROPICAL AGRICULTURAL SCIENCE

Journal homepage: http://www.pertanika.upm.edu.my/

Bazzania spiralis Extracts Exhibit Effective Toxicity and Oviposition Deterrence against *Bemisia tabaci*

Norlyiana N. R. Azmee[1], Chin Wen Koid[1], Gaik Ee Lee[2], Thilahgavani Nagappan[1], Muhammad Zulhilmi Ramlee[3], Wahizatul Afzan Azmi[1] and Nur Fariza M. Shaipulah[1]*

[1]Faculty of Science and Marine Environment, Universiti Malaysia Terengganu, 21030 Kuala Nerus, Terengganu, Malaysia

[2]Institute of Tropical Biodiversity and Sustainable Development, Universiti Malaysia Terengganu, 21030 Kuala Nerus, Terengganu, Malaysia

[3]Centre of Research and Field Service (CRaFS), Universiti Malaysia Terengganu, Kuala Nerus 21030, Terengganu, Malaysia

ABSTRACT

The silverleaf whitefly, *Bemisia tabaci*, is a major agricultural pest that has developed resistance to many synthetic pesticides, necessitating the search for effective, eco-friendly alternatives. This study investigated the insecticidal potential of crude methanol extracts from the liverwort *Bazzania spiralis* against *B. tabaci*. Toxicity assays demonstrated 100% mortality achieved at 1000µg/ml after 48 hours of exposure. The LC_{50} values ranged from 699.37µg/ml (12 hours) to 22.00µg/ml (60 hours). The extracts exhibited strong oviposition deterrence (31.5%) and reduced egg hatchability (39.39%) at 500µg/ml. Gas chromatography-mass spectrometry analysis revealed eleven compounds in the extract, with sesquiterpenes (59%) and fatty acids (35.4%) as major constituents. The predominant compounds were spathulenol (48.7%) and palmitic acid ethyl ester (22.2%). These findings suggest that *Bazzania spiralis* extracts have potential as a natural alternative to synthetic pesticides for *B. tabaci* management. Further research is needed to isolate active compounds, evaluate field efficacy, and assess environmental persistence and effects on beneficial insects.

Keywords: Biopesticide, GC-MS, insecticidal activity, liverwort, whitefly

ARTICLE INFO

Article history:
Received: 29 July 2024
Accepted: 27 September 2024
Published: 16 May 2025

DOI: https://doi.org/10.47836/pjtas.48.3.22

E-mail addresses:
lyianaazmee2813@gmail.com (Norlyiana N. R. Azmee)
wenkoid@gmail.com (Chin Wen Koid)
gaik.ee@umt.edu.my (Gaik Ee Lee)
thila.vani@umt.edu.my (Thilahgavani Nagappan)
zulramlee@umt.edu.my (Muhammad Zulhilmi Ramlee)
wahizatul@umt.edu.my (Wahizatul Afzan Azmi)
fariza@umt.edu.my (Nur Fariza M. Shaipulah)
*Corresponding author

INTRODUCTION

The silverleaf whitefly (*Bemisia tabaci*) is a major pest of chili plants in Malaysia. Whitefly nymphs and adults damage the plants by sucking the sap from leaves,

causing physiological disorders in plants such as chlorotic spots on leaves and abortion of immature fruits. Moreover, the feeding process by adult whiteflies may transmit the lethal begomovirus from one plant to another (Czosnek et al., 2017). The begomovirus-type pepper yellow leaf curl virus (PepYLCV) has been reported to infect chili plants in Indonesia, Thailand and Malaysia, which then exhibit symptoms of leaf deformity and yellowing, resulting in the yield loss of chili production (Fadhila et al., 2020; Laprom et al., 2019; Sau et al., 2020).

Systemic insecticides are preferred for most farmers as they have shown immediate effects against *B. tabaci* and other plant-sucking pests. Carbaryl, malathion and imidacloprid are the world's most utilized and effective pesticides against *B. tabaci* (Abubakar et al., 2022). Humans exposed to imidacloprid have a high likelihood of developing cancer (Caron-Beaudoin et al., 2016). Meanwhile, other neonicotinoid pesticides have been associated with negative effects on non-target organisms, such as honey bees (Mengoni Goñalons & Farina, 2018), vertebrates (Hallmann et al., 2014) and invertebrates (Berheim et al., 2019). A few studies indicate that several biotypes of *B. tabaci* are developing resistance to chemical insecticides. For instance, the Q biotype exhibited significant resistance to commercial insecticides, as observed in a population isolated from Cameron Highland, Pahang, Malaysia (Shadmany et al., 2015).

Terpenes, phenolic and fatty acids are associated with repellent properties to *B. tabaci* (Islam et al., 2017; Yang et al., 2010). Phytochemical investigations on bryophytes have resulted in the isolation of a wide variety of secondary metabolites, namely green leaf volatiles, flavonoids, terpenoids and phenolic compounds (Asakawa et al., 2013; Ludwiczuk & Asakawa, 2019), indicating that these compounds can promote and expand their use as biological insecticides. Among bryophytes, liverworts possess specialized organelles known as oil bodies, a unique structure absent in other bryophytes. The accumulation of secondary metabolites, such as terpenoids and benzenoids, in the oil bodies has been reported (Tanaka et al., 2016). Polygodial sesquiterpenes isolated from *Porella vernicosa* killed mosquito larvae at a concentration of 40 ppm, which was stronger than commercial insect-repellent diethyltoluamide (DEET; Asakawa & Ludwiczuk, 2018). Clavigerins sesquiterpenes from the *Lepidolaena clavigera* have similar efficiency to the active ingredient in pesticide, azadirachtin, against *Anthrenocerus australis* and *Tineola bisselliella* (Perry et al., 2008). It suggests that the production of secondary metabolites in liverworts may have significant implications for plant-herbivore interactions.

Bazzania is the largest genus of the Lepidoziaceae family. Malaysia has documented approximately 66 *Bazzania* species, with 33 identified in Peninsular Malaysia (Lee et al., 2022). Most *Bazzania* sp. are composed of sesquiterpenoid and aromatic compounds (Asakawa et al., 2013). The chemical compositions of Malaysian *Bazzania*, *Bazzania spiralis*, *Bazzania praerupta*, and *Bazzania harpago* have been identified (Ludwiczuk &

Asakawa, 2010). Only *B. harpago* extracts have been tested for antifungal activity (Ng et al., 2021). While in vitro culture has been reported for *Marchantia* sp., similar techniques could potentially be applied to liverworts like *B. spiralis*, offering advantages for biopesticide development due to their ease of culture, rapid life cycles, and ability to establish genetically homogeneous lines through asexual reproduction (Ishizaki et al., 2015; Krishnan et al., 2015). Moreover, their promising terpene profiles make them potential alternatives to chemical pesticides. To investigate the potential of *Bazzania* extracts further, this study aimed to evaluate the insecticidal effects of crude methanol extracts of *B. spiralis* against *B. tabaci* through toxicity and oviposition deterrent assays conducted in a laboratory.

MATERIALS AND METHODS

Sampling Collection

The liverwort species, *Bazzania spiralis*, was collected from Mossy Forest in Cameron Highlands between 8:00 am and 10:00 am in November 2020. The sampling site was located at coordinates 4°31.459'N 101°23.340'E, at 1602 m alt. The recorded temperature was between 15°C and 18°C. The tools and techniques employed for liverwort sample collection in the field adhere to the guidelines provided by Lee and Gradstein (2021). The voucher specimens were identified and deposited in the Herbarium of Universiti Malaysia Terengganu (UMTP). The samples were identified based on morphological characteristics using identification keys (Lee & Gradstein, 2021).

Preparation of Crude Extracts

The preparation of crude extracts was carried out in accordance with Nagappan et al. (2019). The sample was cleaned to remove the substrate and other impurities prior to being air-dried. The air-dried samples were powdered and soaked in 500 ml 80% methanol (Merck, Germany) for four days. The methanol-liverwort mixtures were then filtered using Whatman No.1 (Merck, Germany) filter paper to remove the liverwort remainder, and the filtrate was collected to be concentrated. About 5 g of sodium sulfate anhydrous (Na_2SO_4, Merck, Germany) was added to remove moisture into the filtrate and was left for 30 min at room temperature. The solvent was then filtered and transferred into a round-bottom flask to be concentrated using a rotary evaporator (BUCHI V-700, Switzerland) to obtain the crude extract. The rotary evaporator was set to 25°C, 500-100 mbar, and 125-80 rpm. The pressure and rotation were adjusted within this range to prevent the sample solution from overheating and bubbling. The evaporated extract was transferred into a 20 ml vial and placed in a desiccator to dry out completely. The weight of the dried extract was recorded. Finally, the crude extracts were stored in a -20^{0}C freezer prior to being used for plant treatment and GC-MS analysis.

Bemisia tabaci Rearing

Colonies of *Bemisia tabaci* were collected from *Capsicum annuum* at Kompleks Pertanian UMT Bukit Kor, Terengganu. Colonies of *B. tabaci* were established and maintained on plants in insect-proof cages in a greenhouse at 28°C–32°C and 70%–80% relative humidity. Prior to conducting the toxicity and oviposition assays, newly emerged adults of *B. tabaci* were collected and immobilized by placing them in a refrigerator at 4°C for 2 to 3 minutes. Their sex was distinguished under a stereomicroscope. The females of *B. tabaci* have rounded abdomens, while the males have pointed abdomens. The insects were then placed in flasks and starved for two hours prior to the experiments.

Toxicity Assay

The crude extract was dissolved in absolute ethanol (Merck, Germany) to prepare stock solutions with a 10 mg/ml concentration. The stock solutions were then diluted with a series of concentrations of (1000µg/ml, 500µg/ml, 250 µg/ ml, 125 µg/ml, and 62.5 µg/ ml) and mixed with 0.02% (v/v) Tween 20 (Thermo Scientific, USA) as a surfactant. As for the negative control, a mock solution consisting of a mixture of 70% ethanol and 0.02% (v/v) Tween 20 was prepared. A commercial pesticide, Imidacloprid (Fusilier, Malaysia), was prepared according to the manufacturer's recommended doses and mixed with 0.02% of Tween 20.

This experiment was conducted by following Chen et al. (2018) with modifications. A young, fully extended leaf from a *Capsicum annuum* (variety Kulai 461) plant was sprayed with 1 ml of liverwort crude extracts at various concentrations and was left to dry for 12 hours. The leaf was placed on fresh agar inside a round plastic container (25oz) with a 1-inch agar layer to prevent desiccation. Ten adult insects (five females and five males) were placed into each container. The number of dead and surviving *B. tabaci* individuals was observed under a stereomicroscope after 48 hours. *Bemisia tabaci* was considered dead when no movements of antennae or legs were observed. For the negative control, a leaf was sprayed with a mock solution before infestation. Three leaves per plant and five *C. annuum* plants were used for this experiment. The assay was carried out in a chamber with a temperature of 24°C–26°C, relative humidity of 60%–70%, and a photoperiod of 12-h lights. The mortality rates of *B. tabachi* were compared between different concentrations of liverwort extract, pesticide and negative control.

Oviposition Deterrent Bioassay

To investigate the effect of liverwort crude extract on *B. tabaci*, an oviposition deterrent assay was conducted following Saad et al. (2017). 1 ml of 500µg/ml of liverwort extract solution was sprayed onto leaves of *C. annuum* plants, and then left for 24 hours. Ten adult males and 10 adult females of *B. tabaci* were collected from a rearing cage and placed in a glass jar containing agar and fresh leaves for 24 hours for copulation. Three leaves

from nodes 12 to 14 of each *C. annuum* plant were covered with an insect-proof clip cage (30 mm diameter). Three female adults of *B. tabaci* from the glass jar were subsequently placed in each clip caged. The *B. tabaci* were allowed to feed and oviposit for two days. The number of eggs laid was counted, and the adults were removed from the leaves. On the seventh day, the leaves were detached, and the number of larvae was counted. For the negative control, each leaf was sprayed with a mock solution. The *C. annuum* leaves were also sprayed with a synthetic pesticide, an Imidacloprid solution, as positive control. Five plants were used for the experiment, with each plant having three clip cages per treatment and placed in a separate insect cage (24°C–26°C, 60%–70% RH, 12:12-h lights: dark). The number of survival larvae was considered as viable eggs. The egg hatching rate was determined by the number of viable eggs relative to the total number of laid eggs and was expressed in percentage. An oviposition deterrent index (ODI) was calculated using the formula:

$$T = 100\ (C - T)/\ (C + T)$$

Where C is the total number of eggs laid on control leaves, and T is the total number of eggs on treated leaves (Huang et al., 1994).

Data Analysis

The percentage of mortality was corrected using Abbott's formula (Abbott, 1925). The lethal concentrations (LC_{50} and LC_{90}) and lethal times (LT_{50} and LT_{90}) were calculated using probit analysis. The mortality data were analyzed using the Kruskal-Walis H-test to calculate mean differences between concentrations, followed by post-hoc Dunn's test (*p*-values corrected according to the Bonferroni method for multiple comparisons). Mean differences among plant treatments for oviposition and hatchling rate were analyzed independently using one-way analysis of variance (ANOVA), followed by post hoc Tukey's test. All statistical analyses were performed using IBM Statistical Package for the Social Sciences (SPSS) version 29.0 software.

Gas Chromatography-mass Spectrometry (GC-MS) Analysis

Approximately 1 mg of crude extracts of *B. spiralis* were dissolved in 1 ml of methanol (GC grade, Sigma-Aldrich, Germany) and filtered using a 0.45 µM syringe filter. The GC-MS was performed using SHIMADZU QP2010 Ultra gas chromatograph–mass spectrometer (Japan) equipped with a Zebron ZB-5ms column (30 m × 250 µm i.d. × 0.25 µm film thickness; Phenomenex, USA). The gas chromatographic parameters were as follows: the initial temperature was fixed at 50°C for 1 min, then increased at a rate of 10 °C min^{-1} to 200°C, then further increased to 300°C at 5°C min^{-1}. The injection temperature was set at 300°C, and an injection volume of 1 µL was used in splitless mode. The MS scan range

was set at 50–600 m/z at 70 eV. Helium was used as the carrier gas at a 1 mL/min flow rate. Before GC-MS analysis, the n-alkane standard, C_7-C_{30} (Sigma-Aldrich, Germany), was used and run using the same parameters described above.

Compounds were identified by comparing the GC-MS mass spectra with NIST library spectra. The retention indices were calculated using the method described in Van Den Dool and Kratz (1963). Experimental retention indices (RI) were compared with reported RI in literature (Babushok et al., 2011) or in NIST (https://webbook.nist.gov/chemistry/). The volatile composition was expressed as the percentage of peak area relative to the total peak area of each compound.

RESULTS

Toxicity and Oviposition Deterrent to *Bemisia tabaci*

The liverworts' crude extracts were tested for toxicity against adult *B. tabaci*. The results showed that *B. tabaci* mortality was recorded as 58.3 ± 3.7% at a concentration of 1000 µg/ml after 12 hours of exposure and reached 100% after 48 hours (Figure 1). The crude extracts of *B. spiralis* showed maximum mortality on *B. tabaci* at concentrations of 500µg/ml and 250 µg/ml after 60 hours (Kruskal-Wallis test: H_6=31.83, p<0.001). After 60 hours of exposure, mortality was recorded as 91.7 ± 3.7% and 86.1 ± 5.1% at 125µg/ml concentrations and 62.5µg/ml, respectively. The mock treatment showed the lowest mortality compared to *Bazzania*-treated leaves, while imidacloprid showed maximum mortality after 24 hours of exposure.

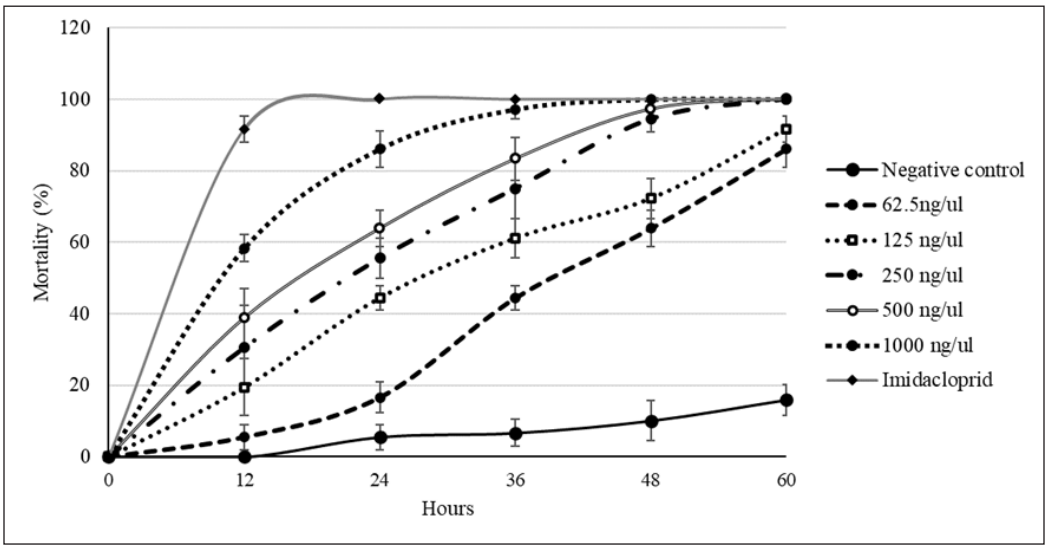

Figure 1. Accumulated mortality of *B. tabaci* in a glass jar exposed to different concentrations of *Bazzania spiralis* crude extracts. The data represents the mean of six replicates for each concentration
Note. Vertical bars represent the standard error (SE) of the mean

The LC_{50} values indicated that *B. tabaci* is sensitive to the *B. spiralis* crude extract, ranging from 699.37µg/ml after 12 hours of exposure to 22.00µg/ml after 60 hours (Table 1). The corresponding LC_{90} values were estimated to be 84.88µg/ml after 60 60-hour exposure period of *B. tabaci* to *B. spiralis* crude extracts. The estimated values of LT_{50} ranged from 10.91 hours to 40.15 hours, while LT_{90} values occurred from 24.25 hours to 78.07 hours at concentrations of 1000µg/ml to 62.5 µg/ml (Table 2).

Table 1
Toxicity of B. spiralis *crude extracts to* B. tabaci *after different exposure time*s (*N*=36)

Exposure time (hours)	**LC_{50} (95% CL)[c] (ug/ml)[a]**	**LC_{90} (95% CL)[c] (ug/ml)[b]**	**Slope ± SE**	x^2
12	699.37 (473.81-1371.25)	6512.82 (2647.33-9914.28)	1.32 ± 0.26	0.96
24	214.30 (152.36-292.83)	1570.76 (917.09-3273.55)	1.48 ± 0.25	2.45
36	81.94 (43.35-118.90)	622.95 (401.84-1423.20)	1.46 ± 0.28	1.14
48	47.11 (20.75-70.07)	215.91 (157.05-370.42)	1.94 ± 0.41	1.95
60	22.00 (6.24-43.82)	84.88 (40.67-141.08)	2.19 ± 0.84	1.44

Notes.
[a] Lethal concentration required to kill 50% of *B. tabaci*
[b] Lethal concentration required to kill 90% of *B. tabaci*
[c] Confidence limit, which was calculated with 95% confidence

Table 2
Toxicity of B. spiralis *crude extracts to* B. tabaci *after different exposure concentrations (N=36)*

Concentration (µg/ml)	**LT_{50} (95% CL)[c] (hours)[a]**	**LT_{90} (95% CL)[c] (hours)[b]**	**Slope ± SE**	x^2
62.50	40.15 (35.51-46.12)	78.07 (63.97-108.49)	4.00 ± 0.57	3.35
125.00	28.98 (24.21-34.24)	74.28 (57.71-114.81)	2.82 ± 0.44	2.35
250.00	19.14 (15.54-22.37)	45.15 (37.67-59.32)	3.44 ± 0.49	5.24
500.00	16.18 (15.59-15.25)	38.17 (32.37-50.94)	3.37 ± 0.58	3.92
1000.00	10.91 (7.38-13.57)	24.25 (20.14-31.81)	3.70 ± 0.70	1.07

Notes.
[a] Lethal time required to kill 50% of *B. tabaci*
[b] Lethal time required to kill 90% of *B. tabaci*
[c] Confidence limit, which was calculated with 95% confidence

The crude extracts of *B. spiralis* strongly deterred oviposition by *B. tabaci*, with a significantly lower number of eggs being laid on *B. spiralis*-treated leaves in comparison with the control ($F_{2,12}$=47.01, p<0.001) (Figure 2). The oviposition deterrent activity of *B. spiralis* extracts was recorded as 31.5% ± 10.44 at 500µg/ml (Table 3). The positive control, imidacloprid, demonstrated a 2-fold higher oviposition deterrent activity than *B. spiralis* extracts. The number of eggs hatching on *B. spiralis*-treated leaves was significantly lower than the control at a concentration of 500 µg/ml after seven days of treatment (Figure 2). The crude extracts of *B. spiralis* reduced the *B. tabaci* eggs' hatchability to 39.39%±4.56 ($F_{2,12}$=200.09, p<0.001).

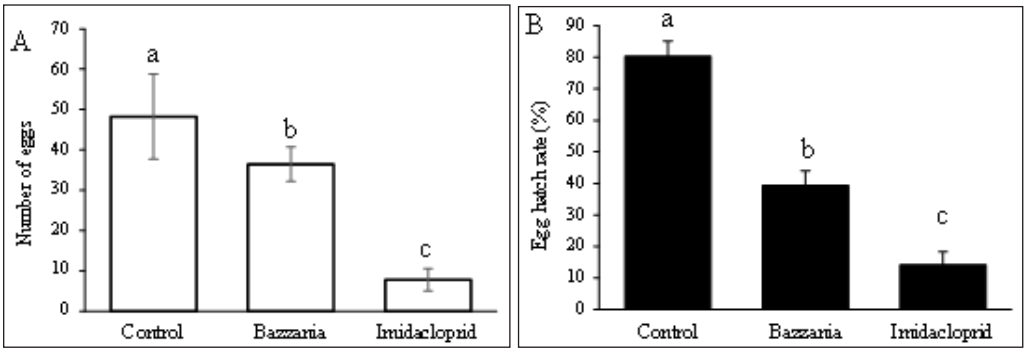

Figure 2. Effects of liverwort extracts (500µg/ml) on oviposition (A) and egg hatching (B) of *B. tabaci*. Mock is the negative control, and imidacloprid is the synthetic pesticide. Different letters indicate significant differences among treatments (ANOVA followed by Tukey's post hoc analysis, p<0.05)

Table 3
The oviposition deterrent effects of liverwort crude extracts on Bemisia tabaci

Liverwort species	Egg number in treated leaves	Egg number in control leaves	Effective deterrence (%)	Egg number in imidacloprid leaves	Effective deterrence (%)
Bazzania spiralis	53 ± 7.44	36.4 ± 4.28	31.5 ± 10.44	7.8 ± 2.77	83.78 ± 7.48

Gas Chromatography-Mass Spectrophotometry (GC-MS) Analysis

The crude extract of *B. spiralis* revealed the presence of eleven compounds, corresponding to 97.8% of the total extract (Table 4). Among these compounds, 64% were fatty acids, representing 35.4% of the total peak area. Despite having the highest number of fatty acids derivatives, sesquiterpene recorded greater peak areas, constituting 59% of the total area. spathulenol exhibited the highest peak area (49.8%), followed by palmitic acid ethyl ester (22.7%).

Table 4
Chemical composition of the crude extracts from Bazzania spiralis

No.	Compounds	RT	RI	RI_{ref}	Peak area (%)
1	Ledene	14.17	1497	1494	2.9
2	Spathulenol	15.57	1608	1605	48.7
3	Aristolone	17.28	1758	1757	2.8
4	Hexahydrofarnesyl acetone	18.21	1843	1843	3.3
5	Palmitic acid, methyl ester	19.07	1914	1920	trace
6	Palmitic acid, ethyl ester	19.94	1960	1976	22.2
7	(9Z,12Z)-9,12-Octadecadien-1-ol	21.33	2067	2069	3.2
8	Trichloroacetic acid, tridec-2-ynyl ester	21.39	2073	2075	8.3
9	cis-10-Heptadecenoic acid	21.45	2080	2084	2.3
10	Heptadecanoic acid, ethyl ester	21.63	2099	2089	1.7
11	Phthalic acid, 2-ethylhexyl tetradecyl ester	24.49	2429	2475	trace
12	Stigmasterol	30.71	3175	3170	2.3
				Total	97.8

Note. RI = Retention indices relative to n-alkanes (C_7-C_{30}). $RI_{ref:}$ Retention indices with those reported in references

DISCUSSION

The present study demonstrates the insecticidal potential of *Bazzania spiralis* crude extracts against the whitefly *Bemisia tabaci*. The extracts exhibited significant toxicity, oviposition deterrence, and egg hatchability reduction, suggesting their potential as a natural alternative to synthetic pesticides for the management of *B. tabaci*. Asakawa et al. (2013) reported that several liverwort species, including the genus *Bazzania*, contain bioactive compounds with insecticidal activities.

To date, no study has reported the toxicity of *Bazzania* sp. extracts against various insect pests. This study showed that the mortality of *B. tabaci* reached 100% at a concentration of 1000 ug/ml after 48 hours of exposure, indicating the potent insecticidal activity of the extracts. Similar studies have reported the toxicity of liverwort extracts against various insect pests. For instance, Mulyani et al. (2024) found that crude extracts of the liverwort *Marchantia paleacea* showed high toxicity against the larvae *Athalia proxima*, with an LC_{50} value of 0.33% after 24 hours of exposure. The LC_{50} values of *B. spiralis* extracts ranged from 699.37µg/ml (12 hours of exposure) to 22.00µg/ml (60 hours of exposure), suggesting that prolonged exposure to lower concentrations can still achieve significant mortality. These findings are consistent with the LC_{50} values of the liverwort *Plagiochila asplenioides* extracts against the diamondback moth, *Plutella xylostella*, which decreased from 245.7 µg/ml (24 hours of exposure) to 76.3 µg/ml (72 hours of exposure) (Zhang et

al., 2020). *Bazzania spiralis* crude extracts significantly deterred oviposition and reduced egg hatchability, demonstrating their potential as oviposition deterrents and ovicides against *B. tabaci*. Similar findings have been reported that crude extracts of the liverwort *Marchantia linearis* exhibited oviposition deterrent activity against the *Spodoptera litura* (Krishnan & Kumara, 2015).

Neonicotinoid pesticides, such as imidacloprid, are highly effective and long-lasting due to their systemic nature. These water-soluble compounds are easily absorbed by plant tissues and transported throughout the plant, providing extended protection against pests like whiteflies and aphids. Imidacloprid affects the central nervous system of insects, leading to paralysis and death. However, it also poses similar risks to beneficial insects, particularly pollinators, contributing to the decline of pollinator populations (Ihara & Matsuda, 2018). Recent studies have shown that imidacloprid triggers a significant oxidative stress response in *B. tabaci*, producing extensive ROS (Li et al., 2024). Our study demonstrates that *B. spiralis* crude extracts achieve 90% mortality of *B. tabaci* within 24 hours of application, suggesting a potential to exhibit similar effects due to the significant increase in *B. tabaci* mortality. Both imidacloprid and *B. spiralis* extracts induce trichome formation in treated plants (unpublished data), indicating absorption into plant tissues. Botanical pesticides like *B. spiralis* extracts typically degrade more quickly than synthetic systemic insecticides (Khursheed et al., 2022). This rapid degradation reduces the risk of toxin accumulation during flowering periods, potentially mitigating harmful effects on beneficial insects. These characteristics suggest that *B. spiralis* extracts could offer a more environmentally friendly alternative to synthetic pesticides, potentially reducing the risk of resistance development and negative impacts on non-target species.

GC-MS analysis of *B. spiralis* crude extracts revealed the presence of eleven compounds, with fatty acids derivatives and sesquiterpenes being the major constituents. Spathulenol, composed of the highest composition of the total compounds in *B. spiralis* extracts, is also isolated from *B. spiralis* and *B. praerupta* (Ludwiczuk & Asakawa, 2010). Diethyl ether extracts of *B. spiralis* from Mount Kinabalu, Sabah, have identified a tetracyclic triterpene, stigmasterol (Kondo et al., 1990), which was also detected in GC-MS of methanolic extracts in this study. Spathulenol has the potential to contribute to the toxicity and inhibition of *B. tabaci*. As a sesquiterpene, spathulenol is lipophilic and volatile, allowing it to penetrate insects rapidly and interfere with their physiological functions (Albouchi et al., 2018; Bakkali et al., 2008). It has been shown to exhibit strong antifeedant activity against phloem feeders, green peach aphids, *Myzus persicae* (Souda et al., 2023), and exhibit neurotoxic effects on the grain aphid, *Metopolophium dirhodum* (Benelli et al., 2020). However, the exact mechanisms by which spathulenol affects *B. tabaci* in our study are not fully understood and merit further investigation.

Palmitic acid, another major component identified in the extracts, has demonstrated significant effects on various insect pests. Palmitic acid showed nymph toxicity and oviposition deterrence against *B. tabaci*, resulting in 55% mortality and 40.5% deterrence in a 24-hour bioassay (Wagan et al., 2018). These effects may be related to palmitic acid's ability to modulate the synthesis and release of insect hormones, such as juvenile hormones and ecdysteroids (Stanley-Samuelson et al., 1988). Disruption of these hormones can lead to developmental abnormalities, reduced fecundity, and increased mortality (Singtripop et al., 2000). The mechanism of action for palmitic acid may also involve neurological effects. Research on the light brown apple moth, *Epiphyas postvittana*, has shown that fatty acids with carbon chains C_{14} to C_{16} can increase the permeability of neuron membranes, affecting ion exchange and provoking stressed excitability of neuron cells (Taverner et al., 2001). Similarly, *Tetranychus cinnabarinus* exposed to palmitate exhibited signs of neural poisoning (Wang et al., 2009). While palmitic acid falls within this category, further research is needed to determine if it acts similarly in *B. tabaci* when exposed to *B. spiralis* extracts.

The presence of fatty acids and sesquiterpenes in *B. spiralis* crude extracts indicates the potential for synergistic effects. Synergistic toxicity commonly occurs among compounds found in essential oils (Pavela, 2014), as well as among the major constituents of these oils in their natural proportions (Hummelbrunner & Isman, 2001). For instance, sesquiterpenes facilitate the penetration or transport of another compound across the insect cuticle or gut membrane (Tak & Isman, 2017). They may enhance the penetration of fatty acids to reach the target sites. Synergistic interactions can also influence changes in insect behavior. One compound may act as a feeding or oviposition deterrent, while another may exhibit toxic effects. The combination of these effects can lead to reduced feeding damage and population growth (Miresmailli & Isman, 2014). The synergistic action of sesquiterpenes and fatty acids in *B. spiralis* extracts may enhance their insecticidal efficacy against *B. tabaci*.

For practical field application of *B. spiralis* extracts, we recommend exploring fumigation methods in greenhouse settings and contact spraying for open-field use. However, the extract's stability under various environmental conditions requires further investigation. Comprehensive field trials are necessary to assess the extract's efficacy and persistence under diverse environmental conditions, which will be crucial for optimizing application strategies.

CONCLUSION

This study demonstrates the insecticidal properties of *B. spiralis* crude extracts against *B. tabaci*, including toxicity, oviposition deterrent activity, and reduction in egg hatchability. Sesquiterpenes, particularly spathulenol, and fatty acids in the extracts may contribute to their insecticidal activity. Moreover, the potential synergistic effects between these

sesquiterpenes and fatty acids could enhance the overall effectiveness of the extracts, highlighting their complexity as a natural insecticidal agent. These findings highlight the potential of liverwort-derived compounds as natural alternatives to synthetic pesticides for managing *B. tabaci*. Further research is needed to isolate and characterize the active compounds responsible for the insecticidal properties, investigate their potential synergistic interactions, and evaluate their efficacy under field conditions.

ACKNOWLEDGEMENTS

This research was funded by the Ministry of Higher Education (MOHE) through the Fundamental Research Grant Scheme (FRGS/1/2020/WAB04/UMT/03/1), a grant awarded to N.F.M.S (VOT59614). We are grateful to Siti Khadijah Ibrahim, Nurfatihah Daud and Nur Ain Ismail for their invaluable assistance and support in the laboratory. This transdisciplinary research is part of a dissertation submitted as partial fulfillment to meet the requirements for the master's degree at Universiti Malaysia Terengganu.

REFERENCES

Abbott, W. S. (1925). A method of computing the effectiveness of an insecticide. *Journal of Economic Entomology*, *18*(2), 265-267. https://doi.org/10.1093/jee/18.2.265a

Abubakar, M., Koul, B., Chandrashekar, K., Raut, A., & Yadav, D. (2022). Whitefly (*Bemisia tabaci*) management (WFM) strategies for sustainable agriculture: A review. *Agriculture*, *12*(9), 1317. https://doi.org/10.3390/agriculture12091317

Albouchi, F., Ghazouani, N., Souissi, R., Abderrabba, M., & Boukhris-Bouhachem, S. (2018). Aphidicidal activities of *Melaleuca styphelioides* Sm. essential oils on three citrus aphids: *Aphis gossypii* Glover; *Aphis spiraecola* Patch and *Myzus persicae* (Sulzer). *South African Journal of Botany*, *117*, 149-154. https://doi.org/https://doi.org/10.1016/j.sajb.2018.05.005

Asakawa, Y., & Ludwiczuk, A. (2018). Chemical constituents of bryophytes: Structures and biological activity. *Journal of Natural Products*, *81*(3), 641-660. https://doi.org/10.1021/acs.jnatprod.6b01046

Asakawa, Y., Ludwiczuk, A., & Nagashima, F. (2013). *Chemical constituents of bryophytes. Bio- and chemical diversity, biological activity, and chemosystematics.* Springer. https://doi.org/10.1007/978-3-7091-1084-3_1

Babushok, V., Linstrom, P., & Zenkevich, I. (2011). Retention indices for frequently reported compounds of plant essential oils. *Journal of Physical and Chemical Reference Data*, *40*(4), 043101. https://doi.org/https://doi.org/10.1063/1.3653552

Bakkali, F., Averbeck, S., Averbeck, D., & Idaomar, M. (2008). Biological effects of essential oils - A review. *Food and Chemical Toxicology*, *46*(2), 446-475. Https://doi.org/10.1016/j.fct.2007.09.106

Benelli, G., Pavela, R., Drenaggi, E., Desneux, N., & Maggi, F. (2020). Phytol, (E)-nerolidol and spathulenol from *Stevia rebaudiana* leaf essential oil as effective and eco-friendly botanical insecticides against

Metopolophium dirhodum. *Industrial Crops and Products*, *155*, 112844. https://doi.org/https://doi.org/10.1016/j.indcrop.2020.112844

Berheim, E. H., Jenks, J. A., Lundgren, J. G., Michel, E. S., Grove, D., & Jensen, W. F. (2019). Effects of neonicotinoid insecticides on physiology and reproductive characteristics of captive female and fawn white-tailed deer. *Scientific Reports*, *9*(1), 4534. https://doi.org/10.1038/s41598-019-40994-9

Caron-Beaudoin, É., Denison, M. S., & Sanderson, J. T. (2016). Effects of neonicotinoids on promoter-specific expression and activity of aromatase (CYP19) in human adrenocortical carcinoma (H295R) and primary umbilical vein endothelial (HUVEC) cells. *Toxicological Sciences*, *149*(1), 134-144. https://doi.org/10.1093/toxsci/kfv220

Chen, G., Klinkhamer, P. G. L., Escobar-Bravo, R., & Leiss, K. A. (2018). Type VI glandular trichome density and their derived volatiles are differently induced by jasmonic acid in developing and fully developed tomato leaves: Implications for thrips resistance. *Plant Sci*, *276*, 87-98. https://doi.org/10.1016/j.plantsci.2018.08.007

Czosnek, H., Hariton-Shalev, A., Sobol, I., Gorovits, R., & Ghanim, M. (2017). The incredible journey of begomoviruses in their whitefly vector. *Viruses*, *9*(10), 273. https://doi.org/10.3390/v9100273

Fadhila, C., Lal, A., Vo, T. T., Ho, P. T., Hidayat, S. H., Lee, J., Kil, E-J., & Lee, S. (2020). The threat of seed-transmissible pepper yellow leaf curl Indonesia virus in chili pepper. *Microbial pathogenesis*, *143*, 104132. https://doi.org/10.1016/j.micpath.2020.104132

Hallmann, C. A., Foppen, R. P., Van Turnhout, C. A., De Kroon, H., & Jongejans, E. (2014). Declines in insectivorous birds are associated with high neonicotinoid concentrations. *Nature*, *511*(7509), 341-343. https://doi.org/10.1038/nature13531

Huang, X. P., Renwick, J., & Chew, F. S. (1994). Oviposition stimulants and deterrents control acceptance of *Alliaria petiolata* by *Pieris rapae* and *P. napi* oleracea. *Chemoecology*, *5*, 79-87. https://doi.org/https://doi.org/10.1007/BF01259436

Hummelbrunner, L. A., & Isman, M. B. (2001). Acute, sublethal, antifeedant, and synergistic effects of monoterpenoid essential oil compounds on the tobacco cutworm, *Spodoptera litura* (Lep., Noctuidae). *Journal of Agricultural and Food Chemistry*, *49*(2), 715-720. https://doi.org/10.1021/jf000749t

Ihara, M., & Matsuda, K. (2018). Neonicotinoids: Molecular mechanisms of action, insights into resistance and impact on pollinators. *Current Opinion in Insect Science*, *30*, 86-92. https://doi.org/10.1016/j.cois.2018.09.009

Ishizaki, K., Nishihama, R., Yamato, K. T., & Kohchi, T. (2015). Molecular genetic tools and techniques for *Marchantia polymorpha* research. *Plant and Cell Physiology*, *57*(2), 262-270. Https://doi.org/10.1093/pcp/pcv097

Islam, M. N., Hasanuzzaman, A. M., Zhang, Z. F., Zhang, Y., & Liu, T. X. (2017). High level of nitrogen makes tomato plants releasing less volatiles and attracting more *Bemisia tabaci* (Hemiptera: Aleyrodidae). *Frontiers in Plant Science*, *8*, 466. https://doi.org/10.3389/fpls.2017.00466

Khursheed, A., Rather, M. A., Jain, V., Wani, A. R., Rasool, S., Nazir, R., Malik, N. A. & Majid, S. A. (2022). Plant based natural products as potential ecofriendly and safer biopesticides: A comprehensive overview of

their advantages over conventional pesticides, limitations and regulatory aspects. *Microbial Pathogenesis*, *173*, 105854. https://doi.org/10.1016/j.micpath.2022.105854

Kondo, K., Toyota, M., & Asakawa, Y. (1990). ent-Eudesmane-type sesquiterpenoids from *Bazzania* species. *Phytochemistry*, *29*(7), 2197-2199. https://doi.org/10.1016/0031-9422(90)83037-2

Krishnan, R., & Kumara, M. (2015). Insecticidal potentiality of flavonoids from cell suspension culture of *Marchantia linearis* lehm. & lindenb against *Spodoptera litura* F. *International Journal of Applied Biology and Pharmaceutical Technology*, *6*(2), 23-32.

Laprom, A., Nilthong, S., & Chukeatirote, E. (2019). Incidence of viruses infecting pepper in Thailand. *Biomolecular Concepts*, *10*(1), 184-193. https://doi.org/10.1515/bmc-2019-0021

Lee, G. E., & Gradstein, S. R. (2021). *Guide to the genera of liverworts and hornworts of Malaysia*. Hattori Botanical Laboratory. https://doi.org/10.3897/phytokeys.199.76693

Lee, G. E., Gradstein, S. R., Pesiu, E., & Norhazrina, N. (2022). An updated checklist of liverworts and hornworts of Malaysia. *Phytokeys 199*, 29-111. https://doi.org/10.3897/phytokeys.199.76693

Li, J., Zhu, C., Xu, Y., He, H., Zhao, C., & Yan, F. (2024). Molecular mechanism underlying ROS-mediated AKH resistance to imidacloprid in whitefly. *Insects*, *15*(6), 436. https://doi.org/10.3390/insects15060436

Ludwiczuk, A., & Asakawa, Y. (2010). Chemosystematics of the liverworts collected in Borneo. *Tropical Bryology*, *31*, 33-42. https://doi.org/10.11646/bde.31.1.8

Ludwiczuk, A., & Asakawa, Y. (2019). Bryophytes as a source of bioactive volatile terpenoids – A review. *Food and Chemical Toxicology*, *132*, 110649. https://doi.org/10.1016/j.fct.2019.110649

Mengoni Goñalons, C., & Farina, W. M. (2018). Impaired associative learning after chronic exposure to pesticides in young adult honey bees. *Journal of Experimental Biology*, *221*(7), jeb176644. https://doi.org/10.1242/jeb.176644

Miresmailli, S., & Isman, M. B. (2014). Botanical insecticides inspired by plant–herbivore chemical interactions. *Trends in Plant Science*, *19*(1), 29-35. https://doi.org/10.1016/j.tplants.2013.10.002

Mulyani, S., Sugiyarto., & Pangastuti, A. (2024). Larvicidal activity of liverworts' (*Marchantia paleacea*) ethyl acetate fraction against *Athalia proxima*. In *IOP conference series: Earth and environmental science* (p. 012042). IOP Publishing. https://doi.org/10.1088/1755-1315/1362/1/012042

Nagappan, T., Tatin, Y., & Skornickova, J. L. (2019). Investigation on bioactive potential of selected wild ginger, genus *Etlingera* from Tasik Kenyir, Terengganu. In M. Abdullah, A. Mohammad, M. Nor Zalipah & M. Safiih Lola (Eds.), *Greater Kenyir landscapes* (pp. 75-82). Springer. https://doi.org/10.1007/978-3-319-92264-5_7

Ng, S. Y., Ang, L. P., Hau, V. L., Suleiman, M., Vairappan, C. S., & Kamada, T. (2021). Structural diversity, anti-fungal activity and chemosystematics of bomean liverwort (De Not.) Schiffner. *Sains Malaysiana*, *50*(1), 101-107. https://doi.org/10.17576/jsm-2021-5001-11

Pavela, R. (2014). Acute, synergistic and antagonistic effects of some aromatic compounds on the *Spodoptera littoralis* Boisd. (Lep., Noctuidae) larvae. *Industrial Crops and Products*, *60*, 247-258. https://doi.org/ https://doi.org/10.1016/j.indcrop.2014.06.030

Perry, N. B., Burgess, E. J., Foster, L. M., Gerard, P. J., Toyota, M., & Asakawa, Y. (2008). Insect antifeedant sesquiterpene acetals from the liverwort *Lepidolaena clavigera*. 2. structures, artifacts, and activity. *Journal of Natural Products*, *71*(2), 258-261. https://doi.org/10.1021/np0706441

Saad, K. A., Roff, M. N. M., & Idris, A. B. (2017). Toxic, repellent, and deterrent effects of citronella essential oil on *Bemisia tabaci* (Hemiptera: Aleyrodidae) on chili plants. *Journal of Entomological Science*, *52*(2), 119-130. https://doi.org/10.18474/jes16-32.1

Sau, A. R., Nazmie, N. M. F., Yusop, M. S. M., Akbar, M. A., Saad, M. F. M., Baharum, S. N., Talip, N., Goh, H. H., Kassim, H., & Bunawan, H. (2020). First report of pepper vein yellows virus and pepper yellow leaf curl virus infecting chilli pepper (*Capsicum annuum*) in Malaysia. *Plant Disease*, *104*(7), 2037-2037. https://doi.org/10.1094/PDIS-10-19-2152-PDN

Shadmany, M., Omar, D., & Muhamad, R. (2015). Biotype and insecticide resistance status of *Bemisia tabaci* populations from Peninsular Malaysia. *Journal of Applied Entomology*, *139*(1-2), 67-75. https://doi.org/ https://doi.org/10.1111/jen.12131

Singtripop, T., Wanichacheewa, S., & Sakurai, S. (2000). Juvenile hormone-mediated termination of larval diapause in the bamboo borer, *Omphisa fuscidentalis*. *Insect Biochemistry and Molecular Biology*, *30*(8), 847-854. https://doi.org/10.1016/S0965-1748(00)00057-6

Souda, B., Andres, M. F., Elfalleh, W., Gonzalez-Coloma, A., & Saadaoui, E. (2023). GC-MS profiling, antifeedant, nematicidal and phytotoxic effects of essential oils of two subspecies of *Eucalyptus flocktoniae* (Maiden) Maiden. *Natural Product Research*, *39*(6), 1444-1451. https://doi.org/10.1080/14786419.2023.2300392

Stanley-Samuelson, D. W., Jurenka, R. A., Cripps, C., Blomquist, G. J., & de Renobales, M. (1988). Fatty acids in insects: Composition, metabolism, and biological significance. *Archives of Insect Biochemistry and Physiology*, *9*(1), 1-33. https://doi.org/10.1002/arch.940090102

Tak, J.-H., & Isman, M. B. (2017). Penetration-enhancement underlies synergy of plant essential oil terpenoids as insecticides in the cabbage looper, *Trichoplusia ni*. *Scientific Reports*, *7*(1), 42432. https://doi.org/10.1038/srep42432

Tanaka, D., Ishizaki, K., Kohchi, T., & Yamato, K. T. (2016). Cryopreservation of gemmae from the liverwort. *Plant and Cell Physiology*, *57*(2), 300-306. https://doi.org/10.1093/pcp/pcv173

Taverner, P. D., Gunning, R. V., Kolesik, P., Bailey, P. T., Inceoglu, A. B., Hammock, B., & Roush, R. T. (2001). Evidence for direct neural toxicity of a "light" oil on the peripheral nerves of lightbrown apple moth. *Pesticide Biochemistry and Physiology*, *69*(3), 153-165. https://doi.org/https://doi.org/10.1006/pest.2000.2527

Van Den Dool, H., & Kratz, P. D. (1963). A generalization of the retention index system including linear temperature programmed gas-liquid partition chromatography. *Journal of Chromatography*, *11*(1963), 463-471. https://doi.org/https://doi.org/10.1016/S0021-9673(01)80947-X

Wagan, T. A., Cai, W., & Hua, H. (2018). Repellency, toxicity, and anti-oviposition of essential oil of *Gardenia jasminoides* and its four major chemical components against whiteflies and mites. *Scientific Reports*, *8*(1), 9375. https://doi.org/10.1038/s41598-018-27366-5

Wang, Y., Wang, H., Shen, Z., Zhao, L., Clarke, S., Sun, J., Du, Y. & Shi, G. (2009). Methyl palmitate, an acaricidal compound occurring in green walnut husks. *Journal of Economic Entomology*, *102*, 196-202. https://doi.org/10.1603/029.102.0128

Yang, N. W., Li, A. L., Wan, F. H., Liu, W. X., & Johnson, D. (2010). Effects of plant essential oils on immature and adult sweetpotato whitefly, biotype B. *Crop Protection*, *29*(10), 1200-1207. https://doi.org/10.1016/j.cropro.2010.05.006

REFEREES FOR THE PERTANIKA
JOURNAL OF TROPICAL AGRICULTURAL SCIENCE

Vol. 48 (3) MAY. 2025

The Editorial Board of the Pertanika Journal of Tropical Agricultural Science wishes to thank the following:

Abdul Hamid Ahmad
(UMS, Malaysia)

Ahmad Muhaimin Roslan
(UPM, Malaysia)

Ahmed Jalal Khan Chowdhury
(UNISSA, Brunei Darussalam)

Ai Nagahama
(Kahaku, Japan)

Aliah Zannierah Mohsin
(UPM, Malaysia)

Amirul Ridzuan Abu Bakar
(UniMAP, Malaysia)

Ankush Saddhe
(CAS, Czech Republic)

Athakorn Promwee
(WU, Thailand)

Aziz Ahmad
(UMT, Malaysia)

Azlina Mansor
(MARDI, Malaysia)

Chodsana Sriket
(KMITL, Thailand)

Chong Khim Phin
(UMS, Malaysia)

Choong Siew Shean
(UMK, Malaysia)

Chuah Tse Seng
(UMT, Malaysia)

Esti Hardi
(UNMUL, Indonesia)

Fernando Carlos Gomez-Merino
(Colpos, Mexico)

Indrastuti Apri Rumanti
(BRIN, Indonesia)

Kadambot H. M. Siddique
(UWA, Australia)

Laura Tomassoli
(CREA, Italy)

Martini Mohammad Yusoff
(UPM, Malaysia)

Mohd Nazre Saleh
(UPM, Malaysia)

Mohd Noor Hisham Mohd Nadzir
(UPM, Malaysia)

Mohd Rakib Mohd. Rashid
(UMS, Malaysia)

Mohd Rakib Mohd. Rashid
(UMS, Malaysia)

Nina Naquiah Ahmad Nizar
(UiTM, Malaysia)

Noor Hidayah Mamat
(UM, Malaysia)

Noor Liyana Yusof
(UPM, Malaysia)

Noorulnajwa Diyana Yaacob
(UniMAP, Malaysia)

Norzainih Jasmin Jamin
(MARDI, Malaysia)

Nur Anuar
(UKM, Malaysia)

Phebe Ding
(UPM, Malaysia)

Piotr Salachna
(ZUT, Poland)

Raimundo Jimenez-Ballesta
(UAM, Spain)

Ramalingam Jegadeesan
(TNAU, India)

Saichol Ketsa
(KU, Thailand)

Samsuri Abdul Wahid
(UPM, Malaysia)

Sandra Arifin Aziz
(IPB, Indonesia)

Shahrizim Zulkifly
(UPM, Malaysia)

BRIN	*-National Research and Innovation Agency*
CAAS	*-Chinese Academy of Agricultural Sciences*
CAS	*-Czech Academy of Sciences*
Colpos	*-Colegio de Postgraduados*
CREA	*-Council for Agricultural Research and Economics*
IPB	*-PB University*
Kahaku	*-Kokuritsu Kagaku Hakubutsukan*
KMITL	*-King Mongkut's Institute of Technology Ladkrabang*
KU	*-Kasetsart University*
MARDI	*-Malaysian Agricultural Research and Development Institute*
TNAU	*-Tamil Nadu Agricultural University*
UAM	*-Autonomous University of Madrid*
UFLA	*-Federal University of Lavras*
UiTM	*-Universiti Teknologi MARA*
UKM	*-Universiti Kebangsaan Malaysia*
UM	*-Universiti Malaya*
UMK	*-Universiti Malaysia Kelantan*
UMPSA	*-Universiti Malaysia Pahang Al-Sultan Abdullah*
UMS	*-Universiti Malaysia Sabah*
UMT	*-Universiti Malaysia Terengganu*
UNIMAP	*-Universiti Malaysia Perlis*
UNISSA	*-Universiti Islam Sultan Sharif Ali*
UNMUL	*-Mulawarman University*
UPM	*-Universiti Putra Malaysia*
UWA	*-University of Western Australia*
WU	*-Walailak University*
ZUT	*-West Pomeranian University of Technology*

While every effort has been made to include a complete list of referees for the period stated above, however if any name(s) have been omitted unintentionally or spelt incorrectly, please notify the Chief Executive Editor, *Pertanika* Journals at executive_editor.pertanika@upm.edu.my

Any inclusion or exclusion of name(s) on this page does not commit the *Pertanika* Editorial Office, nor the UPM Press or the university to provide any liability for whatsoever reason.

Pertanika Journal of Tropical Agricultural Science
Vol. 48 (3) May. 2025

Content

Pertanika Editorial Office, Journal Division,
Putra Science Park,
1st Floor, IDEA Tower II,
UPM-MTDC Center,
Universiti Putra Malaysia,
43400 UPM Serdang,
Selangor Darul Ehsan
Malaysia

http://www.pertanika.upm.edu.my
Email: executive_editor.pertanika@upm.edu.my
Tel. No.: +603- 9769 1622

PENERBIT UPM
UNIVERSITI PUTRA MALAYSIA
PRESS

http://penerbit.upm.edu.my
Email: penerbit@upm.edu.my
Tel. No.: +603- 9769 8855

e-ISSN 2231-8542